CRANFIELD UNIVERSITY

DEBORAH LUCINDA HARRISON

A MULTI PROXY INVESTIGATION INTO THE EFFECTS OF BURIAL ENVIRONMENTS ON NUCLEAR DNA IN BONE OVER FORENSIC AND ARCHAEOLOGICAL TIMESCALES

CRANFIELD FORENSIC INSTITUTE

PhD thesis
Academic Year: 2014 -2015

Supervisor: Dr Karl Harrison
July 2015

CRANFIELD UNIVERSITY

CRANFIELD FORENSIC INSTITUTE

PhD

Academic Year 2014 -2015

DEBORAH LUCINDA HARRISON

A MULTI PROXY INVESTIGATION INTO THE EFFECTS OF BURIAL ENVIRONMENTS ON NUCLEAR DNA IN BONE OVER FORENSIC AND ARCHAEOLOGICAL TIMESCALES

Supervisor: Dr Karl Harrison
July 2015

ABSTRACT

This research conducted a two-pronged approach to study the effects of taphonomic processes by conducting analysis of experimental burials of porcine femora and parallel analysis of ancient human archaeological remains from geologically distinct cemeteries. The aim of this study was to identify the major degradative factors from depositional environments that affect the bone composition and the retention and retrieval of nucleic DNA from archaeological bone. Four different experimental burial environments of clay, compost, lime and sand were designed, displaying different properties of soil type, pH, water content and organic content. Analysis of the burial mediums and bones were conducted at regular intervals over an 18 month period. Observations of changes in the burial medium, comparisons of the rates and degree of soft tissue decomposition, bone diagenesis from compositional assessment, and bone colour change were made and analysed in correspondence with the different environments. The analytical data collected on the diagenesis of the archaeological bone from both studies, was compared to the DNA profiling success rates.

The research and optimisation of sample preparation and DNA analysis enabled the most cost-effective and appropriate methods to be identified and utilised in accordance with the preservation state of the bone samples. This allowed the analysis of ancient archaeological bone to be analysed in-line with forensic protocols, to enable a uniform accessible approach to produce comparable results across different laboratories.

Drawing together the results from the various analytical techniques made it possible to identify the variables that affect bone diagenesis and the survival of nuclear DNA, and provide evidence that the rate of decomposition and bone degradation is affected more significantly by the burial environment than duration of burial, as stated in the research hypothesis. The presence of water, sand and the level of organic content were found to be the most degradative variables within the experimental burial conditions; causing changes in bone crystallinity, and infiltration of contaminants into the bone. The presence of lime, chalk or limestone

in an environment was found to have preserving properties in both the porcine and human burials, by retarding the rate and degree of soft tissue decomposition, and reducing the diagenetic changes in bone composition evident from the other environments.

Despite previous reports of success using analytical techniques as predictive models for DNA and bone preservation, no correlations with DNA survival could be established. However the use of a multi-disciplinary approach enabled the detection and identification of soil contaminants affecting the bone structure and the ability to amplify DNA, in relation to burial environments. This research highlighted the importance of utilising multiple analytical techniques, such as colourimetry, ATR-FTIR, XRF and genetic analysis in order to avoid misinterpretation and false reporting of the state of bone diagenesis or preservation and the survival of DNA, due to environmental contaminants within the hard tissue.

The research confirms the idea that in order to establish optimised sampling and DNA analysis of archaeological bone, it is imperative that certain protocols are adhered to. Precautions must be implemented from excavation through to laboratory analysis to avoid contamination; and correct recording of burial environment is essential to enable consideration of extrinsic factors and contaminants when reporting results.

Keywords:

ancient, ATR-FTIR, burial, capillary electrophoresis, colourimetry, diagenesis, DNA, forensic, human, mini-STR, porcine, soil, XRF

ACKNOWLEDGEMENTS

Firstly I would like to thank my supervisor Dr Karl Harrison for his continued encouragement and support throughout this project, and for the direction and guidance he has provided me.

I would like to thank my colleagues at the Cranfield Forensic Institute for their support with the research and advice, especially Adrian Mustey for his technical knowledge and engineering assistance with equipment, and for always being on hand.

I would like to thank Joanna Caruth from Suffolk County Council and Professor John Hines from Cardiff University for allowing me access to the Eriswell collection and to Dr Clive Waddington and the rest of the team at Archaeological Research Services Ltd for enabling me to assist in the excavation at Fin Cop and for granting permission to analyse the skeletal remains.

My PhD experience would not have been the same without my fellow researchers, Danae Prokopiou, Paraskevi Christiogianni and Oznur Gulhan, who I thank for their support, and sharing of ideas and knowledge.

To my friends, family, parents and grandparents, I owe so much gratitude for the continued love, support and encouragement throughout this PhD, and especially to my sister Melanie for the motivation and for cheering me up when I needed it most. Thank you to my Godparents Susan and Ken Rolfe, for setting me on this path and for the advice and encouragement throughout my education.

Lastly I would like to thank my partner Matt Ryder for his knowledge and expertise and who has supported me through the hard times, and celebrated the good times with me. Regardless of whether you are by my side or far away, you are always with me, and for that I will always be eternally grateful.

TABLE OF CONTENTS

LIST OF FIGURES

LIST OF TABLES

LIST OF ABBREVIATIONS

aDNA	ancient DNA
ATR-FTIR	Attenuated Total Reflectance Fourier Transform Infrared Spectroscopy
bp	base pairs
DNA	deoxyribonucleic acid
dsDNA	double stranded DNA
FTIR	Fourier Transform Infrared Spectroscopy
LCN	low copy number
mtDNA	mitochondrial DNA
nDNA	nuclear DNA
PCR	polymerase chain reaction
SNP	single nucleotide polymorphism
STR	short tandem repeat
St. Dev.	Standard deviation of sample
UV	ultra-violet
XRF	X-ray Fluorescence

Chapter 1: INTRODUCTION

1.1 Background

As DNA technology advances the possibility of profiling samples which were previously too small in quantity, too degraded or too contaminated by inhibitors to analyse, has increased. These improvements in technology have allowed information to be gained from not only trace forensic samples (Fattorini et al., 1999; Prinz et al., 2007; Senge et al., 2011) but also more generally from skeletal remains – both forensic (Prado et al., 1997; Alonso et al., 2001; Bille et al., 2004) and archaeological (Colson et al., 1997; Paabo et al., 2004; Schotsmans et al., 2011). The term archaeological can be defined as the excavation and the study of past populations through human remains, artefacts and sites (Stevenson, 2010).

The ability to analyse trace samples in forensic cases has improved the investigative powers of the police allowing a higher number of positive identifications of victims and perpetrators to be made, from analysis of biological stains or trace evidence left at crime scenes (Mann and Ashworth, 2006). In cases where human skeletal remains are present, information that can now be gained from the analysis of samples enables identifications to be made from minute or damaged DNA (Jeffreys et al., 1992; Gill et al., 1994; Edson et al., 2009; Ambers et al., 2013; Maeda et al., 2013). The development of these DNA techniques has also enabled researchers to study ancient DNA from hard tissue samples revealing information on phylogenetics, migration, pathological conditions and familial relationships providing a new perspective on the history of our ancestors (Salo et al., 1994; Mays et al., 2001; Kaestle and Horsburgh, 2002).

Extensive research has been carried out into the process of decomposition of human remains (Gill-King, 1997; Haglund et al., 2002; Dent et al., 2004; Wilson et al., 2007; Adler et al., 2011; Schotsmans et al., 2011) but there are still unanswered questions about the interactions between the hard tissues, their burial environments and the effect on DNA survival. Pokines (2014a) in particular has highlighted the need for in-depth investigations of these processes in order to develop a better understanding of these interactions.

Cranfield Forensic Institute accommodates an extensive collection of analytical equipment, so by utilising various technology, as discussed later, it was possible to conduct a multi-disciplinary investigation into the different aspects of bone diagenesis and the effect on biomolecules.

1.2 Applications of research

The results from this research can be used across the disciplines of archaeology, anthropology, forensic science, ancient DNA research and archaeological history.

1.2.1 Forensic applications

In the majority of murder and coronial cases, the identity of the deceased is already known, but in cases where this is under dispute, establishing the identity is at the forefront of the investigation (National Centre for Policing Excellence, 2006). In cases where the remains of an unknown individual are found there can be limited resources available to attempt an identification of the deceased, depending on the state in which the remains are recovered. Whether a body is subjected to burial or exposure, decomposition of the soft tissue occurs as one of the first processes. Depending on the deposition environment, the post-mortem interval at the time of discovery and recovery, and more importantly – the state of decay, it is possible that fingerprinting, facial recognition, odontology (Cattaneo et al., 2006, Stavrianos et al., Hartman et al., 2011) or identification by clothing, tattoos and personal effects may not be successful, due to a lack soft tissue, or ante-mortem records for comparison. If soft tissues are still present, these are generally the preferred choice to attempt the recovery of DNA, due to the complicated and time consuming preparation required for bone or teeth extraction. If the presence of pink, deep muscle tissue is evident at post-mortem examination, this is generally the sample of choice (Zehner, 2007). However in cases of multiple interments, or in situations where a number of bodies are stored together such as mass disasters, contamination can occur within both the bone marrow and soft tissue due to the infiltration of putrefaction fluids from surrounding bodies (Zehner, 2007). In cases where this type of contamination is possible, no soft tissue is present, or where soft tissue has already undergone degradation via cellular autolysis or formation of

adipocere; it is necessary to attempt identification by the analysis of DNA extracted from the bones and teeth.

The fragile nature of decomposing soft tissue is a commanding reason why improvements to the analysis of hard tissue are vital in forensic investigations for the identification of unknown individuals; however hard tissue profiling causes a challenge for forensic providers due to the differences in methodologies from trace forensic samples. The majority of forensic samples submitted to laboratories consist of trace samples suitable for automated processes, however this process is not suitable for the most part of DNA extraction from hard tissues. At present it is a commonly held belief in forensic science that when profiling from hard tissue, a tooth is best for analysis (Gaytmenn and Sweet, 2003; Higgins and Austin, 2013) however this is not always possible, especially within an archaeological context. If a tooth is found loose at the bottom of a grave it may not be possible to conclusively assign to a particular individual therefore cannot provide a positive identification. This problem is compounded still further in the case of multiple interments such as mass graves, where association of skeletal elements may be difficult, or remains may be incomplete due to trauma, secondary deposition or scavenging (Haglund, 2002; Ubelaker, 2009; Moraitis and Spiliopoulou, 2010; Hines et al., 2014). However, with technical advancements in DNA analysis and more comparative studies being conducted, recent research shows that femurs provide a better yield of nuclear DNA than teeth, even from degraded skeletal remains (Johnston and Stephenson, 2016).

A better understanding of the decomposition processes in relation to individual skeletal elements from different environments, enable relationships between variables and degradation factors to be identified. Acknowledgement of these factors will enable practitioners to be better informed when it comes to sample selection depending on the nature of the burial, and could subsequently result in a higher number of positive identifications through the use of DNA from archaeological bone for both forensic purposes, and provide better results for interpretation from anthropological and historical contexts.

1.2.2 Archaeological applications

Whilst osteoarchaeological techniques have traditionally been used to estimate the sex of remains, there are instances where this is not possible. For example, the absence of grave goods in Christian burials, indeterminate morphological traits such as where the pelvis and skull are missing, or infant/juvenile remains make this estimate challenging if not impossible. Current methods for the sex estimation of juvenile remains such as the base of the skull, long bones and vertebrae elements are possible but these bones can be missed during excavations due to the small size from lack of fusing and failure to recognise incomplete elements. Other methods include elements that are sexually dimorphic in adults such as the sciatic notch in the pelvis, the shape of the cranium, and the shape of the mandible, but these tend to only be useful around the adolescent period (Dirkmaat and Sienicki, 1995).

Anthropological methods to assess the sex of skeletal remains have also been found to be subject to cognitive bias (Nakhaeizadeh et al., 2014). For these reasons, it has recently become necessary to turn to DNA analysis to provide answers (Colson et al., 1997; Faerman et al., 1998; Fregel et al., 2011; Seidenberg et al., 2012; Bauer et al., 2013).

At the beginning of the project, it was hoped that information obtained from analysing Iron Age remains from Fin Cop Hill Fort in Derbyshire would shed light on the nature of this non-normative deposition and associated events that occurred on the site by providing sex identification and possible familial relationships between the remains.

It was hoped that analysis of the skeletal remains from the Eriswell Anglo-Saxon cemetery at RAF Lakenheath, Suffolk would provide information for the investigation into the historical burial practises, and identification of any familial relationships. In addition, the nature of the geology of the Eriswell cemetery, discussed later, offered an unparalleled opportunity to consider DNA survival over a range of deposition environments. The dramatic contrast between sand and

chalk burial environments at Eriswell, provide an opportunity to contrast DNA survival in hard tissue.

1.3 Aims, objectives and hypothesis

This section provides the overall aims of the research in order to answer the research question of whether different burial environments affect the taphonomic changes that result in bone diagenesis, and changes in the biomolecules contained within. The objectives set out how the research will be conducted in order to answer this question.

1.3.1 Aims of the research

The overall aims of this research project is to improve the understanding of the chemistry of the degradation of nuclear DNA (nDNA) by investigating differences in environmental taphonomic effects on specific skeletal elements from different burial sites. In so doing this research hoped to discover the best practises to improve success rates of nDNA from degraded hard tissue samples, and produce sampling strategies for nDNA extraction across a range of environments and skeletal remains. By implementing the use of analytical techniques in the investigation of diagenesis of the bone, considering aspects such as composition, colour change, and compromise of outer cortex, it was hoped that possible predictors of DNA survival can be identified and studied, ultimately providing techniques that might triage and optimise archaeological DNA research.

1.3.2 Objectives of the project

1. To collect information on the degradation of nuclear DNA, and identify which variables affect this process.
2. To determine how the degradation of nuclear DNA is related to the mineral and organic components of the bone.
3. To measure the interactions between different burial environments and various skeletal elements by quantifying colour change, collagen content and DNA survival.
4. To improve sampling strategies for the best DNA recovery from hard tissue.

5. To quantify and consider the utility of predictive modelling when related to success rates of nuclear DNA extraction.
6. To suggest a triage system for bone sampling and analysis, in relation to the burial environment, that could be utilised by archaeologists to optimise nuclear DNA extraction success from recovered human remains.

1.3.3 Research hypotheses

The hypotheses of the research for the porcine samples, and human samples stated prior to commencement of the work are detailed in the following section.

1.3.3.1 Null hypothesis

1.a. There will be no significant difference in the quantity and quality of amplifiable DNA in bones buried in different environments.

1.b. There will be no significant difference in the quantity and quality of amplifiable DNA from different skeletal elements of femur and metatarsal from the human burials.

1.c. There will be no significant difference in the quantity and quality of amplifiable DNA in bones buried for different durations.

1.d. There will be no quantifiable relationship between the nature of physical characteristics observed in bone and the survival of DNA.

1.3.3.2 Alternative hypothesis

2.a. The bones buried in alkaline soil will retain more amplifiable DNA than those buried in acidic soil. Bones buried in the lime environment will show the best preservation of DNA. Bones buried in the sand environment will show the worst level of preservation of DNA.

2.b. There will be differences in the quantity of DNA retained by the human femora in comparison to the metatarsals.

2.c. The longer the burial duration of the bones, the lower the quality and quantity of amplifiable DNA.

2.c. There will be a quantifiable relationship between the nature of physical characterisation observed in bone and the survival of DNA.

1.4 Project overview

The purpose of this section is to introduce the project, with an overview of what each chapter contains. This project took a two-pronged approach to encompass information from both human remains and human analogues from different burial environments, in an effort to improve the understanding of how burial environments affect decomposition rates, diagenetic alterations of bone, and the preservation of biomolecules. The results from controlled burials of porcine bones in containers of clay, compost, lime or sand over varying durations were compared to results from analysis of ancient human remains from similar burial environments to identify any correlations found due to the burial environment. By examining the manner in which decomposition and diagenesis occur within different environments, a comparison with similar environments over an exaggerated timescale such as ancient remains, enable patterns to be identified.

This chapter provides an introduction to the research, with the aims and objectives, and the application of the completed project. The two-pronged approach of using human archaeological remains and human analogue burials is explained, with a brief introduction to the analysis conducted.

The current understanding of bone biology and diagenesis is detailed in chapter two, with an introduction to bone structure and how it differs between elements, and a literature review on the presence of DNA in bone. The section concludes with a discussion on taphonomy – encompassing the decomposition process, both in terms of human remains and biomolecules.

Chapter three provides a literature review on burial environments, and the current understanding on how different variables such as pH, water content and soil type can affect decomposition and the taphonomic processes of bone. The two archaeological sites studied during the research are then presented, with

archaeological and geological information pertaining to the environments in which the human remains were buried.

A literature review of past and current methods used within archaeological science, and DNA analysis – both forensic and ancient, are presented in chapter four with critical reviews of their use within this research. The chapter continues with a section on the optimisation of current established methods conducted, in which protocols, and methods were tailored to meet the objectives set out in chapter one. The concluding section of chapter four presents the selected methods used to analyse the human archaeological remains, and the experimental procedures conducted with the human analogue samples, and subsequent analysis of the bones and burial environments.

Chapter five is separated into two parts presenting the results from this research. Part A presents the results from the buried human analogue samples, with data from the soil analysis, colour determination, composition information and DNA analysis. The results are presented independently according to environment in order to allow detailed investigation, prior to comparison between all burials at the end of each section. Part B presents the human archaeological results, beginning with the results of analyses conducted on skeletal elements from the Iron Age burial site at Fin Cop in Derbyshire; and secondly the Anglo-Saxon site at Eriswell in Suffolk. The colour, composition and DNA analysis results are presented for each site, prior to a cross-comparison at the end of the chapter. Interpretation of the DNA results in relation to sex determination, familial relationships or burial practise are also discussed.

Chapter six discusses the results from the research, encompassing information from both approaches to the investigation, and identifies the different environmental variables responsible for the diagenetic alterations to bone, and the DNA degradation.

The conclusions from the research are detailed in chapter seven, along with details of the contribution to science that this research has provided. Details of future work are also described.

Supplementary information is provided in Appendix A for the human analogue data, and Appendix B for the human archaeological data.

1.5 Chapter summary

This chapter has detailed the necessity for a better understanding of the taphonomic processes in relation to burial environment in order to optimise sampling and analysis of bone. The applications of the research for both forensic and archaeological contexts have been presented, and the research hypothesis and objectives have been outlined.

Chapter 2: BONE BIOLOGY AND DIAGENESIS

The previous chapter detailed the introduction to the research, and outlined the necessity for a better understanding of taphonomic processes in relation to changes observed in human bone. This chapter provides an introduction to DNA, bone biology, and taphonomy, detailing previous research that has contributed to the understanding of bone diagenesis. Bone diagenesis by definition means the alteration of bone after burial, including chemical, physical and biological changes due to intrinsic and extrinsic factors (Lyman, 2001).

2.1 Cell biology and DNA

Each human body contains billions of cells, which with the exception of red blood cells, all contain genetic material in the nucleus, called deoxyribonucleic acid (DNA). Due to the location of this DNA, it is referred to as nucleic DNA, as opposed to mitochondrial DNA which is contained with the mitochondria of the cell, outside of the nucleus (Butler, 2001; Alberts and Johnson, 2014) as shown in Figure 2-1.

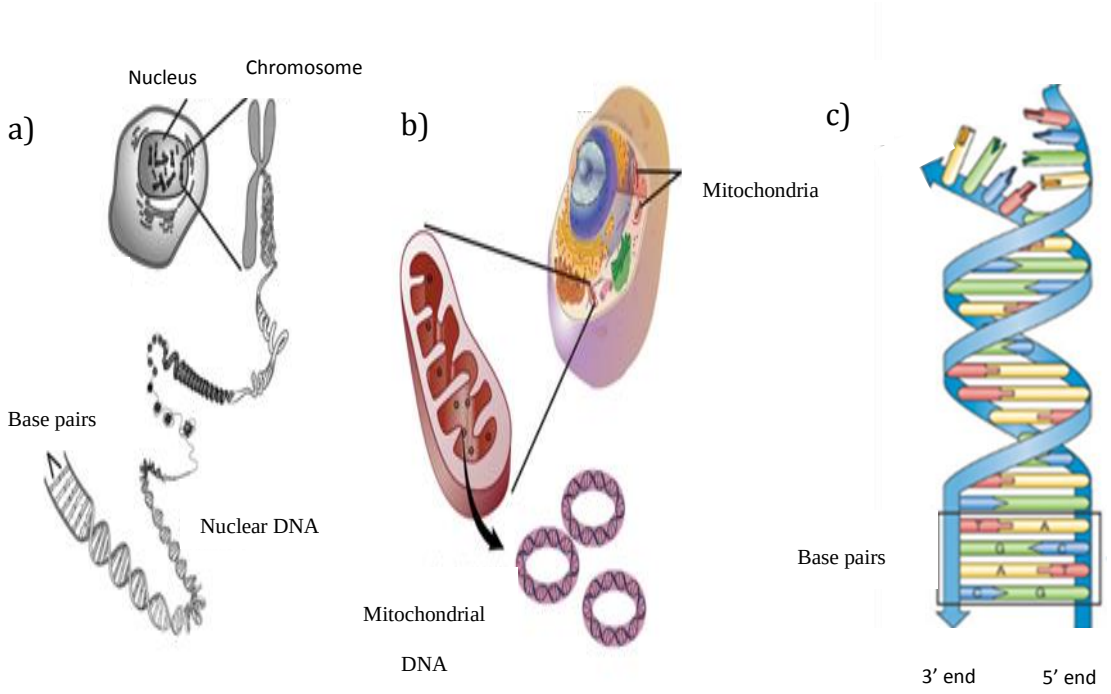

Figure 2-1: Diagrams depicting: a) a cell containing a nucleus and nuclear DNA from Heintzman (2013); b) a cell showing the location of mitochondrial DNA from Heintzman (2013); c) a double stranded DNA helix with complementary base pairs from Pray (2008)

DNA is responsible for storing information for cell replication and development, and also provides a genetic program to be passed on to future generations. Nuclear DNA (nDNA) is found within chromosomes which reside in the nuclei of cells in the body, providing the genetic information for the living organism which is passed down from both parents. Along the length of the chromosome are genes found at specific points or 'loci'. At any given locus, the coding region of DNA is referred to as an allele. It is the location of these alleles that can be used to determine genotypes and population statistics used in forensic DNA studies (Cattaneo et al., 2006; Prinz et al., 2007; Jakovski et al., 2010).

Mitochondrial DNA (mtDNA) is located outside the nucleus, in the cells cytoplasm and is present in abundance compared to nDNA. This larger quantity of genetic information, and therefore higher survivability rate, means mtDNA is used more commonly in archaeological analysis where DNA degradation is likely, and nDNA may be limited. Despite this, cases have been reported of the successful amplification of nucleic DNA from archaeological samples that did not yield any mitochondrial DNA (Chilvers et al., 2008). The natural repetition of mtDNA within the cell means that whilst copies might suffer damage and degradation just as nDNA might, they are unlikely to be damaged in the same locations, allowing resulting 'gaps' to be filled and the ultimate effect to be one of greater resilience and longevity.

Despite these advantages of mtDNA over nDNA, the limitations also need to be acknowledged. Due to its location, mtDNA generates free radicals, which leads to advanced degeneration of the DNA (Hochmeister et al., 1991) due to oxidative damage, and the analysis is a laborious process lacking the automation of the forensic nDNA system. As mtDNA is passed to the offspring solely by the mother, its analysis is useful for tracing maternal lineage, which can be useful for archaeologists and forensic practitioners, but it is inadequate for discriminating identification of individuals due to the wide-scale homogeneity across population groups (Biesecker et al., 2005).

As the aim of this research was to facilitate forensic investigations of unidentified individuals rather than familial lines, the focus was on nDNA rather than mtDNA, but an understanding of the archaeological literature drawing on mtDNA analysis remains apposite to this work where the effect of environmental factors coincide in its survival.

2.2 Bone biology and structure

Bone is composed of an organic matrix (20-40% total live mass), an inorganic mineral component (50-70%), cellular elements (5-10%) and lipids (3%). The organic matrix of the bone consists of different types of collagen that are interwoven to stabilise the matrix, whilst hydroxyapatite is the predominant molecule of the inorganic mineral component which provides rigidity (Li and Jee, 2005) as illustrated in Figure 2-2.

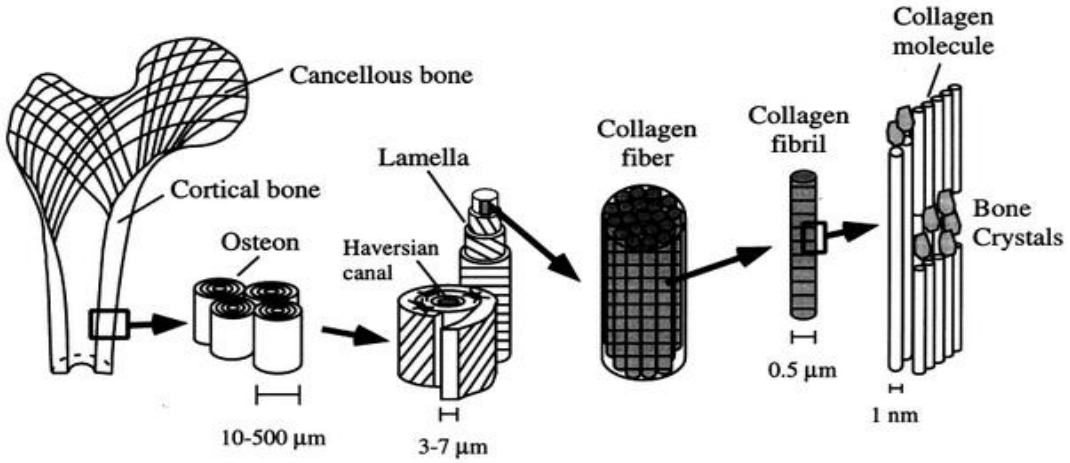

Figure 2-2: The structure of bone, illustrating the collagen and hydroxyapatite bone crystals matrix (Rho et al., 1998)

Research has shown that there is a significant difference between the composition of modern and archaeological bone due to the effects of diagenetic changes (Reiche et al., 1999). These changes occur to bones of the skeleton during decomposition, in the form of exchange of ions between the bone and surrounding soil, an uptake of ions and circulating organics, a breakdown of collagen, an alteration of mineral matrix, infill of mineral deposits and microbiological attack (Hedges, 2002). However, due to the physical and chemical barrier properties of the protein/mineral matrix of bone, it can be the most efficient biological tissue to

attempt DNA extraction because of the protection it provides from environmental and biological deterioration and attack (Loreille et al., 2007).

2.2.1 Skeletal elements

When choosing skeletal elements for targeted extraction, the general process of skeletonisation should be considered as different bones have different decay rates, both in terms of soft tissue loss and diagenetic bone loss. Generally, the first element to be defleshed and reduced to hard tissue is the cranium, followed by clavicles and sternum; cervical vertebrae; arms and hands; thoracic and abdominal region, vertebral column, ribs; and lastly legs and feet (Rolsandic, 2002). This suggests lower regions of the body may yield a higher quantity/quality of DNA as they have been subjected to environmental degradation less than other elements of the skeleton.

This research focusses on DNA in bone, however, researchers and practitioners conducting both forensic and ancient DNA analyses have also used teeth as a source of DNA - particularly with archaeological or badly degraded human remains due to the good survival rate in archaeological conditions due to the protective qualities of the enamel and position in the jaw from extrinsic contaminants (Alonso et al., 2001; Gaytmenn and Sweet, 2003; Ricaut et al., 2005; Rohland and Hofreiter, 2007; Kitayama et al., 2010; Adler et al., 2011; Higgins and Austin, 2013; Higgins et al., 2015; Hughes-Stamm et al., 2016). Other incidences where teeth may be more beneficial for analysis than bone include human remains that have been subjected to fires or explosions (Sweet and Sweet, 1994; Williams et al., 2004). However, femurs have been known to survive fires, better than other skeletal elements in the body, and one case reports the ability to obtain an identifying DNA sample from a decomposed and charred femur from a major forest fire in Galicia, Spain (Fondevila et al., 2008).

Researchers have been comparing the DNA content in different skeletal elements for many years, as discussed in this section. Perry et al (1988) who found that when comparing the DNA degradation in a clavicle bone with a rib bone from the same individual, the DNA in the clavicle had degraded slower. However these

bones were not from an archaeological context, instead were incubated in a laboratory setting using humidity as the environmental factor, as a means of assessing the DNA degradation in relation to the time interval since death. The quality and quantity of DNA recovered from a bone can also be affected by the state of putrefaction (Hochmeister et al., 1991) as the accumulation of body fluids can affect specific bones or aspects of bone depending on the body position or deposition type.

The distribution of cortical and cancellous bone differs between different bones in the body: Short bones such as carpals, and irregular bones such as vertebrae are blocky in shape and consist of cancellous bone surrounded by cortical bone; Flat bones such as scapulae are flat and tabular consisting of cancellous covered by cortical bone; Long bones such as femora consist of a shaft of tubular medullar cavity surrounded by compact bone, whilst the ends are cancellous bone which is covered by cortical bone (Parsons and Weedn, 1997). These differences in bone structure also affect the level of DNA contained within. Cortical bone contains high molecular weight (HMW) DNA, up to 1µg per gram of bone, whereas cancellous bone can yield 10-20 times greater DNA quantities, but does not survive over long periods of time (Hochmeister et al., 1991).

Another aspect to consider is the structural strength of the element, and how this may affect the integrity and subsequent preservation. The cranium and scapulae are often fractured in the context of a burial (Moraitis et al., 2009) most likely due to the inability to withstand force due to the hollow sphere or plate-like structure and the associated pressure of soil overlying the burial. However the petrous bone, part of the temporal bone in the cranium, is a very dense bone and shows good survival rates in archaeological contexts (Pinhasi et al., 2015). Fractures and post-mortem breaks allow further degradation to occur due to the penetration of the surface and therefore most likely affect the survival of DNA. Long bones display a weakness of a different kind, due their hollow rod structure (Currey, 1984). By contrast, elements such as carpals and tarsals are more compact and structurally denser so can withstand a greater force, although phalanges which display a rod-like shape are relatively easily broken (Darwent and Lyman, 2002).

With regards to archaeological skeletal remains, or those subject to surface deposition, factors may affect the availability/presence and feasibility of the recovery and collection of certain bones.

The action of scavengers can affect by the rate of decomposition by consuming soft tissue, and can affect skeletal remains by disarticulating, dispersing, damaging and destroying skeletal elements (Moraitis and Spiliopoulou, 2010; O'Brien et al., 2010). Interference from scavengers can be affected by the depth of burial, degree of clothing and also the location of the body in relation to human presence (Kjorlien et al., 2009). Skeletal components which are small in size and those rich in marrow are also more likely to be subject to scavenging by animals (Pokines, 2014b) whereas flat bones could be lost due to the movement of water through the remains (Gill-King, 1997). Taking these factors into account, although tarsals may appear to be a good element to target for DNA extraction, it is possible they will not be present at deposition sites (Janjua and Rogers, 2008). In addition to loss of elements from single burials, disassociation of elements such as phalanges within an internment of multiple individuals, may be misidentified and be hard to individuate, resulting in the potential for multiple profiles of the same individual. The absence of target elements may often be an issue when sampling from archaeological sites, and highlights the necessity to target several skeletal elements for analysis, subject to cost and authorisation for destructive analysis.

In addition to the variables discussed, a host of other factors can potentially affect the preservation or degradation of soft and hard tissue such as the depth of the burial (Campobasso et al., 2001), the presence or absence of a coffin (Dent et al., 2004), and possible root action which disturb the remains (Tibbett and Carter, 2009).

2.3 Genetic material in bone

Currently we lack a definitive understanding of the location of DNA in bone, and different researchers have posed counteracting hypotheses. Brundin et al. (2013) concluded the survivability of DNA in bone is due to its affinity to hydroxyapatite; whilst Campos et al. (2012) detailed the importance of considering both the

collagen, and the hydroxyapatite for bound DNA for analysis. Research on the use of sodium hypochlorite as a means of eliminating exogenous contaminants from bone, proposes that the DNA binds to the hydroxyapatite – the component which provides rigidity to the bone structure (Kemp and Smith, 2005), a belief shared by others (Parsons and Weedn, 1997). Therefore, bones containing high levels of hydroxyapatite should yield the highest levels of intrinsic DNA.

One commonly held belief is that compact bone it is thought the majority of the DNA present resides in the osteocytes which saturate the matrix at 20,000 to 26,000 cells present per cubic millimetre, higher than that in cancellous bone, therefore providing adequate DNA for extraction (Hochmeister et al., 1991). For this reason, compact bone is often regarded the preferential sample for DNA analysis (Parsons and Weedn, 1997; Milos et al., 2007; Latham and Madonna, 2013).

Recent research by Pinhasi et al. (2015) investigated endogenous DNA content in the dense part of the temporal bone, the petrous bone. The results showed even when poor yields were found from other skeletal elements, the dense petrous bone could still yield high levels of endogenous DNA from the same skeleton. Different areas of the bone were also found to contain different levels of DNA, showing the location of sample site is just as important as the element itself.

In terms of identifying appropriate sites on the bone for analysis, it has been highlighted by several researchers over an extended period that there is a lack of information regarding the relative amounts of DNA contained within different sites on bone (Perry et al., 1988; Adler et al., 2011). This presents difficulties in the estimation of quality and quantity of potential DNA to be retrieved, and how different sampling techniques could affect the results.

2.3.1 Predictors of DNA in bone

Due to the expensive, laborious, destructive, and sometimes less than successful process of DNA analysis, many researchers have tried to establish procedures to predict whether a bone sample will yield DNA. These indicators include gross morphology, nitrogen and collagen content.

There is evidence that suggests observations of the surface of the bone can be utilised as predictors of DNA integrity in that sample (Haynes et al., 2002). If cracks, surface pitting and poor histology are visible then it is probable that no DNA can be profiled due to the degradation of the biomolecules (Al-enizi et al., 2008). Bollongino et al (2008) suggested estimating the presence of well-preserved DNA, by checking physical signs of the bones that can be characteristic to those of good samples; stating that heavy and hard compact bones, that have no or few cracks, and no signs of microbial activity yield the best results.

Microscopy has been used as a common method for histological examination of preservation state of DNA (Hedges and Millard, 1995; Richards et al., 1995; Colson et al., 1997) where a fragment of bone is embedded in epoxy resin, polished and viewed at 100x magnification. However, this method is both destructive and time consuming.

Other methods to assess the state of bone preservation include assessing the quantity of collagen survival within the bone via measurement of the nitrogen content by the use of mass spectrometry (Hedges and Millard, 1995; Colson et al., 1997). Research indicated that high levels of nitrogen, similar to those seen in modern bone, could be used as an indicator to the level of DNA in archaeological bone (Hiller et al., 2004), however more recent research has shown that the nitrogen content in bone cannot be used as a predictor in bone as it is a poor indicator of the preservation state of the molecules (Al-enizi et al., 2008).

Bone mineral is considered an important factor in the preservation of biomolecules within archaeological bone and over time screening methods have been developed to investigate this further. Fourier-Transform Infrared (FTIR) can be used to calculate changes in crystal indices (Lebon et al., 2010; Squires et al., 2011; Hollund et al., 2013; Grunenwald et al., 2014), PIXE (Particle-Induced X-ray Emission) examines any chemical changes within the mineral structure(Elliott and Grime, 1993; Reiche et al., 1999), and XRD (X-ray Diffraction) can be used to identify the composition of the crystal (Stathopoulou et al., 2008; Adamiano et al., 2013).

Further research into the collagen content in bone has shown that there is a clear correlation between the high content and thermal stability of the organic phase and the successful amplification of DNA (Hiller et al., 2004; Gilbert et al., 2005; Koon et al., 2008; Fredericks et al., 2012a) which suggests that the assessment of collagen can be used as an indicator for successful profiling of archaeological samples. However, due to the exchange of ions that occurs during the recrystallization of bone, compounds from surrounding burial environments and groundwater, such as calcium, phosphate and carbonate can be incorporated into the bone mineral (Wright and Schwarcz, 1996; Hollund et al., 2013) which can affect the results of the diagenetic analysis.

Other methods used to assess molecular preservation include amino acid racemization and is commonly within ancient DNA research to screen bones prior to conducting DNA analysis (Bada et al., 1994; Poinar et al., 1996; Kolman and Tuross, 2000; Hofreiter et al., 2001). However this technique is not cost effective in terms of time or equipment (Haynes et al., 2002)

In order to interpret how the post-mortem duration affects the bone structure and DNA content it is necessary to first understand the taphonomic processes which lead to the diagenetic changes in bone.

2.4 Taphonomy

Taphonomy was first conceptualised as a scientific discipline by Efremov (1940) and can be described as the study of the processes which occur to an organism from the moment of death to the point of detection. The interest in taphonomy first began with the analysis of fossils, and the investigation into processes of preservation by geologists and palaeontologists (Pokines, 2014a). Focus turned to the decomposition and preservation of remains from bone depositions and post-mortem changes in bone structure was identified (Jans et al., 2004). The taphonomic processes which occur are all affected by a number of factors to be discussed later in this section, such as the rate and progression of decomposition of soft tissue (Damann and Carter, 2014), differences in the structure/size of skeletal elements (Lyman, 2014), environmental influences, (Pokines and Baker,

2014) and any interference by animal or human activity (Pokines, 2014b). In a forensic context, taphonomic processes, decay, and depositional environments are all studied for information which may assist investigations (Pokines, 2014a) collated with information provided by the anthropologists and archaeologists.

Traditionally human analogues such as pigs are used in order to study the taphonomic effects, due to the similar composition of soft tissue and fat composition. Other animal analogues that have been used include sheep, dogs, rats, deer and bison all of which have been shown to display differences in the manner and rate of decomposition when compared to human cadavers (Stokes et al., 2013).

Although porcine bone is close to human bone in a structural sense, there are differences in the micro-structure (Pearce et al., 2007) and therefore may be different interactions within burial environments so this needs to be considered when analysing results. Research has highlighted these differences and shown that in an archaeological context bacterial attack is twice as likely to occur within human bone, than it is in animal bone (Lee-Thorp and Sealy, 2008), which is most likely due to the de-fleshing of the animal bone, whereas human burials are generally whole bodies (Bell et al., 1996). Despite these differences, pig cadavers are often used in taphonomic studies due to the ease of availability and the 'sterile' nature of the animal due to its presence in the food chain.

More recently, these taphonomic processes are being investigated at taphonomic facilities containing human cadavers, such as the Anthropological Research Facility at the University of Tennessee (Bass and Jefferson, 2003) therefore eliminating the problem of differences in composition, and the structure of bone that exists between species. These facilities provide a means of obtaining vital information to develop understanding and knowledge in taphonomy, by studying the different stages of decay and decomposition, and identifying the variables which affect these processes.

2.4.1 Decomposition

Decomposition of a human body begins as a sequence of events shortly after death, the rate and order of which are dependent on the surrounding environmental conditions, and can cause exceptions such as peat-bog bodies (Painter, 1991) and mummification (Weitzel, 2005). Different authors suggest variants to the stages of decomposition but generally the process of decay has been identified as four different stages: fresh, bloat, decay and dry, although some researchers refer to a fifth stage in regards to buried remains of disintegration between decay and dry (Tibbett and Carter, 2009). The first stage begins with the break-down of cells within the body, due to a process referred to as autolysis. This involves the action of intrinsic enzymes digesting cells, causing the rupture and subsequent release of cellular fluids. This action marks the beginning of the putrefaction stage, where intrinsic bacteria residing within the intestinal tracts breaks down surrounding soft tissue (Parkinson et al., 2009). Gases are produced due to the bacterial action, which lead to bloating of the body, and subsequent rupture, releasing gas and decomposition fluid into the surrounding environment. Active decay is the next stage in the sequence which involves the decomposition of soft tissue due to bacteria and insect activity. The final 'dry' stage refers to the skeletal state of the remains, from which the bone diagenesis will continue (Pokines and Baker, 2014) and will subject the bone to staining, weathering and fragmentation (Dupras and Schultz, 2014; Junod and Pokines, 2014).

In terms of the sequence of skeletonisation, again this is dependent upon the surrounding environment, general observations were published by Dirkmaat and Sienicki (1995) from decomposition of human remains from an open air deposition. Due to the accessibility for flies and insects into orifices, the cranium is the first element to skeletonise, followed by the clavicle and the sternum, the vertebrae, the pelvis and ribs, and lastly the legs and the feet.

In some cases, and dependent of surrounding conditions, soft tissue may survive in the form of desiccation or adipocere. Soft tissue desiccation can be identified as dark and leathery in texture, which are formed due to the rapid drying of tissue, due to a dry environment or exposed to airflow (Aturaliya and Lukasewycz, 1999).

The formation of adipocere occurs in anaerobic conditions where sufficient moisture is available for bacteria to convert subcutaneous fat into a grey-white lipid solution, which can progress into a shell covering the remains (Schotsmans et al., 2011; Forbes et al., 2005).

2.4.2 Diagenetic changes in archaeological bone

The term diagenesis in anthropology refers to any post-mortem changes that occur affecting the physical, chemical and composition of the bone, (Jans et al., 2004) which alters the bone from its original ante-mortem state. Such changes include adsorption, mineral replacement, and precipitation and dissolution (Elliott and Grime, 1993). The presence of these changes and the extent to which they occur will depend on not only the intrinsic factors, but also extrinsic factors provided by the surrounding burial environment (Fernández-Jalvo et al., 2010).

The intrinsic changes that take place in the post-mortem interval, are subject to the morphology of the bone, in terms of size, shape and structure. The diagenesis of the organic matrix of the bone involves the decomposition of proteins into amino acids due to the hydrolysis of the proteins and subsequently the peptides. The inorganic phase of the bone also undergoes changes in structure, becoming more crystalline which in turn weakens the protective matrix. This alteration leaves the bones vulnerable to ion substitution, infiltration of soil contaminants from the environment, and loss of proteins and minerals (Henderson, 1987).

The extrinsic factors that affect the bone diagenesis involve water movement, soil type and soil pH. Collagen is thought to be most stable within a pH of 3-7.5, but any changes in this level can increase or decrease the rate of naturally occurring hydrolysis. The mineral component can also be affected by any pH change deviating from its optimal survival level of pH 7-8 (Turner-Walker, 2007).

The importance of more detailed research into the degradation of bone is imperative for the ability of researchers to identify which skeletal elements have the potential to provide DNA (Adler et al., 2011). Researchers have concluded that the organic content of ancient bone is significantly lower than that in modern bone

(Ariffin et al., 2007) which may relate to the abundance of DNA. But it remains unclear whether this is a simple association or a more complex relationship.

2.4.3 The breakdown of DNA

"As a highly reactive chemical residue, DNA is the target of several physical agents and chemical reactions" (Alaeddini et al 2010, p.149). These processes involve those of a chemical nature which break down the helical spines of the DNA molecule leading to the loss or alteration of nucleotide bases (Campos et al., 2012). In life the process of cell growth and regeneration limit the degradation of DNA, and in bone the action of osteoblasts and osteoclasts ensure a homeostatic 'turnover' of skeletal material. After death there are no mechanisms to repair the DNA therefore the actions of endogenous and exogenous nuclease activity, oxidative nucleotide modifications and hydrolytic cleavage result in strand breakage and the DNA degrades into short fragments of linked base pairs (Martín et al., 2006a; Adler et al., 2011).

2.4.4 Ancient DNA

The investigation of ancient DNA (aDNA) can be used in association with other techniques to provide information about sex estimation, pathology, population migration, community interaction and interbreeding and genetic analyses of our ancestors (Faerman et al., 1998; Hofreiter et al., 2001; Götherström et al., 2002; Adachi et al., 2004; Bollongino et al., 2008; Gamba et al., 2008; Haile et al., 2010; Adler et al., 2011; Hanna et al., 2012; Hofreiter et al., 2012; Kirsanow and Burger, 2012).

The field of ancient DNA analysis stemmed from an interest in our ancestors and the manner in which they lived. This diverse field now includes on-going research and advances in scientific knowledge regarding bioarchaeology, human and animal evolution and even forensic identification. The first article to be published in ancient DNA regarded animal evolution and detailed the cloning of DNA of an extinct equid known as a Quagga (Higuchi et al., 1984) followed a year later by Svente Paabo who reportedly cloned human DNA from a 2,400 year old Eqyptian mummy (Pääbo, 1985). After DNA previously reported to be that from a dinosaur

and a dinosaur egg (Woodward et al., 1994) was later reported to be human DNA due to contamination (Hedges and Schweitzer, 1995), the field of ancient DNA attracted stricter controls and precautions to confirm authenticity of findings.

Studies with aDNA have continued to develop and have allowed the analysis of samples previously stored such as natural history specimens (Mulligan, 2005), have attempted to shed light on familial relationships within burial grounds (Chilvers et al., 2008), to corroborate historical records of people and animal movements (Haile et al., 2010) and to solve the puzzle of multiple skeletons used to construct one individual (Hanna et al., 2012). Most recently, aDNA analysis has been used to determine the origins of those buried in previously undocumented cemeteries (Ozga et al., 2016; Santana et al., 2016).

Ancient DNA has also been used within forensic science since 1991 when DNA extracted from bone was used to identify a murder victim (Hagelberg et al., 1991). In 1992 aDNA analysis of buried remains was able to positively identify the suspected grave of The Angel of Death, Josef Mengele in Brazil (Jeffreys et al., 1992), and analyses conducted in 1994 and 2007 positively identified the remains of the Romanov family (Gill et al., 1994). Some forensic protocols are now using techniques designed by the aDNA community for the purpose of DNA repair from degraded forensic samples (Hall et al., 2016).

But the study of aDNA comes with both more and greatly exacerbated problems compared with the analysis of modern DNA. DNA from recent remains which has not been subject to the extremes of environmental damage, can be found saturated within soft tissue and bone alike, whereas aDNA is less abundant and also irregularly distributed due to diagenetic changes and degradation. In addition, the survival of archaeological soft tissues is rare and is practically unheard of without the action of physical and cellular alteration (Turner-Walker and Peacock, 2008). These changes can not only lead to base modifications in the DNA sequence but also will shorten the DNA fragments, breaking the 'ladders' of preserved linked base pairs still further (Kirsanow and Burger, 2012).

The most significant issue concerned with that of aDNA analysis is the risk of contamination of samples with modern DNA as detailed previously. Considerations of this problem and precautions required to limit the probability of this occurrence is discussed later in section 4.1.3.

In addition to overcoming the potential complications it is also necessary to prove the authenticity of the aDNA. This links to the consideration of contamination, and the importance of obtaining reference/elimination samples. In a forensic context, the process of taking and analysing reference samples from individuals who have processed the sample, from the scene to the laboratory, is common place. However, in a historical archaeological context, when the number or identity of individuals that have had contact with the skeletal remains is unknown, the process of eliminating reference DNA from a potentially contaminated piece of evidence is difficult. Without taking proper precautions, archaeological DNA analysis runs the risk of extracting, amplifying and sequencing the modern DNA of all individuals involved in the process of excavation, storage and osteological analysis.

In an effort to limit the risk of incorrectly reporting contaminant DNA as aDNA, Cooper and Poinar (2000) proposed a 'criteria of authenticity' in order to establish guidelines for researchers working with ancient DNA, however these guidelines have been deemed unreasonable by many due to the multiple extractions and PCR reactions expected when dealing with minute samples (Chilvers et al., 2008).

There is no definitive timeline for the differentiation between aDNA and modern DNA in forensic situations as the categorisation refers to the state of the biomolecules, rather than a set period of time. This is not dissimilar to the distinction between remains deemed forensic or 'of coronial interest', or those regarded as archaeological, which varies country to country. As interest increases in archaeology of World War I and II with the inevitable recovery of remains, the discipline of forensic and archaeological DNA analysis form a continuous spectrum distinguished by cellular survival rates, rather than set periods of time.

Parsons and Weedn (1997) state that DNA preservation is more dependent on the interactions between the sample and its environment rather than time elapsed, and therefore the age of the sample will not dictate the quality or quantity of the DNA within. As protocols differ between aDNA and modern DNA, this statement suggests it is more important to base the differences of protocols on the preservation state of the bone rather than the age of it, again, this refinement of understanding tows a similar line to archaeology, where concepts of time-derived degradation (Ascher, 1968) were replaced with a more complex understanding of site formation processes (Schiffer, 1983). Therefore the development of a reliable method of preservation identification needs to be established, to enable researchers to select the most relevant protocol for the sample.

2.5 Chapter summary

This chapter has introduced the structure of DNA and bone, and how diagenetic alterations enable analytical techniques to be applied in order to establish information of taphonomic changes.

In historical archaeological contexts, the capability of DNA investigation can provide an insight into the burial practises of previous populations, offer information regarding the migration and lifestyles of the past, and provide supporting evidence for human evolution hypotheses.

The ability to detect and interpret DNA in bone has advantageous effects on the positive identification of unknown individuals in a forensic context. Whether the circumstances are down to mass fatalities or single deaths, the emphasis on identifying the individual(s) is paramount. Improvements and advances in DNA technologies are enabling increasing success with degraded samples, but knowledge surrounding the decomposition and diagenesis processes are still not understood.

Chapter 3: BURIAL ENVIRONMENTS

Where the last chapter detailed decomposition, the taphonomic effects on DNA degradation and bone diagenesis, this chapter introduces the ways in which burial environments affects those taphonomic changes.

When bodies are subjected to burial, environmental conditions change the elemental composition of bone by processes of degradation due to uptake of chemical components or erosion as a consequence of contamination from soil (Reiche et al., 1999).

Initial taphonomic variables relate to the manner of disposal of the remains – whether they were buried, scattered, surface, submerged or frozen (Gill-King, 1997) these variations make a huge difference in the nature and extent of decomposition, the long term preservation of tissues that comprise the remains, and ultimately the abundance of extractable DNA. Burials conducted in air-tight coffins or wrapped in clothing have been found to slow the rate of decomposition (Ross and Cunningham, 2011) by creating a barrier between the soft tissues and the burial environment. But by the same token, a coffin will retain decomposition fluids, and produce an increase in temperature and microbial activity in the environment due to the decomposition and fermentation of the wood.

If the remains are buried, the environment will affect the preservation of the bone and therefore the denaturation of the DNA contained. The environmental factors which may affect the preservation of the bone and in turn that of DNA, include the available oxygen, the pH and type of soil, the presence and movement of water, and the activity of soil microbes (Burger et al., 1999; Campos et al., 2012). It has been suggested that the environmental conditions surrounding skeletal remains have more of an influence on the DNA preservation than time elapsed (Burger et al., 1999). Despite the findings of published research in this area, Pokines (2014a) stated there is still an absence of a comprehensive study of taphonomic processes across different environment conditions that identifies and explains the variables which cause the alterations.

Research conducted to date has identified the main environmental variables as temperature, water and oxygen, pH, soil type and content, and microbial activity.

3.1 Temperature

Temperature plays a fundamental role in the preservation of DNA in archaeological bone, which will vary depending on location, season, and depth of burial. An increased temperature in the surrounding environment encourages the development of microorganisms, in the form of bacteria and fungi, which metabolise the collagen and DNA; and also accelerates the chemical decomposition of the bone (Bollongino et al., 2008). Consistently low temperatures of approximately 8^{o}C in the surrounding burial environment, have been shown to preserve DNA exceptionally well (Burger et al., 1999), whereas a 10^{o}C increase can double the rate of chemical reactions (Henderson, 1987).

3.2 Water and oxygen

The presence and movement of water in the deposition site of the body has long been thought to be the main degradative factor and influence on survival for bone, due to the leaching effect. Water is known to dissolve bone apatite, encourage the growth of microorganisms and supports their metabolism, and can lead to damage caused by hydrolytic and oxidative reactions (Turner-Walker, 2007; Bollongino et al., 2008). The existence of water in soil provides a medium for the majority of chemical reactions that occur (Turner-Walker, 2007), however its presence is also thought to act as a buffer between tissue and the acidity/alkalinity of the environment, and has a stabilising effect on the surrounding temperature so therefore can also reduce the rate/intensity of decomposition (Gill-King, 1997).

In the context of assessing survival over archaeological durations, it is important to separate considerations of water and oxygen. Whilst free-draining soils might be subject to high levels of oxygenated water, other environments such as standing bodies of stagnant water are likely to feature different chemical effects. This variation in preservation states due to chemical effects of mineral-rich and mineral-poor groundwater was reported by (Turner-Walker and Peacock, 2008)

when investigating the diagenetic changes in bone of the 'bog bodies' from Scandinavian bogs.

It is not just the presence or absence of water that will affect the survival rate of bone, but also the fluctuation of that water that will lead to either poor preservation or permanent saturation of the skeletal material. Burials that are below the water table, will result in permanent submersion of bones in water, which once the bones become porous, will allow the penetration of calcium and potassium ion saturated water. Once these ions have saturated the pores of the bones, they will resist any water flow out (Turner-Walker, 2007). This submersion can be beneficial for the preservation of the bone, as long as the water level is stable, the water and contained ions will remain in the pores. In free-draining environments such as sand and gravel, once the soil dries, hydraulic potential occurs drawing the water, and associated ions from the bone (Hedges and Millard, 1995). If this process is repeated with the rising and receding water levels leading to reoccurring submersion and drying, total leaching of the bone will occur with the removal of all ions from the bone itself and possible total disintegration of skeletal material as seen in the 'sand bodies' at Sutton Hoo (Carver, 2000).

In respect of the oxygen content in burials, the depth of the burial will affect the level of not only temperature but also aeration of the remains. Higher levels of oxygen in an environment will encourage a faster rate of decay than burials in a deeper and less aerated environment. This effect can also be seen depending on the aeration of the soil type – light porous soils with a higher oxygen content are more likely to provide an environment conducive to decomposition, in contrast with dense soils such as clay. In this instance, it is also necessary to consider the difference in pressure between a heavy clay soil and light porous soil, and how it may affect the preservation of the bone (Henderson, 1987).

3.3 pH

When considered in the context of soil science, the term pH refers to the level of hydrogen ions (H^+) in relation to concentration of hydroxide ions (OH^-) in the soil composition. The more H^+ ions present, the lower the concentration of OH^- ions,

therefore a lower pH and an acidic soil. The opposite is true for alkaline soils – a higher pH due to a higher quantity of OH^- ions in comparison to H^+ ions.

The pH of the soil in which a burial is contained makes an impact on the erosion of the bone surface (Fernández-Jalvo et al., 2010) and decomposition of bone, with preservation thought to be best in neutral or slightly alkaline pH (Henderson, 1987). Acidic soils are known to destroy the bone apatite by dissolving the calcium phosphate, whilst alkaline soils stabilise the apatite by acting as a buffer against the effects on carbonic acid of rainfall in a permeable groundsoil or in the event of it being a surface deposition (Bollongino et al., 2008). The optimal conditions for the preservation of DNA are thought to be neutral or slightly alkaline, cool, dry, anaerobic conditions (Burger et al., 1999; Bollongino et al., 2008).

The pH of any water present is also a factor when discussing bone diagenesis, as this will ascertain the level and type of ions that are present, and also the function capability of soil bacteria (Schotsmans et al., 2012). The type of ions present in water in burials will affect the bone mineral due to the ability of providing ion exchange (Turner-Walker, 2007).

3.4 Soil type and content

The presence of humic and fulvic acid in the surrounding soil, found naturally due to the decomposition of organic material, can result in a decreased success rate of DNA typing from bone as these substances infiltrate the bone matrix and act as inhibitors during PCR (Burger et al., 1999). Humic substances also affect the properties of soil, providing aeration, microbe support, water holding capacity, ion exchange and the reduction of contaminant metals (Lovley and Coates, 1997). Urea present in the soil has also been found to encourage DNA damage by reducing its stability within the bone matrix (Burger et al., 1999).

Research conducted into bone diagenesis in bogs concluded that soil content can play a significant role in the degradation of bone. Bones submerged in a peat-rich environment displayed rapid demineralisation and considerable loss of calcium

and phosphorous (Turner-Walker and Peacock, 2008). DNA analysis conducted on degraded skeletal remains from a lime burial environment also stated evidence of degradation, detailing the inability to identify and amplify DNA within (Parsons et al., 2007). The term lime refers to an alkaline calcium containing substance derived from limestone or chalk (Oates, 1998).

3.5 Microbial activity

If the deposition site is in an area of cultivation, it is likely that increased organic material and bacteria will be present in the soil which will lead to accelerated decomposition of the soft tissue (Haglund et al., 2002), depending on the chemicals used this could also have a detrimental effect on the preservation state of the hard tissues. Soil contaminants may affect the ability to amplify the DNA from a sample, although if the bone is intact and well-preserved the contaminant should not penetrate the surface of the bone (Bollongino et al., 2008). Bones may also be dispersed from their original deposition site or damaged due to the use of machinery. If the remains are deposited on the surface, or partially buried in shallow graves rather than securely interred in deep ones, decay will tend to be more rapid due to the exposure to insects and scavengers (Rolsandic, 2002). In the past it has been known for forensic cases to show curious processes of degradation due to bacterial action from depositions in manure and potting composts, but this information is currently unpublished. In contrast, Child (1995) states it's not the microbiology that affects bone preservation, but rather the soil chemistry.

3.6 Burial environments of case studies

The archaeological human skeletal remains used in this research were excavated from two different sites in the UK, an Iron Age burial ground in Derbyshire and an Anglo-Saxon cemetery in Suffolk. These sites were chosen due to the difference in time scales since burial of the human remains, the dissimilar burial environments, and the authorisation to use destructive techniques for the purpose of DNA and compositional bone analysis. An introduction to the sites and the burial environments are presented in the following section.

3.6.1 Fin Cop

'Fin Cop' comes from Old English meaning a high point in the landscape, and is the location of the remains of an Iron Age hillfort situated on a hilltop overlooking Monsal Dale in Derbyshire. Radiocarbon dating suggests that the hillfort was constructed 440-390 BC and the destruction of the site occurred less than two hundred years later (Waddington et al., 2011).

Evidence of burial practice through the Iron Age shows a diverse practice of cremation burials, and inhumations in single graves, together in cemeteries, or placed in barrows (Hedeager, 1992). It is believed that the comparative lack of human burials as seen from other time periods is because rather than burial in a grave, bodies were left to decompose on the surface, or discarded in pits (Bradley, 1984). Towards the end of the Iron Age, there was a change in rituals, and cremation burials and inhumations with grave goods became more common place. Figure 3-1 shows the ditch burial of Skeleton 8 from the 2010 excavation season at Fin Cop.

Figure 3-1: Skeleton 8 from the 2010 excavation at Fin Cop (Waddington, 2011)

Since 2009, three seasons of excavations have been conducted at Fin Cop, and to date remains have been found representing a minimum of thirteen individuals. The interpretation of these findings and anthropological assessment suggests that these individuals are women and children that have been deposited in the ditch of the hillfort with rocks from the wall placed on top. Information pertaining to the depth of the burials and the body positions of the individuals was not available.

The underlying geology at Fin Cop is Carbonifierous Limestone bedrock with overlying loamy base-rich fertile soils which are mostly humose, sometimes calcareous with relatively shallow topsoil (Waddington et al., 2011). This environment would provide an alkaline pH, which would suggest the preservation state of the bones from this site may be fairly good, but more than likely contaminated with humic substance. The preservation of the bones and the degree of fragmentation is discussed in Chapter 4.

3.6.2 Eriswell

Four Early Saxon cemeteries were first excavated in the late 1980's at RAF Lakenheath, Suffolk, and have uncovered 426 inhumations and 17 cremation burials. Analytical techniques have dated these remains between 475AD and 625AD, with many of the burials also containing grave goods that were characteristic of that era (Caruth and Anderson, 2005).

Prior to the migration of the Germanic people from Angeln, Saxony and Jutland on the North Sea coast of modern day Germany and Denmark, the post-Roman populations of the eastern UK tended towards cremation as the dominant form of mortuary practise. With the arrival of Saxon influence, either through displacement of incipient native populations or through the dispersion of new mortuary rites, the balance of practice altered to Saxon inhumation at first pagan in character with associated grave goods, and later markedly Christianised with graves orientated east-west largely devoid of any other items (Härke, 1990).

From the 6th Century the Anglo-Saxon society burial 'rule' is thought to have been 'as in life, so in death' (Brown, 1978) with the burial style being associated with the social class of the individual, (Härke, 1990; Williams, 1998) for the men: the

swordsman, the spearman and the unarmed man. The swordsmen would have been members of the aristocracy, buried with swords and shields and were the least common of all the burials. The spearmen were average men in society buried with spears, knives, and furnishings of the belt, and these were the most common type of burials found. The unarmed men would have been slaves with an absence of weapons in the grave (Thurlow, 1913). The social class of the women could also be suggested by the burial style. All women were buried with iron knives tucked in a waist belt, with beads and brooches around their neck. The average woman would have two brooches and beads, more than this would indicate the burial of an aristocrat (Brown, 1978). The design of the brooch suggests the age and origin of the deceased (Thurlow, 1913).

The start of the 8th Century saw the open country Pagan cemeteries being mainly abandoned as the Church took control over the burial of the dead with acceptance of Christianity across the country (Brown, 1978; Thurlow, 1913). Whilst some open burials still continued, they did so without the deposition of grave goods (Thurlow, 1913). The orientation of the human remains could also be used as an indicator of the religion of the deceased. As Anglo-Saxons accepted the Christian faith, the remains were buried with the head to the west and feet to the east, although there is evidence for mis-aligned burials alongside (Thurlow, 1913; Williams, 1998). The orientation of the burials at Eriswell cemetery can be seen in Figure 3-2 which illustrates the different areas of the burials.

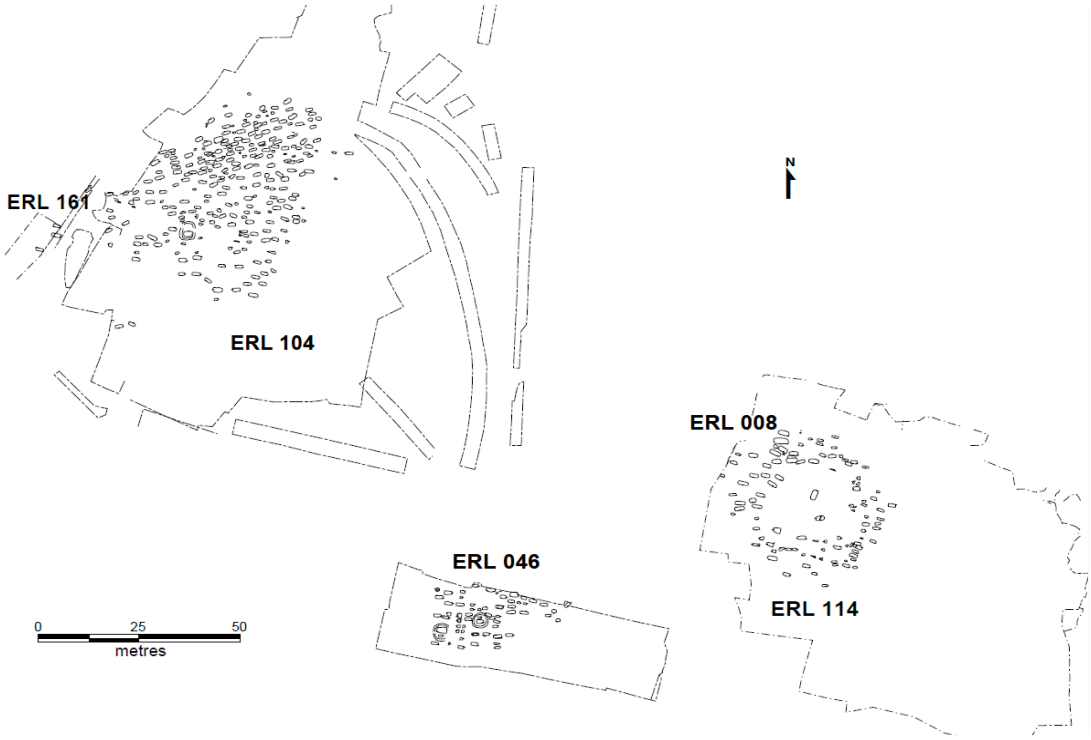

Figure 3-2: The burial site at Lakenheath showing the different areas of Eriswell cemetery, with the location of the human burials (Caruth and Anderson, 2005)

Soil analysis at RAF Lakenheath shows three distinct contexts. The lowest excavated context displays calcareous sands and chalk, topped with a sub-soil of non-calcareous sandy loam with chalk, and a topsoil of non-calcareous loamy sand. The variation of the soil type throughout the site at Lakenheath suggests a varying state of preservation of the skeletal remains depending upon the context it was excavated from, with remains from the calcareous sands and chalk expected to have the best preservation.

3.7 Chapter summary

This chapter has presented the different aspects involved within a burial environment and how those variables may affect human remains. A brief introduction to the human archaeological sites at Fin Cop and Eriswell have also been presented.

Chapter 4: MATERIALS AND METHODS

The previous chapters have introduced and discussed published research regarding archaeological remains, and the general taphonomic effects associated with burial environments. This chapter focusses on the materials and methods that are currently being used, how they were optimised for this research, and finally the methodologies selected for the research and analysis.

Preliminary reading at the beginning of this research exposed the wide variety of techniques and methods used by researchers, for the identification of human remains, and the investigation into decomposition and diagenesis. This literature review highlighted the necessity for researchers around the world to be able to compare results, especially with ancient DNA, and therefore it is necessary to establish optimisation of methods in order to standardise the manner in which they are reported.

This chapter sets out the process of research into different methodologies and techniques available for the analysis of forensic and ancient archaeological human remains. The optimisation of the chosen techniques are reported in this project, which allow effective, economical and time-saving methodologies that will allow data to be compared, and collaborative research to be produced to achieve a common goal. The methods chosen for this project are detailed at the end of this chapter in section 4.3.

4.1 Method research

Many different processes and techniques are currently used on archaeological bone for DNA extraction, screening methods and compositional analysis, although it is still unclear how these may affect the recovery of DNA. Adler et al., (2011) conducted a trial examining the common techniques used to recover DNA and concluded many of the methods are damaging to the genetic material. These findings underlined the need to research and choose the right methods for this project, in order to gain informative data.

It is the intention of this research to provide a better understanding of the taphonomic and diagenetic processes that human remains undergo during burial in relation to different environments, in the hope that the knowledge will lead to improved results for human identification and forensic investigation.

4.1.1 Ethical considerations

Prior to selecting and sampling of any skeletal elements, the factor of ethics must be considered. Recommendations for the destructive sampling and analysis of archaeological human remains for the purpose of scientific research has been published by the Advisory Panel on the Archaeology of Burials in England, in an attempt to curb any unnecessary work and provide guidance to guardians of skeletal collections. The main recommendations include a weighing up of the scientific knowledge that will be gained in contrast to the destruction of the remains; the consideration of whether any other non-destructive techniques could be used instead; how the destructive methods could prevent future research of the material; and the experience and competence of those conducting the work (Mays et al., 2013).

These guidelines were used during the planning and sampling phase of this research, and affected the decisions that were made. Small window cuts were sampled from the bone, taking as less material as possible for the analysis; areas on the bone that displayed any pathology, trauma or of anthropological interest were avoided; the cutting and use of tools was first conducted on animal bone to ascertain a suitable method prior to sampling of human bone; and methods were chosen based on small sample size (FT-IR) and non-destructive techniques (colourimetry).

4.1.2 Sample selection

At present there is no standard protocol that is used by all researchers that has been peer reviewed regarding which skeletal element is best for obtaining a DNA profile. The standard operating procedure produced by International Commission on Missing Persons (ICMP) presents a list of preferred bones to be sampled (Vennemeyer et al., 2015) however no information pertaining to the research or

process of how this list was generated is provided. Skeletal sample selection for the identification of soldiers who died in the Battle Of Fromelles 1916, states two samples should be taken from each individual – a tooth and a bone. Priority is given to the selection of whole bones to reduce contamination issues, and metacarpals and metatarsals are listed first for ease of transportation due to the small size. Femurs are listed as last resort after fibula and other long bones (Loe et al., 2014). A study of past and present literature regarding DNA extraction from forensic or archaeological bone shows that a majority of researchers use long bones, especially the femur for analysis (Kaestle and Horsburgh, 2002; von Wurmb-Schwark et al., 2003; Gilbert et al., 2005) however there is no justification by any author as to why this is used in preference to other bones. Much of the research examined does not state which bone was used stating simply 'human bone fragments' (Alonso et al., 2001; Alonso et al., 2004; Bille et al., 2004) therefore no conclusions can be made about the success in terms of individual bones.

Some researchers have named long bones as the most successful bones from which to retrieve DNA, but not mentioned which other elements were tested, whereas Anðelinoviæ et al (2005) goes into more detail regarding the identification work conducted on skeletal remains in Bosnia, Croatia and Herzegovina from the conflicts during 1991-1995. The majority of the analysis was conducted on long bones with the results showing the femoral bones giving the best DNA result, with good results also from the fibula. Alonso et al., (2001) also stated preferential use of long bones after finding the quality of DNA obtained is higher than that extracted from skulls or ribs.

Conflicting information was reported by Desmyter and Greef (2008) who described a significantly higher DNA yield from the os coxae, as compared to the femur, fibula, phalanges, humerus, and scapula. Nevertheless, full profiles were obtained from all skeletal elements. Prado et al., (1997) also reported the success of DNA extraction from the pelvis with the successful amplification of nine microsatellite loci from the iliac bone.

Bollongino et el (2008) stated that in order to obtain a good quality DNA profile, the analysed bone needs to possess a compact structure (cortical) such as the diaphysis of long bones; as opposed to the porous spongy structure (trabecular) of skeletal elements such as the vertebrae, scapulae, pelvis and parts of the skull. Use of compact bone, as opposed to cancellous bone, was also recommended by Imaizumi et al., (2005) and Anðelinoviæ et al (2005).

Zoledziewska et al. (2003) obtained high quality DNA samples from human rib bones, but the samples were not from an archaeological collection, so had not suffered the damage and fragmentation frequently found from burials.

Research conducted over the last decade shows greater robusticity of comparative analyses between skeletal elements in relation to DNA recovery. Imaizumi et al., (2005) analysed the femur, humerus, rib, parietal, talus, tibia, proximal foot phalange and mandible, and succeeded in extracting and sequencing DNA from all the elements.

Staiti et al. (2008) investigated the analysis of degraded DNA and found the highest DNA quantities were obtained from the femur, tibia, humeral epiphyses and the cranial theca. The ischial tuberosity of the pelvis gave fairly good profiles, whereas only partial profiles were obtained from the glenoid cavity of the scapula, distal epiphysis (styloid process) of the radius, olecranon of the ulna, body and tranverse process of the cervical vertebra, lateral side and transverse process of the thoracic vertebra, body of the lumbar vertebra, rib shaft, acromial end of the clavicle, diaphysis of the fibula, and articular process surface and anterior side of the sacral bone.

A selection of the elements researched for the suitability for DNA analysis over the last 15 years is presented in Table 4-1. While the skeletal terms listed are not presented in standard anthropological nomenclature the elements are described as per the original publications.

Table 4-1: Table of skeletal elements used by other researchers for DNA analysis

Skeletal element	Colson et al., 1997	Prado et al., 1997	Alonso et al., 2001	Kaestle & Horsburgh, 2002	Von Wurumb-Schwark et al., 2003	Zoledziewska et al., 2003	Alonso et al., 2004	Bille et al., 2004	Andelinovic et al., 2005	Gilbert et al., 2005	Imaizumi et al., 2005	Milos et al., 2007	Chilvers et al., 2008	Gamba et al., 2008	Fernàndez et al., 2009	Gamba et al., 2011	Caputo et al., 2013	Ambers et al., 2013	Bauer et al., 2013	Caputo et al., 2013	Fredericks et al., 2013	Mundorff & Davoren., 2014
Skull											X	X	X									X
Mandible													X					X				X
Clavicle												X	X								X	X
Scapula												X									X	X
Humerus		X									X	X	X						X			X
Ulna												X	X								X	X
Radius												X	X				X			X	X	X
Metacarpal												X					X			X	X	X
Rib						X					X		X								X	X
Sternum																						X
Vertebrae												X					X			X	X	X
Pelvis		X										X									X	X
Sacrum																					X	X
Femur	X			X	X				X	X	X	X	X				X	X	X	X	X	X
Patella													X									X
Fibula									X			X									X	X
Tibia											X	X	X				X	X		X	X	X
Tarsal											X										X	X
Metatarsal												X	X								X	X
Phalanges											X											X
Not stated			X				X	X						X	X	X						

Milos et al. (2007) highlighted the need for a more in-depth analysis and examined 15 different skeletal elements for success rates. The results obtained are displayed in Table 4-2, alongside the positive identification rates from DNA analysis on

different fragmented elements as reported by Mundorff (2009) when analysing a subset of samples from the World Trade Centre Human Remains Database.

Table 4-2: Success rates in percentage of DNA amplification and identification from DNA extracted from human bone, with the sample size of each skeletal element displayed within brackets

Skeletal element	Amplification success rate Milos et al., 2007	Positive identification rate Mundorff., 2009
Skull	40% (757)	47% (494)
Mandible	Not analysed	65% (46)
Clavicle	26% (128)	54% (97)
Scapula	57% (35)	54% (92)
Humerus	46% (2415)	61% (110)
Ulna	23% (444)	61% (87)
Radius	25% (469)	60% (120)
Metacarpal	61% (18)	44% (211)
Hand phalanx	Not analysed	57% (83)
Rib	Not analysed	64% (1301)
Vertebrae	62% (146)	61% (72)
Pelvis	53% (185)	63% (62)
Sacrum	Not analysed	59% (27)
Femur	87% (11356)	71% (143)
Patella	Not analysed	80% (83)
Fibula	63% (160)	60% (159)
Tibia	76% (1329)	70% (125)
Tarsal	Not analysed	51% (37)
Metatarsal	33% (120)	72% (257)
Foot phalanx	Not analysed	80% (25)

Results from Milos et al. (2007) showed the femur, tibia and fibula as the top three for the best success rates, followed by vertebrae, metacarpals, scapulae, mandibular body, and illium; with the metatarsals, arm bones and clavicle showed the lowest success rates. Whereas Mundorff (2009), reported the patella, foot phalanx and metatarsal providing the highest percentage of positive identification from DNA analysis, followed by the femur and tibia at 71% and 70% respectively. Remaining elements were between 50-70% successful, with the lowest identification success rate from metacarpals at 44%.

The results reported by numerous researchers appear contradictory on the success rates of amplification and the obtaining of full profiles, but this is expected due to the varying nature of the samples. For example, Milos et al. (2007) reports on skeletal elements from different geological locations from mass graves resulting from the conflicts in the former Yugoslavia in the 1990s; whereas Mundorff (2009) reports on fragmented skeletal remains recovered after the World Trade Centre disaster in 2001.

As previously discussed at the beginning for this section, details of which bone the researcher has used is often omitted from publications, therefore limited the case studies with ancient DNA studies that can be compared for methodologies and skeletal element success. However, the following case studies all include detailed information of samples used. Ancient and forensic DNA analyses were used to confirm the removal and deposit of human remains from the tomb of Francesco Petrarca. Confirming the anthropological assessment, the DNA results from the skull and ribs confirmed the skull belonged to a female, and the rest of the skeletal remains belonged to a male (Pilli et al., 2008). Another case of utilising ancient DNA analysis to confirm the sex of a skeleton comes from an archaeological site in Pompeii. A selection of eight femora, four tibia and one humerus were used for amplification of the sex marker amelogenin and a Y-specific sequence which only DNA from males would display - DNA results were obtained from all elements (Cipollaro et al., 1998).

Despite the apparent differences, there appears to be a trend in the success of lower limbs for positive DNA amplification. It is possible that these weight-bearing bones provide a higher amount of DNA than non-weight bearing bones. This would explain why the lower limbs especially the femur tend to contain more DNA than the humerus, even though they have similar bone structures of compact bone. Femurs also tend to survive better than most other bones due to its stronger composition of compact bone (Mays, 2010). The foot bones can also in some circumstances, be better protected from degradative elements and fracturing due to the covering of boots or shoes (Cox et al., 2007). By this rationale, the femur and

foot bones are likely to provide an optimal DNA sample for successful amplification and analysis.

In conclusion, when choosing skeletal elements to analyse, the factors that need consideration are: the preservation state of the bone – the best samples need to be heavy, hard and show little evidence of microbial activity; the elements need to contain a high percentage of compact bone; the selected elements need to be those that survive well in a burial environment to ensure the samples are as intact as possible; and if using skeletal remains from a museum collection or similar, samples need to be of low anthropological interest (avoiding the skull and pelvis) and sampling needs to be discreet.

After considering all the factors discovered in the relevant literature regarding the successful amplification of DNA from skeletal elements, the two skeletal elements chosen to be analysed in this project are femora and metatarsals. These elements have been chosen based on the criteria mentioned earlier: heavy, hard and show little evidence of microbial activity; contain a high percentage of compact bone, and need to have good survivability in a burial environment. Although metatarsals can be absent in archaeological contexts, a main reason for this is the excavation methodology – small bones can be lost if the grave sides cannot be found or the appropriate level of care and attention is not applied to the process (Tuller and Đurić', 2006). By choosing the largest metatarsal, it is hopeful that the majority of skeletons to be investigated will have a metatarsal present and therefore comparative data can be obtained.

4.1.3 Contamination precautions

Due to the fragile nature of ancient DNA molecules, anti-contamination controls need to be tightly monitored or modern DNA may infiltrate the sample and overpower the original ancient DNA sequence in the sample. These potential contamination risks make the extraction of ancient DNA from archaeological bone very challenging, and depending on the stage of decay of the bone and the denaturation of DNA, the process of obtaining a profile is a complicated and not always successful one.

These contamination issues also exist with forensic DNA samples where strict guidelines need to be followed in order to eliminate the risk of contamination and provide results that are admissible in court (von Wurmb-Schwark et al., 2008).

By acknowledging and understanding the factors of the contamination associated with ancient DNA, in particular those associated with bone analysis these challenges can be addressed. Table 4-3 outlines the contamination issues affecting ancient DNA analysis, and methods that can be used to mitigate the risks.

Table 4-3: Contamination issues affecting aDNA analysis (after (Kirsanow and Burger, 2012)

Contamination source	Manner of contamination	Mitigating methods
Excavation, transportation, washing and anthropological assessment	Close contact between personnel and the skeletal material. Contamination can be transferred via touching, breathing, shedding of cellular components or washing with water.	Ensure all personnel are aware of the risks. Protective clothing to be worn – clothes, lab coats/suits, gloves, face masks. Use brushes to remove dirt.
Sampling of the bone	Drilling / sawing of the bone, and removal of the bone surface exposes previously protected areas of the bone to the environment.	Cleaning of the bone surface and using a decontamination process on the bone surface.
Laboratory equipment and consumables	Any piece of equipment / workspace/ consumable in the lab has potential to become contaminated with modern of sample DNA.	All equipment needs to be assigned to a particular process and thoroughly cleaned before and after each use. Blank controls to be run to pinpoint any contamination occurring.
General environment and storage environment	Movement of people in the laboratory causing a build-up of molecular material.	Restricted access to the laboratory and storage sites. Storage bags / boxes clean of DNA.
Amplification products	The cross over between previously amplified products and new samples.	Processes split between a 'clean room' and 'dirty room' to contain PCR products.

4.1.4 Sample preparation

In order to process bone samples it is necessary to cut, drill, or powder the samples, however these physical methods can be detrimental to the quality and quantity of DNA recovered due to the associated increase in temperature (Adler et al., 2011). In order to combat these difficulties, precautions were taken with the preparation of bone samples.

Researchers (Adler et al., 2011) have investigated the effects of physical sampling methods on the recovery of DNA and concluded that providing the build-up of heat is kept to a minimum by drilling at a maximum speed of 100 RPM, excess DNA damage can be avoided. One way of reducing the temperature is to use a water coolant system but this can introduce more contaminants to the sample, especially in the case of archaeological bone where the surface may be compromised.

Many protocols for DNA extraction use bone powder (Colson et al., 1997; Götherström et al., 2002; Hartman et al., 2011) however powdering of bone can lead to airborne contamination between samples (Kitayama et al., 2010). Instead of powdering the bone for analysis, thin slices can be used in order to decrease the amount of physical preparation (Caputo et al., 2013). However, by not powdering the bone, there is a risk that the sample may not be homogenous and by not using a uniform method it will be harder to produce comparable results between samples.

When the archaeological human skeletons in this study were excavated, DNA analysis was not considered, therefore no precautions were in place to limit DNA contamination. By not enforcing anti-contamination measures, the possibility of contamination of exogenous DNA from archaeologists and anthropologists on the bone surface is high, and therefore is a critical issue for this study. Importantly though, this manner of unprotected excavation and handling of skeletons is common place within archaeology, so therefore an important aspect of this research.

A literature review was conducted on the impact of DNA contamination on bone samples which showed that providing an adequate cleaning protocol of the bone

surface was followed, contamination from individuals touching the bones did not reproduce any STR signals (von Wurmb-Schwark et al., 2008). Therefore choosing the appropriate cleaning method for this research is imperative.

4.1.4.1 Bone cutting vs drilling vs milling

The cutting, drilling or milling of bone sections all have their advantages and disadvantages as described in Table 4-4. Methods that result in the generation of bone dust must be carefully contained with suitable apparatus and PPE. Although heat will unavoidably be produced which can lead to denaturation of DNA and changes to the bone structure and composition, measures can be taken to minimise this effect.

Table 4-4: Advantages and disadvantages of different sample preparation techniques

	Advantages	Disadvantages
Bone cutting	Less preparation time	Heat and dust generation
	Lower risk of contamination	Longer analysis period
Bone drilling	Homogenous sample	Contamination risk
	Less destructive for bone	Heat and dust generation
Bone milling	Homogenous sample	Contamination risk
	Quicker analysis period	Heat generation

4.1.4.2 Surface decontamination vs surface removal

Many researchers have used the addition or submersion of bones into water or chemical solutions in order to remove the possible exogenous DNA and other contaminants from the surface (Richards et al., 1995). Amory et al., (2012) found that extensive testing of soaking bone samples in 10% bleach (0.5% sodium hypochlorite) to remove surface contaminants proved that this method does not damage the DNA residing within the internal matrix of compact bone, but whilst some methods of soaking have been shown to remove contaminants, these

methods also provide a medium of transportation, and risk conveying impurities into the bone cortex from the surface, or in cases of bone with bad preservation, could cause irreparable damage to the biomolecules themselves. For this reason, this method may not be possible on highly degraded archaeological samples due to the fragility of their structure.

Other researchers chose to remove the surface of the bone, (Lambert et al., 1990; Gamba et al., 2011; Ambers et al., 2013) either as an alternative to sodium hypochlorite submersion or as a pre-cursor (Bauer et al., 2013). Bouwman et al., (2006) intentionally contaminated ancient bone with modern DNA and found that by removing the top 1-2 mm of the bone surface the contaminants were removed.

Surface removal can be achieved with a sander that can be cleaned and de-contaminated between each sample to ensure there is no carry-over of bone material, and can achieve removal of contaminants without the addition of harsh chemicals or by providing a method of passage for water to possibly damage biomolecules or the bone. Although heat will be generated using this method, by using for short durations, any damage by heat can be minimised.

The removal of the bone surface not only removes contaminates in a safer manner, but also enables colourimetric analysis of the bone cortex to be conducted, therefore this method was chosen to be implemented in this research.

4.1.5 Demineralisation

Demineralisation of a bone sample is essential due to the mineral properties acting as a physical barrier to extraction reagents, which therefore prevents the release of DNA molecules. By digesting the mineral fraction of the bone, more DNA will be accessible, and the DNA bound to the hydroxyapatite mineral matrix of bone will also be made accessible (Götherström et al., 2002; Amory et al., 2012).

Loreille et al. (2007) proposed a protocol for DNA extraction from bone involving complete demineralisation of the sample by full physical dissolution of the sample. Results showed this method produced significantly higher DNA yields in comparison to standard extraction methods, and produced adequate DNA

quantities from small amounts of material. This is vital for obtaining profiles from degraded skeletal elements.

In order to ascertain to what degree of demineralisation would be suitable for the biological material in this research, tests were conducted on both porcine and human archaeological bone samples.

4.1.6 Extraction

There are many variations on detergents, chemicals, methodologies, and available commercial kits for DNA extractions, however there is a general protocol that many adhere to. These steps are detailed in Table 4-5.

Table 4-5: General DNA extraction protocol

Stage	Description
1	Tissue is sectioned, ground or sonicated to break open cells in order to expose contained DNA
2	Various detergents are added in order to remove the membrane lipids
3	The enzyme Proteinase K is added to remove proteins
4	DNA is precipitated in alcohol to form a pellet for analysis

Desmyter and Greef (2008) tested the efficiency of the extraction methods mentioned previously by Loreille et al. (2007) and a method by Rohland and Hofreiter (2007), on eight human bone fragments derived from forensic casework. The bone fragments used included femur, fibula, os coxae, phalanges, humerus and scapula. Results suggested that the complete decalcification of bone in the presence of the detergent SDS (sodium dodecyl sulphate) resulted in the recovery of more DNA from standard protocols but also enabled full STR profiling for all samples. By contrast, decalcification without the addition of SDS yielded even higher quantities of DNA and STR profiling was still of high quality. The addition of the bond cleaver PTB (N-phenacylthiazolium bromide) decreased DNA yield and

resulted in incomplete or absent STR profiles. The highest yield of DNA was recovered from the os coxae, but full profiles were obtained from all samples after the decalcification of the bones. This suggests that all skeletal elements mentioned above are worth considering for extraction even though long bones and teeth are the most commonly recommended.

4.1.7 Amplification using polymerase chain reaction (PCR)

The choice of technique available for the extraction and subsequent analysis of the DNA is dictated by the quantity and quality of the DNA available. For this reason and the fact that many if not all of the samples for this project were degraded or minute, techniques such as RFLP (Restriction Fragment Length Polymorphisms) was not possible. Polymerase Chain Reaction (PCR) is a technique used to amplify a DNA segment by the use of numerous cycles of denaturing and annealing of DNA and primers which results in replication of the target DNA (Parsons and Weedn, 1997). Using PCR is an obvious choice and often stated as essential (Ariffin et al., 2007).

The concept of the PCR technique was established in 1983 by Kary Mullis by the amalgamation of the synthesis of oligonucleotides (single strands of DNA) and using target-specific synthesis to amplify the region between them on complementary opposite strands of DNA (Bartlett and Stirling, 2003). Advances in the technique have improved dramatically and PCR is now routinely used in all forensic DNA laboratories to amplify small traces of DNA. However, the use of PCR does require care as the prevalent risk of contamination can easily be moved around a workspace and contaminate pre-PCR samples. For this reason it is essential to restrict all PCR work to a designated room and control the personnel and workflow from this space.

In order to recover DNA from bone with a sufficient quality and quantity to produce a profile, STR (short tandem repeat) system markers can be used. Due to their ability to improve results from low template (LT) DNA they are used extensively in forensic DNA analysis (Lopes et al., 2009). The multiplex STR typing kits simultaneously amplify up to 17 loci, generating amplicon sizes from 100-450

base pairs (bp). In cases of severe DNA degradation, even STR profiles may only be a partial, or exposed to stochastic effects (Pizzamiglio et al., 2006). This problem can be overcome or improved by using mini-STRs – primers which use smaller amplicons of less than 150bp by implementing markers closer to the coding region, allowing for additional genetic information to be retrieved (Martín et al., 2006b).

In cases where STRs and mini STRs fail to analyse autosomal DNA samples, mtDNA analysis can be conducted in order to gain information (Catelli et al., 2008). SNPs (single nucleotide polymorphisms) can be used in forensic DNA typing for amplicons ranging from 40-50bp. SNP analysis looks at the variations of specific single points in the genome and are therefore very useful for degraded DNA samples (Senge et al., 2011).

4.1.8 PCR inhibitors

One of the most complex problems with aDNA extraction from bone is the large presence of PCR inhibitors. These inhibitors if not removed, can interfere with the amplification of the aDNA (Rohland and Hofreiter, 2007) by binding or competing with reaction components, or inactivating the polymerase (Eilert and Foran, 2009).

These inhibitors can be present in the burial environment, occur due to intrinsic processes or as a result of the laboratory techniques. The most common PCR inhibitors are calcium ions, Maillard products, molecular damage, humic substances and chelating agents such as EDTA (Simón et al., 2012).

Maillard products are the result of a Maillard reaction of an amino acid and a reducing sugar, such as glucose, which can cause breakage of the DNA strands (Hiramoto et al., 1995). These products cause cross-linking of the DNA molecules which act as PCR inhibitors by obstructing the PCR reaction (Simón et al., 2012).

As discussed earlier in section 2.4.3, molecular damage occurs when the organism dies, due to oxidation and hydrolysis which degrades the DNA.

Humic substances that act as PCR inhibitors include humic acid, fulvic acid and tannin – all which are components of soil. The presence of humic substances in the

excavated archaeological bone samples can be indicated by colour, and depending on the concentration, can lead to total inhibition of the PCR reaction (Simón et al., 2012).

Chelating agents such as EDTA are introduced to the bone during the demineralisation process, but act as PCR inhibitors if not completely removed (Simón et al., 2012).

Calcium ions can be found in acidic soil and in the human remains themselves, and can act as PCR inhibitors by precipitating with DNA (Simón et al., 2012).

4.1.9 DNA separation methods

After amplification, the DNA sample consists of many copies of different lengths and areas of genetic code, depending on the primers used. In order for the amplified PCR products to be meaningful, the DNA needs to be separated into mini-STR fragments enabling each allele to be identified. It is the differences in these alleles that differentiate individuals from one another.

In order to achieve separation by the size of the target fragments, a method called electrophoresis is used. This method applies an electrical charge to negatively charged DNA molecules, causing them to migrate from a negative electrode (cathode), towards a positive electrode (anode) (Butler, 2001). As the smaller molecules will migrate faster than large molecules, separation of the DNA fragments is achieved.

During this research, two types of electrophoresis were used - slab gel electrophoresis and capillary electrophoresis, both of which will now be discussed.

4.1.9.1 Slab gel electrophoresis

Slab gels are composed of a solid matrix, agarose gels were used in this case, which contain pores through which the DNA molecules pass during electrophoresis. For this research agarose was used, which is presented in powder form, but when added to a buffer solution such as TBE (Tris/Borate/EDTA) and heated, the agarose dissolves into the solution, enabling the mixture to be poured into a tray to set. Toothed combs are placed into the molten liquid in order to generate wells in

the set gel upon removal. The gel is then submerged into a tank containing running buffer such as TBE, which provides a cooling system once the current is applied. DNA is loaded into the wells in a solution containing a dye enabling visualisation of the DNA, and sucrose to ensure the samples remain at the bottom of the well. Positive and negative controls are run alongside the samples to provide confidence that the technique is working and the absence of contamination; and DNA of known molecular weight is injected into lanes either side of the samples to provide a 'ladder' to compare lengths of unknown DNA to.

Following the loading of the samples, a lid is placed onto the tank, and electrodes are attached at either end to enable the flow of current through the gel and migration of DNA. The size of the DNA molecules and pore size of the agarose gel, as well as the level of voltage applied will dictate the duration that the electric current is applied in order to achieve separation of DNA.

Once the electrophoresis is complete, the gel is removed from the tank and placed under a ultra-violet light in order to visualise the dye attached to the DNA. Photographs can then be taken for analysis purposes and record keeping.

This technique was used throughout this research to confirm the absence or presence of DNA in the porcine samples, and also provide an indication into the length of remaining DNA fragments. However, a major drawback to this technique with determining the quantity of aDNA is that the quantity will be very low and therefore may not be visible by using the standard dye of ethidium bromide, other dyes such as SYBR Green or SYBR Gold may need to be used (Rohland and Hofreiter, 2007). Therefore, for the ancient human DNA samples, capillary electrophoresis was used to separate the DNA molecules and identify the alleles present.

4.1.9.2 Capillary electrophoresis

Capillary electrophoresis works on the same principle to that of slab gel electrophoresis, with the application of electric current to separate DNA molecules by causing migration from a cathode to an anode. However, instead of samples

passing through a gel, this is replaced by a polymer which runs through a capillary between two buffers.

PCR products are added to a loading cocktail of internal lane standard which will provide the 'ruler' of DNA strand size, and Hi-Di formamide which re-suspends the DNA and assists with the denaturation of the DNA required for separation. The samples are loaded onto the auto-sampler tray along with a negative and positive control and an allelic ladder to verify the calibration and correct 'calling' of alleles.

One at a time, the samples are automatically injected into the capillary, and migrate past an oven heated to 60^{o}C, which heats the samples facilitating the separation of the PCR products. These products are then separated by mobility and pass through a detection window in size order. The fluorescent dyes which were added during the PCR process to label the STR markers are excited by a laser, at a primary excitation wavelength of 488 nm. The light emitted by this excitation is separated by a diffraction grating into a colour spectrum which illuminates the CCD (charge-coupled device) camera. When each photon of light hits the millions of pixels in the CCD, it is converted to an electron, of which the intensity is recorded by data collection software which converts the signal intensity to a value known as the Reflective Fluorescence Unit (RFU). Analysis software such as GeneMapper, displays these RFUs of the STR PCR products as colour-separated peaks on an electropherogram, which can then be analysed for the interpretation of the biological profile.

4.1.10 Electropherogram interpretation

Due to the combination of hardware components, chemicals and dye-labelled fragments within a capillary electrophoresis system such as the ABI 310, artefacts and noise are generated which can appear on the electropherogram as pull-up peaks and electrical spikes. It is not possible to remove this background noise so careful interpretation of the data must be undertaken. Figure 4-1 shows a typical electropherogram of a full profile from a single source, showing heterozygous alleles at all loci apart from D22S1045 which has a homozygous peak. The peaks show good morphology with -4 and +4 stutter peaks.

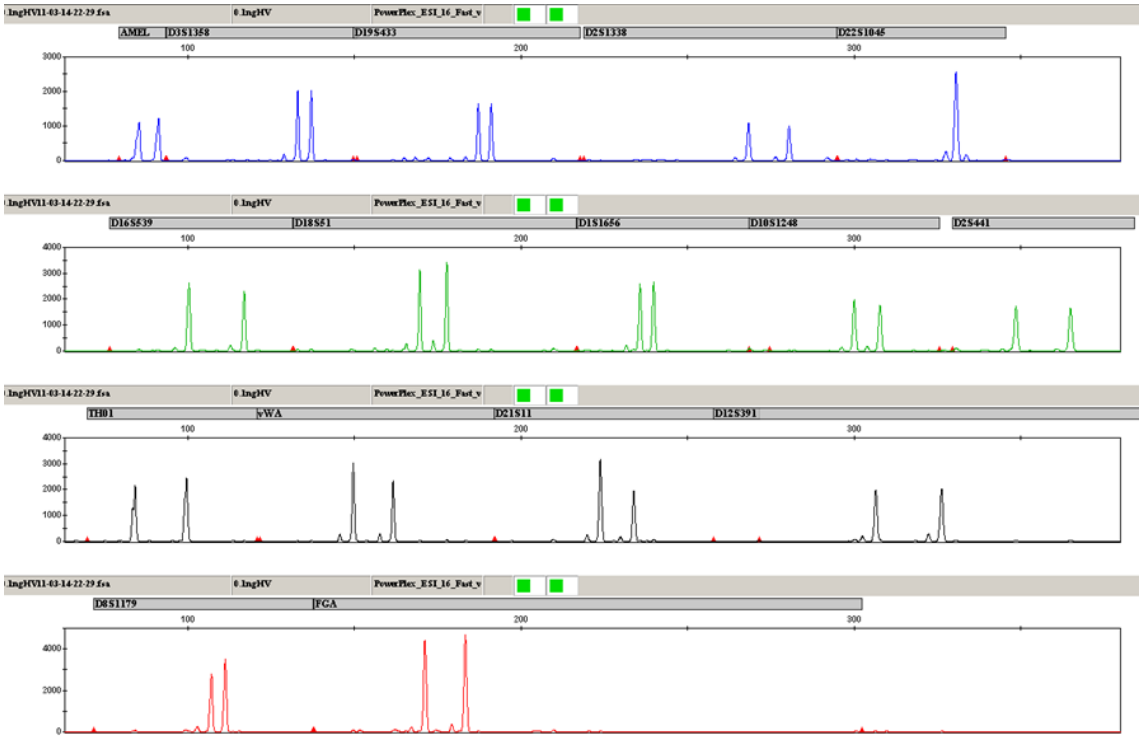

Figure 4-1: Electropherogram showing a characteristic full DNA profile from a single source, with alleles displaying at each loci.

Figure 4-2 shows an example of pull-up from peaks in vWA into D18S51, and electrical spikes caused by fluctuations in the equipment.

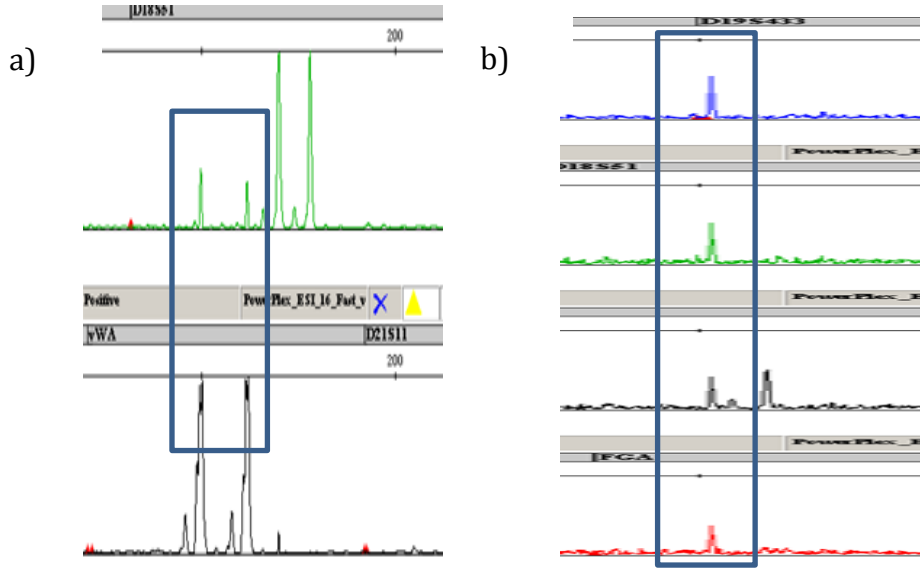

Figure 4-2: Electropherograms displaying a) pull-up of peak signal, and b) electrical spikes displaying on all dyes.

One way to discriminate between real allelic peaks and noise is to set a RFU threshold, so the data collection software will only detect peaks above a certain value, hence ignoring the baseline noise. The manufacturers default setting is 50 RFU, and this is the level many laboratories adhere to. In cases of degraded DNA analysis where it may be necessary to look below the 50 RFU threshold for true peaks, peak height can be used to calculate a ratio – where peak height of alleles should be at least three times greater than the background noise.

The nature of PCR amplification, the addition of primers, and the process of capillary electrophoresis can result in the production of signal which can appear on the electropherogram as artefacts, such as stutter, pull-up, spikes and dye blobs. By recognising these artefacts they can be eliminated from the analysis, leaving just true alleles to be identified.

One way to determine true heterozygous peaks is to perform a Peak Height Ratio (PHR) calculation, which compares the heights of peaks to provide an estimate of heterozygosity. A common equation used for this calculation is shown below: (Leclair et al., 2004).

$$\frac{Lowest\ Intensity\ Allele\ (RFU)}{Highest\ Intensity\ Allele\ (RFU)} \times 100 \qquad \textbf{(4-1)}$$

The value of the cut-off of the PHR value to determine whether a peak is heterozygous or not, varies from researcher to researcher (Butler, 2015) and when analysing DNA in low concentration and quality, preferential amplification can occur causing peak imbalance between heterozygous sister peaks. Due to the degraded nature of the samples involved in this research, performing PHR calculations may not be useful, due to this phenomenon and therefore tests were performed to establish whether a suitable PHR threshold could be set.

4.1.11 Analytical techniques

In addition to DNA analysis the bones involved in this research were also assessed using colourimetry to determine any staining on the bone, and to approximate the depth at which contamination may have occurred. Additionally compositional analysis was performed using FT-IR to identify diagenetic changes.

4.1.11.1 Colourimetry

Determination of colour has been used for decades by using human visual perception in many industries (Ansorena et al., 1997; Wilson et al., 2008; Korifi et al., 2013; Sharifzadeh et al., 2014) including its application in soil analysis to determine composition (Viscarra Rossel et al., 2009; Aitkenhead et al., 2013) and in archaeology with the use of Munsell Colour charts for the colour determination of soil (Hester et al., 1997).

The determination of bone colour has been used previously as an interpretative tool in the investigation of distinguishing human cremated bone from animal origins (Devlin and Herrmann, 2008), and estimating the maximum temperatures reached on heated bone (Shipman et al., 1984). Previous research has also found it a useful technique to indicate the presence of Maillard reactions and cross-linking which will affect the amplification and profiling of DNA samples (Koon et al., 2008).

The problem with using human colour perception is that everyone perceives colours differently, and slight differences may not be detectable (Wilson et al., 2008). Hence for this research a colourimeter was used in order to record colours in a numerical form, by using one of the most common colour spaces: CIE L*a*b*. The colourimetric system converts colours into coordinates in a colour space as detailed in Figure 4-3.

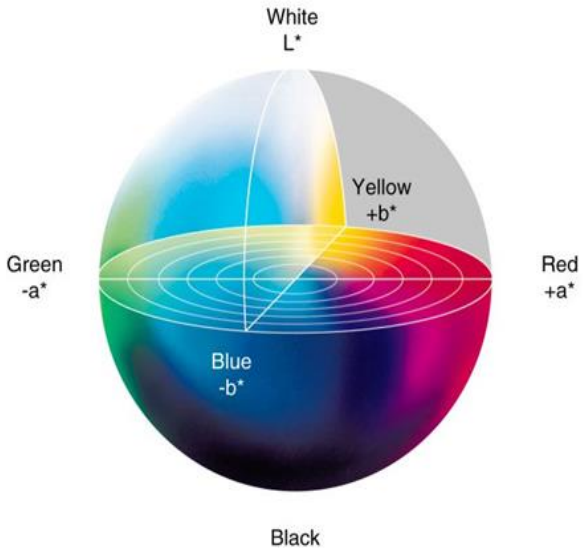

Figure 4-3: The CIE L*a*b* colour space, showing the three axis of lightness, hue and chroma after Williams (2002)

L* represents the lightness variable of a colour, with an axis white to black, where 0 corresponds to black and 100 corresponds to white. The other axis represent the hue and the chroma of the colour, where: a* defines the red (+127) and green (-128), and b* represents the yellow (+127) and blue (-128).

By using the CIE L*a*b* colour coordinate system, not only can numerical values of colours be recorded, but it is also possible to calculate the colour differences and changes that occur to the samples, by using the equation (4-2):

$$\Delta E* = \sqrt{\Delta L^{*2} + \Delta a^{*2} + \Delta b^{*2}} \quad \textbf{(4-2)}$$

Where Δ is the difference between the sample and the standard of the particular coordinate.

The use of the CIE L*a*b* system for this project will enable the overall differences in colour due to the burial conditions of the porcine bone to be calculated, and also variations in bone colour from the human archaeological samples. These documented colour changes and differences in lightness, chroma and hue allow another aspect of comparison to the compositional and structural changes detected by the other techniques mentioned in this section.

4.1.11.2 Fourier Transform Infrared Spectroscopy

As this research seeks to document variables of the bone that have changed in relation to burial environment, it is necessary to assess the structural state of the bones in order to determine the state of diagenesis.

In archaeological science, the possible relationship between diagenetic indicators such as the ratios of the mineral and organic portions, and the splitting factor, in relation to burial environments have been studied intently (Hedges and Millard, 1995; Wright and Schwarcz, 1996; Lozano et al., 2002; D'Elia et al., 2007; Trueman et al., 2008). Wright and Schwarcz (1996) concluded using FTIR permitted alterations in bone carbonate, and crystallinity to be detected and used as a screening tool for diagenesis. Trueman et al (2008) did not find any correlations with carbonate, but summarised that differences were observed in the splitting factor between the surface and sub-surface of weathered bone, which increased in severity the longer the post-mortem duration.

The technique chosen to assess this diagenesis is Fourier Transform Infrared Spectroscopy (FTIR) as it provides structural information about molecules in a sample, by passing infrared radiation through the sample and collecting the absorbance and transmission data that is produced. As different bonds and groups of bonds within molecular compounds vibrate at different frequencies, energy will be absorbed at different frequencies depending on the compound and a spectrum is produced that can be compared to known molecules in a library.

An example of an FTIR spectrum of bone is shown in Figure 4-4, with the identification of major peaks and vibration bands, and functional groups reported in Table 4-6 with approximate wave numbers.

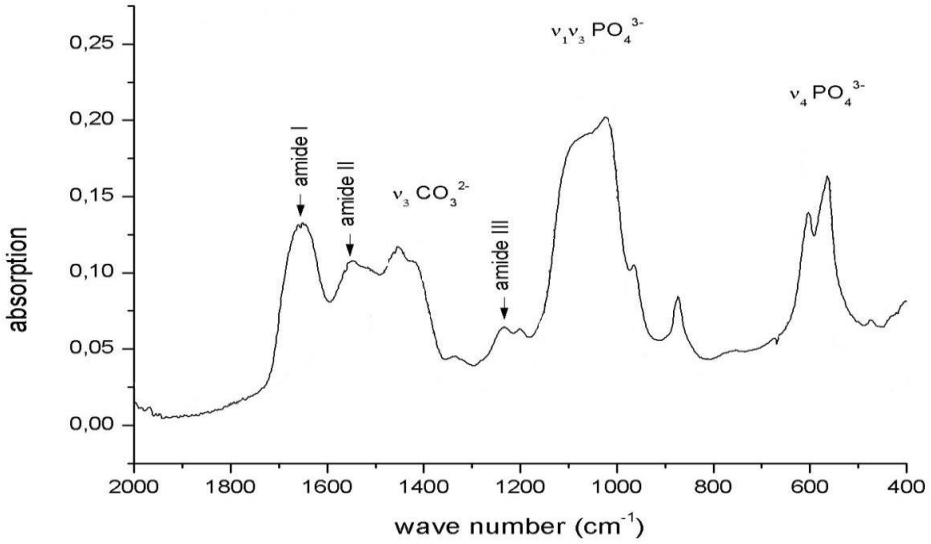

Figure 4-4: FTIR spectra of a typical bone sample with major peaks and characteristic vibration bands identified (Chaumat et al., 2011)

Table 4-6: Wavelength and functional group of major bone components (after Thompson et al., 2013)

Approximate wave number	Functional group
565	v_4PO_4 phosphate
605	v_4PO_4
632-650	OH group
874	$v_2CO_3^{2-}$ group
960	$v_1(PO_4)$ apatite
1028-1100	v_3(PO4) apatite
1400-1550	CO_3^{2-} groups (lattice carbonate)
1630-1660	Organic tissue and water
3400	OH water
3573	OH group

FTIR analysis is used widely across many disciplines, but for the purpose of this research, the main areas to be investigated are the integrity, maturity and content of collagen in a bone, by assessing the mineral and the matrix components.

Researchers have used FTIR in the past to estimate the carbonate content by assessing the ratio of carbonate to phosphate peaks, and assessed the crystallinity of hydroxyapatite in phosphate as an estimate of diagenetic change (Weiner and Bar-Yosef, 1990; Wright and Schwarcz, 1996; Nielsen-Marsh et al., 2000; Fredericks et al., 2012b). In addition to using FTIR to establish diagenetic information from crystallinity, it can also be used to identify contamination such as humic acid (D'Elia et al., 2007), carbon minerals such as calcite (Lee-Thorp and van der Merwe, 1991; Trueman et al., 2008), and francolite (Shemesh, 1990; Wright and Schwarcz, 1996) and can be used as a screening tool for the likelihood of DNA success from heated bone (Fredericks et al., 2012b).

Over the last few years, researchers such as D'Elia et al (2007) have been using a combination of FTIR and ATR (attenuated total reflectance), which is the addition of an ATR unit in the form of a crystal, to an FTIR. As the infra-red beam penetrates the surface of the sample, the ATR measures the intensity loss as the sample absorbs the energy (Thompson et al., 2011; Hollund et al., 2013). This provides a higher sensitivity due to the direct contact between the crystal and the sample (Hollund et al., 2013) therefore a better identification of the presence of collagen, and an improved ability to identify contaminants present in the bone sample. Other advantages over using standalone FTIR include the reduced sample preparation time (Thompson et al., 2011) by negating the need for pellet preparation, eliminates the risk of damage the preparation can do to the sample, which affects the splitting factor (Surovell and Stiner, 2001) and a smaller sample mass is required.

It is due to these advantages over standard FTIR, that ATR-FTIR was chosen to be used to analyse the archaeological samples in this research.

4.1.11.3 X-ray Fluorescence Spectrometry (XRF)

The fundamental principles of XRF are founded on the interactions of atoms with radiation and how this affects their behaviour. When radiation is applied to a material, it becomes ionised due to the energy of X-rays, which when high enough, will displace electrons making the atom unstable. This is achieved by the movement of tightly bound inner shell electrons, which are replaced by outer electrons, causing radiation emission. It is the measure of this release of energy, also known as fluorescent radiation or fluorescence that identifies the compositional nature of a sample by comparing the energy differences to a library from known elements (Shackley, 2010).

The use of XRF within the archaeological community has increased over the years for elemental composition analysis, due to its non-destructive nature, minimum preparation of samples, and ease of use.

4.2 Method optimisation

Due to the numerous techniques and methods currently used, the lack of detailed methodologies discussion in published material, and the limited samples available, it was necessary to thoroughly investigate, develop and ascertain methods that would not only work for this study, but could also provide assistance and guidance to other researchers.

After the method research had been conducted, as discussed in section 4.1, the optimisation of chosen methods began in order to identify the most successful, time effective, and possible due to tight resources and available equipment. The results from this method optimisation section led to the selection of protocols to be used on the research material. This optimisation process is detailed in the following section.

4.2.1 Colourimetry tests

As discussed in section 4.1.11.1, colour analysis was used to assess bone colour in comparison to different burial environments, identify areas of possible soil contamination, and investigate any correlations with DNA survival and bone diagenesis.

Where possible, colour tests would be performed on the flattest part of the bone, however tests were performed on a pipe section of similar curvature to that of bone, in order to calculate the possible error limits associated with a curved surface.

Tests were performed using two different masks in order to optimise the best results with the lowest standard deviation, and conducted 10 times, using 10 measurements per reading. The results from the tests are shown in the following tables: Table 4-7 and Table 4-8.

Table 4-7: Colourimetry error tests on a flat surface

	SAV mask (6 mm) on a flat surface						MAV mask (11 mm) on a flat surface					
	SCI			SCE			SCI			SCE		
	L*	a*	b*	L*	a*	b*	L*	a*	b*	L*	a*	b*
1	95.12	1.49	-6.60	95.06	1.62	-7.11	94.88	1.38	-6.64	94.81	1.51	-7.18
2	95.08	1.52	-6.69	95.02	1.64	-7.20	95.13	1.40	-6.49	95.06	1.53	-7.03
3	95.02	1.46	-6.73	94.96	1.58	-7.25	95.09	1.39	-6.43	95.02	1.52	-6.97
4	95.08	1.49	-6.71	95.02	1.61	-7.22	94.93	1.39	-6.71	94.86	1.51	-7.25
5	95.07	1.48	-6.71	95.01	1.60	-7.22	94.91	1.39	-6.72	94.84	1.51	-7.25
6	94.96	1.48	-6.92	94.90	1.60	-7.44	94.85	1.37	-6.68	94.77	1.49	-7.21
7	94.88	1.44	-6.87	94.83	1.56	-7.38	94.98	1.37	-6.63	94.90	1.49	-7.16
8	94.96	1.48	-6.84	94.90	1.61	-7.35	94.88	1.38	-6.69	94.80	1.51	-7.23
9	94.94	1.48	-6.85	94.88	1.60	-7.36	94.99	1.42	-6.61	94.91	1.54	-7.14
10	94.89	1.44	-6.85	94.84	1.56	-7.36	94.93	1.40	-6.71	94.86	1.52	-7.25
Mean	95.00	1.48	-6.78	94.9	1.60	-7.29	94.96	1.39	-6.63	94.88	1.51	-7.17
St. Dev.	0.09	0.02	0.10	0.08	0.03	0.10	0.09	0.02	0.10	0.09	0.02	0.10

As the table shows, there is negligible difference between using the SAV mask and MAV mask on a flat surface. The standard deviation is the same for the SCI readings, and only slight differences with the SCE readings.

Table 4-8: Colourimetry error tests on a curved surface

	SAV mask (6 mm) on a curved surface						MAV mask (11 mm) on a curved surface					
	SCI			SCE			SCI			SCE		
	L*	a*	b*	L*	a*	b*	L*	a*	b*	L*	a*	b*
1	94.84	1.30	-6.45	94.73	1.41	-6.95	94.63	1.24	-6.24	94.54	1.35	-6.73
2	94.83	1.32	-6.47	94.76	1.42	-6.95	93.73	1.33	-6.35	93.67	1.44	-6.81
3	94.82	1.30	-6.40	94.75	1.40	-6.89	94.45	1.22	-6.19	94.39	1.33	-6.66
4	94.85	1.34	-6.42	94.80	1.45	-6.89	94.59	1.23	-6.19	94.51	1.34	-6.67
5	94.74	1.32	-6.18	94.67	1.42	-6.64	94.73	1.26	-6.18	94.65	1.37	-6.67
6	94.14	1.36	-6.45	94.04	1.46	-6.91	93.22	1.26	-6.15	93.10	1.36	-6.59
7	93.26	1.35	-6.26	93.18	1.45	-6.82	94.20	1.26	-5.99	94.11	1.36	-6.45
8	93.48	1.34	-6.18	93.26	1.44	-6.61	94.77	1.21	-6.06	94.37	1.31	-6.55
9	92.62	1.40	-6.07	92.38	1.50	-6.48	93.72	1.25	-6.05	93.59	1.35	-6.51
10	94.08	1.35	-6.22	93.95	1.45	-6.67	92.14	1.25	-5.94	91.99	1.34	-6.37
Mean	94.17	1.33	-6.31	94.05	1.44	-6.78	94.02	1.25	-6.13	93.89	1.36	-6.60
St. Dev.	0.80	0.03	0.14	0.85	0.03	0.17	0.84	0.03	0.12	0.84	0.03	0.13

The variation observed from the measurements taken from the curved surface versus the flat surface show an increase, especially on the L* coordinate, however deviation is still minimal.

Colourimetry readings were taken on the flattest part of the bone in order to reduce this error. As the error levels between the SAV mask and the MAV mask are negligible, the SAV mask was used in order to accommodate some of the smaller bone samples to be used, without the issue of background incorporation.

For the purpose of this research, the SCE readings were measured, as this excludes the reflectance from the sample, and therefore resembles the way the human eye perceives a colour, better than SCI.

4.2.2 Sample preparation and DNA extraction

In order to decide upon the best sample preparation and extraction method that would provide the highest yield of DNA, and also keep the contamination risk to a low level, research was conducted into the available commercial extraction kits.

The two kits that were chosen for comparative tests were Genial First-DNA all-tissue DNA-extraction kit due to the successful reported by Fredericks (2011) and PrepFiler® BTA Forensic DNA Extraction Kit (Applied Biosystems®) due to their proposed ability to extract DNA from degraded hard tissue in the presence of inhibitors, whilst using less tube transfers than comparable kits – reducing the risk of contamination.

Due to the limited availability of human bone, porcine bone was used to conduct the tests. Variables were changed and tested in order to ascertain the most optimal method for extraction from the archaeological bone. For all conditions tested, the surface of the bone had been removed in order to reduce any inhibitors associated with soil contact, or potential DNA contamination. The variables and samples tested are listed in Table 4-9.

Table 4-9: Preparation and extraction kit samples

Sample number	Extraction kit	Physical state	Demineralised?
1.	Prepfiler	Powder	No
2.	Prepfiler	Powder	Yes
3.	Prepfiler	Shavings	Yes
4.	Genial	Powder	Yes
5.	Genial	Shavings	Yes

Bone samples were sectioned with a Dremel hand tool and a diamond cutting wheel, which was decontaminated prior to, and after each sample, with 10% bleach.

Samples that were to be de-mineralised were then placed into 50 mL tubes, and submerged in EDTA. Tubes were placed onto a roller mixer with the EDTA which was changed daily for 5-7 days. When the bones had become pliable, they were rinsed repeatedly with distilled water and cut into slithers with disposable forceps and scalpels and placed 100 mg was placed into labelled sterile 2 mL Eppendorf tubes.

The remaining samples were milled using a Retsch mixer mill, running two minutes at a time, with a two minute break to ensure there was no detrimental effect from any heat generated. 100 mg powdered bone sample was weighed into labelled sterile 2 mL Eppendorf tubes for extraction.

Individual manufacturer's extraction protocols were followed for both the Prepfiler and the Genial kits. Once extracted these samples were stored at 4^{o}C overnight to be amplified the next day.

Amplification was performed using the PCR technique as detailed in section 4.3.8.2, and were separated and visualised by gel electrophoresis as stated in section 4.3.9. The results are shown in Figure 4-5.

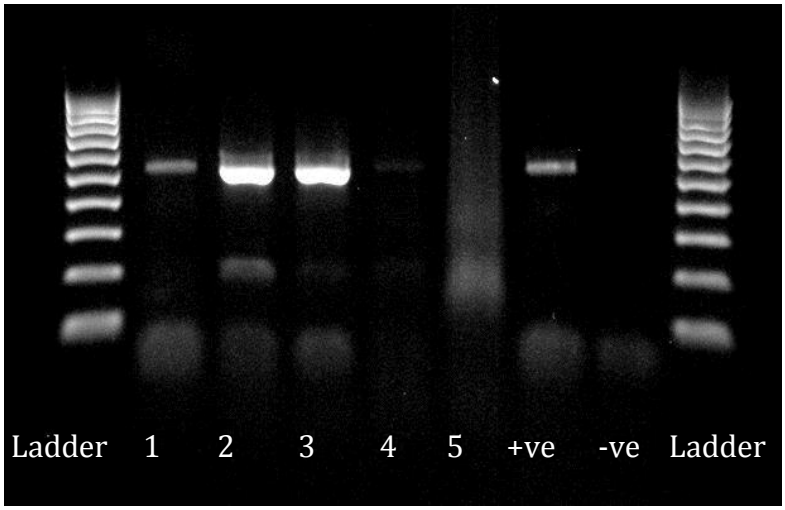

Figure 4-5: Extraction kit test results

The results of the extraction kits showed Prepfiler to be more effective compared to Genial for the skeletal material, and that demineralising the sample prior to extraction provided a higher yield of DNA. Lanes 2 and 3 showed a similar quantity of DNA, despite different preparation methods, resulting in the decision to use shavings of bone rather than powdered due to the lower contamination risk. Based on these findings, the chosen method for the extraction of the porcine samples is detailed in Table 4-10.

Tests were also run on ancient human archaeological samples, using the Fin Cop skeletal samples. Preparation for extraction was conducted using two different methods – demineralisation and non-demineralisation.

Due to the structural differences of ancient human archaeological bone compared to modern porcine bone, the results from demineralisation were significantly different. The ancient samples disintegrated in the EDTA resulting in difficulty in the changing of the EDTA, and increasing the risk of loss of material. Due to the fragile nature of the bones, milling was not necessary, as the bones could be powdered with a pestle and mortar. This not only reduced the risk of heat damage from the millers, but also limited the risk of contamination, as the equipment could be thoroughly decontaminated and dried between each sample.

All extractions were analysed on the ABI 310 genetic analyser to provide a comparison of how techniques affect the ability to amplify alleles.

Of the 20 samples analysed, five returned no amplified alleles, all of which were demineralised prior to extractions. The sister samples of the same skeletal elements that had not undergone demineralisation prior to extraction, all returned amplified alleles.

By comparing the number of amplified alleles across the number of different loci, a comparison can be made of the successful amplifications from different elements, and different preparation techniques.

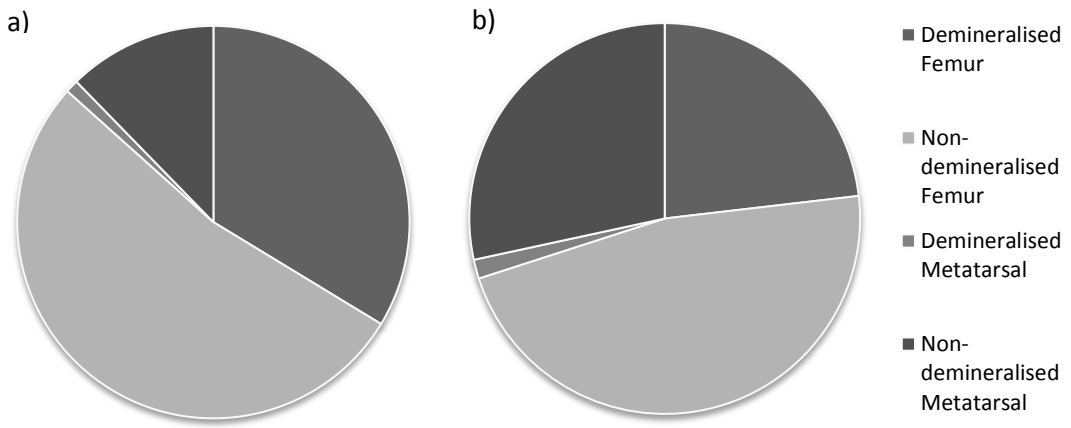

Figure 4-6: Comparison of a) number of amplified alleles, and b) number of loci from different sample preparation on metatarsals and femora, expressed as a percentage.

As Figure 4-6 illustrates, the femur samples that did not undergo demineralisation prior to extraction, showed the highest percentage of successful amplified alleles, across the highest number of loci, whilst the demineralised metatarsal samples showed the least success of amplification. Based on these findings, the Eriswell samples were not demineralised prior to extraction, and the methods chosen for preparation and DNA extraction from the human bone samples is detailed in Table 4-10.

Table 4-10: Methods for sample extraction for porcine and human archaeological samples

Stage	Porcine samples	Human samples
Treatment:	Demineralised into EDTA for 5-7 days	No prior demineralisation
Preparation:	Sliced into shavings prior to extraction	Powdered with a pestle and mortar
Extraction kit:	PrepFiler® BTA Forensic DNA Extraction Kit	PrepFiler® BTA Forensic DNA Extraction Kit

4.2.3 PCR optimisation

Validation of the porcine PCR protocol was required prior to any sample testing. By running a series of dilutions of known concentration DNA, altering the number of cycles, and changing the annealing temperature, it was possible to identify a protocol which provided the strongest amplified DNA sample.

By adjusting variables one at a time, it was possible to determine the ideal PCR thermal parameters and the number of cycles for the chosen primers, which enabled good quality bands for all three primers, as seen in Figure 4-7. The protocol is detailed in 4.3.8.

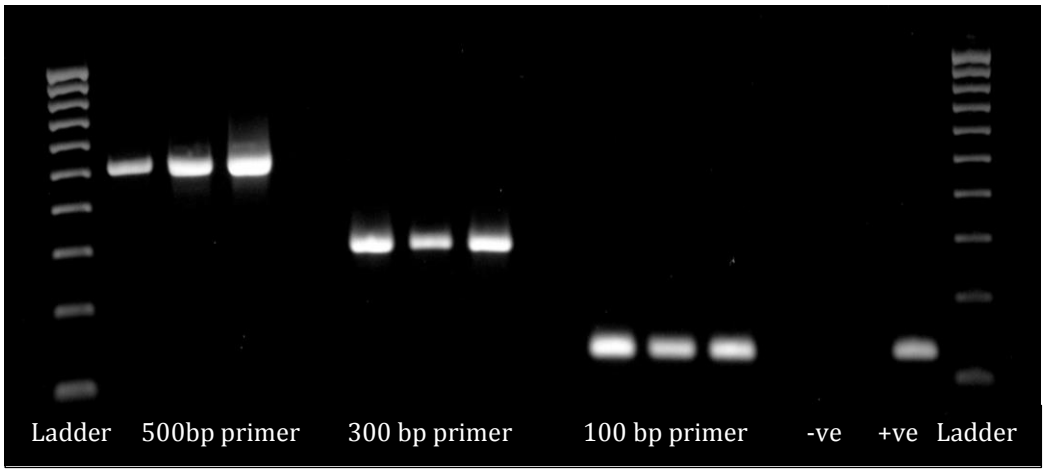

Figure 4-7: Optimisation of 500, 300 and 100 base pair primers

By performing serial dilutions of known quantity calf thymus DNA, it was possible to achieve amplification of control samples down to 1 ng/µl, as shown in Figure 4-8.

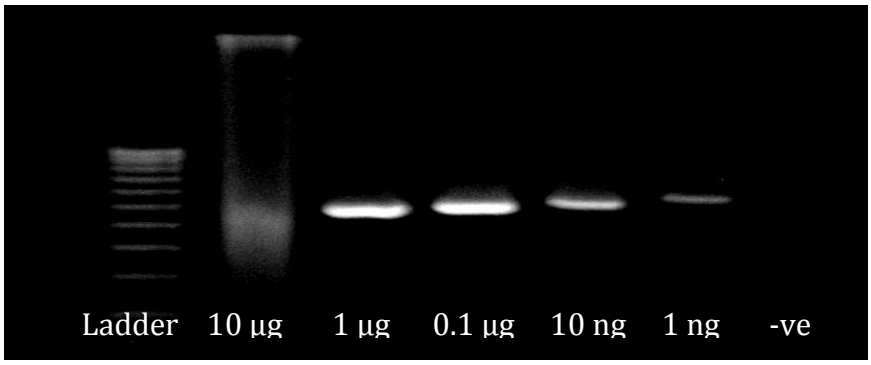

Figure 4-8: Optimisation of PCR sensitivity

Due to the costly nature of the PCR components chosen for the analysis of the human archaeological samples as discussed in section 4.3.8.1, tests were conducted to ascertain whether reduced volumes could be used for the research in order to analyse a higher number of samples for the same cost.

Serial dilutions were prepared using 2800M Control DNA (Promega), and reactions were set up as directed in the manufacturers protocol, in addition, half volume reactions were prepared from the same serial dilution stocks. Results verified using half volume reactions would be as effective, if not more so, than the standard volume - as shown in Figure 4-9.

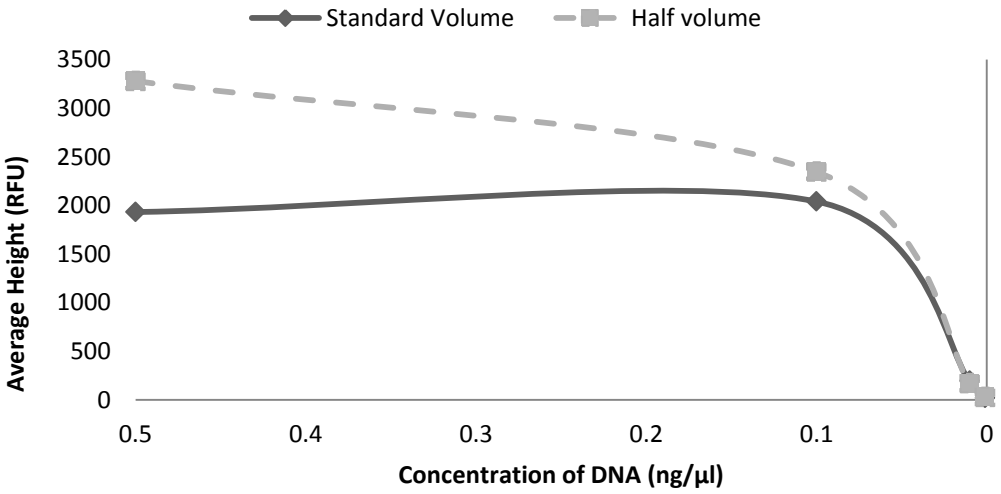

Figure 4-9: Comparison of average RFU from serial dilutions using standard volume reactions and half volume reactions

4.2.4 Fragment analysis optimisation

The analysis parameters used with the Applied Biosystems ABI Prism 310 were validated by the adjustment of injection time, injection volume, polymer type and software and compared to peak height and correct calling of known alleles of known DNA as shown in Figure 4-10. The optimised settings decided upon and used are discussed in section 4.3.10.

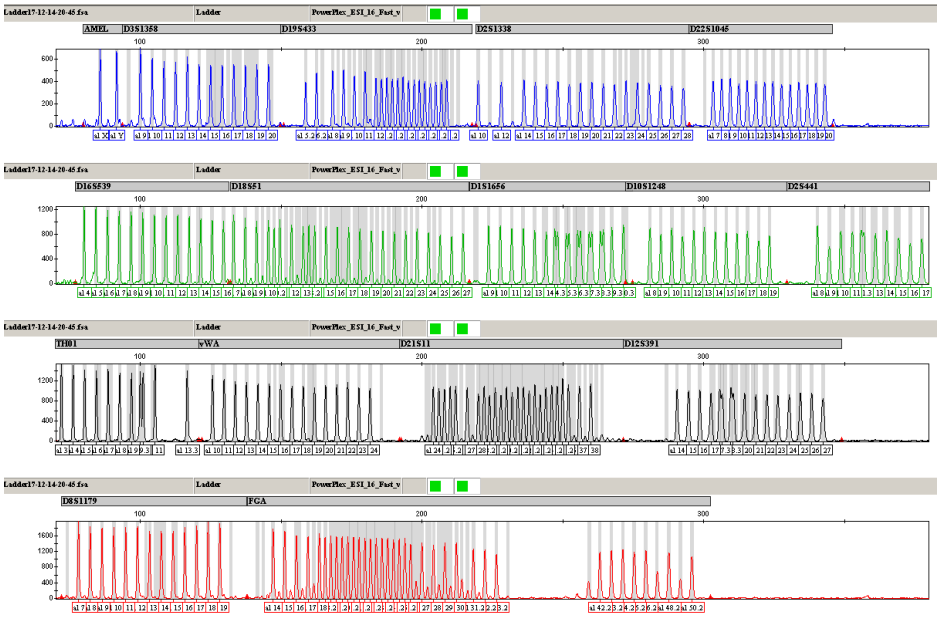

Figure 4-10: The ladder sample showing correct calling of all alleles

Tests using 2800M control DNA (Promega) were performed to establish the rate of allelic drop-out across various loci at different concentrations of DNA, and to verify whether Peak Height Ratio (PHR) calculations could be used to determine the relationship of peaks and probability of heterozygosity for the ancient DNA samples.

Table 4-11: Peak Height Ratio results from serial dilutions of control DNA, with drop-out occurrence, expressed as a percentage

Marker	0.5ng/µl	0.1 ng/µl	0.01 ng/µl	0.001 ng/µl
Amelogenin	82.00	90.67	21.25*	Drop-out
D3S1358	86.01	99.36	53.75*	No alleles
D19S433	82.24	99.21	58.18*	91.67
D2S1338	88.09	92.28	58.51*	75.00
D16S539	86.51	87.56	99.38	20.00*
D18S51	94.04	91.53	49.88*	No alleles
D1S1656	92.80	96.45	92.77	90.41
D10S1248	85.52	89.92	65.25	No alleles
D2S441	98.02	94.75	97.98	No alleles
TH01	66.28	88.64	91.24	66.67
vWA	99.08	77.61	75.21	Drop-out
D21S11	96.38	61.57	91.86	No alleles
D12S391	83.61	98.03	32.89*	Drop-out
D8S1179	99.94	79.57	72.10	No alleles
FGA	95.63	94.67	52.29*	93.63
Average	89.08	89.45	67.50	72.90

*Value below the threshold of PHR for heterozygous peaks

Results in Table 4-11 illustrate that when analysing DNA of a concentration of 0.1ng/µl to 0.5ng/µl the PHR calculations indicate a high probability of heterozygosity, and therefore the peaks are of similar height as no preferential amplification is taking place.

The tests using 0.01ng/µl DNA showed peak imbalance due to preferential amplification at the seven of the 16 markers: Amelogenin, D3S1358, D19S433, D2S1338, D18S51, D12S391, and FGA, resulting in a probability of less than 60% and therefore below the threshold used to estimate the heterozygosity of peaks.

Analysis of the 0.001 ng/µl sample showed allelic drop-out occurring at three markers: Amelogenin, vWA, and D12S391, where only one allelic peak was present at the loci. No allelic peaks were seen at six of the 16 markers: D3S1358, D18S51, D10S1248, D2S441, D21S11 and D8S1179.

These tests illustrate that if the DNA samples from the human archaeological collection are below 0.1ng/µl, preferential amplification will occur, making PHR calculations and the determination of heterozygous peaks difficult. Analysis of

samples ~ 0.001 ng/µl, will likely display allelic drop-out, and absence of peaks at several markers.

Surprisingly, it appears that the base pair size of the target DNA fragment does not have an effect on the allelic drop-out, as this phenomenon occurs at the smallest marker - amelogenin (80-100 bp) from a concentration of 0.01 ng/µl, whereas at the largest loci - D2S441 (325-375bp), no evidence of drop-out occurs until a concentration of 0.001 ng/µl.

The PHR threshold is illustrated in Figure 4-11, and shows how heterozygote peaks would be incorrectly eliminated due to preferential amplification and allelic drop-out, as the concentration of the DNA in the sample decreases.

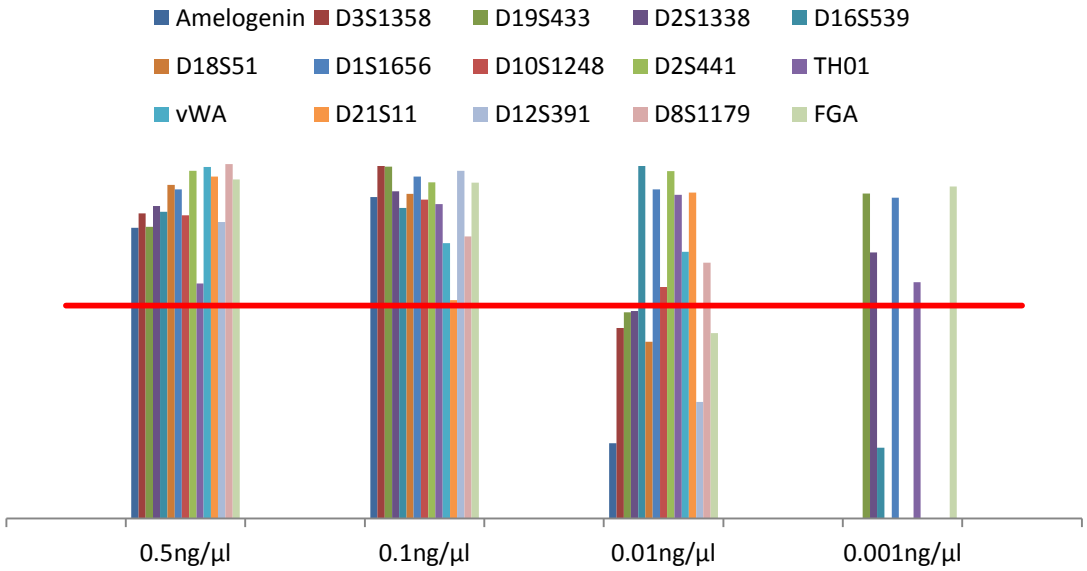

Figure 4-11: Illustration of PHR values across the loci, where allelic drop-out and peak absence is represented by zero, and the PHR threshold of 60% is represented by a red line.

This possible inability of utilising the PHR calculations for means of identifying heterozygote peaks could cause issues in interpreting of data when more than one contributor is suspected. Other methods of data interpretation would need to be used.

4.3 Selected methodologies

This section details the methodologies used as a result of the previous literature review and the optimisation tests that were conducted. The methods were chosen based on available equipment that would provide an analysis of multiple aspects of bone diagenesis, non-destructive methods were chosen where possible to enable multiple analyses to be made with a small sample, and techniques that were time effective and cost-effective were used in an attempt to make analysis available to a wider community. Figure 4-12 shows a flowchart of the methodology used.

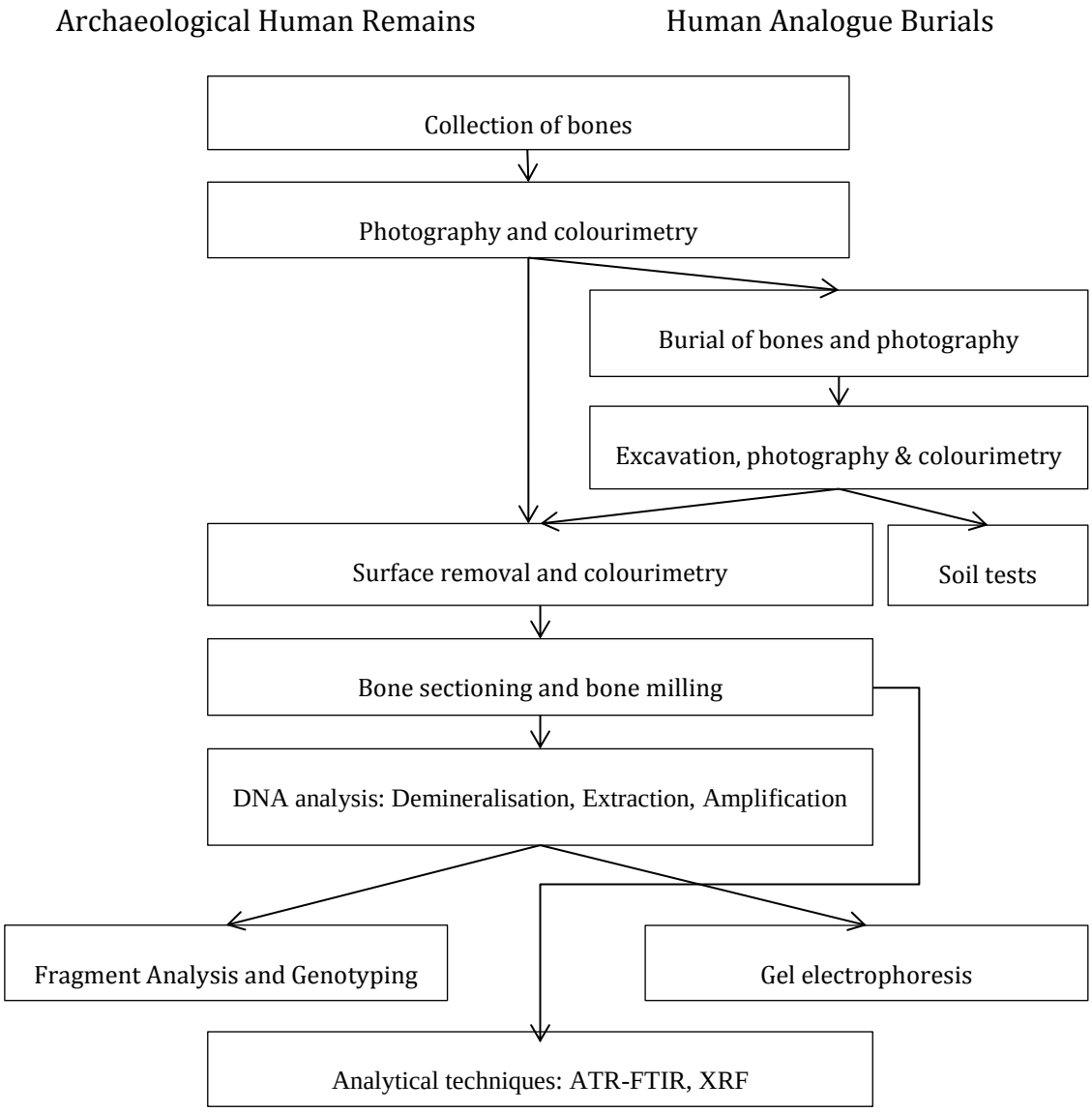

Figure 4-12: Flowchart of methods

4.3.1 Contamination precautions

In order to minimise the risk of DNA contamination, as discussed in section 4.1.3, the following precautions were taken.

4.3.1.1 Laboratory personnel and personal protective equipment (PPE)

Access to the DNA laboratory was strictly limited to a small number of authorised personnel; all of whom had reference samples taken in order to be able to eliminate individuals in the case of sample contamination.

In order to limit the potential contaminations of exogenous DNA onto the samples, full PPE was worn at all time when handling or working on either the porcine or archaeological human bones; face mask, clean laboratory coats, and double gloves. To eliminate the transfer of DNA between samples, gloves were changed between each sample.

Due to the nature of the skeletal material, and the lack of PPE worn during excavation and handling, it is possible that contamination from exogenous DNA has already occurred, and therefore removal techniques will need to be applied.

4.3.1.2 Laboratory protocols

All laboratory protocols for extraction, amplification, gel electrophoresis analysis and fragment analysis included positive controls and negative controls to detect any evidence of contamination that may have occurred during the procedures.

4.3.1.3 Laboratory layout and equipment

Work was carried out in dedicated clean rooms or laboratories that had been cleaned and decontaminated prior to, and after all work had been completed.

The laboratory made use of the two existing rooms to separate the processes into pre-amplification (clean) and post-amplification (dirty) rooms and a one-way system was adhered to, in terms of samples and personnel. Pre-amplification work was conducted in the clean room in the morning, and post-amplification work was conducted in the afternoon in the dirty room with no re-entry into the pre-amplification laboratory on the same day or in the same clothing.

Laboratory equipment was designated to particular processes and only used for either pre-amplification or post-amplification work. Equipment was cleaned and decontaminated with 10% bleach and 70% ethanol prior to and after every use.

4.3.2 Archaeological human remains

Excavated archaeological human remains were collected from two archaeological sites from distinctly different geological environments in order to investigate if burial variables influence the colour, composition and the state of DNA contained within.

4.3.2.1 Sample selection

With the previous research taken into consideration, the elements chosen to be investigated in this study were metatarsals and femora. Metatarsals were chosen due to the small compact nature of the element, meaning they are less likely to have been crushed or damaged in the burial environment and subsequent excavation. Femurs were chosen because of their robusticity and composition, and a higher percentage of compact bone than other elements.

4.3.2.2 Sample collection

The human remains from Eriswell and Fin Cop had been excavated prior to knowledge of this study; therefore no influence could be made over the procedure for excavation of the remains, the use of PPE, or the facilities in which the human archaeological bones have been stored. Some of this handling was documented (i.e. anthropological work), but general handling, by whom, movement and storage was undocumented. All these factors may have had a detrimental effect on the level of preservation, the state of DNA contained within the bone, and levels of exogenous DNA contamination, therefore must be taken into account when discussing any results.

Fin Cop

The skeletons from Fin Cop were stored at the premises of the Archaeological Research Services Ltd in Bakewell, Derbyshire, and were chosen on the basis of available material. Two of the available skeletons were neo-natal and as such

sampling would have consumed the whole skeleton, therefore only six skeletons were selected for sampling. The samples were bagged, labelled and placed in a protective box for transportation back to the DNA laboratory for sampling and analysis.

Table 4-12 details an inventory of the skeletons sampled for investigation presenting information on condition, age at death, sex estimation and a preservation score as analysed and provided by the standard anthropological assessment (exact method used unknown) prior to collection (Waddington et al., 2011). Skeleton 6 was originally collected in two separate parts, before being assigned as one.

Table 4-12: Inventory of sampled skeletons from Fin Cop

Skeleton number	Burial Environment	Condition	Overall preservation score*	Sex estimation	Age estimation	Elements sampled	Preservation of element
Skeleton 1	Lime-rich sediment and limestone boulders over limestone geology	Articulated, fragmented, 65% recovered	3	Probable female	Young adult 25-35 years	Femur Metatarsal	3 2
Skeleton 3		Articulated, very fragmented, almost entire skeleton recovered	3	Probable female	Young adult 20-30 years	Femur Metatarsal	3 3
Skeleton 5		Disarticulated, only small percentage recovered	4	Indeterminate due to lack of elements	Young adult 20 – 30 years	Femur Metatarsal	5 3
Skeleton 6 (1 & 2)		Commingled skeletons, fragile and fractured	3.5	Not possible due to young age	~ 40 weeks pre-natal - neonate	Femur	4
Skeleton 7		Disarticulated and commingled with skeleton 5 & 6	3	Indeterminate due to young age	1 year 4 months – 2 years 8 months	Femur	3
Skeleton 8		Articulated	3	More likely male (many indicators indeterminate)	15-16 years	Femur Metatarsal	3 3

* Where grade 0 bone has a clear visible morphology with no modifications, and 5+ shows heavy modifications and erosion.

Eriswell / Lakenheath

The human skeletons available for sampling at Lakenheath totalled 425 rendering a whole site analysis impossible due to time and resources. Selection of the material was prioritised on the basis of results from other analytical techniques, such as C14 dating, carbon and nitrogen isotope analysis, or those identified by excavation as being of special interest from an archaeological or bio-archaeological context (double burials, wealthy burials, or those displaying non-metric traits).

From this priority list 60 skeletons were selected for investigation, from across the entire site including all 3 cemeteries, (as introduced in Figure 3-2) ensuring samples from different burial environments. This number was chosen to provide a diverse sample range whilst adhering to time and cost restrictions. Where possible, both femora and metatarsals were sampled from the same skeleton. The exception being skeleton 4222 whose remains were largely unobtainable due to its presence in a museum display in Suffolk, therefore available samples were limited to a femur fragment and a sternum fragment. In order to follow protocol, the sternum fragment was sampled to enable two samples to be analysed per skeleton. This resulted in the collection of 57 femur samples, 47 metatarsal samples and one sternum fragment. The collected bones were bagged, labelled and stored in a protective box for transportation to the DNA laboratory for sampling and analysis.

Due to the expense of DNA analysis, genetic investigation concentrated on cemetery 104, since this was the location of the skeleton 4222 whose wealthy grave contained a sword and horse skeleton, and appeared to be of high status and a centre-piece in the cemeteries. From cemetery 104, 35 skeletons were analysed for DNA, testing both femora and metatarsals where possible, totalling 63 elements. Table 4-13 provides an inventory of the skeletons from Eriswell cemeteries that were selected for investigation along with information regarding the reason for sampling (from the skeletal collection guardians), preservation condition, and other anthropological data such as estimated sex and age at death (Caruth and Anderson, 2005). Methods used for estimations are unknown. Unless otherwise stated all burials were single inhumations.

Table 4-13: Inventory of sampled Eriswell skeletons

Skeleton	Cemetery	Burial environment	Overall condition*	Elements sampled	Criteria for sampling	Age	Sex	DNA analysis
0067	104	Sand & chalk	4	Femur & metatarsal	Isotopes, C14 dating	c.20-23	Female	Yes
0145	46	Sand & Chalk	4	Femur & metatarsal	Child with brooch	c. 8-9	Child	
0158	46	Sand & Chalk	4	Femur & metatarsal	Non-metric traits	Y-MA	Female	
0201	46	Sand & Chalk	5	Femur & metatarsal	Isotopes	MA-Old	Male	
0203	46	Sand & Chalk	7	Femur & metatarsal	Isotopes	Y-MA	Female	
0235	104	Chalk	5	Femur & metatarsal	Isotopes, wealthy burial	MA-Old	Male	Yes
0241	46	Sand & Chalk	7	Femur	Isotopes	MA	Male	
0251	46	Sand & Chalk	5	Femur & metatarsal	Non-metric traits	Y-MA	Female	
0255	46	Sand & Chalk	6	Femur & metatarsal	Isotopes, C14 dating	c.18-20	Male	
0259	46	Chalk	3	Femur & metatarsal	Double burial	MA-Old	Female	
0309	46	Chalk	5	Femur & metatarsal	Isotopes, C14 dating	MA?	Female	
0310	46	Sand & Chalk	6	Femur	Isotopes	MA	Female	
0317	46	Sand & Chalk	5	Femur & metatarsal	Non-metric traits	MA	Male	
0318	114	Sand & Chalk	5	Femur & metatarsal	Isotopes, non-metric traits	Y-MA	Male	
0326	104	Chalk	7	Femur & metatarsal	C14 dating	Y-MA	Male?	Yes
0343	46	Chalk	5	Femur & metatarsal	Wealthy burial	c.15-16	Child	
0346	46	Chalk	5	Femur & metatarsal	C14 dating	MA-Old	Male	
0363	114	Sand & Chalk	4	Femur & metatarsal	Isotopes, related to others?	Y-MA	Male	
0392	114	Sand & Chalk	5	Femur & metatarsal	Isotopes, C14 dating	Y-MA	Male	
0395	46	Sand & Chalk	3	Femur & metatarsal	Isotopes, non-metric traits	Y-MA	Female	
0425	104	Unknown	3	Femur & metatarsal	Double burial	c.11-13	Child	Yes
0426	104	Unknown	5	Femur & metatarsal		c.15	Child	Yes

Skeleton	Cemetery	Burial environment	Overall condition*	Elements sampled	Criteria for sampling	Age	Sex	DNA analysis
0474	114	Sand & Chalk	2	Femur	Related to others?	Y-MA	Male	
0477	104	Chalk	4	Femur & metatarsal	Non-metric traits	c.12	Child	Yes
0554	104	Sand & Chalk	3	Femur	C14 dating	Young	Male	
0570	104	Chalk	6	Femur & Metatarsal	Isotopes, C14 dating	MA-Old	Female	Yes
0571	114	Sand & Chalk	3	Metatarsal	Related to others?	c.8	Child	
0580	114	Sand & Chalk	6	Femur & metatarsal	Isotopes	c.20-23	Female	
0612	104	Chalk	6	Femur & metatarsal	Isotopes, non-metric traits	Young	Female	Yes
0692	104	Chalk	3	Femur & metatarsal	C14 dating, wealthy burial near skeleton 4222	MA	Female	Yes
0717	104	Chalk	4	Femur & metatarsal	Non-metric traits	c.15	Male?	Yes
0759	104	Chalk	6	Femur & metatarsal	Isotopes, C14 dating	Old	Male	Yes
0791	104	Chalk	4	Femur & metatarsal	Isotopes, C14 dating, non-metric traits	Old	Female	Yes
0799	104	Chalk	4	Femur & metatarsal	Isotopes	MA?	Female	Yes
0808	104	Sand & Chalk	3	Femur & metatarsal	Isotopes, non-metric traits	MA	Female	Yes
0809	104	Chalk	5	Femur & metatarsal	Non-metric traits	Young	Male	Yes
0851	114	Sand & Chalk	4	Femur & metatarsal	Isotopes, C14 dating,	Y-MA	Female	
0888	104	Chalk	3	Femur	Wealthy burial	Old	Female	
0907	114	Sand & Chalk	4	Femur	Isotopes, C14 dating	MA	Female	
0991	104	Sand & Chalk	6	Femur & metatarsal	Non-metric traits	Y-MA	Female?	Yes
0994	104	Chalk	4	Femur & metatarsal	Effect of coffin	MA	Male	Yes
4040	104	Chalk	3	Femur & metatarsal	Related to others?	Young	Female	Yes
4046	104	Chalk	2	Femur & metatarsal	Non-metric traits	Y-MA	Male	Yes
4067	104	Chalk	6	Femur & metatarsal	Isotopes	MA?	Male	Yes

Skeleton	Cemetery	Burial environment	Overall condition*	Elements sampled	Criteria for sampling	Age	Sex	DNA analysis
4095	104	Chalk	4	Femur	Multiple burial, Isotopes, C14 dating, Related to others?	c.4-5	Child	Yes
4098	104	Chalk	4	Femur		MA+	Female?	Yes
4099	104	Chalk	6	Femur & metatarsal	Isotopes, non-metric traits	MA	Male	Yes
4191	104	Sand & Chalk	3	Femur	Related to others?	MA-old	Male	Yes
4127	104	Sand & Chalk	1	Metatarsal	Non-metric traits	Y-MA	Male	
4222	104	Chalk	7	Femur & sternum	Isotopes, wealthy burial, sword & horse	Young	Male	Yes
4226	104	Chalk	4	Femur & metatarsal	C14 dating, non-metric traits	c.20	Male?	Yes
4288	104	Unknown	4	Femur & metatarsal	Good bone	c.20-23	Male?	Yes
4291	104	Chalk	4	Femur	Isotopes, related to others?	Old	Male	Yes
4295	104	Sand & Chalk	2	Femur	Related to others?	Y-MA	Male	Yes
4340	104	Chalk	4	Femur & metatarsal	Non-metric traits	16-18	Male?	Yes
4411	104	Chalk	6	Femur	Non-metric traits	c.8	Child	Yes
4462	104	Sand	2	Femur & metatarsal	Related to others?	Y-MA	Male	Yes
4473	104	Chalk	2	Femur	Non-metric traits	MA	Male	Yes
4503	104	Chalk	3	Femur & metatarsal	Related to others?	Adult	Male	Yes
4561	104	Chalk	4	Femur & metatarsal	Isotopes, non-metric traits	Young	Male	Yes

* Where grade 0 bone has a clear visible morphology with no modifications, and 5+ shows heavy modifications and erosion

Key for age estimation: Y = young

MA = middle aged

4.3.2.3 Sample preparation

Bones were cleaned by removing the dried dirt with clean soft brushes. Water was not used for cleaning the bones as this can lead to further degradation of the structure of the bone, and can also provide a medium for contamination to travel inside the bone as discussed in section 4.1.4. No record had been kept as to how bones may have been previously cleaned.

A Dremel hand-tool with a sterilised diamond cutting blade was used to section a 'window-cut' from the shaft of all the bones, avoiding any areas of apparent pathologies, landmarks or post-mortem damage. Areas of staining or possible contact with any metal grave goods were also avoided. Where the mid-shaft was missing, another area of the shaft was sampled. The blade and Dremel were decontaminated with bleach between each sample to ensure no carry-over of material from bone to bone and gloves were changed. The cutting was conducted within a custom-made Perspex box to contain bone dust and provide protection from the environment. Bone samples were stored in individual sealable labelled plastic bags prior to colourimetry analysis described in section 4.3.4.

Figure 4-13: Example of Eriswell right femur pre- and post-sectioning

After colourimetry analysis had been conducted, 1-2mm of the surface of the bone was stripped using a sandpaper attachment on the Dremel hand-tool, in order to remove contamination caused by soil interaction and potential exogenous from prior handling from individuals. Colourimetry of the exposed cortex of the bone was then conducted in order to estimate the penetration of colour and potential contaminates through the bone.

The surface-exposed bone was then sectioned for different analytical techniques. A section was returned to the individual labelled plastic bags to await DNA analyses, and a section was milled using a Retsch M2000 ball mill and sieved through a 106 μm stainless steel mesh. The homogenous powders were stored in individual labelled sterilised glass jars with airtight plastic lids at room temperature, until required for downstream analysis such as FT-IR.

4.3.3 Human analogue burials

The human analogue samples used for the study were *Sus scrofa* or *Sus scrofa domesticus* (domestic pigs) due to the comparable bone composition to that of humans as discussed in section 2.4, and easy availability due to presence in the food chain which also negates the concern over disease when handling the samples. In total, 60 porcine femurs were used for the research.

4.3.3.1 Sample collection

The porcine samples were obtained from the local butcher, to ensure kill dates could be determined and that no processing or cooking of the bones had occurred. All bones were stored in the fridge in labelled bags, processed within 3-5 days of the kill date, and pigs were aged between 8 and 12 months at time of death.

4.3.3.2 Sample preparation

If an excessive amount of soft tissue was still found to be covering the bone shaft surface, this was removed with a scalpel to ensure exposure of the bone to the burial medium. Soft tissue was left in place at the bone diaphysis, and this is the tissue referred to later when observations of decomposition are noted. Soft tissue was also removed from the control bones so that the bone could be examined with no other variables.

4.3.3.3 Burial conditions

Different burial conditions are known to have varying effects on the rate of decomposition of soft tissues, as discussed in Chapter 3, but there is limited research available regarding these effects on the different components of the bone and the subsequent effect on the endogenous DNA. This study will concentrate on

the effects of differing pH in soils, soil type and the duration of burial on the composition and colour of the bone, and quality and quantity of the DNA retrieved from the buried porcine bones. All burial mediums were purchased from gardening stores.

Dependent variables

The elements of the study which remained constant for all trials:

- The location of the trials: a dark room with no access to sunlight or exposure to heat sources, close to the DNA laboratory with restricted access
- The ratio of soil to bone: all bones were placed surrounded by the burial medium of the same volume to ensure no other factors such as air
- The containers: 4 litre plastic containers with airtight plastic lids and sealed with parafilm, all wrapped in black plastic – all brand new and cleaned prior to the study to ensure no added bacteria / moisture.

Independent variables

Elements of the study independent to each trial:

- Soil type: clay, compost, hydrated lime or sand.
- pH: varied depending on soil type
- Moisture content: varied depending on soil type
- Organic content: varied depending on soil type
- Duration of burial: 1.5 months, 3 months, 6 months, 12 months, 18 months.

Control samples

The control samples consisted of samples stored in the same conditions but without the burial medium, and were analysed in parallel with identical time durations to the tested variable samples.

List of burials

Pig bones were buried in duplicate for each burial medium / duration period in order to duplicate data recovered. The categories of burials and sample names are listed below in Table 4-14.

Table 4-14: Porcine burial sample categories and sample names

Burial duration	Controls	Clay	Compost	Lime	Sand
0 months	C0m	0mCl	0mCo	0mLi	0mSa
1.5 months	C1.5m	1.5mCl	1.5mCo	1.5mLi	1.5mSa
3 months	C3m	3mCla	3mCo	3mLi	3mSa
6 months	C6m	6mCl	6mCo	6mLi	6mSa
12 months	C12m	12mCl	12mCo	12mLi	12mSa
18 months	C18m	18mCl	18mCo	18mLi	18mSa

4.3.3.4 Burial methodology

Porcine bones were photographed and bone surface colour recorded prior to burial, as discussed in section 4.3.4. To house the bones within distinct burial environments, individual four-litre plastic containers were half-filled with the appropriate burial medium, the bone was placed on top, and the container filled with the same medium, ensuring no air voids at the top. The containers were sealed with an airtight plastic lid, sealed with parafilm, labelled with sample name, burial and excavation date and wrapped in black plastic before being stored in a dark room.

Figure 4-14: Photographs depicting porcine burial methodology of the porcine bones, in plastic boxes filled with the chosen medium, sealed with parafilm and labelled with burial/excavation date and burial medium

4.3.3.5 Excavation recording methodology

At the end of the specified time period, chosen in order to provide a snapshot of the processes over the available time frame, the samples were removed from the dark room and unwrapped from the black plastic. Prior to removing the lid and during the excavation process, visual observations of presence of water, condensation and mould were made and recorded, along with observations of any odours present.

The burial medium was removed using standard archaeological excavation techniques, removing layers with a trowel and recording any observations, such as presence and appearance of mould, condensation, olfactic observations of odour and general appearance. Once the bone was uncovered, in-situ photography was conducted, and the bone was carefully removed, prior to photography and soil sample collection from directly under the bone.

Soil samples were stored in labelled 50mL plastic screw-top tubes prior to undergoing soil testing, as discussed in section 4.3.3.6. Bones were cleaned with sterile clean brushes, moistened with deionised water, and placed into individual labelled plastic sealable bags and stored at 4^{o}C prior to analysis described in the following sections.

4.3.3.6 Soil analysis

Soil analysis was conducted on the control soil samples of clay, compost, lime and sand prior to any experimental work in order to provide reference values to calculate any change due to the burials. The experimental soil samples were tested in the same way, after each burial.

Three different tests were performed on each sample - water content determination, organic content determination and pH. All mass readings were recorded in grams and measured to 2 decimal places.

Water content determination

The protocol for the water determination test followed the standard reference ASTM D 2216 – Standard test method for laboratory determination of water (moisture) content of soil, rock, and soil-aggregate mixtures (Tan, 2005).

Clean, dry, labelled crucibles were weighed prior to the addition of 1-3g of either clay, compost, lime and sand, and weighed again. The crucibles were then placed into a wire holding rack and placed into a pre-heated furnace at 105^{o}C, and left for 24 hours. After this time, the crucibles were re-weighed immediately, and the mass recorded.

Figure 4-15: Crucibles containing control soils after 24 hours at 105^{o}C

Using the different measurements and the following equations - (4-3)(4-4)(4-5), the water content can then be determined as a ratio percentage to that of the soil solids.

To determine the mass of soil solids:

$$M_S = M_{CDS} - M_C \qquad \textbf{(4-3)}$$

where M_S is the mass of soil solids, M_{CDS} is the mass of the crucible containing dry soil and M_C is the mass of the dry crucible

To determine the mass of pore water:

$$M_W = M_{CWS} - M_{CDS} \quad \textbf{(4-4)}$$

where M_W is the mass of pore water, and M_{CWS} is the mass of the crucible containing wet soil

To determine the water content:

$$W = \frac{M_W}{M_S} \times 100 \quad \textbf{(4-5)}$$

where W is water content in percentage

Organic matter determination

The protocol for the organic matter determination test followed the standard reference ASTM D 2974 – Standard Test Methods for Moisture, Ash, and Organic Matter of Peat and Organic Soils.

Clean, dry, labelled crucibles were weighed prior to the addition of a dried soil sample, and weighed again. The crucibles were then placed into a wire holding rack and placed into a furnace with a gradual increase of temperature to 440°C, and left for 24 hours. After this time, the crucibles were cooled prior to being re-weighed.

Figure 4-16: Crucibles containing control 'ashed' soils after 24 hours at 440°C

Using the different measurements and the following equations - (4-6)(4-7)(4-8) and (4-9), the organic matter can then be determined as a ratio percentage to that of the dry soil solids.

To determine the mass of the dry soil:

$$M_D = M_{CDS} - M_C \quad \textbf{(4-6)}$$

where M_D is the mass of dried soil

To determine the mass of the ashed soil:

$$M_A = M_{CA} - M_C \quad \textbf{(4-7)}$$

where M_A is the mass of ashed soil, and M_{CA} is the mass of the crucible containing ashed soil

To determine the mass of the organic matter:

$$M_O = M_D - M_A \quad \textbf{(4-8)}$$

where M_O is the mass of the organic matter

To determine the organic matter content (%):

$$OM = \frac{M_O}{M_D} \times 100 \quad \textbf{(4-9)}$$

where OM is organic matter in %

pH determination

The pH of the soil samples was determined using a standard soil:water suspension test and a pH meter and pH electrode. The pH meter was calibrated, using ph4, pH7 and pH10 buffers - depending on the soil type being tested.

Solutions of the soils were prepared in 50 mL plastic tubes in a suspension of 1:5 soil:ionised water, and placed on a roller mixer for one hour. After this time, the electrode was submerged into the solution, and once equilibrium was reached, the value was recorded. The electrode was thoroughly rinsed between each sample.

4.3.3.7 Bone sectioning

Following excavation and cleaning of bones, a Dremel hand-tool with diamond cutting blades were used to section the bones. As mentioned earlier in section

4.3.2.3 a custom-made Perspex box was used to contain the bone dust and protect the bones from the environment. The Dremel blade and Perspex box was decontaminated between each sample with bleach to ensure no-carry-over of material from sample to sample.

Visual examination and recording of the bone marrow colour and consistency was conducted as a means of comparative data between bone samples. Bones were sectioned in preparation for various analytical investigations – a section for colourimetric analysis (section 4.3.4) and demineralisation (section 4.3.7.1) and downstream DNA analysis (section 4.3.7) and a section to powder for ATR-FTIR analysis (section 4.3.5).

4.3.4 Colourimetric analysis

The colourimetric analysis was conducted with a Konica Minolta Spectrophotometer CM-700d/600d using the following parameters detailed in Table 4-15.

Table 4-15: Display conditions for colourimetric analysis

Target Mask:	SAV	**Illuminant 2:**	None
Colour space:	L*a*b*	**Mode:**	SCI and SCE
Equation:	dE00	**Wait time:**	0.0
Colour index:	YI (E313-73)	**Auto average:**	10
Observer:	10^{o}	**Manual average:**	1
Illuminant 1:	D5		

In order to minimise error and deviation in colour determination, a total of 30 measurements were taken on the flattest part of the bone, enabling the calculation of a mean average and standard deviation of the data.

4.3.5 Fourier-Transform Infra-Red Spectroscopy (FT-IR)

A Bruker Alpha Fourier Transform Infrared (FTIR) spectrophotometer coupled with a platinum diamond ATR module was used to analyse the bone samples to

investigate the mineral and organic components. Data was analysed with OPUS software, version 7.2.

A small sample of powdered bone was placed onto the diamond, pressure was then applied by the anvil to allow good contact between the diamond and the bone sample. A scan resolution of 2 cm^{-1} was used for each run within the range of 400-2000cm^{-1}, performing 16 scans on each sample.

Three peak ratios were chosen in order to estimate: the splitting factor (crystallinity), collagen content and carbonate content of the bone, as illustrated in Figure 4-17.

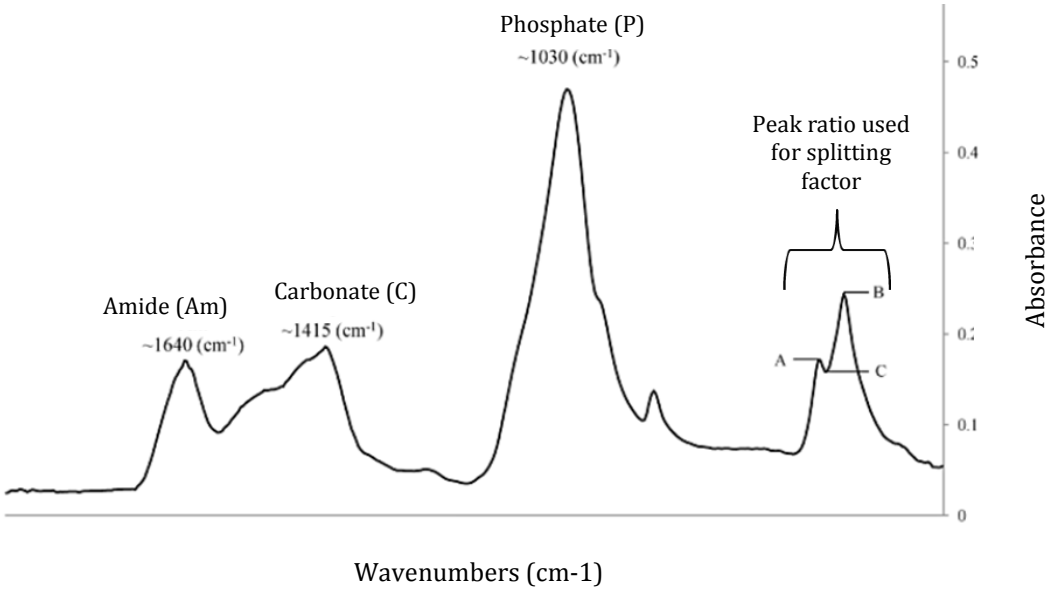

Figure 4-17: ATR-FTIR spectra identifying the peaks used for calculation of collagen (Am/P) and carbonate (C/P), and splitting factor; where A and B indicate the phosphate peaks, and C indicates the trough. After Hollund et al.,(2013)

To establish the splitting factor, the height of the two phosphate peaks at ~565 cm-1 and ~605 cm-1 were summed and divided by the trough between the peaks at ~590 cm-1 (Weiner and Bar-Yosef, 1990). To estimate the collagen content, the ratio between the height of the amide peak at ~1640 cm-1, and the height of the

phosphate peak at ~1030 cm-1 was calculated (Trueman et al., 2008). To estimate the carbonate content, the ratio between the phosphate peak at ~1030 cm-1 and the carbonate peak at ~1415 cm-1 was calculated (Wright and Schwarcz, 1996).

4.3.6 X-ray Fluorescence Spectrometry (XRF)

A Seiko SII SEA60000VX Fluorescent X-ray Analyser was used for XRF analysis on a selection of the bone samples. A small sample of bone fragments were placed onto a sticky sheet on a Plastazote white plastic board and placed onto the sample platform. Measurements were taken in triplicate using the measurement parameters seen in Table 4-16.

Table 4-16: Measurement parameters for XRF analysis

Measurement system:	SEA60000VX	**Tube voltage (kV):**	50
Measurement time (seconds):	30	**Tube current (uA):**	589
Live Time (seconds):	17	**Filter:**	OFF
Environment:	Air	**Focus:**	Normal
Collimator:	1.2mmx1.2mm	**Peaking time:**	1.0usec

The samples were run against a library of known elements commonly found in soils, in order to identify any contaminants present in the bone samples. The elements that were checked are detailed in Table 4-17. The results from the analysis were expressed as peak intensity measured in counts per second (cps) which relates to the concentration of elements.

Table 4-17: Elements searched for within XRF analysis to identify possible soil contaminants in bone samples

Element	Element Name	Line	ROI keV
Si	Silicon	Ka	1.60- 1.88
P	Phosphorus	Ka	1.88- 2.15
Ca	Calcium	Ka	3.54- 3.84
Ti	Titanium	Ka	4.35- 4.67
Fe	Iron	Ka	6.23- 6.57
Mn	Manganese	Ka	5.73- 6.07
Cu	Copper	Ka	7.86- 8.23
Zn	Zinc	Ka	8.44- 8.82
Sr	Strontium	Ka	13.92-14.36
Zr	Zirconium	Ka	15.51-15.98
Cr	Chromium	Ka	5.25- 5.58
Ni	Nickel	Ka	7.29- 7.65
K	Potassium	Ka	3.16- 3.46

4.3.7 DNA extraction

The most effective commercial DNA extraction kit for the purpose of this research was found to be BTA Forensic Extraction kit (Promega) as established by tests performed and described in section 4.2.2. The same extraction kit was used on both the porcine and human bone samples, but with slightly different protocols at the initial stage. Porcine bones and Fin Cop samples were demineralised prior to DNA extraction as described in the next section.

The processing of human bone samples followed the manufacturers' protocol, with the exception of using double the recommended bone powder. Therefore 100mg of whole bone powder was weighed on an analytical scale and transferred into a sterile 2 mL Eppendorf tube.

Lysis buffer was prepared according to the reaction number detailed in Table 4-18 and mixed gently. 230 µL buffer was added to each sample, tightly capped and sealed with parafilm. The tubes were then vortexed for 5 seconds, centrifuged briefly and placed in a shaking water bath at 1100 rpm at 56^{o}C for 2 hours.

Table 4-18: Lysis buffer preparation per reaction plus 5% excess for pipetting error

Reagent	Number of reactions			
	1	**1 + 5%excess**	**8 + 5% excess**	**16 + 5% excess**
BTA Lysis buffer	220 µL	231 µL	1848 µL	3696 µL
DTT	3 µL	3.15 µL	25.2 µL	50.4 µL
Proteinase K	7 µL	7.35 µL	58.8 µL	117.6 µL
Total	230 µL	241.5 µL	1932 µL	3864 µL

After incubation, the sample tubes were removed and allowed to equilibrate to room temperature prior to centrifugation at 10,500 rpm (10,000 x g) for 90 seconds to separate the lysate from the sediment. This lysate was then pipetted into a 1.5mL tube without disturbing the pellet at the bottom of the tube. Add 300 µL of Lysis Buffer was added and vortexed briefly to mix.

In order to bind the genomic DNA, 15 µL of magnetic particles were pipetted into each sample tube, which were capped and vortexed for 10 seconds. 300 µL isopropanol was added to each tube individually, capped and vortexed for 5 seconds before briefly centrifuging to collect any liquid from the sides and lid of the tube. Tubes were placed in a shaker at 20^{o}C at 700rpm for 10 minutes

To wash the DNA now bound to the magnetic particles, the tubes were vortexed for 10 seconds and briefly centrifuged to collect any residual contents. The tubes were then placed in a magnetic stand for 10 minutes until the particles formed a pellet against the back on the tube. The liquid phase was then aspirated and discarded and 600 µL Wash Buffer A was added to each tube, which was then capped, and removed from the stand to vortex for 15 seconds, and returned to the stand for 1 minute.

This process was repeated again with 300 µL Wash Buffer A, and again with 300 µL Wash Buffer B. The tubes were then centrifuged briefly, placed back on the

magnetic stand for 60 seconds, and any residual liquid was collected using a 20 µL tip and discarded.

Bound and washed DNA was then eluted by pipetting 50 µL of Elution Buffer to the sample DNA tube and vortexed until the pellet had re-suspended. Tubes were placed in a shaking water bath at 900rpm, and 70°C, for 10 minutes. The sample tube was then vortexed until there were no visible magnetic particles, and centrifuged to collect any residual contents.

Tubes were then placed back into the magnetic stand for 5 minutes until the pellet size stopped increasing. The isolated genomic DNA was then transferred into 1.5mL tubes and stored at 4°C for up to one week or at -20°C for longer storage.

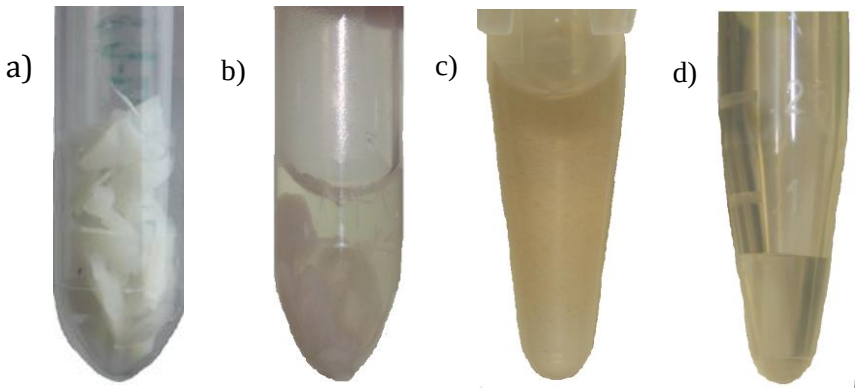

Figure 4-18: Photographs depicting the different stages of DNA extraction from bone, a) bone cut into slithers and placed into tube, b) bone being lysed, c) DNA adhering to magnetic beads, d) DNA resuspended in elution buffer.

4.3.7.1 Bone demineralisation

Bone samples were placed into 15 mL plastic tubes with corresponding labels and filled to the 14 mL marker with 0.5M EDTA pH 7.5. The tubes were sealed with screw-top plastic lids and parafilm and placed onto a roller mixer for 5-7 days (until the bone was pliable) with daily changes of EDTA.

Samples were then repeatedly washed with distilled water and returned to the roller mixer four times for 15 minute durations to remove any residual EDTA which may affect downstream analysis.

For the porcine samples, sterile scalpels and forceps were used to take shavings of the bone which were placed into 2 mL Eppendorf tubes ready for DNA extraction. For the Fin Cop samples, the demineralisation led to, in most cases, complete disintegration of the sample, therefore slicing was not necessary.

4.3.8 PCR amplification

PCR amplification was conducted on all extracted DNA samples in order to amplify specific areas of the DNA strand. The areas of interest differed between the archaeological human samples and the human analogue samples so different primers and conditions were used as discussed in the following sections.

4.3.8.1 Archaeological human amplification

Due to the degraded nature of the archaeological human DNA samples, the Powerplex ESI 16 Fast system (Promega) was chosen for the analysis. This multiplex system amplifies 16 loci and has been specifically designed for low quality and quantity of DNA with small base pairs, as shown in Figure 4-19.

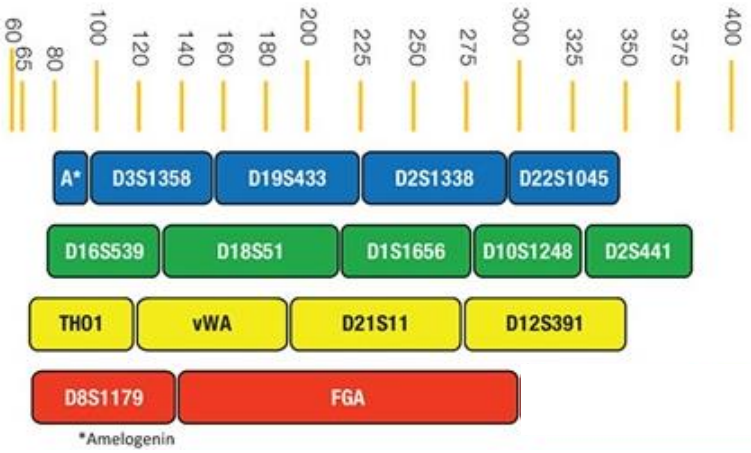

Figure 4-19: PowerPlex® ESI loci as miniSTRs, showing size and in base pairs Sprecher et al (2009)

As discussed in section 4.1.7 half volumes of the multiplex kit were used in order to lower the cost of analysis, and no additional water was added during the reaction in order to prevent the DNA sample being diluted. Aside from these modifications the manufacturers' protocol was followed.

An amplification mix containing 2.5µl PowerPlex® ESI Fast 5X Master Mix, 1.25µl PowerPlex® ESI 16 Fast 10X Primer Pair Mix, was gently mixed and 3.75µl was pipetted into individual 0.2ml reaction tubes, before adding 9µl sample DNA. Controls were prepared at the same time, replacing sample DNA with 0.5ng 2800M Control DNA for the positive control, and amplification grade water for the negative controls.

The sample tubes were placed into a G-Storm thermocycler, software version 3.4.0.1 using the following program, with the ramp speed set at maximum.

96°C for 1 minute	
96°C for 5 seconds	30 cycles
60°C for 35 seconds	
72°C for 5 seconds	
60°C for 2 minutes	
4°C soak	

After completion of the thermal cycling protocol, the amplified samples were stored at –20°C in a light-protected box to protect against the production of artefacts, in a freezer in the post amplification laboratory.

4.3.8.2 Human analogue amplification

Amplification of the human analogue DNA samples was conducted in order to assess the length of surviving DNA strands, as opposed to specific loci used for the human archaeological samples. Primers designed by researcher Fredericks (2012) were used to amplify sequences of certain amplicon lengths; 131 bp, 290 bp and 506 bp.

1µl forward primer and 1µl reverse primer were added to an amplification mix of 7.5µl ReddyMix PCR Master Mix (ABgene) and 4.5µl PCR grade water (Severn Biotech), before adding 1µl sample DNA.

The 0.2mL sample tubes were then amplified using the following PCR protocol as determined during optimisation, as detailed in section 4.2.3:

94°C for 5 minutes	
94°C for 30 seconds	34 cycles
55°C for 30 seconds	
72°C for 30 seconds	
72°C for 10 minutes	
4°C soak	

Post-amplification samples were stored in a freezer in the post-amplification laboratory prior to DNA quantitation.

4.3.9 DNA quantitation

Gel electrophoresis was used to visualise and confirm the presence of the amplified human analogue DNA samples by running on a 2% agarose gel for 30 minutes. Positive and negatives controls were used to confirm the analysis was working correctly, and to confirm the absence of contamination.

The completed gel was then recorded using a Photodoc-it gel recording system (UVP) and the results were recorded as either negative or positive.

As multiplex DNA amplifications do not tend to illuminate well on agarose gels, quantitation of the human DNA samples was established using peak height determination from the capillary electrophoresis results as detailed in section 5.6.3 and section 5.7.3.

4.3.10 Fragment analysis

An ABI PRISM 310 genetic analyser (Applied Biosystems) was used to analyse the amplified archaeological human DNA samples, following the manufacturers' protocol as detailed in the following section.

A loading cocktail was prepared by combining the thawed and vortexed CC5 Internal Lane Standard 500 Pro and Hi-Di™ formamide as follows:

[(2.0µl CC5 ILS 500 Pro) × (# samples)] + [(23.0µl Hi-Di™ formamide) × (# samples)] **(4-10)**

The loading cocktail was vortexed for 10–15 seconds to mix, before combining 25.0µl with 1.0µl of amplified sample (or 1µl of PowerPlex® ESI 16 Fast Allelic Ladder Mix).

The samples and ladder were then denatured just prior to loading onto the ABI 310, by heating at 95°C for 3 minutes, and immediately chilled on crushed ice for 3 minutes. Tubes were then placed in the appropriate autosampler tray and the tube positions detailed in the software with sample details.

The run was conducted using POP-6™ polymer, and the GS STR POP4 (1mL) G5v2.md5 module, with the following parameters:

Inj. Secs: 5

Inj. kV: 15.0

Run kV: 15.0

Run °C: 60

Run Time (minutes): 50

Data analysis was conducted using GeneMapper v3.2 (Applied Biosystems) where the generated electropherograms were analysed in accordance with guidelines. Interpretation guidelines as those described in 4.1.10 were followed to separate the identification of true peaks from background noise and analysis artefacts such as pull-up, spikes and dye blobs.

The height or Relative Fluorescence Unit (RFU) of each peak was recorded, not only as a means of quantitation, but also to allow calculations for the identification of heterozygous alleles. This information was then used to establish the presence

or absence of modern contamination, and to identify or exclude any possible familial relationships between individuals.

4.3.11 Limitations of selected methodologies

Whilst care was taken to choose the best methods for this project, as discussed in sections 4.1 and 4.2, every technique and protocol comes with limitations. The main limitations of methods for this research was the necessity for the destructive sampling of the archaeological human remains. By following guidelines and sampling the smallest amount of material possible, the choice of methods and available results became more limited. For this reason, the DNA analysis of the human remains was limited to duplicate or triplicate analyses and no additional work was conducted in outside laboratories to provide confirmation of results.

Due to the nature of ancient archaeological human remains, interpretation of results is limited to not being able to confirm the identity of the individuals – if forensic samples from known individuals could be used, the DNA methodology and results could be interrogated at a much more in-depth level. The quantitation of the DNA also had limitations due to using a standard PCR machine, rather than a more up-to-date qPCR machine which would have provided a 'real-time' concentration of DNA in the sample during PCR.

For the analytical techniques such as colourimetry, a limitation includes the analysis of only a small area – this was reduced by doing multiple readings along the area of the sample and taking an overall average. Use of the XRF provided high sensitivity analysis and therefore included information on all elements, whether found naturally in the bone or contamination from the ground.

The method design for the experimental burials in contained units, can be argued that without all the other factors such as rainfall and temperature change experienced outside, the processes would not be representative of 'real life', however enabled this methodology provided the opportunity to study individual aspects of the environments at one time.

Due to the form of the data this research produced, it was not possible to conduct any statistical analysis on the findings, however to combat this, the levels of accuracy were assessed via repetitions of experiments, and the use of averaged results with standard deviations and error bars where necessary.

4.4 Chapter summary

This chapter has provided a critical review of the methods presently used in similar research, and identified those suitable for this research. The method optimisation section has explained the process of developing suitable protocols, with the selected methods then presented. Data interpretation of the different analytical techniques used, including electropherograms for DNA analysis has also been explained. The next chapter presents the results from the research split into two parts. Part A presents the human analogue burial data, and Part B shows the human archaeological results.

Chapter 5: RESULTS

This chapter is separated into Part A which presents the results from the human analogue burials and Part B where the results from the human archaeological results are presented.

Part A: HUMAN ANALOGUE BURIALS

This chapter presents the results from the analysis of the controlled human analogue burials, conducted as described in Chapter 4.

A total of 60 porcine femora used as a human analogue were buried in differing controlled environments for varying durations, in order to assess diagenetic changes in comparison to the unburied control bones. Analytical techniques were used to assess the changes in the environment; and how the decomposition rates, and diagenetic changes were affected by the burials. Analysis of changes in colour, composition, and DNA content and quality were measured to identify the differences due to burial environments and varying durations of burial.

The chapter begins with the results from the analysis of the soil control samples and the soil samples taken from the each burial during excavation. Observations recorded at excavation of the bones in terms of presence/absence of mould, moisture and smell are discussed, and the manner in which the bones are observed to change over time within each environment. The pH, organic content and water content of each sample are presented, with a comparison of the differences between the environments.

Following this, the colour analysis of the control and buried bones are presented, along with the changes in colour that occur in the different environments over the range of durations of burial. Observations of changes in the bone marrow are also detailed. The results from the composition analysis of the bones are then described, showing the differences found from the different burials, and how these changes differ to those seen in unburied bones. Results from the DNA analysis of the bone samples are then presented, which provide an indication of the survivability and success of the extraction and amplification of the genetic

material. Finally, the results from the four aforementioned sections are collated to provide an overview of the different interactions between the analysed components of the research.

5.1 Soil Analysis

Soil analysis was conducted as per protocols stated in Chapter 4. Prior to burial, a small sample of each burial medium – clay, compost, lime and sand were taken and analysed – the information was then used as controls for comparison to assess the level of change, if any, from the separate burial mediums and different time intervals.

5.1.1 Control soil samples

The control samples were analysed for water content, organic content, pH, and colour, the results of which are presented in the following sections.

5.1.1.1 Composition analysis of control soil samples

Soil analysis of each of the control samples were conducted in triplicate, in order to provide reference values for the assessment of taphonomic effects of the burial mediums. The results of the analysis to determine the water content, organic content and pH of the samples are detailed in Figure 5-1.

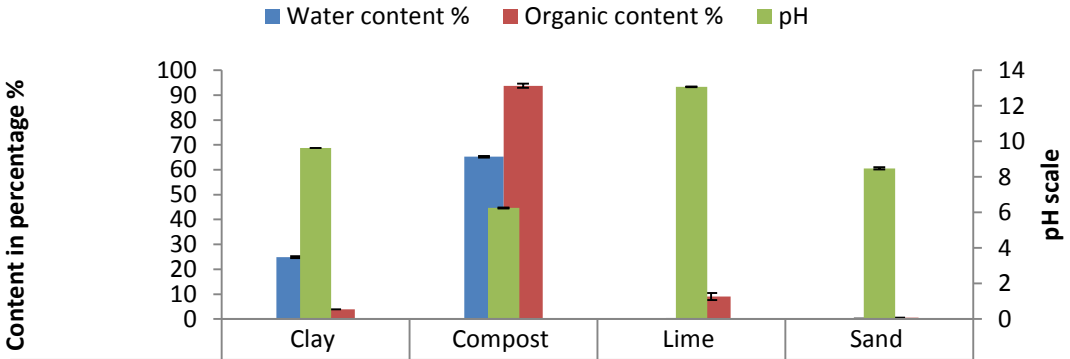

	Clay	Compost	Lime	Sand
Water content %	24.9	65.25	0	0.2
Organic content %	3.93	93.76	9	0.6
pH	9.63	6.25	13.07	8.48

Figure 5-1 Soil analysis of control soil samples, with water and organic content shown in percentage from the primary axis, and pH shown in logarithmic scale on the secondary axis.

All values show a low standard deviation from the mean, (as illustrated by the error bars on the figure) identifying the clay, compost, lime and sand tested were homogenous samples.

Compost contained the highest percentage of water, followed by clay, sand and finally the lime which showed almost no water content. This information is important as water presence in the burial medium is thought to be an important aspect contributing to changes in taphonomy, as previously discussed in section 3.2.

Compost showed the highest organic content, suggesting the bones buried in this medium would be most likely to display evidence of microbial action; in contrast to sand which showed a very small presence. The organic content reported for the lime sample is thought to be misleading as this may be due to the loss of tightly bound water as a result of the heat treatment.

The results from the pH tests showed a range from strong alkaline in the lime sample, to a medium alkaline in clay, sand at slightly alkaline, and compost at a slightly acidic value.

In order to assess any changes in pH, organic content or water content from the soil after the respective time durations of porcine bone burial, two soil samples were removed from directly below the bone after excavation, and analysed in triplicate in order to compare to the control soil sample results. These results were then collated to provide an average, which are detailed in the following sections with the associated standard deviations. Only in cases where disparities are identified will the individual samples be considered separately. All graphs are plotted on the same axis of 100% in order to provide a comparison across the data sets.

5.1.1.2 Colour analysis of the control soil samples

The colour analysis of the soils was conducted to see whether this variable had any impact of any staining of the bones that may appear later, and also as it is known to be an indicator of the soil content.

As described in section 4.3.4, four readings from an average of ten measurements were recorded from duplicate samples. The summary data can be seen in Table 5-1, with the complete data in Table A-1 in the appendix.

Table 5-1: Colour analysis of control soil samples

	Mean average			Standard deviation		
Soil sample	L*	a*	b*	L*	a*	b*
Clay 1 average	41.65	3.57	5.89	1.07	0.42	0.89
Clay 2 average	42.81	3.12	5.06	1.60	0.53	0.97
Average clay	42.23	3.34	5.47	1.40	0.51	0.97
Compost 1average	34.54	1.37	1.33	0.40	0.89	0.59
Compost 2average	35.36	1.43	1.24	0.73	0.43	0.51
Average compost	34.95	1.40	1.29	0.70	0.65	0.52
Lime 1 average	94.54	0.44	3.40	0.68	0.06	0.33
Lime 2 average	94.04	0.49	3.63	0.82	0.06	0.23
Average lime	94.29	0.47	3.52	0.75	0.06	0.29
Sand 1 average	62.52	4.59	19.60	0.39	0.06	0.09
Sand 2 average	62.59	4.70	19.69	0.98	0.29	0.56
Average sand	62.56	4.65	19.65	0.69	0.20	0.37

The colours of the soils vary from the lightest shown as lime with an average L* reading of 94.29 (where white is 100, and black is zero as described in 4.1.11.1), followed by sand at an average of 62.56, then clay at 42.23 and the darkest is compost with an average of 34.95. This would suggest that compost is the most likely of the mediums to stain the bone due to the intense colour, and therefore a larger colour difference between the bone surface and cortex would be expected. The darkness of the colour also indicates a high content of organic material and humic substances which also affect the bone surface, together with good drainage of the soil matrix. The grey colour of the clay indicates the presence of iron in the form of ferrous oxides, whereas the red and yellow present in the sand samples show the presence of iron in the form of ferric oxide.

5.1.2 Clay burials

For each individual excavation, photographs were taken and observations were recorded regarding the appearance of the burial medium and any odours that were present. The photographs taken are collated in Figure 5-2, and recorded observations for the clay burials are detailed in Table 5-2 , before a discussion in terms of the results of the soil analysis conducted. For each different burial medium and duration, samples were conducted in duplicate – the results collaborated, therefore the results are presented once for each instance.

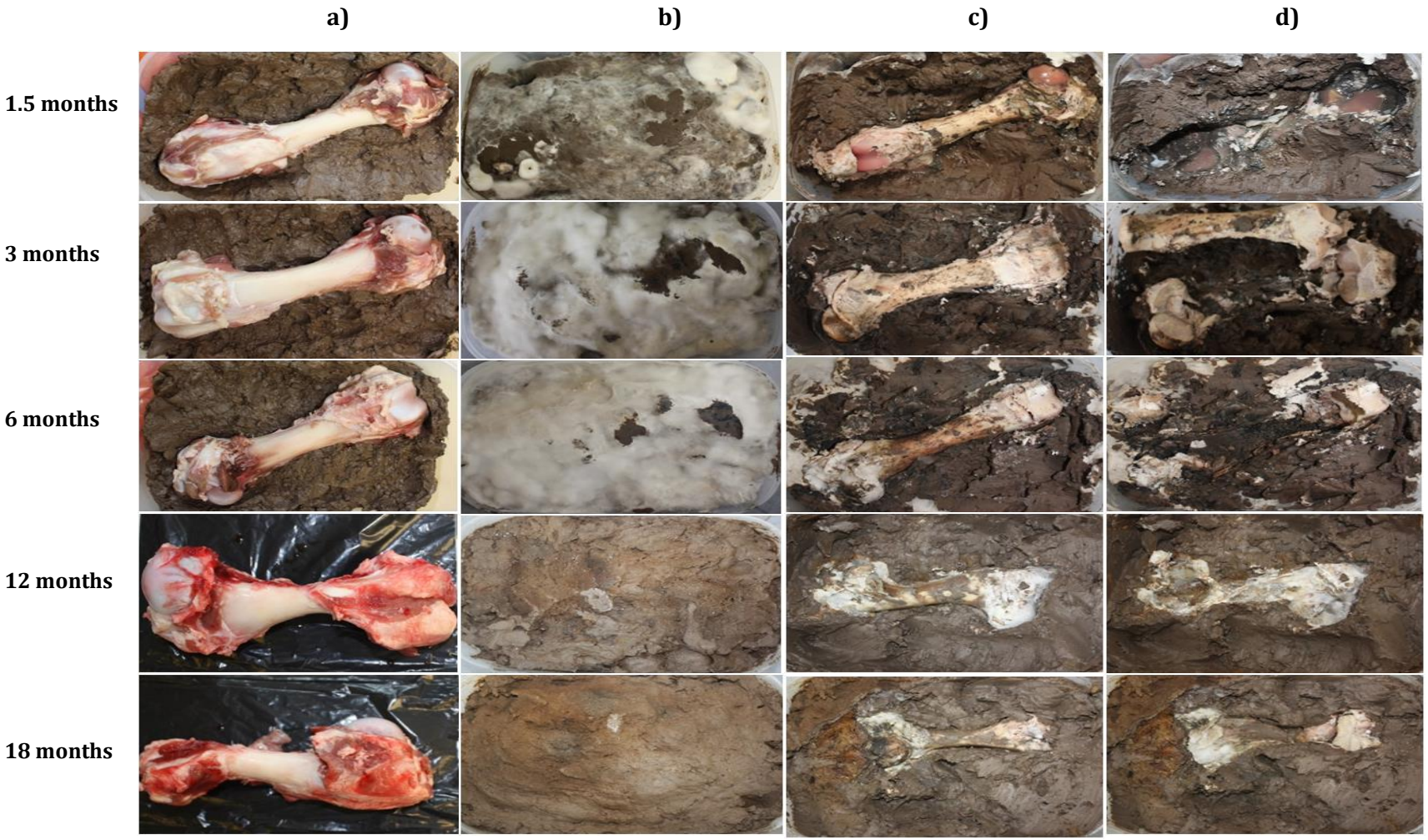

Figure 5-2: Photographs depicting the clay burials from different burial durations: a) prior to burial, b) surface prior to excavation, c) uncovered bone, d) underneath the bone after removal

Evidence of moisture within the burial was evident due to the collection of condensation on the lid from 1.5, 3 and 6 month burials. Upon removal of the bone from the 1.5 month burial, significant pooling of liquid was found accumulated beneath the bone, and submerging the underside. The 3 month burial also had a pooling of liquid but not to the same extent, yet after this it was not evident in the longer duration burials, however the clay was still visibly wet.

Table 5-2: Observations from clay burials

Burial duration	Moisture	Mould	Soft tissue	Odour	Other
1.5 months	Condensation Excessive pooling of liquid under the bone	White mould on the top of the clay	Wet white fatty tissue – beginning of adipocere formation	Strong odour upon removal of lid	Black inclusions
3 months	Condensation Pooling of liquid under the bone	White mould on top of the clay	White adipocere around bone	Strong odour upon removal of the lid	Black inclusions
6 months	Condensation No liquid pool under the bone	White and green mould on top and throughout	White adipocere around and under the bone Soft tissue no longer attached	Odour only when the bone uncovered	Black inclusions
12 months	No liquid pool under the bone Clay very wet	White and grey mould on top and throughout	No soft tissue remaining White adipocere underneath the bone, and dried on the ends	Odour only when the bone uncovered	Black inclusions around the bone
18 months	No liquid pool under the bone Clay damp	White mould on top and beneath the bone	No soft tissue remaining	No odour	Brown / orange substance around bone

The covering of white mould, as identified through observation, over the surface of the burial also mirrors the same information from the observations of moisture, with an abundance of mould from 1.5 months to 6 months and then a decrease with the 12 month and 18 month burials.

The first sign of white adipocere formation (previously discussed in section 2.4.1) was found to be present in the 1.5 month burial and persisted throughout all the burials, gradually increasing in the amount and becoming waxier.

A strong odour was present immediately upon lid removal for both the 1.5 and 3 month burials. This suggests that proteolysis has broken down proteins, and the deamination of amino acids which leads to release of gases such as ammonia and nitrogen. As the odour was strong, it was possible that ammonium ions released into the clay have been converted to ammonia due to the alkaline environment. The odour associated with the 6 month and 12 month burials is only present when the bone is uncovered, and absent by the 18 month burial. This suggests that the majority of the proteolysis and deamination occurs within the first 6 months of decomposition in a clay burial environment, and therefore the production of ammonia decreases, and therefore no foul odour.

Black inclusions were present in the clay burial from the first burial at 1.5 months, and throughout the entire duration to1 8 months. This indicates the production of ferrous sulphide due to the presence of iron in the clay and the process of bacterial decomposition of amino acids.

Another observation made was the presence of a wet brown / orange substance around the bone. This could be brown adipocere forming from brown fat deposits from the bone (Forbes et al., 2005).

The soil analysis from the samples taken beneath the bone, calculated the changes observed in the pH, water content and organic content are depicted in Figure 5-3 where the results are plotted against duration of burial, started with the results from the control samples prior to burial.

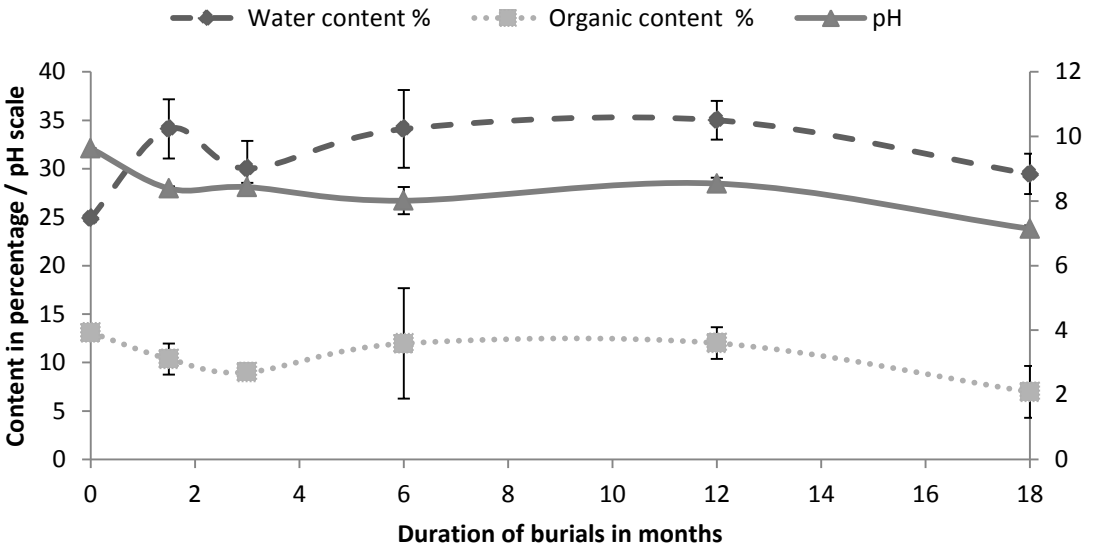

Figure 5-3: Changes in the composition of clay from control sample to 18 month burial, where water content is on the primary left axis, and organic content and pH are displayed on the secondary right axis

An initial increase in water content of 9.21% can be identified from pre-burial to 1.5 month burial which is likely to be the release of fluid due to the beginning of the decomposition process. A larger variance in the water content was observed between the individual samples than the initial control sample, showing the infiltration of water through the clay has not occurred in a uniform manner, and the burial medium is no longer a homogenous soil matrix. The decline in water content between 1.5 months and 3 months can be explained by the filtration of water down through the clay after the initial 'pooling' due to the excess of decomposition fluid, as discussed previously. The water content then appears to gradually increase and then decrease before 18 months due to the progression of decomposition and the drying out of the biological material. The changes in the level of water content mirrors the level of pH for the first 3 months – as the water content goes up, the pH goes down; thus showing the water level having a neutralising effect on the pH.

The changes in both the organic content in the clay and the pH appear to be very similar, with a slight decrease in both during the initial stages of burial. The absence of an increase in organic content suggests the biological by-product of the

decomposition is not infiltrating the clay, but rather pooling underneath the bone, or filtering down through the pores in the medium, without being absorbed into the matrix.

The increase in acidity is most likely attributed to the release of acidic decomposition fluids such as lactic acid, butyric acid and acetic acid which are formed by the decomposition of sugars due to an anaerobic environment.

5.1.3 Compost burials

The observations recorded from the changes seen in the compost burials are shown in photographs in Figure 5-4 and are detailed in Table 5-3, with the soil analysis results presented after.

Condensation was present on the lid of the burials from 1.5 months through till 12 months, with no pooling of liquid at any stage, although the compost appeared to be moister at 18 months than any time.

Mould was present on top of the burial surface from 1.5 months to 12 months, and absent on the 18 month burial, suggesting a reduction in the environment moisture as shown by the lack of condensation.

Soft tissue was still present after 1.5 months and the formation of dry adipocere was present at this stage and gradually progressed through to 18 months. From 6 months onwards, the bone left an imprint of adipocere in the compost.

No strong odours were present from any of the burials, even when the bone was uncovered. The lack of ammonia and gases suggest a retarded process of proteolysis where a slower decomposition of proteins and amino acids has occurred.

The formation of white adipocere from 1.5 months confirms the presence of water in the environment was high enough for this to develop, although due to dry and waxy nature it was not in excess.

Other observations noted including the ‘feel’ of the bone – which appeared noticeably lighter by 12 months and lighter and drier by 18 months.

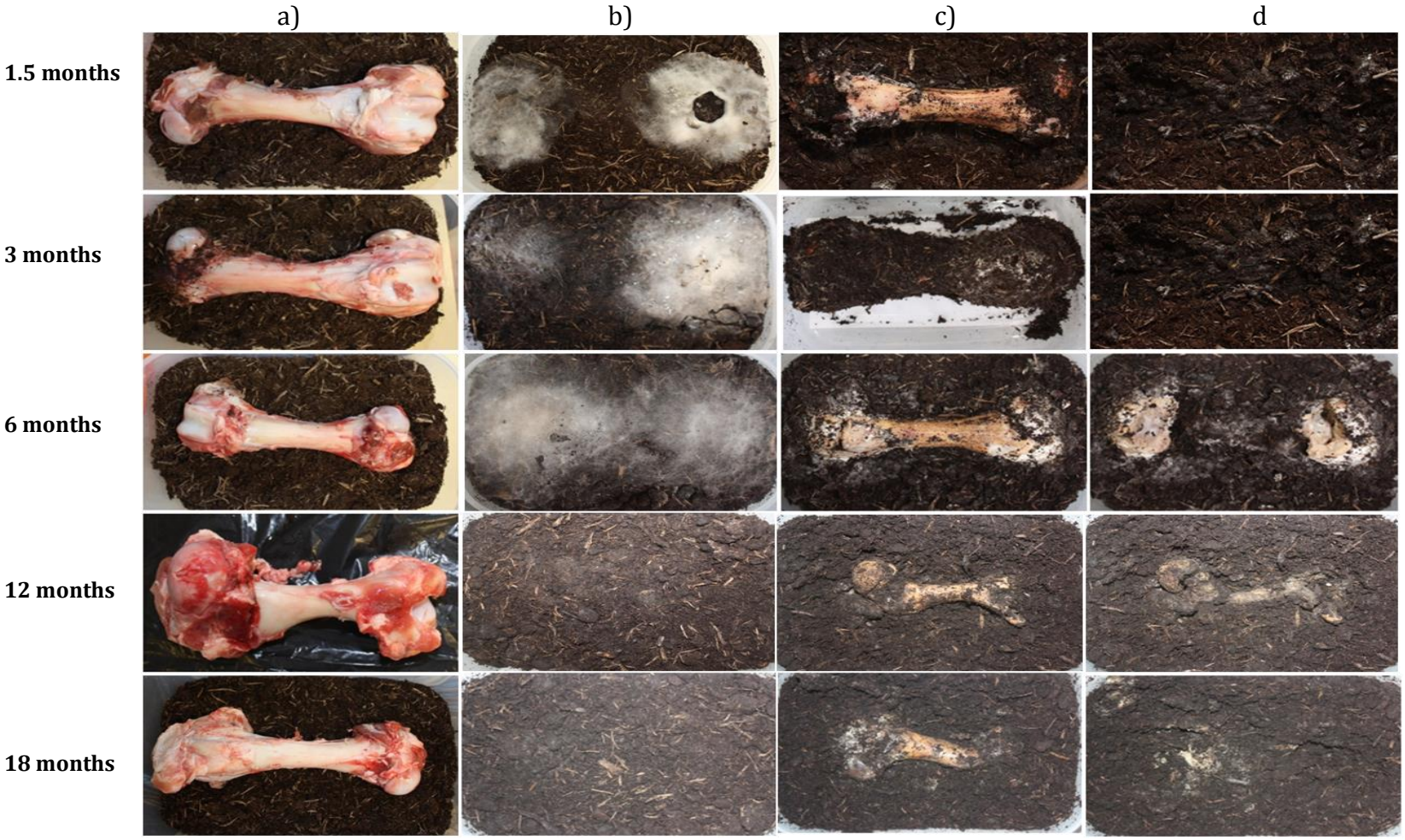

Figure 5-4: Photographs depicting the compost burials from different burial durations: a) prior to burial, b) surface prior to excavation, c) uncovered bone, d) underneath the bone after removal.

Table 5-3: Observations from compost burials

Burial duration	Moisture	Mould	Soft tissue	Odour	Other
1.5 months	Condensation No liquid	White mould in soil and on bone ends	Still present on bone ends Dry adipocere	No odour	
3 months	Condensation No liquid	White mould on top	Dry adipocere	No odour	
6 months	Condensation No liquid	White mould on top	Dry adipocere	No odour	
12 months	Condensation No liquid	White and brown mould	Dry adipocere	No odour	Bone feels light
18 months	No liquid Compost moist	No mould	Dry adipocere	No odour	Bone feels light and dry

The measured organic content fluctuated between 0 months and 6 months of burial, in the same manner as the pH – as the organic content rose, so did the pH, both in a mirror image of the water content. This suggests the decomposition products being released into the compost are not acidic or liquid, and the ammonium ions produced from the breakdown of proteins are remaining in the soil, rather than being converted to ammonia; this would also explain the lack of odour.

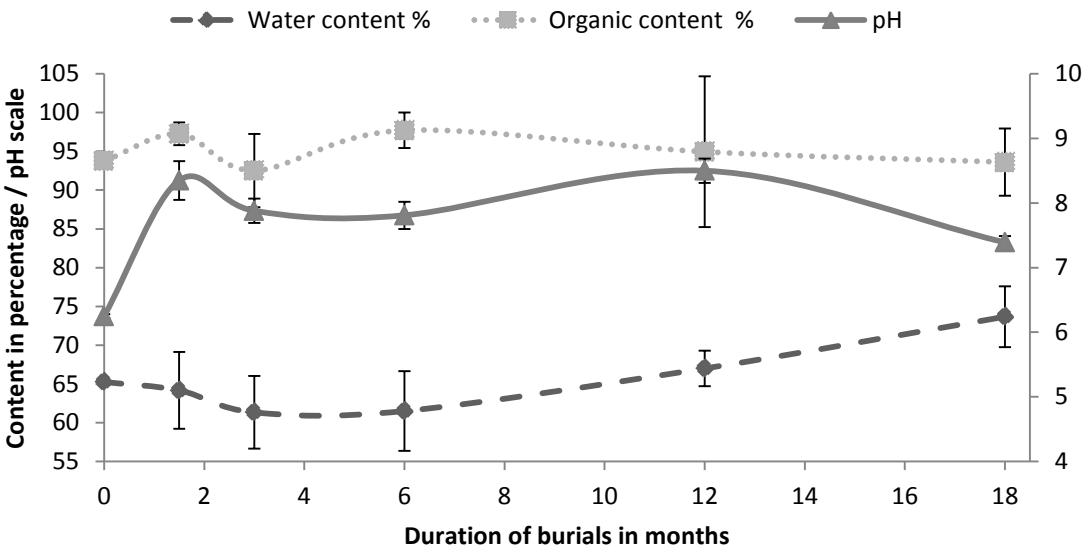

Figure 5-5: Changes in the composition of compost from pre-burial to 18 months, where water content and organic content are on the primary left axis, and pH is on the secondary right axis

From 6 months, the water content increases steadily to 18 months, as the pH level begins to become more acidic, suggesting the release of acidic fluids into the compost from proteolysis and the deamination of amino acids.

5.1.4 Lime burials

The lime burials showed an absence of evidence of moisture and mould as depicted in Figure 5-6 and Table 5-4. No liquid was present underneath the bone or in the environment and no condensation was evident on the lid of the burial container. The absence of mould supports the notion of no excess moisture in the environment.

Soft tissues were still present around the bone, but in a desiccated form, where the lime had caused a 'cast' to be formed, protecting the soft tissue which was still present at the 18 month stage.

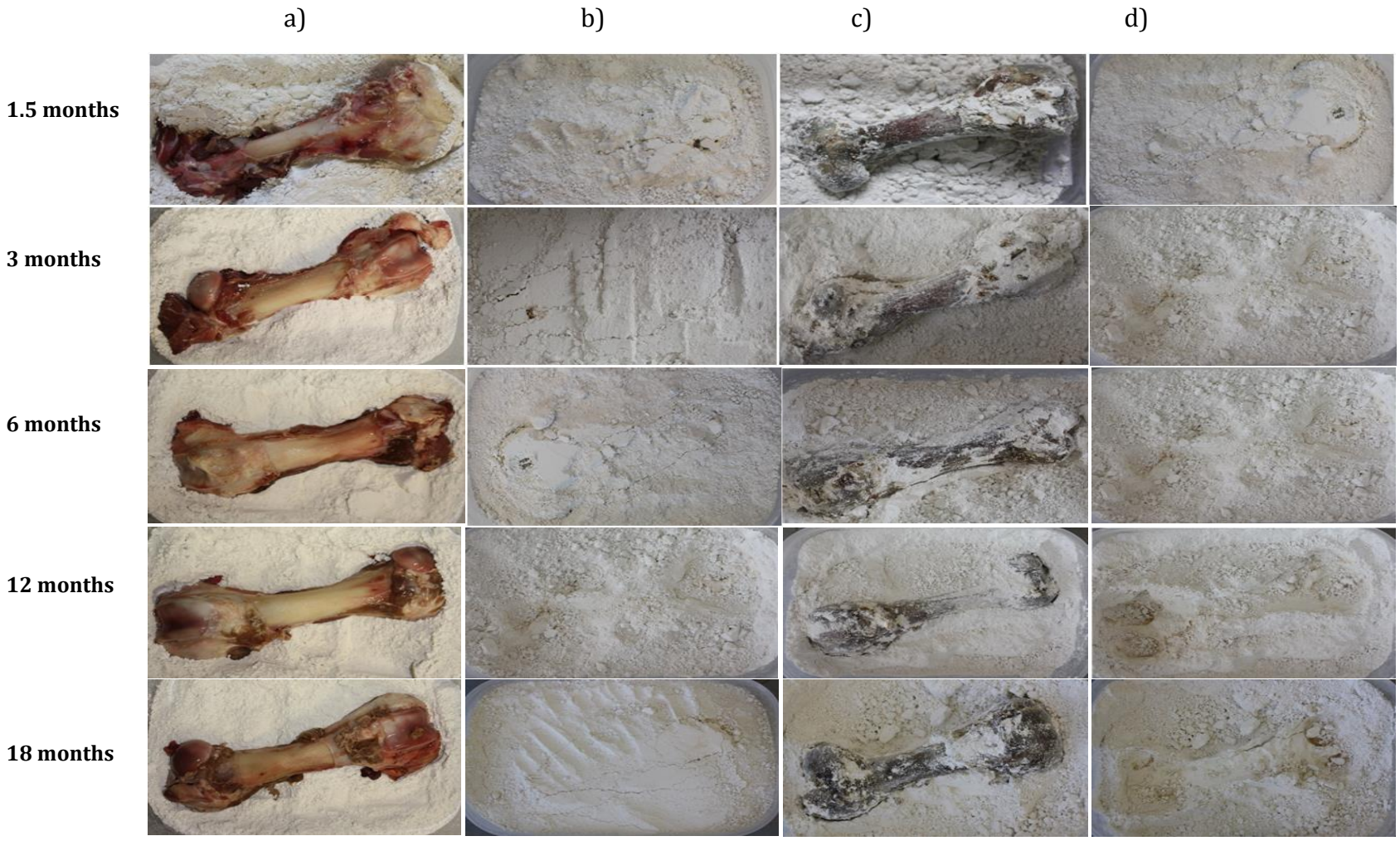

Figure 5-6: Photographs depicting the lime burials from different burial durations: a) prior to burial, b) surface prior to excavation, c) uncovered bone, d) underneath the bone after remova

There was an absence of strong odour throughout all the burials, suggesting the lack of nitrogen or ammonia release due to the breakdown of proteins, confirming the lack of decomposition of soft tissue. Slight odour was present in the 12 month and 18 month burials along with a slight orange/yellow discolouration of the lime above and below the bone, suggesting proteolysis was beginning to occur in the soft tissues with the release of fluid into the lime.

Table 5-4: Observations from lime burials

Burial duration	Moisture	Mould	Soft tissue	Odour	Other
1.5 months	No liquid	No mould	Soft tissue present but desiccated	Faint odour	Cast formed around the bone
			Blood tissue under tissue		
3 months	No liquid	No mould	Soft tissue desiccated	No odour	Cast formed around the bone
6 months	No liquid	No mould	Soft tissue desiccated	No odour	Cast formed around the bone
12 months	No liquid	No mould	Soft tissue desiccated	Slight odour	Cast formed around the bone
					Slight orange discolouration in lime above bone
18 months	No liquid	No mould	Soft tissue desiccated	Slight odour	Cast formed around the bone
					Slight yellow discolouration in lime above bone

The results of the soil analysis of the lime samples shown in Figure 5-7, showed an increase in water content of almost 10% from pre-burial to 1.5 months, which mirrored the organic content and the pH of the lime.

The 3 month burial showed the pH at its most acidic level of 12.68, despite a reduction in the water content, suggesting the addition of acids into the lime.

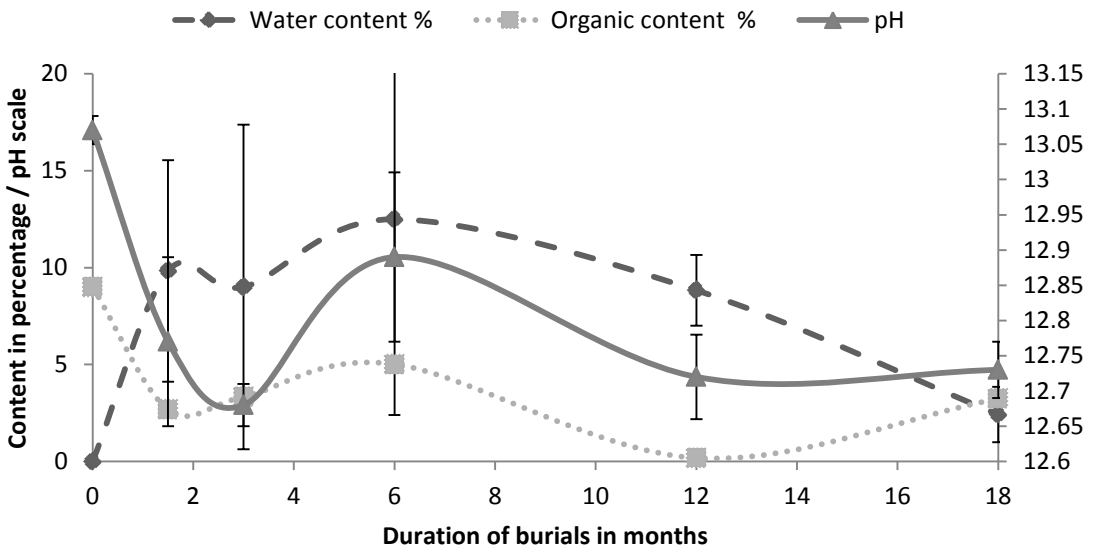

Figure 5-7: Changes in the composition of lime from pre-burial to 18 months, where water content and organic content are on the primary left axis, and pH is on the secondary right axis.

The organic content reached a high of 5% at the 6 month interval. This increase also coincided with the water content and the pH in the lime samples at this stage and therefore suggests this raise is due to the release of decomposition products into the environment.

The correlation between water content and organic content continues until the 18 month burial where the organic content raises again, showing the further breakdown of tissue as confirmed by the presence of orange discolouration in the lime beneath the bone.

5.1.5 Sand burials

The photographs taken from the sand burials are displayed in Figure 5-8 with the observational data detailed in Table 5-5.

The moisture in the sand burial environment was shown to be low in observations due to the lack of condensation and mould over the top. An area of dark soil indicating wet sand directly over the bone was evident in all burials from 1.5 months to 18 months.

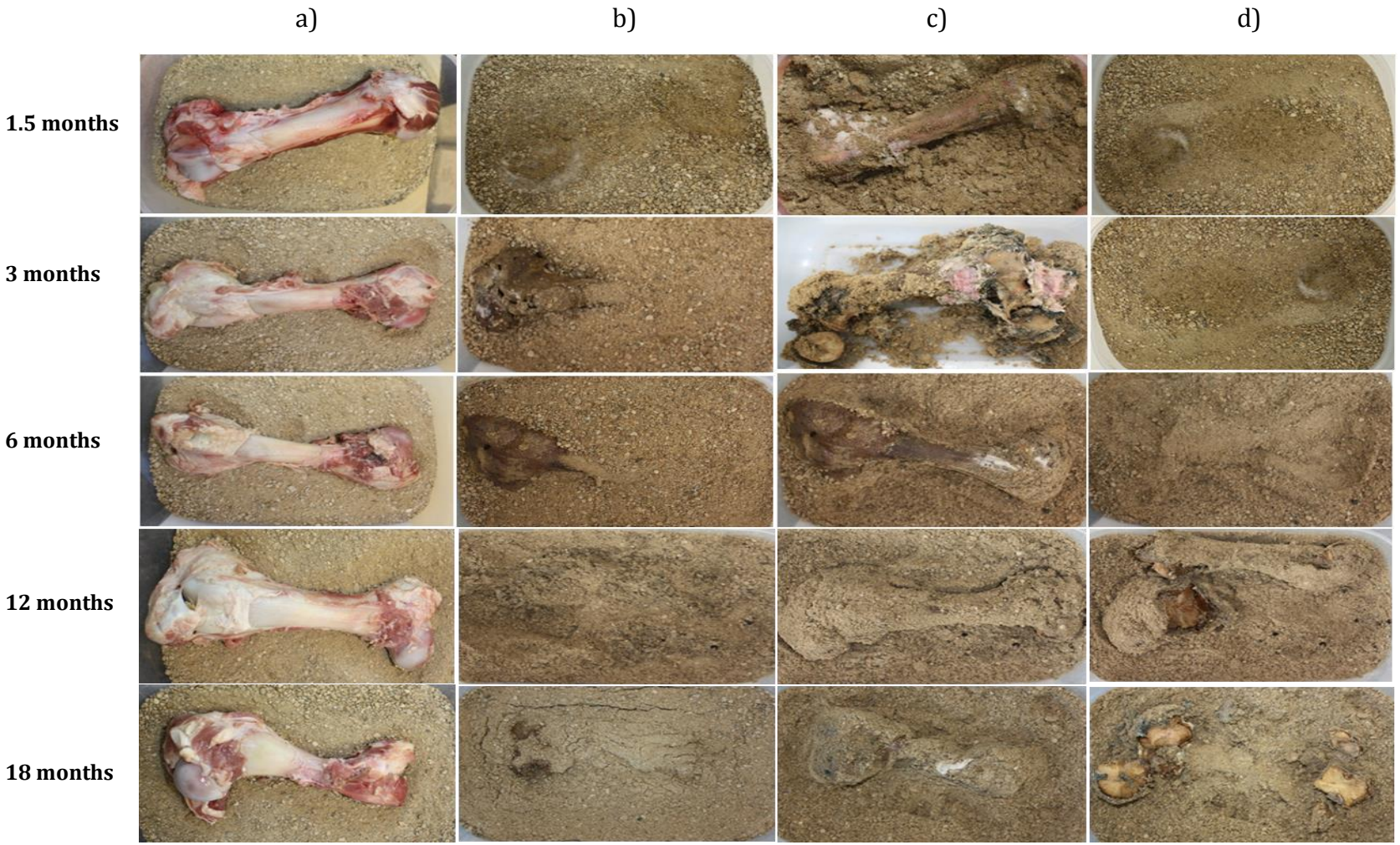

Figure 5-8: Photographs depicting the sand burials from different burial durations: a) prior to burial, b) surface prior to excavation, c) uncovered bone, d) underneath the bone after removal

During excavation of the bones, wet sand was noted around the bone from 1.5 months to 6 months, after which the sand was noticeably drier but still moist at 12 months and 18 months.

Table 5-5: Observations from sand burials

Burial duration	Moisture	Mould	Soft tissue	Odour	Other
1.5 months	Moisture strip present in sand above bone Sand very wet around bone	No mould	Dry white adipocere Wet brown substance	Strong odour when bone uncovered	
3 months	Sand wet around bone	No mould	Dry white adipocere Wet brown substance	Strong odour when lid removed	
6 months	Moisture on bone Sand wet	No mould	Dry white adipocere Wet brown substance	Strong odour when lid removed	
12 months	Condensation Moist sand	No mould	Dry white adipocere Wet brown substance	Strong odour when lid removed	
18 months	Wet patch over the bone Moist sand	No mould	Dry white adipocere Wet brown substance	Strong odour when lid removed	Dry bone

Dry white adipocere was evident from the 1.5 month burial, and throughout all the others until 18 months. This confirms the fact that enough moisture was present within the environment for adipocere to form. A brown wet substance was also present, most likely to be liquefied soft tissue.

A strong odour was present throughout all the sand burials, yet at 1.5 months the odour was only present after the bone was uncovered; with the other burials, the odour was present as soon as the lid was taken off. The strong odour is due to the

process of proteolysis and the breakdown of the proteins, and the deamination of the amino acids which produces the gas ammonia, among other gases. Due to alkaline nature of the burial environment, the ammonium ions are likely to have been converted to ammonia, resulting in a strong odour. This presence of the odour confirms the other observations of an accelerated decomposition process. Another observation noted, was the dryness of the bone from the 18 month burial.

The results from the soil analysis tests show the water content was highest after 3 months of burial, increasing from 0.2% to 14.03%, which is a mirror image of the pH – showing the water may be neutralising the environment. Although, the increase in organic content at this point, also suggests the release of decomposition products into the sand, therefore acidic decomposition fluid such as lactic acid may also be contributing to the lower pH.

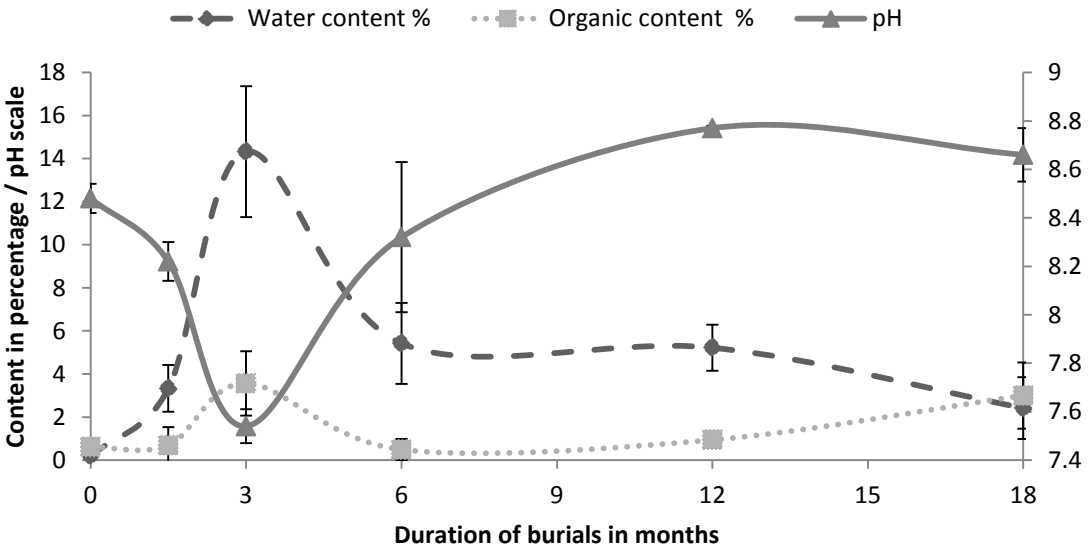

Figure 5-9: Changes in the composition of sand from pre-burial to 18 months, where water content and organic content are on the primary left axis, and pH is on the secondary right axis

The 6 month burial shows a reversal in the trends of pH and water content from the previous sample, with the pH rising above its original value suggesting the presence of ammonium ions in the sand from the breakdown of proteins.

5.1.6 Soil analysis comparisons across environments

In order to put the individual soil analysis results from the four different burial environments into context, it is necessary to compare the data directly to ascertain the differences.

Observations from the burials show the differences between the presence of moisture as shown in Figure 5-10.

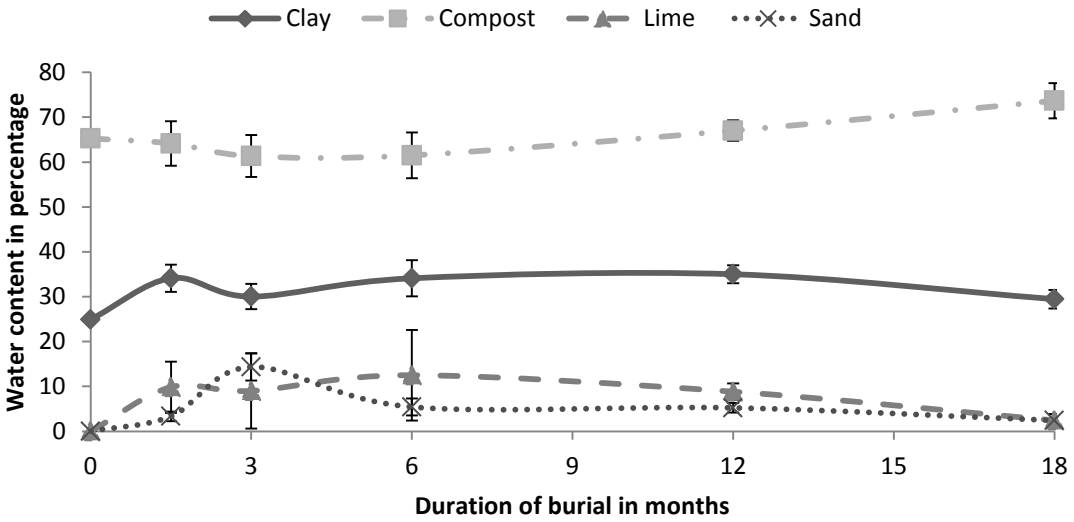

Figure 5-10: Comparison of water content across the different environments

Clay and compost burials both showed excess moisture present due to condensation and production of mould, but was absent in the lime and sand burials.

Peaks in the water content of the burial mediums occurred earlier for clay and lime suggesting initial release of decomposition fluids occurred during the first 1.5 months of burial, whereas the highest content of water in sand occurred at 3 months, and 18 months for compost.

The differences in the organic content across the different burial environments are shown in Figure 5-11, providing the variance in samples with error bars on the figures.

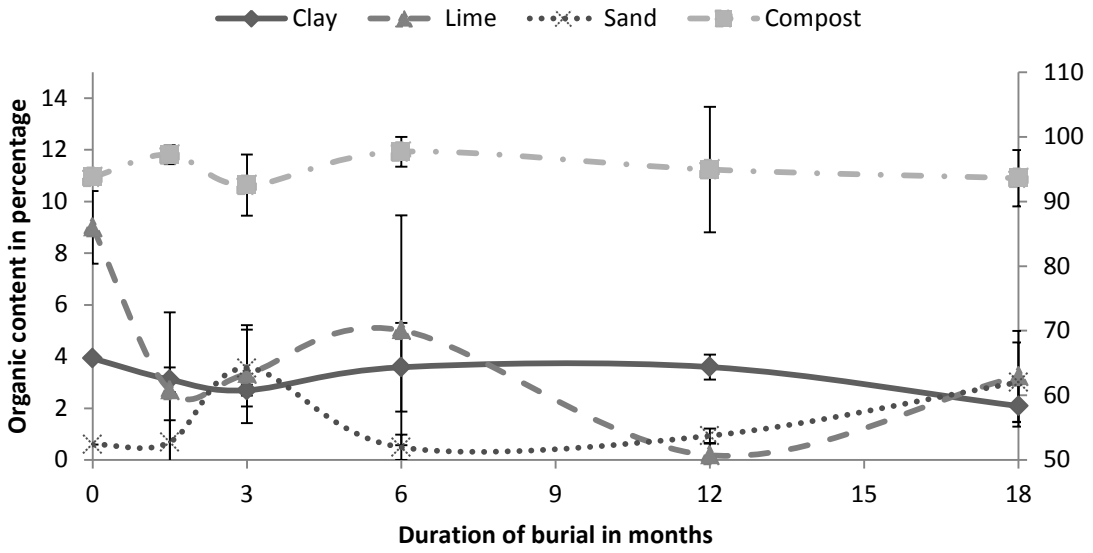

Figure 5-11: Comparison of organic content across the different environments, due to the high content in compost, a secondary axis on the left has been used in order to allow comparisons of trends

The first soil sample to show an increase in organic content is compost at 1.5 months, followed by sand at 3 months, and lime and clay at 6 months. The organic content in clay and compost show a similar trend of then stabilising, yet both the lime and sand show a drop before both rising again from 12 months to 18 months.

Differences were observed in the pH changes within the burial mediums across the 18 month duration, and are detailed in Figure 5-12.

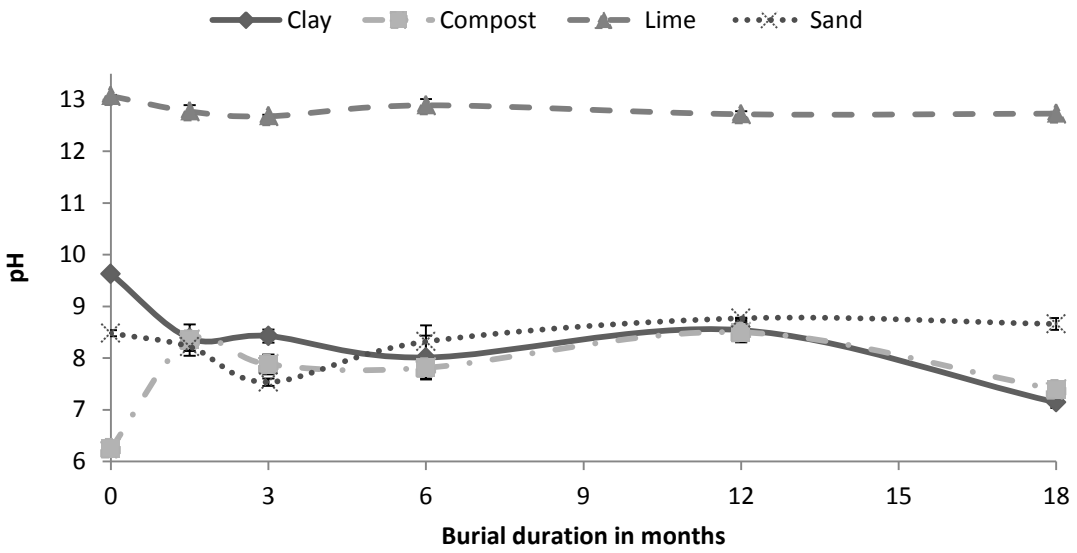

Figure 5-12: Comparison of pH across different environments

Compost was the only burial medium to become more alkaline within the first 1.5 months of burial, and also showed the largest change from 6.25 at pre-burial to 8.21. Sand showed an initial decrease until 3 months before a steady increase until 18 months. Despite the initial differences in pH for clay and compost, from 6 months to 18 months they showed similar trends. The pH of the lime burial remains the most constant throughout the 18 month period, with the biggest difference occurring within the first 3 months.

5.2 Colour Analysis of Bone

The colourimetric analysis of the bones was conducted as detailed in section 4.3.4, and the results of the porcine analysis is presented in this section. First, the results from the control bones are detailed, in order to provide a reference for buried samples. Followed by the data analysis from the clay, compost, lime and sand burials, prior to a comparison across the sample set.

5.2.1 Control burial bones

As detailed in section 4.3.3, the control bones were unburied, and analysed at the same time duration as that of the buried samples. Photographs were taken at each

stage to record the appearance of the bones, in addition to colour data measured with a colourimeter.

The photographs are presented in Figure 5-13, and show the surface of the control bones, after sectioning prior to removal of the surface, and the control after surface removal had been conducted. The control bones were assessed at the same intervals as the buried bones, at 0 months (within 3-5 days of the kill date), 1.5 months, 3 months, 6 months, 12 months and 18 months.

The 0 month control samples show a smooth, creamy colour bone surface, which bled when the soft tissue was removed with a scalpel. After surface removal, the bones appeared slightly darker, and evidence of the blood staining was still present.

The photographs from the 1.5 month control bones showed a cream bone but with evidence of blood staining on the surface. After removal of soft tissue, there was still a slight bleed from the disruption of the blood vessels, but to a lesser extent than those from 0 months. Surface removal revealed a colour and texture very similar to 0 month controls.

At 3 months the surface of the bone has visibly changed colour, with a patchy green tinge, no blood was evident after sectioning, and the surface removal provided a cream colour.

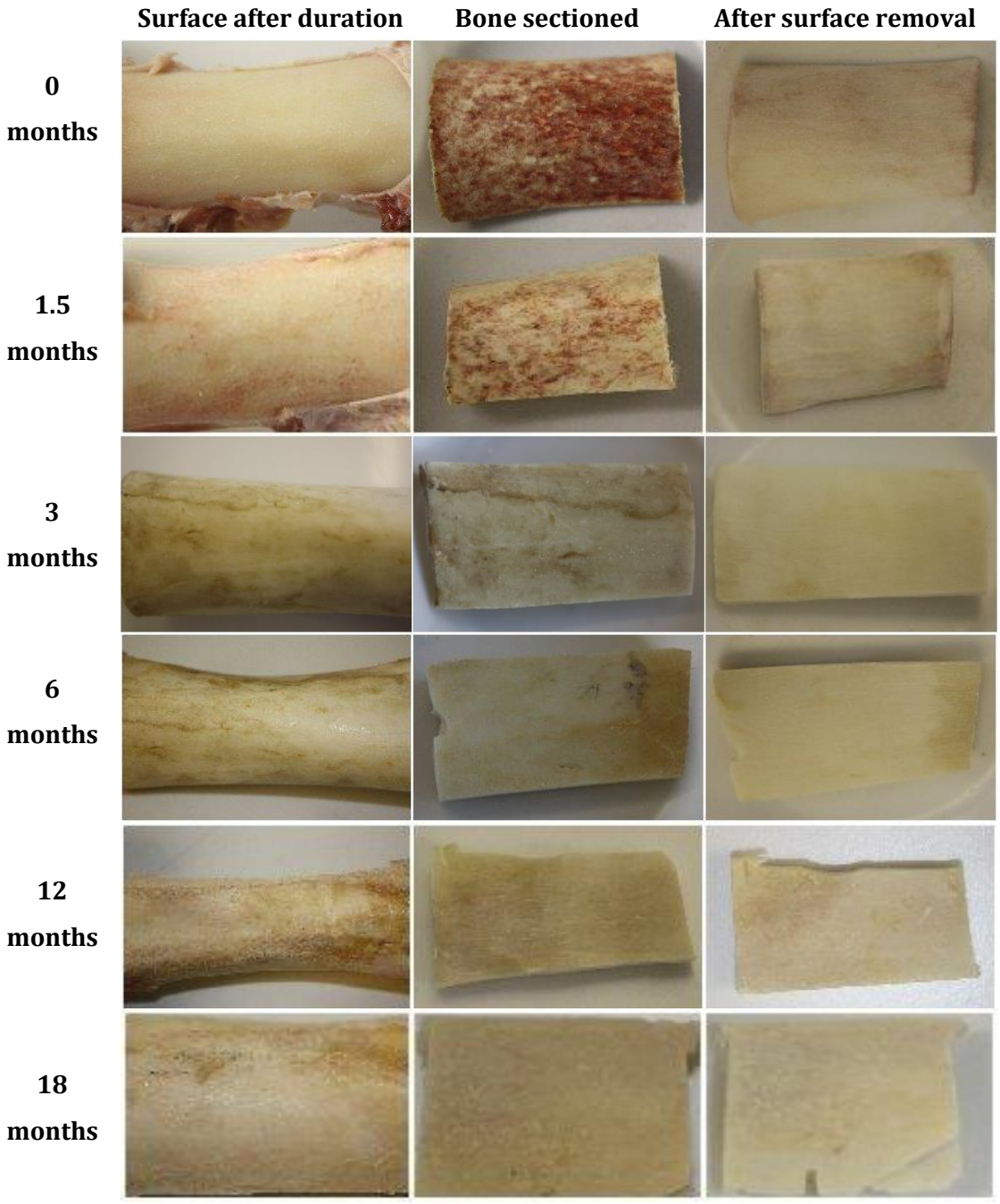

Figure 5-13: Photographs depicting the colour change of control unburied porcine bone over controlled durations.

This change continued as the durations were increased, resulting in a mottled colouration of the bone surface, which upon removal, revealed a creamy bone surface.

In order to analyse the overall colour difference between the pre-burial, post-burial and surface removal of the bone, calculations from the colourimetry data were performed as discussed in 4.1.11.1, and the results are shown in Figure 5-14. Although the bones were not buried in a soil matrix, the duration has still been referred to as burial duration for clarity.

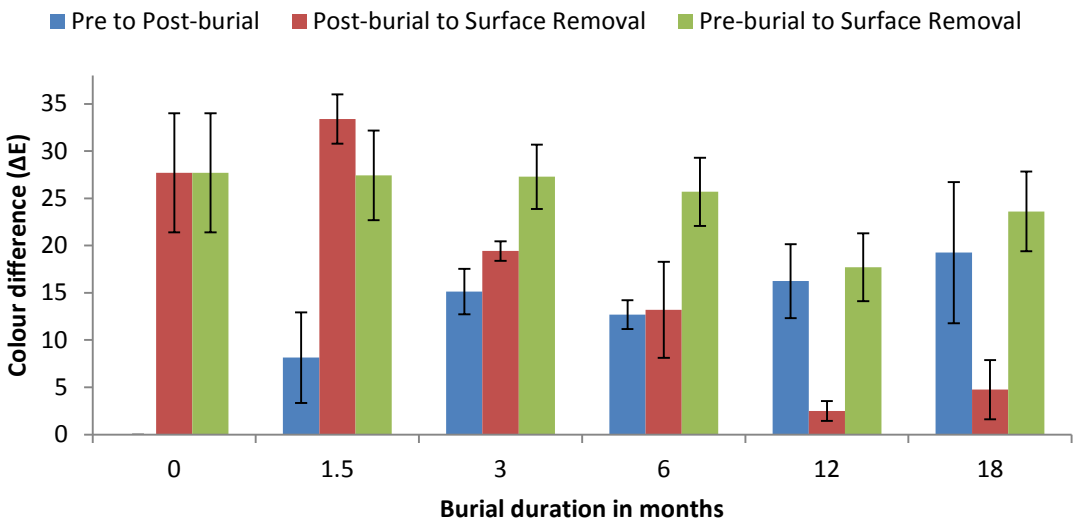

Figure 5-14: Overall colour difference of the control bones at the different stages

The biggest colour difference between the post-burial surface of the bone and the colour after surface removal is shown at 1.5 months, after which this difference decreases, and the difference from the colour of the pre-burial surface to post-burial surface increases. Although this analysis provides information as to the colour change of the bone, it does not explain how the colour change occurs.

By analysing the individual components from the colourimetry measurements, it is possible to numerically see how the colour of the bone surface changes over the three different axes of lightness, hue and chroma, over the 18 month period.

The data in Figure 5-15 shows how the L*a*b* colour values of the bone surface change over the duration of 18 months, from the post-burial surface and after the surface has been removed.

L* is the axis that co-ordinates with the lightness of a colour from white (100) to black (0) – it can be seen that from 0 months it darkens to 1.5 months - this reflects the information from the photographs, where the bone surface changes from cream to pink due to the blood vessels within from 0 to 1.5 months. The figure then shows a steep increase in lightness at 3 months followed by a gradual increase through to 18 months. This contradicts the images from the photographs which appear to be getting darker, but this can be explained by the other two axis.

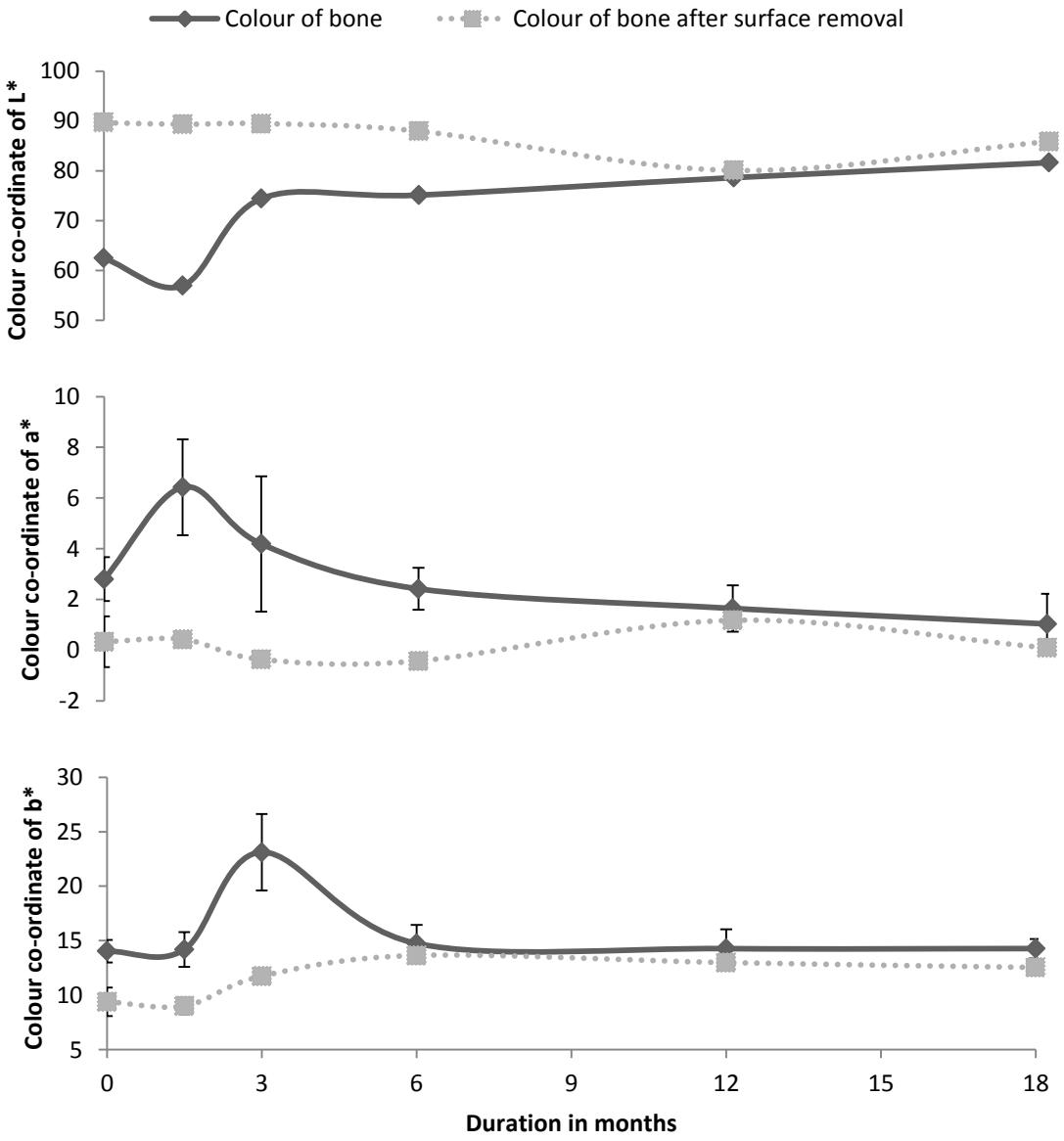

Figure 5-15: Colour data analysis of individual axis – L*, a*, and b* with a comparison between the colour of the bone before and after surface removal

The L* values after surface removal can be seen to remain stable around 90 for the first 3 months, before gradually becoming darker until 12 months as the decomposition progresses, before another increase in lightness at 18 months back to 85. This shows how the greatest change is occurring on the bone surface, with less diagenetic changes occurring underneath.

a* is the axis between red (+127) and green (-128) which can be seen to increase between 0 to 1.5 months on the surface of the bone, moving further towards a red colour - confirming the presence of the blood seen in the photographs; before a subsequent steady decrease until 18 months, towards green. This can also be seen in the photographs, and can be explained by the decomposition of the proteins and cells within the bone. After surface removal, the a* values can be seen to decrease in redness from 0 months, to 1.5 months when evidence of blood can still be seen, to 3 months where the value of -0.365 shows the surface is more green than red and even further to -0.427 at 6 months as the decomposition progresses. This migration towards green can be explained by the breakdown in the haemoglobin from the blood present within the bone. The values at 12 months and 18 months show a slight increase back to the red side of the scale. Once again this shows more diagenetic changes occurring on the surface and not throughout the whole bone.

The last values to be discussed – b*, is the axis between yellow (+127) and blue (-128). On the bone surface this value remains stable from 0 months to 1.5 months, before increasing towards yellow at 3 months, in line with increase in lightness, before dropping again at 6 months and remaining relatively stable until 18 months. This again is confirmed by the photographs, where you see the original cream colour of the bone becoming yellower. After surface removal, the b* values mirror those of the a* axis, with a slight decrease in yellow from 0 to 1.5 months, before a steady increase in yellow to 6 months, before levelling out towards 18 months. This steady increase in yellow could be due to the decomposition of fat tissue.

Comparison of the individual colour scales of lightness, colour and hue are detailed in Figure 5-15 showing the differences between the bone colour before and after surface removal. This clearly illustrates the biggest colour difference between the surface of the bone, and below the surface occurs within the first 6 months. By 12 months, the colour of the surface and below can be seen to equilibrate on all three axis.

It was also noted during the processing of the bones, that a distinct difference in colour was observed from the bone marrow. In order to allow a comparison of the difference Figure 5-16 shows the appearance of bone marrow from 0 month control bone.

Figure 5-16: Bone marrow from 0 month control porcine bone

The photograph displays the bright red haematopoietic form of fresh bone marrow. Observations on the changes that occur in the different burial environments can be seen in the following sections.

5.2.2 Clay burial bones

The photographs in Figure 5-17 illustrate the colour change of the bone from pre-burial, to post-excavation to post-surface removal. Patchy staining of the bone can be seen in the post-excavation photographs, as a result of contact with the clay. Most of the staining is removed with the surface removal, but is not as homogenous in colour as the control bones. Other observations include changes to the texture of the bone, the surface became much rougher after burial.

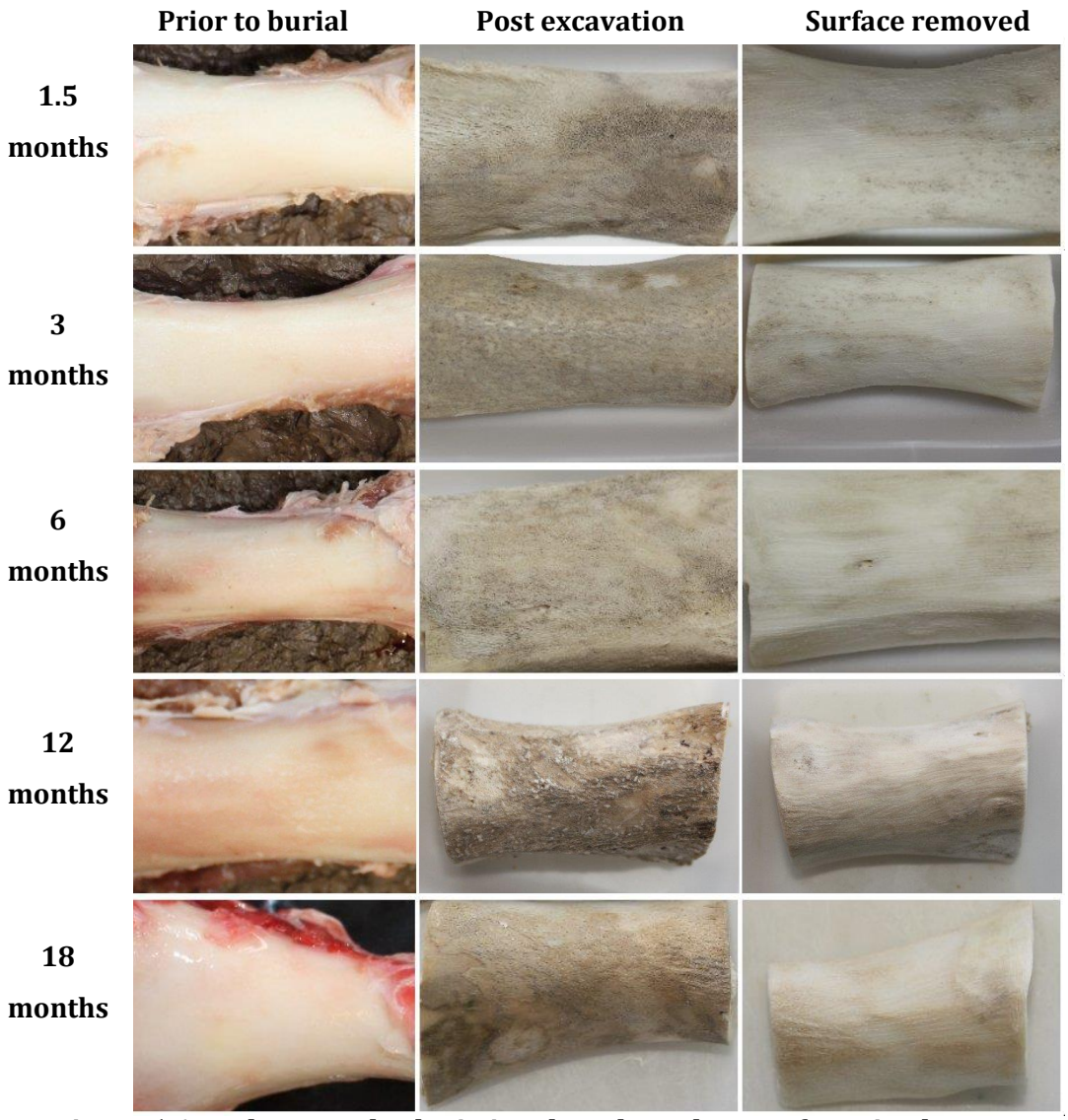

Figure 5-17: Photographs depicting the colour change of porcine bone from the clay environment over a period of 18 months

After colourimetry was conducted, the overall colour differences between the stages were calculated as a single number and are presented in Figure 5-18. The largest difference in colour can be seen from the pre-burial surface to the removal of surface after excavation. The difference in the surface colour from pre-burial to post-burial increases at a uniform rate. The changes in the colour from post-burial to surface removal remain relatively constant throughout the 18 month period.

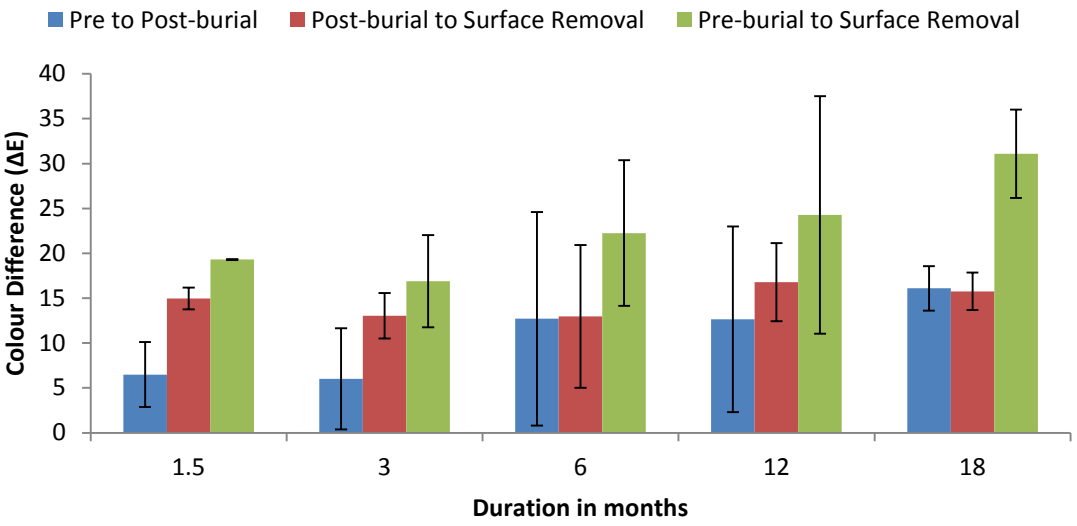

Figure 5-18: Overall colour differences of the bones buried in clay, over the 18 month period.

By looking at the axes individually, a more detailed description about the direction of the colour changes in the bone can be ascertained. By utilising the three axes for analysis, instead of a single number for the overall colour change, three co-ordinates are given, and therefore looked at independently but collated together in Figure 5-23 to allow comparison across the axes at the given burial durations. The values shown are the averages of the duplicate samples that were tested, with error bars to show the variance of the samples.

The value at 0 months for the post-burial bone surface colour is an average of all 10 bone samples prior to burial in order to provide a baseline from which the colour begins from. No data is provided for bone colour after surface removal at 0 months, as no surface was removed prior to burial, apart from the control bones.

The co-ordinate of L* can be seen to increase in parallel for both the post-burial bone surface colour and the bone colour after surface removal until 6 months of burial. This shows that the clay is lightening not only the bone surface, but also infiltrating the surface to the cortex of the bone. The colour of both the bone surface and the cortex then darkens slightly prior to a plateau. For the duration of 0-18 months, the surface is always darker than the underlying bone.

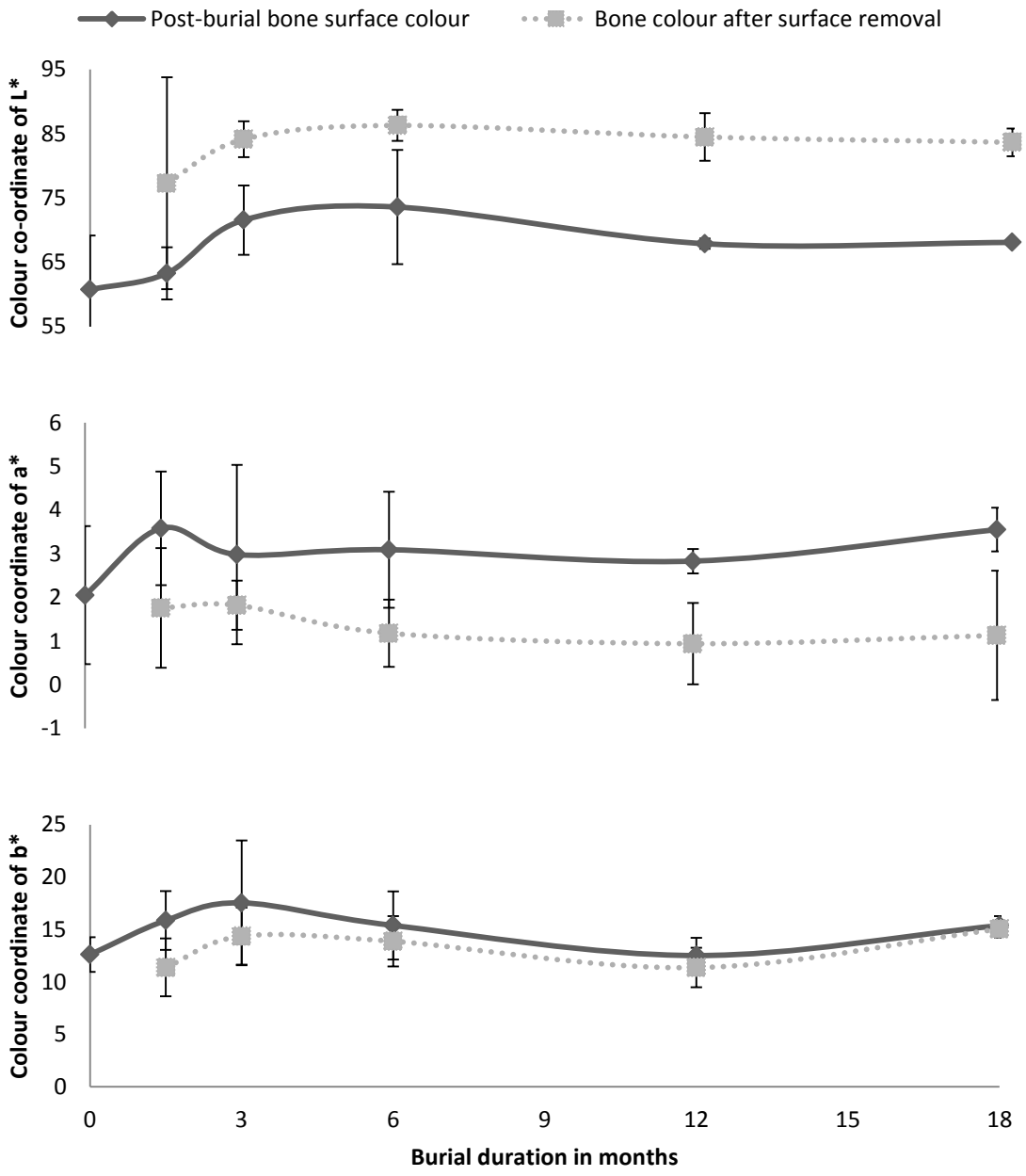

Figure 5-19: Colour data analysis of individual axes – L*, a*, and b* from clay burials, with a comparison between the colour of the bone before and after surface removal

The a* axis shows an initial increase in red in the surface colour of the bone until 1.5 months, where it then decreases again before levelling out with a slight incline towards 18 months. The colour of the bone after surface removal appears to mirror this trend, decreasing as the post-burial surface increases in red.

The third axis, b*, shows parallel similarities in the colour trend – with both increasing towards yellow until 3 months, before a gradual decrease until 12 months and a slight incline again towards 18 months. The longer the duration of burial, the more similar in colour, in terms of the b* axis, the outside surface and the cortex of the bone become.

5.2.2.1 Clay bone marrow colouration

As shown in Figure 5-16, bone marrow shortly after death is bright red due to the content of haematopoietic tissue. The images in Figure 5-20 show the changes that occur to bone marrow within porcine bones when buried in clay for 3-18 months.

Figure 5-20: Bone marrow from bones buried in clay; showing left to right – 3 months, 6 months, 12 months, 18 months

The bone marrow contained within the bone after burial for 3 months in clay, shows a loss of haematopoietic tissue, which has been replaced with adipose tissue, with a pink and cream colouration. From 6 months to 18 months burial, the bone marrow continues to darken, with the cream turning grey and resulting in a grey bone marrow with pink areas along the edges next to the bone.

5.2.3 Compost burial bones

The photographs in Figure 5-21 display the visual differences in the bone from the compost burials, from pre-burial to surface removal across the 18 month duration. The photographs show the mottled colour and texture of the bone, which is still evident after surface removal, which increases with the duration of burial. Areas

where soft tissue was still present are still pale in colour, where the bone surface was not in contact with the compost

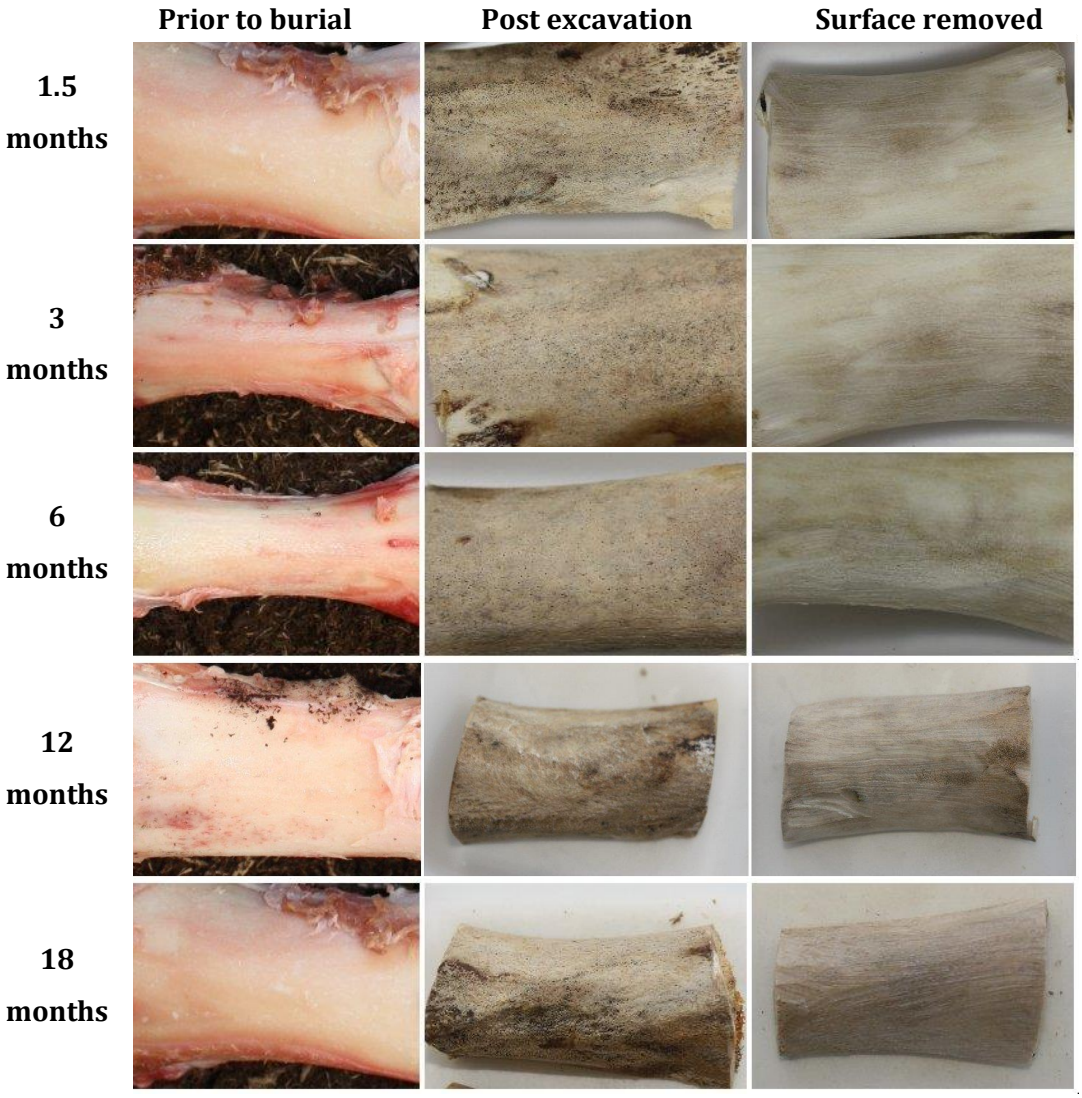

Figure 5-21: Photographs depicting the colour change of porcine bone from the compost environment over a period of 18 months

From the colourimetry data, the overall colour differences were calculated and the results are shown in Figure 5-22. The results show the largest difference in colour was present at 1.5 months between the surface of the bone after burial, and after surface removal; this was also accompanied by the largest difference in results, showing how the staining from the compost was mottled and therefore did not result in a uniform colour across the bone surface. This difference between post

burial and surface removal decreased throughout the duration from pre-burial to 18 months, showing how the colour was infiltrating down through the cortex as shown in the photographs.

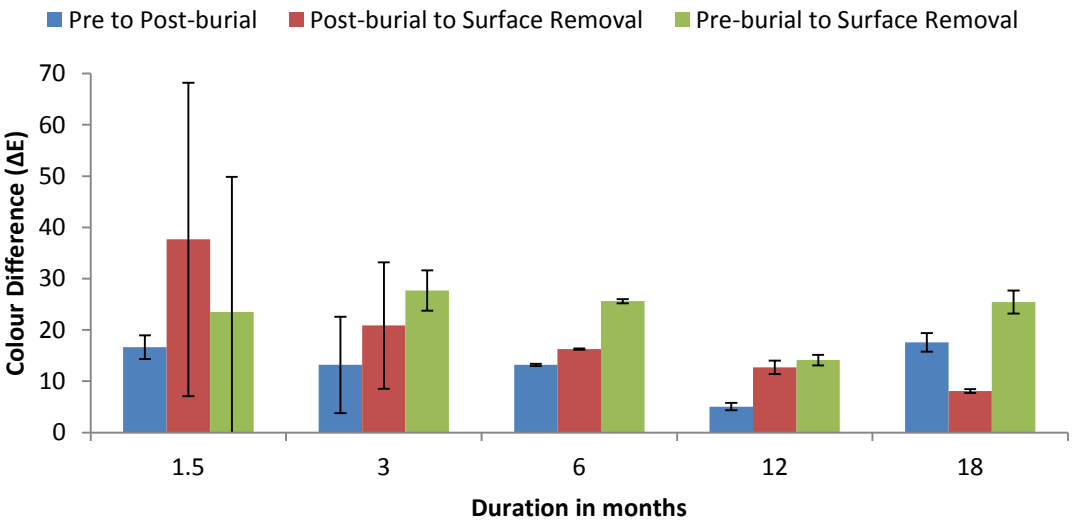

Figure 5-22: Overall colour differences of the bones buried in compost, over the 18 month period.

The difference shown between the pre-burial colour and after surface removal remained relatively constant throughout, suggesting the staining is due to the contact with the compost rather than internal processes of decomposition.

Overall colour differences from the surface of the bone from pre-burial to post-burial remained similar from 1.5 months to 6 months before a decline and then increased to its highest point at 18 months.

In order to get a more detailed picture of the direction in which the colour was changing, the three individual axes of the colour space were investigated and results of the colour values, as opposed to colour change are displayed in Figure 5-23. By comparing the post-burial surface colour and the bone colour after surface removal at the same, is possible to see how the burial type and duration affects the surface and any infiltration through the bone

The L* axis is detailed first, showing the post-burial bone surface becoming darker within the first 1.5 months where initial staining from the compost is taking place.

The level of staining then decreases at 3 months showing the bone becoming lighter again, and remaining relatively constant until 18 months, confirming observations from the photographs. The results from the surface removal are distinctly different, showing an almost mirror image of the post-burial surface becoming darker from 1.5 months with a dramatic darkening at 3 months, resulting in a cross-over of the data between 6 and 12 months, before another rise at the 18 month stage.

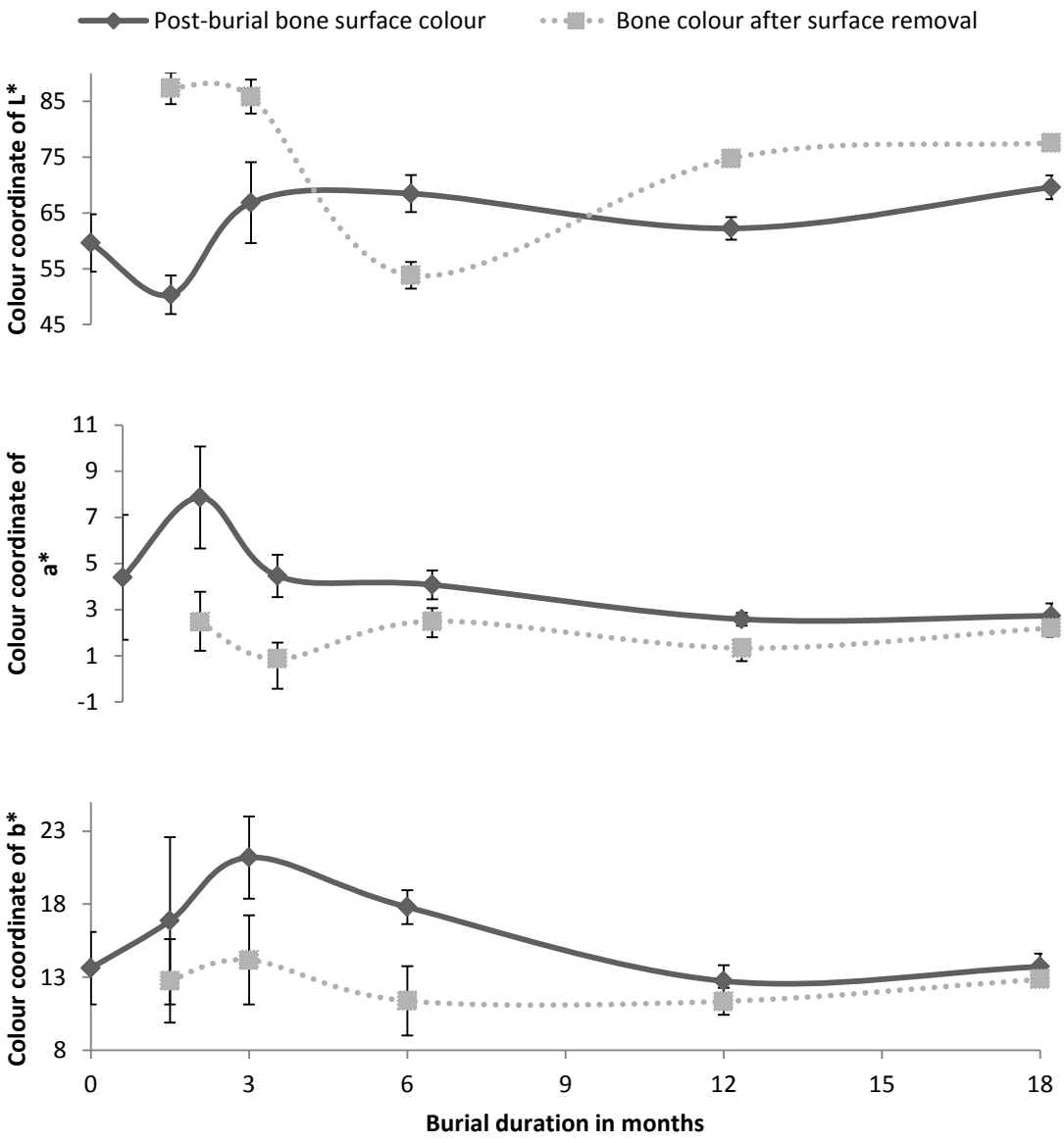

Figure 5-23: Colour data analysis of individual axis – L*, a*, and b* from compost burials, with a comparison between the colour of the bone before and after surface removal

The a* axis show the bone surface becoming more red from pre-burial to 1.5 months, before a decrease at 3 months moving towards to green, and a gradual decrease until 18 months. This pattern is matched by the data after surface removal.

The final axis of b* shows a steep increase in the yellowness of the bone from pre-burial to 3 months, before a gradual decrease to 12 months and a slight increase to 18 months. This pattern is also matched by the colour after surface removal but to a much less extent.

5.2.3.1 Compost bone marrow colouration

The photographs displayed in Figure 5-24 show the changes in bone marrow after 3 to 18 months burial in compost.

Figure 5-24: Bone marrow from bones buried in compost; showing left to right – 3 months, 6 months, 12 months, 18 months

After 3 months, the bone marrow had turned cream and orange, showing the loss of haematopoietic tissue. The bone marrow from the 6 month burials showed further degradation of the cells with brown colouration appearing with the orange and cream, before the grey colouration at 12 months. After 18 months burial, the bone marrow had turned dark orange in colour with dark brown and black areas.

5.2.4 Lime burial bones

The photographs showing the visual changes in the bone from the lime burials are depicted in Figure 5-25. The photographs showing the post-burial image of the bone at 1.5 months show the presence of not only soft tissue, but also wet blood that dispersed when the soft tissue was disturbed during cleaning of the bone. After surface removal of the bone, this blood can still be seen on the bone, where blood vessels have been broken.

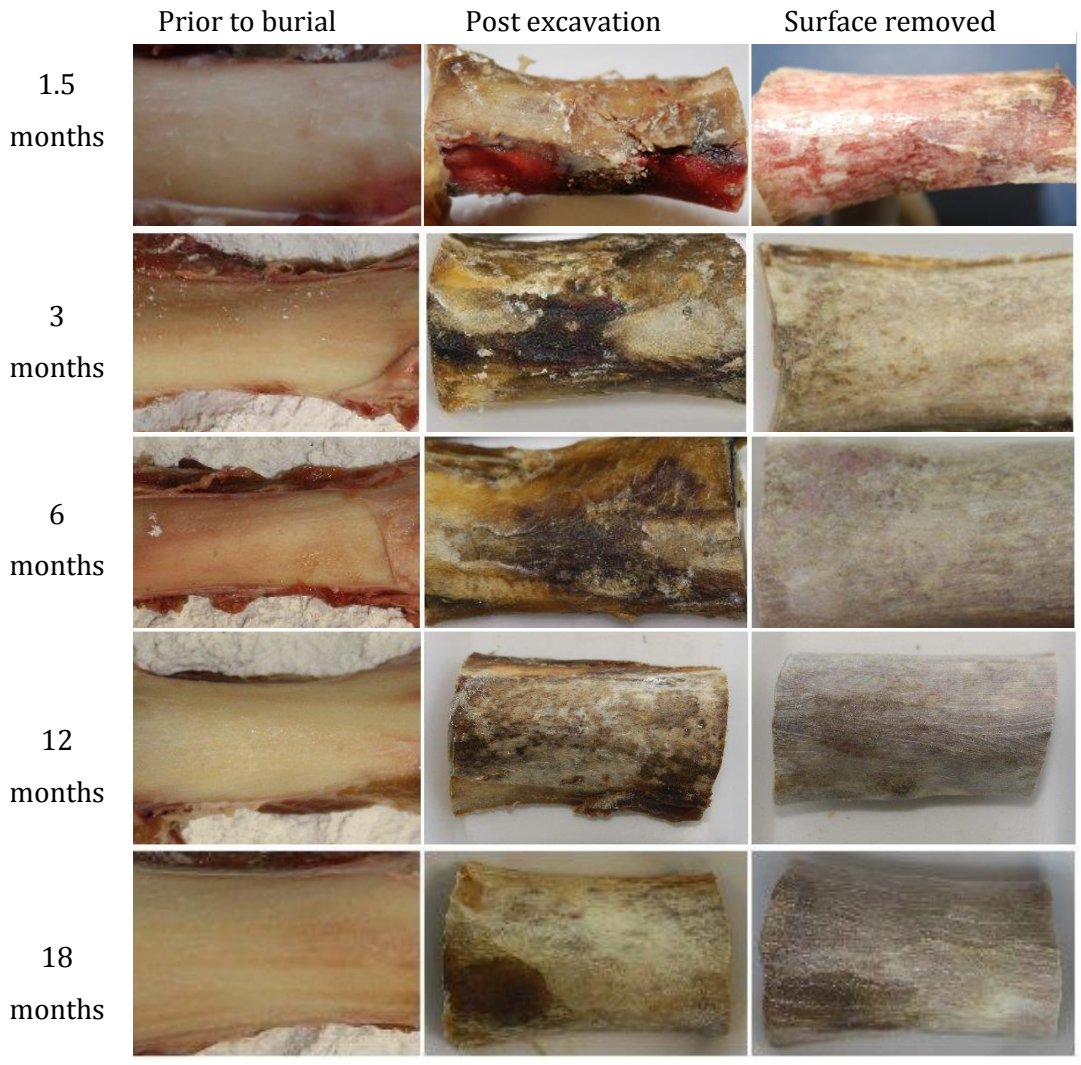

Figure 5-25: Photographs depicting the colour change of porcine bone from the lime environment over a period of 18 months

The preservation of the soft tissue continued throughout the burials and was still present, albeit dried, at the 18 month burial. The photographs depict how the colour change at post-excavation appeared to be mainly due to the soft tissue decomposition. The surface removal photographs show a gradual increase in the darkening and colouration of the bone through the 18 months.

The total colour change between the different time points were investigated, to establish when the biggest colour change occurred, the results are shown in Figure 5-26.

The biggest total colour difference can be seen at 1.5 months between the colour of the post-burial surface and colour after the surface removal. This value then decreases dramatically at 3 months, followed by small fluctuations until 18 months. This confirms the information presented in the photographs.

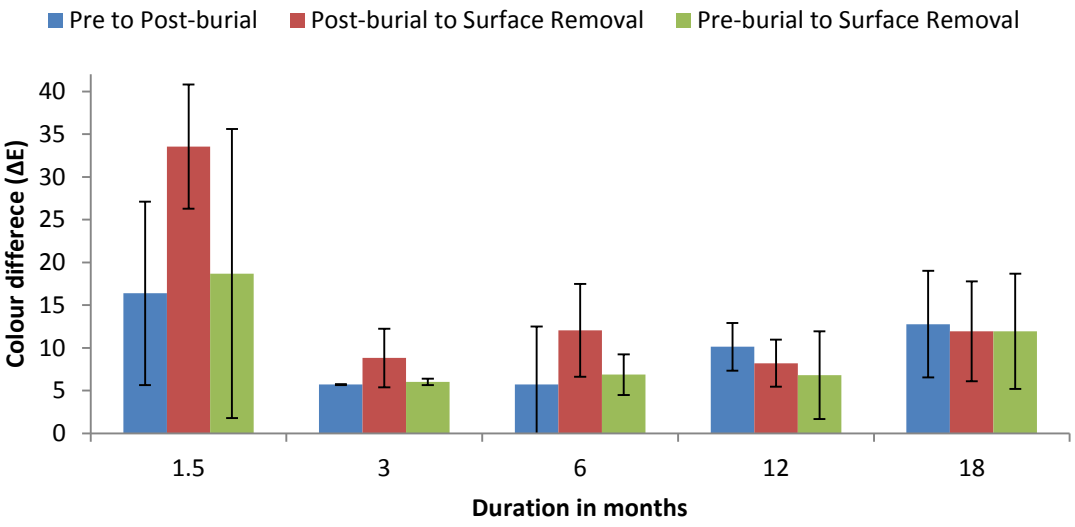

Figure 5-26: Overall colour differences of the bones buried in lime, over the 18 month period.

The difference in pre to post-burial surface colour is biggest at the 1.5 month burials, primarily due to the presence of soft tissue and blood. This value then decreases at 3 months before another increase up until 18 months where it is the largest difference between the analyses at that point.

Total colour difference between the pre-burial surface colour and the surface removal is also largest at 1.5 months, with a decrease at months and another increase at the 18 month burials.

The individual axes of the colour analysis were also investigated to provide a more comprehensive understanding of the manner of the colour change across the burials, as shown in Figure 5-27.

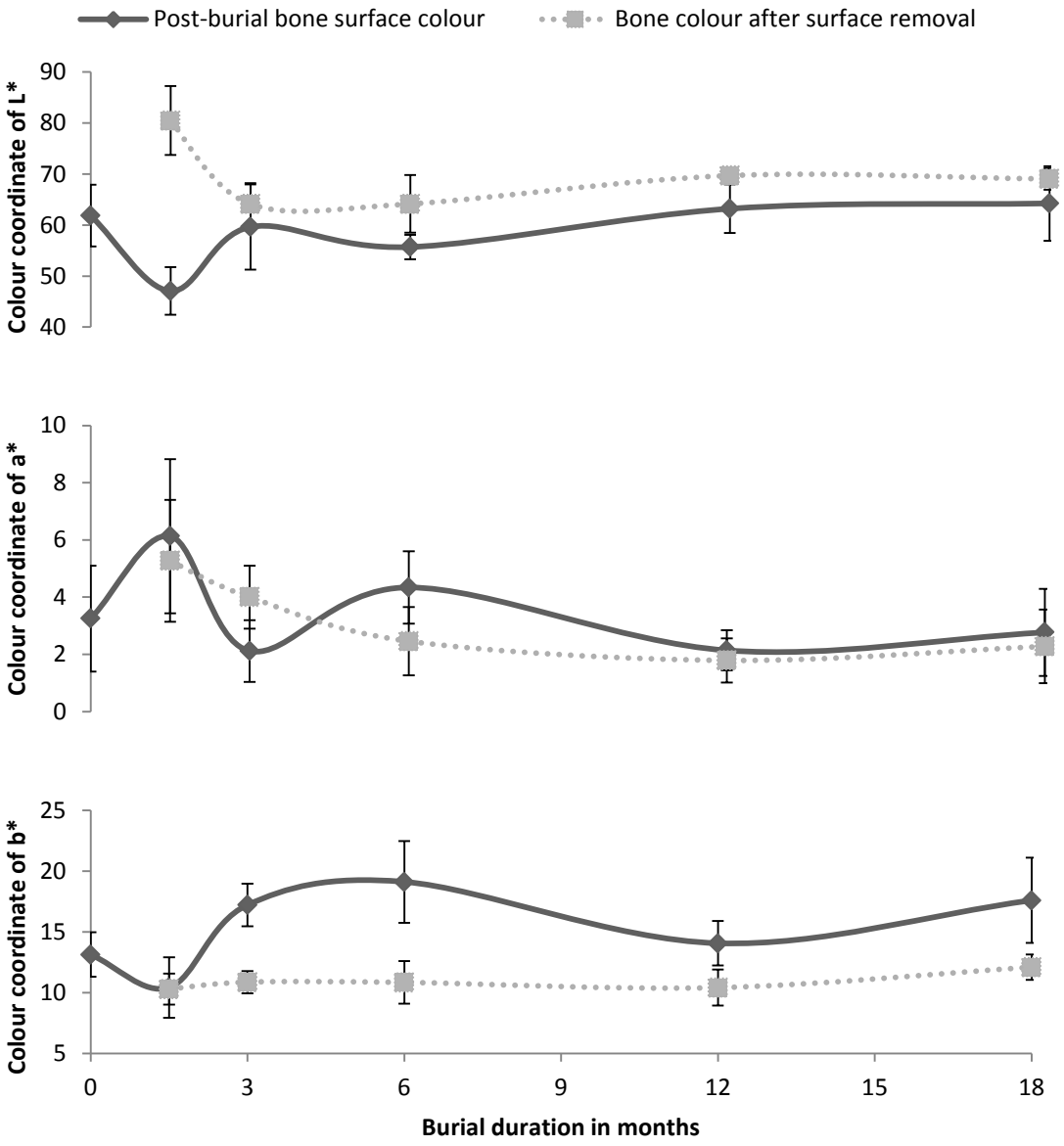

Figure 5-27: Colour data analysis of individual axis – L*, a*, and b* from lime burials, with a comparison between the colour of the bone before and after surface removal

On the L* axis, the largest difference in colour change of the post-burial bone surface colour was between pre-burial and 1.5 months where the bone became darker. The 3 month burial showed an increase in lightness, which increased until 18 months with a slight fluctuation at 3 months. The colour after surface removal showed an initial darkening between 1.5 and 3 months before a steady increase parallel to the post-burial surface colour.

The a* axis displayed a variable colour change in the post-burial surface colour, varying from an increase in red from pre-burial to 1.5 months, as seen by the presence of blood, to a decrease at 3 months moving towards green, another increase at 6 months, before running parallel to the surface removal colour from 12 to 18 months. The surface removal colour showed an exponential decrease from red towards green from 1.5 months through to 18 months, due to haemoglobin decomposition.

Analysis of the b* axis showed an initial decrease in yellow from pre-burial to 1.5 months, before doubling in value towards yellow until 6 months, before a slight decrease and final rise at 18 months. The colour after surface removal remained consistent in comparison, with the only difference in units observed at 18 months with an increase towards yellow, which could be attributed to the decomposition of the adipose tissue.

5.2.4.1 Lime bone marrow colouration

The visual changes in the colour of the bone marrow from the lime burials can be seen in Figure 5-28. Traces of haematopoietic tissue can still be seen at 3 months – although degraded as shown by the brown and purple colouration rather than red.

Figure 5-28: Bone marrow from bones buried in lime; showing left to right – 3 months, 6 months, 12 months, 18 months

The marrow at the 6 month burial, appeared to contain pink, purple, cream and yellow areas, which change to orange, grey and purple at 12 months, and just orange and at 18 months.

5.2.5 Sand burial bones

The photographs from the observed visual changes in the bones from the sand burials are displayed in Figure 5-29.

The photographs show how a dark uniform staining of the bones occurred during the burial, from 1.5 months through to 18 months. The surface of the bone appeared porous, and very dry with a rough texture.

Once the surface had been removed, a paler area was uncovered, although staining is still evident in places, especially from the 18 month burial. The texture of the bone appeared smoother to that of the post-burial surface.

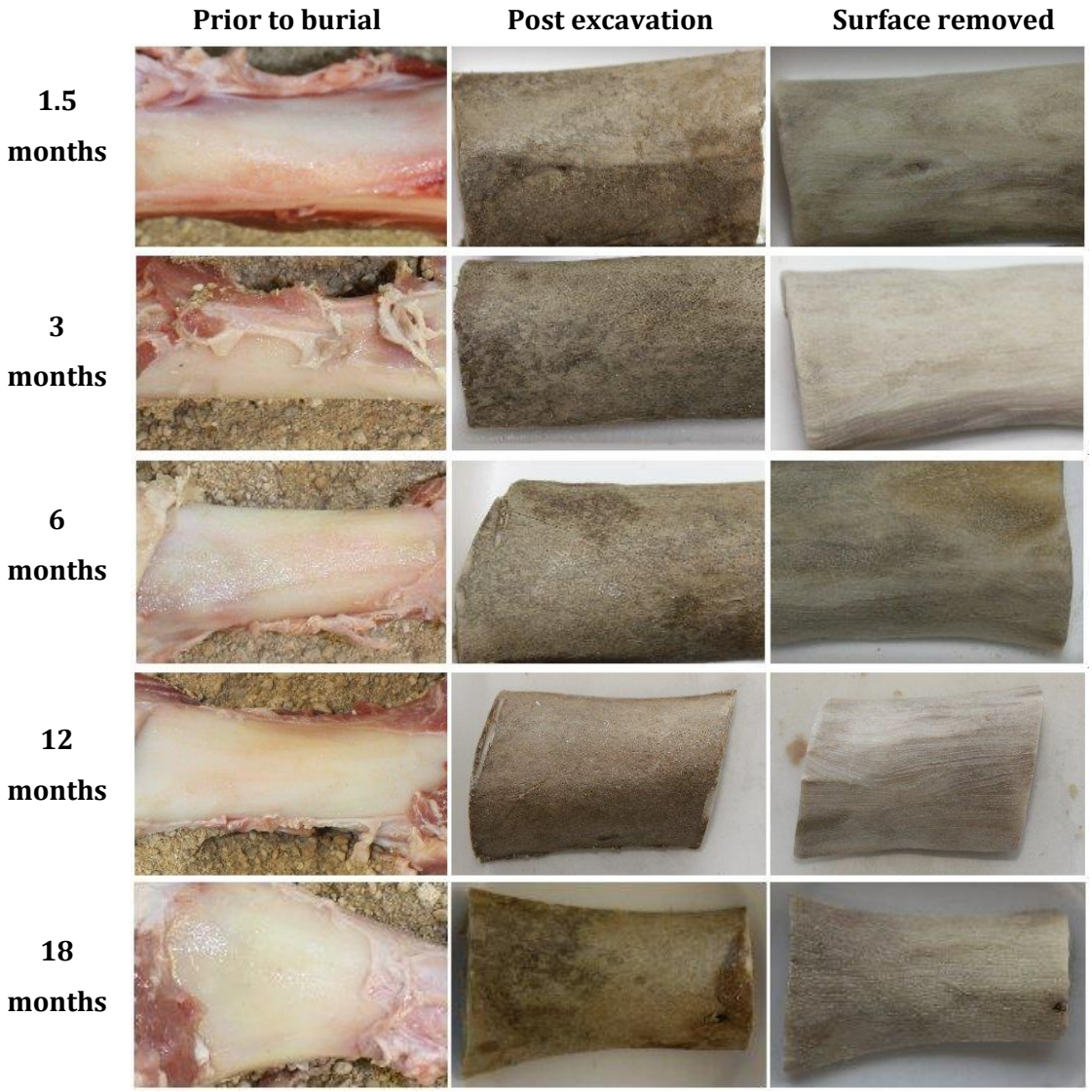

Figure 5-29: Photographs depicting the colour change of porcine bone from the sand environment over a period of 18 months

The results from the total colour difference analysis are displayed in Figure 5-30, and show the biggest difference can be seen between the post-burial surface and once the surface had been removed. This difference is largest at 1.5 months, and can be seen to steadily decrease across the whole duration until 18 months. This shows how the colour staining is gradually infiltrating the cortex of the bone through the surface.

The difference in colour between the pre-burial surface and post-burial surface remains relatively constant for the first 6 months, with decreased difference showing at 12 and 18 months.

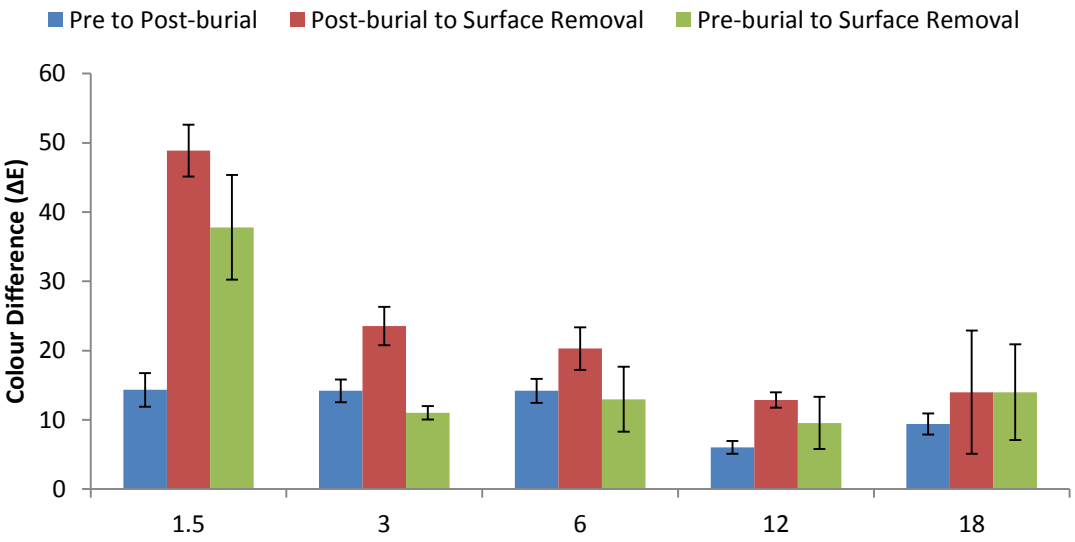

Figure 5-30: Overall colour differences of the bones buried in sand, over the 18 month period

The biggest difference between the colour of the pre-burial surface of the bone, and after surface removal is seen at 1.5 months, decreasing at 3 months and then fluctuating until 18 months.

The individual axes were then assessed to identify the direction in which the colour change was occurring. Figure 5-31 displays the colours recorded on the L*, a* and b* axes.

The L* axis shows an initial darkening of the bone colour from 0-1.5 months, where it remains around the same until an increase in lightness around 12 months and a slight decrease at 18 months. The lightness of the bone after the surface removal, showed a similar pattern but with a larger initial decrease seen from 1.5 months to 3 months. The difference in the pattern between the post-burial surface and after removal, suggests more changes are occurring internally than on the surface.

Values from the analysis of the a* axis can be seen to make a big increase towards red from 0 to 1.5 months for the post burial bone surface colour. This could indicate a rapid period of decomposition from the presence of bacteria, causing the colour to become greener. The pattern of colour fluctuations on this axis, are mirrored by those of the colour of bone after surface removal.

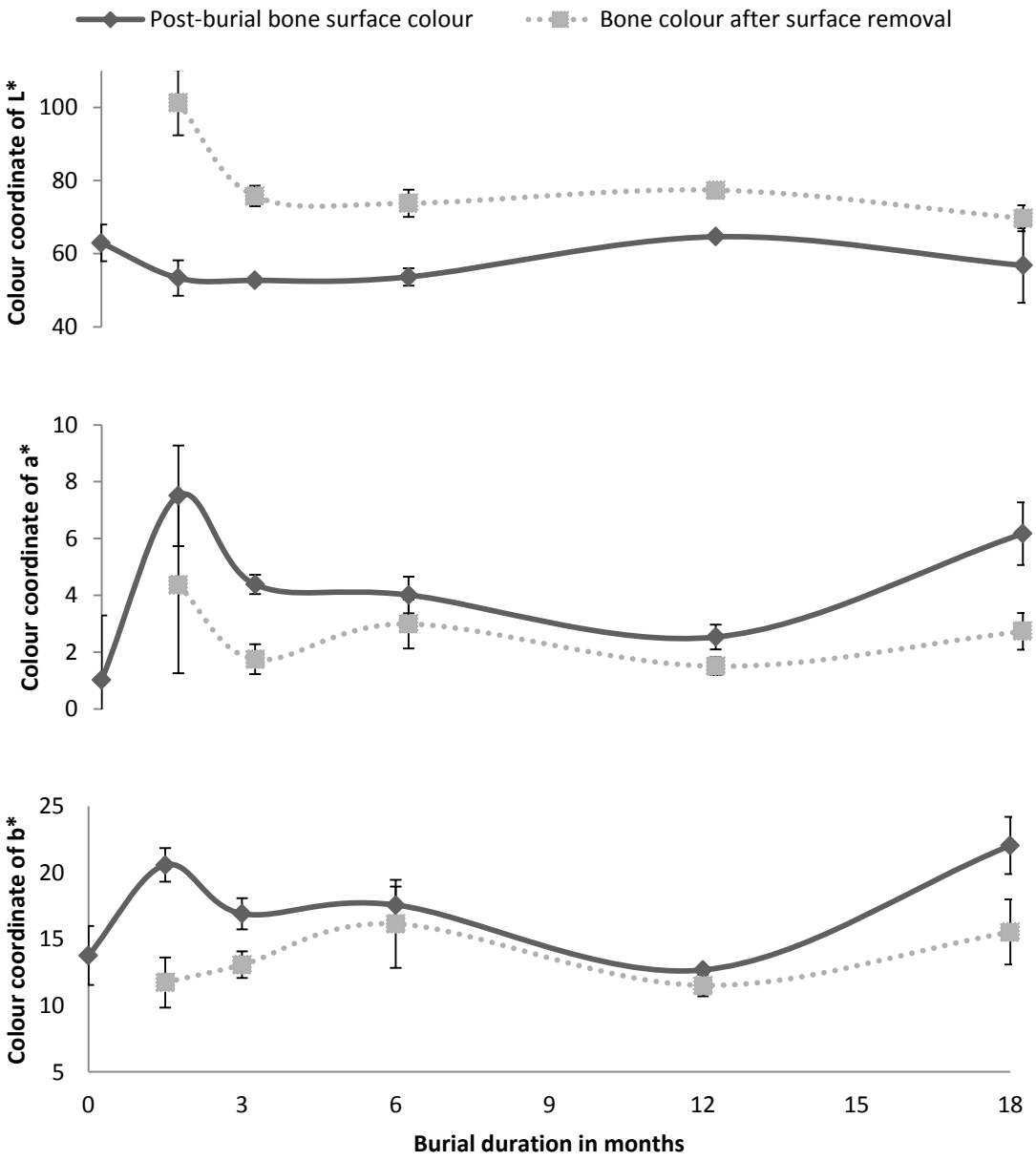

Figure 5-31: Colour data analysis of individual axis – L*, a*, and b* from sand burials, with a comparison between the colour of the bone before and after surface removal

Analysis of the b* axis showed resemblance not only between the post-burial surface and surface removed colour, but also to the a* axis. The increase in yellow at 1.5 months could indicate the presence of yellow decomposition fluid on the outside of the bone, which is not present within the bone, whereas the increase in both measurements at 18 months could indicate the decomposition of adipose tissue from inside of the bone.

5.2.5.1 Sand bone marrow colouration

The photographs of the colour changes in bone marrow from sand burials are shown in Figure 5-32.

Figure 5-32: Bone marrow from bones buried in sand; showing left to right – 3 months, 6 months, 12 months, 18 months

The bone marrow from 3 months of burial shows a dark red and purple colouration, suggesting the presence of degraded haematopoietic tissue. After 6 months the red colouration has gone and is replaced with purple and brown. The 12 month burial shows the bone marrow to be of a purple, pink and cream colour, before a purple, pink, brown and pink colouration at 18 months.

5.2.6 Colour analysis comparisons across environments

The results from the colour analysis were then collated in order to compare how the different burial environments affect the colour change in the bones, and how this relates to an unburied control. Total colour difference between pre-burial and post-burial colour was looked at first, with the results shown in Figure 5-33. For purposes of clarity of the figure, the standard deviation error bars have been omitted, but can be found on previous figures in this chapter.

All four burial environments and the control bone showed different trends in the amount of total colour difference that occurred during the 18 month period, although some similarities can be observed.

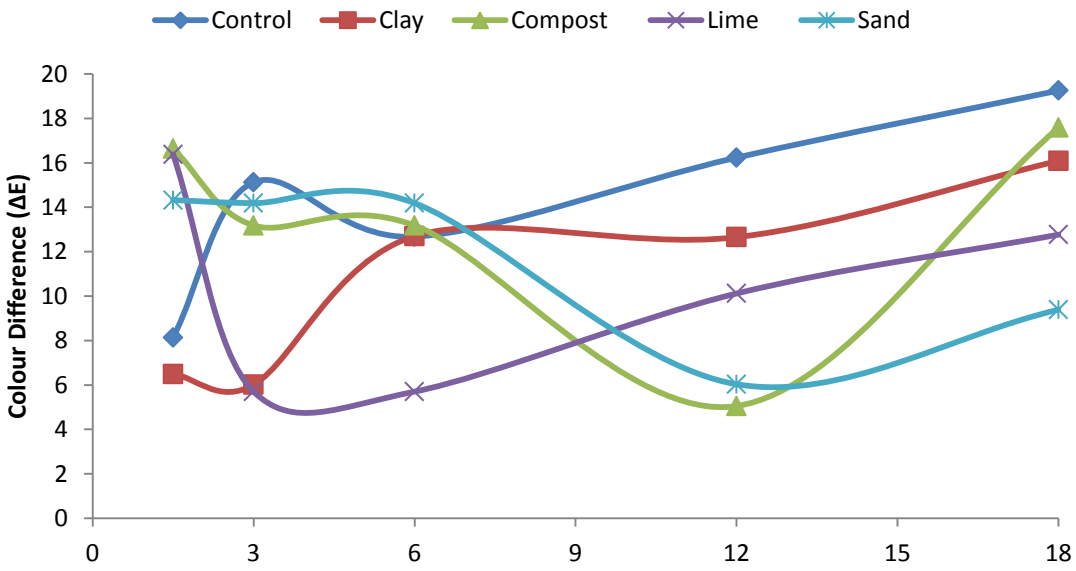

Figure 5-33: Total colour difference: pre to post burial surface colour

The compost, lime and sand burials show their highest colour difference between pre-burial and post-burial colour at 1.5 months, suggesting an aggressive attack on the bone surface from the environment. The differences observed in colour of the bones at this interval can be seen in Figure 5-34.

Figure 5-34: Comparison of the colour of bone sections after 1.5 months of burial from the control and experimental burials

In contrast to the compost, lime and sand bones, the colour difference shown at 1.5 months for the control bones, and those from the clay environment show a much smaller difference, which increases with time over the 18 month duration, suggesting a much slower diagenetic rate of the bone surface. From 3 months, the colour difference from the bones in compost and sand behave similarly, with a stabilising of colour for 3 months prior to a reduction in colour change for the next 6 months. An increase is evident from both environments from 12 – 18 months but with a much bigger difference seen in the compost environment. The colour difference evident on the bone surface from the lime environment is almost opposite to that shown in the control sample within the first 6 months, with the biggest difference occurring at 1.5 months, with a significant drop at 3 months followed by a steady increase in difference to 18 months, running parallel to the control bone.

The colour difference between the surface of the post-burial bones and once removal had occurred was also compared to understand whether colour penetration was occurring from the burial environments. The results are shown in Figure 5-35.

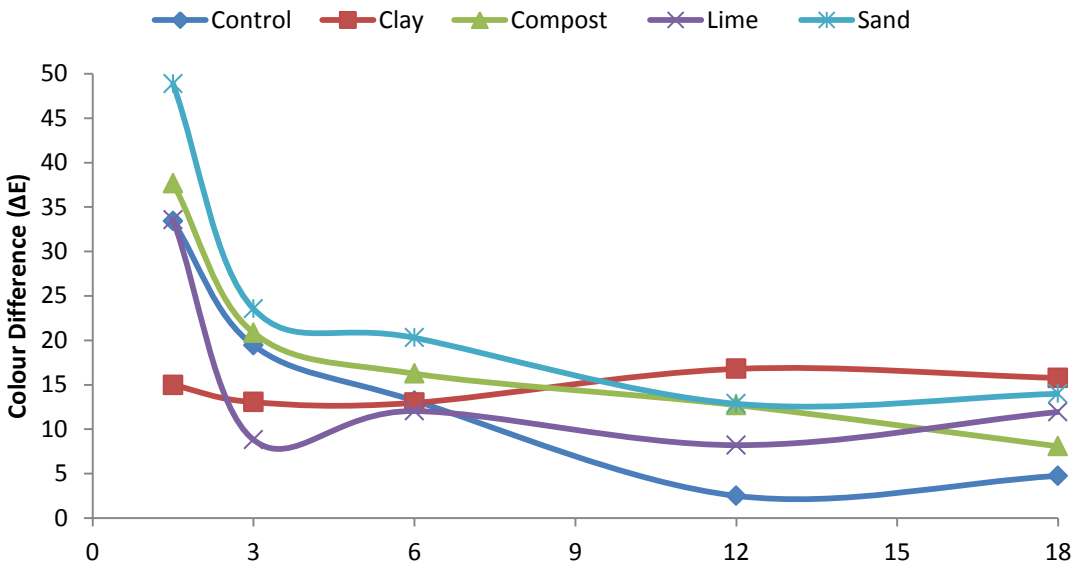

Figure 5-35: Total colour difference: post burial to surface removal

The biggest total colour difference between the post-burial surface and post-removal, was seen after 1.5 months in all environments apart from the bones from the clay environment. This colour difference then followed a trend with a large decrease to 3 months and then a steady decline for the control bones, and bones from the compost, lime and sand environments. The clay data displays a different trend, with the colour difference remaining relatively stable with an increase from 6 months, opposite from the other environments. This analysis suggests that either contaminants from the clay environment take longer to penetrate the surface of the bone, or different intrinsic processes are occurring within the bone due to the clay in order for a smaller colour difference showing above and below the bone surface.

Another way to look at the data is to examine how the difference in colour between the pre-burial surface and post-removal, is affected by different environments, as shown in Figure 5-36. In this incidence, similarities in value and trend are shown between the control bones and those from the compost environment. The sand and lime burials also show distinct similarities with an initial decline from a high value between 1.5 months and 3 months before a gradual increase until 18

months. Once again, the bones from the clay environment show a different trend to all the other environments, with an initial decrease between 1.5 months and 3 months before a steady increase where the largest colour difference is seen at 18 months.

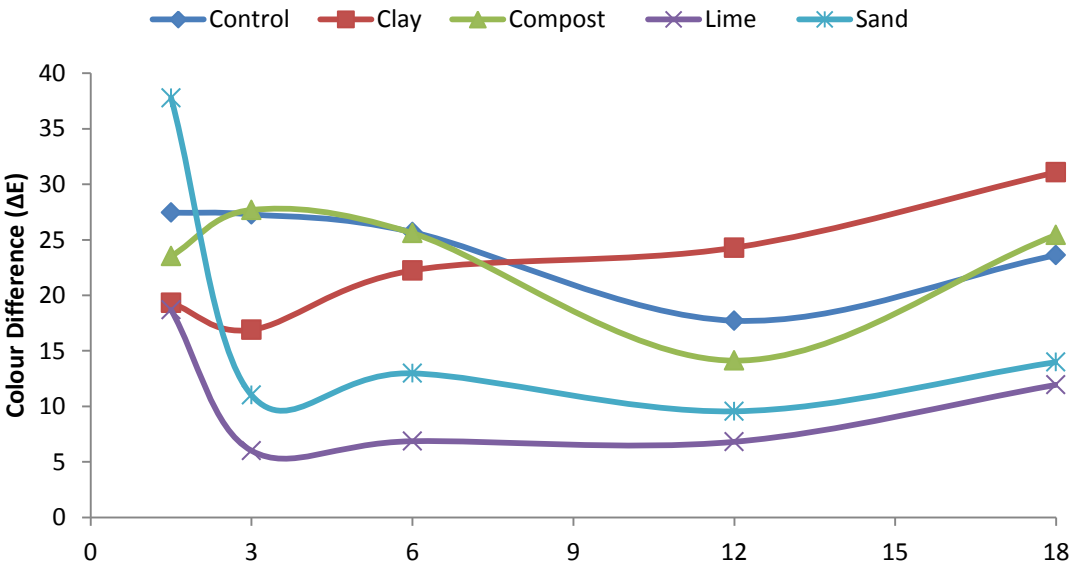

Figure 5-36: Total colour difference: pre-burial to surface removal

These differences confirm that the diagenetic processes occurring within the bone are influenced by the burial environment, and results in colour changes that are not only different to each other, but also to those of the control bone. The individual analysis of the axes - L*, a* and b* were also compared across the different burial environments and to the control bones, as shown in Figure 5-37.

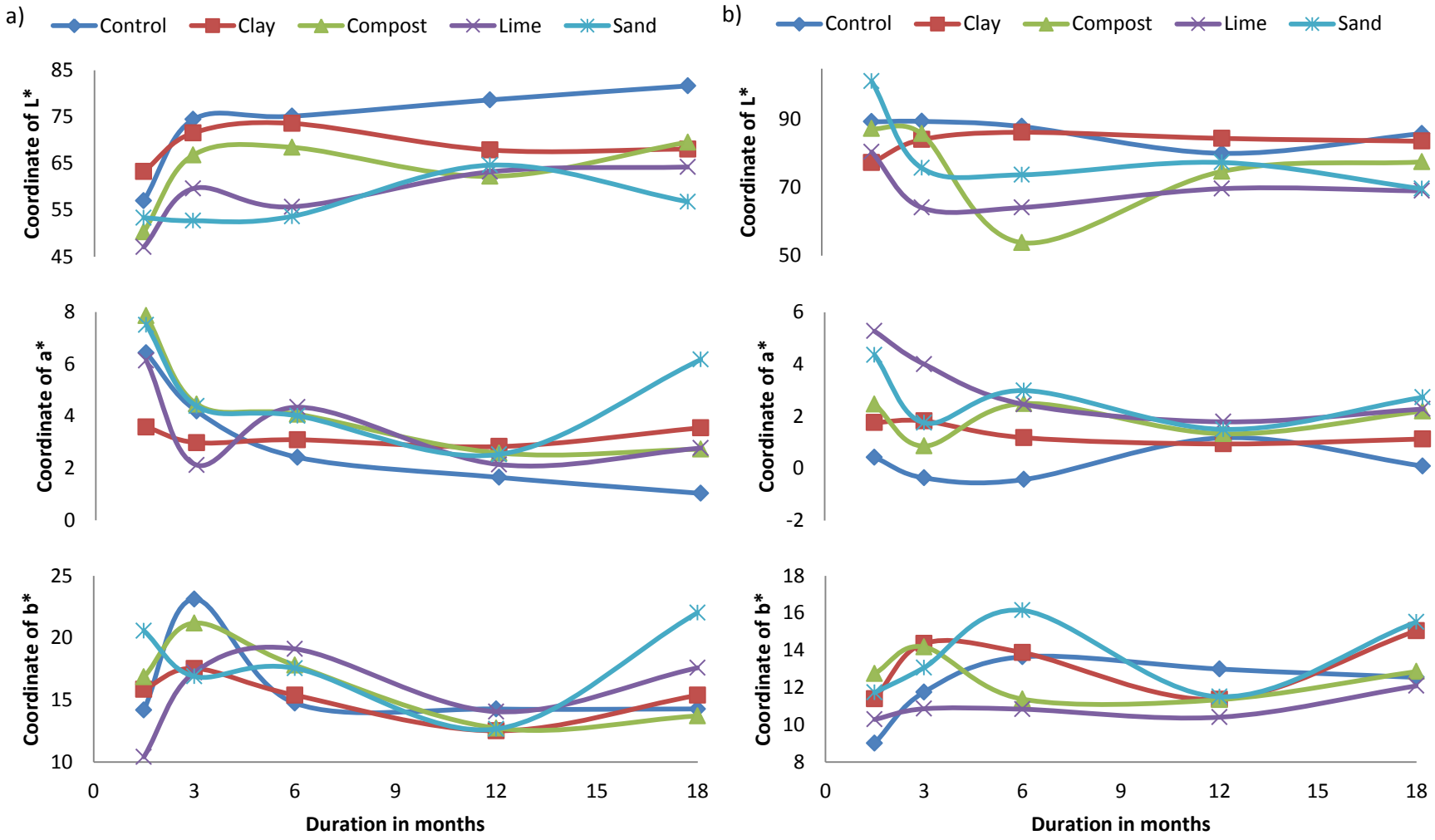

Figure 5-37: Individual axes coordinates of L*, a* and b* for a) Post-burial colour and b) Post-surface removal colour

The post burial colour data on the L* axis shows the control bone is the lightest of all the samples, and shows increase in lightness from all the way from 1.5 to 18 months with the biggest change occurring between 1.5 and 3 months. The clay and compost show a very similar trend – with intense lightening between 1.5 and 3 months then slightly darker between 6 and 12 months before the compost bones displaying a lighter colour at 18 months. The sand samples show the darkest colour at 3 to 6 months prior to becoming lighter at 12 months, and darker by 18 months. Lime shows initial lightening like control, clay and compost, darkening slightly at 6 months before a gradual lightening 6-18 months.

On the a* axis, the control sample shows a continual drop in red towards the green end of the spectrum from 1.5 months through to 18 months. This can be explained by the increase in bacteria causing the breakdown of the haemoglobin present within the bone, causing the production of hydrogen sulphide. Once again, this trend in the control bones is different to all the buried samples. The clay samples show the least variable of the samples, with only slight fluctuations, whereas sand shows the most variation with a steep decrease from 1.5 months to 3 months, a further decrease to 12 months before an increase to 18 months to almost the same redness at 1.5 months. The compost, lime and sand show similar trends within the first 12 months, with a reduction in the red colour, starting with a larger change initially.

Results from the analysis of the b* axis, showed the control bone having the most dramatic change between 1.5 and 3 months, moving further towards the yellow end of the spectrum, this value then dropped again and remained relatively constant until 18 months. The clay and compost showed the most similarities to the control samples, but with a less intense change at 3 months, followed by a reduction to 12 months and both displayed an increase in yellow up to 18 months. This increase in yellow could be explained by the presence of yellow decomposition fluid, released as decomposition progresses. The lime samples can be seen to be less yellow than all the other samples at 1.5 months, with an increase at 6 months – later than the control, compost and clay, followed by a decrease at 12

months and another increase in yellow at 18 months. The sand samples are the only bones that displayed a reduction in yellow at 3 months, and after a further decrease at 12 months, the degree of yellow then increased higher than all the other samples at 18 months.

The results from the post-surface removal colour show some similarities, but also big differences in the colour direction on the axes. The control sample on the L* axis shows a steady decrease in lightness from 1.5 months through to 12 months with a slight increase up to 18 months. The clay samples show the least variance, with a slight increase up to 6 months, where it then remains constant throughout. The lime and sand samples show similarities with an initial darkening from 1.5 to 3 months and then a steady lightening until 12 months, where sand then begins to darken again. The compost samples showed the largest variance with only a slight change between 1.5 months and 3 months, but then a dramatic darkening at 6 months, and an increase to 18 months, where the results is in the middle of all samples.

The analysis of the a* axis showed the control sample reducing in red onto the green half of the scale at 3 months, where it remained apart from a slight increase to red at 12 months. The sand and compost showed the most similarities running parallel in trend throughout, both moving towards green at 3 months and then fluctuating until 18 months. Clay showed the least variance, remaining just on the red side of the scale for the duration. The lime samples were the only samples which showed a continual smooth decrease in redness from 1.5 months to 18 months.

The control sample on the b* axis showed a slow increase in yellow prior to 6 months before slowly decreasing slightly to 18 months. The lime samples showed the least variance, with the biggest change 12 to 18 months. The sand samples were most similar to the control samples in the first 6 months, but followed with a fluctuation resulting in an increase at 18 months. Compost and clay both displayed an increase between 1.5 months and 3 months, reaching the peak of yellow earlier than the other samples.

5.2.6.1 Changes observed in bone marrow

The colour changes observed in the bone marrow, varied between the different environments. The fresh bone marrow displayed the bright red colour of haematopoietic tissue, which changed within the first 1.5 months in all burials but to different extents. The sand showed the least evidence of decomposition, with a dark red composition showing presence of haematopoietic tissue, but darkened from the autolysis of the tissue, due to the shrinking and darkening of the nuclei cells (Tattoli et al., 2014).

The bone marrow in the clay and lime burials displayed pink and cream colouration, suggesting the overriding presence of adipose tissue rather than haematopoietic tissue. The decomposition process of the bone marrow appears to then change to purple, grey, orange, brown and black, although some stages appear to be absent in certain conditions.

Bones from the compost environment appear to have the biggest change with evidence of black tissue suggesting putrefaction has occurred and also the drying out of tissue which is reportedly the last stage in decomposition. The lime bones then appear to be the most advanced decomposition with orange bone marrow, followed by clay at grey, with the least changes seen in the sand bone marrow with a colour of brown.

A lack of forensic research published on the detailed colour changes in bone marrow, results in the lack of comparison, however research into the different packaging of meat products provides a colour scale of bone marrow in a low oxygen environment. Grobbel et al. (2006) reported seven different stages of bone marrow colouration as depicted in Figure 5-38.

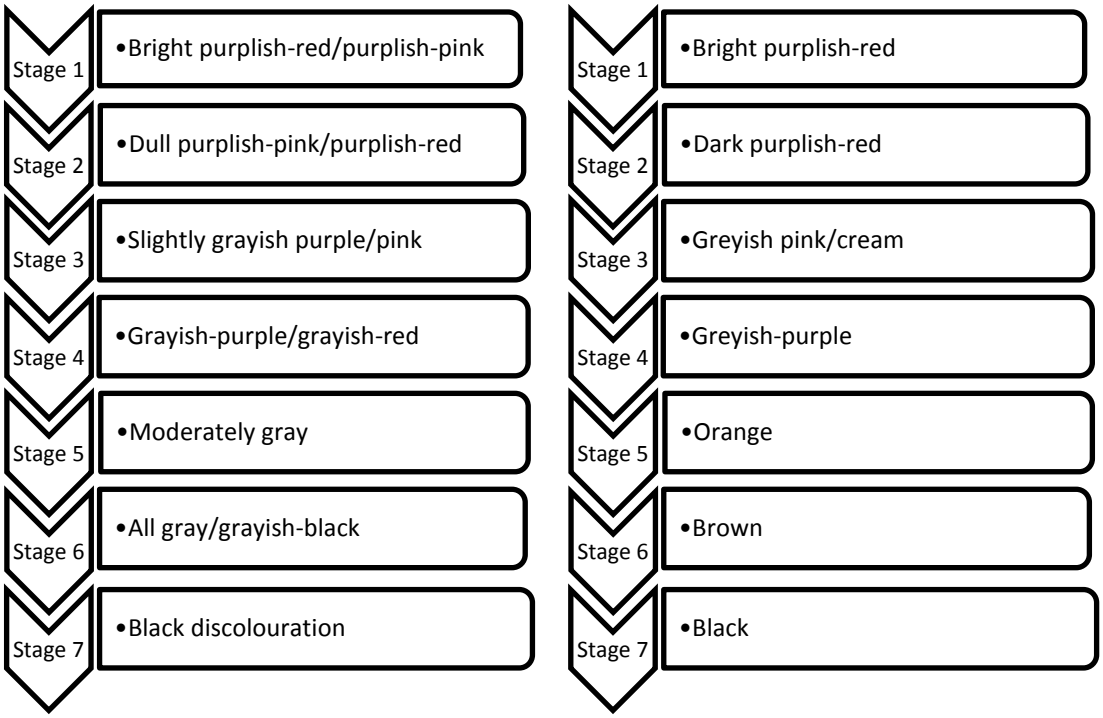

Figure 5-38: Colour changes in bone marrow as described by Grobbel et al., 2006 on the left; Visual observations from the decomposition of porcine bones from this research, on the right

No orange or brown stages were mentioned in the research by Grobbel et al., however, the research was conducted over a period of only four days and the conditions were different, therefore decomposition of the soft tissues would not have occurred to the same extent. Based on these results, more support can be given to the earlier observations from the bone marrow colouration, in relation to the process of decomposition.

5.3 Composition Analysis

The investigation into the composition of the bones was conducted using FTIR-ATR as discussed in 4.1.11.2, to estimate the diagenetic changes that have occurred within the bone, in relation to the different environments. The results are displayed together in order to allow direct comparison across the different environments, and to the results on the unburied control samples. The complete data sets are presented in Appendix A, with standard deviations from the mean. The results displayed in Figure 5-39 show the average of the sample results.

The diagenetic changes of the bones were investigated by assessing the crystallinity of the mineral, (splitting factor) the collagen content (Amide/Phosphate) and the carbonate content (Carbonate/Phosphate), as discussed in Chapter 4. Researchers have commonly used these parameters to assess diagenesis in archaeological bones (Weiner and Bar-Yosef, 1990; Price et al., 1992; Sosa et al., 2013) including Stiner et al (1995) who observed no difference in splitting factor and carbonate content between burned and unburned archaeological bones. Since this time, others have simulated artificial diagenesis by heating bones in order to develop an understanding of the changes that occur. As a general rule, it has been found that the splitting factor increases with diagenesis, and the collagen content and carbonate content both decrease (Fredericks et al., 2012; Hollund et al., 2013).

The splitting factor is a quantitative measurement of the crystalline structure of the mineral (hydroxyapatite) in bone, as determined by the ratio of the phosphate absorption bands. Researchers have estimated that the splitting factor of modern bone samples range between 2.5-2.9 (Stiner et al., 1995; Hollund et al., 2013). Hydroxyapatite has a poorly crystalline structure due to small crystal size and irregularities in the lattice such as ion substitutions, but becomes more crystalline as a result of diagenesis. For this reason, it was expected that the splitting factor would increase in all samples over the duration of 18 months.

The results from the control bones show a steady increase in splitting factor from fresh bone to 3 months, before a plateauing around 3 months to 18 months.

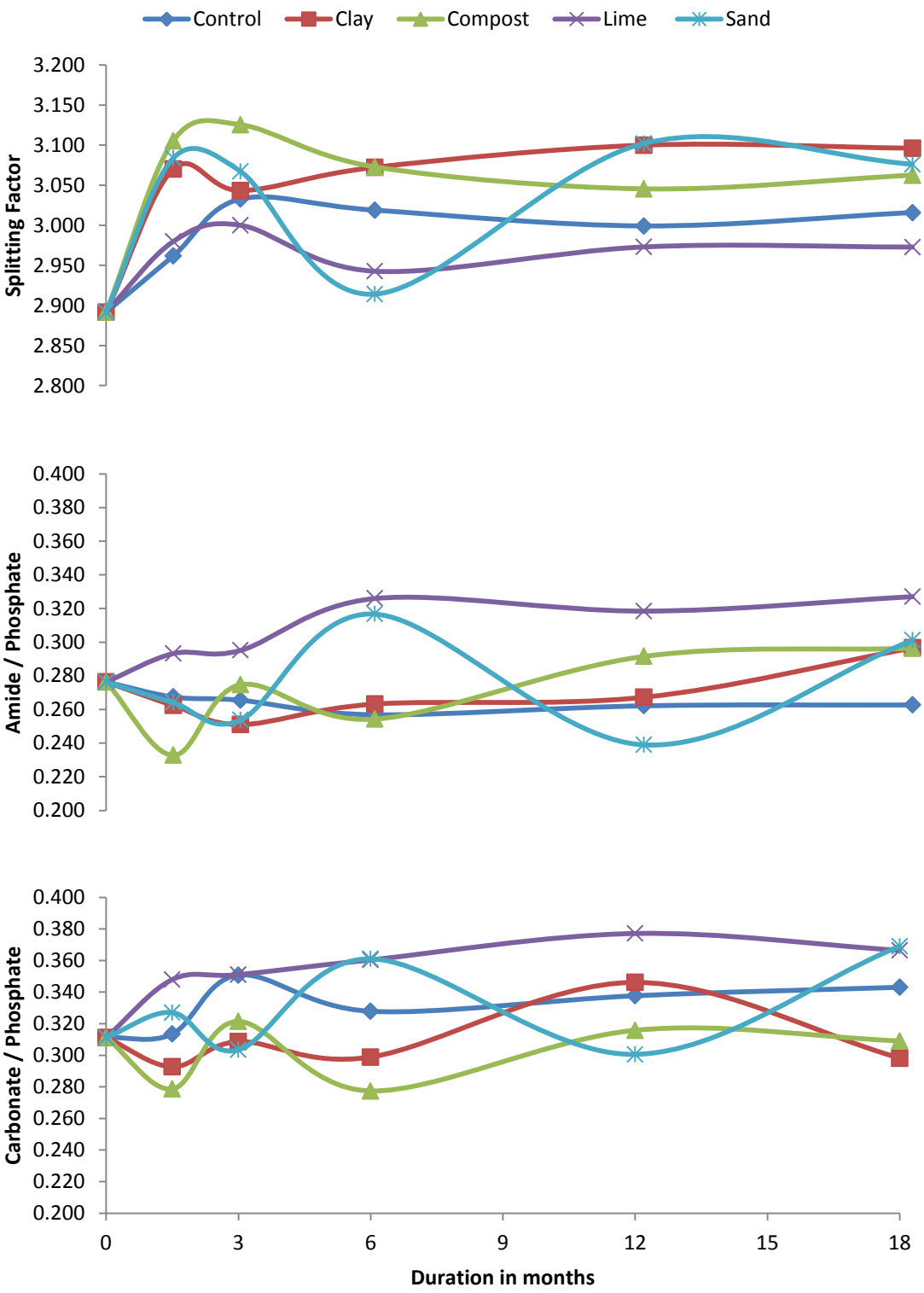

Figure 5-39: Splitting factor, amide/phosphate, and carbonate/phosphate of control and experimental porcine bones

The buried bones all showed variances in the degree of change of the splitting factor, but all showed an initial increase in the first 1.5 months. The bones from the sand environment showed the biggest difference from the control bones, with a decrease in splitting factor back to that of a fresh bone, at 6 months. The bones from the clay environment showed the largest increase in splitting factor, supposedly showing a higher degree of diagenesis, contradicting the findings of Weiner and Bar-Yosef (1990) who found that despite no direct correlation was found between bone preservation and sediment type, bones that had contact with clay deposits were better preserved. However, Price et al (1992) detailed how the presence of water in an environment encourages the action of microorganisms in destruction of apatite mineral, therefore as the clay environment had the highest water content, the change in crystallinity may be due to water presence rather the clay itself. Bones from the lime environment showed the highest degree of preservation with the lowest splitting factor, even lower than that of the control bones.

The Amide / Phosphate ratio can be used as an indication of collagen in a bone sample, as when the collagen denatures, the Amide I band will also decrease. Not much information has been cited in the literature, in terms of expected values, but Hollund et al (2013) reports bones one year after death should be between 0.2 and 0.8 and decrease with a larger post-mortem interval. This decrease in content can be seen in the control bones across the 18 month duration. The biggest deviation from this trend can be seen in the bones from the lime environment, which showed an increase throughout the burials. The bones from the sand environment showed the most variation, with a large increase at 6 months followed by a decrease at 12 months and another increase at 18 months. The bones from the compost and clay environment also showed an increase from 6 to 18 months, suggesting phosphate from the environments is infiltrating the bone matrix as reported by Álvarez-Lloret et al. (2006) who noted how environmental contamination can cause differences in bone metabolism, resulting in higher concentrations of carbonate and acid phosphatase and changes in crystallinity.

The Carbonate / Phosphate ratio can be used to assess the degree of diagenesis, by estimating the content of carbonate in a bone, which is predicted to decrease with ongoing diagenesis, with a value of 0.36 in modern bones (Hollund et al., 2013). The control bones show a slight increase in the C/P ratio, with the largest increase occurring at the 3 month stage. Similar to the Am/P ratio, the bones from the lime environment show a steady increase across the 18 month burial duration. This result indicates that ion substitution from the environment is occurring within the bone matrix. The bones buried in sand, once again showed the biggest variance in change, resulting in an increase between 12 and 18 months. The bones from the clay and compost environment showed similarities in the patterns of change, and showed a decrease between 12 and 18 months.

No published research has been found on the short term diagenesis in bone from different environments, so comparison of findings is difficult due to the huge difference in burial duration to that of archaeological studies. Many researchers comment that mineral recrystallisation does not occur until complete removal of the organic content has occurred (Sillen et al., 1989; Price et al., 1992; Fredericks et al., 2012) which suggests that any changes in bone composition in this research may be due to ion substitution in the mineral lattice from deposition contaminants from the environmental conditions rather than the bone remodelling. Price et al., (1992) stated that the duration and environment conditions of burial are important factors in diagenetic modification of bone, and Hedges et al., (1995) suggested that the processes which results in bone modification (porosity change, protein content and crystallinity) all work on different timescales to one another after finding no correlation between these parameters and environmental factors from three different archaeological sites.

5.4 DNA analysis

The DNA analysis of the porcine bones, were conducted as described in section 4.3, with the amplification of different DNA amplicon lengths. The lengths of the amplicons were designed to imitate the DNA lengths used for different techniques used within forensic science laboratories.

During the demineralisation of the bones, and during the extraction process, any colour changes observed were recorded. This information and the results from the DNA analysis are indicated in this section.

All samples were treated in the same way in order to provide a comparison of the success or failures in amplification. Each sample was extracted and amplified in triplicate.

5.4.1 Control bones

The results from the control bones DNA analysis and discolouration during the overall process are displayed in Table 5-6.

Table 5-6: DNA results from control porcine bones

Duration	Discolouration of EDTA	Discolouration during extraction	DNA amplicon length								
			~100bp			~300bp			~500bp		
0 weeks	None	None	X	X	X	X	X	X	X	X	X
0 weeks	None	None	X	X	X	X	X	X	X	X	X
1.5 months	None	None	X	X	X	X	X	X	X	X	X
1.5 months	None	None	X	X	X	X	X	X	X	X	X
3 months	None	None	X	X	X	X	X	X	X	X	X
3 months	None	None	X	X	X	X	X	X	X	X	X
6 months	None	None	X	X	X	X	X	X	X	X	X
6 months	None	None	X	X	X	X	X	X	X	X	X
12 months	None	None	X	X	X	X	X	X	X	X	X
12 months	None	None	X	X	X	X	X	X	X	X	X
18 months	None	None	X	X	X	X	X	X	X	X	X
18 months	None	None	X	X	X	X	X	X	X	X	X

As shown, there was no discolouration of the EDTA during the demineralisation or of the extraction liquids during the process. All of the samples, in triplicate showed successful amplification of all 100, 300 and 500 base pair amplicons, from fresh bone all the way through to 18 months. This concludes that although some degradation of the biomolecules may have occurred, the processes used were still adequate for amplification of the DNA over a period of 18 months.

5.4.2 Clay burial bones

The DNA results and observations from the clay burials are shown in Table 5-7, and show how the clay burial affects the bones in comparison to the control bones.

Table 5-7: DNA results from clay burial porcine bones

Duration	Discolouration of EDTA	Discolouration during extraction	DNA amplicon length								
			~100bp			~300bp			~500bp		
1.5 months	None	Yellow	X	X	X	X	X	X	X	X	X
1.5 months	None	Yellow	X	X	X	X	X	X	X	X	X
3 months	None	Yellow	X	X	X	X	X	X	X	X	X
3 months	None	Yellow	X	X	X	X	X	X	X	X	X
6 months	None	Orange	X	X	X	X	X	X	X	X	X
6 months	None	Orange	X	X	X	X	X	X	X	X	X
12 months	None	Orange									
12 months	None	Orange									
18 months	None	Orange									
18 months	None	Orange									

There was no colour change in the EDTA during demineralisation, despite the colour staining on the surface of the bones. However, colour change of the extraction liquids did occur. At 1.5 months and 3 months, the colour had changed from clear to yellow, which progressed to orange from 6 months to 18 months. The reason for this change could be attributed to contamination within the membranes of the DNA that is released during lysis of the cells.

It is also noted that no amplification was successful after 6 months of burial. As no gradual degradation of DNA is noted, with a drop-off in the ability to amplify the larger amplicons opposed to the smaller fragments, it is possible that PCR inhibitors are present. The gradual darkening of the colour change during lysis suggests that a higher degree of humic acid from soil contamination was leaching into the bone matrix, and therefore affecting the ability of the extraction components.

5.4.3 Compost burial bones

Observations of colour change and the results from the DNA analysis of the compost porcine bones are displayed in Table 5-8.

Table 5-8: DNA results of compost burial porcine bones

Duration	Discolouration of EDTA	Discolouration during extraction	DNA amplicon length								
			~100bp			~300bp			~500bp		
1.5 months	None	Orange	X	X	X	X	X	X	X	X	X
1.5 months	None	Orange	X	X	X	X	X	X	X	X	X
3 months	None	Yellow	X	X	X	X	X	X	X	X	X
3 months	None	Yellow	X	X	X	X	X	X	X	X	X
6 months	None	Yellow	X	X	X	X	X	X	X	X	X
6 months	None	Yellow	X	X	X	X	X	X	X	X	X
12 months	None	Orange									
12 months	None	Orange									
18 months	None	Orange									
18 months	None	Orange									

The lack of discolouration of the EDTA was the same as that found from the control and bones from the clay environment. However a lager colour difference during extraction was observed with an orange discolouration at 1.5 months, yellow for 3and 6 month burials, and returning to orange for the 12 and 18 months burials.

The lack of amplification of DNA products after 6 months matches that seen in the clay burials, once again suggesting the infiltration of humic acid from the compost acting as PCR inhibitors and obstructing the amplification of the DNA.

5.4.4 Lime burial bones

The results from the DNA analysis and colour changes observed during that process are presented in Table 5-9.

Table 5-9: DNA results from lime burial porcine bones

Duration	Discolouration of EDTA	Discolouration during extraction	DNA amplicon length								
			~100bp			~300bp			~500bp		
1.5 months	None	Orange	X	X	X	X	X	X	X	X	X
1.5 months	None	Orange	X	X	X	X	X	X	X	X	X
3 months	Slight	Orange	X	X	X	X	X	X	X	X	X
3 months	Slight	Orange	X	X	X	X	X	X	X	X	X
6 months	Yellow	Brown	X	X	X	X	X	X	X	X	X
6 months	Yellow	Brown	X	X	X	X	X	X	X	X	X
12 months	Yellow	Brown	X	X	X	X	X	X			
12 months	Yellow	Brown	X	X	X	X	X	X			
18 months	Yellow	Brown	X	X	X	X	X	X			
18 months	Yellow	Brown	X	X	X	X	X	X			

Unlike the control, clay and compost burials, discolouration of EDTA occurred whilst demineralising the bones from the lime environment. No discolouration was present whilst processing the 1.5 month burials, but from 3 months onwards, the colour change steadily increased until 18 months. This would suggest that elements from the lime burial are infiltrating the bone into the mineral matrix, which are being released as the mineral aspect of the bone is broken down.

Discolouration of the samples was also observed during extraction, from orange at 1.5 months progressing to brown at the 6 month and 18 month burials. This shows the contamination from the lime burials was more advanced in these samples than the aforementioned samples.

The DNA results show how from the 12 month burials, it was not possible to amplify any 500 base pairs amplicons, but both 300 and 100 base pairs were still successful. This suggests that breakdown of the DNA has occurred.

5.4.5 Sand burial bones

Observations of colour change during the demineralisation process and the DNA analysis are displayed in Table 5-10.

Table 5-10: DNA results from sand burial porcine bones

Duration	Discolouration of EDTA	Discolouration during extraction	DNA amplicon length								
			~100bp			~300bp			~500bp		
1.5 months	None	Yellow	X	X	X	X	X	X	X	X	X
1.5 months	None	Yellow	X	X	X	X	X	X	X	X	X
3 months	None	Yellow	X	X	X	X	X	X			
3 months	None	Yellow	X	X	X	X	X	X			
6 months	None	Orange	X	X	X	X	X	X			
6 months	None	Orange	X	X	X	X	X	X			
12 months	None	Orange	X	X	X	X	X	X			
12 months	None	Orange	X	X	X	X	X	X			
18 months	None	Orange	X	X	X	X	X	X			
18 months	None	Orange	X	X	X	X	X	X			

No discolouration of the EDTA was seen during the demineralisation of the bone, suggesting the staining of the exterior of the bone was not attached to the mineral of the bone. Yellow discolouration during extraction showed immediately from the 1.5 month burials with a darkening to orange from 6 months onwards, showing contamination from the burial environment throughout all the samples.

The DNA analysis showed amplification of the 500 base pair amplicon was only achieved from the 1.5 month burial, after which only the 100 and 300 base pair amplicons were amplified. This could be due to the presence of PCR inhibitors in the sample affecting the amplification, however as the smaller DNA fragments are still amplified, it is more likely due to the degradation of the DNA.

5.5 Human analogue burial summary

A general summary of the results from the human analogue results can be tabulated to show the effect of the burial environment on the different aspects investigated as shown in Table 5-11.

Table 5-11: Ranking order of human analogue bones according to environment

Ranking Order	Soft tissue preservation	Bone preservation	DNA preservation
Best	Lime	Lime	Lime
↓	Clay	Sand	Compost and Clay
	Compost	Compost and Clay	
Worst	Sand		Sand

The next section displays the results from the analysis of the human archaeological remains.

Part B: HUMAN ARCHAEOLOGICAL RESULTS

This part presents the results from analysis of the human archaeological samples from the Fin Cop site in Derbyshire and Eriswell cemetery in Suffolk. As detailed in Chapter 4, analysis was conducted in order to produce detailed information in regards to colour, composition and biomolecules of the skeletons, to allow both intra- and inter-site comparisons to be made.

The analysis of the human bones derived from archaeological contexts comprised of collating information on the burial environment and comparing this to data obtained from the DNA, colour, and composition analysis. This information provided the ability to identify diagenetic patterns in accordance to the burial environments, and to ascertain how different burial environments affect different skeletal elements. The analysis allowed both an inter-site comparison (Fin Cop to Eriswell), as well as an intra-site analysis, due to geological complexity of the Eriswell cemetery site.

5.6 Fin Cop

Ten samples from six skeletons (as described in section 4.3.1.1) were assessed for colour, composition and DNA content. The results are presented separately from Eriswell initially, with a comparison between findings at the end of the chapter.

5.6.1 Colour Analysis

The colour analysis was performed on the bones prior to and after surface removal in order to assess whether changes in colour, or depth of colour is relevant to the burial environment and other factors tested such as collagen and carbonate content, splitting factor and DNA content. A full table of colour data can be found in Appendix B, with summary data presented in Figure 5-40 along with the colour difference value between the surface colour and cortex colour of the bones.

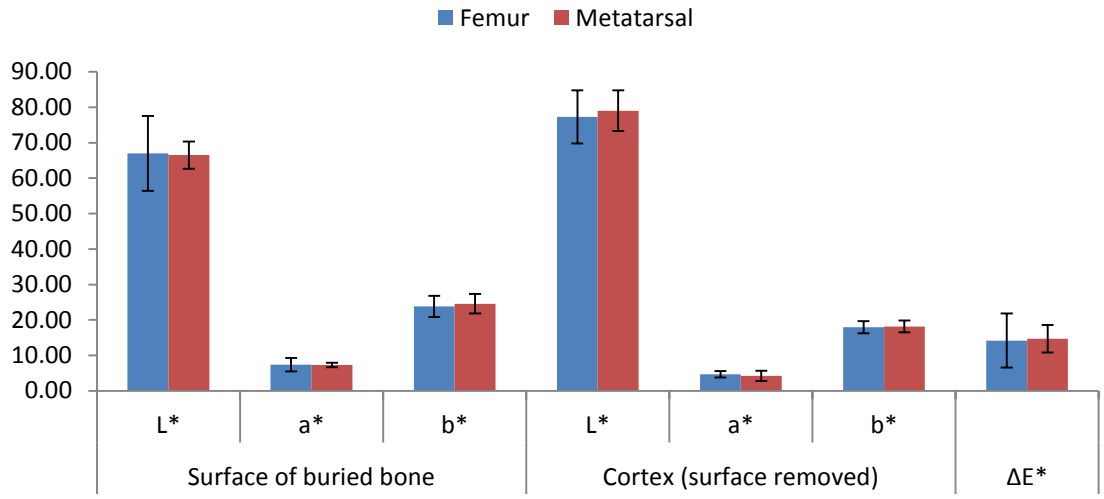

Figure 5-40: Combined data from the colourimetry data from the Fin Cop femurs and metatarsals, showing the individual L*a*b* values

Overall the femurs were lighter than the corresponding metatarsals, with the exception of Skeleton 3; which displayed the largest colour difference between the surface colour and the exposed cortex colour. All elements were lighter when the bone surface was removed, apart from the femur from skeleton 5 which became slightly darker, and also the only element to move higher on the red scale on the a* axis. This difference can be explained by the infiltration of soil into the cavity of the femur as shown in Figure 5-41.

Figure 5-41: Infiltration of soil into the cavity of the femur from Fin Cop skeleton 5

The b* axis (yellow/blue) showed the highest similarity between the two elements from the same skeletons. The femur from skeleton 7 was the only element that showed an increase further towards yellow, but the amount is negligible.

The overall colour difference calculations showed there was no pattern showing one element with a higher colour difference than the other, although more variance was observed with the femur samples.

No remarkable difference between the different colour axis on the different elements can be identified. The highest variation was observed on the L* axis, which increased in lightness for both the femurs and the metatarsals once the surface was removed. Both the a* and b* decreased in value after surface removal, becoming less red and yellow, respectively.

5.6.2 Composition Analysis

The bones from the Fin Cop skeletons were analysed using FTIR-ATR as discussed in section 4.1.11.2 to estimate the degree of diagenetic change that had occurred. Full results are detailed in Appendix B, with summary data and analysis provided in Figure 5-42. During analysis of the results it was noted that unidentified peaks were present in some of the samples, therefore XRF was used in order to identify the origin of the peaks, full results are detailed in Appendix B and summary information is provided after the FTIR-ATR results.

5.6.2.1 ATR-FTIR results

Of the six skeletons that were analysed from the Fin Cop site, only four had both the femur and metatarsal available for analysis, of which, preferential preservation was not observed in one element over the other. The metatarsals from skeleton 1 and 8 both showed better preservation than the femurs, in terms of splitting factor, collagen content and carbonate content; whereas skeleton 2 and 3 both showed better preservation in the femurs than metatarsals, in all three of the results.

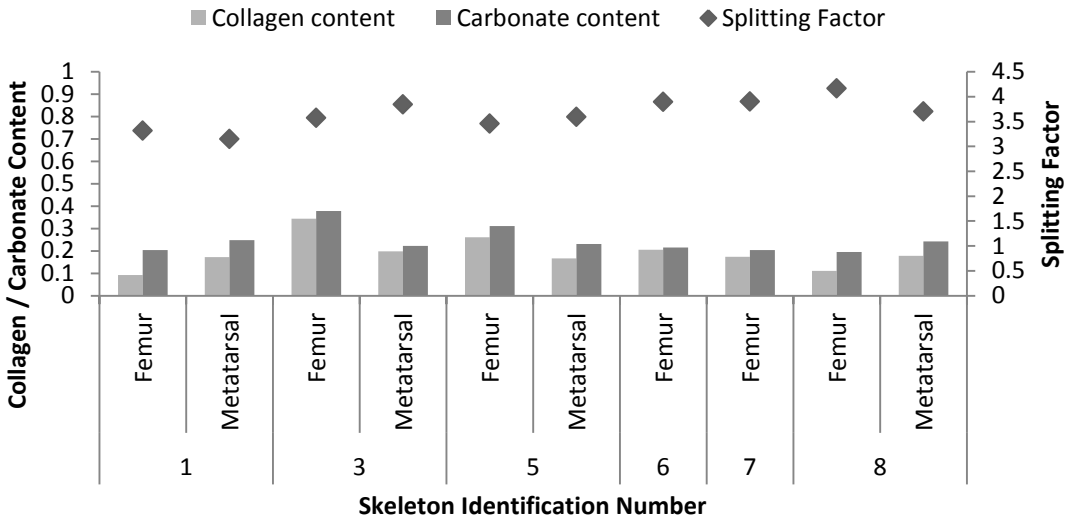

Figure 5-42: FTIR-ATR results of Fin Cop Skeletons showing Splitting Factor (secondary right axis), Collagen content (primary left axis) and Carbonate content (primary left axis)

The splitting factor of the samples ranged from 3.15 to 4.17, which matches with those previously reported for archaeological human remains (Weiner and Bar-Yosef, 1990; Sosa et al., 2013). The lowest splitting factor was observed from the metatarsal from skeleton 1, and the highest from the femur of skeleton 8.

The highest collagen and carbonate content was seen in the femur from skeleton 2, and the lowest in the femur from skeleton 8, supporting the notion of bad preservation shown by the high splitting factor results.

During analysis extra peaks were observed in the spectra, as indicated in Figure 5-43 showing absorbance on the y-axis and wavenumber on the x-axis. Due to the location of the peaks between 460-470nm, and the close proximity to the phosphate peaks used to calculate the splitting factor of the bones, the samples displaying the highest peaks were investigated using XRF in order to ascertain the contamination present.

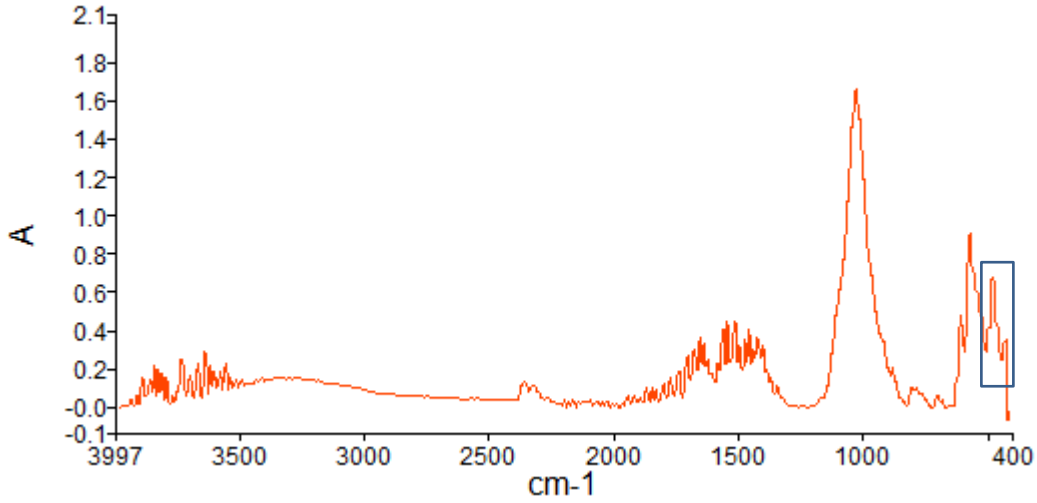

Figure 5-43: ATR-FTIR spectra of Fin Cop skeleton 6 femur sample, showing additional peaks indicated with a box

5.6.2.2 XRF results

XRF was utilised in order to identify the origin of unknown peaks appearing in some of the FTIR spectra. The tests were run in triplicate, with the full data sets displayed in appendix B. The summary data in the form of sample averages of identified elements are presented in Table 5-12.

Table 5-12: XRF results showing the averages of three readings from Fin Cop bone samples, expressed as area in counts per second

Element	Skeleton 6 Femur	Skeleton 7 Femur	Skeleton 8 Femur	Skeleton 8 Metatarsal
Silicon	1030.67	734.99	375.08	514.70
Phosphorus	4142.83	5740.46	6263.64	5851.30
Calcium	63001.31	75379.30	79679.59	77880.58
Titanium	442.76	132.27	21.33	161.16
Iron	10240.70	2196.39	594.21	3233.27
Manganese	542.48	298.05	238.93	306.82
Copper	553.30	293.75	601.79	573.95
Zinc	937.86	297.82	749.50	717.39
Strontium	477.39	450.10	562.63	503.41
Zirconium	244.68	117.42	91.35	82.48
Chromium	119.87	129.87	158.16	129.57
Nickel	862.51	959.46	1392.93	1291.14
Potassium	1200.34	820.22	640.68	806.53

The data shows the top three elements identified in all the bone samples were calcium, iron and potassium – all of which are known to be present in soil samples.

By observing the FTIR-ATR spectra, the sample displaying the biggest anomaly from the expected peaks, was the femur sample from skeleton 6. The XRF results show the amount of calcium and potassium are similar between all samples, but the iron is much higher in the skeleton 6 femur sample, with a peak area of 10240.70 cps, therefore this element could be the cause of the unexpected peaks in the FTIR-ATR spectra.

There is also a significant difference between the levels of iron between the femur and the metatarsal from skeleton 8, despite being from the same grave. Figure 5-44 shows the difference observed in the XRF spectrum. The metatarsal spectrum shown in red shows a much larger peak area of iron.

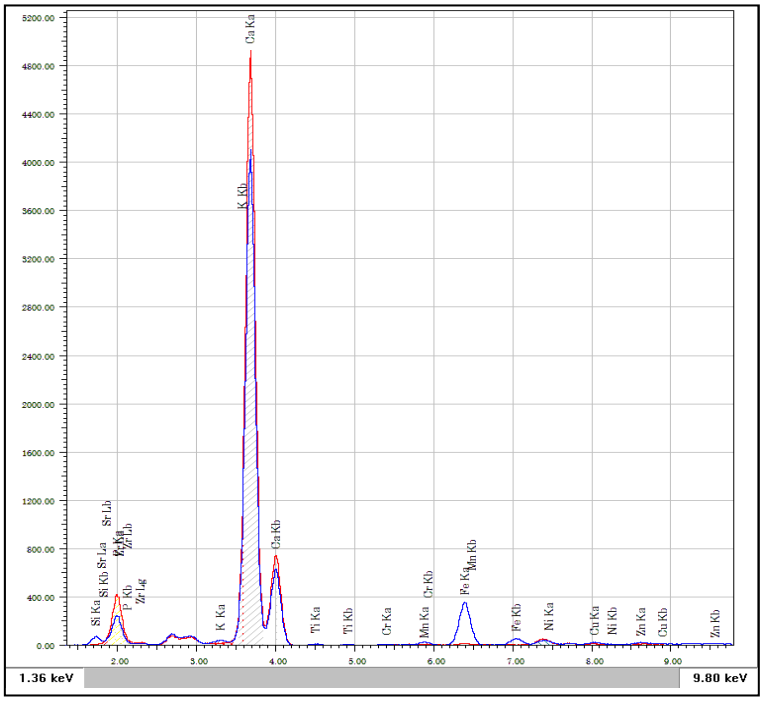

Figure 5-44: Comparison of XRF spectrum of the femur sample shown in red, and the metatarsal sample shown in blue, from skeleton 8

The relationship between the iron content in the bone samples as identified by the XRF analysis, and the height of the peak between 460-470nm from the FT-IR ATR analysis was then investigated, and the results are shown in Figure 5-45.

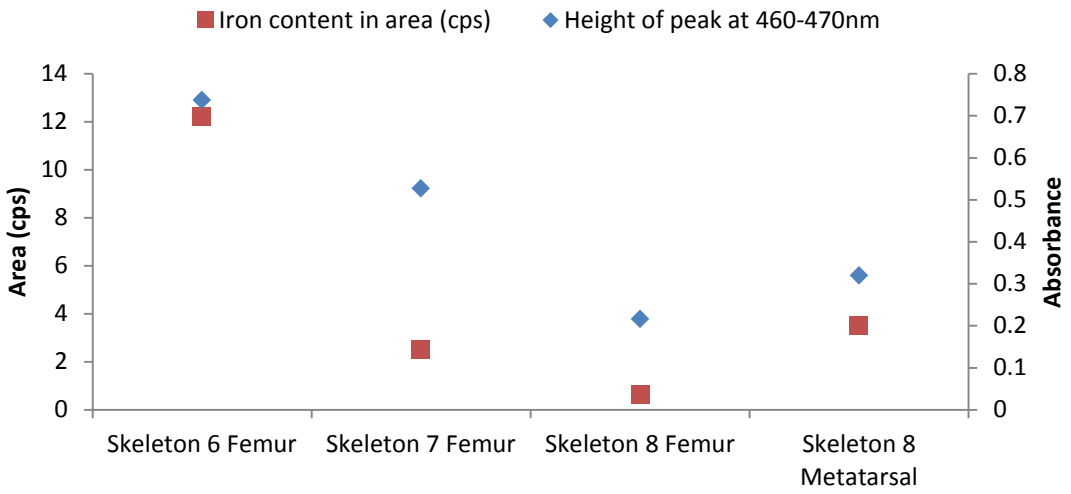

Figure 5-45: The relationship between the height of the unidentified peak in FT-IR ATR spectra (460-470nm) and peak area of iron in Fin Cop samples

A clear correlation can be seen between the two sets of data, demonstrating the unknown peaks in the FTIR-ATR spectra are at least partly caused by the concentration of iron in the sample. Due to the red colouration often seen with iron deposits in soil, this information was related back to the colour data, which showed the femur from skeleton 6 had the highest red value for the bone surface colour, in comparison to the other bone samples tested with XRF.

5.6.3 DNA analysis of Fin Cop skeletons

The data produced from the genetic analyser were analysed following guidelines set out by SWGDAM 2010, and those presented by John Butler (2005) as detailed in section 4.3.10.

To interpret the data, the individual electropherograms were first analysed for the identification of true peaks, with the elimination of artefacts. Allelic pairings were estimated from PHR calculations as discussed in section 4.1.10. As also discussed in the mentioned section, PHR calculations can be unreliable in cases of severely degraded DNA, so after the initial assessment of present alleles in individual samples, allele exclusion was conducted to remove any potential contamination from the analysis.

5.6.3.1 Fin Cop Skeleton 1

Analysis of the electropherograms of Fin Cop skeleton 1 showed no amplified alleles in the samples that had undergone demineralisation prior to extraction, the amplified alleles in the other femur and metatarsal samples are displayed in Table 5-13.

Table 5-13: Fin Cop skeleton 1 DNA results

Femur				Metatarsal			
Marker	**Allele**	**RFU**	**PHR**	**Marker**	**Allele**	**RFU**	**PHR**
Amelogenin	Y	43		**Amelogenin**	X	21	85.71
D19S433	13	19	79.17	**Amelogenin**	Y	18	
D19S433	14	24		**D1S1656**	16.3	62	
D2S1338	17	27		**D10S1248**	13	36	
D22S1045	15	19	90.48	**TH01**	6	30	34.09
D22S1045	16	21		**TH01**	8	88	
D16S539	10	49	87.76	**vWA**	14	39	89.74
D16S539	13	43		**vWA**	17	35	
D18S51	16	38	92.11	**vWA**	18	65	
D18S51	18	35		**D21S11**	31	37	
TH01	6	54	96.43				
TH01	7	56					
vWA	18	30	63.83				
vWA	19	47					
D8S1179	11	52					
FGA	13	35	97.14				
FGA	23	34					

The femur 1 showed a partial profile with a maximum of two peaks at each loci, therefore there is no evidence to suggest there is more than one contributor to the profile. All peaks observed were below 60 RFU, reducing the possibility that the DNA is modern contaminant.

Although the Y allele in the amelogenin marker is off ladder, it appears to be a true allele with N-4 stutter, and it exhibits good morphology, suggesting that this could just be due to a shift in the ladder during analysis. There is no evidence of a peak for the X allele, which must be due to allelic drop-out.

The calculation of PHR on the observed allele pairs all resulted in values over 60%, suggesting that they are heterozygous peaks.

Both the markers of D2S1338 and D8S1179 show a single peak which could either mean this allele is homozygous, (although the heterozygosity of these markers for European population are reported at 88% and 80%, respectively) (Welch et al., 2012); or there has been allelic drop-out, of which the probability is calculated at 95-99% and 70-80%, respectively (Tvedebrink et al., 2009).

Analysis of the metatarsal showed ten amplified alleles, across six loci. Alleles on the amelogenin marker show 2 peaks off-ladder, yet the morphology suggests there are in fact true alleles in the form of X and Y, and PHR calculations suggest they are paired.

The markers D1S1656, D10S1248 and D21S11 show only single peaks – the probability of these markers being heterozygous is 90%, 76% and 85% respectively, therefore it may be due to allele drop-out. By using the RFU of the allele at D21S11, the probability of allele drop-out of a sister allele is 80-90%.

The TH01 marker displays two peaks but calculation of their PHR is only 34.09% which suggests that either the peaks are not paired and they are from 2 separate individuals, or preferential amplification has happened during PCR.

The three alleles at vWA show that there is either more than 1 contributor to this DNA profile, or it could be due to a tri-allelic pattern where an extra chromosome fragment in the sample has led to the amplification of extra PCR products. A tri-allelic pattern at vWA of alleles 14, 17 and 18 has previously been observed (Butler, 2006) but no guidance is provided as to how similar the peak heights should be. Another possibility is that there is a second contributor, although this seems unlikely due to no other contamination present in the profile – unless the peaks at TH01 are also not from the same individual. If in fact the three peaks at vWA are due to more than one contributor to the profile, there are 12 possible genotypes if using an un-restricted approach of considering all possibilities of genotype due to the data being close to the limit of detection, and therefore stochastic effects and allelic drop-out are a possibility.

Based on the PHR and the peak heights of the alleles, the highest probability for allele pairings is a heterozygous 14 and 17, and a homozygous 18, 18. This is

possible as the peak height of 18 is double that of the smaller alleles of 14 and 17. Another possibility is that allele 18 is heterozygote and a sister allele has dropped out – the probability of this is 50-60%.

5.6.3.2 Fin Cop Skeleton 3

The analysis of the electropherograms from skeleton 3, showed allelic peaks on both femur samples, and the metatarsal sample which had not undergone initial demineralisation – no alleles were seen from the demineralised metatarsal. Compiled results can be seen in Table 5-14.

Table 5-14: Fin Cop skeleton 3 DNA results

Demineralised Femur			
Marker	**Allele**	**RFU**	**PHR**
D19S433	15	26	
D2S1338	20	24	
D18S51	15	46	
D1S1656	16	43	60.47
D1S1656	18	26	
D10S1248	13	26	
THO1	9.3	55	
D8S1179	14	28	
FGA	20	24	92.31
FGA	23	26	

Non-demineralised Femur			
Marker	**Allele**	**RFU**	**PHR**
AMEL	Y	13	
THO1	9.3	49	
D8S1179	14	24	
FGA	20	19	100
FGA	23	19	

Non-demineralised metatarsal			
Marker	**Allele**	**RFU**	**PHR**
D16S539	8	31	
D18S51	16	34	65.38
D18S51	17	52	
vWA	10	56	
vWA	15	38	
vWA	16	60	
vWA	17	81	
vWA	18	38	
vWA	19	31	
vWA	22	39	

The electropherograms of the demineralised femur sample showed 10 alleles on 8 different loci, whilst the non-demineralised sample displayed 4 alleles on 3 different loci.

Both the femur samples analysed provide partial profiles and neither of them displayed more than two alleles at each loci. This along with relatively low RFU values of the peaks there is no reason to suspect more than one contributor to the samples. All alleles present in the non-demineralised femur sample match with alleles displayed on the same loci on the demineralised sample, suggesting it came from the same donor.

Electropherograms from the metatarsal samples from skeleton 3 show no allelic peaks present in the demineralised DNA sample, in comparison to the non-demineralised sample which shows peaks on 10 peaks on 3 loci.

The partial profile shows two alleles 16,17 at D18S51, and have a PHR of 65% so it is likely these peaks at sister alleles. Seven alleles at vWA shows contamination but only at one loci, which suggests it may be due to analysis error, rather than contamination of multiple contributors at only one loci.

As mentioned earlier, tri-allelic patterns have been reported at the vWA marker before, but the only combination which could work here is 15,16,17 but the peak heights do not coincide with either type 1 or 2. Although some peaks are in the correct positions for stutter, the percentages are too high in order to be so. By using peak heights, one allele pairing could be 3 heterozygous pairs: 10,16 (93.34%), 15,18 (100%) 19,22 (79.49%) and one homozygous 17,17; however, with the possibility of stacking, and no known profiles to compare to, it is not possible to determine how many individuals might be represented.

5.6.3.3 Fin Cop Skeleton 5

Analysis of the elements of skeleton 5, shown in Table 5-15, displayed a maximum of 2 peaks per loci, with peak heights between 25-59 RFU, therefore displaying no evidence of contamination from modern DNA.

Table 5-15: Fin Cop skeleton 5 DNA results

Femur 5				Demineralised Metatarsal 5				Metatarsal 5		
Marker	**Allele**	**RFU**	**PHR**	**Marker**	**Allele**	**RFU**	**PHR**	**Marker**	**Allele**	**RFU**
D3S1358	15	29	86.21	**vWA**	11	36	83.72	**D16S539**	10	59
D3S1358	16	25		**vWA**	18	43				
D19S433	13	36								
D16S539	12	95								
TH01	6	59	54.24							
TH01	9.3	32								

The demineralised femur sample displayed no alleles, with six alleles on four loci on the sister sample. PHR calculations suggests the alleles on D3S1358 are true heterozygous peaks at 86.21%, yet the two alleles at TH01 only have a PHR of 54.24% - due to the lack of any other alleles, this could be due to preferential amplification rather than DNA from two origins.

The demineralised metatarsal displayed two alleles on the vWA marker with a PHR of 83.72%, with the non-demineralised counterpart only displaying one allele at

D16S539. Due to the low allele count and lack of corresponding peaks, it is not possible to conclude these profiles originate from the same individual, but there is no evidence to suggest any contamination.

5.6.3.4 Fin Cop Skeleton 6

Electropherograms from the analysis of skeleton 6, show allelic peaks on both femur samples tested, both demineralised and non-demineralised, as seen in Table 5-16. No metatarsal samples were available for analysis.

Table 5-16: Fin Cop skeleton 6 DNA results

Demineralised Femur 6			
Marker	**Allele**	**RFU**	**PHR**
D3S1358	15	66	21.57
D3S1358	16	306	
D19S433	12	63	
D16S539	10	152	
D16S539	11	55	80.00
D16S539	13	44	
D18S51	13	79	51.90
D18S51	15	180	43.89
D18S51	16	41	22.78
TH01	8	58	63.79
TH01	9	144	77.42
TH01	9.3	186	
TH01	10.3	37	
vWA	15	34	77.27
vWA	16	44	
vWA	17	117	72.65
vWA	18	85	
D21S11	30	30	68.18
D21S11	31	44	

Femur 6			
Marker	**Allele**	**RFU**	**PHR**
AMEL	X	35	
D16S539	10	81	62.31
D16S539	11	130	
D18S51	13	105	48.57
D18S51	16	51	
TH01	9	177	39.55
TH01	9.3	70	
vWA	15	51	74.51
vWA	17	38	
FGA	21	46	

Analysis of the peak heights from the electropherograms of the Skeleton 6 femurs, suggests contamination is possible within both samples, yet only the demineralised sample shows multiple peaks within alleles. Allelic pairing using PHR calculations is possible for some peaks in the demineralised sample, but severe peak imbalance is still present especially at the D3S1358 loci, which only displays 2 peaks. Peak imbalance is also seen at D18S51 and TH01 on the non-demineralised femur sample.

If the peak imbalance is in fact due to DNA from different donors, rather than preferential amplification, it is possible there are 2 contributors on each sample.

5.6.3.5 Fin Cop Skeleton 7

Analysis of the two femur samples from Skeleton 7 showed a much stronger DNA presence on the non-demineralised sample, displaying 13 peaks in 10 loci as opposed to two peaks on the demineralised sample, as seen in Table 5-17.

Table 5-17: Fin Cop skeleton 7 DNA results

Demineralised femur		
Marker	**Allele**	**RFU**
AMEL	Y	28
D12S391	21.3	32

Femur			
Marker	**Allele**	**RFU**	**PHR**
AMEL	Y	12	
D19S433	15	32	
D2S1338	20	30	
D16S539	8	40	95.00
D16S539	11	38	
D18S51	13	52	
D1S1656	12	40	
TH01	7	68	85.29
TH01	8	58	
vWA	21	32	
D12S391	17	152	
FGA	21	87	

No multiple peaks were present in any of the loci, and all peaks were relatively low in height, with PHR calculations confirming heterozygous peaks on all paired alleles.

Apart from the Amelogenin loci that displays an ‘X’ drop-out, the only peak present in the demineralised sample was allele 21.3 on the D12S391 loci, which when compared to allele 17 in the other extract, showed discrepancy due to peak height. At a height of 152RFU, it would be expected to be a homozygous peak therefore 21.3 must originate from another individual.

This may be due to preferential amplification therefore it is not possible to state contamination has occurred.

5.6.3.6 Fin Cop Skeleton 8

Of the four samples analysed from Skeleton 8, DNA was identified in all apart from the demineralised metatarsal sample as shown in Table 5-18, the three remaining samples showed corresponding peaks on eight loci.

Table 5-18: Fin Cop skeleton 8 DNA results

Demineralised Femur			
Marker	**Allele**	**RFU**	**PHR**
D3S1358	17	16	69.57
D3S1358	18	23	
D16S539	9	93	87.74
D16S539	10	106	
D18S51	12	48	75.00
D18S51	16	36	
D18S51	17	73	
TH01	9	40	52.63
TH01	9.3	76	
vWA	16	33	94.29
vWA	18	35	

Femur			
Marker	**Allele**	**RFU**	**PHR**
AMEL	X	1213	65.64
AMEL	Y	1848	
D3S1358	8	76	90.48
D3S1358	9	84	
D3S1358	18	1117	
D19S433	13	162	55.56
D19S433	15	90	
D2S1338	22	24	
D22S1045	13	26	
D16S539	10	1595	93.10
D16S539	12	1485	
D18S51	12	402	81.59
D18S51	16	328	
D10S1248	13	79	
D2S441	14	30	
TH01	7	64	52.03
TH01	8	123	
TH01	9	2147	84.86
TH01	9.3	1822	
vWA	17	809	82.32
vWA	18	666	
D21S11	28	115	
D12S391	18	34	44.16
D12S391	20	77	
D8S1179	10	3259	26.42
D8S1179	17	861	
FGA	19.2	50	80.65
FGA	21	62	
FGA	24	550	62.18
FGA	26	342	

Metatarsal			
Marker	**Allele**	**RFU**	**PHR**
AMEL	X	16	
D19S433	15	29	
D2S1338	23	38	
D22S1045	11	46	76.09
D22S1045	16	35	
D16S539	10	27	
D18S51	15	83	
D10S1248	13	56	
D21S11	31	70	
FGA	18	38	77.55
FGA	19.2	49	

Contamination was found to be present on the non-demineralised femur sample, due to multiple peaks on three loci – D3S1358, TH01 and FGA. PHR calculations showed imbalance in peak height of possible sister alleles on both the demineralised femur and the non-demineralised sample, some of which could be

due to preferential amplification; however with some peak heights exceeding 1000/2000/3000 RFU, contamination from modern DNA is most likely.

Three peaks were identified on D18S51 of the demineralised femur sample, yet peak heights show this can be explained by a tri-allelic pattern, as previously reported (Tvedebrink et al., 2012).

5.6.3.7 Fin Cop DNA result interpretation

For the purpose of comparison, all alleles that were identified as possible modern DNA contamination, and all alleles matching reference profiles were removed from the analysis and the remaining alleles are displayed in Table 5-19. Potentially, some ancient DNA alleles may also have been removed, but this approach allows confidence in the recording of genetic material without contamination. By removing the alleles suspected to be from an external source, comparisons can be made from the remaining genetic information across the elements from each skeleton and related back to the archaeological information.

The results from skeleton 1 show no alleles were amplified in either of the demineralised samples, but share the Y allele at the amelogenin marker, and allele 6 at TH01. The anthropological data about the Fin Cop collection indicate the sex estimation of skeleton 1 to be probable female, yet the genetic information shows a Y chromosome and therefore the sample belonged to a male. Discrepancies can be seen at vWA with the femur showing 18,19; whereas the metatarsal sample shows 14,17. These differences indicate that either the femur and metatarsal originate from a different source, or some of the alleles present are a source of external DNA but without any indications of contamination it is not possible to say which is true.

Skeleton 3 shows similarities between the demineralised and non-demineralised femur samples with allele 9.3 at TH01, and alleles 20,23 at FGA; although there is a discrepancy that can be seen at loci D18S51 with allele 15 on the femur, and alleles 16,17 from the metatarsal sample. The anthropological data once again estimates the sex of the skeleton to be female, yet the presence of a Y chromosome shows the DNA belongs to a male.

Table 5-19: Fin Cop DNA results from skeletal elements, after evidence of modern DNA contamination has been excluded.

Sample	Amelogenin	D3S1358	D16S539	TH01	D8S1179	D19S433	D18S51	vWA	D2S1338	D1S1656	D21S11	FGA	D22S1045	D10S1248	D2S441	D12S391	Number of alleles	Number of loci?	Matching alleles	Discrepancies
DF1																	0	0		
F1	Y			6		14	16,18	19	17			13,23	15				10	8	2	1
DM1																	0	0		
M1	X,Y			6				14,17		16.3							6	4		
DF3				9.3	14				20	18		20,23					6	5		
F3	Y			9.3	14							20,23					5	4	4	0
DM3																	0	0		
M3			8				16										2	2		
DF5																	0	0		
F5			12	6,9.3													3	2	0	0
DM5								11									1	1		
M5																	0	0		
DF6			11,13	9,9.3		12	13,16	15,17									9	5	7	0
F6	X		11	9,9.3			13,16	15,17									8	5		
DF7	Y															21.3	2	2	1	0
F7	X,Y		8,11				13	21	20	12		21					9	7		
DF8		17,18	9	9,9.3			12,16	16									8	5		
F8		8,9	12	9,9.3	10,17		12,16	17	22		28	19.2,26	13			18,20	17	11	5	4
DM8																	0	0		
M8	X		10									18,19.2					4	3		

Key: D = Demineralised, F = Femur, M = Metatarsal

Analysis of the two femur samples from skeleton 6, showed no discrepancies and shared 8 of the same alleles: 10,11 at D16S539; 9,9.3 at TH01; 13,16 at D18S51 and 15,17 at vWA, showing no evidence of contamination, just confirmation of alleles present. Anthropological data states skeleton 6 was commingled with skeleton 7 and 8, yet as the age of the skeleton was 40 weeks pre-natal, it is unlikely that the femur from skeleton 6 could be mis-identified with the others.

Matches between the samples from skeleton 8 can be seen at allele 10 at D16S539, 15 at D19S433,19.2 at FGA, and 13 at D10S1248. But discrepancies can be seen at D3S1358, TH01, between the demineralised and non-demineralised sample showing that external DNA is present in either or both of the samples. Discrepancies can also be seen at D18S51, FGA and D22S1045; concluding that these samples contain DNA that has originated from different sources.

By comparing the genetic information back to the original archaeological records, the discrepancies between alleles on skeleton 8 can be explained by the commingled nature of the burial. It is reported that skeleton 6, 7 and 8 were all commingled and heavily fragmented (Waddington et al., 2011), so it is possible that the skeletal elements have not been assigned to the correct skeleton.

Analysis of skeleton 5 showed no matches and no discrepancies between the results, and the only matching allele from skeleton 7 is the Y allele at the amelogenin marker.

Sex determination

Osteological reports on the skeletons from Fin Cop, suggest that skeleton 1 and 3 are 'probable female', based on the mandible and pelvis for skeleton 1, and fragmented pelvis and skull for skeleton 3. However, the Y allele was found on both the metatarsal and femur from both skeletons, suggesting the remains are in fact both male.

The sex of skeleton 5 was deemed 'indeterminate' due to lack of elements, and no amelogenin alleles were amplified on either of the elements, so there is no DNA evidence to assist with this categorisation.

Due to the young age of skeleton 6, no sex estimation could be made by the osteologist, however the DNA results returned one report of an X allele. Due to the low height of 35RFU, it is possible that allelic drop-out of the Y allele has occurred.

Skeleton 7 is also reported as indeterminate in the osteological report due to the young age, but the DNA analysis suggests the skeleton is male, with the presence of a Y allele in both the femur samples (demineralised and non-demineralised).

The DNA results for skeleton 8 display a very low peak of 16 RFU for the X allele on the metatarsal suggesting female, but nothing on the femur. Due to the height, it is possible that allelic drop-out has caused the Y allele absence. Osteological reports suggest the sex of the skeleton to be 'more likely male' but many indicators are indeterminate.

5.7 Eriswell

Due to the large number of skeletons excavated from the Eriswell site it was not possible to analyse them in entirety. As discussed in section 4.3, 60 skeletons were selected from across the three cemeteries, and 57 femurs, 47 metatarsals and 1 sternum fragment were sampled. These elements were all analysed to determine colour and composition. For the DNA analysis, 36 skeletons were selected from cemetery ERL 104, and 64 elements were sampled.

This section presents the results from the analysis of the Eriswell samples independently, and then a cross comparison with the Fin Cop results are presented in section 5.8.

5.7.1 Colour Analysis

The colour analysis for the Eriswell samples was conducted and analysed in the same way as that for the Fin Cop samples previously detailed. However, due to the different cemeteries and burial environment encased within the Eriswell area, the results are presented firstly as a whole, then across the different cemeteries from which they were excavated from; and finally in terms of the burial environment description from archaeological reports.

The overall results from the Eriswell cemeteries are presented in Figure 5-46 and show the individual colour axes of all the elements, and the femurs and metatarsals separately. The average colour of the bones prior to, and after surface removal, has been shown including the overall colour difference.

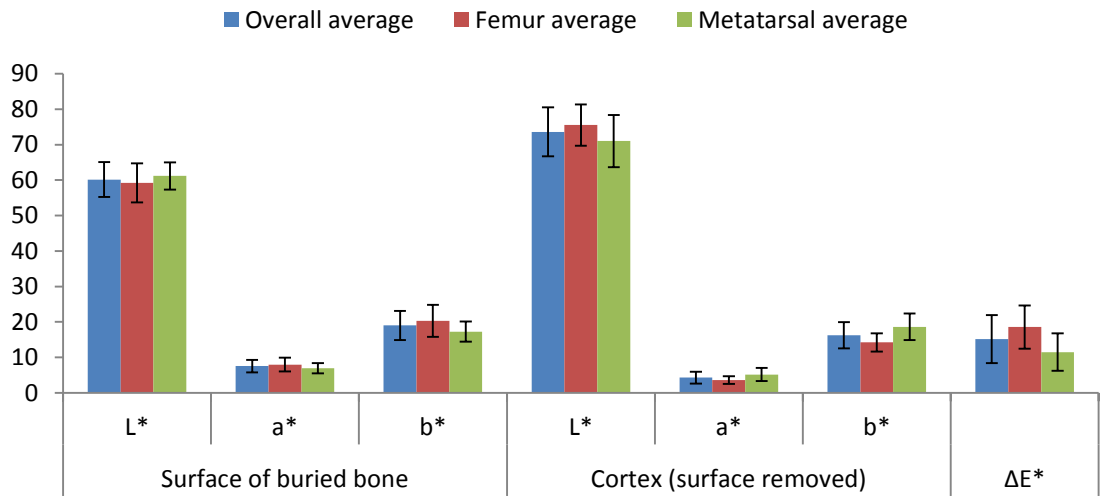

Figure 5-46: Overall colour analysis of averages from all tested skeletal elements from the Eriswell cemetery

The L* axis shows all elements become lighter after surface removal, although the femurs were darker prior to surface removal and lighter after removal; showing the largest difference in lightness. The a* axis shows all elements become less red after surface removal, with the biggest change seen in the femurs. The b* axis shows the femur average decreasing in yellow, whereas the metatarsal average increases slightly. Overall, the femurs show the largest colour change from after removal of the bone surface.

The data was then analysed in accordance with the area of the cemetery from which they were excavated, and this information is shown in Figure 5-47.

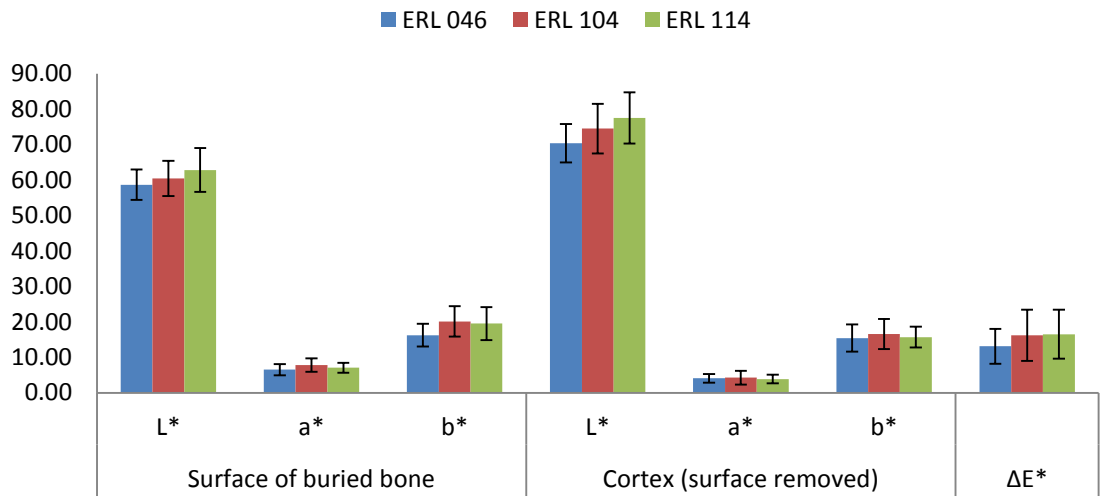

Figure 5-47: Colour analysis of overall averages from metatarsals and femurs, from ERL 046, 104, and 114 cemeteries

The L* axis shows the darkest bones, both before and after surface removal, to be those from ERL 046, followed by ERL 104 and lastly ERL 114 being the lightest bones, and also showing the smallest overall colour change. The a* and b* both show decreasing values in a uniform manner, showing all the bones becoming less red and less yellow after surface removal.

In order to assess whether these differences are the same in both femurs and metatarsals, the data in Figure 5-48 is separated into cemeteries, and also into elements: femurs and metatarsals.

The L*axis shows the metatarsals from ERL 046 have a lighter colour, both prior to and after surface removal. The femurs from ERL 104 are also darker initially, but after surface removal, a much lighter bone colour than the metatarsals is observed. The femurs from ERL 114 are different from the other cemeteries in the respect that they are lighter than the metatarsals from the same cemetery, both before and after surface removal.

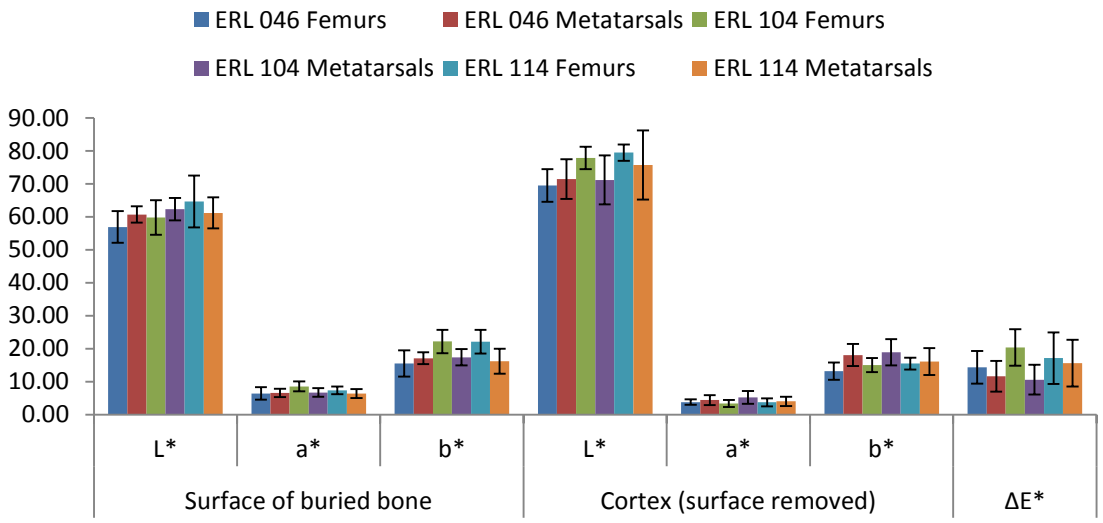

Figure 5-48: Colour analysis of femora and metatarsals from the cemeteries ERL 046, 104 and 114

The femurs from ERL 104 have the highest red value (a* axis), yet after surface removal, it shows the lowest value. All the other elements also reduce in redness after surface removal.

The b* axis value reduces in all the element averages, showing similar values for all the metatarsals. The femurs from ERL 104 show the highest value of yellow, with the femurs from ERL 114 only slightly below. Femurs from the ERL 046 cemetery show the lowest value both before and after surface removal.

Overall the largest colour difference between the elements and the cemeteries can be seen in the data from the femurs from the ERL 104 cemetery, however the metatarsals from the same cemetery show the least colour difference between all the elements.

In order to assess whether the localised burial environment or the location of the cemetery within the Eriswell site had a larger effect on the differences observed in bone colour, the results were then analysed according to the burial environment as described by the excavating archaeologists. The overall results are presented in Figure 5-49, with more detailed analysis of the elements is shown in Figure 5-50.

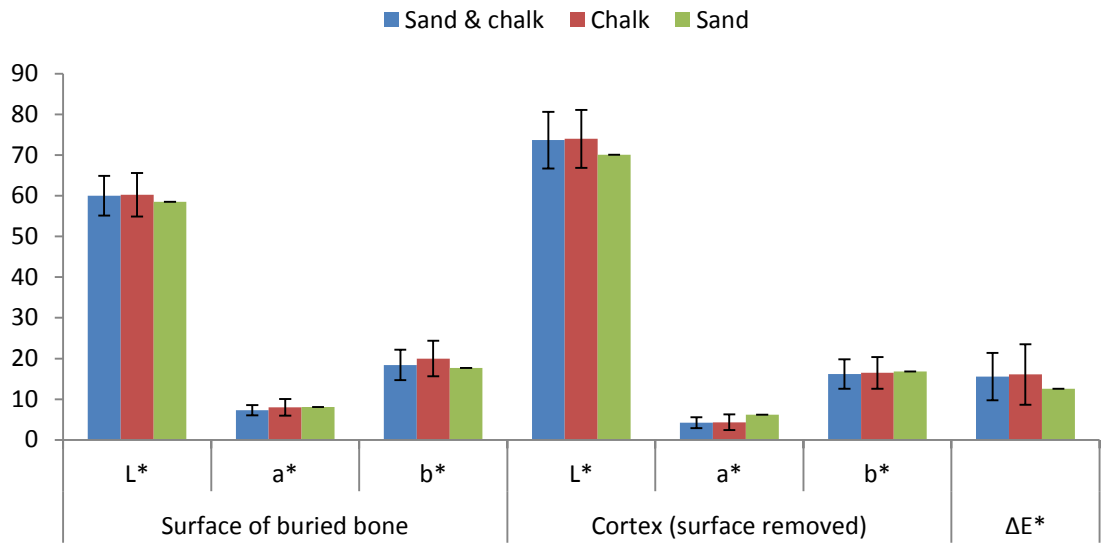

Figure 5-49: Colour analysis of overall averages from the sand and chalk, chalk, and sand burial environments from Eriswell cemeteries.

The sand and chalk environment show very similar results to those elements buried in a chalk environment. Differences can be seen in the sand environment, however these results are provided from only two elements from one skeleton.

All elements become lighter, less red and less yellow after surface removal. The largest colour difference can be seen in the bones from the chalk environment, but all values are very similar. By breaking the data down into individual elements, more information can be ascertained from the results.

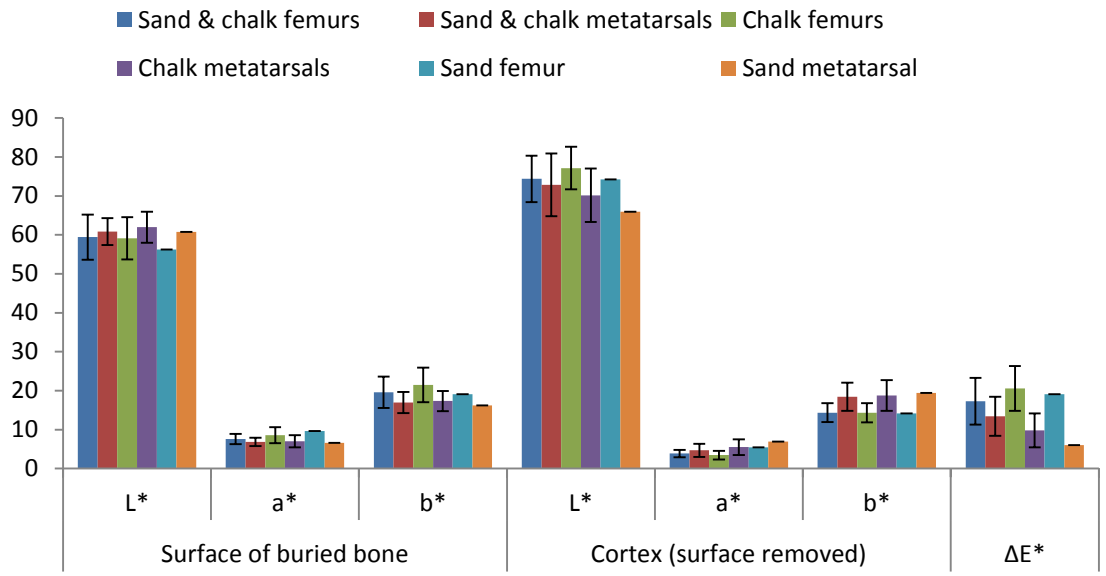

Figure 5-50: Individual elements from environments

Analysis of the L* axis shows all metatarsals across the different environments are lighter than the femurs prior to surface removal, but darker than the femurs after surface removal. The lightness of the sand and chalk femurs and chalk femurs are very similar to each other, whereas the sand femur is darker.

The a* axis shows the metatarsal from the sand environment is the only element across the environments that becomes redder after surface removal.

Values from analysis of the b* axis, show the femurs and metatarsals from the different environments behaving differently – all the metatarsals become more yellow after surface removal, whereas all the femurs become less yellow.

The biggest overall colour difference can be seen in the femora – chalk shows the largest difference, followed by sand and then sand and chalk. The order is different with the metatarsals, showing the largest difference occurring with the sand and chalk metatarsals, followed by the chalk, and lastly those from the sand environment.

5.7.2 Composition Analysis

The composition analysis on the Eriswell skeletons was conducted in order to assess the diagenetic changes that occurred in the bone. The complete results tables are presented in Appendix B.

The sample set showed a range of splitting factors from 2.88-4.63 showing varying degrees of preservation across the whole site. The femurs showed the largest range: 2.88-4.63, and the metatarsals a slightly smaller range 2.99-4.36.

By organising the results into associated cemeteries, the results can be observed in accordance to their location within the entire area. Figure 5-51 shows the average and range of splitting factor from the bones from each cemetery, in comparison to each other. The metatarsals in each cemetery showed a higher average splitting than the associated femurs from the same burials, suggesting a higher preservation rate in the femurs. ERL 114 showed the highest splitting factor of both the femurs and metatarsals, followed by ERL 104, and ERL 046 displaying the best overall preservation with the lowest average splitting factor of both the metatarsals and the femurs.

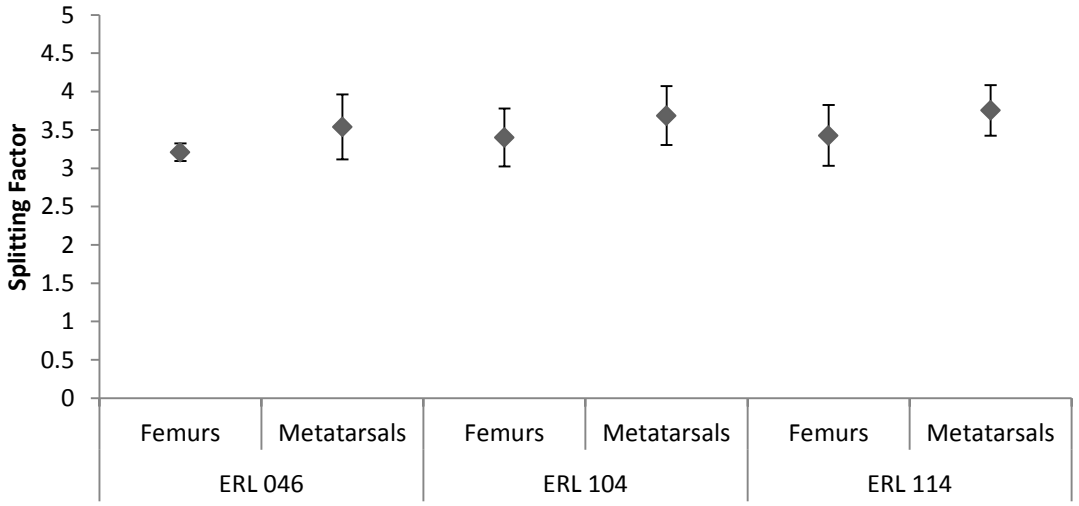

Figure 5-51: Range of splitting factors from femurs and metatarsals across cemeteries at Eriswell

The ratio of Carbonate/Phosphate is an indication of the level of carbonate preservation in the bone, which ranged from 0.11-0.72 across the Eriswell cemeteries. Overall the femurs showed a lower rate of preservation with a range of 0.11-0.43, whereas the metatarsals were slightly higher with a range of 0.12-0.72. When the results were analysed within the individual cemeteries, different trends could be seen - the femurs from both ERL 046 and ERL 114 showed a higher average of preservation than the metatarsals. ERL 104 showed the highest carbonate content in metatarsals than the other sites, and was also higher than that of the associated femurs.

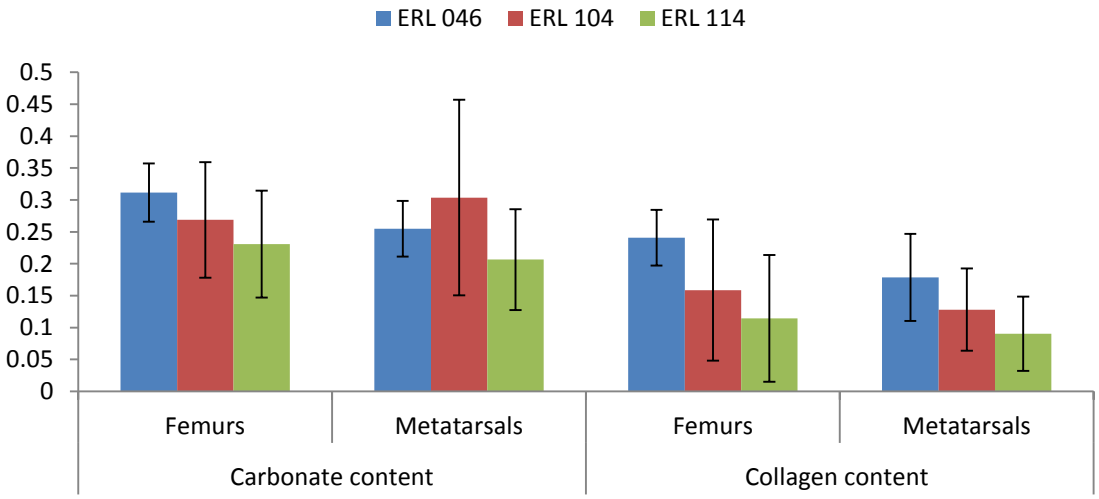

Figure 5-52: Carbonate and collagen content estimates from calculated ratios of femurs and metatarsals across cemeteries at Eriswell

The collagen content in the bones was indicated by the ratio of the Amide I band and phosphate, and showed an overall range of 0.03 – 0.35. The femurs and metatarsals showed similar ranges of 0.03-0.35, and 0.05-0.34, respectively. When analysed within individual cemetery areas, all areas showed the average femur content to be higher than that of the metatarsals from the same burials. ERL 046 showed the highest collagen content, followed by ERL 104 and the lowest preservation state was seen from the ERL 114 cemetery. This data is supported by the splitting factor reported earlier.

The elements from ERL 104 showed the highest variance in carbonate and collagen content, showing a variation in the preservation level in the elements.

The data was also analysed in relation to the burial environment stipulated by the archaeological excavation report. The splitting factor results from this analysis are shown in Figure 5-53. There appears to be no obvious difference to those results shown from the cemetery assessment, with the metatarsals again slightly higher. Due to the lack of skeletons from the sand environment, results are based on two elements from one skeleton; therefore this may not be a true representation of bone material preservation from a sand environment.

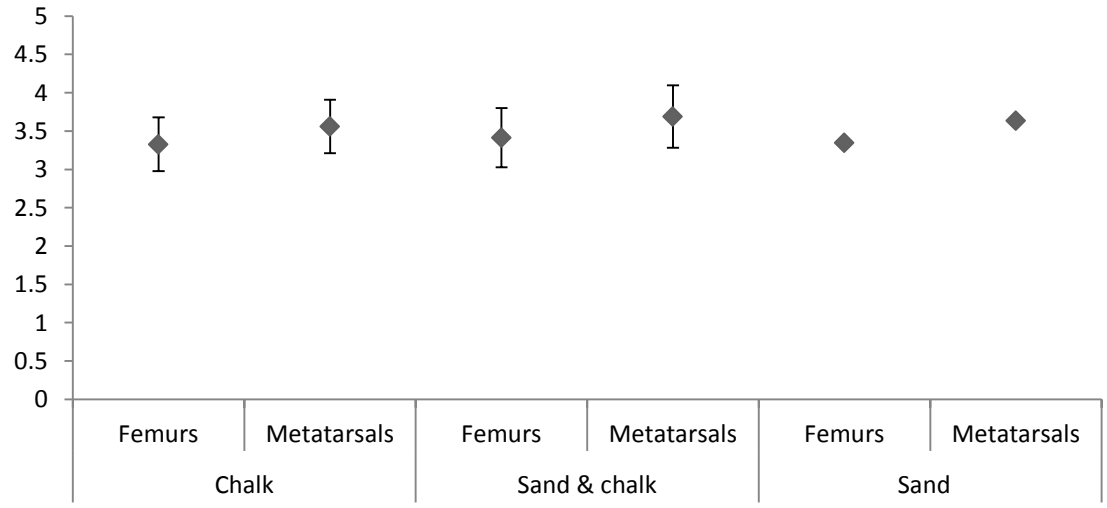

Figure 5-53: Range of splitting factors from femurs and metatarsals across the different burial environments at Eriswell

The estimated carbonate and collagen content from the bones was also analysed in relation to the individual burial environments at Eriswell and the results are shown in Figure 5-54.

The elements with the largest carbonate content were calculated to be metatarsals from the chalk environment, however when relating to the high splitting factor, it would appear the high carbonate content may be due to ion exchange from the environment rather than preservation of the carbonate intrinsic to the bone; the femurs from the chalk environment also showed the highest content of carbonate from all the environments.

The bones from the sand and chalk environment again showed the femurs to have a higher content in comparison to the metatarsals, which supports the information provided by the splitting factor; this is also shown in the results from the collagen content estimation.

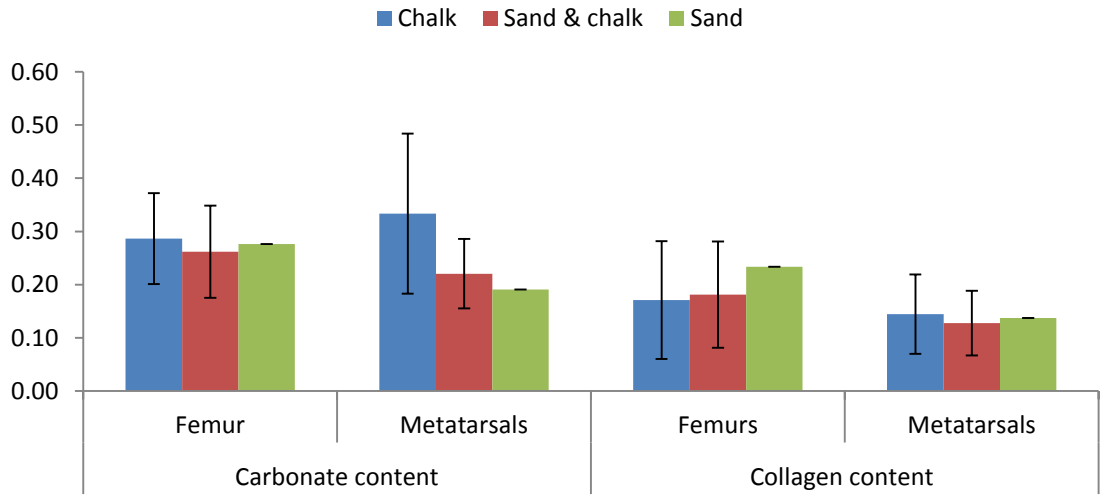

Figure 5-54: Carbonate and collagen content estimates from calculated ratios of femurs and metatarsals across the different burial environments at Eriswell

Results from the collagen content estimation, show the average of all the femurs is higher than that displayed by corresponding metatarsals, however the range of content in both elements is high. The femurs from the chalk environment show the lowest content from all the burial environments, which contradicts the splitting factor results which showed this group of data to have the lowest splitting factor and therefore the best preservation.

The femur from the sand environment displayed the highest collagen content, with the metatarsal at the same level as the chalk metatarsal – it must be noted that this result is based on only one skeleton.

The same extra peaks noted in some of the Fin Cop samples also appeared in a minority of the Eriswell bone samples (see Figure 5-55) and therefore six samples were selected for XRF analysis to determine what the identity of the contamination present.

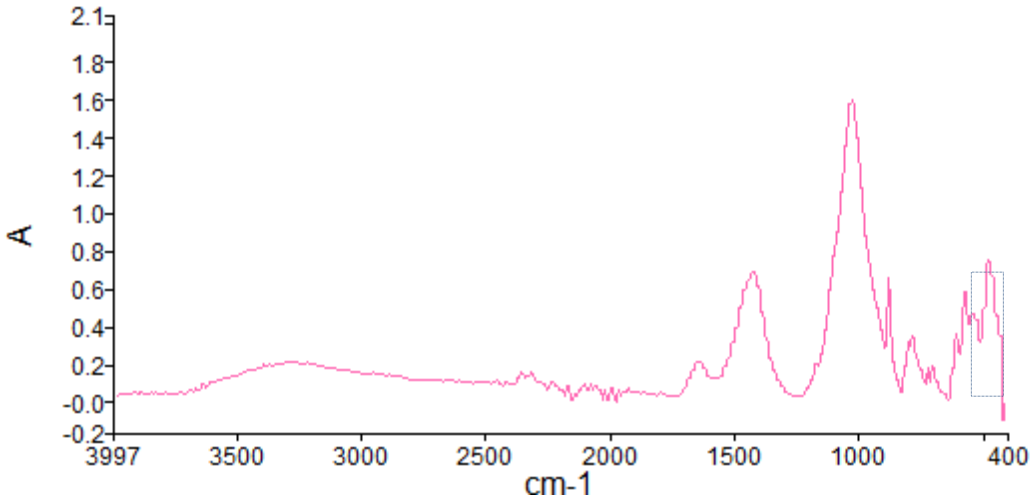

Figure 5-55: ATR-FTIR spectra of Eriswell skeleton 4226 metatarsal sample, showing additional peaks indicated with a box

5.7.2.1 XRF results

Using the same analysis parameters as Fin Cop, the results from the analysis of six samples from three Eriswell skeletons are shown in Table 5-20.

Table 5-20: XRF results showing the averages of three readings from Eriswell bone samples, expressed as area in counts per second

Element	Skeleton 0570		Skeleton 0809		Skeleton 4226	
	Femur	Metatarsal	Femur	Metatarsal	Femur	Metatarsal
Silicon	396.30	1131.83	369.56	1119.81	377.30	707.40
Phosphorus	6528.86	4179.55	6455.74	3920.88	6538.01	5001.29
Calcium	78369.95	63596.15	76884.02	64404.74	78012.26	71253.62
Titanium	18.79	438.50	17.36	183.78	15.15	95.00
Iron	189.28	4730.79	321.30	6019.79	291.33	2236.67
Manganese	210.02	872.87	298.85	612.65	396.72	704.83
Copper	291.95	574.64	379.18	638.60	355.49	335.83
Zinc	284.34	707.50	345.08	694.17	470.50	546.51
Strontium	234.26	350.47	231.82	323.67	420.22	415.79
Zirconium	24.79	1152.46	46.82	747.65	60.96	94.34
Chromium	112.58	142.91	139.50	174.92	123.57	118.63
Nickel	1004.19	1011.81	1117.38	1057.61	1072.66	879.62
Potassium	612.44	945.59	602.37	952.78	605.78	730.44

The results are similar to those obtained from the Fin Cop samples, with the content of iron varying between the samples. Interestingly a pattern can be seen in iron content between the femurs and metatarsals from the same skeletons, with a significantly larger level in metatarsals than femurs. Figure 5-56 shows the XRF spectrum comparison of the femur and metatarsal from skeleton 4226.

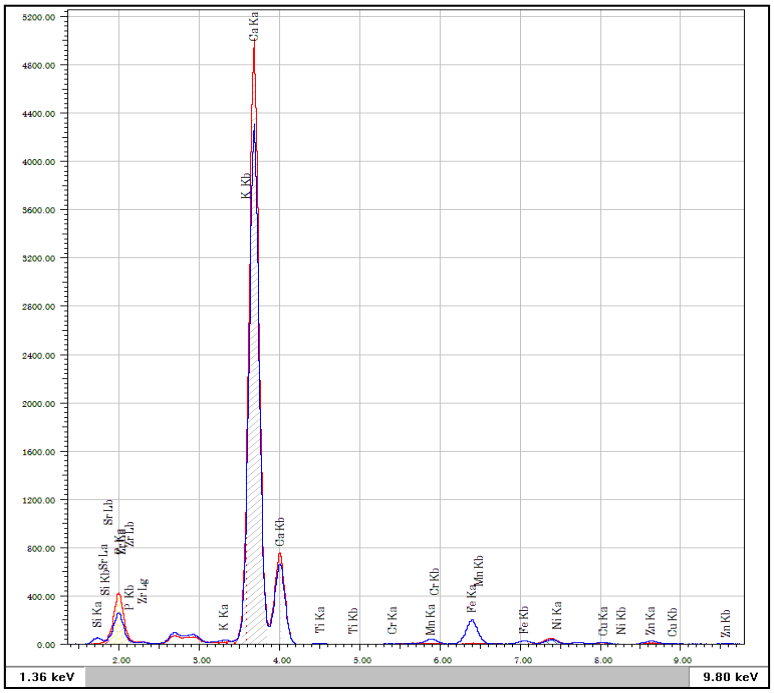

Figure 5-56: Comparison of XRF spectrum of the femur sample shown in red, and the metatarsal sample shown in blue, from skeleton 4226.

The spectrum clearly shows the iron peak from the metatarsal sample (shown in blue) larger than that from the femur sample.

When relating back to the colour data, both metatarsals from skeletons 0809 and 4226 show a slight increase in red from the femurs, but not significantly, and the femur from skeleton 0570 displays more red than the metatarsal.

5.7.3 DNA analysis

This section reports the results from the DNA analysis of the skeletal elements from the Eriswell cemeteries. The results from each individual skeleton are presented initially, with collation of data at the end of the section.

5.7.3.1 Skeleton 0067

Multiple peaks were observed at D16S539, TH01 and vWA on the femur sample, and vWA on the metatarsal sample from Skeleton 0067, showing contamination of the elements from an external DNA source, results can be seen in Table 5-21.

Table 5-21: Skeleton 0067 DNA results

Femur			
Marker	**Allele**	**RFU**	**PHR**
D3S1358	15	39	88.64
D3S1358	17	44	
D19S433	13	38	
D2S1338	19	34	
D16S539	10	42	82.35
D16S539	11	51	73.68
D16S539	13	57	89.47
D18S51	16	64	55.17
D18S51	17	116	
D1S1656	16	36	
TH01	6	64	91.43
TH01	7	70	
TH01	9.3	43	72.09
TH01	13.3	31	
vWA	13	57	84.21
vWA	15	48	
vWA	17	137	81.55
vWA	18	168	

Metatarsal			
Marker	**Allele**	**RFU**	**PHR**
D19S433	14	35	
D10S1248	9	36	59.02
D10S1248	13	61	
TH01	8	38	
vWA	14,14	106	
vWA	17	45	91.11
vWA	20	41	
D21S11	30	43	

The heights of the multiple peaks on the femur show a distinction between a major and minor contributor at TH01 and vWA, but not at D16S539 which displays three peaks of equal height. The metatarsal displays no alleles on this marker, therefore is it not possible to exclude or confirm the potential endogenous alleles.

The heights of the three allelic peaks on the vWA marker on the metatarsal of Skeleton 0067, suggest a heterozygous of 17,20 with an PHR of 91.11%, and a

homozygous 14,14 as with a height of 106 RFU it is over double the height of the heterozygous peaks, and the chances of a sister peak drop-out is only 10-20%. The presence of different alleles on the vWA marker on both the femur and metatarsal suggests as many as four contributors present.

5.7.3.2 Skeleton 0235

DNA data obtained from the femur and metatarsal of Skeleton 0235, showed partial profiles from both elements but with a larger quantity from the femur, as seen in Table 5-22.

Table 5-22: Skeleton 0235 DNA analysis

Femur			
Marker	**Allele**	**RFU**	**PHR**
AMEL	X	106	
D3S1358	12	36	
D3S1358	15	256	64.06
D3S1358	16	164	
D3S1358	17	88	
D19S433	15	35	
D2S1338	19	32	
D16S539	10	77	
D18S51	15	103	
D18S51	17	58	75.32
D18S51	18	77	
D1S1656	16	99	
D2S441	14	36	
TH01	7	684	77.63
TH01	8	531	
TH01	9.3	133	
vWA	13	59	78.67
vWA	16	75	
vWA	17	183	30.91
vWA	18	592	
D21S11	24	80	91.95
D21S11	29	87	
D21S11	30	361	
D12S391	17	56	57.14
D12S391	21	98	
FGA	22.2	85	

Metatarsal			
Marker	**Allele**	**RFU**	**PHR**
D10S1248	13	52	
D2S441	10	59	96.72
D2S441	14	61	
vWA	18	91	

The partial DNA profile from the femur sample of Skeleton 0235 shows more than two alleles at five different loci, suggesting more than one contributor to the genetic information – and this is confirmed by the extensive difference in peak heights at these loci, showing a major contaminant.

By calculating PHR for the peaks, heterozygous peaks can be identified, however, peak imbalance can be seen at D3S1358, vWA and D12S391, but without evidence of further contamination, this imbalance could be explained by preferential amplification. The profile from the metatarsal shares alleles with both the minor and the major contributor from the femur sample, suggesting it is possible the DNA has originated from the same source, however without more alleles it is not possible to give a conclusive result.

5.7.3.3 Skeleton 0326

Analysis from the femur of Skeleton 0326 showed strong contamination from a single source with high RFU, with an underlying minor profile. In contrast, analysis of the DNA data from the metatarsal showed only six alleles, all below 70 RFU, as seen in Table 5-23.

Analysis of the femur data showed no more than four peaks at each loci after stutter peaks, and noise had been eliminated so therefore it is unlikely that there are more than two contributors to the DNA results. The major component of the data is very high in RFU with the highest homozygous peak at 3486 RFU, therefore any peaks lower down would have be washed out due to preferential amplification, overlapping peaks and stutter.

When all the data from the femur and the metatarsal is compared, similarities can be seen between the metatarsal and the minor component of the DNA mixture from the femur, as can be seen in

Although there is not enough data to make a confirmed match, potentially the minor profile on the femur and the DNA present in the metatarsal is in fact endogenous DNA.

Table 5-23: Skeleton 0326 DNA results

Femur				Metatarsal			
Marker	**Allele**	**RFU**	**PHR**	**Marker**	**Allele**	**RFU**	**PHR**
AMEL	X	327	97.90	**D16S539**	13	65	
AMEL	Y	334		**D18S51**	17	41	
D3S1358	15	76	58.91	**D10S1248**	15	57	
D3S1358	16	129		**D8S1179**	6	44	81.82
D3S1358	17	603	96.48	**D8S1179**	13	36	
D3S1358	18	625		**FGA**	24	41	
D19S433	13	739	59.27				
D19S433	14	438					
D2S1338	16	177	83.05				
D2S1338	18	147					
D2S1338	19	49					
D22S1045	11	400	52.00				
D22S1045	15	208					
D22S1045	16	66					
D16S539	9	2600					
D16S539	13	223					
D18S51	12	1332	76.50				
D18S51	14	1019					
D18S51	15	362	42.82				
D18S51	17	155					
D1S1656	12	57	91.94				
D1S1656	15	62					
D1S1656	16	533	87.24				
D1S1656	17	465					
D10S1248	13	134	68.66				
D10S1248	15	92					
D10S1248	14	310	76.13				
D10S1248	17	236					
D2S441	10	82					
D2S441	11	224					
D2S441	14	155	69.20				
TH01	4	30	75.00				
TH01	6	40					
TH01	8	2506					
vWA	18	250					
vWA	16	1119	90.53				
vWA	19	1013					
D21S11	29	933	75.56				
D21S11	30	705					
D12S391	21	216					
D12S391	18	643	61.28				
D12S391	22	394					
D8S1179	10	843	69.61				
D8S1179	12	1211					
D8S1179	11	202	77.72				
D8S1179	13	157					
FGA	23	3486					

5.7.3.4 Skeleton 0425

Analysis of the femur from Skeleton 0425 showed evidence of contamination on the markers: vWA, D21S11 and FGA, whereas the metatarsal data shows no evidence of contamination, as only two peaks are present, both with heights below 50 RFU. Results displayed in Table 5-24.

Table 5-24: Skeleton 0425 DNA results

Femur				Metatarsal		
Marker	**Allele**	**RFU**	**PHR**	**Marker**	**Allele**	**RFU**
AMEL	X	178		**D3S1358**	16	44
D3S1358	14	76		**vWA**	18	42
D2S1338	19	39				
D16S539	11	109	69.72			
D16S539	13	76				
D18S51	14	275	20.00			
D18S51	15	55				
D1S1656	16	41				
D10S1248	13	38	81.58			
D10S1248	15	31				
TH01	7	252				
TH01	8	66				
vWA	16	62	74.19			
vWA	18	46				
vWA	19	36	80.00			
vWA	22	45				
D21S11	28	53	89.83			
D21S11	31	59				
D21S11	36	37				
D12S391	17	90	61.64			
D12S391	21	146				
D8S1179	13	356				
FGA	17	82				
FGA	21	90				
FGA	23.2	81				
FGA	24	96				
FGA	46.2	83				

Multiple peaks on vWA and D21S11 can be categorised into two profiles, by using PHR, although due to similar peak heights there is not a strong 'major' profile. Due to the similar heights of five peaks at the FGA marker, (all within a range of 15

RFU) it is not possible to distinguish individual profiles due to the many possibilities of allelic pairing.

The markers D18S51, and TH01 show two peaks at each loci, but display severe peak imbalance of 20% and 26.19% respectively. It is possible that the smaller allele at D18S51 is a large stutter peak at +4 bp, however the probability of a heterozygous allele at this loci is 88%. Similarly the probability of heterozygous alleles at TH01 is 79%, therefore with the absence of more peaks, this peak imbalance may be due to preferential amplification as the probability of sister allele drop-out is less than 1%.

As shown in Table 5-24 (with the exception of FGA) the potential profiles are detailed, showing a minimum number of contributors of two to the femur and no evidence of contamination from the metatarsal.

Due to the lack of information from the metatarsal, it is not possible to comment on the inclusion or exclusion of the DNA originating from the same individual.

5.7.3.5 Skeleton 0426

Analysis of the elements from Skeleton 0426 resulted in no peaks from the femur, but the generated a full profile from the metatarsal, with two peaks at each of the markers as seen in Table 5-25. The lack of multiple peaks at the markers suggests that no contamination is present, however peak imbalance is evident at three loci – D3S1358 (44.99%), TH01 (44.09%) and D2S11 (23.22%), although this could be due to preferential amplification during the PCR.

Despite the heights of the peaks having a relatively high RFU at majority of the markers, the Amelogenin marker shows significantly lower peaks, suggesting amplification had not been as successful at this loci.

Table 5-25: Skeleton 0426 DNA results

	Metatarsal		
Marker	**Allele**	**Height**	**PHR**
AMEL	X	53	90.57
AMEL	Y	48	
D3S1358	14	184	44.99
D3S1358	17	409	
D19S433	11	433	64.90
D19S433	12	281	
D2S1338	17	150	88.67
D2S1338	20	133	
D22S1045	11	186	82.80
D22S1045	15	154	
D16S539	11	523	94.75
D16S539	13	552	
D18S51	12	651	82.64
D18S51	13	538	
D1S1656	15	359	60.44
D1S1656	16.3	594	
D10S1248	13	236	89.73
D10S1248	16	263	
D2S441	11	235	96.71
D2S441	14	243	
TH01	6	499	44.09
TH01	9.3	220	
vWA	17	641	78.55
vWA	19	816	
D21S11	29	435	23.22
D21S11	32.2	101	
D12S391	19	201	92.20
D12S391	20	218	
D8S1179	13	133	94.33
D8S1179	14	141	
FGA	20	245	85.96
FGA	24	285	

5.7.3.6 Skeleton 0477

No allelic peaks were present from the femur of Skeleton 0477, in comparison with 15 of the 16 loci present in the metatarsal sample, as displayed in Table 5-26.

Table 5-26: Skeleton 0477 DNA results

	Metatarsal		
Marker	**Allele**	**Height**	**PHR**
D3S1358	15	65	
D19S433	13	56	73.21
D19S433	15	41	
D2S1338	19	30	
D22S1045	11	213	33.33
D22S1045	16	71	
D16S539	13	32	
D18S51	15	186	87.63
D18S51	17	163	
D1S1656	16	141	
D10S1248	13	95	33.22
D10S1248	15	286	
D2S441	10	75	89.29
D2S441	14	84	
TH01	7	77	43.75
TH01	8	176	
vWA	18	316	
D21S11	30	342	
D12S391	17	117	66.67
D12S391	21	78	
D8S1179	11	41	70.69
D8S1179	13	58	
FGA	24	284	

No more than two peaks were present at each loci, yet unusually for expected degraded DNA samples, the bigger DNA fragments amplified more efficiently than the smaller ones – Amelogenin is the only marker displaying no peaks yet the region is less than 150 bp. PHR calculations indicated peak height imbalance at D22S1045, D10S1248 and TH01.

Upon comparison to the reference samples, it was found that all present alleles matched with the researcher, and therefore confirmed as exogenous contamination from modern DNA. The peak imbalance of the three loci, were actually sister alleles, and therefore due to preferential amplification. The allelic drop-out could also be observed at six different loci, where only one peak was present.– this information would be taken into account for future analysis.

5.7.3.7 Skeleton 0570

Both samples from skeleton 0570 confirmed evidence of DNA, with 11 loci on the femur sample displaying peaks and 16 loci on the metatarsal sample as seen in Table 5-27.

Table 5-27: Skeleton 0570 DNA results

Femur				Metatarsal			
Marker	**Allele**	**Height**	**PHR**	**Marker**	**Allele**	**Height**	**PHR**
AMEL	X	26		**AMEL**	X	163	
D3S1358	17	49	83.67	**D3S1358**	17	328	92.39
D3S1358	18	41		**D3S1358**	18	355	
D19S433	14	43	95.35	**D19S433**	14	348	87.64
D19S433	15	41		**D19S433**	15	305	
D16S539	10	178	74.16	**D2S1338**	20	57	68.42
D16S539	13	132		**D2S1338**	23	39	
D18S51	16	155	83.87	**D22S1045**	11	60	85.00
D18S51	17	130		**D22S1045**	17	51	
D1S1656	13	55		**D16S539**	10	535	78.69
TH01	6	155	76.13	**D16S539**	13	421	
TH01	9.3	118		**D18S51**	16	248	60.05
vWA	14	133	100.00	**D18S51**	17	413	
vWA	18	133		**D1S1656**	13	128	55.41
D21S11	30	58		**D1S1656**	17.3	231	
D8S1179	9	35		**D10S1248**	15	225	
FGA	21	61	96.83	**D2S441**	11	188	27.13
FGA	22	63		**D2S441**	14	51	
				TH01	6	1548	60.59
				TH01	9.3	938	
				vWA	14	754	98.41
				vWA	18	742	
				D21S11	30	441	
				D12S391	18	76	46.05
				D12S391	22	35	
				D8S1179	9	237	59.92
				D8S1179	10	142	
				FGA	21	215	96.85
				FGA	22	222	

No multiple peaks were seen within any of the loci, showing no evidence of DNA from more than one individual being present in the samples.

PHR calculations on the allelic peaks from the femur confirmed true sister peaks, whilst peak imbalance was seen at D1S1656 (55.41%), D2S441 (27.13%), D12S391 (46.05%) and D8S1179 (59.92%) from the metatarsal.

5.7.3.8 Skeleton 0612

The results from the DNA analysis of the femur and the metatarsal are displayed in Table 5-28.

Table 5-28: Skeleton 0612 DNA results

Femur				Metatarsal			
Marker	**Allele**	**Height**	**PHR**	**Marker**	**Allele**	**Height**	**PHR**
AMEL	X	56		**AMEL**	X	48	
D19S433	13	49		**D3S1358**	14	59	
D18S51	17	45		**D19S433**	13	51	
TH01	7	30		**D22S1045**	11	99	
vWA	15	33	96.97	**D16S539**	12	31	
vWA	18	32		**D18S51**	15	133	33.83
FGA	21	30	65.22	**D18S51**	16	45	
FGA	22	46		**D1S1656**	16	65	
				D10S1248	13	58	
				TH01	7	111	83.78
				TH01	9.3	93	
				vWA	15	83	61.48
				vWA	18	135	
				D21S11	28	50	
				D12S391	17	174	
				D12S391	18.3	52	92.31
				D12S391	21	48	
				D8S1179	11	89	78.76
				D8S1179	13	113	
				FGA	21	37	

Eight peaks were determined from the Skeleton 0612 femur at six different loci including amelogenin. Sister peaks were observed at vWA and FGA, both of which met the criteria using PHR at 96.97% and 65.22% respectively. Single peaks were seen at D19S433, D18S51 and TH01, of which the calculated probability of allelic drop-out was 90-95%, ~80%, and 99% respectively.

Analysis of the metatarsal resulted in more DNA present than the femur, with 20 peaks across 14 loci. Sister alleles can be identified by PHR at TH01, vWA, D12S391 and D8S1179; however multiple loci were displayed at D12S391 suggesting contamination from an external source, and severe peak imbalance at D18S51 also supports this occurrence.

Similarities can be seen between the DNA from the femur and the minor profile from the metatarsal, where four alleles match at D19S433, TH01, vWA and FGA. They are no conflicting alleles in the profile, supporting the possibility that the profiles obtained from the femur and metatarsal (minor) result from intrinsic DNA.

5.7.3.9 Skeleton 0692

Analysis of the metatarsal and femur from skeleton 0692 displayed evidence of the potential of two profiles on each element, as displayed in Table 5-29.

Table 5-29: Skeleton 0692 DNA results

Femur				Metatarsal			
Marker	**Allele**	**Height**	**PHR**	**Marker**	**Allele**	**Height**	**PHR**
AMEL	X	83	19.28	**D3S1358**	14	92	
AMEL	Y	16		**D19S433**	15.2	41	
D3S1358	15	24	95.83	**D16S539**	11	129	
D3S1358	16	23		**D18S51**	15	94	
D19S433	15.2	18		**D18S51**	16	31	93.94
D16S539	11	84	84	**D18S51**	18	33	
D16S539	13	100		**D1S1656**	12	42	
TH01	7	62		**TH01**	6	188	82.98
TH01	8	35	71.43	**TH01**	9	156	
TH01	9	25		**vWA**	17	488	
vWA	17	96	40.63	**D21S11**	29	23	88.46
vWA	18	39		**D21S11**	30	26	
D21S11	29	17	50	**D12S391**	20	33	93.94
D21S11	30	34		**D12S391**	22	31	
FGA	18	35	94.29	**D8S1179**	15	38	
FGA	21	33					

Only two incidences of multiple peaks at loci were reported, TH01 on the femur and D18S51 on the metatarsal, however severe peak imbalance was seen at multiple loci.

Similarities can be seen between the two minor profiles: allele 15.2 at D19S433, alleles 29,30 at D21S11, and with no conflicting alleles present, it is possible that the profiles originate from the same source, and may be intrinsic DNA.

None of the genotypes match that of the researcher or any reference profiles, therefore the major profile contamination present must have occurred prior to submission.

5.7.3.10 Skeleton 0717

DNA quantity from the elements of skeleton 0717 was extremely low, with the highest peak height resulting in the X allele at the Amelogenin marker on the femur at 43 RFU , and no detectable DNA from the metatarsal as seen in Table 5-30.

Table 5-30: Skeleton 0717 DNA results

	Femur	
Marker	**Allele**	**Height (RFU)**
AMEL	X	43
D3S1358	17	21
D2S1338	19	24
D16S539	10	30
TH01	7	42
FGA	21	34

Only single peaks were observed above the noise threshold on the femur sample, so no PHR calculations were necessary to establish pairings. All peaks identified were below 50 RFU which is the standard detection limit used in the majority of forensic laboratories.

5.7.3.11 Skeleton 0759

Analysis of the femur and metatarsal from skeleton 0759 showed low quantity DNA in both elements – eight peaks over five loci on the femur, and three peaks at the vWA marker on the metatarsal, as result of a tri-allelic pattern.

Majority of the peaks identified, as shown in Table 5-31, were below 50 RFU so it is possible that more peaks are present but are disguised by the background noise.

Table 5-31: Skeleton 0759 DNA results

Femur				Metatarsal		
Marker	**Allele**	**Height**	**PHR**	**Marker**	**Allele**	**Height**
D19S433	13	38		**vWA**	15	36
D18S51	15	41	97.56	**vWA**	16	39
D18S51	17	40		**vWA**	17	42
TH01	7	43	81.13			
TH01	9.3	53				
vWA	16	32	87.50			
vWA	18	28				
FGA	19	59				

The only marker to display alleles on both elements is vWA – and conflicting results are reported. This can be explained, by either the skeletal elements originating from different individuals, which is unlikely due to the reported single burial environment; or due most likely due to contamination of one or both of the elements by an external DNA source.

5.7.3.12 Skeleton 0791

No detectable DNA was found from the femur sample of skeleton 0791, and only eight alleles were found present over six loci from the metatarsal analysis, as shown in Table 5-32.

Table 5-32: Skeleton 0791 DNA results

Metatarsal			
Marker	**Allele**	**Height**	**PHR**
D3S1358	15	42	
D18S51	14	53	
D1S1656	12	33	
D10S1248	13	46	69.57
D10S1248	17	32	
TH01	8	52	63.46
TH01	9.3	33	
vWA	15	78	

Two heterozygous allelic pairs were calculated on D10S1248 and TH01, with the rest of the loci displaying a single peak or no peaks.

Based on the peak height of allele 15 at the vWA marker in relation to the other peaks present, and with a probability of allele drop-out of 30-40% it appears likely that this is a homozygous allele. The remaining loci displaying single peaks have a minimum of 70% probability of drop-out, due to the low RFU.

The absence of any data from the femur results in no ability to comment further on the origin of the DNA, but there is no evidence of contamination.

5.7.3.13 Skeleton 0799

Analysis of the elements from skeleton 0799 showed the presence of DNA on both the femur and metatarsal, results of which are shown in Table 5-33. Interpretation of the data concludes six peaks over five loci for the femur, and four peaks over three loci for the metatarsal sample.

Table 5-33: Skeleton 0799 DNA results

Femur				Metatarsal			
Marker	**Allele**	**Height**	**PHR**	**Marker**	**Allele**	**Height**	**PHR**
AMEL	X	25		**D18S51**	14	46	
D16S539	10	72		**vWA**	18	49	93.88
D2S441	14	96		**vWA**	19	46	
D8S1179	11	78		**D12S391**	21	65	
FGA	21	30	71.43				
FGA	24	42					

FGA displayed two alleles, providing a PHR of 71.43% on the femur, and the metatarsal – two alleles at vWA had a PHR of 93.88% confirming both sets of sister peaks as heterozygous. Low RFU of the single peak heights detected, suggest it is likely that allele drop-out has occurred at the remaining loci.

Due to the presence and location of electrical spikes on the electropherogram of the femur sample, it is not possible to comment on the presence or absence of the Y allele at the amelogenin marker.

Upon comparison of the data between the elements, no corresponding alleles are shown due to different loci being populated with data, therefore no comment can be made on the origin of the samples, however no evidence contamination was detected.

5.7.3.14 Skeleton 0808

The electropherogram of the femur sample from skeleton 0808 displayed high levels of noise from the instrument and electrical spikes, which may have resulted in the masking of peaks, however two alleles were detected at two different loci, as shown in Table 5-34.

In contrast, analysis of the metatarsal resulted in the identification of 22 alleles at 14 loci. Three alleles were detected at the D3S1358 marker, resulting from either more than one DNA contributor to the sample, or the presence of a tri-allelic pattern. Although this pattern has been previously reported at this locus, the peak heights do not correlate with type 1 or type 2, and the peak imbalance noted at other loci on the electropherogram, suggests the possibility that the detection of three alleles may be due to contamination. Working on this assumption, the potential genotypes of the DNA sample based on peak heights and PHR calculations is illustrated in Table 5-34.

Table 5-34: Skeleton 0808 DNA results

Femur		
Marker	**Allele**	**Height**
vWA	18	74
D21S11	38.2	68

Metatarsal			
Marker	**Allele**	**Height**	
AMEL	X	186	
D3S1358	15	43	
D3S1358	17	84	67.86
D3S1358	18	57	
D19S433	13	28	
D22S1045	16	36	
D16S539	11	146	93.15
D16S539	12	136	
D18S51	13	128	29.69
D18S51	16	38	
D1S1656	11	75	
D2S441	14	33	
TH01	6	234	68.80
TH01	9	161	
vWA	16	87	
D21S11	30.3	32	
D12S391	19	80	63.75
D12S391	20	51	
D8S1179	10	134	49.26
D8S1179	12	272	
FGA	20	68	57.14
FGA	22	119	

Despite the possibility of the tri-allelic pattern explanation, and the lack of any conflicting alleles from the analysis of the femur and metatarsal, due to the complication of the three alleles at D3S1358, and the peak imbalance throughout the electropherogram it is not possible to conclusively state the number of contributors within this sample, or whether this DNA is in fact intrinsic DNA.

5.7.3.15 Skeleton 0809

Data analysis of skeleton 0809 resulted in the identification of four alleles at three markers on the femur and five alleles at four loci on the metatarsal as shown in Table 5-35.

Table 5-35: Skeleton 0809 DNA results

Femur				Metatarsal			
Marker	**Allele**	**Height**	**PHR**	**Marker**	**Allele**	**Height**	**PHR**
TH01	8	51		**D16S539**	11	50	
D8S1179	17	51		**D18S51**	15	52	
FGA	31	35	94.29	**TH01**	7	89	
FGA	31.2	33		**vWA**	15	129	65.12
				vWA	16	84	

Heterozygous peaks are confirmed by PHR at both loci displaying two alleles. Calculations of allele drop-out show high probability of occurrence where single alleles are present.

No conflicting or duplicating alleles were identified at the represented loci, and with a maximum of two alleles at each loci and low RFU of the peaks, there is no evidence of contamination from an external source.

5.7.3.16 Skeleton 0991

An abundance of DNA was discovered in the samples from skeleton 0991, with the femur displaying alleles at 13/16 of the markers tested, and the metatarsal analysis producing a full profile as seen in Table 5-36.

Table 5-36: Skeleton 0991 DNA results

Femur				Metatarsal			
Marker	**Allele**	**Height**	**PHR**	**Marker**	**Allele**	**Height**	**PHR**
AMEL	X	453		**AMEL**	X	1130	
D3S1358	15	98	96.94	**D3S1358**	15	1066	88.18
D3S1358	18	95		**D3S1358**	18	940	
D3S1358	16	52	48.08	**D19S433**	14	776	76.55
D3S1358	17	25		**D19S433**	15	594	
D19S433	14	153	53.15	**D2S1338**	20	466	
D19S433	15	76		**D22S1045**	15	253	86.17
D19S433	13	48		**D22S1045**	16	218	
D2S1338	20	32		**D16S539**	12	1636	90.71
D16S539	10	69	57.97	**D16S539**	13	1484	
D16S539	11	40		**D18S51**	12	1172	83.12
D16S539	12	279	80.65	**D18S51**	17	1410	
D16S539	13	225		**D1S1656**	14	544	87.60
D18S51	12	309	37.22	**D1S1656**	15	621	
D18S51	17	115		**D10S1248**	13	461	75.49
D18S51	14	75	64.10	**D10S1248**	16	348	
D18S51	15	117		**D2S441**	13	177	85.51
D1S1656	14	88	76.52	**D2S441**	14	207	
D1S1656	15	115		**TH01**	8	2288	97.15
D10S1248	13	48	64.58	**TH01**	9.3	2355	
D10S1248	16	31		**vWA**	16	1841	98.19
D10S1248	14	50	68.00	**vWA**	17	1875	
D10S1248	15	34		**D21S11**	29	746	78.53
TH01	8	570	78.07	**D21S11**	31	950	
TH01	9.3	445		**D12S391**	17	460	43.48
vWA	12	54	36.24	**D12S391**	24	200	
vWA	18	149		**D8S1179**	12	1762	51.87
vWA	16	602	57.81	**D8S1179**	14	914	
vWA	17	348		**FGA**	20	1903	80.40
D21S11	29	51	25.76	**FGA**	25	1530	
D21S11	31	198					
D21S11	33.2	32	100.00				
D21S11	36	32					
D8S1179	12	240	97.96				
D8S1179	14	245					
FGA	20	284	76.34				
FGA	25	372					
FGA	21	141					

Evidence of contamination within the femur sample was evident with eight loci displaying multiple alleles. The RFU of the peaks of the major component in the femur, and the peaks in the metatarsal sample strongly suggest that the DNA present is not intrinsic to the skeleton, but more likely to be contamination from a modern source. This modern profile does not match the reference samples held of the researcher, or any personnel with access to the laboratory where analysis was conducted, and therefore must belong to an archaeologist / anthropologist or another unknown individual who handled the bones prior to submission to the researcher.

Given the strength of the data and no evidence of more than one profile in the metatarsal sample, inferences could be made to confirm the allocation of allele pairings within the femur sample. By utilising the comparison of the modern profile, it is possible to confirm that the alleles described in the minor component of the femur sample, do not belong to the same contaminant, and with the low RFU and characteristic evidence of degradation of larger alleles, it is possible this profile belongs to skeleton 0991.

Skeleton 0994Table 5-37 shows the results of the DNA analysis of skeleton 0994, where allelic peaks were identified on both the femur and metatarsal samples.

Electropherograms from skeleton 0994, showed the metatarsal exhibiting seven alleles over five alleles, with PHR calculations identifying the pairs at D10S1248 and vWA as sister alleles.

Interpretation of the results from analysis of the femur proved much more complicated with evidence of contamination in the form of multiple peaks at nine loci. The peaks were assigned to minor or major contributors using peak heights and PHR calculations. Peak imbalance is evident and so is allele drop-out which further complicates the interpretation.

Table 5-37: Skeleton 0994 DNA results

Femur			
Marker	**Allele**	**Height**	**PHR**
AMEL	X	240	90.42
AMEL	Y	217	
D3S1358	15	226	51.77
D3S1358	18	117	
D3S1358	16	77	87.01
D3S1358	17	67	
D19S433	13	89	95.70 (13,14)
D19S433	14	93	86.02 (14,16.2)
D19S433	16.2	80	89.89 (13,16.2)
D2S1338	19	60	85.00
D2S1338	23	51	
D22S1045	11	62	79.49
D22S1045	16	78	
D16S539	10	183	55.74
D16S539	13	102	
D16S539	12	644	
D18S51	13	412	71.84
D18S51	14	296	
D18S51	15	149	63.76
D18S51	17	95	
D1S1656	13	71	91.03
D1S1656	16	78	
D10S1248	13	262	42.75(13,14)
D10S1248	14	112	15.65(13,15)
D10S1248	15	41	36.61(14,15)
D2S441	10	55	33.95
D2S441	14	162	
TH01	7	124	99.19
TH01	8	123	
TH01	9	326	63.80
TH01	9.3	511	
vWA	14	42	
vWA	17	267	
vWA	18	993	
D21S11	28	46	
D21S11	29	146	83.91
D21S11	30	174	
D12S391	17	46	100.00
D12S391	21	46	
D8S1179	11	720	19.17
D8S1179	13	138	
FGA	21	295	90.49
FGA	25	326	
FGA	22	233	59.66
FGA	24	139	

Metatarsal			
Marker	**Allele**	**Height**	**PHR**
D18S51	15	35	
D1S1656	16	38	
D10S1248	13	63	82.54
D10S1248	15	52	
TH01	7	31	
vWA	17	56	69.14
vWA	18	81	

When these profiles were compared to reference samples, similarities were discovered with the profile of the researcher, providing evidence that peak imbalance and allele drop-out had occurred. The contamination from the researcher displayed as a minor contributor in the most case, and therefore it is unlikely the remaining DNA present is intrinsic to the bone due to the levels of concentration. The major component did not match any reference samples therefore must belong to an unknown individual (male) who had contact with the bones prior to DNA analysis.

5.7.3.17 Skeleton 4040

Analysis of the femur showed no evidence of contamination as no multiple peaks were found, and majority of peaks were of low height; however allele 29 at D21S11 displayed a relatively high RFU in relation to the rest of the electropherogram, as evident in Table 5-38, but this could be explained as a homozygous peak.

Interpretation of the metatarsal data showed no evidence of contamination due to multiple peaks, nonetheless with some peak heights in excess of 1000 RFU – this is way above the expected level for ancient DNA, and therefore may have been compromised by modern DNA; which does not match the reference samples on file.

All allele pairings were confirmed with high PHR values and no evidence of allele drop-out – as expected with peaks of this height.

Table 5-38: Skeleton 4040 DNA results

Femur				Metatarsal			
Marker	**Allele**	**Height**	**PHR**	**Marker**	**Allele**	**Height**	**PHR**
D19S433	9	35		**AMEL**	X	653	
D18S51	17	35		**D3S1358**	16	141	91.56
TH01	7	33	82.50	**D3S1358**	18	154	
TH01	8	40		**D19S433**	14	315	91.84
D21S11	29	94		**D19S433**	16	343	
D8S1179	10	43		**D22S1045**	16	34	65.38
				D22S1045	17	52	
				D16S539	11	512	72.07
				D16S539	12	369	
				D18S51	12	738	70.33
				D18S51	14	519	
				D1S1656	15.3	121	
				D10S1248	14	444	
				D2S441	11	47	
				TH01	7	994	93.51
				TH01	8	1063	
				vWA	17	617	91.41
				vWA	18	564	
				D21S11	29	311	
				D12S391	20	42	
				D8S1179	10	703	84.92
				D8S1179	13	597	
				FGA	24	626	94.57
				FGA	25	592	

By comparing the major profile from the metatarsal to the profile obtained from the femur, it is possible that the alleles at TH01, D21S11 and D8S1179 have also originated from an external source, however, only allele 29 on D21S11 showed comparatively high peak height.

5.7.3.18 Skeleton 4046

Analysis of the electropherograms from skeleton 4046 identified alleles on both the femur and the metatarsal samples, as seen in Table 5-39.

Table 5-39: Skeleton 4046 DNA results

Femur		
Marker	**Allele**	**Height**
D2S1338	23	48
vWA	18	71
D12S391	21	75
FGA	22	57

Metatarsal			
Marker	**Allele**	**Height**	**PHR**
D3S1358	15	49	90.74
D3S1358	16	54	
D19S433	13	93	67.74
D19S433	15	63	
D2S1338	23	32	
D22S1045	15	31	93.94
D22S1045	16	33	
D18S51	15	216	
D1S1656	16	132	
D10S1248	13	162	
TH01	7	135	98.52
TH01	8	133	
vWA	15	48	26.23
vWA	18	183	
D21S11	30	151	91.39
D21S11	31	138	
D12S391	17	56	67.86
D12S391	21	38	
FGA	24	41	

At first glance there was no evidence of more than one DNA contributor to the elements from skeleton 4046, however when comparing the results to reference samples it became apparent that contamination from modern DNA from the researcher may have occurred.

The four alleles from the femur sample could all be assigned to a reference sample, and only two alleles from the metatarsal profile could be positively eliminated from the contamination – allele 15 at D22S1045, and allele 15 at vWA. The two alleles at D22S1045 displayed a very high PHR of 93.94, and low RFU so it is possible that alleles do not belong to the researcher; PHR calculations on the alleles 15 at vWA, showed the allele not assigned to the researcher was unlikely to be heterozygous with allele 18 and had very low RFU so it is unlikely to be contamination.

5.7.3.19 Skeleton 4067

Analysis of the femur and metatarsal from skeleton 4067 identified a high number of alleles as seen in Table 5-40. Although the RFU values on the metatarsal are high at some of the loci, there are no more than two peaks at each, therefore no evidence of more than one contributor.

Table 5-40: Skeleton 4067 DNA analysis

Femur			
Marker	**Allele**	**Height**	**RFU**
AMEL	X	378	78.57
AMEL	Y	297	
D3S1358	15	211	89.57
D3S1358	17	189	
D3S1358	16	107	
D19S433	13	119	91.54 (13&14)
D19S433	14	130	89.04 (14&15)
D19S433	15	146	81.51 (13&15)
D2S1338	17	76	71.05
D2S1338	23	54	
D2S1338	18	38	90.48
D2S1338	19	42	
D16S539	10	355	71.14
D16S539	13	499	
D16S539	12	1053	
D18S51	13	497	
D18S51	15	231	54.11
D18S51	17	125	
D1S1656	10	82	
D1S1656	16	120	75.47
D1S1656	16.3	159	
D10S1248	13	241	94.19
D10S1248	15	227	
D10S1248	17	41	
D2S441	10	94	76.42
D2S441	14	123	
TH01	7	348	79.02
TH01	8	275	
TH01	9.3	1307	
vWA	17	570	77.55
vWA	18	735	
D21S11	30	467	23.13
D21S11	31	108	
D12S391	17	408	
D12S391	21	169	40.83
D12S391	23	63	
D8S1179	11	435	84.63
D8S1179	12	514	
D8S1179	13	794	
FGA	21	578	89.89
FGA	24	643	

Metatarsal			
Marker	**Allele**	**Height**	**RFU**
AMEL	X	59	79.73
AMEL	Y	74	
D3S1358	16	168	89.84
D3S1358	17	187	
D19S433	14	82	50.00
D19S433	15	41	
D16S539	12	603	
D18S51	13	539	
D1S1656	16.3	42	
D10S1248	14	82	82.00
D10S1248	17	100	
vWA	17	273	59.71
vWA	18	163	
D21S11	30	226	
D12S391	17	66	75.76
D12S391	21	50	
D8S1179	12	140	94.29
D8S1179	13	132	
FGA	21	232	82.86
FGA	24	280	

However multiple alleles are present at nine loci on the femur, showing at least two contributors to the DNA profile. PHR calculations were performed to identify heterozygous peaks to assist with the allocation of alleles to genotypes. However, some the peak height of the alleles varies greatly from 38RFU at the smallest, to 1307 at the highest. This shows it is likely that preferential amplification has occurred, rendering the PHR calculations as a means of identifying sister peaks, inaccurate. Instead, the profile was compared to reference samples, in order to eliminate the contamination.

5.7.3.20 Skeleton 4095

Analysis of the femur from skeleton 4095 resulted in the presentation of only three alleles at three different loci, as shown in Table 5-41. The lack of allele presence or multiple alleles, and low RFU of the peaks suggest no evidence of contamination.

Table 5-41: Skeleton 4095 DNA results

	Femur	
Marker	**Allele**	**Height**
TH01	9.3	80
vWA	18	44
D21S11	30	35

5.7.3.21 Skeleton 4098

Electropherograms from the femur of skeleton 4098 showed 11 alleles distributed across eight loci, as shown in Table 5-42, there was no metatarsal to available to analyse.

Table 5-42: Skeleton 4098 DNA results

	Femur		
Marker	**Allele**	**Height**	**PHR**
D3S1358	15	52	80.77 (15,16)
D3S1358	16	42	78.57 (16,17)
D3S1358	17	33	63.46(15,17)
D16S539	12	70	82.35
D16S539	13	85	
D18S51	13.2	36	
D1S1656	11	72	
D10S1248	13	30	
vWA	18	81	
D21S11	31	34	
FGA	23	31	

Three alleles were located at the D3S1358 marker, but peak heights and previous reported occurrence of this pattern suggest this may be a tri-allelic pattern rather than more than one contributor. There is no other evidence in the data to suggest contamination has occurred.

The only other pair of alleles is reported at D16S539 where PHR confirm the probability of sister alleles.

5.7.3.22 Skeleton 4099

Results from the analysis of the femur and metatarsal samples from skeleton 4099, show very low and degraded quantities of DNA - as reported in Table 5-43.

Table 5-43: Skeleton 4099 DNA results

Femur			Metatarsal			
Marker	**Allele**	**Height**	**Marker**	**Allele**	**Height**	
D10S1248	13	58	**D3S1358**	14	33	56.90
vWA	18	59	**D3S1358**	16	58	
D21S11	31	41	**D8S1179**	13	44	
D8S1179	11	34	**FGA**	24	55	

After comparison with reference samples, all but one of the alleles present – allele 14 at D3S1358, can be attributed to the researcher's reference sample.

5.7.3.23 Skeleton 4191

Six alleles were identified from the analysis from the femur of skeleton 4191, as seen in Table 5-44.

Table 5-44: Skeleton 4191 DNA analysis

Femur			
Marker	**Allele**	**Height**	**PHR**
D16S539	12	35	71.43
D16S539	13	49	
TH01	7	78	42.31
TH01	8	33	
vWA	18	79	
FGA	24	37	

Five of the observed alleles are shared with the researcher, and although further peaks can be seen at low RFUs, due to the noise level it is not possible to accurately assign them as true alleles.

5.7.3.24 Skeleton 4222

Due to the unavailability of the metatarsal of skeleton 4222, a section of sternum was used for DNA analysis, in addition to the femur. Results from the analysis are shown in Table 5-45.

Table 5-45: Skeleton 4222 DNA analysis

Femur			
Marker	**Allele**	**Height**	**PHR**
D22S1045	16	36	
TH01	7	63	65.08
TH01	9	41	
D21S11	30	47	

Sternum			
Marker	**Allele**	**Height**	**PHR**
D3S1358	14	50	80.00
D3S1358	16	40	
D19S433	14	33	62.26
D19S433	17.2	53	
D16S539	11	91	63.74
D16S539	12	58	
D18S51	14	169	
TH01	6	111	83.78
TH01	8	93	
vWA	17	150	81.97
vWA	18	183	
D21S11	29	38	84.21
D21S11	30.2	32	

Both elements displayed genetic information, however conflicting alleles were presented at both TH01 and D21S11, suggesting that either the two elements originate from two different individuals or contamination from an external source has occurred. Knowledge of the extensive handling of this skeleton prior to submission to the researcher increase the possibility for contamination. The RFU of the allelic peaks from both elements are low and show characteristic degradation, although PHR results are all within the limit.

5.7.3.25 Skeleton 4226

Analysis of the femur from skeleton 4226 displayed the possibility of contamination due to three allelic peaks at the TH01 marker, as can be seen in Table 5-46.

Table 5-46: Skeleton 4226 DNA analysis

Femur				Metatarsal			
Marker	**Allele**	**Height**	**PHR**	**Marker**	**Allele**	**Height**	**PHR**
Amelogenin	X	20	57.14	**Amelogenin**	X	16	80.00
Amelogenin	Y	35		**Amelogenin**	Y	20	
D3S1358	15	25	40.98	**D19S433**	14	62	
D3S1358	16	61		**D16S539**	6	43	
D19S433	15	52		**D18S51**	16	56	
D16S539	14	215		**TH01**	6	47	
TH01	6	56	71.43 (6,8)	**vWA**	11	60	70.00
TH01	7	78	71.79(6,7)	**vWA**	18	42	
TH01	8	40	51.28 (7,8)	**D12S391**	18	33	
vWA	18	119		**D8S1179**	15	31	
D8S1179	13	39					

Similarities can be seen between the metatarsal and the femur, at Amelogenin, TH01, and vWA. Alleles at Amelogenin and D3S1358 show low PHR values, suggesting the peaks are not heterozygous, or have been subject to preferential amplification.

5.7.3.26 Skeleton 4288

Six alleles were detected from the analysis of the femur from skeleton 4288, as seen in Table 5-47.

Table 5-47: Skeleton 4288 DNA analysis

Femur			
Marker	**Allele**	**Height**	**PHR**
AMEL	X	28	
D3S1358	16	34	
D16S539	8.3	31	81.56
D16S539	10	38	
TH01	7	50	
vWA	18,18	100	

The two alleles at D16S539 show a PHR of 81.58% suggesting they true sister alleles, whilst the height of allele 18 at vWA, in comparison to the other peaks, suggests a homozygous peak. A low RFU was observed on all loci present, and no evidence of contamination.

No allelic peaks were observed from the metatarsal sample, therefore no comparisons between the elements is possible.

5.7.3.27 Skeleton 4291

Only the femur from skeleton 4291 was available for DNA testing, but no allelic peaks were found.

5.7.3.28 Skeleton 4295

Data interpretation of the electropherogram of the femur from skeleton 4295 displayed evidence of contamination with multiple peaks evident at both the D3S1358 and the D16S539 markers, as illustrated in Table 5-48.

Table 5-48: Skeleton 4295 DNA results

	Femur		
Marker	**Allele**	**Height**	**PHR**
AMEL	X	65	81.54
AMEL	Y	53	
D3S1358	14	50	
D3S1358	16	26	92.31
D3S1358	18	24	
D16S539	10	34	57.63
D16S539	11	59	
D16S539	13	152	
D18S51	14	69	56.56
D18S51	17	122	
TH01	8	92	92.00
TH01	9.3	100	
vWA	15	49	25.00
vWA	18	196	
D8S1179	10	98	38.78
D8S1179	14	38	
FGA	21	72	93.06
FGA	23	67	

Further interpretation of the data showed peak imbalance and comparatively high RFUs on some alleles, affecting the PHR value between allelic pairing. As evidence of contamination is present, the results were compared to the researchers profile, however they were not a match, therefore external contamination occurred prior to analysis.

5.7.3.29 Skeleton 4340

Data interpretation, shown in Table 5-49, from the analysis of skeleton 4340 shows the observed alleles from the femur and metatarsal.

Table 5-49: Skeleton 4340 DNA results

Femur				Metatarsal			
Marker	**Allele**	**Height**	**PHR**	**Marker**	**Allele**	**Height**	**PHR**
AMEL	X	39		**D19S433**	13	89	40.45
D19S433	10	21	70.00	**D19S433**	15	36	
D19S433	13	30		**D16S539**	13	104	
D22S1045	11	55		**D10S1248**	15	98	
D16S539	10	47		**TH01**	8	43	
D18S51	15	50	56.18	**vWA**	18	61	
D18S51	17	89		**D21S11**	30	59	90.77
D1S1656	16	54		**D21S11**	31	65	
D10S1248	13	36	65.45				
D10S1248	15	55					
TH01	6	27	96.43				
TH01	7	28					
TH01	8	88	40.91				
TH01	10	36					
vWA	18	87					
D12S391	17	40					
FGA	21	47	76.60				
FGA	24	36					

Comparison with the researcher's profile, showed some similarities to alleles on both elements, therefore it appears contamination has occurred. Smaller peaks can also be seen, but as they do not meet the requirements of 'true alleles' they cannot be assigned.

5.7.3.30 Skeleton 4411

Analysis of the femur from skeleton 4411 displayed only four alleles at three loci., as shown in Table 5-50. Due to the metatarsal being absence, no comparisons to other elements can be made.

Table 5-50: Skeleton 4411 DNA analysis

Femur			
Marker	**Allele**	**Height**	**PHR**
TH01	8	31	
vWA	18	51	70.59
vWA	19	36	
D8S1179	11	38	

5.7.3.31 Skeleton 4462

Data interpretation of the DNA results from skeleton 4462 displayed DNA on both the femur and metatarsal, as shown in Table 5-51.

Table 5-51: Skeleton 4462 DNA analysis

Femur			
Marker	**Allele**	**Height**	**PHR**
AMEL	X	27	74.07
AMEL	Y	20	
D3S1358	15	55	49.09
D3S1358	16	27	
D22S1045	11	44	
D16S539	13	61	
D18S51	16	59	
D1S1656	17.3	41	
D10S1248	15	44	
D2S441	14	58	
TH01	7	54	62.96
TH01	8	34	
vWA	18	126	
D12S391	21	48	
D8S1179	13	42	

Metatarsal			
Marker	**Allele**	**Height**	**PHR**
D16S539	13	26	
D18S51	15	94	
D1S1656	16	47	
D10S1248	15	61	
TH01	7	57	
vWA	16.1	30	81.08
vWA	18	37	
FGA	24	46	

Peak imbalance was observed at the two peaks at D3S1358 with a PHR calculation below the threshold, but the other paired alleles at amelogenin and TH01 were

confirmed. The heights of the remaining single alleles at the other loci showed high probability of allele drop-out due to the low range of RFU from the peaks.

The only discrepancy between the two elements is observed at the vWA allele, with the femur exhibiting a homozygous allele 18, and the metatarsal with a heterozygous 16.1,18.

When compared with the reference sample from the researcher, it was observed that many of the alleles correspond.

5.7.3.32 Skeleton 4473

Only the femur was available for analysis from skeleton 4473, which resulted in the identification of six alleles across five loci, as displayed in Table 5-52.

Table 5-52: Skeleton 4473 DNA results

	Femur		
Marker	**Allele**	**Height**	**PHR**
D16S539	10	45	
D18S51	17	31	
TH01	6	30	76.92
TH01	8	39	
D12S391	17	39	
D8S1179	13	78	

The TH01 marker was the only loci which displayed more than one peak – PHR calculations gave a result of 76.92% that there are true heterozygous alleles. Due to the low quantity of peak heights, the probability of allele drop-out is high.

5.7.3.33 Skeleton 4503

Analysis of the femur and metatarsal from skeleton 4503 showed they both displayed alleles, as can be seen in Table 5-53.

Table 5-53: Skeleton 4503 DNA analysis

Femur		
Marker	**Allele**	**Height**
AMEL	X	71
D16S539	4	30
D10S1248	13	53
TH01	7	64
D21S11	30	49
D12S391	21	33
D8S1179	9	62

Metatarsal			
Marker	**Allele**	**Height**	**PHR**
D3S1358	15	27	57.45
D3S1358	16	47	
D19S433	13	101	41.58
D19S433	15	42	
D2S1338	19	35	
D22S1045	11	69	92.75
D22S1045	16	64	
D16S539	10	193	42.49
D16S539	13	82	
D18S51	15	58	81.03
D18S51	17	47	
D1S1656	16	104	
D10S1248	13	60	73.17
D10S1248	15	82	
TH01	7	71	74.65
TH01	8	53	
vWA	16	52	32.10
vWA	18	162	
D21S11	30	48	42.11
D21S11	31	114	
D12S391	17	40	53.33
D12S391	21	75	
FGA	21	44	68.18
FGA	24	30	

The femur sample displays only seven alleles of a low RFU value, and display characteristic degradation patterns.

The data from the metatarsal shows a maximum of two alleles at each loci, however with severe peak imbalance, it is possible that more than one individual has contributed to the DNA profile.

5.7.3.34 Skeleton 4561

The electropherograms from the femur and metatarsal analysis displayed numerous alleles of very high RFU, as shown in Table 5-54, strongly suggesting the presence of modern DNA.

Table 5-54: Skeleton 4561 DNA results

Femur				Metatarsal			
Marker	**Allele**	**Height**	**PHR**	**Marker**	**Allele**	**Height**	**PHR**
AMEL	X	310		**AMEL**	Y	35	
D3S1358	15	103	29.77	**D3S1358**	15	59	
D3S1358	16	346		**D3S1358**	16	150	78.67
D19S433	13	214	82.71	**D3S1358**	17	118	
D19S433	15	177		**D19S433**	13	65	
D2S1338	19	165	84.85	**D16S539**	11	70	
D2S1338	23	140		**D18S51**	12	87	67.97
D22S1045	11	167	28.14	**D18S51**	20	128	
D22S1045	16	47		**D18S51**	17	44	
D16S539	10	402	57.71	**D1S1656**	16	56	
D16S539	13	232		**vWA**	17	130	
D18S51	15	288	45.93	**D21S11**	28	65	68.42
D18S51	17	627		**D21S11**	30	95	
D1S1656	16	425		**D12S391**	19	58	
D10S1248	13	618	26.54	**FGA**	22	297	28.96
D10S1248	15	164		**FGA**	24	86	
D2S441	10	322	80.30				
D2S441	14	401					
TH01	7	236	84.89				
TH01	8	278					
vWA	18	731					
D21S11	30	721	27.88				
D21S11	31	201					
D12S391	17	177	90.31				
D12S391	21	196					
D8S1179	11	238	59.66				
D8S1179	13	142					
FGA	21	460	83.04				
FGA	24	382					

Although no multiple peaks were found within the femur data, severe peak imbalance suggests that more than one contributor may be present. The data was compared with reference samples, and despite the peak imbalance in the femur sample suggesting more than one contributor – all the alleles compiled together provide a complete profile of the researcher.

Analysis of the metatarsal showed the presence of three alleles at D3S1358 and D18S51, confirming the presence of more than one contributor. Comparisons with the profiles found on the metatarsal display some alleles that do not match any of the reference profiles.

5.7.3.35 Eriswell DNA result interpretation

Due to the nature of the skeletal collection being analysed, the possibility of contamination from modern DNA was always high. After individual analysis of each element, the results were compared to the profile of the researcher, and other reference samples from individuals that had had contact with the bones. It was not possible to profile every individual, due to the time lapse between excavation and analysis.

In order to eliminate any DNA from the analysis that does not belong to the skeleton, it was necessary to not only exclude any alleles associated with the researcher, but also any alleles that displayed characteristics of DNA originating from modern DNA, such as high RFU. Although this method is likely to also remove intrinsic DNA information due to the commonality of the researcher's profile, it is the only way to provide confidence in the results that are remaining.

The results from this elimination process are presented in Table 5-55, alongside the reported number of alleles and loci identified, with the number of matching alleles between the elements of the same skeleton. No discrepancies were found within elements from the same skeleton, which would otherwise suggest different origins.

The strongest connections found between elements were from skeletons 0570 and 4067 which both displayed 9 matching alleles between the femurs and metatarsals and no discrepancies at any of the loci, providing strong evidence that both elements are representative of intrinsic DNA.

Table 5-55: Eriswell DNA results from skeletal elements, after evidence of modern DNA contamination has been excluded.

Sample	Amelogenin	D3S1358	D16S539	TH01	D8S1179	D19S433	D18S51	vWA	D2S1338	D1S1656	D21S11	FGA	D22S1045	D10S1248	D2S441	D12S391	Number of alleles	Number of loci	Matching alleles	Discrepancies
0067F		17		9.3,13.3			16	13,15									6	4	0	0
0067M														9			1	1		
0235F		12,17		9.3			18	13,16			24,29	22.2					9	6	0	0
0235M																	0	0		
0326F				4,6						12,15			15				5	3	0	0
0326M					6												1	1		
0425F	X	14	11				14	19,22			36						7	6	0	0
0425M																	0	0		
0426F																			0	0
0426M	X,Y	14,17	11	6,9.3	14	11,12	12,13	17,19	17,20	15,16.3	29,32.2	20	15	16	11	19,20	26	16		
0477F																	0	0	0	0
0477M																	0	0		
0570F	X	17,18			9	14	16	14		13		22					9	8	9	0
0570M	X	17,18			9,10	14	16	14	20	13,17.3		22	17		11	18,22	16	12		
0612F	X							15				22					3	3	2	0
0612M	X	14	12	9.3			16	15			28						7	7		

Sample	Amelogenin	D3S1358	D16S539	TH01	D8S1179	D19S433	D18S51	vWA	D2S1338	D1S1656	D21S11	FGA	D22S1045	D10S1248	D2S441	D12S391	Number of alleles	Number of loci	Matching alleles	Discrepancies
0692F	X		11	9		15.2		17			29	18							5	0
0692M		14	11	6,9	15	15.2	16,18	17		12	29					20,22	14	10		
0717F	X	17															2	2	0	0
0717M																				0
0759F				9.3				16				19					3	3	1	0
0759M								15,16,17									3	1		
0791F																	0	0	0	0
0791M				9.3			14	15		12				17			5	5		
0799F	X														14		2	2	0	0
0799M							14	19									2	2		
0808F											38.2						1	1	0	0
0808M	X		11,12	6,9	10,12		13,16	16		11	30.3	20,22				19,20	16	10		
0809F					17							31,31.2					2	2	0	0
0809M			11	7				15,16									4	3		
0991F	X	18	11				14	12			33.2,36			14			8	7	0	0
0991M																	0	0		
0994F		17,18	12			14,16.2	13,14	14,17		13	28,29	22,25		14			15	9	0	0
0994M																	0	0		
4040F					10	9					29						3	3	2	0
4040M		18			10			17		15.3	29		17		11	20	8	8		

Sample	Amelogenin	D3S1358	D16S539	TH01	D8S1179	D19S433	D18S51	vWA	D2S1338	D1S1656	D21S11	FGA	D22S1045	D10S1248	D2S441	D12S391	Number of alleles	Number of loci	Matching alleles	Discrepancies
4046F												22					1	1	0	0
4046M								15					15,16				3	2		
4067F	X,Y	17	12	9.3			13	17,18	17,18	10,16.3	30			17			14	10	9	0
4067M	X,Y	17	12				13	17,18		16.3	30			14,17			11	8		
4095F				9.3													1	1	-	-
4098F		17	12				13.2			11		23					5	5	-	-
4099F																	0	0	0	0
4099M		14															1	1		
4191F			12														1	1	-	-
4222F				9													1	1	0	0
4222S		14	11,12	6		14,17.2	14	17			29,30.2						10	7		
4226F	X,Y		14	6													4	3	3	0
4226M	X,Y		6	6	15	14	16	11								18	9	8		
4288F	X		8.3														2	2	0	0
4288M																	0	0		
4291																	0	0	0	0
4295F	X,Y	14,18	11	9.3	10,14		14	15				23					11	8	0	0
4340F						10,13											2	1	0	0
4340M																	0	0		
4411F								19									1	1	-	-

Sample	Amelogenin	D3S1358	D16S539	TH01	D8S1179	D19S433	D18S51	vWA	D2S1338	D1S1656	D21S11	FGA	D22S1045	D10S1248	D2S441	D12S391	Number of alleles	Number of loci	Matching alleles	Discrepancies
4462F	X,Y						16			17.3							4	3	0	0
4462M								16.1									1	1		
4473F				6													1	1	-	-
4503F	X		4		9												3	3	0	0
4503M								16									1	1		
4561F																	0	0	0	0
4561M	Y	17	11				12,20	17			28	22				19	9	8		

By comparing the DNA evidence to the original osteological reports and archaeological records from Eriswell cemetery, more information can be provided on the burial context. Allelic similarities were observed between the femurs of skeleton 0067 - a female aged to be approximately 20-23 years, and skeleton 0235 – a middle-aged male. Similarities were found at three different loci, showing the possibility of a familial relationship. No conflicting alleles were present, but with the absence of DNA on the metatarsals, these similarities cannot be confirmed.

Skeletons 0425 was aged between 11-13 years, in osteological reports, and was buried in a double grave with skeleton 0426 – estimated as a 15 year old at the time of burial. DNA profiles were only possible on one element per skeleton, so confirmation of alleles is not possible. Similarities were seen on three alleles, suggesting a possible familial relationship. Amplification of the amelogenin suggested skeleton 0425 was female, and skeleton 0426 was male. Similarities can also be seen with skeleton 0692, estimated as a wealthy middle-aged female. Skeleton 4067, reported as a middle-aged male in osteological reports, also showed similarities with this group, especially with skeleton 0426.

DNA analysis of skeletons 4226 and 4295 confirmed the estimation of sex as male as reported in the osteology report.

The skeleton 4222, buried with a horse and a sword, showed similarities to several of the skeletons, but the partial profiles did not allow any positive associations to be made.

5.8 Comparison of Fin Cop and Eriswell Results

This section presents a summary of the data already discussed from Fin Cop and Eriswell in order to provide a comparison between the different burial environments. The results from the colour, composition and DNA analysis are compared in relation to the skeletal element and burial environment from which the human remains were excavated.

5.8.1 Colour comparison

The colour data from the limestone burial environment at Fin Cop and from the different environments are Eriswell is presented as average values in Figure 5-57. The results are reported on individual axes to allow the direction of colour difference to be identified.

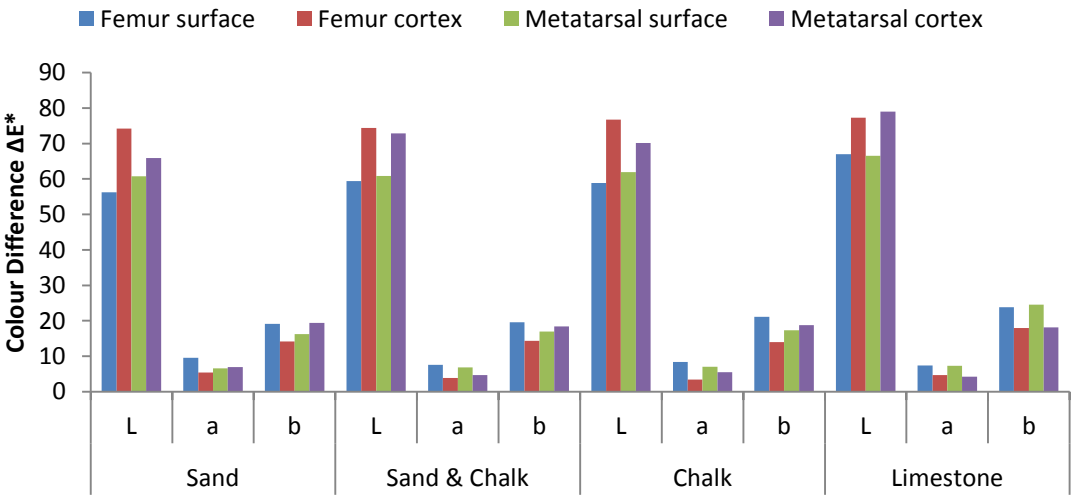

Figure 5-57: Colour data of surface and colour of femurs and metatarsals from the limestone environment at Fin Cop and the sand, sand and chalk, and chalk environments at Eriswell

The femur from the sand environment showed the darkest surface colour, but the colour did not penetrate deeply, leaving the cortex colour similar to the other environments. Both the surface and cortex of the metatarsal from the sand environment were darker than the other metatarsals. The metatarsal from sand was the only element to increase on the a axis after surface removal, therefore increasing in the colour red.

Limestone was the only environment from which the metatarsal cortex was lighter than that on the femurs, and the limestone metatarsal was the only element to decrease on the b axis after surface removal, showing the cortex to be more yellow than the surface. All the lightness measurements from the femora and metatarsals, both surface and cortex were highest from the limestone samples than any other environment.

5.8.2 Composition comparison

The composition data, as calculated by ATR-FTIR, of the skeletal elements from Eriswell and Fin Cop analysis are displayed in Figure 5-58, in order to allow comparisons from the different burial environments to be visualised.

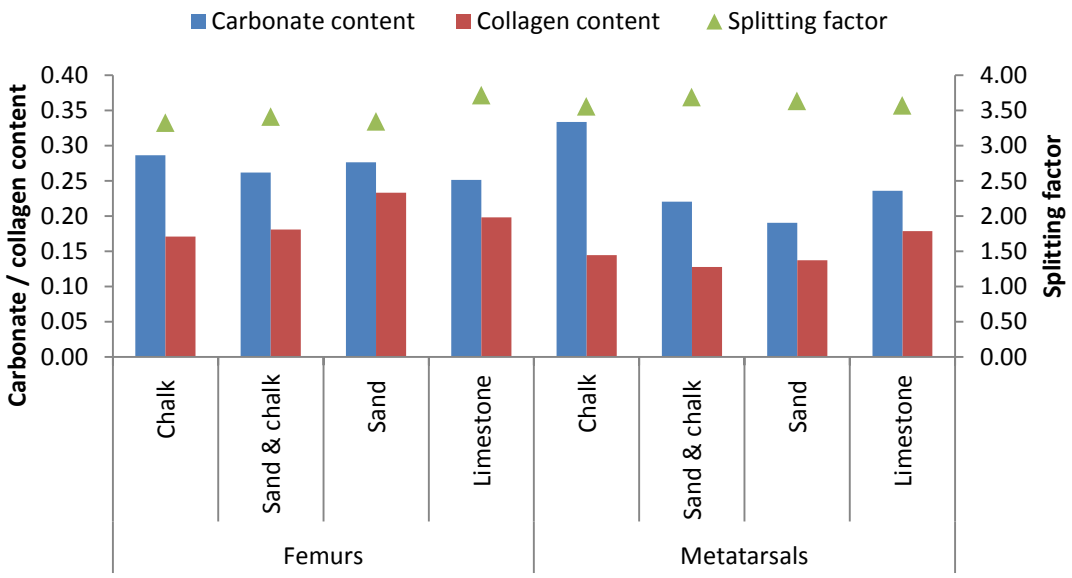

Figure 5-58: Comparison of average carbonate content, collagen content, and splitting factor (secondary right axis) of metatarsals and femurs from chalk, sand and chalk and sand burial environments from Eriswell and limestone from Fin Cop

Overall the metatarsals displayed worse collagen preservation than the femurs, with the sand, and sand and chalk environments showing the worst preservation for the metatarsals, and chalk and sand and chalk being the worst for the femur samples.

The limestone femur average shows the highest splitting factor in relation to all the skeletal elements from all four different burial environments, whereas the limestone metatarsal has the second lowest splitting factor of all the metatarsals, the lowest being metatarsals from the chalk environment. The limestone environment is the only environment that shows the metatarsals with a lower average spitting factor than the femurs.

The highest carbonate content can be seen in the chalk environment for both the femurs and the metatarsals, and also shows the biggest difference between this parameter and the collagen content. As both calculations include the peak height of the phosphate peak, the results are generally similar, as shown by results from the other environments. These high results, especially in the metatarsal samples, may be due to the uptake of carbonate from the burial environment. Given the similar composition of the limestone burial medium, it is surprising the same cannot be seen in these burials.

The least differences observed between skeletal elements from the same environments can be seen in the limestone samples, of which the results seem to display a similar diagenetic state. The biggest differences can be observed between the elements from the sand burials – however, the sample size of tested elements is much lower than the other environments.

XRF analysis was also conducted on the bone samples in an attempt to identify the unknown peaks that were present in some of the spectra during ATR-FTIR analysis. A comparison of the estimated iron content from a small sample set of bone samples from Fin Cop and Eriswell can be seen in Figure 5-59.

The highest iron content can clearly be seen in skeleton 6 from Fin Cop, more than double than the other elements from Fin Cop and also higher than any of the Eriswell elements. The samples from Fin Cop show a varying amount of iron present, between the femurs and the metatarsal, whereas the analysis of the Eriswell samples show a significant difference between the femurs and the metatarsals.

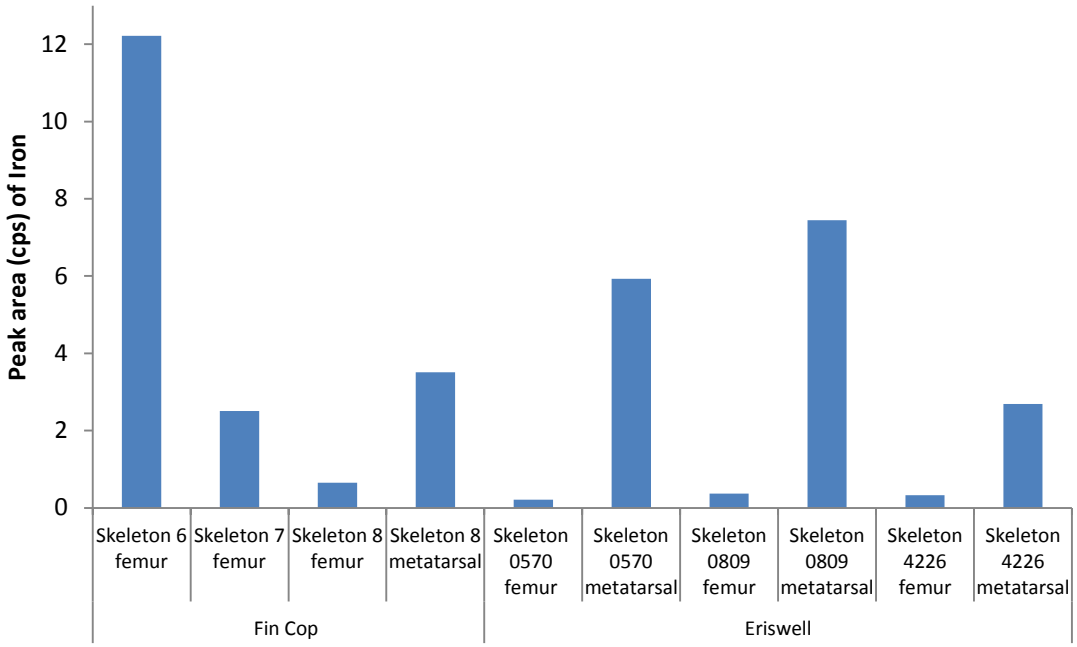

Figure 5-59: XRF results of iron quantitation in bone samples from Fin Cop and Eriswell burials

The quantity of iron can be seen to be much higher in the metatarsals, than the associated femurs from the same skeletons.

5.8.3 DNA comparison

In order to allow a crude comparison of the amount of DNA contained within the archaeological samples, the average of the peak heights from samples containing DNA, from both collections, were compared to the average peak heights from the serial dilutions of control DNA analysed as part of the optimisation process outlined in section 4.2.4. The Fin Cop samples displayed a higher concentration of DNA than the elements from the Eriswell skeletons, although both at very low concentrations as shown in Figure 5-60.

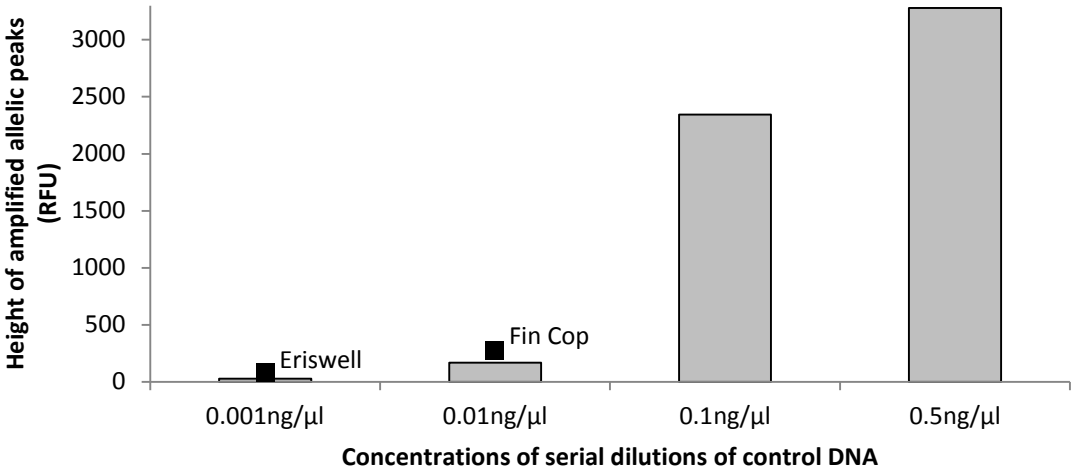

Figure 5-60: Comparison of average peak heights from serial dilutions of control DNA, and the average peak heights from samples containing DNA from Eriswell and Fin Cop analysis.

As all samples were prepared and analysed in the same way, this suggests that the quantity of DNA preservation of the Fin Cop samples in relation to the Eriswell samples was much better, despite the vast difference of centuries in age of the samples.

By looking at the two burial grounds together, more information can be obtained about the difference of the quality of DNA preservation. Figure 5-61 shows the overall percentage of the allele amplification at the different loci from both the Eriswell and Fin Cop skeletal samples.

The Fin Cop samples show better amplification than Eriswell in the smaller amplicon loci of amelogenin, TH01 and D16S539; FGA at mid-range, and the larger amplicons of D21S1338 and D22S1045. However, less loci were amplified from the Fin Cop collection, than the Eriswell collection which showed amplification was possible at all loci. A 'ski slope' pattern characteristic to degraded or inhibited DNA (McCord, 2011) is observed from both the burial grounds, but with decreased amplification at certain loci. This observation, along with the absence of some loci in the Fin Cop samples, shows evidence of inhibition displaying at certain loci. As this has not occurred purely at the large base pairs amplicons, it suggests sequence

specific inhibition is occurring rather than just DNA degradation leading to strand breakage.

Figure 5-61: Percentage of Fin Cop and Eriswell samples displaying alleles at the 16 loci, in relation to the base pair size of the amplicons

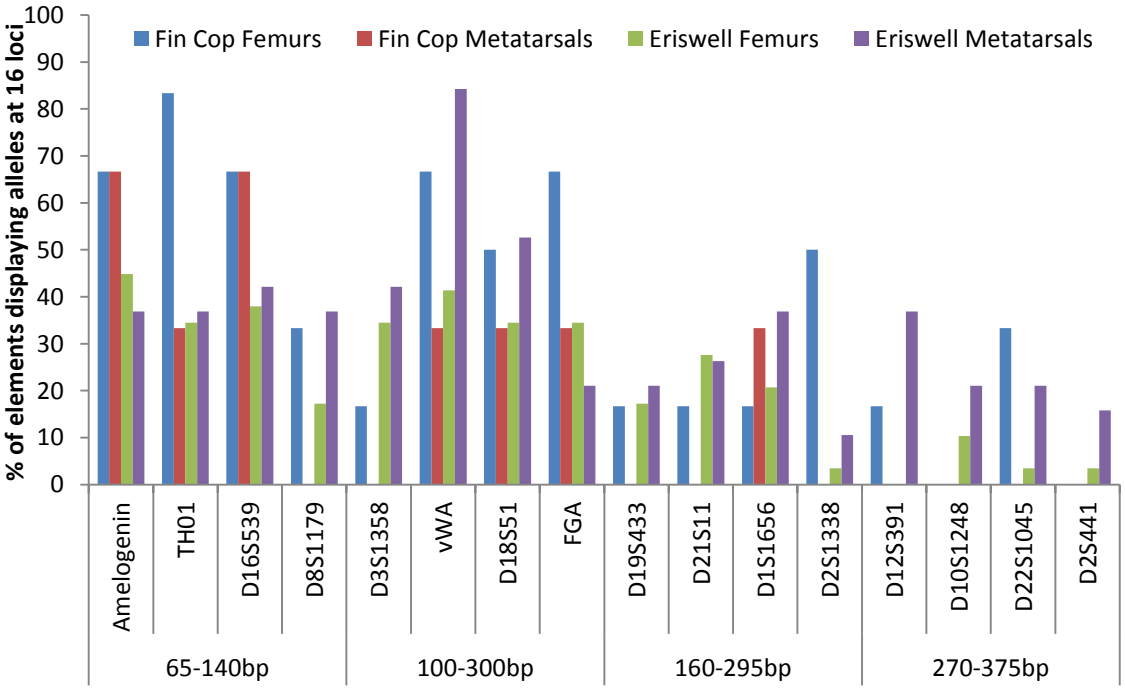

Figure 5-62: Percentage of elements from Fin Cop and Eriswell displaying alleles at the 16 loci

Figure 5-62 shows the loci amplification in more detail, with the percentage of metatarsals and femurs (separated by burial ground) shown rather than just an overall average shown in the last figure.

The loci Amelogenin and D16S539 are the only two that show better amplification in both the femurs and metatarsals from the Fin Cop samples than the Eriswell bones, although the Fin Cop femurs show strong amplification in comparison to the metatarsals and the Eriswell samples.

In contrast, the Eriswell metatarsals were the only elements where amplification was successful at all loci, showing much better DNA preservation than that of the Eriswell femurs.

In terms of the differences observed between the skeletal elements, D1S1656 is the only locus that shows better amplification in metatarsals than the femurs, from both the Fin Cop and Eriswell sites.

By looking at the results in terms of burial environments rather than site, additional information can be gained in regards to DNA preservation, but more importantly, DNA inhibition.

Figure 5-63 shows the percentage of both femurs and metatarsals that displayed alleles at the 16 loci, in relation to the reported burial environment. Due to the differences in sample sizes these have been reported on the figure in order to be able to put the results of the sand burials into context.

As the previous three figures have displayed, a decline in the successful amplification of alleles diminishes as the length of the target amplicon increases, indicative of DNA degradation. However, this figure also portrays that the inability of amplification is likely due to inhibition in some places, rather than just DNA degradation. In some instances, this inhibition appears to be related to the burial environment and skeletal element.

The metatarsals from the limestone environment (Fin Cop) show a larger degree of inhibition occurring than in the femurs from the same environment; with no amplification of alleles at some of the smaller loci of D8S1179 and D3S1358, but

amplifying successfully at D1S1656. However, the lack of any DNA at any loci past this suggest DNA degradation is more advanced in the metatarsals than the femurs that showed successful amplification with the larger amplicons.

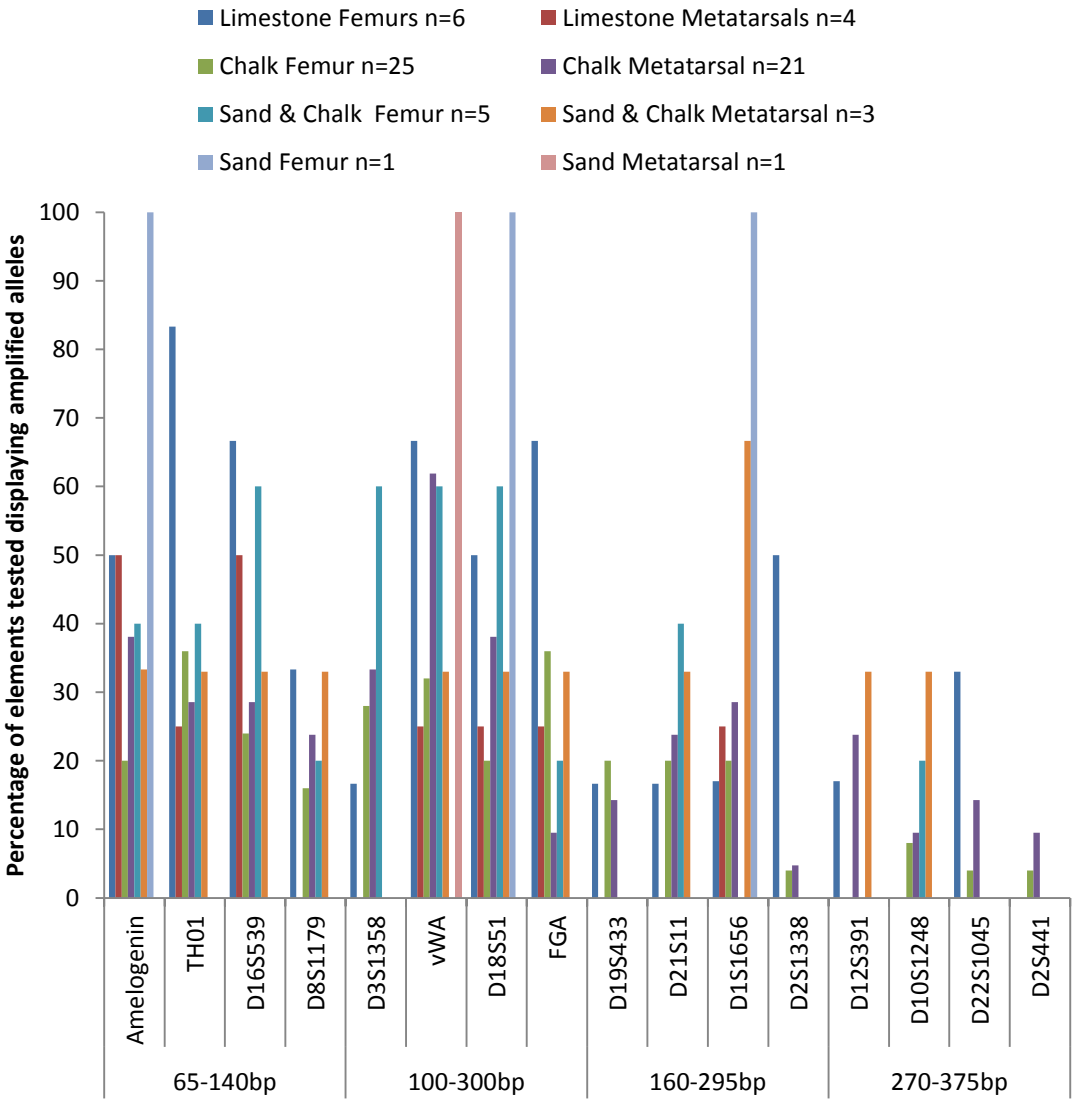

Figure 5-63: Percentage of samples displaying allelic amplification in relation to burial environments from both the Fin Cop and Eriswell site

The metatarsals from the chalk environment (Eriswell) were the only sub-section of samples to display successful amplification at all of the 16 loci. The femur samples from the same environment produced results at 15 of the loci, failing only at D12S391.

The results of the elements from the sand burials showed inhibition in both the femur and metatarsal, with no allelic amplification possible at the five smallest loci (except amelogenin in the femur) yet possible with larger amplicons. However these results are purely based on elements from one skeleton.

The possible inhibition seen at loci D19S433 and D2S1338 only show successful amplification from samples from the limestone (Fin Cop) and the chalk (Eriswell) environments, suggesting more inhibitions present in burial environments containing sand. The largest two loci also only display results from the limestone and chalk environments, however this could be due to DNA degradation rather than inhibition – in either case it would appear that the limestone and especially the chalk environments best promote the survivability and successful amplification of ancient human DNA.

5.9 Chapter summary

This chapter has presented the results from the human analogue experimental burials and the ancient human archaeological remains. The results of this chapter are discussed in the next chapter, with comparisons of both data sets.

Chapter 6: DISCUSSION

Chapter 5 presented the results from both the experimental porcine burials and the archaeological human remains, with comparisons made between the data sets.

This chapter presents a critical discussion of the data obtained throughout the research, with collation of all the results presented in the previous section. The intention is to identify associations observed between bone preservation and soil conditions observed in the porcine burials, to correlate with findings from the human archaeological remains.

6.1 Decomposition of human analogue burials

In order to assess whether decomposition rates were affected by different attributes within a burial environment, observations in relation to soil properties and behaviours were made and related to the analytic data.

In terms of observations, a strong odour was noted immediately with the clay burials, which was correlated with the decomposition of the soft tissue and associated fluid pooling beneath the bone. The odour reduced at 6 months when there was no pooling or soft tissue remaining, and dissipated completely by 18 months. As expected within a wet and poorly drained environment (Schotsmans et al., 2011), adipocere formation was observed from 1.5 months and persisted for 12 months.

The level of odour from the sand burials mimicked that of the clay burials, yet it persisted for the entire 18 month duration. Unlike the clay burials, there was no pooling of liquid, due to the draining nature of the sand, however the sand was visibly wet. These observations of odour and sand wetness has also been reported by Janaway et al (2009) when studying decomposition using pig carcases in a sandy desert in Peru. The persistence of the odour has also been reported when conducting controlled laboratory experiments, of burying pig carcases in sandy soil (Stokes et al., 2009). No soft tissue was present at any of the excavations, but dry adipocere and a wet brown substance were present throughout – showing the decomposition of the soft tissues has been the most aggressive out of all the

burials. The production of adipocere formation has previously been reported in sandy burial conditions, despite the non-ideal environment of well-draining soil (Schotsmans et al., 2011).

In contrast, the lime burials displayed the best soft tissue preservation, albeit in the form of desiccated tissue, being evident throughout the 18 month burials. The lime environment provided the perfect conditions for tissue desiccation with a dry and porous environment wicking moisture away from the bone. The desiccation of the tissue also minimised the odour released, with only a slight odour present at the 12 and 18 month burials, in addition to a discolouration in the lime above the bone suggesting some decomposition fluid present also.

No odour was evident with any of the compost burials, no pooling of fluids occurred, and tissue was only evident at 1.5 months, after which only dry adipocere was evident. Forbes et al (2005) reports an optimal pH level for adipocere formation is 5-9, and a highly acidic environment is not favourable for adipocere formation. For this reason, adipocere was not expected in the compost environment, however, within the first 1.5 months of burial, pH levels in the compost changed from acidic to neutral, and therefore became an acceptable level for adipocere formation.

Based on these observations, the decomposition rate of the soft tissue was quickest with the bones buried in the sand environment, followed by the compost and clay burials, with the best soft tissue preservation seen in the lime burials.

6.2 Effects of burial environments

By conducting soil analysis, similarities were observed between certain aspects of the decomposition process from the compost and clay environments, despite the differences in soil properties. In terms of burial medium composition, the biggest difference separating compost and clay from sand and lime was the water content of the burial medium, and the presence of mould and condensation within the burial, therefore the effect of water was investigated.

Within the clay environment, the soil particles served as a 'holding' platform for the decomposition products released and prevented drainage therefore partly submerging the bone in a mix of water and decomposition fluids.

The compost burials displayed a gradual increase in the water content of the compost, with no pooling of liquid, and the bone felt dry. It would appear that the compost wicked the moisture and liquid away from the bone, behaving like a sponge.

Despite a lack of water in the lime environment, the moisture from the bone enabled the production of a covering or cast to be produced around the bone and the soft tissue, limiting the release of any decomposition fluids into the surrounding medium, and appeared to slow the decomposition process.

The presence of water in a burial environment remains a point of dispute as to whether it is a help or a hindrance in the preservation of skeletal remains and associated soft tissue (Turner-Walker, 2007). Standing water can often be seen to act like a buffer by resisting change in temperature and stabilising any changes in pH, whereas running water many result in the movement of water through the bone matrix leading to subsequent ion loss leading to breakdown of the matrix, but also providing a means of transport for soil contaminants into the bone (Hedges and Millard, 1995; Carver, 2000). In this case, it would appear that the standing water (or decomposition products from the bone) actually provides a hindrance to preservation, due to its ability of transporting soil contaminants such as humic acids into the bone which act as PCR inhibitors and therefore prevent the subsequent amplification of the DNA products held within.

By monitoring the pH levels of the burials, it was possible to record the changes which occurred at different times during the burials. Prior to the burial of the porcine bones, the pH levels in the compost, sand, clay, and lime were 6.25, 8.48, 9.63 and 13.07 respectively. The changes in the pH varied between the different burial environments, narrowing the range of difference between them, by converging at equilibrium. Compost as the most acidic environment was the only burial medium seen to become more alkaline due to the increased ammonia levels

as a result of the decomposition process. This increase in pH in an acidic environment has previously been reported by Stokes et al (2009). The remaining environments all became more acidic although with varying changes and fluctuations. This change is different to previous studies reported, which found during early and intermediate periods of decomposition, the pH of the soil increased initially, with a decrease in the later stages (Stokes et al., 2009; Schotsmans et al., 2014). However these studies used pig carcases as opposed to individual bones with minimal soft tissue. Therefore these differences in pH change can be explained by the putrefaction and release of abdominal fluids and decomposition of other soft tissues not present in this study.

The pH range seen in the sand, clay and compost environments are all within the range of pH4-10 reported to be acceptable for activity by soil bacteria (Schotsmans et al., 2012). Research by Fernández-Calviño et al. (2011) demonstrated small changes in pH can be tolerated by the native soil bacteria, acclimatising to the different levels readily; therefore the changes seen in the burials would not have affected the activity of the microbial bacteria. The lime environment showed the smallest change in pH, only fluctuating between pH 12-13, remaining outside of the optimal range for soil bacteria. This small increase of pH during decomposition in an alkaline environment has also been reported by Schotsmans et al (2014).

The organic content within the compost and clay environment was another assessed parameter which showed similar patterns of fluctuation throughout the 18 month duration. Fluctuating patterns were expected due to the periodical release of fluids at different stages of decomposition; however more activity can be seen from the lime and the sand burials. Within the sand burials, a large increase is seen at 3 months, which coincides with the rise in water content, and a drop in pH – confirming the initial release of acidic decomposition products. The lime burials showed similar trends to that of sand but it occurs three months later at the 6 months point – a rise in water content, organic content and this time an increase in pH, once again shows the release of decomposition products into the lime. This delay suggests a relatively retarded decomposition process is occurring within the lime environment, compared to that seen in the sand burials, as previously

reported by Schotsmans et al. (2012) who compared the decomposition rate of pigs concluding that the limed pigs were better preserved that the unlimed pigs. Schotsmans et al (2012), whilst researching the changes in pH of hydrated and quicklime pits, reported that the pH values of control pits which contained no pigs both increased in alkalinity, therefore the rise seen in this research may not be due to the decomposition process, however with the water and organic levels also changing, it seems to be the case.

In terms of pH the compost and clay samples show the opposite effects within the first 1.5 months with an increase in pH in the compost, and a decrease in the clay environment – possibly due to the higher percentage of soil bacteria and microbes present in the compost. From this 1.5 month point they follow very similar fluctuating trends that ultimately decrease by 18 months.

6.3 Colourimetry of porcine bones from experimental burials

These findings of decomposition rates can also be confirmed by the other analysis conducted upon the bones, as well as analysis the burial environments. The observation of the bone submersion within the clay environment, providing passage of contaminants into the bone is reflected in the colourimetry data. The colour of the surface of the bone progressively shows an increase in the colour change from that of pre-burial, and so does the colour of the cortex of bone, showing penetration of contamination of the bone is occurring, and is becoming progressively worse over the 18 month period.

The trend seen from the compost burials differs from that of clay burials, with a distinct trend of decreasing colour difference between the post-burial surface and the cortex colour, their colour becoming more similar over time. Although this suggests that the colour is penetrating the surface, the colour difference between pre-burial and surface removal does not dramatically change throughout the 18 months. However, by examining the individual colour axes, it is possible to identify it is the lightness of the bone which is changing dramatically, especially at 6 months, where the bone cortex is darker than the surface, showing extreme infiltration of contaminants, possibly humic acid from the compost into the bone

cortex. Previous research has indicated the change in bone to a darker colour when in an acidic environment, can also be due to exchange of metal ions such as iron and manganese from the environment (Turner-Walker, 2007).

The lime burials show the highest colour differences in all categories tested at the 1.5 month stage, with a large difference seen between the post-burial surface and the cortex colour, after which a more constant cortex colour on all 3 axes can be seen. Within the first 6 months, fluctuations can be seen on the a* axis, (red/green) which were also recorded as observations during excavation with the presence of blood and soft tissue still surrounding the bone. The colour change on the b*(yellow/blue) axis, or lack thereof, due to the big difference of a higher and fluctuating yellow value on the surface compared to consistent lower value on the cortex. The highest value of yellow on the surface of the lime bones, also coincides with the rise in water content, organic content and pH, providing another indicator of decomposition processes.

The sand bones showed the biggest colour differences between surface and cortex occurring within the first 1.5 months coinciding with the changes observed in the soil of water, organic content and pH, after which the cortex and surface displayed similar colouration, suggesting slight staining on the bone exterior, but no signs of infiltration into the cortex occurring.

The colour of the bone marrow also provides another perspective on the rate of decomposition. As with the bone colour, the bone marrow also changed the least within the sand burials with the presence of haematopoietic tissue still present at a later stage, and a slower colour progression than others – showing a slower decomposition rate. The bones from the compost burials showed the fastest decomposition of bone marrow, being the only samples to show black discolouration by the 18 month period. The lime and compost showed similarities in the orange colouration, whereas clay and sand showed similarities in the grey colouration of the marrow.

The control bone showed the largest colour difference between the bone surface colour at 0 months to that at the 18 month period – without any burial this change

is purely to do with intrinsic factors occurring due to the diagenesis of the bone and the air. By investigating the individual axes, the change could be calculated by direction – after variable colour change on all three axes in the first three months, the lightness showed a steady increase, the degree of red steadily decreased, and the yellowness of the surface plateaued. The initial changes showed the bone becoming darker, redder and more yellow, presumably caused by the breakdown of proteins and fats with the bone matrix.

Compost showed the next highest difference with a huge increase in the last period of 12- 18 months, with increases in lightness, redness and yellowness occurring on the surface. Clay was the next largest with the biggest change between 3-6 months. Lime burials showed the largest increase in colour difference between 1.5 months and 3 months of burial, followed by a gradual increase. Sand mirrored that of compost without the increase at the end of the burials – resulting in the smallest overall colour difference of the surface.

Despite the largest colour difference of the surface, the control bones showed the least difference between the bone surface and the underlying cortex, showing uniformity in the colouration without the soil contaminants. Within the first 3 months, the control bones along with those from the sand, lime, and compost burials showed the largest colour difference between surface and cortex, suggesting staining was purely on the surface and infiltration had not occurred within this period. This difference was due to changes in all three of the colour axes, but to varying degrees for each burial type. Sand burials were the only bones not to increase in lightness, and the only bones to decrease in yellowness of the surface colour within this period. The control, sand and lime burial samples all showed small decreases of colour difference after the initial change, showing gradual decreases in lightness suggesting infiltration of contaminants was occurring at a gradual pace. The control, lime and sand showed a slight increase between 12 and 18 months suggesting the attack on the surface of the bone had stopped moving through the cortex, or the bone surface was at this stage, more vulnerable to a different type of attack. Bones from the clay environment showed a completely different trend from the other environments, with the rate of colour

change remaining relatively constant throughout the duration of burial. This resulted in the largest colour difference between the surface and cortex by the 18 month point, suggesting slower but more persistent penetration of contaminants from the clay into the bone.

Observations of the total colour difference between the bone surface prior to burial and after surface removal show how the compost and control bones had similarities during the 18 month period, suggesting the surface colour change of the compost burials was in fact only surface deep and infiltration has occurred no more than seen in the control bones. The clay bones showed the largest colour difference suggesting the highest diagenetic change or infiltration of contamination. The bones from the sand and lime environment also showed similarities in trend and values, showing the largest change within the first 3 months – most likely due to the retarded decomposition process seen through data collection from other variables.

6.4 Bone diagenesis of human analogue burials

The results from ATR-FTIR analysis provided more information of the preservation of the bones. The first 1.5 months showed a step increase in splitting factor for all samples, as expected due to intrinsic alterations of the structure associated with decay. After this initial increase the control samples showed a plateau, with the same observed in the carbonate content and collagen content. Due to the lack of a burial environment, these changes in composition and structure must be due to intrinsic factors or exposure to air prompting the diagenesis. Samples from all the experimental burials showed differences to those recorded from the control bones, showing changes to the normal bone taphonomic metabolism. The data shows the lime bones remain the best preserved after the 18 month burial period, with a splitting factor remaining below that of the control bone from 1.5 months onwards. However, these results were not indicative of the amount of DNA present as no 500 base pair amplicons were able to be amplified after 6 months of burial – the same point from which an increase in water content,

organic content and pH were observed in the environment, and an increase in yellow colouration on the surface on the bone.

The composition results showed that overall the compost and clay samples showed the worst bone preservation with high splitting factors, and low carbonate and collagen content. As the clay and compost both showed high water content, these diagenetic changes of the bone could be due to the presence of water, dissolving the apatites in the bone and changing the structure.

Although not widely reported, it is a common thought between archaeologists and researchers that clay has preserving qualities (Gabbott, 1998; O'Connor et al., 2011), however, in this case it would appear the water content had a dramatically deleterious effect on the bone preservation. This has been previously reported after analysis of skeletal material from waterlogged clay burials (Rahtz and Hurst, 1976) and assessment of weathering rates in defleshed bones in a high clay environment (Janjua and Rogers, 2008).

The sand burials also showed high splitting factors, but in a more variable manner with a decrease after 1.5 months. At 6 months the splitting factor was lower than that of the control and the lime, after which no 500 base pair amplicons were amplifiable. The standard deviation between samples at this point was 0.04 so the results do not appear to as a consequence of inter-sample variability. Rather this highlights the fact that other processes were occurring within the bone due to interactions with the environment which affected the mineral matrix of the bone. The good preservation of the bones noted in the sand burials, in contrast with the observations of archaeologists in the case of Sutton Hoo (Carver, 2000) and from the ancient human archaeological remains from this research, could be due to the lack of water movement that would occur in an open space. By containing the burial in a plastic box and not providing a simulated rainfall, there is no water movement through the particles of the sand which would occur naturally. This eliminates both the effect of the water percolation on the bone and surrounding environment, and also the chemical "refreshment" that rainfall would provide by the changes in pH, and movement of decomposition fluid.

For comparative analysis, other sites containing burials in sand were examined, and while Sutton Hoo offers the most striking perspective on the effect of sand on the degradation of human remains, other patterns of preservation are evident elsewhere. Recent excavations at St Patrick's Chapel, Whitesands, Dyfed, have revealed well preserved coffined skeletal remains lying within dune sand deposits (Murphy et al., 2015). These inhumations, some centuries later than the Sutton Hoo burials, are strikingly well preserved by comparison. Similarly, Bronze Age cist burials recovered from the dune system of Low Hauxley, Tyne and Wear, while not so strikingly well preserved as the burials at Whitesands, are robust in comparison with the far later Sutton Hoo (Waddington, 2014).

These processes occurring in the experimental samples at 6 months in the sand samples can also be seen in the other FTIR data in the ratios of Amide/Phosphate and Carbonate/Phosphate, with sharp inclines in both, and again variable trends very different to those from the control bones, and bones from other environments.

The bones from the lime burials also displayed increases in Amide/Phosphate and Carbonate/Phosphate, but with steady increases over the 18 month period, despite the continually low splitting factors. This provides more support to the notion that these changes in carbonate, phosphate and crystallinity must be due to the uptake of environmental contaminants altering the bone metabolism, as previously reported by Álvarez-Lloret et al (2006) whilst analysing bones from contaminated soil. This shows that other factors are occurring due to the properties of the sand, which due to its aggressive nature in the degradation of DNA at 3 months and onwards, penetration from the environment is occurring, allowing ions to infiltrate the bone matrix.

The results of the control bone showed that the highest degree and fastest rate of diagenesis, as observed via the splitting factor, occurred within the first three months. However the splitting factor then decreased again between 3 and 12 months before an increase at 18 months, suggesting other processes occurring within the bone, confirmed by the rise in Carbonate/Phosphate, suggesting

splitting factor cannot be used independently as an assessment of early-stage diagenesis.

Considerations of rates of chemical change have been discussed above and indicate how results from the porcine burials show how the passage of time affects bone diagenesis. The rate and extent of the bone diagenesis was dependent on the burial environment in which the bone resided. In terms of colour changes, and structural changes, the majority of this appears to occur within the first 6 months, before a plateauing of changes, of either increasing or decreasing values. Schotsmans et al (2014) also reported preservation differences in bone buried in different environments to be highest during the first 6 months.

6.5 Bone diagenesis of human remains

In regards to the human archaeological results, due to the vast difference in duration of burials, in excess of thousands of years, a much higher state of diagenesis in the Fin Cop samples than the Eriswell samples might be expected, however this was not observed in all cases. The ATR-FTIR results showed varying degrees of diagenesis - with some results showing better preservation in terms of higher Carbonate/Phosphate and Amide/Phosphate levels in metatarsals compared to those from different burial conditions from Eriswell. A greater quantity of DNA preservation, measured by height in RFU, was observed in the Fin Cop samples when compared to the Eriswell samples. However, amplification was not possible at all loci from the Fin Cop samples, in contrast to the Eriswell samples which showed allelic amplification was possible at all loci. The Fin Cop analysis also showed a higher percentage of samples exhibiting alleles at the amelogenin marker. As the smallest amplicon in the multiplex analysis, it was expected the amelogenin marker would have amplified in all cases where DNA was amplifiable. This suggests a higher level of inhibition at this locus in the Eriswell bones than those from the Fin Cop site.

Analysis of the human archaeological samples highlighted the differences observed in results from the different skeletal elements. The extent of preservation as observed from the ATR-FTIR results, showed that overall the metatarsals were

found to have worse preservation with lower collagen and carbonate levels estimated from Amide/Phosphate and Carbonate/Phosphate ratios, and a higher splitting factor than the femurs. This coincides with research previously reported by Janjua and Rogers (2008) who found femora were more resilient than metatarsals, when assessing weathering modifications such as cracking, colour change, soft tissue presence and odour. Metatarsals from Eriswell showed the highest rate of contamination from Iron– most likely to do with the differences in cancellous bone structure and size, showing vulnerability to penetration from contamination; despite this, the same samples were the only elements that showed amplification on all loci tested.

6.6 DNA survival in human remains

This vulnerability due to element structure is also observed when comparing the environment in which the skeletons were buried, to the DNA results. The metatarsals from the limestone environment (Fin Cop) showed a much higher level of inhibition that the femurs from the same skeletons buried in the same environment, but also a higher level of DNA degradation with no amplification in the larger amplicons. However, the same pattern of inhibition and degradation was not observed in the chalk environment at Eriswell, where the metatarsals display amplification on all alleles, but the same was not achieved from the femurs. The highest level of inhibition was seen in the femur and metatarsal from the sand burial, with the inability of amplification noted at the five smallest loci.

This observation brings into question the proposed relationship between the survival of DNA and that of the mineral and organic components of the bone. Due to the uptake of carbonate, phosphate, calcium and other contaminants derived from the environment and groundwater, it is difficult to state a simple relationship between the DNA survival in the bone compared to the native mineral and organic components of the bone. In past research Fredericks (2012) reported it was possible to use splitting factor as an indicator of preservation and DNA survival, but that this was dependent on the preservation of collagen, which in turn was related to the presence of bone mineral. However, Fredericks' research

investigated controlled thermal diagenesis using bovine bone and not human archaeological bone which had been exposed to many other diagenetic factors. Stiner et al (1995) did use archaeological bone, primarily from goats, and found no significant differences between burnt and non-burnt bones when investigating the carbonate content and splitting factor which all fell within the range of 3-4.

Research by Trueman (2008) used archaeological human bone and determined that the change in crystallinity and trace element uptake from the environment was correlated, and controlled by the decomposition of the organic phase up until the point of exposure of the crystal structure due to collagen degradation. From this point, Trueman stated that chemical alteration is then "site-specific" in terms of environments, and will only provide a broad indication of collagen survival and is not an appropriate tool for assessment of diagenetic alteration. The results from this research, supports Trueman's statement as the control porcine bones showed a systematic diagenetic process, whereas the bones from the experimental burials did not.

6.7 Relationship between archaeological conditions and DNA survival

Although difficulties are associated with the determination of the nature of the structural changes due to different environments, a relationship between burial conditions and the survival of DNA can be seen within the experimental porcine burials, and also the human archaeological remains. Degradation of DNA could be seen with the lime and sand analogue burials, however due to the sudden drop out of all amplifiable DNA from the clay and compost samples from 12 months, and the notable colour change indicating ion exchange, this is more likely to be due to inhibition. PCR inhibitors are present in substances in the soil, as discussed in section 4.1.8 which can prevent the amplification of the target DNA (Anðelinoviæ et al., 2005). Inhibitors such as humic acid can reduce the apparent DNA concentration in a sample by binding to the structures. This inhibition process is thought to be specific to certain DNA sequences, but is also concentration dependent and may be responsible for overwhelming all sizes of base pair

amplicons (McCord et al., 2011). Inhibition of DNA amplification can also be seen in the archaeological human remains, with some larger amplicons being preferentially amplified over the smaller ones, providing further evidence to support the concept of this effect being sequence specific. Further investigation also discovered the loci D3S1358 and D8S1179 which displayed inhibition on the Fin Cop metatarsals, were the only loci to contain the same sequence. The inhibition was less pronounced in the elements from the chalk and the limestone environments, and most apparent in the sand bones, and generally the metatarsals were affected worse than the femurs.

Another source of PCR inhibition is collagen which binds to the Taq polymerase in the PCR mastermix. The ATR-FTIR results show bones such as those from the lime environment with a higher collagen content than the clay and compost bones which were not affected, therefore this does not appear to be a simple relationship with collagen.

The sand environment appeared to be the most aggressive in terms of DNA degradation with the inability to amplify 500 base pair amplicons after 1.5 months. Lime appeared to have a preserving effect on the soft tissue yet the inability to amplify 500 base pair amplicons occurred after 6 months. Although this may also be due to PCR inhibition as calcium is present in high quantities in lime and acts as a PCR inhibitor by binding to the Taq polymerase in the mastermix (McCord et al., 2011). The darkening colour change seen in the lysis during extraction (section 5.4), may be due to the removal of inhibitors such as calcium from the sample, until the point of saturation at which PCR inhibition occurred. A similar correlation between the colour of a DNA extract and inhibition has been reported by Eilert and Foran (2009), who proposed the colour was due to the presence of iron and humic substances.

The human archaeological bones from the sand environment showed the worst preservation of DNA, both in the number of loci amplified and the estimated quantity of DNA measured in RFU of the peak heights as discussed in section 4.3.10, but also the highest level of inhibition. The presence of limestone at Fin

Cop or chalk at Eriswell, appeared to increase the survivability of the DNA, and also showed less effect from inhibitors.

By looking at the individual variables, it was possible to identify those which may be responsible for the changes seen in composition, colour and biomolecules in relation to their environmental conditions. The clay and compost bones all showed drop out of amplifiable alleles after 6 months of burials. Both clay and compost soils contained the highest organic and water content of all the burials, and also showed the biggest difference between the pre-burial surface colour and the bone colour after surface removal, when compared with sand and lime. These variables suggest it is the organic content of the burial medium providing the bacteria that promoted the bone degradation, with the water acting as a passage into the bone which is confirmed by the difference seen in the cortex colour of the bone.

The lime samples showed the best preservation in relation to amplifiable DNA and showed a darker colour of lysis during extraction. This dark lysis may indicate a more complete inhibitor removal therefore leaving less inhibitors in the bone to obstruct amplification. The lime environment had the highest pH level, which is reported to be outside of the optimal pH range for soil bacteria, potentially limiting the development and efficiency of bacterial attack. Lime bones showed the slowest degradation of bone matrix reported by the lowest splitting factor from all the environments, however an uptake of carbonate from the environment was evident.

The sand samples showed a dropout of DNA after 1.5 months, at the same time the biggest colour difference for pre-burial to surface removal and post-burial to surface removal started at this point and continued for the whole duration. A steady increase in colouration of yellow on the b* axis, suggests the infiltration of iron (Viscarra Rossel et al., 2009) or fluvic acid into the bone. Dramatic fluctuations were also seen in the FTIR results – suggesting the presence of iron or other contaminants from the environment affecting the results (Cheshire et al., 2000).

6.8 Relationship between archaeological environment and bone diagenesis

Despite the similarities in burial composition between the limestone burials from Fin Cop (Iron Age) and the chalk burials from Eriswell (Anglo-Saxon) the results from the analysis showed big differences. The bones from the limestone environment showed the highest average splitting factor from all four environments, and also the lightest surface colour and the lightest cortex colour – showing that the limestone had a bleaching effect on the bones. This effect has been reported previously in alkaline soils and is thought to be due to the presence of metal ions bound on the surface as insoluble carbohydrates (Turner-Walker, 2007). In contrast, the bones from the chalk environment displayed the lowest average splitting factor, but did have the largest range observed from the sample set. They were second lightest in surface and cortex colour (like the limestone) but also exhibited the smallest colour difference. The bones showed the highest Carbonate/Phosphate content – presumably due to environment contamination due to the uptake of carbonate as seen in the porcine burials in lime. Despite the differences reported above, when analysing the DNA results in relation to individual burial environments from across both sites, those remains from the chalk and the limestone burial environments showed the best DNA preservation and amplification.

The bones derived from sandy burials at Eriswell, showed the largest colour difference, but the lowest difference on the L* axis – showing the colour change from the a* and b* axis – possible infiltration of iron and fulvic acids, confirmed by the lowest recorded DNA content, and the evidence of inhibition.

Interestingly, the results of the bones from the 'sand and chalk' environment sat within those from both the sand environment and the chalk environment, in terms of Amide/Phosphate results. The bones showed the highest difference in lightness between the surface and the cortex – possibly due to a combined geological effect; the aggressive nature of the sand destroying the integrity of the bone surface and the chalk subsequently bleaching the cortical bone. Analysis also showed these

bones contained the second highest Carbonate/Phosphate content after the chalk environment, and the highest allele number amplified from the bones.

Lambert (1990) showed by removing 1-3mm of bone surface, contaminants such as iron, and manganese were removed, however the XRF results illustrated earlier that contamination can persist after surface removal. This research has shown that contamination of cortical bone and bone marrow results from the infiltration of inhibitors and bacteria via soil water, and the degree of infiltration is dependent on environment. In some instances this infiltration will be both total, throughout the whole sample and indelibly grossly affect any attempt to derive a DNA sample.

6.9 Importance of method optimisation

The method optimisation chapter has shown the importance of choosing the correct demineralisation technique based on the preservation state of the bone – complete demineralisation of the bone was found not to be appropriate for the ancient bones, however it was essential for the less degraded porcine bones, in order to remove inhibiting collagen and mineral. While the majority of archaeological bones are expected to fit the first description, some may be more like the porcine bones in integrity.

The colour of lysis chemicals showed the extraction of environmental contamination from the bones, as seen in the lime bones – show the importance of using a extraction kit which is designed to wash these contaminants away, in order to limit the issue of PCR inhibition in downstream analysis.

6.10 Summary

This research has shown that it is possible to analyse ancient human remains in the same manner in which degraded forensic samples are already analysed. Inhibition has been observed at certain loci, across the board, suggesting not all the loci used for forensic analysis is applicable for ancient work. However, as the inhibition appears to be sequence dependent in certain instances, as it is not purely the larger amplicons which are affected.

This research has highlighted the difficulties associated with using analytical techniques to predict the survival of DNA, but has also highlighted the necessity of using a combination of analyses to confirm results obtained. The use of XRF to identify the extra peaks seen in the ATR-FTIR spectra, showed how iron contamination can affect the splitting factor result and other composition information. Using ATR-FTIR in relation to the burial environment information showed the contamination of carbonate into metatarsals in chalk environments giving an incorrect preservation value.

Colour analysis was not found to be as accurate a predictor of preservation state in buried bones as it has proved to be in the past with burnt bones (as discussed in 4.1.11.1), and did not provide an accurate indication of collagen preservation (Shipman et al., 1984; Walker et al., 2008) but can be used as an indicator of the penetration of contamination of humic bones into the cortex, and therefore the possible inhibition of humic acid.

Comparison of the analytical results with the osteological reports of the human remains appeared to be effective in broad prediction of diagenesis and DNA content. Although classification of bone preservation by observations of surface integrity (as discussed in section 2.3.1) can be subject to objectivity, the bones with the lowest osteological preservation scores provided analytical results of good preservation state and DNA content, demonstrating the importance of using traditional methods alongside modern analytical techniques to obtain optimum results.

Chapter 7: CONCLUSION

The purpose of this research was to analyse the degradation of nucleic DNA, and bone diagenesis in relation to different burial environments in order to improve the understanding of taphonomic processes. The objectives of the research prior to the commencement of the study have all been fulfilled and will be summarised in this chapter.

At the beginning of the research it was hoped that the DNA results from the archaeological human remains would provide an insight into the burial practises at the individual cemeteries. This was achieved but in a limiting manner in such some suggested familial relationships could be discounted, and others were shown to be a possibility. The use of sex identification at Fin Cop also assisted in changing the opinion of the manner of events that led to the burial of the individuals.

Investigation of the controlled porcine burials using different burial mediums, allowed the ability to monitor individual aspects of decomposition and bone diagenesis. Analysis of the results showed distinct differences in the process of decomposition due to the different soil properties in the environments used, and also different behaviours in terms of bone diagenesis. The results from the porcine burials allowed comparisons with the ancient human archaeological samples, in order to identify the common variables in relation to the burial environments.

The human analogue burials showed that the sand burials provided the most aggressive environment for the decomposition of the soft tissue, even without the movement of water which would be commonplace in a sand environment due to the draining properties of that medium. The water content, in addition to the microbial activity from the high organic content in the clay and compost environments, appeared to have an effect on burials which presented the next quickest decomposition of soft tissues. The lime burials promoted the best preservation of soft tissues, with the lowest water and organic content in the burial medium.

Chapter 7: CONCLUSION

During this research, the importance of differentiating between the terms preservation state and decomposition rate became apparent. Although the sand burials showed the fastest decomposition rate of soft tissues, the rate of diagenesis of the bone did not coincide. Further analysis indicated the clay and compost samples displayed the same level of bone preservation state with high splitting factors and low results for carbonate and collagen preservation, despite the slower decomposition of the associated soft tissue.

By studying the effects of different burial environments, it was possible to identify the similarities and contrasting behaviours occurring within. The production of adipocere was observed in both clay and compost burials, despite the dissimilar properties of the environments; whereas variable bone preservation was observed in sand environments. These observations confirm the notion that decomposition and diagenesis cannot simply be related to one parameter, but rather it is the combination and interaction between multiple factors which affect the physical, chemical and biological decomposition of archaeological remains.

Analysis of bone composition of the human analogue samples in the lime environment showed how the environmental contaminants can cause alteration to the bone structure, thus affecting an accurate calculation of collagen and carbonate, and in addition affect the assessment of bone crystallinity from the splitting factor. The continued increase in Amide/Phosphate and Carbonate/Phosphate readings, were opposite to those expected with increasing burial duration, and did not correlate with the calculated splitting factors. This problem using composition information from ATR-FTIR analysis to identify preservation level was also identified in the unburied control bones which showed fluctuations in the splitting factors between 3 and 12 months, resulting in the conclusion that these estimations of bone structure and composition cannot be used solely as an indicator of preservation in archaeological bones, and the effect of the burial environment must be taken into account in order to fully understand the results.

By analysing both the metatarsals and femurs from the same skeletons of the human archaeological remains, it was possible to make assessments of the bone and DNA preservation in relation to one another. Overall, the research collated across all environments showed the metatarsals had the worst bone preservation with higher splitting factors, lower estimated collagen and carbonate contents, and higher levels of environmental contamination. When looking at each environment independently, the metatarsals from the limestone environment showed a higher level of inhibition due to infiltration of environmental contaminants and higher level of DNA degradation. However the observed differences in levels of degradation and inhibition between the skeletal elements was dependent on the environment, as DNA amplification was more successful in the metatarsals than the femurs from the chalk environment and the sand environment. This result can assist in the sampling strategies of archaeological remains for DNA analysis and also suggests a triage system for archaeologists for further analysis based upon the burial environment.

The analysis of both experimental porcine burials and ancient human archaeological samples allow correlations to be drawn in regards to the environments. The worst preservation of DNA was observed in the sand environments with both the porcine burials and the human burials, despite the differences in water movement. This shows that even without the degradation from water percolation, the sand provides an aggressive environment for the destruction of bone and DNA. The use of colourimetry and XRF in the research was able to identify the higher colouration of yellow in the bones from both the human and porcine bone samples from sand environments, was likely due to the infiltration of fulvic acid and iron from the environment, which in the porcine bones was linked to the lack of amplification of DNA. The porcine burials showed that the best preservation of DNA was from bones buried in the lime environment – results which are mirrored in the human remains from the chalk and limestone environments.

This research highlights the importance of assessing environmental conditions prior to sample choice for expensive and time-consuming DNA analysis. The

observation of contamination shown from the XRF and FTIR and colourimetry data show the importance of using additional analytical techniques to study the bone in order to identify inhibition which may produce incorrect preservation calculations, leading to decisive moves regarding to DNA extraction methods and analysis. Using a variety of techniques such as these to assess the bone, allows a basic form of predictive modelling prior to commencement of DNA analysis by identifying possible issues, or areas of concern from known inhibitive or diagenetic environments or observations. To allow full comprehension of the diagenetic factors which may have affected archaeological bones in order to analyse appropriately, it is vital that accurate and detailed notes and samples are recorded and taken from burial grounds at the time of archaeological excavation. It is also imperative appropriate PPE and handling is adhered to if DNA analysis is potentially to be performed at any time in the future.

The process of optimising methodologies during this research shows the significance of choosing the appropriate protocols for the analysis of archaeological bone. Methods of cleaning, surface removal, and sample preparation can all be detrimental to bones, and it is important to ascertain the most appropriate method for each individual sample.

The overall aims of this research to investigate diagenesis and nucleic DNA degradation has been achieved, and the null hypotheses of no differences in decomposition, bone diagenesis and DNA degradation between samples from different burial environments can be rejected. In terms of the alternative hypotheses stated, it is not primarily the pH of the burial environment that has an effect on the state of DNA preservation, but other variables such as organic content providing microbial decomposition and the water content providing a passage into the bone which affect degradation. As predicted, the lime environment provided the best environment for preservation of DNA (although also caused inhibition of DNA during amplification), and the sand environment the most destructive. As previously reported, there was a difference observed between the quantity of DNA retained by the femurs in comparison to metatarsals, however the reason for the

differences were more complicated than first thought due to the different ways in which the elements interact with the burial environments.

This research showed that the burial environment had a more significant effect on soft tissue decomposition, bone diagenesis and DNA degradation than the passage of time for which the remains were buried. This statement can be seen to be true in the results from both the human analogue, and the human archaeological samples which were separated by several thousand years.

Although similarities can be seen between the state of bone diagenesis and DNA degradation, it is not possible to quantify the relationship due to many other variables which are at play within each burial environment. The results of this research show that in order to provide a comprehensive assessment of the preservation state of the bone it is necessary to use a multi-disciplinary approach of both traditional osteological observations, and modern analytical techniques in order to evaluate the bone in relation to its burial environment.

The time and cost implications of the management of a DNA-led identification strategy are huge, and it is hoped that one of the products of this study is an improved understanding of the complex interaction between this relationship, and therefore, the more efficient any subsequent DNA profiling may be. This will assist not only forensic science practitioners and investigators, but also archaeologists and historians who are looking for answers. By having a better understanding of the whole process, the information recorded by the excavation team, archaeologists, geologists and anthropologists, will also benefit the DNA analysts and assist in the decision making process of sampling, and protocol selection.

7.1 Limitations of the research

Although every attempt was made to make the investigations comparable in the experimental burials, with porcine bones being collected from the same butcher, with similar age at deaths, and post-mortem intervals, some differences observed in the bone structure may be due to individual differences. Different bones were used for each experiment, in order to eliminate addition variables such as lack of

bone integrity which would have occurred by excavating and sampling the bone at each time interval.

Individual porcine bones were used as the primary investigation was concentrated on the bone diagenesis, however the decomposition of a whole carcass will alter the burial environment in a manner which was not observed in this study.

The methodology for the experimental burials allowed for the control of environmental factors such as movement of water, and the ability to measure any pH changes without loss of material. However, these burials may not be comparable to natural environments where natural rainfall would have changed the conditions, and provided different variables.

The sample size of the human archaeological remains available and archaeological reports of the burials provided some limitations to the research. Due to the lack of geological samples taken and in-depth records it was only possible to relate the results to the broad geological assessments provided within the original archaeological reports. The natural context of the burial grounds, meant it was not possible to use balanced sample sets of skeletal remains for comparison; this was especially a problem with the lack of burials from the sand environment.

7.2 Future work

In reference to the taphonomic side of this research, future work in this area would benefit from the use of whole carcasses in different environments, in an outside facility where an in-vivo assessment of decomposition and diagenesis might be conducted with the monitoring of environmental variables. Furthermore, by testing the burial environment for contaminants with XRF, colourimetry and soil analysis prior to burial, would enable an opportunity to develop predictions for the most optimal protocols and methodologies for subsequent analysis of the archaeological remains upon excavation.

In order to further improve the success of DNA amplification from archaeological bone, further research into the inhibition effects of environmental contaminants would be advantageous. The identification of DNA sequences most likely to be

inhibited due to environmental contaminates such as fulvic and humic acid, would enable a multiplex primer set to be developed to assist in the successful amplification of archaeological samples.

In addition, by utilising a technique such as X-ray diffraction (XRD), differentiation between hydroxyapatite in the bone and mineral contaminants could be achieved, therefore providing a more accurate assessment of bone diagenesis, than found during this research. If correlations between the crystallinity results and DNA amplification were established, this technique could be used for cost-effective and rapid identification of the probability of successful amplification of forensic and archaeological remains.

REFERENCES

Adachi, N., Umetsu, K., Takigawa, W. and Sakaue, K. (2004), "Phylogenetic analysis of the human ancient mitochondrial DNA", *Journal of Archaeological Science,* vol. 31, no. 10, pp. 1339-1348.

Adamiano, A., Fabbri, D., Falini, G. and Giovanna Belcastro, M. (2013), "A complementary approach using analytical pyrolysis to evaluate collagen degradation and mineral fossilisation in archaeological bones: The case study of Vicenne-Campochiaro necropolis (Italy)", *Journal of Analytical and Applied Pyrolysis,* vol. 100, no. 0, pp. 173-180.

Adler, C. J., Haak, W., Donlon, D. and Cooper, A. (2011), "Survival and recovery of DNA from ancient teeth and bones", *Journal of Archaeological Science,* vol. 38, no. 5, pp. 956-964.

Aitkenhead, M. J., Coull, M., Towers, W., Hudson, G. and Black, H. I. J. (2013), "Prediction of soil characteristics and colour using data from the National Soils Inventory of Scotland", *Geoderma,* vol. 200–201, no. 0, pp. 99-107.

Alaeddini, R., Walsh, S. J. and Abbas, A. (2010), "Forensic implications of genetic analyses from degraded DNA—A review", *Forensic Science International: Genetics,* vol. 4, no. 3, pp. 148-157.

Alberts, B. and Johnson, A. (eds.) (2014), *Molecular Biology of the Cell,* Sixth ed, Taylor & Francis Inc , Garland Publishing Inc, San Francisco.

Al-enizi, M., Hadi, S. and Goodwin, W. (2008), "The development of visual and chemical methods for predicting the likelihood of obtaining a DNA profile from degraded bone samples", *Forensic Science International: Genetics Supplement Series,* vol. 1, no. 1, pp. 2-3.

Alonso, A., Anðelinoviæ, S., Martín, P., Sutloviæ, D., Erceg, I., Huffine, E., Fernández de Simón, L., Albarrán, C., Definis-Gojanoviæ, M., Fernández-Rodriguez, A., García, P., Drmiæ, I., Rezic, B., Kuret, S., Sancho, M. and Primorac, D. (2001), "DNA Typing from Skeletal Remains: Evaluation of Multiplex and Megaplex STR Systemson DNA Isolated from Bone and Teeth Samples", *Croatian Medical Journal,* vol. 42, no. 3, pp. 260-266.

Alonso, A., Martín, P., Albarrán, C., García, P., Primorac, D., García, O., Fernández de Simón, L., García-Hirschfeld, J., Sancho, M. and Fernández-Piqueras, J. (2004), "Specific Quantification of Human Genomes from Low Copy Number DNA Samples inForensic and Ancient DNA Studies", *Croatian Medical Journal,* vol. 44, no. 3, pp. 273-280.

Álvarez-Lloret, P., Rodríguez-Navarro, A. B., Romanek, C. S., Gaines, K. F. and Congdon, J. (2006), "Quantitative analysis of bone mineral using FTIR", *MACLA,* vol. 6, pp. 45-47.

Ambers, A., Gill-King, H., Dirkmaat, D., Benjamin, R., King, J. and Budowle, B. (2013), "Autosomal and Y-STR Analysis of Degraded DNA from the 120-Year-Old Skeletal Remains of Ezekiel Harper", *Forensic Science International: Genetics,* vol. 9, pp. 33-41.

Amory, S., Huel, R., Bilić, A., Loreille, O. and Parsons, T. J. (2012), "Automatable full demineralization DNA extraction procedure from degraded skeletal remains", *Forensic Science International: Genetics,* vol. 6, no. 3, pp. 398-406.

Anđelinoviæ, S., Sutloviæ, D., Ivkošiæ, I. E., Škaro, V., Ivkošiæ, A., Paiæ, F., Rezic, B., Definis-Gojanoviæ, M. and Primorac, D. (2005), "Twelve-year Experience in Identification of Skeletal Remainsfrom Mass Graves", *Croatian Medical Journal,* vol. 46, no. 4, pp. 530-539.

Ansorena, D., De Peña, M. P., Astiasarán, I. and Bello, J. (1997), "Colour evaluation of chorizo de Pamplona, a Spanish dry fermented sausage: Comparison between the CIE L∗a∗b∗ and the Hunter lab systems with illuminants D65 and C", *Meat Science,* vol. 46, no. 4, pp. 313-318.

Ariffin, S. H. Z., Wahab, R. M. A., Zamrod, Z., Sahar, S., Razak, M. F. A., Ariffin, E. J. and Senafi, S. (2007), "Molecular Archeology of Ancient Bone From 400 Year Old Shipwreck", *Asia Pacific Journal of Molecular Biology and Biotechnology,* vol. 15, no. 1, pp. 27-31.

Ascher, R. (1968), "Time's Arrow and the Archaeology of a Contemporary Community", in Chang, K. (ed.) *Settlement Archaeology,* National Press Books, Palo Alto, CA, pp. 43-52.

Aturaliya, S. and Lukasewycz, A. (1999), "Experimental Forensic and Bioanthropological Aspects of Soft Tissue Taphonomy: 1. Factors Influencing Postmortem Tissue Desiccation Rate", *Journal of Forensic Sciences,* vol. 44, no. 5, pp. 893-896.

Bada, J. L., Wang, X. S., Poinar, H. N., Pääbo, S. and Poinar, G. O. (1994), "Amino acid racemization in amber-entombed insects: Implications for DNA preservation", *Geochimica et Cosmochimica Acta,* vol. 58, no. 14, pp. 3131-3135.

Bartlett, J. and Stirling, D. (2003), "A short history of the Polymerase Chain Reaction", in Bartlett, J. and Stirling, D. (eds.) *PCR protocols,* 2nd ed, Humana Press Inc, Totowa, pp. 3-4.

Bass, B. and Jefferson, J. (2003), *Death's Acre: Inside the legendary 'body farm',* Time Warner Books, London.

Bauer, C. M., Niederstätter, H., McGlynn, G., Stadler, H. and Parson, W. (2013), "Comparison of morphological and molecular genetic sex-typing on mediaeval human skeletal remains", *Forensic Science International: Genetics,* vol. 7, no. 6, pp. 581-586.

Bell, L. S., Skinner, M. F. and Jones, S. J. (1996), "The speed of post mortem change to the human skeleton and its taphonomic significance", *Forensic science international,* vol. 82, no. 2, pp. 129-140.

Biesecker, L. G., Bailey-Wilson, J. E., Ballantyne, J., Baum, H., Bieber, F. R., Brenner, C., Budowle, B., Butler, J. M., Carmody, G. P., Conneally, M., Duceman, B., Eisenberg, A., Forman, L., Kidd, K. K., Leclair, B., Niezgoda, S., Parsons, T. J., Pugh, E., Shaler, R., Sherry, S. T., Sozer, A. and Walsh, A. (2005), "DNA Identifications After the 9/11 World Trade Center Attack", *Epidemiology,* vol. 310, pp. 1122-1123.

Bille, T., Wingrove, R., Holland, M., Holland, C., Cave, C. and Schumm, J. (2004), "Novel method of DNA extraction from bones assisted DNA identification of World Trade Center victims", *International Congress Series,* vol. 1261, no. 0, pp. 553-555.

Bollongino, R., Tresset, A. and Vigne, J. (2008), "Environment and excavation: Pre-lab impacts on ancient DNA analyses", *Comptes Rendus Palevol,* vol. 7, no. 2–3, pp. 91-98.

Bollongino, R. and Vigne, J. (2008), "Temperature monitoring in archaeological animal bone samples in the Near East arid area, before, during and after excavation", *Journal of Archaeological Science,* vol. 35, no. 4, pp. 873-881.

Bouwman, A. S., Chilvers, E. R., Brown, K. A. and Brown, T. A. (2006), "Brief communication: Identification of the authentic ancient DNA sequence in a human bone contaminated with modern DNA", *American Journal of Physical Anthropology,* vol. 131, pp. 428--431.

Bradley, R. (1984), *The Social Foundations of Prehistoric Britain: Themes and Variations in the Archaeology of Power,* Longman Archaeology Series, London.

Brown, D. (1978), *Anglo-Saxon England,* Book Club Associates, London.

Brundin, M., Figdor, D., Sundqvist, G. and Sjögren, U. (2013), "DNA Binding to Hydroxyapatite: A Potential Mechanism for Preservation of Microbial DNA", *Journal of endodontics,* vol. 39, no. 2, pp. 211-216.

Burger, J., Hummel, S., Herrmann, B. and Henke, W. (1999), "DNA preservation: A microsatellite-DNA study on ancient skeletal remains", *Electrophoresis,* vol. 20, pp. 1722--1728.

Butler, J. M. (2001), *Forensic DNA Typing,* Elsevier Academic Press, London.

Butler, J. M. (2015), *Advanced Topics in Forensic DNA Typing: Interpretation,* Academic Press, San Diego.

Butler, J. M. (2006), "Genetics and Genomics of Core Short Tandem Repeat Loci Used in Human Identity Testing", *Journal of Forensic Sciences,* vol. 51, no. 2, pp. 253-265.

Campobasso, C. P., Di Vella, G. and Introna, F. (2001), "Factors affecting decomposition and Diptera colonization", *Forensic science international,* vol. 120, no. 1–2, pp. 18-27.

Campos, P. F., Craig, O. E., Turner-Walker, G., Peacock, E., Willerslev, E. and Gilbert, M. T. P. (2012), "DNA in ancient bone – Where is it located and how should we extract it?", *Annals of Anatomy - Anatomischer Anzeiger,* vol. 194, no. 1, pp. 7-16.

Caputo, M., Irisarri, M., Alechine, E. and Corach, D. (2013), "A DNA extraction method of small quantities of bone for high-quality genotyping", *Forensic Science International: Genetics,* vol. 7, pp. 488--493.

Caruth, J. and Anderson, S. (2005), *An assessment of the potential for analysis and publication for archaeological work carried out at RAF Lakenheath between 1987 and June 2005,* 2005/94, Suffolk C.C. Archaeological Service, Suffolk, UK.

Carver, M. (2000), *Sutton Hoo: Burial Ground of Kings?* British Museum Press, London.

Catelli, L., Borosky, A., Romanini, C., Salado, M., Bernardi, P. and Vullo, C. (2008), "Skeletal reassociation from an illegal common grave of Argentina by using STR, miniSTR, and mtDNA analysis", *Forensic Science International: Genetics Supplement Series,* vol. 1, no. 1, pp. 408-410.

Cattaneo, C. D., Angelis, D. and Porta, D. (2006), "Personal identification of cadavers and human remains", in Schmitt, A., Cunha, A. and Pinheiro, J. (eds.) *Forensic Anthropology and Medicine: Complementary Sciences From Recovery to Cause of Death,* Humana Press Inc., Totowa, NJ, pp. 359-379.

Chaumat, G., Müller, K. and Reiche, I. (2011), "Preliminary Experiments on Model Artificially Altered Samples to Consolidate Degraded and Wet Archaeological Bone with Azelaic Acid", *Archeo Sciences,* vol. 3, pp. 213--222.

Cheshire, M. V., Dumat, C., Fraser, A. R., Hillier, S. and Staunton, S. (2000), "The interaction between soil organic matter and soil clay minerals by selective removal and controlled addition of organic matter", *European Journal of Soil Science,* vol. 51, pp. 497-509.

Child, A. M. (1995), "Towards and Understanding of the Microbial Decomposition of Archaeological Bone in the Burial Environment", *Journal of Archaeological Science,* vol. 22, no. 2, pp. 165-174.

Chilvers, E. R., Bouwman, A. S., Brown, K. A., Arnott, R. G., Prag, A. J. N. W. and Brown, T. A. (2008), "Ancient DNA in human bones from Neolithic and Bronze Age sites in Greece and Crete", *Journal of Archaeological Science,* vol. 35, no. 10, pp. 2707-2714.

Cipollaro, M., Di Bernardo, G., Galano, G., Galderisi, U., Guarino, F., Angelini, F. and Cascino, A. (1998), "Ancient DNA in Human Bone Remains from Pompeii Archaeological Site", *Biochemical and biophysical research communications,* vol. 247, no. 3, pp. 901-904.

Colson, I. B., Richards, M. B., Bailey, J. F., Sykes, B. C. and Hedges, R. E. M. (1997), "DNA Analysis of Seven Human Skeletons Excavated from the Terp of Wijnaldum", *Journal of Archaeological Science,* vol. 24, no. 10, pp. 911-917.

Cooper, A. and Poinar, H. N. (2000), "Ancient DNA: Do it right or not at all ", *Science,* vol. 289, no. 5482, pp. 1139.

Cox, M., Hanson, I., Laver, J. and Wessling, R. (2007), *The Scientific Investigation of Mass Graves: Towards Protocols and Standard Operating Procedures,* Cambridge University Press, Cambridge.

Currey, J. (1984), *The Mechanical Adaptations of Bones,* Princeton University Press, New Jersey.

Damann, F. E. and Carter, D. O. (2014), "Human Decomposition Ecology and Postmortem Microbiology", in Pokines, J. T. and Symes, S. A. (eds.) *Manual of Forensic Taphonomy,* CRC Press, London, pp. 37-45.

Darwent, C. M. and Lyman, R. L. (2002), "Detecting the postburial fragmentation of carpals, tarsals and phalanges", in Haglund, W. D. and , S., Marcella. H. (eds.) *Advances in Forensic Taphonomy: Method, Theory and Archaeological Perspectives,* CRC Press, , pp. 335-377.

D'Elia, M., Gianfrate, G., Quarta, G., Giotta, L., Giancane, G. and Calcagnile, L. (2007), "Evaluation of possible contamination sources in the 14C analysis of bone samples by FTIR spectroscopy", *Radiocarbon,* vol. 49, no. 2, pp. 201-210.

Dent, B. B., Forbes, S. L. and Stuart, B. H. (2004), "Review of human decomposition processes in soil", *Environmental Geology,* vol. 45, pp. 576-585.

Desmyter, S. and Greef, C. D. (2008), "A more efficient extraction method of human bone resulting in improved DNA profiling", *Forensic Science International: Genetics Supplement Series,* vol. 1, pp. 24-25.

Devlin, J. B. and Herrmann, N. P. (2008), "6 - Bone Color as an Interpretive Tool of the Depositional History of Archaeological Cremains", in Christopher W. Schmidt and Steven A. Symes (eds.) *The Analysis of Burned Human Remains,* Academic Press, San Diego, pp. 109-128.

Dirkmaat, D. C. and Sienicki, L. A. (1995), "Taphonomy in the northeast woodlands: four cases from western Pennsylvania", *Proceedings of the 47th Annual Meeting of the American Academy of Forensic Sciences,* Vol. 1 (10), Seattle, .

Dupras, T. L. and Schultz, J. J. (2014), "Taphonomic Bone Staining and Colour Changes in Forensic Contexts", in Pokines, J. T. and Symes, S. A. (eds.) *Manual of Forensic Taphonomy,* CRC Press, London, pp. 315-340.

Edson, S. M., Christensen, A. F., Barritt, S. M., Meehan, A., Leney, M. D. and Finelli, L. N. (2009), "Sampling of the cranium for mitochondrial DNA analysis of human skeletal remains", *Forensic Science International: Genetics Supplement Series,* vol. 2, no. 1, pp. 269-270.

Efremov, J. A. (1940), "Taphonomy: New branch of Paleontology", *Pan American Geologist,* vol. LXXIV, no. 2.

Eilert, K. D. and Foran, D. R. (2009), "Polymerase Resistance to Polymerase Chain Reaction Inhibitors in Bone", *Journal of Forensic Science,* vol. 54, no. 5, pp. 1001-1007.

Elliott, T. A. and Grime, G. W. (1993), "Examining the diagenetic alteration of human bone material from a range of archaeological burial sites using nuclear microscopy", *Nuclear Instruments and Methods in Physics Research Section B: Beam Interactions with Materials and Atoms,* vol. 77, no. 1–4, pp. 537-547.

Faerman, M., Bar-Gal, G. K., Filon, D., Greenblatt, C. L., Stager, L., Oppenheim, A. and Smith, P. (1998), "Determining the Sex of Infanticide Victims from the Late Roman Era through Ancient DNA Analysis", *Journal of Archaeological Science,* vol. 25, no. 9, pp. 861-865.

Fattorini, P., Ciofuli, R., Cossutta, F., Giulianini, P., Edomi, P., Furlanut, M. and Previderè, C. (1999), "Fidelity of polymerase chain reaction-direct sequencing analysis of damaged forensic samples.", *Electrophoresis,* vol. 20, pp. 3349-3357.

Fernández-Calviño, D., Rousk, J., Brookes, P. C. and Bååth, E. (2011), "Bacterial pH-optima for growth track soil pH, but are higher than expected at low pH", *Soil Biology and Biochemistry,* vol. 43, no. 7, pp. 1569-1575.

Fernández-Jalvo, Y., Andrews, P., Pesquero, D., Smith, C., Marín-Monfort, D., Sánchez, B., Geigl, E. and Alonso, A. (2010), "Early bone diagenesis in temperate environments: Part I: Surface features and histology",

Palaeogeography, Palaeoclimatology, Palaeoecology, vol. 288, no. 1–4, pp. 62-81.

Fondevila, M., Phillips, C., Naveran, N., Fernandez, L., Cerezo, M., Salas, A., Carracedo, Á and Lareu, M. V. (2008), "Case report: Identification of skeletal remains using short-amplicon marker analysis of severely degraded DNA extracted from a decomposed and charred femur", *Forensic Science International: Genetics,* vol. 2, no. 3, pp. 212-218.

Forbes, S. L., Dent, B. B. and Stuart, B. H. (2005), "The effect of soil type on adipocere formation", *Forensic Science International,* vol. 154, no. 1, pp. 35-43.

Fredericks, J. D., Bennett, P., Williams, A. and Rogers, K. D. (2012a), "FTIR spectroscopy: A new diagnostic tool to aid DNA analysis from heated bone", *Forensic Science International: Genetics,* vol. 6, no. 3, pp. 375-380.

Fredericks, J. D., Bennett, P., Williams, A. and Rogers, K. D. (2012b), "FTIR spectroscopy: A new diagnostic tool to aid DNA analysis from heated bone", *Forensic Science International: Genetics,* vol. 6, no. 3, pp. 375-380.

Fredericks, J. D. (2011), *Development of new tools for forensic analysis of DNA from compromised bone* (Ph.D. thesis), Cranfield Univeristy, .

Fregel, R., Almeida, M., Betancor, E., Suárez, N. M. and Pestano, J. (2011), "Reliable nuclear and mitochondrial DNA quantification for low copy number and degraded forensic samples", *Forensic Science International: Genetics Supplement Series,* vol. 3, no. 1, pp. e303-e304.

Gabbott, S. E. (1998), "Taphonomy of the Ordovician Soom Shale Lagerstätte: an example of soft tissue preservation in clay minerals", *Palaeontology,* vol. 41, pp. 631-667.

Gamba, C., Fernández, E., Oliver, A., Tirado, M., Baeza, C., López-Parra, A. M. and Arroyo-Pardo, E. (2008), "Population genetics and DNA preservation in ancient human remains from Eastern Spain", *Forensic Science International: Genetics Supplement Series,* vol. 1, no. 1, pp. 462-464.

Gamba, C., Fernández, E., López-Parra, A. M. and Arroyo-Pardo, E. (2011), "Statistical evaluation of pre-laboratory and laboratory factors that influence DNA recovery from archaeological material", *Forensic Science International: Genetics Supplement Series,* vol. 3, no. 1, pp. e109-e110.

Gaytmenn, R. and Sweet, D. (2003), "Quantification of forensic DNA from various regions of human teeth", *Journal of Forensic Science,* vol. 48, no. 3, pp. 1--4.

Gilbert, T. M., Rudbeck, L., Willerslev, E., Hansen, A. J., Smith, C., Penkman, K. E. H., Prangenberg, K., Nielsen-Marsh, C. M., Jans, M. E., Arthur, P., Lynnerup, N.,

Turner-Walker, G., Biddle, M., Kjølbye-Biddle, B. and Collins, M. J. (2005), "Biochemical and physical correlates of DNA contamination in archaeological human bones and teeth excavated at Matera, Italy", *Journal of Archaeological Science,* vol. 32, no. 5, pp. 785-793.

Gill, P., Ivanov, P. L., Kimpton, C., Piercy, R., Benson, N., Tully, G., Evett, I., Hagelberg, E. and Sullivan, K. (1994), "Identification of the remains of the Romanov family by DNA analysis", *Nature Genetics,* vol. 6, pp. 130-135.

Gill-King, H. (1997), "Chemical and ultrastructural aspects of decomposition", in Haglund, W. D. and Sorg, M., H. (eds.) *Forensic taphonomy - The post-mortem fate of human remains,* CRC Press, , pp. 93-108.

Götherström, A., Collins, M. J., Angerbjörn, A. and Lidén, K. (2002), "Bone preservation and DNA amplification", *Archaeometry,* vol. 44, pp. 395-404.

Grobbel, J. P., Dikeman, M. E., Smith, J. S., Kropf, D. H. and Milliken, G. A. (2006), "Effects of polyvinyl chloride overwrap film, high-oxygen modified atmosphere packaging, or ultra-low- oxygen modified atmosphere packaging on bone marrow discolouration in beef humerus, rib, thoracic vertebra, and scapula", *Journal of Animal Science,* vol. 84, pp. 694-701.

Grunenwald, A., Keyser, C., Sautereau, A. M., Crubézy, E., Ludes, B. and Drouet, C. (2014), "Revisiting carbonate quantification in apatite (bio)minerals: a validated FTIR methodology", *Journal of Archaeological Science,* vol. 49, no. 0, pp. 134-141.

Hagelberg, E., Gray, I. C. and Jeffreys, A. J. (1991), "Identification of the skeletal remains of a murder victim by DNA analysis.", *Nature,* vol. 352, no. 6334, pp. 427-429.

Haglund, W. D. (2002), "Recent mass graves, an introduction", in Haglund, W., D. and Sorg, M. H. (eds.) *Advances in forensic taphonomy: Method, theory and archaeological perspectives.* CRC Press, , pp. 243-261.

Haglund, W. D., Connor, M. and Scott, D. D. (2002), "The effect of cultivation on buried human remains", in Haglund, W. D. and Sorg, M. H. (eds.) *Advances in forensic taphonomy: Method, theory and archaeological perspectives,* CRC Press, , pp. 133-150.

Haile, J., Larson, G., Owens, K., Dobney, K. and Shapiro, B. (2010), "Ancient DNA typing of archaeological pig remains corroborates historical records", *Journal of Archaeological Science,* vol. 37, no. 1, pp. 174-177.

Hall, A., Sims, L., Foster, A. and Ballantyne, J. (2016), "DNA Damage and Repair in Forensic Science", in Katz, E. and Halámek, J. (eds.) *Forensic Science: A Multidisciplinary Approach,* Wiley-VCH, New York, pp. 208-211.

Hanna, J., Bouwman, A. S., Brown, K. A., Parker Pearson, M. and Brown, T. A. (2012), "Ancient DNA typing shows that a Bronze Age mummy is a composite of different skeletons", *Journal of Archaeological Science,* vol. 39, no. 8, pp. 2774-2779.

Härke, H. (1990), ""Warrior Graves"? The Background of the Anglo-Saxon Weapon Burial Rite", *The Past and Present Society, Oxford University Press, Oxford,* vol. 126, pp. 22-43.

Hartman, D., Drummer, O., Eckhoff, C., Scheffer, J. W. and Stringer, P. (2011), "The contribution of DNA to the disaster victim identification (DVI) effort", *Forensic Science International,* vol. 205, no. 1–3, pp. 52-58.

Haynes, S., Searle, J. B., Bretman, A. and Dobney, K. M. (2002), "Bone Preservation and Ancient DNA: The Application of Screening Methods for Predicting DNA Survival", *Journal of Archaeological Science,* vol. 29, no. 6, pp. 585-592.

Hedeager, L. (1992), *Iron-Age Societies,* Blackwell Publishers, Oxford.

Hedges, S. and Schweitzer, M. (1995), "Detecting dinosaur DNA", *Science,* vol. 268, no. 5214, pp. 1191-1192.

Hedges, R. E. M. (2002), "Bone diagenesis: An overview of processes", *Archaeometry,* vol. 44, no. 3, pp. 319-328.

Hedges, R. E. M. and Millard, A. R. (1995), "Bones and Groundwater: Towards the Modelling of Diagenetic Processes", *Journal of Archaeological Science,* vol. 22, no. 2, pp. 155-164.

Heintzman, P. D. (2013), "Patterns in palaeontology: An introduction to ancient DNA", *Palaeontology Online,* [Online], vol. 3, no. 10, pp. 01/07/2015-1-10 available at: http://www.palaeontologyonline.com/articles/2013/patterns-in-palaeontology-an-introduction-to-ancient-dna/.

Henderson, J. (1987), "Factors determining the state of preservation of human remains", in Boddington, A., Garland, A. N. and Janaway, R. C. (eds.) *Death, decay and reconstruction: approaches to archaeology and forensic science,* , pp. 43-54.

Hester, T. R., Shafer, H. J. and Feder, K. L. (1997), *Field methods in archaeology,* 7th ed, Mayfield, London.

Higgins, D. and Austin, J. (2013), "Teeth as a source of DNA for forensic identification of human remains: A Review", *Science & Justice : Journal of the Forensic Science Society,* vol. 53, no. 4, pp. 433-441.

Higgins, D., Rohrlach, A. B., Kaidonis, J., Townsend, G. and Austin, J. J. (2015), "Differential Nuclear and Mitochondrial DNA Preservation in Post-Mortem Teeth with Implications for Forensic and Ancient DNA Studies", *PLOS ONE,* vol. 10, no. 5, pp. e0126935.

Higuchi, R., Bowman, B., Freiberger, M., Ryder, O. A. and Wilson, A. C. (1984), "DNA sequences from the quagga, an extinct member of the horse family", *Nature,* vol. 312, pp. 282-284.

Hiller, J. C., Collins, M. J., Chamberlain, A. T. and Wess, T. J. (2004), "Small-angle X-ray scattering: a high-throughput technique for investigating archaeological bone preservation", *Journal of Archaeological Science,* vol. 31, no. 10, pp. 1349-1359.

Hines, D. Z. C., Vennemeyer, M., Amory, S., Huel, R. L. M., Hanson, I., Katzmarzyk, C. and Parsons, T. J. (2014), "Chapter 13 - Prioritized Sampling of Bone and Teeth for DNA Analysis in Commingled Cases", in Byrd, B. J. A. E. (ed.) *Commingled Human Remains,* Academic Press, San Diego, pp. 275-305.

Hiramoto, K., Sekiguchi, K., Aso-O, R., Ayuha, K., Ni-Iyama, H., Kato, T. and Kikugawa, K. (1995), "Dna strand breaks induced through active oxygen radicals by fragrant component 4-hydroxy-2-hydroxymethyl5-methyl-3(2H)-furanone in maillard reaction of hexose/amino acid", *Food and Chemical Toxicology,* vol. 33, no. 10, pp. 803-814.

Hochmeister, M. N., Budowle, B., Borer, U. V., Eggmann, U., Comey, C. T. and Dirnhofer, R. (1991), "Typing of deoxyribonucleic acid (DNA) extracted from compact bone from human remains", *Journal of Forensic Science,* vol. 36, no. 6, pp. 1649-1661.

Hofreiter, M., Serre, D., Poinar, H. N., Kuch, M. and Paabo, S. (2001), "Ancient DNA", *Nature Reviews - Genetics,* vol. 2, pp. 353-359.

Hofreiter, M., Collins, M. and Stewart, J. R. (2012), "Ancient biomolecules in Quaternary palaeoecology", *Quaternary Science Reviews,* vol. 33, no. 0, pp. 1-13.

Hollund, H. I., Ariese, F., Fernandes, R., Jans, M. M. E. and Kars, H. (2013), "Testing an alternative high-thoroughput tool for investigating bone diagenesis: FTIR in attenuated total reflection (ATR) mode", *Archaeometry,* vol. 55, no. 3, pp. 507-532.

Hughes-Stamm, S., Warnke, F. and van Daal, A. (2016), "An alternate method for extracting DNA from environmentally challenged teeth for improved DNA analysis", *Legal medicine,* vol. 18, pp. 31-36.

Imaizumi, K., Noguchi, K., Shiraishi, T., Sekiguchi, K., Senju, H., Fujii, K., Yoshida, K., Kasai, K. and Yoshino, M. (2005), "DNA typing of bone specimens—the potential use of the profiler test as a tool for bone identification", *Legal medicine,* vol. 7, no. 1, pp. 31-41.

Jakovski, Z., Nikolova, K., Janeska, B., Cakar, Z., Stankov, A., Poposka, V., Palvovski, G. and Duma, A. (2010), "Forensic DNA analysis in the identification of human remains in mass graves", *Journal of Clinical Pathology and Forensic Medicine,* vol. 1, no. 1, pp. 001-004.

Janaway, R. C., Wilson, A. S., Carpio Díaz, G. and Guillen. S. (2009), "Taphonomic changes to the buried body in arid environments: an experimental case study in Peru. ", in Ritz, K., Dawson, L. and . Miller, D. (eds.) *Criminal & Environmental Soil Forensics: 341-356.* Springer, New York, pp. 341-356.

Janjua, M. A. and Rogers, T. L. (2008), "Bone weathering patterns of metatarsal v. femur and the postmortem interval in Southern Ontario", *Forensic science international,* vol. 178, no. 1, pp. 16-23.

Jans, M. M. E., Nielsen-Marsh, C. M., Smith, C. I., Collins, M. J. and Kars, H. (2004), "Characterisation of microbial attack on archaeological bone", *Journal of Archaeological Science,* vol. 31, no. 1, pp. 87-95.

Jeffreys, A. J., Allen, M. J., Hagelberg, E. and Sonnberg, A. (1992), "Identification of the skeletal remains of Josef Mengele by DNA analysis", *Forensic Science International,* vol. 56, no. 1, pp. 65-76.

Johnston, E. and Stephenson, M. (2016), "DNA Profiling Success Rates from Degraded Skeletal Remains in Guatemala.", *Journal of Forensic Sciences,* [Online], , pp. 05/05/2016 available at: doi:10.1111/1556-4029.13087.

Junod, C. A. and Pokines, J. T. (2014), "Subaerial Weathering", in Pokines, J. T. and Symes, S. A. (eds.) *Manual of Forensic Taphonomy,* CRC Press, London, pp. 287-314.

Kaestle, F. A. and Horsburgh, K. A. (2002), "Ancient DNA in Anthropology: Methods, Applications,and Ethics", *Yearbook of Physical Anthropology,* vol. 45, pp. 92-130.

Kemp, B. M. and Smith, D. G. (2005), "Use of bleach to eliminate contaminating DNA from the surface of bones and teeth", *Forensic science international,* vol. 154, no. 1, pp. 53-61.

Kirsanow, K. and Burger, J. (2012), "Ancient human DNA", *Annals of Anatomy - Anatomischer Anzeiger,* vol. 194, no. 1, pp. 121-132.

Kitayama, T., Ogawa, Y., Fujii, K., Nakahara, H., Mizuno, N., Sekiguchi, K., Kasai, K., Yurino, N., Yokoi, T., Fukuma, Y., Yamamoto, K., Oki, T., Asamura, H. and Fukushima, H. (2010), "Evaluation of a new experimental kit for the extraction of DNA from bones and teeth using a non-powder method", *Legal medicine,* vol. 12, no. 2, pp. 84-89.

Kjorlien, Y. P., Beattie, O. B. and Peterson, A. E. (2009), "Scavenging activity can produce predictable patterns in surface skeletal remains scattering: Observations and comments from two experiments", *Forensic science international,* vol. 188, no. 1–3, pp. 103-106.

Kolman, C. J. and Tuross, N. (2000), "Ancient DNA analysis of human populations", *American Journal of Physical Anthropology,* vol. 111, no. 1, pp. 5-23.

Koon, H. E. C., Loreille, O. M., Covington, A. D., Christensen, A. F., Parsons, T. J. and Collins, M. J. (2008), "Diagnosing post-mortem treatments which inhibit DNA amplification from US MIAs buried at the Punchbowl", *Forensic Science International,* vol. 178, no. 2–3, pp. 171-177.

Korifi, R., Le Dréau, Y., Antinelli, J., Valls, R. and Dupuy, N. (2013), "CIE L*a*b* color space predictive models for colorimetry devices – Analysisof perfume quality", *Talanta,* vol. 104, pp. 58-66.

Lambert, J. B., Weydert, J. M., Williams, S. R. and Buikstra, J. E. (1990), "Comparison of methods for the removal of diagenetic material in buried bone", *Journal of Archaeological Science,* vol. 17, no. 4, pp. 453-468.

Latham, K. E. and Madonna, M. E. (2013), "DNA Survivability in Skeletal Remains", in Pokines, J. T. and Symes, S. A. (eds.) *Manual of Forensic Taphonomy,* CRC Press, London, pp. 403-426.

Lebon, M., Reiche, I., Bahain, J. -., Chadefaux, C., Moigne, A. -., Fröhlich, F., Sémah, F., Schwarcz, H. P. and Falguères, C. (2010), "New parameters for the characterization of diagenetic alterations and heat-induced changes of fossil bone mineral using Fourier transform infrared spectrometry", *Journal of Archaeological Science,* vol. 37, no. 9, pp. 2265-2276.

Leclair, B., Frégeau, C. and Bowen KL, F. R. (2004), "Systematic analysis of stutter percentages and allele peak height and peak area ratios at heterozygous STR loci for forensic casework and database samples", *Journal of Forensic Sciences,* vol. 49, no. 5, pp. 968-980.

Lee-Thorp, J. A. and van der Merwe, N. J. (1991), "Aspects of the chemistry of modern and fossil biological apatites", *Journal of Archaeological Science,* vol. 18, no. 3, pp. 343-354.

Lee-Thorp, J. and Sealy, J. (2008), "Beyond documenting diagenesis: The fifth international bone diagenesis workshop", *Palaeogeography, Palaeoclimatology, Palaeoecology,* vol. 266, no. 3–4, pp. 129-133.

Li, X. J. and Jee, W. S. S. (2005), "Chapter 2: Integrated bone tissue anatomy and physiology", in Deng, H. and Liu, Y. (eds.) *Current topics in bone biology.* World Scientific, , pp. 11-56.

Loe, L., Barker, C., Brady, K., Cox, M. and Webb, H. (2014), *'Remember Me to All': The archaeological recovery and identification of soldiers who fought and died in the battle of Fromelles 1916,* Oxford Archaeology Monograph, Oxford.

Lopes, V., Andrade, L., Carvalho, M., Serra, A., Balsa, F., Bento, A. M., Batista, L., Oliveira, C., Corte-Real, F. and Anjos, M. J. (2009), "Mini-STRs: A powerful tool to identify genetic profiles in samples with small amounts of DNA", *Forensic Science International: Genetics Supplement Series,* vol. 2, no. 1, pp. 121-122.

Loreille, O. M., Diegoli, T. M., Irwin, J. A., Coble, M. D. and Parsons, T. J. (2007), "High efficieny DNA extraction from bone by total demineralisation.", *Forensic Science International: Genetics,* vol. 1, pp. 191-195.

Lovley, D. R. and Coates, J. D. (1997), "Bioremediation of metal contamination", *Current opinion in biotechnology,* vol. 8, no. 3, pp. 285-289.

Lozano, L. F., Pena-Rico, M. A., Jang-Cho, H., Heredia, A., Villarreal, E., Ocotlan-Flores, J., Gomez-Cortes, A. L., Aranda-Manteca, F. J., Orozco, E. and Bucio, L. (2002), *Thermal properties of mineralized and non mineralized type I collagen in bone,* 724, Material Research Society Symposium Proceedings, Mexico.

Lyman, R. L. (2001), *Vertebrate Taphonomy,* Cambridge University Press, Cambridge.

Lyman, R. L. (2014), "Bone Density and Bone Attrition", in Pokines, J. T. and Symes, S. A. (eds.) *Manual of Forensic Taphonomy,* CRC Press, London, pp. 51-70.

Maeda, K., Murakami, C., Hara, M., Irie, W., Oishi, M., Sasaki, C., Nakamura, S., Takahashi, S., Takada, A. and Saito, K. (2013), "DNA identification of skeletal remains by using a new extraction kit", *Forensic Science International: Genetics Supplement Series,* vol. 4, no. 1, pp. e242-e243.

Mann, L. and Ashworth, D. (2006), *Crime-fighting successes of DNA*, available at: http://news.bbc.co.uk/1/hi/uk/5405470.stm (accessed 18/06/15).

Martín, P., Albarrán, C., García, P. and Alonso, A. (2006a), "Application of mini-STR loci to severely degraded casework samples

", *International Congress Series,* vol. 1288, pp. 522-525.

Martín, P., García, O., Albarrán, C., García, P. and Alonso, A. (2006b), "Application of mini-STR loci to severely degraded casework samples", *International Congress Series,* vol. 1288, no. 0, pp. 522-525.

Mays, S., Taylor, G. M., Legge, A. J., Young, D. B. and Turner-Walker, G. (2001), "Paleopathological and Biomolecular Study of Tuberculosis in a Medieval Skeletal Collection from England", *American Journal of Physical Anthropology,* vol. 114, pp. 298-311.

Mays, S. (2010), *The Archaeology of Human Bones,* 2nd Edition ed, Routledge, Oxon.

Mays, S., Elders, J., Humphrey, L., White, W. and Marshall, P., (2013), *Science and the Dead: A guidleine for the destructive sampling of archaeological human remains for scientific analysis.*, English Heritage, Swindon.

McCord, B., Opel, K., Funes, M., Zoppis, S. and Meadows Jantz, L. (2011), "An investigation of the effect of DNA degradation and inhibition on PCR amplification of single source and mixed forensic samples", *National Criminal Justice Reference Service,* vol. NCJ 236692.

Milos, A., Selmanovic, A., Smajlovic, L., Huel, R. L. M., Katzmarzyk, C., Rizvic, A. and Parsons, T. J. (2007), "Success rates of nuclear short tandem repeat typing from different skeletal elements", *Croatian Medical Journal,* vol. 45, pp. 489--493.

Moraitis, K., Eliopoulos, C. and Spiliopoulou, C. (2009), "Fracture characteristics of perimortem trauma in skeletal material", *Internet Journal of Biological Anthropology,* vol. 3, no. 2.

Moraitis, K. and Spiliopoulou, C. (2010), "Forensic implications of carnivore scavenging on human remains recovered from outdoor locations in Greece.", *Journal of forensic and legal medicine,* vol. 17, no. 6, pp. 298-303.

Mulligan, C. J. (2005), "Isolation and Analysis of DNA from Archaeological, Clinical, and Natural History Specimens", in *Methods in Enzymology,* Academic Press, , pp. 87-103.

Mundorff, A. (2009), *Human idenfication following the world trade center disaster: Assessing management practises for highly fragmented and commingled human remains.* (Ph.D. thesis), Simon Fraser University, Canada.

Murphy, K., Shiner, M. and Wilson, H. (2015), *Excavation at St Patrick's Chapel 2015 Interim Report,* 2015/35, Dyfed Archaeological Trust, Pembrokeshire.

Nakhaeizadeh, S., Dror, I. E. and Morgan, R. M. (2014), "Cognitive bias in forensic anthropology: Visual assessment of skeletal remains is susceptible to confirmation bias", *Science & Justice,* vol. 54, no. 3, pp. 208-214.

National Centre for Policing Excellence (2006), *Murder Investigation Manual,* , United Kingdom.

Nielsen-Marsh, C. M., Hedges, R. E. M., Mann, T. and Collins, M. J. (2000), "A preliminary investigation of the application of differential scanning calorimetry to the study of collagen degradation in archaeological bone", *Thermochimica Acta,* vol. 365, no. 1–2, pp. 129-139.

O'Connor, S., Ali, E., Al-Sabah, S., Anwar, D., Bergström, E., Brown, K. A., Buckberry, J., Buckley, S., Collins, M., Denton, J., Dorling, K. M., Dowle, A., Duffey, P., Edwards, H. G. M., Faria, E. C., Gardner, P., Gledhill, A., Heaton, K., Heron, C., Janaway, R., Keely, B. J., King, D., Masinton, A., Penkman, K., Petzold, A., Pickering, M. D., Rumsby, M., Schutkowski, H., Shackleton, K. A., Thomas, J., Thomas-Oates, J., Usai, M., Wilson, A. S. and O'Connor, T. (2011), "Exceptional preservation of a prehistoric human brain from Heslington, Yorkshire, UK", *Journal of Archaeological Science,* vol. 38, no. 7, pp. 1641-1654.

Oates, J. A. H. (1998), *Lime and Limestone: Chemistry and Technology, Production and Uses.* Wiley-VCH, Weinheim.

O'Brien, R. C., Forbes, S. L., Meyer, J. and Dadour, I. (2010), "Forensically significant scavenging guilds in the southwest of Western Australia.", *Forensic Science International,* vol. 198, no. 1-3, pp. 89-91.

Ozga, A. T., Tito, R. Y., Kemp, B. M., Matternes, H., Obregon-Tito, A., Neal, L. and Lewis Jr, C. M. (2016), "Origins of an unmarked Georgia cemetery using ancient DNA analysis.", *Human Biology,* vol. 87, no. 2, pp. 3.

Paabo, S., Poinar, H., Serre, D., Jaenicke-Despres, V., Hebler, J., Rohland, N., Kuch, M., Krause, J., Vigilant, L. and Hofreiter, M. (2004), "Genetic analyses from ancient DNA", *Annual Review of Genetics,* vol. 38, pp. 645-679.

Pääbo, S. (1985), "Molecular cloning of Ancient Egyptian mummy DNA", *Nature,* vol. 314, pp. 644-645.

Painter, T. J. (1991), "Lindow man, tollund man and other peat-bog bodies: The preservative and antimicrobial action of Sphagnan, a reactive glycuronoglycan with tanning and sequestering properties", *Carbohydrate Polymers,* vol. 15, no. 2, pp. 123-142.

Parkinson, R. A., Dias, K. -., Horswell, J., Greenwood, P., Banning, N., Tibbett, M. and Vass, A. A. (2009), "Microbial community analysis of human decomposition on soil", in Ritz, K., Dawson, L. and Miller, D. (eds.) *Criminal and Environmental Soil Forensics,* Springer, new York, pp. 379-394.

Parsons, T. J. and Weedn, V. W. (1997), "Preservation and recovery of DNA in post-mortem specimens and trace samples", in *The post-mortem fate of human remains,* CRC Press, , pp. 109-138.

Parsons, T. J., Huel, R., Davoren, J., Katzmarzyk, C., Miloš, A., Selmanović, A., Smajlović, L., Coble, M. D. and Rizvić, A. (2007), "Application of novel "mini-amplicon" STR multiplexes to high volume casework on degraded skeletal remains", *Forensic Science International: Genetics,* vol. 1, no. 2, pp. 175-179.

Pearce, A., Richards, R. G., Milz, S., Schneider, E. and Pearce, S. G. (2007), "Animal models for implant biomaterial research in bone: a review", *European Cells and Materials,* vol. 13, pp. 1-10.

Perry, W. L., Bass, W. M., Riggsby, W. S. and Sirotkin, K. (1988), "The autodegradation of Deoxyribonucleic Acid (DNA) in human rib bone and its relationship to the time interval since death", *Journal of Forensic Science,* vol. 33, no. 1, pp. 144-153.

Pilli, E., Fox, C. L., Capelli, C., Lari, M., Sampietro, L., Gigli, E., Milani, L., Guimaraes, S., Chiarelli, B., Marin, V. T. W., Casoli, A., Stanyon, R., Barbujani, G. and Caramelli, D. (2008), "Ancient DNA and forensics genetics: The case of Francesco Petrarca", *Forensic Science International: Genetics Supplement Series,* vol. 1, no. 1, pp. 469-470.

Pinhasi, R., Fernandes, D., Sirak, K., Novak, M., Connell, S., Alpaslan-Roodenberg, S., Gerritsen, F., Moiseyev, V., Gromov, A., Raczky, P., Anders, A., Pietrusewsky, M., Rollefson, G., Jovanovic, M., Trinhhoang, H., Bar-Oz, G., Oxenham, M., Matsumura, H. and Hofreiter, M. (2015), "Optimal Ancient DNA Yields from the Inner Ear Part of the Human Petrous Bone", *PloS one,* vol. 10, no. 6, pp. e0129102.

Pizzamiglio, M., Marino, A., Coli, A., Floris, T. and Garofano, L. (2006), "The use of mini-STRs on degraded DNA samples", *International Congress Series,* vol. 1288, no. 0, pp. 498-500.

Poinar, H. N., Höss, M., Bada, J. L. and Pääbo, S. (1996), "Amino Acid Racemization and the Preservation of Ancient DNA ", vol. 272, no. 5263, pp. 864-866.

Pokines, J. T. (2014a), "Collection of macroscopic osseous taphonomic data and the recognition of taphonomic suites of characteristics", in Pokines, J. T. and Symes, S. A. (eds.) *Manual of forensic taphonomy,* CRC Press, London, pp. 1--17.

Pokines, J. T. (2014b), "Faunal Dispersal, Reconcentration, and Gnawing Damage to Bone in Terrestrial Environments", in Pokines, J. T. and Symes, S. A. (eds.) *Manual of Forensic Taphonomy,* CRC Press, London, pp. 201-241.

Pokines, J. T. and Baker, J. E. (2014), "Effects of Burial Environment on Osseous Remains", in Pokines, J. T. and Symes, S. A. (eds.) *Manual of Forensic Taphonomy,* CRC Press, London, pp. 73-108.

Prado, V. F., Castro, A. K. F., Oliveira, C. L., Souza, K. T. and Pena, S. D. J. (1997), "Extraction of DNA from human skeletal remains: practical applications in forensic sciences", *Genetic Analysis: Biomolecular Engineering,* vol. 14, no. 2, pp. 41-44.

Pray, L. (2008), "Discovery of DNA structure and function: Watson and Crick", *Nature Education,* vol. 1, no. 1.

Price, T. D., Blitz, J., Burton, J. and Ezzo, J. A. (1992), "Diagenesis in prehistoric bone: Problems and solutions", *Journal of Archaeological Science,* vol. 19, no. 5, pp. 513-529.

Prinz, M., Carracedo, A., Mayr, W. R., Morling, N., Parsons, T. J., Sajantila, A., Scheithauer, R., Schmitter, H. and Schneider, P. M. (2007), "DNA Commission of the International Society for Forensic Genetics (ISFG): Recommendations regarding the role of forensic genetics for disaster victim identification (DVI)", *Forensic Science International: Genetics,* vol. 1, no. 1, pp. 3-12.

Rahtz, P. and Hurst, S. (1976), "Bordesley Abbey", *British Archaeological Reports,* vol. 23, no. British Series.

Reiche, I., Favre-Quattropani, L., Calligaro, T., Salomon, J., Bocherens, H., Charlet, L. and Menu, M. (1999), "Trace element composition of archaeological bones and post-mortem alteration in the burial environment", *Nuclear Instruments and Methods in Physics Research Section B: Beam Interactions with Materials and Atoms,* vol. 150, no. 1–4, pp. 656-662.

Rho, J., Kuhn-Spearing, L. and Zioupos, P. (1998), "Mechanical properties and the hierarchical structure of bone", *Medical engineering & physics,* vol. 20, no. 2, pp. 92-102.

Ricaut, F., Keyser-Tracqui, C., Crubézy, E. and Ludes, B. (2005), "STR-genotyping from human medieval tooth and bone samples", *Forensic science international,* vol. 151, no. 1, pp. 31-35.

Richards, M. B., Sykes, B. C. and Hedges, R. E. M. (1995), "Authenticating DNA extracted from ancient skeletal remains", *Journal of Archaeological Science,* vol. 22, pp. 291-299.

Rohland, N. and Hofreiter, M. (2007), "Ancient DNA extraction from bones and teeth", *Nature Protocols,* vol. 2, no. 7, pp. 1756-1762.

Rolsandic, M. (2002), "Position of skeletal remains as a key to understanding mortuary behaviour", in Haglund, W. D. and Sorg, M. H. (eds.) *Advances in forensic taphonomy: Method, theory and archaeological perspectives,* CRC Press, , pp. 99-117.

Ross, A. H. and Cunningham, S. L. (2011), "Time-since-death and bone weathering in a tropical environment", *Forensic Science International,* vol. 204, no. 1–3, pp. 126-133.

Salo, W. L., Aufderheide, A., C., Buikstra, J. and Holcomb, T. A. (1994), "Identification of Mycobacterium tuberculosis DNA in a pre-Columbian Peruvian mummy", *Proceedings of the National Academy of Sciences USA,* vol. 91, no. Microbiology, pp. 2091-2094.

Santana, J., Fregel, R., Lightfoot, E., Morales, J., Alamón, M., Guillén, J., Moreno, M. and Rodríguez, A. (2016), "The early colonial atlantic world: New insights on the African Diaspora from isotopic and ancient DNA analyses of a multiethnic 15th-17th century burial population from the Canary Islands, Spain. ", *American Journal of Physical Anthropology,* vol. 159, no. 2, pp. 300-312.

Schiffer, M. B. (1983), "Toward the identification of formation processes", *American Antiquity,* vol. 48, no. 4, pp. 675-706.

Schotsmans, E. M. J., Denton, J., Dekeirsschieter, J., Ivaneanu, T., Leentjes, S., Janaway, R. C. and Wilson, A. S. (2012), "Effects of hydrated lime and quicklime on the decay of buried human remains using pig cadavers as human body analogues", *Forensic Science International,* vol. 217, no. 1–3, pp. 50-59.

Schotsmans, E. M. J., Fletcher, J. N., Denton, J., Janaway, R. C. and Wilson, A. S. (2014), "Long-term effects of hydrated lime and quicklime on the decay of human remains using pig cadavers as human body analogues: Field experiments", *Forensic Science International,* vol. 238, no. 0, pp. 141.e1-141.e13.

Schotsmans, E. M. J., Van de Voorde, W., De Winne, J. and Wilson, A. S. (2011), "The impact of shallow burial on differential decomposition to the body: A temperate case study", *Forensic Science International,* vol. 206, no. 1–3, pp. e43-e48.

Seidenberg, V., Schilz, F., Pfister, D., Georges, L., Fehren-Schmitz, L. and Hummel, S. (2012), "A new miniSTR heptaplex system for genetic fingerprinting of ancient DNA from archaeological human bone", *Journal of Archaeological Science,* vol. 39, no. 10, pp. 3224-3229.

Senge, T., Madea, B., Junge, A., Rothschild, M. A. and Schneider, P. M. (2011), "STRs, mini STRs and SNPs – A comparative study for typing degraded DNA", *Legal medicine,* vol. 13, no. 2, pp. 68-74.

Shackley, M. S. (2010), *X-ray fluorescence spectrometry (XRF) in geoarchaeology,* Springer, London.

Sharifzadeh, S., Clemmensen, L. H., Borggaard, C., Støier, S. and Ersbøll, B. K. (2014), "Supervised feature selection for linear and non-linear regression of L*a*b* color from multispectral images of meat", *Engineering Applications of Artificial Intelligence,* vol. 27, pp. 211-227.

Shemesh, A. (1990), "Crystallinity and diagenesis of sedimentary apatites", *Geochimica et Cosmochimica Acta,* vol. 54, no. 9, pp. 2433-2438.

Shipman, P., Foster, G. and Schoeninger, M. (1984), "Burnt bones and teeth: an experimental study of color, morphology, crystal structure and shrinkage", *Journal of Archaeological Science,* vol. 11, no. 4, pp. 307-325.

Simón, M., González-Ruiz, M., Prats-Muñoz, G. and Malgosa, A. (2012), "Comparison of two DNA extraction methods in a Spanish Bronze Age burial cave", *Quaternary International,* vol. 247, no. 0, pp. 358-362.

Sosa, C., Vispe, E., Núñez, C., Baeta, M., Casalod, Y., Bolea, M., Hedges, R. E. M. and Martinez-Jarreta, B. (2013), "Association between ancient bone preservation and dna yield: A multidisciplinary approach", *American Journal of Physical Anthropology,* vol. 151, no. 1, pp. 102-109.

Sprecher, C. J., McLaren, R. S., Rabbach, D. R., Ensenberger, M. G., Fulmer, P. M., Krenke, B. E., Corona, C., Scurria, M. A., Good, T. D., Dwight, S. J., McDougall, M. G. and Storts, D. R. (2009)*, The PowerPlex® ESX and ESI Systems: Meeting the New European Standard*, available at: http://www.promega.co.uk/resources/profiles-in-dna/2009/the-powerplex-esx-and-esi-systems-meeting-the-new-european-standard/ (accessed 06/06/2015).

Squires, K. E., Thompson, T. J. U., Islam, M. and Chamberlain, A. (2011), "The application of histomorphometry and Fourier Transform Infrared Spectroscopy to the analysis of early Anglo-Saxon burned bone", *Journal of Archaeological Science,* vol. 38, no. 9, pp. 2399-2409.

Staiti, N., Di Luise, E., Ciuna, I., Piscitello, D., Quadrana, F. and Romano, C. (2008), "Old cadaver identification from severely spoiled bones: Analytical approach to degraded DNA", *Forensic Science International: Genetics Supplement Series,* vol. 1, no. 1, pp. 444-445.

Stathopoulou, E. T., Psycharis, V., Chryssikos, G. D., Gionis, V. and Theodorou, G. (2008), "Bone diagenesis: New data from infrared spectroscopy and X-ray diffraction", *Palaeogeography, Palaeoclimatology, Palaeoecology,* vol. 266, no. 3–4, pp. 168-174.

Stevenson, A. (ed.) (2010), *Oxford Dictionary of English,* Third Edition ed, Oxford University Press, Oxford.

Stiner, M. C., Kuhn, S. L., Weiner, S. and Bar-Yosef, O. (1995), "Differential Burning, Recrystallization, and Fragmentation of Archaeological Bone", *Journal of Archaeological Science,* vol. 22, no. 2, pp. 223-237.

Stokes, K. L., Forbes, S. L., Benninger, L. A., Carter, D. O. and Tibbett, M. (2009), "Decomposition studies using animal models in contrasting environments: Evidence from temporal changes in soil chemistry and microbial activity.", in Ritz, K., Dawson, L. and Miller, D. (eds.) *Criminal and Environmental Soil Forensics,* Springer, New York, pp. 357--378.

Stokes, K. L., Forbes, S. L. and Tibbett, M. (2013), "Human Versus Animal: Contrasting Decomposition Dynamics of Mammalian Analogues in Experimental Taphonomy", *Journal of Forensic Sciences,* vol. 58, no. 3, pp. 583-591.

Surovell, T. A. and Stiner, M. C. (2001), "Standardizing Infra-red Measures of Bone Mineral Crystallinity: an Experimental Approach", *Journal of Archaeological Science,* vol. 28, no. 6, pp. 633-642.

Sweet, D. and Sweet, C. (1994), "DNA Analysis of Dental Pulp to Link Incinerated Remains of Homicide Victim to Crime Scene", *Journal of Forensic Sciences,* vol. 40, no. 2, pp. 310-314.

Tan, K. H. (2005), *Soil sampling, preparation and analysis,* 2nd ed, CRC, New York.

Tattoli, L., Tsokos, M., Sautter, J., Anagnostopoulos, J., Maselli, E., Ingravallo, G., Delia, M. and Solarino, B. (2014), "Postmortem bone marrow analysis in forensic science: Study of 73 cases and review of the literature", *Forensic Science International,* vol. 234, pp. 72-78.

Thompson, T. J. U., Islam, M., Piduru, K. and Marcel, A. (2011), "An investigation into the internal and external variables acting on crystallinity index using Fourier Transform Infrared Spectroscopy on unaltered and burned bone", *Palaeogeography, Palaeoclimatology, Palaeoecology,* vol. 299, no. 1–2, pp. 168-174.

Thurlow, E. (1913), *The Archaeology of the Anglo-Saxon Settlements,* Clarendon Press, Oxford.

Tibbett, M. and Carter, D. O. (2009), "Research in forensic taphonomy: A soil-based perspective", in Ritz, K., Dawson, L. and Miller, D. (eds.) *Criminal and Environmental Soil Forensics,* Springer, New York, pp. 317-331.

Trueman, C. N., Privat, K. and Field, J. (2008), "Why do crystallinity values fail to predict the extent of diagenetic alteration of bone mineral?", *Palaeogeography, Palaeoclimatology, Palaeoecology,* vol. 266, no. 3–4, pp. 160-167.

Tuller, H. and Đurić', M. (2006), "Keeping the pieces together: Comparison of mass grave excavation methodology", *Forensic Science International,* vol. 156, no. 2–3, pp. 192-200.

Turner-Walker, G. (2007), "The Chemical and Microbial Degradation of Bones and Teeth", in Pinhasi, R. and Mays, S. (eds.) ***Advances in Human Palaeopathology,*** Wiley, England, pp. 11--14.

Turner-Walker, G. and Peacock, E. E. (2008), "Preliminary results of bone diagenesis in Scandinavian bogs", *Palaeogeography, Palaeoclimatology, Palaeoecology,* vol. 266, no. 3–4, pp. 151-159.

Tvedebrink, T., Eriksen, P. S., Mogensen, H. S. and Morling, N. (2009), "Estimating the probability of allelic drop-out of STR alleles in forensic genetics", *Forensic Science International: Genetics,* vol. 3, no. 4, pp. 222-226.

Tvedebrink, T., Eriksen, P. S., Mogensen, H. S. and Morling, N. (2012), "Statistical model for degraded DNA samples and adjusted probabilities for allelic drop-out", *Forensic Science International: Genetics,* vol. 6, no. 1, pp. 97-101.

Ubelaker, D. H. (2009), "The forensic evaluation of burned skeletal remains: A synthesis", *Forensic science international,* vol. 183, no. 1–3, pp. 1-5.

Viscarra Rossel, R. A., Cattle, S. R., Ortega, A. and Fouad, Y. (2009), "In situ measurements of soil colour, mineral composition and clay content by vis–NIR spectroscopy", *Geoderma,* vol. 150, no. 3–4, pp. 253-266.

von Wurmb-Schwark, N., Harbeck, M., Wiesbrock, U., Schroeder, I., Ritz-Timme, S. and Oehmichen, M. (2003), "Extraction and amplification of nuclear and mitochondrial DNA from ancient and artificially aged bones", *Legal medicine,* vol. 5, Supplement, no. 0, pp. S169-S172.

von Wurmb-Schwark, N., Heinrich, A., Freudenberg, M., Gebühr, M. and Schwark, T. (2008), "The impact of DNA contamination of bone samples in forensic case analysis and anthropological research", *Legal medicine,* vol. 10, no. 3, pp. 125-130.

Waddington, C., Beswick, P., Brightman, J., Mapplethorpe, K., Marshall, P., Meadows, J., Thornton, A. and Longstone Local History Group. (2011), *Fin Cop Excavation Archive Report for 2010,* 2011/27, Archaeological Research Services Ltd.

Waddington, C. (2014), *Rescued from the sea: An Archaeologist's Tale,* Archaeological Research Services Ltd, Derbyshire.

Walker, P. L., Miller, K. W. P. and Richman, R. (2008), "7 - Time, Temperature, and Oxygen Availability: An Experimental Study of the Effects of Environmental Conditions on the Color and Organic Content of Cremated Bone", in Schmidt, C. W. and Symes, S. A. (eds.) *The Analysis of Burned Human Remains,* Academic Press, San Diego, pp. 129-xi.

Weiner, S. and Bar-Yosef, O. (1990), "States of preservation of bones from prehistoric sites in the Near East: A survey", *Journal of Archaeological Science,* vol. 17, no. 2, pp. 187-196.

Weitzel, M. (2005), "A Report of Decomposition Rates of a Special Burial Type in Edmonton, Alberta from an Experimental Field Study", *Journal of Forensic Sciences,* vol. 50, no. 3, pp. 1-7.

Welch, L. A., Gill, P., Phillips, C., Ansell, R., Morling, N., Parson, W., Palo, J. U. and Bastisch, I. (2012), "European Network of Forensic Science Institutes (ENFSI): Evaluation of new commercial STR multiplexes that include the European Standard Set (ESS) of markers", *Forensic Science International: Genetics,* vol. 6, no. 6, pp. 819-826.

Williams, A. (2002), "Greybalance: a key element in colour reproduction", *The International Journal of Newspaper Technology,* .

Williams, H. (1998), "Monuments and the past in early Anglo-Saxon England ", *World Archaeology,* vol. 30, no. 1, pp. 90--108.

Williams, D., Lewis, M., Franzen, T., Lissett, V., Adams, C., Whittaker, D., Tysoe, C. and Butler, R. (2004), "Sex determination by PCR analysis of DNA extracted from incinerated, deciduous teeth", *Science & Justice,* vol. 44, no. 2, pp. 89-94.

Wilson, C. A., Gies, P. H., Niven, B. E., Mclennan, A. and Bevin, N. K. (2008), "The relationship between UV transmittance and colour - Visual description and instrumental measurement", *Textile research journal,* vol. 78, pp. 128--137.

Wilson, A. S., Janaway, R. C., Holland, A. D., Dodson, H. I., Baran, E., Pollard, A. M. and Tobin, D. J. (2007), "Modelling the buried human body environment in upland climes using three contrasting field sites", *Forensic science international,* vol. 169, no. 1, pp. 6-18.

Woodward, S. R., Weyand, N. J. and Bunnell, M. (1994), "DNA sequence from Cretaceous period bone fragments.", *Science,* vol. 266, no. 5188, pp. 1229-1232.

Wright, L. E. and Schwarcz, H. P. (1996), "Infrared and Isotopic Evidence for Diagenesis of Bone Apatite at Dos Pilas, Guatemala: Palaeodietary Implications", *Journal of Archaeological Science,* vol. 23, no. 6, pp. 933-944.

Zehner, R. (2007), ""Foreign" DNA in tissue adherent to compact bone from tsunami victims", *Forensic Science International: Genetics,* vol. 1, no. 2, pp. 218-222.

Zoledziewska, M. and Dobosz, T. (2003), "Gender determination in highly degraded DNA samples", *International Congress Series,* vol. 1239, no. 0, pp. 593-595.

APPENDICES

Appendix A : Human Analogue Data

Table A-1: Colour analysis of control soil samples

		Aggregate average					Aggregate average		
	Readings	L*	a*	b*		Readings	L*	a*	b*
Clay 1	1-10	40.63	2.94	4.55	Clay 2	1-10	43.56	2.53	4.16
	11-20	40.82	3.71	6.21		11-20	44.26	3.41	5.49
	21-30	42.50	3.82	6.42		21-30	42.83	3.70	6.22
	31-40	42.64	3.79	6.36		31-40	40.57	2.82	4.35
	Mean	41.65	3.57	5.89		Mean:	42.81	3.12	5.06
	St. Dev:	1.07	0.42	0.89		St. Dev:	1.60	0.53	0.97
Compost 1	1-10	35.06	1.51	1.43	Compost 2	1-10	35.62	1.46	1.38
	11-20	34.09	1.98	1.77		11-20	36.22	0.87	0.49
	21-30	34.46	0.08	0.47		21-30	34.52	1.91	1.64
	31-40	34.55	1.92	1.66		31-40	35.09	1.49	1.46
	Mean:	34.54	1.37	1.33		Mean:	35.36	1.43	1.24
	St. Dev:	0.40	0.89	0.59		St. Dev:	0.73	0.43	0.51
Lime 1	1-10	93.57	0.51	3.74	Lime 2	1-10	93.14	0.55	3.89
	11-20	94.58	0.46	3.51		11-20	93.57	0.51	3.74
	21-30	94.88	0.42	3.38		21-30	94.58	0.46	3.51
	31-40	95.11	0.38	2.96		31-40	94.88	0.42	3.38
	Mean:	94.54	0.44	3.40		Mean:	94.04	0.49	3.63
	St. Dev:	0.68	0.06	0.33		St. Dev:	0.82	0.06	0.23
Sand 1	1-10	62.84	4.65	19.73	Sand 2	1-10	61.42	4.99	20.34
	11-20	62.78	4.61	19.54		11-20	62.28	4.83	19.89
	21-30	62.47	4.60	19.56		21-30	62.90	4.67	19.48
	31-40	61.98	4.50	19.58		31-40	63.75	4.31	19.04
	Mean:	62.52	4.59	19.60		Mean:	62.59	4.70	19.69
	St. Dev:	0.39	0.06	0.09		St Dev:	0.98	0.29	0.56

Table A-2: Data from soil analysis of clay control soils and experimental soils. All mass measurements are presented in grams.

Sample information			Wet weight			Dry weight	Water content			Ash weight		Organic content		pH
Type	Duration	Sample.	Pot	Soil	Pot & soil	Pot & Soil	Soil solids	Pore water	%	Pot & soil	Ash mass	Organic matter	%	
Clay	0 months	a	8.00	5.00	13.00	11.77	3.83	1.23	24.60	11.68	3.68	0.15	3.92	9.63
Clay	0 months	b	8.31	5.00	13.31	12.05	3.81	1.26	25.20	11.97	3.66	0.15	3.94	9.62
Clay	1.5 months	a (1)	8.26	3.00	11.26	10.30	2.04	0.96	32.00	10.23	1.97	0.07	3.43	8.32
Clay	1.5 months	a (2)	8.32	3.00	11.32	10.23	1.91	1.09	36.33	10.18	1.86	0.05	2.62	8.42
Clay	1.5 months	a (3)	8.46	3.00	11.46	10.40	1.94	1.06	35.33	10.34	1.88	0.06	3.09	8.37
Clay	1.5 months	b (1)	7.99	3.00	10.99	9.86	1.87	1.13	37.67	9.80	1.81	0.06	3.21	8.43
Clay	1.5 months	b (2)	8.34	3.00	11.34	10.46	2.12	0.88	29.33	10.38	2.04	0.08	3.77	8.32
Clay	1.5 months	b (3)	8.29	3.00	11.29	10.27	1.98	1.02	34.00	10.22	1.93	0.05	2.53	8.47
Clay	3 months	a (1)	8.49	5.00	13.49	11.95	3.46	1.54	30.80	11.85	3.36	0.10	2.89	8.46
Clay	3 months	a (2)	8.32	3.00	11.32	10.43	2.11	0.89	29.67	10.37	2.05	0.06	2.84	8.53
Clay	3 months	a (3)	8.49	3.00	11.49	10.64	2.15	0.85	28.33	10.58	2.09	0.06	2.79	8.58
Clay	3 months	b (1)	8.52	3.00	11.52	10.46	1.94	1.06	35.33	10.41	1.89	0.05	2.58	8.44
Clay	3 months	b (2)	8.01	3.00	11.01	10.16	2.15	0.85	28.33	10.11	2.10	0.05	2.33	8.26
Clay	3 months	b (3)	8.32	3.00	11.32	10.49	2.17	0.83	27.67	10.43	2.11	0.06	2.76	8.29
Clay	6 months	a (1)	8.23	5.00	13.23	11.35	3.12	1.88	37.60	11.13	2.90	0.22	7.05	7.43
Clay	6 months	a (2)	7.96	3.00	10.96	9.82	1.86	1.14	38.00	9.77	1.81	0.05	2.69	7.75
Clay	6 months	a (3)	8.06	3.00	11.06	10.15	2.09	0.91	30.33	10.08	2.02	0.07	3.35	7.77
Clay	6 months	b (1)	8.36	3.00	11.36	10.23	1.87	1.13	37.67	10.18	1.82	0.05	2.67	8.53
Clay	6 months	b (2)	8.30	3.00	11.30	10.38	2.08	0.92	30.67	10.32	2.02	0.06	2.88	8.30
Clay	6 months	b (3)	8.01	3.00	11.01	10.10	2.09	0.91	30.33	10.04	2.03	0.06	2.87	8.29
Clay	12 months	a (1)	8.22	3.00	11.22	10.13	1.91	1.09	36.33	10.06	1.84	0.07	3.66	8.44
Clay	12 months	a (2)	8.18	3.00	11.18	10.03	1.85	1.15	38.33	9.96	1.78	0.07	3.78	8.42
Clay	12 months	a (3)	8.32	3.00	11.32	10.30	1.98	1.02	34.00	10.22	1.90	0.08	4.04	8.39
Clay	12 months	b (1)	8.17	3.00	11.17	10.18	2.01	0.99	33.00	10.12	1.95	0.06	2.99	8.60
Clay	12 months	b (2)	8.34	3.00	11.34	10.33	1.99	1.01	33.67	10.27	1.93	0.06	3.02	8.88
Clay	12 months	b (3)	8.35	3.00	11.35	10.31	1.96	1.04	34.67	10.23	1.88	0.08	4.08	8.51
Clay	18 months	a (1)	8.05	5.00	13.05	11.49	3.44	1.56	31.20	11.47	3.42	0.02	0.58	7.12
Clay	18 months	a (2)	8.46	3.00	11.46	10.55	2.09	0.91	30.33	10.51	2.05	0.04	1.91	7.02
Clay	18 months	a (3)	8.32	3.00	11.32	10.48	2.16	0.84	28.00	10.42	2.10	0.06	2.78	7.08
Clay	18 months	b (1)	8.30	5.00	13.30	11.69	3.39	1.61	32.20	11.60	3.30	0.09	2.65	7.33
Clay	18 months	b (2)	8.33	3.00	11.33	10.49	2.16	0.84	28.00	10.44	2.11	0.05	2.31	7.17
Clay	18 months	b (3)	8.54	3.00	11.54	10.73	2.19	0.81	27.00	10.68	2.14	0.05	2.28	7.13

Table A-3: Data from soil analysis of compost control soils and experimental soils. All mass measurements are presented in grams.

Sample information			Wet weight			Dry weight	Water content			Ash weight		Organic content		pH
Type	Duration	Sample.	Pot	Soil	Pot & soil	Pot & Soil	Soil solids	Pore water	%	Pot & soil	Ash mass	Organic matter	%	
Compost	0 months	a	8.22	2.00	10.23	8.93	0.73	1.30	65.00	8.27	0.05	0.68	93.15	6.27
Compost	0 months	b	8.22	2.00	10.21	8.90	0.71	1.31	65.50	8.26	0.04	0.67	94.37	6.22
Compost	1.5 months	a (1)	8.18	1.00	9.18	8.54	0.36	0.64	64.00	8.18	0.00	0.36	100.00	8.01
Compost	1.5 months	a (2)	8.01	1.00	11.01	8.46	0.45	0.55	55.00	8.03	0.02	0.43	95.56	8.09
Compost	1.5 months	a (3)	8.24	1.00	11.24	8.56	0.32	0.68	68.00	8.25	0.01	0.31	96.88	8.13
Compost	1.5 months	b (1)	8.05	1.00	11.05	8.42	0.37	0.63	63.00	8.06	0.01	0.36	97.30	8.56
Compost	1.5 months	b (2)	8.48	1.00	11.48	8.80	0.32	0.68	68.00	8.49	0.01	0.31	96.88	8.67
Compost	1.5 months	b (3)	7.83	1.00	10.83	8.16	0.33	0.67	67.00	7.84	0.01	0.32	96.97	8.63
Compost	3 months	a (1)	8.34	1.00	9.34	8.72	0.38	0.62	62.00	8.35	0.01	0.37	97.37	8.00
Compost	3 months	a (2)	7.86	1.00	8.86	8.23	0.37	0.63	63.00	7.91	0.05	0.32	86.49	8.05
Compost	3 months	a (3)	8.20	1.00	9.20	8.67	0.47	0.53	53.00	8.26	0.06	0.41	87.23	8.10
Compost	3 months	b (1)	8.50	1.00	9.50	8.90	0.40	0.60	60.00	8.53	0.03	0.37	92.50	7.66
Compost	3 months	b (2)	8.48	1.00	9.48	8.81	0.33	0.67	67.00	8.49	0.01	0.32	96.97	7.72
Compost	3 months	b (3)	7.83	1.00	8.83	8.20	0.37	0.63	63.00	7.85	0.02	0.35	94.59	7.74
Compost	6 months	a (1)	8.35	1.00	9.35	8.69	0.34	0.66	66.00	8.35	0.00	0.34	100.00	7.64
Compost	6 months	a (2)	8.46	1.00	9.46	8.89	0.43	0.57	57.00	8.47	0.01	0.42	97.67	7.89
Compost	6 months	a (3)	8.23	1.00	9.23	8.67	0.44	0.56	56.00	8.23	0.00	0.44	100.00	7.72
Compost	6 months	b (1)	8.01	1.00	9.01	8.43	0.42	0.58	58.00	8.02	0.01	0.41	97.62	8.20
Compost	6 months	b (2)	8.24	1.00	9.24	8.56	0.32	0.68	68.00	8.26	0.02	0.30	93.75	7.73
Compost	6 months	b (3)	7.99	1.00	8.99	8.35	0.36	0.64	64.00	8.00	0.01	0.35	97.22	7.70
Compost	12 months	a (1)	7.92	1.00	8.92	8.29	0.37	0.63	63.00	7.92	0.00	0.37	100.00	8.33
Compost	12 months	a (2)	8.39	1.00	9.39	8.72	0.33	0.67	67.00	8.41	0.02	0.31	93.94	8.32
Compost	12 months	a (3)	8.22	1.00	9.22	8.55	0.33	0.67	67.00	8.30	0.08	0.25	75.76	8.32
Compost	12 months	b (1)	8.46	1.00	9.46	8.78	0.32	0.68	68.00	8.46	0.00	0.32	100.00	8.70
Compost	12 months	b (2)	8.33	1.00	9.33	8.63	0.30	0.70	70.00	8.33	0.00	0.30	100.00	8.68
Compost	12 months	b (3)	8.40	1.00	9.40	8.73	0.33	0.67	67.00	8.40	0.00	0.33	100.00	8.64
Compost	18 months	a (1)	7.92	1.00	8.92	8.17	0.25	0.75	75.00	7.93	0.01	0.24	96.00	7.41
Compost	18 months	a (2)	8.22	1.00	9.22	8.56	0.34	0.66	66.00	8.24	0.02	0.32	94.12	7.35
Compost	18 months	a (3)	8.28	1.00	9.28	8.54	0.26	0.74	74.00	8.30	0.02	0.24	92.31	7.30
Compost	18 months	b (1)	8.58	1.00	9.58	8.82	0.24	0.76	76.00	8.58	0.00	0.24	100.00	7.29
Compost	18 months	b (2)	8.38	1.00	9.38	8.64	0.26	0.74	74.00	8.40	0.02	0.24	92.31	7.52
Compost	18 months	b (3)	8.40	1.00	9.40	8.63	0.23	0.77	77.00	8.43	0.03	0.20	86.96	7.49

Table A-4: Data from soil analysis of lime control soils and experimental soils. All mass measurements are presented in grams

Sample information			Wet weight			Dry weight	Water content			Ash weight		Organic content		pH
Type	Duration	Sample.	Pot	Soil	Pot & soil	Pot & Soil	Soil solids	Pore water	%	Pot & soil	Ash mass	Organic matter	%	
Lime	0 months	a	8.15	2.00	10.15	10.15	2.00	0.00	0.00	9.99	1.84	0.16	8.00	13.05
Lime	0 months	b	8.34	2.00	10.34	10.34	2.00	0.00	0.00	10.14	1.80	0.20	10.00	8.52
Lime	1.5 months	a (1)	8.43	1.00	9.43	9.34	0.91	0.09	9.00	9.30	0.87	0.04	4.40	12.67
Lime	1.5 months	a (2)	8.40	1.00	9.40	9.34	0.94	0.06	6.00	9.28	0.88	0.06	6.38	12.63
Lime	1.5 months	a (3)	8.34	0.50	8.84	8.79	0.45	0.05	10.00	8.79	0.45	0.00	0.00	12.77
Lime	1.5 months	b (1)	8.50	1.00	9.50	9.29	0.79	0.21	21.00	9.29	0.79	0.00	0.00	12.73
Lime	1.5 months	b (2)	7.79	0.50	8.29	8.26	0.47	0.03	6.00	8.26	0.47	0.00	0.00	12.89
Lime	1.5 months	b (3)	8.39	1.00	9.39	9.32	0.93	0.07	7.00	9.27	0.88	0.05	5.38	12.94
Lime	3 months	a (1)	8.16	1.00	9.16	9.08	0.92	0.08	8.00	9.08	0.92	0.00	0.00	12.70
Lime	3 months	a (2)	8.15	0.50	8.65	8.62	0.47	0.03	6.00	8.60	0.45	0.02	4.26	12.68
Lime	3 months	a (3)	8.19	0.50	8.69	8.67	0.48	0.02	4.00	8.65	0.46	0.02	4.17	12.64
Lime	3 months	b (1)	7.98	1.00	8.98	8.86	0.88	0.12	12.00	8.84	0.86	0.02	2.27	12.71
Lime	3 months	b (2)	8.15	0.50	8.66	8.65	0.50	0.00	0.00	8.63	0.48	0.02	4.00	12.69
Lime	3 months	b (3)	8.23	0.50	8.73	8.61	0.38	0.12	24.00	8.59	0.36	0.02	5.26	12.65
Lime	6 months	a (1)	8.07	1.00	9.07	8.75	0.68	0.32	32.00	8.75	0.68	0.00	0.00	12.77
Lime	6 months	a (2)	7.89	0.50	8.39	8.36	0.47	0.03	6.00	8.33	0.44	0.03	6.38	12.94
Lime	6 months	a (3)	8.24	0.50	8.74	8.70	0.46	0.04	8.00	8.68	0.44	0.02	4.35	12.99
Lime	6 months	b (1)	8.44	1.00	9.44	9.29	0.85	0.15	15.00	9.29	0.85	0.00	0.00	12.71
Lime	6 months	b (2)	8.03	0.50	8.53	8.50	0.47	0.03	6.00	8.46	0.43	0.04	8.51	13.00
Lime	6 months	b (3)	7.83	0.50	8.33	8.29	0.46	0.04	8.00	8.24	0.41	0.05	10.87	12.93
Lime	12 months	a (1)	8.19	1.00	9.19	9.10	0.91	0.09	9.00	9.09	0.90	0.01	1.10	12.71
Lime	12 months	a (2)	8.39	1.00	9.39	9.28	0.89	0.11	11.00	9.28	0.89	0.00	0.00	12.73
Lime	12 months	a (3)	8.16	1.00	9.16	9.05	0.89	0.11	11.00	9.05	0.89	0.00	0.00	12.74
Lime	12 months	b (1)	8.55	1.00	9.55	9.47	0.92	0.08	8.00	9.47	0.92	0.00	0.00	12.75
Lime	12 months	b (2)	8.44	1.00	9.46	9.37	0.93	0.07	7.00	9.37	0.93	0.00	0.00	12.61
Lime	12 months	b (3)	8.01	1.00	9.01	8.94	0.93	0.07	7.00	8.94	0.93	0.00	0.00	12.77
Lime	18 months	a (1)	7.99	1.00	8.99	8.98	0.99	0.01	1.00	8.95	0.96	0.03	3.03	12.69
Lime	18 months	a (2)	8.15	1.00	9.15	9.13	0.98	0.02	2.00	9.07	0.92	0.06	6.12	12.73
Lime	18 months	a (3)	8.02	1.00	9.02	8.99	0.97	0.03	3.00	8.95	0.93	0.04	4.12	12.76
Lime	18 months	b (1)	8.21	1.00	9.21	9.18	0.97	0.03	3.00	9.17	0.96	0.01	1.03	12.76
Lime	18 months	b (2)	8.24	1.00	9.24	9.21	0.97	0.03	3.00	9.19	0.95	0.02	2.06	12.68
Lime	18 months	b (3)	8.39	1.00	9.39	9.37	0.98	0.02	2.00	9.34	0.95	0.03	3.06	12.76

Table A-5: Data from soil analysis of sand control soils and experimental soils. All mass measurements are presented in grams

Sample information			Wet weight			Dry weight	Water content			Ash weight		Organic content		pH
Type	Duration	Sample.	Pot	Soil	Pot & soil	Pot & Soil	Soil solids	Pore water	%	Pot & soil	Ash mass	Organic matter	%	
Sand	0 months	a	8.41	5.00	13.40	13.39	4.98	0.01	0.20	13.36	4.95	0.03	0.60	8.52
Sand	0 months	b	8.24	5.00	13.24	13.23	4.99	0.01	0.20	13.20	4.96	0.03	0.60	8.43
Sand	1.5 months	a (1)	8.06	4.00	12.06	11.90	3.84	0.16	4.00	11.82	3.76	0.08	2.08	8.10
Sand	1.5 months	a (2)	8.16	2.00	10.16	10.12	1.96	0.04	2.00	10.12	1.96	0.00	0.00	8.27
Sand	1.5 months	a (3)	8.03	2.00	10.03	9.98	1.95	0.05	2.50	9.98	1.95	0.00	0.00	8.25
Sand	1.5 months	b (1)	7.81	4.00	11.81	11.67	3.86	0.14	3.50	11.63	3.82	0.04	1.04	8.14
Sand	1.5 months	b (2)	7.89	1.00	8.89	8.86	0.97	0.03	3.00	8.85	0.96	0.01	1.03	8.29
Sand	1.5 months	b (3)	8.22	1.00	9.22	9.17	0.95	0.05	5.00	9.17	0.95	0.00	0.00	8.26
Sand	3 months	a (1)	8.36	4.00	12.36	11.65	3.29	0.71	17.75	11.46	3.10	0.19	5.78	7.59
Sand	3 months	a (2)	8.31	2.00	10.31	9.96	1.65	0.35	17.50	9.92	1.61	0.04	2.42	7.57
Sand	3 months	a (3)	7.94	2.00	9.94	9.69	1.75	0.25	12.50	9.66	1.72	0.03	1.71	7.55
Sand	3 months	b (1)	8.26	4.00	12.24	11.87	3.61	0.39	9.75	11.71	3.45	0.16	4.43	7.61
Sand	3 months	b (2)	8.43	2.00	10.43	10.14	1.71	0.29	14.50	10.09	1.66	0.05	2.92	7.47
Sand	3 months	b (3)	7.94	2.00	9.94	9.66	1.72	0.28	14.00	9.59	1.65	0.07	4.07	7.43
Sand	6 months	a (1)	7.81	4.00	11.81	11.57	3.76	0.24	6.00	11.56	3.75	0.01	0.27	8.70
Sand	6 months	a (2)	8.21	2.00	10.21	10.13	1.92	0.08	4.00	10.12	1.91	0.01	0.52	8.41
Sand	6 months	a (3)	8.39	2.00	10.39	10.30	1.91	0.09	4.50	10.30	1.91	0.00	0.00	8.50
Sand	6 months	b (1)	8.47	4.00	12.47	12.11	3.64	0.36	9.00	12.07	3.60	0.04	1.10	8.42
Sand	6 months	b (2)	8.00	2.00	10.00	9.91	1.91	0.09	4.50	9.89	1.89	0.02	1.05	7.90
Sand	6 months	b (3)	8.27	2.00	10.27	10.18	1.91	0.09	4.50	10.18	1.91	0.00	0.00	7.98
Sand	12 months	a (1)	8.27	3.00	11.27	11.13	2.86	0.14	4.67	11.09	2.82	0.04	1.40	8.79
Sand	12 months	a (2)	7.95	3.00	10.95	10.82	2.87	0.13	4.33	10.80	2.85	0.02	0.70	8.78
Sand	12 months	a (3)	8.02	3.00	11.02	10.87	2.85	0.15	5.00	10.85	2.83	0.02	0.70	8.76
Sand	12 months	b (1)	7.88	3.00	10.88	10.73	2.85	0.15	5.00	10.70	2.82	0.03	1.05	8.77
Sand	12 months	b (2)	8.40	3.00	11.40	11.25	2.85	0.15	5.00	11.22	2.82	0.03	1.05	8.76
Sand	12 months	b (3)	7.79	3.00	10.79	10.57	2.78	0.22	7.33	10.55	2.76	0.02	0.72	8.76
Sand	18 months	a (1)	8.20	2.00	10.20	10.14	1.94	0.06	3.00	10.09	1.89	0.05	2.58	8.80
Sand	18 months	a (2)	8.23	2.00	10.23	10.13	1.90	0.10	5.00	10.03	1.80	0.10	5.26	8.76
Sand	18 months	a (3)	8.27	2.00	10.27	10.23	1.96	0.04	2.00	10.19	1.92	0.04	2.04	8.72
Sand	18 months	b (1)	7.88	2.00	9.88	9.84	1.96	0.04	2.00	9.75	1.87	0.09	4.59	8.57
Sand	18 months	b (2)	7.95	2.00	9.95	9.93	1.98	0.02	1.00	9.90	1.95	0.03	1.52	8.57
Sand	18 months	b (3)	8.15	2.00	10.15	10.12	1.97	0.03	1.50	10.08	1.93	0.04	2.03	8.54

Table A-6: 1.5 month clay burial bone colour analysis

	Readings	Aggregate average L*	a*	b*		Readings	Aggregate average L*	a*	b*
Pre-burial (a)	1-10	55.16	3.74	15.15	Pre-burial (b)	1-10	61.11	0.87	11.05
	11-20	60.42	1.88	13.77		11-20	56.34	1.10	12.51
	21-30	54.99	4.83	14.89		21-30	63.72	0.14	10.79
	Mean	56.86	3.48	14.60		Mean:	60.39	0.70	11.45
	St. Dev:	3.09	1.49	0.73		St. Dev:	3.74	0.50	0.93
Post-burial (a)	1-10	59.70	4.66	13.99	Post-burial(b)	1-10	68.63	2.91	19.26
	11-20	61.16	4.67	12.78		11-20	68.31	1.54	19.06
	21-30	60.46	4.65	13.83		21-30	61.54	3.02	16.29
	Mean:	60.44	4.66	13.53		Mean:	66.16	2.49	18.20
	St. Dev:	0.73	0.01	0.66		St. Dev:	4.00	0.82	1.66
Cortex (a)	1-10	75.00	0.69	10.07	Cortex (b)	1-10	50.94	4.03	13.52
	11-20	77.51	0.36	9.27		11-20	86.79	2.48	11.94
	21-30	72.88	1.01	8.11		21-30	100.75	2.01	15.41
	Mean:	75.13	0.69	9.15		Mean:	79.49	2.84	13.62
	St. Dev:	2.32	0.33	0.99		St. Dev:	25.69	1.06	1.74

Table A-7: 3 month clay burial bone colour analysis

	Readings	Aggregate average L*	a*	b*		Readings	Aggregate average L*	a*	b*
Pre-burial (a)	1-10	60.62	4.48	12.14	Pre-burial (b)	1-10	73.27	-0.01	11.87
	11-20	63.34	2.56	13.48		11-20	74.64	3.09	17.78
	21-30	61.38	1.24	12.92		21-30	72.24	3.15	14.9
	Mean	61.78	2.76	12.85		Mean:	73.38	2.08	14.85
	St. Dev:	1.40	1.63	0.67		St. Dev:	1.20	1.81	2.96
Post-burial (a)	1-10	63.7	5.06	23.57	Post-burial (b)	1-10	75.53	0.06	11.95
	11-20	65.74	5.24	26.02		11-20	74.36	3.72	17.24
	21-30	74.00	2.08	12.53		21-30	76.1	1.71	13.92
	Mean:	67.81	4.13	20.71		Mean:	75.33	1.83	14.37
	St. Dev:	5.45	1.77	7.19		St. Dev:	0.89	1.83	2.67
Cortex (a)	1-10	82.67	2.39	15.04	Cortex (b)	1-10	84.52	2.05	11.5
	11-20	82.78	1.71	17.29		11-20	88.02	0.83	12.37
	21-30	80.37	2.24	17.69		21-30	86.47	1.68	12.25
	Mean:	81.94	2.11	16.67		Mean:	86.34	1.52	12.04
	St. Dev:	1.36	0.36	1.43		St. Dev:	1.75	0.63	0.47

Table A-8: 6 months clay burial bone colour analysis

		Aggregate average					Aggregate average		
	Readings	L*	a*	b*		Readings	L*	a*	b*
Pre-burial (a)	1-10	59.09	-0.34	12.80	Pre-burial (b)	1-10	66.87	2.35	12.29
	11-20	61.88	-0.50	15.35		11-20	67.37	3.88	13.68
	21-30	60.16	-0.35	12.82		21-30	69.80	3.81	14.20
	Mean	60.38	-0.40	13.66		Mean:	68.01	3.35	13.39
	St. Dev:	1.41	0.09	1.47		St. Dev:	1.57	0.86	0.99
Post-burial (a)	1-10	84.78	0.82	10.13	Post-burial (b)	1-10	64.45	4.21	17.48
	11-20	78.57	3.46	17.42		11-20	69.26	4.39	18.96
	21-30	80.65	2.33	13.61		21-30	63.91	3.31	14.72
	Mean:	81.33	2.20	13.72		Mean:	65.87	3.97	17.05
	St. Dev:	3.16	1.32	3.65		St. Dev:	2.95	0.58	2.15
Cortex (a)	1-10	87.44	-0.01	11.44	Cortex (b)	1-10	83.03	1.83	13.77
	11-20	87.95	1.07	13.90		11-20	85.44	1.68	16.45
	21-30	89.52	0.60	11.03		21-30	84.41	1.90	16.69
	Mean:	88.30	0.55	12.12		Mean:	84.29	1.80	15.64
	St. Dev:	1.08	0.54	1.55		St. Dev:	1.21	0.11	1.62

Table A-9: 12 months clay burial bone colour analysis

		Aggregate average					Aggregate average		
	Readings	L*	a*	b*		Readings	L*	a*	b*
Pre-burial (a)	1-10	56.05	4.98	11.76	Pre-burial (b)	1-10	76.19	0.29	13.02
	11-20	60.21	7.80	14.49		11-20	67.98	1.46	12.99
	21-30	29.71	1.89	4.45		21-30	72.77	0.67	13.92
	Mean	48.66	4.89	10.23		Mean:	72.31	0.81	13.31
	St. Dev:	16.54	2.96	5.19		St. Dev:	4.12	0.60	0.53
Post-burial (a)	1-10	67.55	3.11	13.62	Post-burial (b)	1-10	67.35	2.77	12.87
	11-20	69.16	3.18	13.71		11-20	67.38	2.76	12.87
	21-30	68.59	2.40	9.18		21-30	67.38	2.76	12.87
	Mean:	68.43	2.90	12.17		Mean:	67.37	2.76	12.87
	St. Dev:	0.82	0.43	2.59		St. Dev:	0.02	0.01	0.00
Cortex (a)	1-10	80.51	1.52	12.10	Cortex (b)	1-10	90.03	-0.24	8.40
	11-20	84.08	1.27	13.35		11-20	82.89	1.67	12.74
	21-30	81.60	1.68	11.79		21-30	87.89	-0.24	9.81
	Mean:	82.06	1.49	12.41		Mean:	86.94	0.40	10.32
	St. Dev:	1.83	0.21	0.83		St. Dev:	3.66	1.10	2.21

Table A-10: 18 months clay burial bone colour analysis

		Aggregate average					Aggregate average		
	Readings	L*	a*	b*		Readings	L*	a*	b*
Pre-burial (a)	1-10	56.78	1.35	12.33	Pre-burial (b)	1-10	58.26	0.63	11.67
	11-20	49.66	1.36	11.88		11-20	54.40	1.38	9.78
	21-30	46.74	1.44	9.29		21-30	51.70	2.34	10.15
	Mean	51.06	1.38	11.17		Mean:	54.79	1.45	10.53
	St. Dev:	5.16	0.05	1.64		St. Dev:	3.30	0.86	1.00
Post-burial (a)	1-10	68.87	3.11	14.77	Post-burial (b)	1-10	67.50	4.07	16.16
	11-20	68.14	3.14	14.69		11-20	67.92	3.97	16.25
	21-30	68.45	3.02	14.24		21-30	67.74	3.96	16.17
	Mean:	68.49	3.09	14.57		Mean:	67.72	4.00	16.19
	St. Dev:	0.37	0.06	0.29		St. Dev:	0.21	0.06	0.05
Cortex (a)	1-10	84.93	0.77	14.84	Cortex (b)	1-10	81.85	2.69	15.49
	11-20	84.30	-0.83	14.49		11-20	82.37	1.63	16.24
	21-30	87.08	-0.21	13.96		21-30	81.46	2.71	15.27
	Mean:	85.44	-0.09	14.43		Mean:	81.89	2.34	15.67
	St. Dev:	1.46	0.81	0.44		St. Dev:	0.46	0.62	0.51

Table A-11: 1.5 months compost burial bone colour analysis

		Aggregate average					Aggregate average		
	Readings	L*	a*	b*		Readings	L*	a*	b*
Pre-burial (a)	1-10	62.11	4.32	16.56	Pre-burial (b)	1-10	69.97	2.82	13.78
	11-20	59.70	3.77	13.95		11-20	70.64	5.60	17.03
	21-30	64.02	3.83	17.99		21-30	67.00	5.02	14.78
	Mean	61.94	3.97	16.17		Mean:	69.20	4.48	15.20
	St. Dev:	2.16	0.30	2.05		St. Dev:	1.94	1.47	1.66
Post-burial (a)	1-10	44.58	6.06	12.19	Post-burial (b)	1-10	53.05	9.05	19.56
	11-20	48.94	6.18	14.30		11-20	51.82	10.26	22.90
	21-30	49.46	5.44	9.40		21-30	54.20	10.17	22.82
	Mean:	47.66	5.89	11.96		Mean:	53.02	9.83	21.76
	St. Dev:	2.68	0.40	2.46		St. Dev:	1.19	0.67	1.91
Cortex (a)	1-10	71.09	1.25	9.48	Cortex (b)	1-10	114.42	1.74	15.00
	11-20	57.12	2.12	9.39		11-20	111.51	1.89	12.26
	21-30	61.95	4.70	16.04		21-30	107.86	3.13	14.33
	Mean:	63.39	2.69	11.64		Mean:	111.26	2.25	13.86
	St. Dev:	7.09	1.79	3.81		St. Dev:	3.29	0.76	1.43

Table A-12: 3 months compost burial bone colour analysis

		Aggregate average					Aggregate average		
	Readings	L*	a*	b*		Readings	L*	a*	b*
Pre-burial (a)	1-10	57.86	0.99	10.21	Pre-burial (b)	1-10	64.30	10.10	16.80
	11-20	58.34	0.68	9.47		11-20	50.30	8.30	11.22
	21-30	60.24	0.29	7.71		21-30	65.80	11.49	18.12
	Mean	58.81	0.65	9.13		Mean:	60.13	9.96	15.38
	St. Dev:	1.26	0.35	1.28		St. Dev:	8.55	1.60	3.66
Post-burial (a)	1-10	72.03	3.61	20.80	Post-burial (b)	1-10	64.35	6.00	21.30
	11-20	73.10	3.52	20.37		11-20	60.97	4.64	19.07
	21-30	73.95	4.13	26.60		21-30	56.53	4.83	19.01
	Mean:	73.03	3.75	22.59		Mean:	60.62	5.16	19.79
	St. Dev:	0.96	0.33	3.48		St. Dev:	3.92	0.74	1.31
Cortex (a)	1-10	78.18	3.32	19.90	Cortex (b)	1-10	88.95	0.22	12.73
	11-20	83.61	1.23	15.30		11-20	89.34	-0.08	11.88
	21-30	86.56	-0.09	12.11		21-30	88.39	0.55	13.18
	Mean:	82.78	1.49	15.77		Mean:	88.89	0.23	12.60
	St. Dev:	4.25	1.72	3.92		St. Dev:	0.48	0.32	0.66

Table A-13: 6 months compost burial bone colour analysis

		Aggregate average					Aggregate average		
	Readings	L*	a*	b*		Readings	L*	a*	b*
Pre-burial (a)	1-10	61.74	2.09	14.56	Pre-burial (b)	1-10	45.51	4.51	8.79
	11-20	58.87	4.42	13.42		11-20	65.47	2.78	12.18
	21-30	56.25	2.58	14.12		21-30	62.52	5.77	15.07
	Mean	58.95	3.03	14.03		Mean:	57.83	4.35	12.01
	St. Dev:	2.75	1.23	0.57		St. Dev:	10.77	1.50	3.14
Post-burial (a)	1-10	70.21	3.80	19.11	Post-burial (b)	1-10	71.78	3.33	15.92
	11-20	69.30	3.84	17.13		11-20	62.11	5.03	17.87
	21-30	68.64	3.81	18.78		21-30	68.72	4.61	17.97
	Mean:	69.38	3.82	18.34		Mean:	67.54	4.32	17.25
	St. Dev:	0.79	0.02	1.06		St. Dev:	4.94	0.89	1.16
Cortex (a)	1-10	83.69	0.34	11.99	Cortex (b)	1-10	85.45	0.60	13.14
	11-20	84.66	0.73	11.94		11-20	80.32	2.31	17.14
	21-30	83.80	1.01	11.68		21-30	84.15	0.73	16.14
	Mean:	84.05	0.69	11.87		Mean:	83.31	1.21	15.47
	St. Dev:	0.53	0.34	0.17		St. Dev:	2.67	0.95	2.08

Table A-14: 12 months compost burial bone colour analysis

		Aggregate average					Aggregate average		
	Readings	L*	a*	b*		Readings	L*	a*	b*
Pre-burial (a)	1-10	52.78	8.35	13.74	Pre-burial (b)	1-10	63.53	5.55	15.41
	11-20	56.34	11.29	16.64		11-20	62.22	6.54	16.20
	21-30	70.05	1.13	13.93		21-30	68.96	5.00	17.58
	Mean	59.72	6.92	14.77		Mean:	64.90	5.70	16.40
	St. Dev:	9.12	5.23	1.62		St. Dev:	3.57	0.78	1.10
Post-burial (a)	1-10	61.23	2.38	11.96	Post-burial (b)	1-10	61.41	2.63	12.75
	11-20	61.41	2.39	12.02		11-20	61.42	2.63	12.76
	21-30	61.59	2.38	12.12		21-30	66.31	3.09	14.84
	Mean:	61.41	2.38	12.03		Mean:	63.05	2.78	13.45
	St. Dev:	0.18	0.01	0.08		St. Dev:	2.83	0.27	1.20
Cortex (a)	1-10	67.90	2.44	13.02	Cortex (b)	1-10	76.42	1.39	11.00
	11-20	74.08	0.94	10.74		11-20	73.83	1.13	10.86
	21-30	77.41	0.96	10.67		21-30	78.99	1.13	11.82
	Mean:	73.13	1.45	11.48		Mean:	76.41	1.22	11.23
	St. Dev:	4.83	0.86	1.34		St. Dev:	2.58	0.15	0.52

Table A-15: 18 months compost burial bone colour analysis

		Aggregate average					Aggregate average		
	Readings	L*	a*	b*		Readings	L*	a*	b*
Pre-burial (a)	1-10	51.76	3.83	12.54	Pre-burial (b)	1-10	55.90	1.19	9.66
	11-20	52.30	3.39	12.83		11-20	51.08	1.12	10.59
	21-30	53.03	3.74	12.74		21-30	49.33	1.38	10.97
	Mean	52.36	3.65	12.70		Mean:	52.10	1.23	10.41
	St. Dev:	0.64	0.23	0.15		St. Dev:	3.40	0.13	0.67
Post-burial (a)	1-10	73.43	2.50	13.72	Post-burial (b)	1-10	68.31	3.47	14.08
	11-20	69.79	2.19	14.46		11-20	68.57	2.70	12.17
	21-30	70.13	2.21	14.61		21-30	67.29	3.29	13.28
	Mean:	71.12	2.30	14.26		Mean:	68.06	3.15	13.18
	St. Dev:	2.01	0.17	0.48		St. Dev:	0.68	0.40	0.96
Cortex (a)	1-10	80.01	2.08	12.73	Cortex (b)	1-10	76.97	2.02	12.54
	11-20	78.65	2.37	13.56		11-20	74.54	2.66	13.38
	21-30	79.33	1.59	12.48		21-30	75.94	2.50	12.44
	Mean:	79.33	2.01	12.92		Mean:	75.82	2.39	12.79
	St. Dev:	0.68	0.39	0.57		St. Dev:	1.22	0.33	0.52

Table A-16: 1.5 months lime burial bone colour analysis

		Aggregate average					Aggregate average		
	Readings	L*	a*	b*		Readings	L*	a*	b*
Pre-burial (a)	1-10	66.07	1.98	12.21	Pre-burial (b)	1-10	71.78	0.88	14.82
	11-20	43.03	2.99	8.33		11-20	69.16	0.31	11.58
	21-30	54.77	4.15	11.65		21-30	71.24	-0.17	11.88
	Mean	54.62	3.04	10.73		Mean:	70.73	0.34	12.76
	St. Dev:	11.52	1.09	2.10		St. Dev:	1.38	0.53	1.79
Post-burial (a)	1-10	40.67	6.31	8.31	Post-burial (b)	1-10	49.67	11.38	12.71
	11-20	52.10	4.90	9.85		11-20	42.52	5.60	11.03
	21-30	46.54	4.58	7.11		21-30	50.94	4.03	13.52
	Mean:	46.44	5.26	8.42		Mean:	47.71	7.00	12.42
	St. Dev:	5.72	0.92	1.37		St. Dev:	4.54	3.87	1.27
Cortex (a)	1-10	85.54	6.75	8.80	Cortex (b)	1-10	82.30	1.75	11.97
	11-20	89.15	4.69	9.81		11-20	71.23	4.58	9.03
	21-30	80.52	7.86	10.91		21-30	74.22	6.00	11.20
	Mean:	85.07	6.43	9.84		Mean:	75.92	4.11	10.73
	St. Dev:	4.33	1.61	1.06		St. Dev:	5.73	2.16	1.52

Table A-17: 3 months lime burial bone colour analysis

		Aggregate average					Aggregate average		
	Readings	L*	a*	b*		Readings	L*	a*	b*
Pre-burial (a)	1-10	69.14	4.57	17.32	Pre-burial (b)	1-10	65.30	4.87	14.86
	11-20	52.51	1.28	13.76		11-20	64.23	5.83	15.84
	21-30	68.96	0.91	14.72		21-30	64.04	5.23	15.61
	Mean	63.54	2.25	15.27		Mean:	64.52	5.31	15.44
	St. Dev:	9.55	2.01	1.84		St. Dev:	0.68	0.48	0.51
Post-burial (a)	1-10	52.78	2.06	17.30	Post-burial (b)	1-10	54.82	1.80	17.40
	11-20	57.25	3.76	19.70		11-20	53.12	1.92	15.52
	21-30	66.66	2.69	18.37		21-30	73.13	0.47	14.95
	Mean:	58.90	2.84	18.46		Mean:	60.36	1.40	15.96
	St. Dev:	7.09	0.86	1.20		St. Dev:	11.09	0.80	1.28
Cortex (a)	1-10	65.35	4.20	11.27	Cortex (b)	1-10	62.35	4.63	11.76
	11-20	67.37	2.09	11.64		11-20	59.17	5.37	10.33
	21-30	69.74	3.82	10.81		21-30	60.75	3.90	9.34
	Mean:	67.49	3.37	11.24		Mean:	60.76	4.63	10.48
	St. Dev:	2.20	1.12	0.42		St. Dev:	1.59	0.74	1.22

Table A-18: 6 months lime burial bone colour analysis

		Aggregate average					Aggregate average		
	Readings	L*	a*	b*		Readings	L*	a*	b*
Pre-burial (a)	1-10	68.79	1.63	17.04	Pre-burial (b)	1-10	68.36	8.11	14.66
	11-20	32.32	5.91	13.76		11-20	61.97	4.76	13.83
	21-30	66.14	2.88	14.59		21-30	57.68	4.23	14.12
	Mean	55.75	3.47	15.13		Mean:	62.67	5.70	14.20
	St. Dev:	20.33	2.20	1.71		St. Dev:	5.37	2.10	0.42
Post-burial (a)	1-10	59.19	3.67	15.12	Post-burial (b)	1-10	54.67	5.74	23.05
	11-20	55.64	3.73	18.41		11-20	55.05	4.84	20.91
	21-30	57.40	2.49	15.36		21-30	52.26	5.58	21.80
	Mean:	57.41	3.30	16.30		Mean:	53.99	5.39	21.92
	St. Dev:	1.78	0.70	1.83		St. Dev:	1.51	0.48	1.08
Cortex (a)	1-10	68.02	1.46	12.23	Cortex (b)	1-10	60.56	4.15	11.60
	11-20	63.22	3.07	8.49		11-20	65.24	2.13	12.14
	21-30	55.85	3.02	8.70		21-30	71.95	0.90	11.87
	Mean:	62.36	2.52	9.81		Mean:	65.92	2.39	11.87
	St. Dev:	6.13	0.92	2.10		St. Dev:	5.73	1.64	0.27

Table A-19: 12 months lime burial bone colour analysis

		Aggregate average					Aggregate average		
	Readings	L*	a*	b*		Readings	L*	a*	b*
Pre-burial (a)	1-10	62.78	5.25	13.63	Pre-burial (b)	1-10	70.87	0.66	11.86
	11-20	56.38	4.44	10.11		11-20	72.99	1.69	15.78
	21-30	62.38	4.27	12.51		21-30	69.31	0.62	12.10
	Mean	60.51	4.65	12.08		Mean:	71.06	0.99	13.25
	St. Dev:	3.59	0.52	1.80		St. Dev:	1.85	0.61	2.20
Post-burial (a)	1-10	65.57	1.58	16.18	Post-burial (b)	1-10	59.55	2.69	13.02
	11-20	69.77	1.06	13.08		11-20	57.88	2.78	12.34
	21-30	66.66	2.13	16.60		21-30	59.82	2.62	13.14
	Mean:	67.33	1.59	15.29		Mean:	59.08	2.70	12.83
	St. Dev:	2.18	0.54	1.92		St. Dev:	1.05	0.08	0.43
Cortex (a)	1-10	71.64	2.05	10.66	Cortex (b)	1-10	69.20	0.95	9.43
	11-20	70.28	2.09	9.69		11-20	68.61	1.78	13.29
	21-30	69.47	2.96	9.47		21-30	69.02	0.93	9.90
	Mean:	70.46	2.37	9.94		Mean:	68.94	1.22	10.87
	St. Dev:	1.10	0.51	0.63		St. Dev:	0.30	0.49	2.11

Table A-20: 18 months lime burial bone colour analysis

		Aggregate average					Aggregate average		
	Readings	L*	a*	b*		Readings	L*	a*	b*
Pre-burial (a)	1-10	64.95	4.38	13.65	Pre-burial (b)	1-10	43.64	2.27	6.70
	11-20	59.96	6.67	10.42		11-20	58.60	1.64	14.25
	21-30	58.70	3.30	10.97		21-30	59.43	2.03	11.17
	Mean	61.20	4.78	11.68		Mean:	53.89	1.98	10.71
	St. Dev:	3.31	1.72	1.73		St. Dev:	8.89	0.32	3.80
Post-burial (a)	1-10	58.35	3.72	16.26	Post-burial (b)	1-10	68.43	1.78	18.88
	11-20	53.61	5.31	23.33		11-20	71.90	1.38	13.77
	21-30	62.62	2.80	18.70		21-30	70.60	1.63	14.58
	Mean:	58.19	3.94	19.43		Mean:	70.31	1.60	15.74
	St. Dev:	4.51	1.27	3.59		St. Dev:	1.75	0.20	2.75
Cortex (a)	1-10	68.06	0.54	11.16	Cortex (b)	1-10	69.18	2.83	11.64
	11-20	69.10	0.72	13.92		11-20	70.76	3.01	12.19
	21-30	65.58	3.26	11.13		21-30	71.56	3.34	12.49
	Mean:	67.58	1.51	12.07		Mean:	70.50	3.06	12.11
	St. Dev:	1.81	1.52	1.60		St. Dev:	1.21	0.26	0.43

Table A-21: 1.5 months sand burial bone colour analysis

		Aggregate average					Aggregate average		
	Readings	L*	a*	b*		Readings	L*	a*	b*
Pre-burial (a)	1-10	66.70	3.70	14.19	Pre-burial (b)	1-10	53.72	1.38	8.36
	11-20	58.97	3.14	11.71		11-20	66.15	1.76	12.50
	21-30	65.05	2.96	14.11		21-30	71.10	0.68	13.28
	Mean	63.57	3.27	13.34		Mean:	63.66	1.27	11.38
	St. Dev:	4.07	0.39	1.41		St. Dev:	8.95	0.55	2.64
Post-burial (a)	1-10	52.20	8.13	19.37	Post-burial (b)	1-10	55.25	6.23	19.15
	11-20	50.18	7.16	22.37		11-20	51.22	7.60	19.99
	21-30	49.11	10.49	21.13		21-30	62.20	5.36	21.38
	Mean:	50.50	8.59	20.96		Mean:	56.22	6.40	20.17
	St. Dev:	1.57	1.71	1.51		St. Dev:	5.55	1.13	1.13
Cortex (a)	1-10	88.91	8.08	9.47	Cortex (b)	1-10	106.75	2.38	11.99
	11-20	107.51	2.63	12.57		11-20	104.15	2.95	9.88
	21-30	91.10	8.54	14.67		21-30	109.42	1.57	11.80
	Mean:	95.84	6.42	12.24		Mean:	106.77	2.30	11.22
	St. Dev:	10.17	3.29	2.62		St. Dev:	2.64	0.69	1.17

Table A-22: 3 months sand burial bone colour analysis

		Aggregate average					Aggregate average		
	Readings	L*	a*	b*		Readings	L*	a*	b*
Pre-burial (a)	1-10	68.69	-1.48	18.46	Pre-burial (b)	1-10	64.85	0.52	13.06
	11-20	66.94	-1.82	15.73		11-20	68.35	0.68	10.86
	21-30	62.40	-1.67	12.28		21-30	60.97	0.64	9.58
	Mean	66.01	-1.66	15.49		Mean:	64.72	0.61	11.17
	St. Dev:	3.25	0.17	3.10		St. Dev:	3.69	0.08	1.76
Post-burial (a)	1-10	51.25	3.91	16.28	Post-burial (b)	1-10	52.77	4.27	15.82
	11-20	52.92	4.69	18.99		11-20	54.11	4.29	16.03
	21-30	51.82	4.27	16.99		21-30	53.39	4.86	17.28
	Mean:	52.00	4.29	17.42		Mean:	53.42	4.47	16.38
	St. Dev:	0.85	0.39	1.41		St. Dev:	0.67	0.34	0.79
Cortex (a)	1-10	76.87	1.77	11.52	Cortex (b)	1-10	73.66	1.68	14.02
	11-20	80.10	0.75	12.25		11-20	73.00	2.15	13.54
	21-30	73.65	2.16	13.94		21-30	77.37	1.98	13.06
	Mean:	76.87	1.56	12.57		Mean:	74.68	1.94	13.54
	St. Dev:	3.23	0.73	1.24		St. Dev:	2.36	0.24	0.48

Table A-23: 6 months sand burial bone colour analysis

		Aggregate average					Aggregate average		
	Readings	L*	a*	b*		Readings	L*	a*	b*
Pre-burial (a)	1-10	65.19	-0.08	18.29	Pre-burial (b)	1-10	65.20	0.49	18.99
	11-20	62.70	2.18	17.69		11-20	60.73	3.80	16.12
	21-30	63.94	0.32	17.09		21-30	48.07	2.43	7.63
	Mean	63.94	0.81	17.69		Mean:	58.00	2.24	14.25
	St. Dev:	1.25	1.21	0.60		St. Dev:	8.89	1.66	5.91
Post-burial (a)	1-10	55.81	4.70	18.70	Post-burial (b)	1-10	51.07	4.02	17.51
	11-20	55.14	3.08	15.40		11-20	54.98	3.74	18.03
	21-30	54.73	4.78	19.10		21-30	50.21	3.71	16.60
	Mean:	55.23	4.19	17.73		Mean:	52.09	3.82	17.38
	St. Dev:	0.55	0.96	2.03		St. Dev:	2.54	0.17	0.72
Cortex (a)	1-10	79.36	1.93	14.51	Cortex (b)	1-10	73.36	3.18	14.14
	11-20	68.80	3.68	18.46		11-20	76.50	1.98	13.74
	21-30	71.73	3.97	21.88		21-30	72.95	3.20	14.12
	Mean:	73.30	3.19	18.28		Mean:	74.27	2.79	14.00
	St. Dev:	5.45	1.10	3.69		St. Dev:	1.94	0.70	0.23

Table A-24: 12 months sand burial bone colour analysis

		Aggregate average					Aggregate average		
	Readings	L*	a*	b*		Readings	L*	a*	b*
Pre-burial (a)	1-10	65.25	-0.86	14.90	Pre-burial (b)	1-10	71.04	-0.89	8.09
	11-20	69.76	-0.89	16.32		11-20	71.47	-0.68	15.66
	21-30	64.40	-0.71	15.54		21-30	70.31	-0.96	8.48
	Mean	66.47	-0.82	15.59		Mean:	70.94	-0.84	10.74
	St. Dev:	2.88	0.10	0.71		St. Dev:	0.59	0.15	4.26
Post-burial (a)	1-10	64.16	2.91	12.66	Post-burial (b)	1-10	65.08	2.16	12.65
	11-20	63.69	2.95	12.60		11-20	65.68	2.09	12.96
	21-30	64.17	2.93	12.63		21-30	65.08	2.14	12.54
	Mean:	64.01	2.93	12.63		Mean:	65.28	2.13	12.72
	St. Dev:	0.27	0.02	0.03		St. Dev:	0.35	0.04	0.22
Cortex (a)	1-10	76.95	1.86	11.07	Cortex (b)	1-10	78.44	1.09	11.94
	11-20	78.64	1.32	10.22		11-20	77.63	1.27	11.95
	21-30	76.83	1.75	11.35		21-30	75.90	1.68	12.53
	Mean:	77.47	1.64	10.88		Mean:	77.32	1.35	12.14
	St. Dev:	1.01	0.29	0.59		St. Dev:	1.30	0.30	0.34

Table A-25: 18 months sand burial bone colour analysis

		Aggregate average					Aggregate average		
	Readings	L*	a*	b*		Readings	L*	a*	b*
Pre-burial (a)	1-10	54.26	0.15	13.02	Pre-burial (b)	1-10	61.46	6.29	16.84
	11-20	64.07	-1.01	13.20		11-20	42.74	6.29	13.33
	21-30	58.77	-0.81	14.60		21-30	55.32	4.97	13.00
	Mean	59.03	-0.56	13.61		Mean:	53.17	5.85	14.39
	St. Dev:	4.91	0.62	0.86		St. Dev:	9.54	0.76	2.13
Post-burial (a)	1-10	61.55	5.05	21.51	Post-burial (b)	1-10	37.10	7.93	18.87
	11-20	62.89	5.17	21.68		11-20	54.18	6.82	22.86
	21-30	62.31	5.66	21.79		21-30	62.69	6.41	25.49
	Mean:	62.25	5.29	21.66		Mean:	51.32	7.05	22.41
	St. Dev:	0.67	0.32	0.14		St. Dev:	13.03	0.79	3.33
Cortex (a)	1-10	70.63	1.73	16.93	Cortex (b)	1-10	72.02	3.65	18.05
	11-20	62.69	2.52	11.08		11-20	71.56	3.19	15.86
	21-30	69.44	2.68	16.54		21-30	71.70	2.61	14.68
	Mean:	67.59	2.31	14.85		Mean:	71.76	3.15	16.20
	St. Dev:	4.28	0.51	3.27		St. Dev:	0.24	0.52	1.71

Table A-26: Overall colour difference between bone surface and cortex expressed as a single numerical value

	Duration	Clay				Compost				Lime				Sand			
Pre-burial to post-burial		Clay 1	Clay 2	Average	S.D.	Compost 1	Compost 2	Average	S.D.	Lime 1	Lime 2	Average	S.D.	Sand 1	Sand 2	Average	S.D.
	1.5	3.92	9.06	6.49	3.63	15.01	18.26	16.64	2.30	8.79	23.96	16.38	10.73	16.04	12.60	14.32	2.43
	3	10.00	2.02	6.01	5.64	19.82	6.54	13.18	9.39	5.66	5.74	5.70	0.06	15.34	13.03	14.19	1.64
	6	21.12	4.29	12.70	11.90	11.31	11.03	13.18	0.20	2.04	11.62	5.70	6.77	9.35	6.88	14.19	1.75
	12	19.97	5.33	12.65	10.35	5.56	4.54	5.05	0.72	8.13	12.10	10.12	2.81	5.37	6.69	6.03	0.93
	18	14.35	17.84	16.09	2.47	16.31	18.87	17.59	1.81	8.36	17.18	12.77	6.24	10.46	8.32	9.39	1.51
		Clay				Compost				Lime				Sand			
Post-burial to surface removal		Clay 1	Clay 2	Average	S.D.	Compost 1	Compost 2	Average	S.D.	Lime 1	Lime 2	Average	S.D.	Sand 1	Sand 2	Average	S.D.
	1.5	15.84	14.10	14.97	1.23	16.05	59.26	37.66	30.55	38.68	28.40	33.54	7.26	46.23	51.50	48.86	3.73
	3	14.83	11.25	13.04	2.53	12.12	29.59	20.85	12.36	11.23	6.38	8.80	3.43	25.49	21.59	23.54	2.76
	6	7.34	18.60	12.97	7.96	16.33	16.17	16.25	0.11	8.20	15.88	12.04	5.43	18.11	22.46	20.28	3.08
	12	13.70	19.87	16.79	4.36	11.77	13.64	12.71	1.32	6.24	10.16	8.20	2.77	13.64	12.08	12.86	1.10
	18	14.28	17.25	15.76	2.10	7.81	8.33	8.07	0.37	12.18	3.92	11.94	5.84	9.15	21.72	13.99	8.88
		Clay				Compost				Lime				Sand			
Pre-burial to surface removal		Clay 1	Clay 2	Average	S.D.	Compost 1	Compost 2	Average	S.D.	Lime 1	Lime 2	Average	S.D.	Sand 1	Sand 2	Average	S.D.
	1.5	19.27	19.34	19.31	0.05	4.92	42.14	23.53	26.32	30.65	6.73	18.69	16.91	32.44	43.13	37.78	7.56
	3	20.53	13.27	16.90	5.14	24.89	30.49	27.69	3.96	5.75	6.26	6.01	0.36	11.70	10.32	11.01	0.98
	6	27.98	16.51	22.25	8.12	25.30	25.90	25.60	0.42	8.54	5.19	6.87	2.37	9.67	16.28	12.98	4.67
	12	33.65	14.93	24.29	13.24	14.85	13.39	14.12	1.03	10.43	3.19	6.81	5.12	12.22	6.89	9.56	3.77
	18	27.60	34.56	31.08	4.92	23.86	27.02	25.44	2.23	7.18	16.70	11.94	6.74	9.11	18.87	13.99	6.90

Table A-27: ATR-FTIR data for control porcine bones and experimental burial porcine bones

Burial Type	Duration	Peak heights as designated wavenumber positions									Mean Average			Standard deviation		
		Peak A (600)	Peak B (560)	Peak C (586)	Phosphate (1015)	Carbonate (1410)	Amide I (1642)	SF	C/P	Am/P	SF	C/P	Am/P	SF	C/P	Am/P
Control	0	0.07	0.12	0.07	0.15	0.05	0.04	2.91	0.32	0.28	2.89	0.31	0.28	0.03	0.01	0.00
	0	0.08	0.13	0.07	0.15	0.05	0.04	2.87	0.31	0.28						
	1.5	0.09	0.15	0.08	0.19	0.06	0.05	2.98	0.31	0.27	2.96	0.31	0.27	0.02	0.00	0.01
	1.5	0.08	0.14	0.08	0.18	0.06	0.05	2.95	0.31	0.26						
	3	0.07	0.12	0.06	0.14	0.05	0.04	3.07	0.35	0.26	3.03	0.35	0.27	0.05	0.00	0.00
	3	0.08	0.14	0.07	0.17	0.06	0.04	3.00	0.35	0.27						
	6	0.09	0.15	0.08	0.17	0.06	0.04	3.03	0.33	0.26	3.02	0.33	0.26	0.01	0.00	0.00
	6	0.10	0.16	0.09	0.20	0.06	0.05	3.01	0.33	0.26						
	12	0.09	0.15	0.08	0.19	0.06	0.05	2.98	0.34	0.27	3.00	0.34	0.26	0.03	0.00	0.01
	12	0.10	0.17	0.09	0.21	0.07	0.05	3.02	0.34	0.26						
	18	0.09	0.14	0.08	0.17	0.06	0.05	3.01	0.35	0.27	3.02	0.34	0.26	0.00	0.01	0.01
	18	0.12	0.20	0.11	0.25	0.09	0.07	3.02	0.34	0.26						
Clay	1.5	0.13	0.22	0.11	0.29	0.07	0.07	3.12	0.24	0.24	3.07	0.29	0.26	0.07	0.08	0.04
	1.5	0.06	0.11	0.06	0.13	0.05	0.04	3.02	0.35	0.29						
	3	0.12	0.20	0.10	0.25	0.08	0.06	3.09	0.32	0.25	3.04	0.31	0.25	0.06	0.02	0.00
	3	0.12	0.19	0.10	0.25	0.07	0.06	3.00	0.29	0.25						
	6	0.13	0.22	0.11	0.30	0.08	0.07	3.10	0.29	0.24	3.07	0.30	0.26	0.03	0.02	0.04
	6	0.17	0.28	0.15	0.38	0.12	0.11	3.05	0.31	0.29						
	12	0.15	0.25	0.13	0.34	0.13	0.09	3.13	0.39	0.27	3.10	0.35	0.27	0.04	0.07	0.00
	12	0.14	0.24	0.13	0.33	0.10	0.09	3.07	0.30	0.27						
	18	0.13	0.23	0.12	0.30	0.09	0.09	3.08	0.29	0.29	3.10	0.30	0.30	0.03	0.01	0.01
	18	0.13	0.22	0.11	0.30	0.09	0.09	3.12	0.31	0.30						

APPENDICES

Burial Type	Duration	Peak heights as designated wavenumber positions									Mean Average			Standard deviation		
		Peak A (600)	Peak B (560)	Peak C (586)	Phosphate (1015)	Carbonate (1410)	Amide I (1642)	SF	C/P	Am/P	SF	C/P	Am/P	SF	C/P	Am/P
Compost	1.5	0.12	0.21	0.10	0.26	0.06	0.05	3.18	0.24	0.20	3.11	0.28	0.23	0.11	0.06	0.05
	1.5	0.08	0.14	0.08	0.18	0.06	0.05	3.03	0.32	0.27						
	3	0.13	0.20	0.11	0.27	0.09	0.07	3.13	0.33	0.26	3.13	0.32	0.28	0.01	0.01	0.02
	3	0.16	0.26	0.14	0.37	0.12	0.11	3.12	0.32	0.29						
	6	0.11	0.18	0.09	0.24	0.07	0.06	3.09	0.29	0.26	3.07	0.28	0.25	0.02	0.02	0.01
	6	0.11	0.19	0.10	0.24	0.06	0.06	3.06	0.26	0.25						
	12	0.13	0.22	0.12	0.29	0.09	0.08	3.03	0.31	0.28	3.05	0.32	0.29	0.02	0.01	0.02
	12	0.14	0.24	0.12	0.34	0.11	0.10	3.06	0.32	0.31						
	18	0.11	0.18	0.10	0.24	0.07	0.08	3.05	0.30	0.31	3.06	0.31	0.30	0.01	0.01	0.02
	18	0.14	0.24	0.12	0.33	0.10	0.09	3.07	0.32	0.29						
Lime	1.5	0.07	0.12	0.06	0.15	0.05	0.04	3.00	0.32	0.27	2.98	0.35	0.29	0.03	0.04	0.04
	1.5	0.11	0.18	0.10	0.24	0.09	0.08	2.96	0.37	0.32						
	3	0.08	0.13	0.07	0.16	0.05	0.05	3.00	0.33	0.28	3.00	0.35	0.30	0.00	0.03	0.02
	3	0.08	0.13	0.07	0.16	0.06	0.05	3.00	0.37	0.31						
	6	0.07	0.11	0.06	0.15	0.06	0.06	2.89	0.42	0.40	2.94	0.36	0.33	0.08	0.08	0.10
	6	0.10	0.16	0.09	0.21	0.06	0.05	3.00	0.31	0.26						
	12	0.13	0.20	0.11	0.28	0.10	0.09	2.95	0.37	0.34	2.97	0.38	0.32	0.04	0.01	0.02
	12	0.12	0.20	0.10	0.26	0.10	0.08	3.00	0.38	0.30						
	18	0.10	0.17	0.09	0.22	0.09	0.08	2.95	0.39	0.36	2.97	0.37	0.33	0.04	0.03	0.04
	18	0.11	0.18	0.10	0.24	0.08	0.07	3.00	0.35	0.30						

APPENDICES

Burial Type	Duration	Peak heights as designated wavenumber positions									Mean Average			Standard deviation		
		Peak A (600)	Peak B (560)	Peak C (586)	Phosphate (1015)	Carbonate (1410)	Amide I (1642)	SF	C/P	Am/P	SF	C/P	Am/P	SF	C/P	Am/P
Sand	1.5	0.07	0.12	0.06	0.14	0.05	0.04	3.14	0.34	0.28	3.08	0.33	0.26	0.08	0.01	0.02
	1.5	0.08	0.13	0.07	0.16	0.05	0.04	3.03	0.32	0.25						
	3	0.12	0.20	0.11	0.27	0.08	0.07	3.04	0.30	0.26	3.07	0.30	0.25	0.04	0.00	0.02
	3	0.12	0.20	0.10	0.26	0.08	0.06	3.10	0.31	0.24						
	6	0.17	0.27	0.15	0.37	0.13	0.12	2.94	0.35	0.31	2.91	0.36	0.32	0.04	0.02	0.01
	6	0.12	0.19	0.11	0.26	0.10	0.08	2.89	0.38	0.32						
	12	0.13	0.22	0.11	0.29	0.08	0.07	3.13	0.28	0.23	3.10	0.30	0.24	0.04	0.03	0.01
	12	0.14	0.24	0.13	0.32	0.10	0.08	3.07	0.32	0.25						
	18	0.10	0.17	0.09	0.22	0.07	0.06	3.01	0.34	0.27	3.08	0.37	0.30	0.09	0.04	0.04
	18	0.20	0.34	0.17	0.41	0.16	0.13	3.14	0.40	0.33						

Appendix B : Human Archaeological Data

Table B-1: Fin Cop skeletal colour data

Sample name		Measurement	Surface colour			Cortex colour		
Skeleton number	Element		L	a	b	L	a	b
Skeleton 1	Femur	Reading 1-10	75.37	5.86	22.04	82.59	4.33	18.21
		Reading 11-20	78.07	5.77	25.11	84.57	3.49	17.92
		Reading 21-30	73.11	9.06	31.60	84.61	3.65	18.44
		Reading 31-40	72.09	8.90	30.61	84.49	3.36	17.52
		Average	74.66	7.40	27.34	84.07	3.71	18.02
		Standard deviation	2.65	1.83	4.54	0.98	0.43	0.40
	Metatarsal	Reading 1-10	66.27	8.83	26.02	81.83	3.94	17.94
		Reading 11-20	72.13	7.49	28.72	76.94	4.67	19.20
		Reading 21-30	62.14	8.06	26.94	76.97	4.63	19.13
		Reading 31-40	69.56	8.05	27.77	79.88	4.57	19.37
		Average	67.53	8.11	27.36	78.91	4.45	18.91
		Standard deviation	4.32	0.55	1.15	2.39	0.34	0.65
Skeleton 3	Femur	Reading 1-10	53.49	9.49	23.22	81.44	4.01	18.87
		Reading 11-20	58.66	9.71	24.84	84.11	3.50	18.12
		Reading 21-30	53.25	10.54	23.31	79.45	4.36	19.60
		Reading 31-40	59.81	10.37	28.08	81.74	4.57	19.14
		Average	56.30	10.03	24.86	81.69	4.11	18.93
		Standard deviation	3.42	0.51	2.27	1.91	0.47	0.62
	Metatarsal	Reading 1-10	67.38	8.76	29.37	80.44	4.29	17.91
		Reading 11-20	71.22	4.70	20.96	81.85	4.03	17.90
		Reading 21-30	61.11	7.36	23.78	81.13	4.26	18.00
		Reading 31-40	71.13	6.36	24.15	81.92	4.09	17.93
		Average	67.71	6.80	24.57	81.34	4.17	17.94
		Standard deviation	4.75	1.71	3.51	0.70	0.13	0.05
Skeleton 5	Femur	Reading 1-10	74.93	5.10	19.77	71.10	5.53	15.06
		Reading 11-20	77.88	4.69	20.40	66.93	6.89	14.00
		Reading 21-30	72.16	5.74	20.12	73.81	4.76	14.95
		Reading 31-40	73.79	5.38	19.41	69.87	5.92	15.72
		Average	74.69	5.23	19.93	70.43	5.78	14.93
		Standard deviation	2.41	0.44	0.43	2.85	0.89	0.71
	Metatarsal	Reading 1-10	63.67	8.73	24.40	82.98	2.96	16.53
		Reading 11-20	62.51	9.03	24.34	81.08	2.74	15.18
		Reading 21-30	67.70	6.24	22.18	83.11	2.94	16.45
		Reading 31-40	67.53	7.70	24.38	80.80	3.35	15.73
		Average	65.35	7.93	23.83	81.99	3.00	15.97
		Standard deviation	2.66	1.26	1.10	1.22	0.26	0.64
Skeleton 6	Femur	Reading 1-10	51.75	8.81	21.20	68.20	5.43	18.74
		Reading 11-20	56.79	7.87	21.85	67.12	5.98	20.34
		Reading 21-30	49.98	9.37	20.80	69.44	5.10	18.40
		Reading 31-40	59.60	7.68	22.45	66.84	5.38	18.47
		Average	54.53	8.43	21.58	67.90	5.47	18.99
		Standard deviation	4.44	0.80	0.73	1.18	0.37	0.91

Sample name		Measurement	Surface colour			Cortex colour		
Skeleton number	Element		L	a	b	L	a	b
Skeleton 7	Femur	Reading 1-10	64.98	5.20	18.51	68.07	6.49	20.49
		Reading 11-20	60.84	7.13	22.27	70.41	5.41	20.63
		Reading 21-30	57.91	7.04	19.69	68.82	7.23	20.33
		Reading 31-40	59.23	7.49	21.22	69.60	6.87	20.56
		Average	60.74	6.72	20.42	69.23	6.50	20.50
		Standard deviation	3.07	1.03	1.66	1.01	0.79	0.13
Skeleton 8	Femur	Reading 1-10	79.27	5.75	27.56	81.24	4.78	18.79
		Reading 11-20	71.64	6.48	24.99	82.95	4.45	19.60
		Reading 21-30	68.52	6.54	23.14	81.88	4.31	18.10
		Reading 31-40	79.87	5.17	26.08	83.37	4.31	19.26
		Average	74.83	5.99	25.44	82.36	4.46	18.94
		Standard deviation	5.63	0.65	1.86	0.98	0.22	0.65
	Metatarsal	Reading 1-10	65.26	8.26	26.41	85.26	2.86	19.08
		Reading 11-20	76.99	5.76	25.90	82.42	3.05	16.06
		Reading 21-30	67.36	7.76	26.26	84.41	3.27	19.34
		Reading 31-40	75.26	6.87	28.68	82.41	3.08	15.71
		Average	71.22	7.16	26.81	83.63	3.07	17.55
		Standard deviation	5.77	1.10	1.26	1.44	0.17	1.93

Table B-2: ATR-FTIR data of Fin Cop skeletal elements

Skeleton Identification number	Skeletal element	Peak heights at designated wavenumber positions						Splitting Factor	Carbonate/ Phosphate	Amide / Phosphate
		Peak A (600)	Peak B (560)	Peak C (586)	Phosphate (1015)	Carbonate (1410)	Amide I (1642)			
Skeleton 1	Femur	1.44	0.85	0.69	1.82	0.37	0.17	3.32	0.20	0.09
	Metatarsal	1.21	0.68	0.60	1.69	0.42	0.29	3.15	0.25	0.17
Skeleton 3	Femur	1.15	0.66	0.51	1.43	0.54	0.49	3.57	0.38	0.34
	Metatarsal	1.35	0.73	0.54	1.71	0.38	0.34	3.84	0.22	0.20
Skeleton 5	Femur	1.32	0.74	0.60	1.64	0.51	0.43	3.45	0.31	0.26
	Metatarsal	1.25	0.66	0.53	1.78	0.41	0.30	3.59	0.23	0.17
Skeleton 6	Femur	0.86	0.38	0.32	1.67	0.36	0.34	3.89	0.22	0.21
Skeleton 7	Femur	0.98	0.43	0.36	1.72	0.35	0.30	3.90	0.20	0.17
Skeleton 8	Femur	1.42	0.79	0.53	1.87	0.37	0.21	4.17	0.20	0.11
	Metatarsal	1.17	0.61	0.48	1.75	0.42	0.31	3.70	0.24	0.18

Table B-3: XRF data of selected Fin Cop skeletal elements

Sample name	Test number	Element peak height in cps												
		Si	P	Ca	Ti	Fe	Mn	Cu	Zn	Sr	Zr	Cr	Ni	K
Femur 6	1	1049.51	4210.83	65045.27	473.94	10645.91	579.11	597.23	987.16	447.53	185.47	128.16	943.10	1239.14
	2	1032.00	4011.09	61264.58	454.10	10488.69	577.44	580.50	942.76	434.05	277.49	147.74	876.43	1176.89
	3	1010.49	4206.57	62694.09	400.24	9587.50	470.90	482.16	883.65	550.58	271.08	83.72	768.01	1185.00
	Average	1030.67	4142.83	63001.31	442.76	10240.70	542.48	553.30	937.86	477.39	244.68	119.87	862.51	1200.34
	s.d.	19.55	114.11	1908.98	38.14	571.13	62.00	62.17	51.93	63.75	51.38	32.80	88.37	33.84
Femur 7	1	682.69	5823.67	75120.74	118.38	1920.25	293.69	297.28	284.74	411.87	98.59	138.39	961.95	763.16
	2	810.04	5678.94	75524.86	154.39	2764.24	326.56	295.41	308.82	467.86	169.77	147.38	941.28	885.71
	3	712.25	5718.75	75492.31	124.03	1904.69	273.91	288.55	299.91	470.59	83.90	103.85	975.15	811.79
	Average	734.99	5740.46	75379.30	132.27	2196.39	298.05	293.75	297.82	450.10	117.42	129.87	959.46	820.22
	s.d.	66.66	74.77	224.51	19.37	491.83	26.59	4.60	12.17	33.14	45.93	22.98	17.07	61.71
Femur 8	1	371.58	6273.58	80484.22	32.62	655.48	262.12	659.28	797.92	523.56	71.22	171.85	1451.13	651.87
	2	405.66	6595.96	82133.23	12.35	590.79	271.15	591.46	763.00	576.03	90.52	166.94	1452.68	665.14
	3	348.00	5921.39	76421.32	19.02	536.38	183.52	554.62	687.58	588.31	112.31	135.69	1274.98	605.05
	Average	375.08	6263.64	79679.59	21.33	594.21	238.93	601.79	749.50	562.63	91.35	158.16	1392.93	640.68
	s.d.	28.99	337.39	2939.74	10.33	59.62	48.20	53.08	56.39	34.39	20.56	19.61	102.15	31.57
Metatarsal 8	1	544.04	5761.19	76562.10	210.61	3634.13	299.37	531.87	683.94	498.41	92.58	110.22	1229.79	819.15
	2	474.75	5913.23	77731.03	81.36	2591.85	305.18	602.47	737.68	503.19	90.35	133.86	1327.08	764.27
	3	525.30	5879.49	79348.60	191.51	3473.82	315.92	587.50	730.54	508.62	64.51	144.62	1316.54	836.16
	Average	514.70	5851.30	77880.58	161.16	3233.27	306.82	573.95	717.39	503.41	82.48	129.57	1291.14	806.53
	s.d.	35.84	79.84	1399.26	69.77	561.24	8.39	37.20	29.19	5.11	15.60	17.59	53.38	37.57

Table B-4: Colour data of Eriswell skeletal elements

Sample name		Surface colour			Cortex colour			Colour change
Skeleton number	Element	L*	a*	b*	L*	a*	b*	
0067	Femur	57.83	6.49	12.22	73.61	5.05	17.01	16.55
	Metatarsal	59.60	7.61	16.98	70.35	7.62	23.03	12.33
0145	Femur	61.13	6.75	19.36	57.54	3.76	9.73	10.71
	Metatarsal	64.20	7.71	20.04	78.21	3.55	19.40	14.63
0158	Femur	57.22	8.39	19.35	69.69	5.07	14.32	13.85
	Metatarsal	64.38	7.48	20.22	81.19	1.95	15.78	18.25
0201	Femur	55.10	8.91	18.97	74.93	4.28	15.76	20.61
	Metatarsal	57.16	6.62	15.92	73.90	4.02	17.18	16.98
0203	Femur	52.63	9.12	19.48	72.37	5.57	16.70	20.24
	Metatarsal	58.24	8.13	16.91	71.48	6.62	23.01	14.65
0235	Femur	68.07	6.58	30.92	79.10	4.49	17.45	17.54
	Metatarsal	62.35	6.41	17.69	80.77	3.60	18.62	18.66
0241	Femur	61.38	7.31	16.87	72.12	4.48	15.82	11.15
0251	Femur	53.37	5.82	11.05	66.83	2.46	8.82	14.04
	Metatarsal	62.16	4.33	15.68	72.38	2.59	14.30	10.45
0255	Femur	52.29	5.31	13.42	74.32	3.25	14.28	22.14
	Metatarsal	60.22	6.65	16.95	73.43	4.22	19.56	13.68
0259	Femur	53.78	6.06	15.40	68.89	3.39	11.86	15.74
	Metatarsal	61.46	4.47	15.51	72.32	3.89	16.34	10.90
0309	Femur	64.66	5.81	15.31	73.99	3.92	14.95	9.53
	Metatarsal	62.02	5.88	17.84	74.63	4.27	20.92	13.08
0310	Femur	52.96	8.64	18.82	68.15	3.76	14.21	16.61
0317	Femur	62.29	5.51	12.86	65.47	3.10	8.97	5.57
	Metatarsal	56.78	7.80	16.64	60.15	4.05	13.94	5.71
0318	Femur	65.86	7.73	23.21	79.39	4.12	16.99	15.33
	Metatarsal	64.85	7.17	19.80	84.75	2.82	15.76	20.77
0326	Femur	58.46	9.29	21.26	73.36	4.34	17.67	16.10
	Metatarsal	58.48	7.82	16.86	67.89	8.70	23.69	11.65
0343	Femur	64.54	3.79	12.12	73.73	3.11	14.57	9.53
	Metatarsal	60.94	7.02	15.59	61.57	6.20	13.56	2.28
0346	Femur	52.04	2.75	6.30	63.74	3.77	11.51	12.84
	Metatarsal	62.23	7.78	19.12	69.13	6.14	21.46	7.47
0363	Femur	63.22	7.30	22.04	77.84	4.55	16.88	15.75
	Metatarsal	53.87	5.35	11.54	66.46	4.24	12.68	12.69
0392	Femur	69.97	9.43	26.50	79.48	5.02	16.54	14.45
	Metatarsal	66.52	8.65	21.63	83.35	3.89	18.64	17.74
0395	Femur	53.90	6.55	18.63	72.25	3.68	13.45	19.28
	Metatarsal	59.29	6.07	15.11	69.55	6.11	21.95	12.33

Sample name		Surface colour			Cortex colour			Colour change
Skeleton number	Element	L*	a*	b*	L*	a*	b*	
0425	Femur	61.22	8.09	22.14	74.72	3.79	15.40	15.68
	Metatarsal	56.78	6.67	13.71	54.75	7.12	19.76	6.40
0426	Femur	63.07	6.98	21.85	75.72	3.70	15.33	14.61
	Metatarsal	61.83	7.31	16.72	72.50	5.22	21.80	12.00
0474	Femur	61.73	9.14	23.84	76.33	3.86	14.30	18.22
0477	Femur	64.93	8.29	22.67	77.26	4.39	16.22	14.45
	Metatarsal	63.81	5.58	14.54	72.80	4.80	21.33	11.29
0554	Femur	61.81	7.45	21.91	68.73	4.08	12.50	12.15
0570	Femur	62.32	8.96	26.36	77.60	1.60	16.19	19.77
	Metatarsal	57.08	4.30	13.46	58.90	3.32	8.17	5.68
0571	Metatarsal	58.48	6.04	14.55	75.28	6.42	22.93	18.77
0580	Femur	50.08	6.49	16.55	82.19	1.53	12.27	32.78
	Metatarsal	63.65	6.35	15.30	84.63	2.34	14.95	21.36
0612	Femur	65.96	11.60	29.57	77.83	4.51	18.50	17.71
	Metatarsal	63.26	6.96	16.23	62.10	6.21	14.99	1.86
0692	Femur	69.08	8.18	24.00	78.86	4.05	15.59	13.54
	Metatarsal	64.14	6.44	17.62	74.77	3.35	17.45	11.07
0717	Femur	68.90	8.52	21.14	77.15	4.49	16.20	10.43
	Metatarsal	68.34	5.89	16.39	73.18	3.80	18.38	5.63
0759	Femur	52.41	12.01	23.57	76.89	3.39	14.29	27.56
	Metatarsal	60.95	9.04	18.68	70.26	9.96	26.27	12.05
0791	Femur	59.47	6.67	19.95	83.77	1.44	10.82	26.48
	Metatarsal	65.96	6.14	19.08	83.16	3.83	18.77	17.36
0799	Femur	60.34	6.88	20.12	79.28	1.58	10.49	21.89
	Metatarsal	66.92	5.94	19.20	76.00	2.29	14.86	10.70
0808	Femur	61.84	8.72	23.42	80.35	2.50	13.31	21.99
	Metatarsal	66.42	7.45	21.50	75.22	6.30	23.03	9.00
0809	Femur	64.13	7.58	22.95	76.98	4.12	15.75	15.13
	Metatarsal	58.40	6.73	16.26	64.13	6.39	19.20	6.44
0851	Femur	66.67	5.94	19.90	75.85	3.71	14.80	10.74
	Metatarsal	60.05	5.00	14.67	60.05	4.69	12.08	2.61
0888	Femur	62.57	7.44	19.30	77.42	3.29	15.37	15.91
0907	Femur	72.49	7.60	24.92	82.31	3.80	15.75	13.95
0991	Femur	56.54	7.75	18.80	78.07	3.24	13.50	22.63
	Metatarsal	61.27	6.77	15.71	72.13	5.98	20.23	11.78
0994	Femur	60.92	8.68	19.36	80.80	2.07	13.80	21.68
	Metatarsal	55.34	7.29	15.14	66.35	4.56	16.07	11.38
4040	Femur	63.16	10.25	24.25	80.24	3.43	17.09	19.73
	Metatarsal	65.16	4.90	18.75	66.17	4.58	13.85	5.02
4046	Femur	61.62	9.16	22.58	84.20	3.36	14.91	24.54
	Metatarsal	66.21	9.31	22.18	82.81	4.02	18.61	17.79

Sample name		Surface colour			Cortex colour			Colour change
Skeleton number	Element	L*	a*	b*	L*	a*	b*	
4067	Femur	52.22	10.32	21.90	76.60	2.38	11.66	27.61
	Metatarsal	63.24	7.84	20.50	68.52	5.80	17.39	6.45
4095	Femur	52.09	7.94	20.67	77.05	2.74	14.44	26.25
4098	Femur	53.66	10.63	23.64	80.42	3.87	16.38	28.54
4099	Femur	61.68	8.37	21.83	82.99	1.96	12.55	24.11
	Metatarsal	68.50	8.31	20.90	77.22	6.08	22.62	9.16
4191	Femur	57.82	8.74	23.68	82.92	3.10	14.76	27.23
	Metatarsal	60.73	7.89	19.32	77.19	3.60	18.72	17.02
4222	Femur	54.81	9.04	25.41	79.84	1.61	17.22	20.46
	Sternum	50.95	10.95	26.69	63.45	7.02	23.40	23.96
4226	Femur	59.10	5.41	15.80	78.88	2.79	13.13	20.13
	Metatarsal	56.59	5.41	12.37	65.27	6.87	18.49	10.72
4288	Femur	52.96	7.50	17.35	73.23	4.23	13.06	20.98
	Metatarsal	59.65	5.47	13.85	63.50	5.18	15.98	4.41
4291	Femur	55.14	9.97	20.79	82.70	2.66	13.40	29.45
4295	Femur	53.25	10.19	20.41	78.30	5.30	17.57	25.68
4340	Femur	52.46	11.09	21.87	71.13	5.12	13.63	21.26
	Metatarsal	56.21	7.35	14.77	60.59	9.27	22.23	8.86
4411	Femur	53.41	6.62	18.81	59.59	2.93	7.74	13.20
4462	Femur	56.24	9.61	19.13	74.22	5.44	14.16	19.11
	Metatarsal	60.80	6.61	16.24	65.92	6.91	19.43	6.03
4473	Femur	59.99	7.39	19.32	71.46	5.43	15.36	12.29
4503	Femur	54.67	11.20	24.92	80.92	3.62	15.28	28.98
	Metatarsal	60.59	10.10	19.28	70.97	7.37	22.45	11.18
4561	Femur	57.35	11.59	25.44	81.72	3.13	14.48	28.04
	Metatarsal	60.12	9.05	18.59	69.24	5.31	21.76	10.35

Table B-5: ATR-FTIR data from Eriswell skeletal elements

Skeleton Identification number	Skeletal element	Peak heights at designated wavenumber positions						Splitting Factor	Carbonate/ Phosphate	Amide / Phosphate
		Peak A (600)	Peak B (560)	Peak C (586)	Phosphate (1015)	Carbonate (1410)	Amide I (1642)			
0067	Femur	1.32	0.81	0.68	1.47	0.49	0.38	3.12	0.33	0.26
	Metatarsal	0.11	0.06	0.04	0.19	0.03	0.02	4.36	0.15	0.09
0145	Femur	1.45	0.89	0.70	1.78	0.53	0.33	3.35	0.30	0.19
	Metatarsal	0.07	0.04	0.03	0.10	0.03	0.02	3.79	0.25	0.18
0158	Femur	1.42	0.91	0.73	1.61	0.56	0.46	3.19	0.35	0.29
	Metatarsal	0.07	0.05	0.03	0.11	0.03	0.02	3.69	0.25	0.16
0201	Femur	1.43	0.86	0.72	1.55	0.56	0.44	3.18	0.36	0.28
	Metatarsal	0.06	0.04	0.02	0.13	0.02	0.01	4.48	0.12	0.08
0203	Femur	1.48	0.92	0.72	1.67	0.40	0.30	3.34	0.24	0.18
	Metatarsal	1.26	0.70	0.64	1.75	0.34	0.26	3.08	0.19	0.15
0235	Femur	1.54	0.93	0.70	1.82	0.36	0.10	3.53	0.20	0.05
	Metatarsal	1.53	0.94	0.74	1.81	0.44	0.13	3.32	0.24	0.07
0241	Femur	1.39	0.85	0.69	1.60	0.55	0.44	3.23	0.34	0.27
0251	Femur	1.47	0.91	0.75	1.56	0.54	0.45	3.16	0.35	0.29
	Metatarsal	1.18	0.75	0.61	1.61	0.50	0.36	3.18	0.31	0.22
0255	Femur	1.45	0.89	0.70	1.70	0.40	0.35	3.36	0.23	0.21
	Metatarsal	1.41	0.91	0.75	1.61	0.49	0.36	3.08	0.30	0.22
0259	Femur	1.34	0.83	0.67	1.59	0.54	0.45	3.21	0.34	0.28
	Metatarsal	1.04	0.67	0.54	1.57	0.54	0.43	3.17	0.34	0.27
0309	Femur	1.48	0.93	0.75	1.71	0.48	0.35	3.21	0.28	0.20
	Metatarsal	0.06	0.03	0.03	0.08	0.03	0.02	3.68	0.31	0.20
0310	Femur	1.39	0.87	0.72	1.63	0.51	0.37	3.16	0.31	0.23
0317	Femur	1.49	0.92	0.72	1.70	0.48	0.38	3.33	0.28	0.22
	Metatarsal	0.06	0.04	0.03	0.09	0.02	0.02	3.76	0.23	0.17
0318	Femur	0.26	0.15	0.12	0.30	0.06	0.02	3.46	0.21	0.05
	Metatarsal	1.39	0.85	0.66	1.79	0.43	0.11	3.40	0.24	0.06
0326	Femur	1.26	0.77	0.69	1.48	0.63	0.51	2.93	0.43	0.35
	Metatarsal	1.35	0.87	0.74	1.65	0.66	0.57	2.99	0.40	0.34
0343	Femur	1.47	0.93	0.76	1.75	0.48	0.32	3.16	0.28	0.18
	Metatarsal	1.31	0.81	0.63	1.68	0.55	0.37	3.37	0.33	0.22

Skeleton Identification number	Skeletal element	Peak heights at designated wavenumber positions						Splitting Factor	Carbonate/ Phosphate	Amide / Phosphate
		Peak A (600)	Peak B (560)	Peak C (586)	Phosphate (1015)	Carbonate (1410)	Amide I (1642)			
0346	Femur	1.38	0.91	0.78	1.62	0.62	0.48	2.95	0.39	0.30
	Metatarsal	1.18	0.65	0.56	1.78	0.33	0.22	3.26	0.19	0.12
0363	Femur	1.39	0.90	0.80	1.66	0.60	0.47	2.88	0.36	0.29
	Metatarsal	1.27	0.74	0.52	1.79	0.28	0.12	3.85	0.16	0.07
0392	Femur	1.49	0.92	0.72	1.78	0.39	0.13	3.36	0.22	0.07
	Metatarsal	1.51	0.89	0.64	1.84	0.33	0.09	3.75	0.18	0.05
0395	Femur	1.43	0.92	0.76	1.57	0.50	0.40	3.08	0.32	0.25
	Metatarsal	0.06	0.04	0.03	0.10	0.02	0.01	3.92	0.23	0.14
0425	Femur	1.51	0.95	0.75	1.80	0.44	0.16	3.28	0.24	0.09
	Metatarsal	1.16	0.71	0.50	1.76	0.36	0.17	3.70	0.20	0.10
0426	Femur	1.51	0.92	0.73	1.81	0.41	0.12	3.32	0.22	0.07
	Metatarsal	1.17	0.70	0.50	1.75	0.36	0.17	3.70	0.21	0.09
0474	Femur	1.40	0.82	0.53	1.85	0.20	0.06	4.19	0.11	0.03
0554	Femur	1.37	0.82	0.57	1.84	0.27	0.10	3.84	0.15	0.05
0570	Metatarsal	0.02	0.01	0.01	0.04	0.02	0.01	3.80	0.39	0.20
0571	Metatarsal	0.10	0.06	0.04	0.17	0.02	0.02	4.32	0.14	0.11
0580	Femur	1.49	0.91	0.68	1.81	0.32	0.10	3.54	0.18	0.05
	Metatarsal	1.41	0.82	0.60	1.82	0.31	0.10	3.74	0.17	0.06
0612	Femur	1.37	0.91	0.77	1.60	0.61	0.47	2.96	0.38	0.29
	Metatarsal	0.04	0.02	0.02	0.06	0.04	0.01	3.50	0.72	0.10
0692	Femur	1.33	0.85	0.72	1.49	0.58	0.44	3.01	0.39	0.29
	Metatarsal	0.07	0.04	0.03	0.10	0.06	0.01	3.26	0.62	0.13
0717	Femur	1.47	0.88	0.68	1.77	0.40	0.12	3.44	0.23	0.07
	Metatarsal	0.11	0.06	0.05	0.17	0.08	0.02	3.72	0.49	0.09
0759	Femur	1.49	0.91	0.70	1.79	0.37	0.12	3.44	0.21	0.06
	Metatarsal	1.15	0.69	0.57	1.67	0.60	0.19	3.22	0.36	0.11
0791	Femur	1.47	0.87	0.66	1.77	0.39	0.10	3.57	0.22	0.06
	Metatarsal	1.14	0.66	0.48	1.72	0.45	0.17	3.76	0.26	0.10
0799	Femur	1.48	0.92	0.72	1.79	0.47	0.14	3.33	0.26	0.08
	Metatarsal	1.23	0.73	0.55	1.74	0.49	0.13	3.56	0.28	0.07
0808	Femur	1.58	0.94	0.65	1.98	0.30	0.14	3.91	0.15	0.07
	Metatarsal	1.17	0.70	0.55	1.67	0.39	0.20	3.43	0.23	0.12

Skeleton Identification number	Skeletal element	Peak heights at designated wavenumber positions						Splitting Factor	Carbonate/ Phosphate	Amide / Phosphate
		Peak A (600)	Peak B (560)	Peak C (586)	Phosphate (1015)	Carbonate (1410)	Amide I (1642)			
0809	Femur	1.41	0.89	0.71	1.63	0.43	0.35	3.27	0.27	0.21
	Metatarsal	0.05	0.03	0.02	0.11	0.04	0.02	4.00	0.32	0.14
0851	Femur	1.51	0.95	0.76	1.73	0.53	0.39	3.23	0.30	0.23
	Metatarsal	1.08	0.65	0.50	1.59	0.56	0.32	3.46	0.35	0.20
0888	Femur	1.34	0.84	0.68	1.50	0.59	0.47	3.21	0.39	0.31
0907	Femur	1.34	0.83	0.65	1.75	0.42	0.14	3.33	0.24	0.08
0991	Femur	1.39	0.85	0.72	1.62	0.59	0.48	3.12	0.36	0.30
	Metatarsal	1.08	0.68	0.51	1.60	0.45	0.31	3.47	0.28	0.19
0994	Femur	1.38	0.86	0.74	1.57	0.57	0.44	3.04	0.36	0.28
	Metatarsal	0.05	0.05	0.03	0.15	0.03	0.02	3.06	0.18	0.10
4040	Femur	1.33	0.84	0.71	1.58	0.62	0.48	3.08	0.39	0.30
	Metatarsal	1.20	0.72	0.62	1.55	0.74	0.45	3.11	0.48	0.29
4046	Femur	1.46	0.90	0.64	1.82	0.28	0.10	3.69	0.16	0.06
	Metatarsal	1.31	0.78	0.53	1.80	0.31	0.13	3.96	0.17	0.07
4067	Femur	1.35	0.85	0.71	1.57	0.62	0.50	3.09	0.40	0.32
	Metatarsal	1.15	0.75	0.53	1.65	0.40	0.34	3.61	0.24	0.20
4077	Femur	1.45	0.89	0.71	1.79	0.46	0.15	3.29	0.26	0.08
	Metatarsal	0.08	0.05	0.04	0.10	0.06	0.01	3.66	0.58	0.14
4095	Femur	1.44	0.91	0.70	1.78	0.45	0.17	3.34	0.25	0.10
4098	Femur	1.54	0.99	0.77	1.79	0.46	0.15	3.30	0.26	0.08
4099	Femur	1.48	0.94	0.75	1.76	0.52	0.16	3.21	0.29	0.09
	Metatarsal	1.20	0.74	0.58	1.73	0.49	0.16	3.36	0.29	0.09
4127	Metatarsal	1.23	0.75	0.49	1.78	0.28	0.13	4.05	0.16	0.07
4191	Femur	1.36	0.80	0.52	1.83	0.21	0.08	4.15	0.11	0.04
4222	Femur	0.15	0.10	0.08	0.18	0.05	0.02	3.28	0.25	0.08
	Sternum	0.03	0.02	0.01	0.09	0.02	0.01	4.15	0.24	0.11
4226	Femur	1.37	0.91	0.76	1.53	0.63	0.51	3.00	0.41	0.33
	Metatarsal	0.04	0.02	0.02	0.07	0.03	0.01	3.67	0.38	0.14
4288	Femur	1.47	0.91	0.60	1.75	0.30	0.22	3.94	0.17	0.12
	Metatarsal	0.07	0.04	0.03	0.13	0.02	0.01	4.50	0.13	0.11
4291	Femur	1.56	0.87	0.61	1.84	0.32	0.11	3.99	0.17	0.06
4295	Femur	1.42	0.92	0.76	1.49	0.52	0.47	3.09	0.35	0.31

Skeleton Identification number	Skeletal element	Peak heights at designated wavenumber positions						Splitting Factor	Carbonate/ Phosphate	Amide / Phosphate
		Peak A (600)	Peak B (560)	Peak C (586)	Phosphate (1015)	Carbonate (1410)	Amide I (1642)			
4340	Femur	1.43	0.91	0.73	1.73	0.54	0.42	3.21	0.31	0.24
	Metatarsal	0.10	0.06	0.04	0.15	0.02	0.02	4.13	0.15	0.13
4411	Femur	1.45	0.91	0.70	1.69	0.45	0.35	3.40	0.27	0.21
4462	Femur	1.46	0.92	0.71	1.63	0.45	0.38	3.34	0.28	0.23
	Metatarsal	1.32	0.82	0.59	1.76	0.34	0.24	3.63	0.19	0.14
4473	Femur	1.41	0.84	0.59	1.85	0.34	0.11	3.80	0.19	0.06
4503	Femur	1.45	0.80	0.49	1.88	0.20	0.06	4.63	0.11	0.03
	Metatarsal	1.26	0.73	0.48	1.82	0.25	0.12	4.16	0.14	0.06
4561	Femur	1.55	0.95	0.77	1.87	0.49	0.13	3.26	0.26	0.07
	Metatarsal	1.24	0.74	0.56	1.75	0.41	0.15	3.49	0.23	0.09

Table B-6: XRF data from Eriswell skeletal elements

Sample name	Test number	Element peak height in cps												
		Si	P	Ca	Ti	Fe	Mn	Cu	Zn	Sr	Zr	Cr	Ni	K
0570 Femur	1	396.37	6533.63	78597.60	20.99	161.03	199.65	270.22	275.83	243.13	34.78	107.59	985.32	625.24
	2	420.32	6541.68	77929.19	20.78	267.45	246.56	372.52	339.97	246.05	29.20	130.67	1075.04	611.43
	3	372.22	6511.26	78583.05	14.61	139.37	183.85	233.12	237.24	213.58	10.39	99.48	952.20	600.65
	Average	396.30	6528.86	78369.95	18.79	189.28	210.02	291.95	284.34	234.26	24.79	112.58	1004.19	612.44
	s.d.	24.05	15.76	381.78	3.62	68.55	32.62	72.20	51.89	17.96	12.78	16.18	63.56	12.33
0809 Femur	1	364.40	6350.33	76145.54	16.37	318.42	278.50	350.03	316.57	223.74	24.43	146.48	1099.54	589.00
	2	380.82	6341.30	75625.40	19.86	293.09	304.30	336.65	291.06	224.50	61.11	122.35	1050.09	602.59
	3	363.45	6675.59	78881.12	15.87	352.41	313.75	450.87	427.62	247.22	54.93	149.67	1202.51	615.51
	Average	369.56	6455.74	76884.02	17.36	321.30	298.85	379.18	345.08	231.82	46.82	139.50	1117.38	602.37
	s.d.	9.76	190.45	1748.98	2.17	29.77	18.25	62.44	72.61	13.34	19.63	14.93	77.76	13.26
4226 Femur	1	385.49	6498.71	77240.91	12.87	195.56	226.50	284.99	257.49	396.32	46.24	112.28	1000.39	599.90
	2	380.27	6492.86	78349.58	13.03	347.56	442.97	399.44	604.48	449.67	75.77	134.64	1100.33	610.79
	3	366.14	6622.47	78446.28	19.57	330.87	520.69	382.05	549.53	414.67	60.88	123.80	1117.26	606.66
	Average	377.30	6538.01	78012.26	15.15	291.33	396.72	355.49	470.50	420.22	60.96	123.57	1072.66	605.78
	s.d.	10.01	73.20	669.75	3.82	83.36	152.45	61.68	186.50	27.10	14.77	11.18	63.16	5.50
0570 Metatarsal	1	1163.25	4075.56	62386.35	327.55	5171.43	805.87	509.97	623.79	335.29	1367.88	90.16	952.53	952.93
	2	934.18	4124.31	63625.82	169.78	3780.65	930.61	650.27	836.55	382.18	1634.62	175.12	1071.47	858.35
	3	1298.06	4338.79	64776.28	818.17	5240.28	882.14	563.69	662.17	333.94	454.89	163.46	1011.42	1025.49
	Average	1131.83	4179.55	63596.15	438.50	4730.79	872.87	574.64	707.50	350.47	1152.46	142.91	1011.81	945.59
	s.d.	183.96	140.04	1195.24	338.13	823.56	62.89	70.79	113.40	27.47	618.67	46.06	59.47	83.81
0809 Metatarsal	1	1185.18	3835.28	63350.48	173.19	6265.94	501.22	580.02	629.77	321.95	1365.95	150.07	944.98	936.63
	2	1092.37	4038.53	65013.69	199.31	5629.47	627.04	611.34	687.97	293.35	434.17	184.90	1063.15	951.29
	3	1081.87	3888.84	64850.04	178.85	6163.95	709.68	724.43	764.76	355.71	442.82	189.80	1164.71	970.42
	Average	1119.81	3920.88	64404.74	183.78	6019.79	612.65	638.60	694.17	323.67	747.65	174.92	1057.61	952.78
	s.d.	56.86	105.35	916.67	13.74	341.85	104.97	75.97	67.71	31.22	535.48	21.66	109.97	16.94
4226 Metatarsal	1	960.05	4053.89	66724.11	153.59	3613.46	859.08	334.95	570.26	428.20	156.66	118.08	769.92	829.03
	2	365.35	6478.47	78339.71	3.29	320.12	424.07	320.72	518.97	416.61	38.29	124.25	1042.60	594.80
	3	796.79	4471.51	68697.04	128.12	2776.42	831.35	351.81	550.31	402.56	88.08	113.57	826.33	767.49
	Average	707.40	5001.29	71253.62	95.00	2236.67	704.83	335.83	546.51	415.79	94.34	118.63	879.62	730.44
	s.d.	307.26	1296.20	6215.51	80.44	1711.73	243.55	15.56	25.86	12.84	59.43	5.36	143.94	121.43

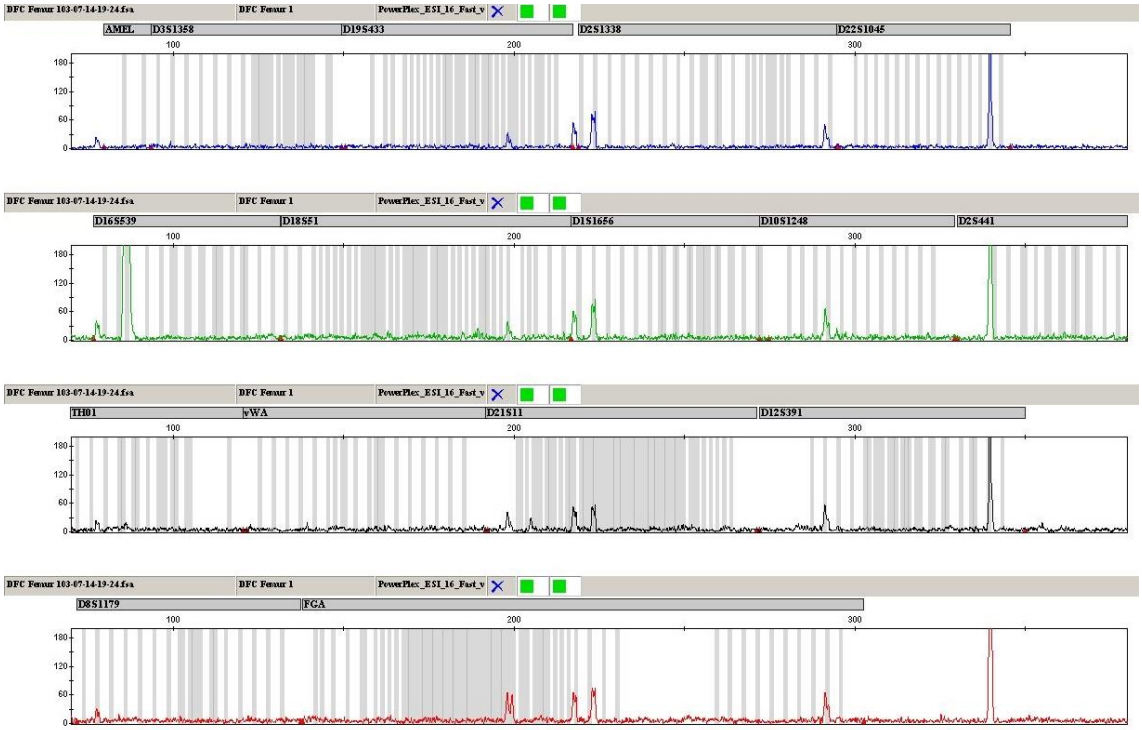

Figure B-1: Fin Cop Skeleton 1 demineralised femur electropherogram

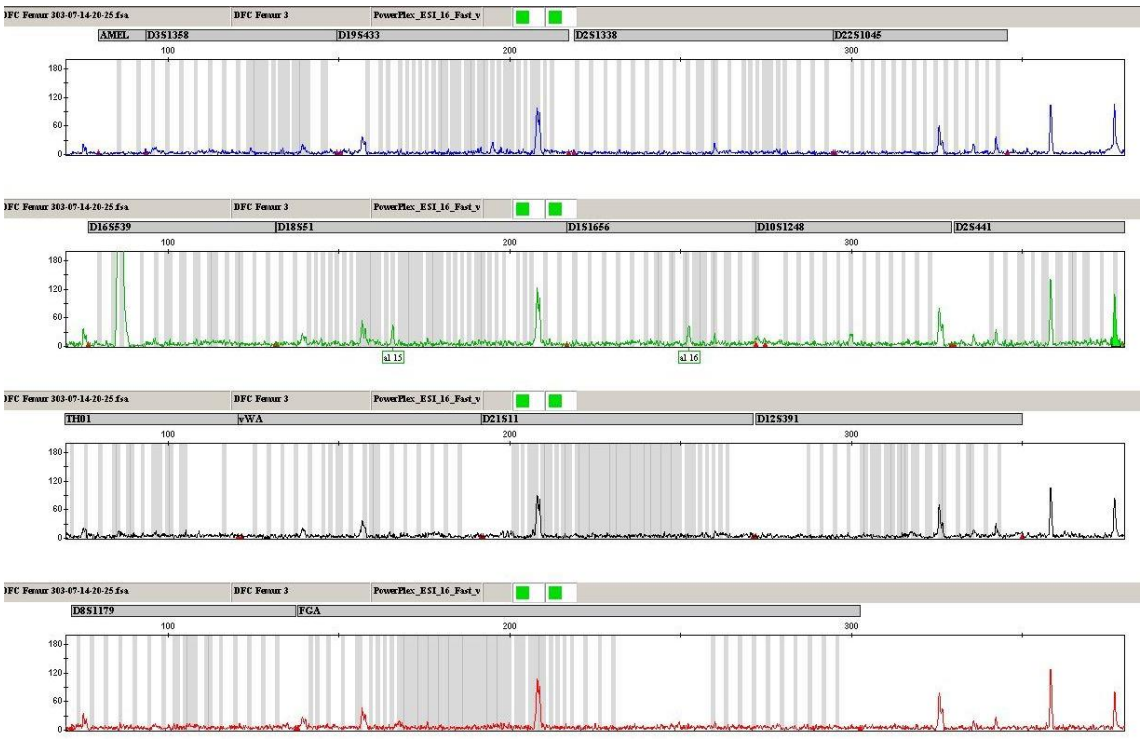

Figure B-2: Fin Cop Skeleton 3 demineralised femur electropherogram

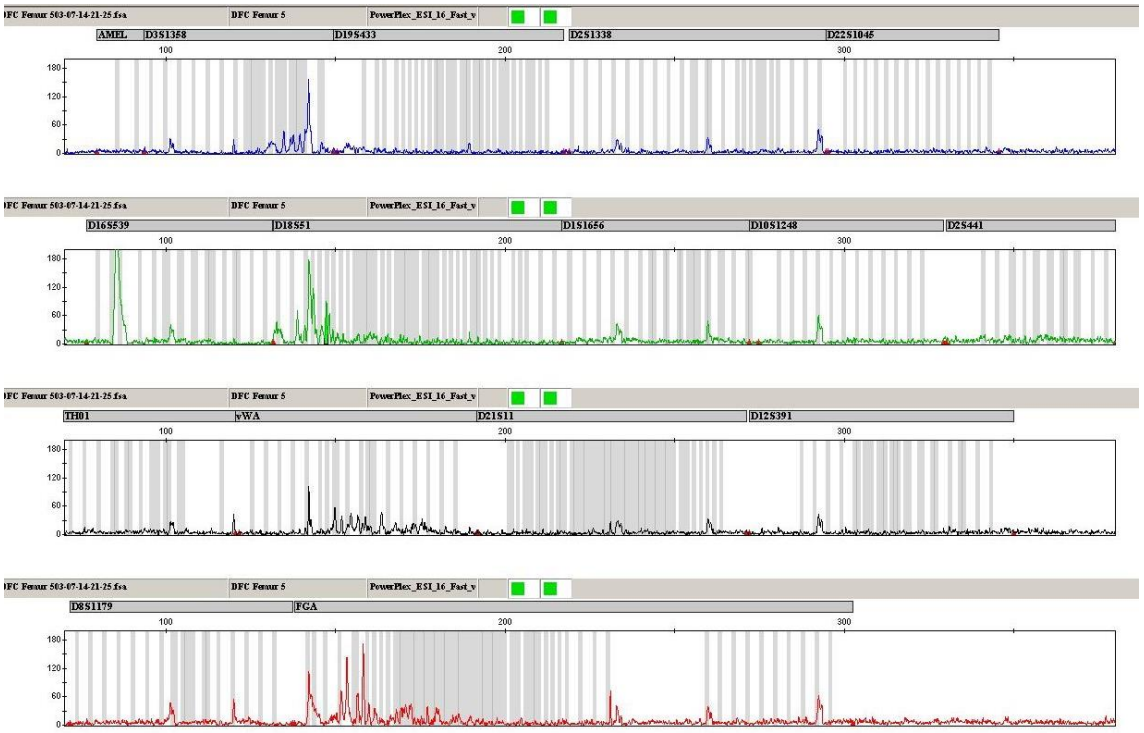

Figure B-3: Fin Cop Skeleton 5 demineralised femur electropherogram

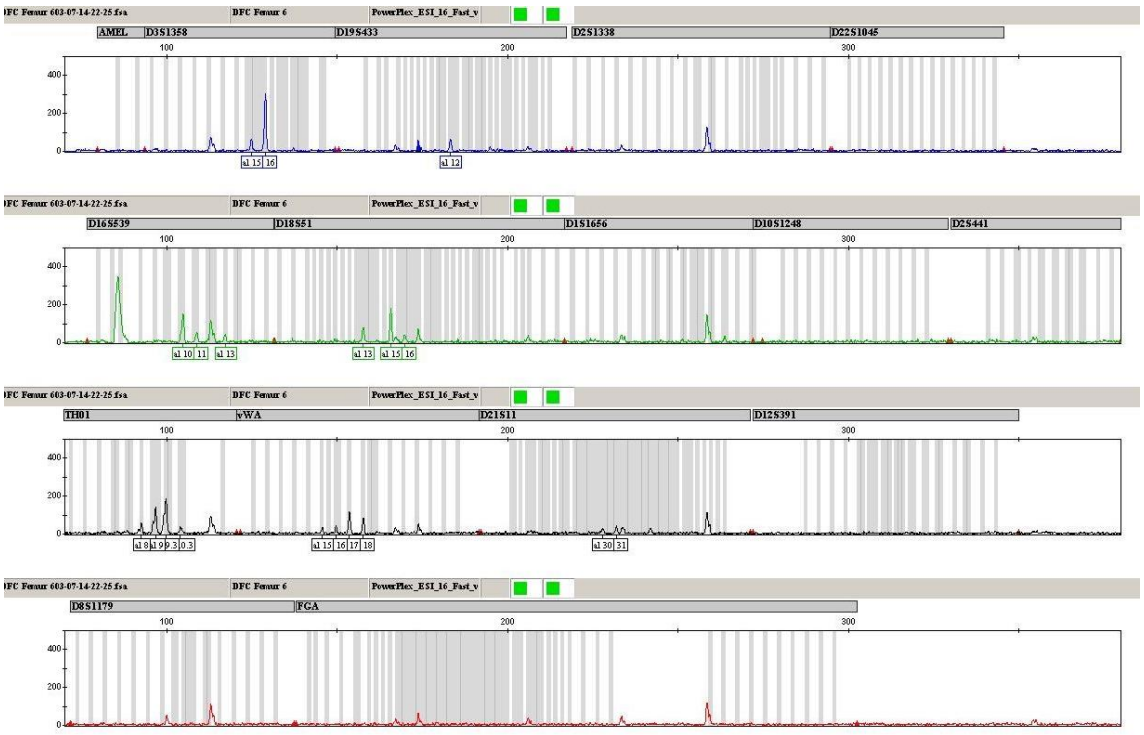

Figure B-4: Fin Cop Skeleton 6 demineralised femur electropherogram

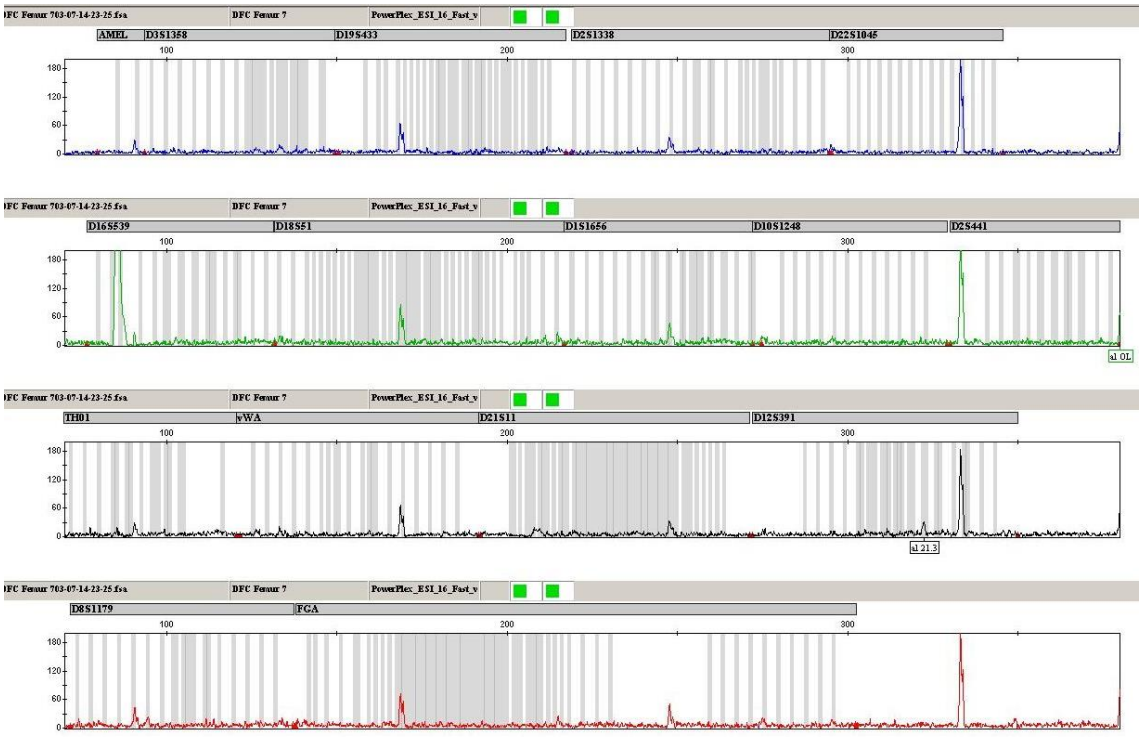

Figure B-5: Fin Cop Skeleton 7 demineralised femur electropherogram

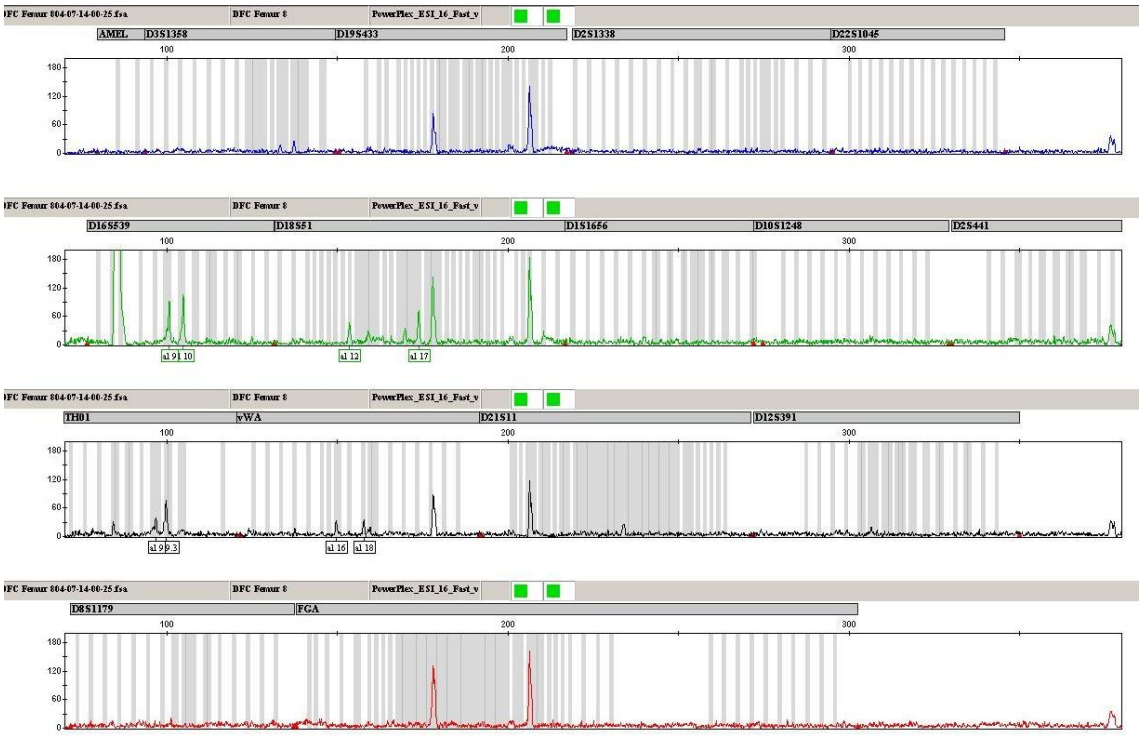

Figure B-6: Fin Cop Skeleton 8 demineralised femur electropherogram

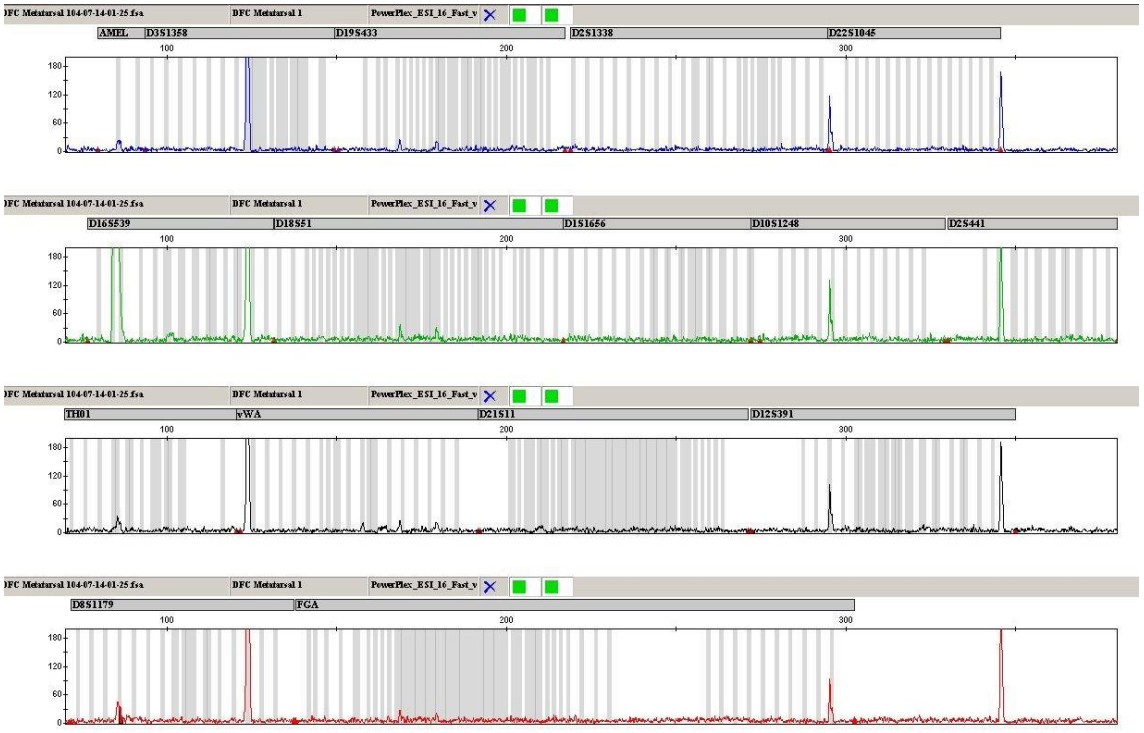

Figure B-7: Fin Cop Skeleton 1 demineralised metatarsal electropherogram

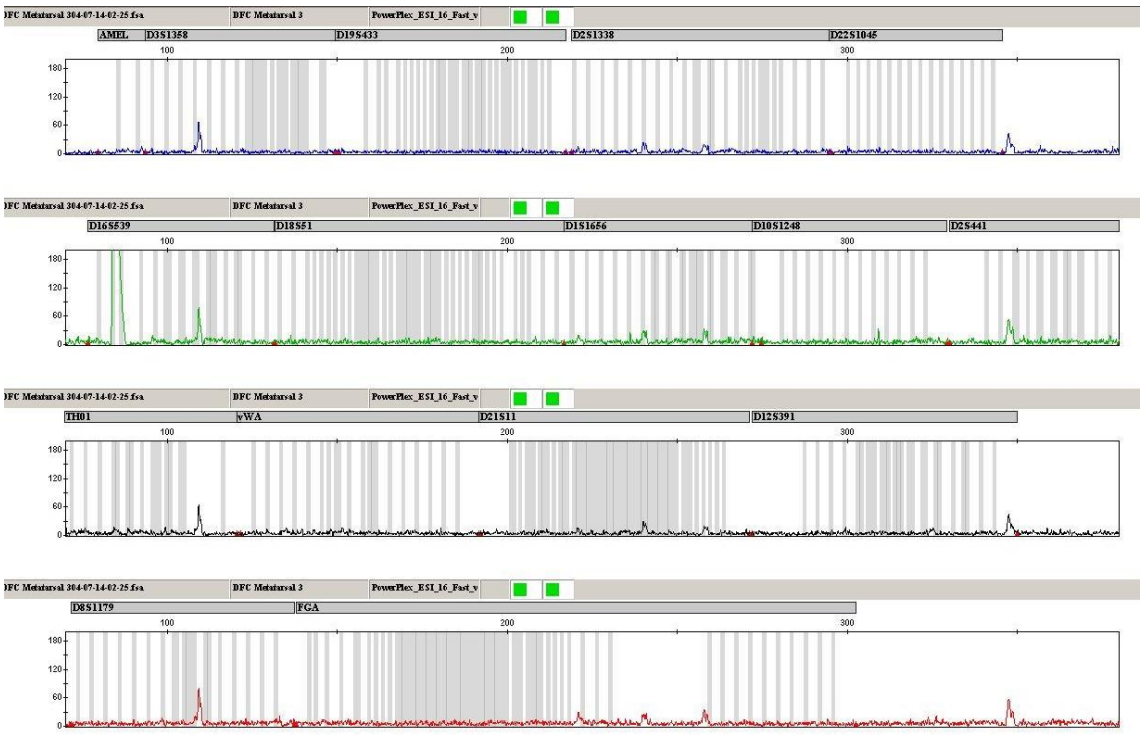

Figure B-8: Fin Cop Skeleton 3 demineralised metatarsal electropherogram

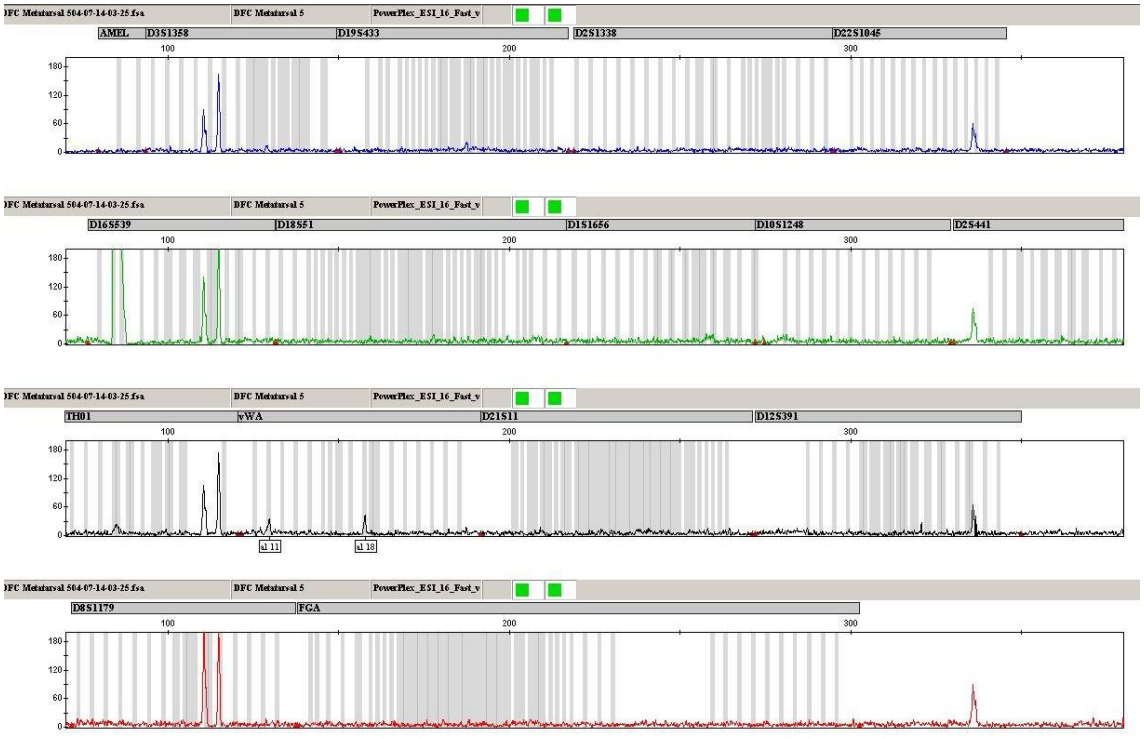

Figure B-9: Fin Cop Skeleton 5 demineralised metatarsal electropherogram

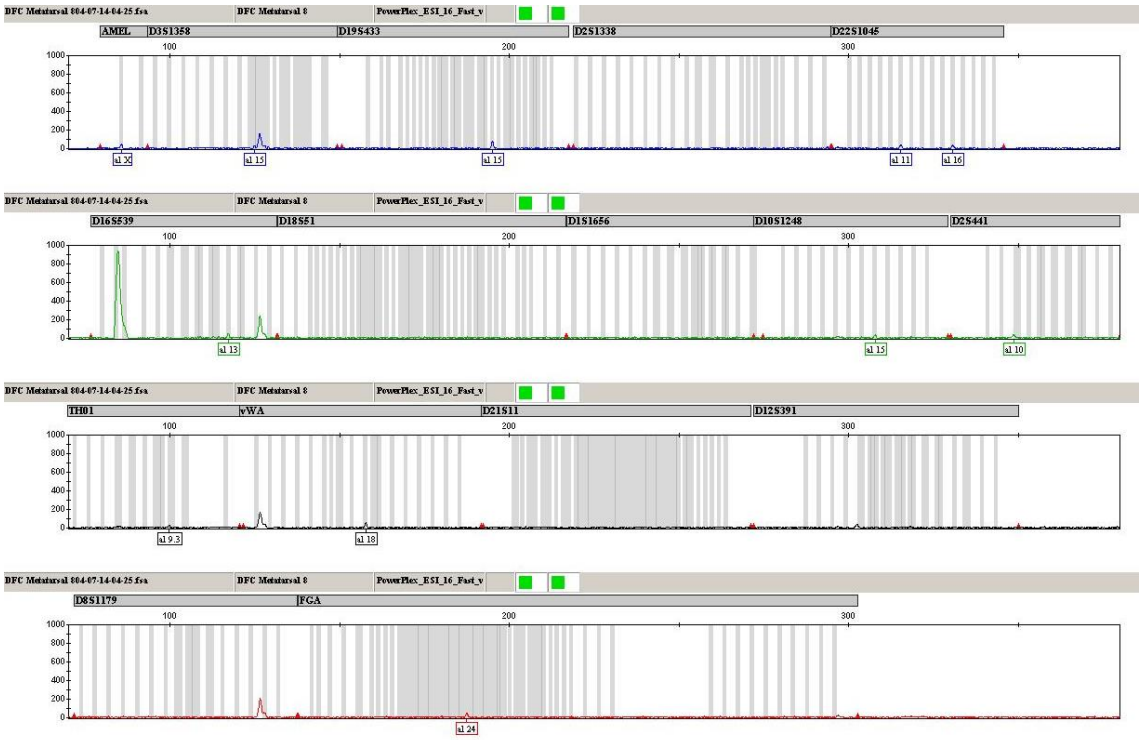

Figure B-10: Fin Cop Skeleton 8 demineralised metatarsal electropherogram

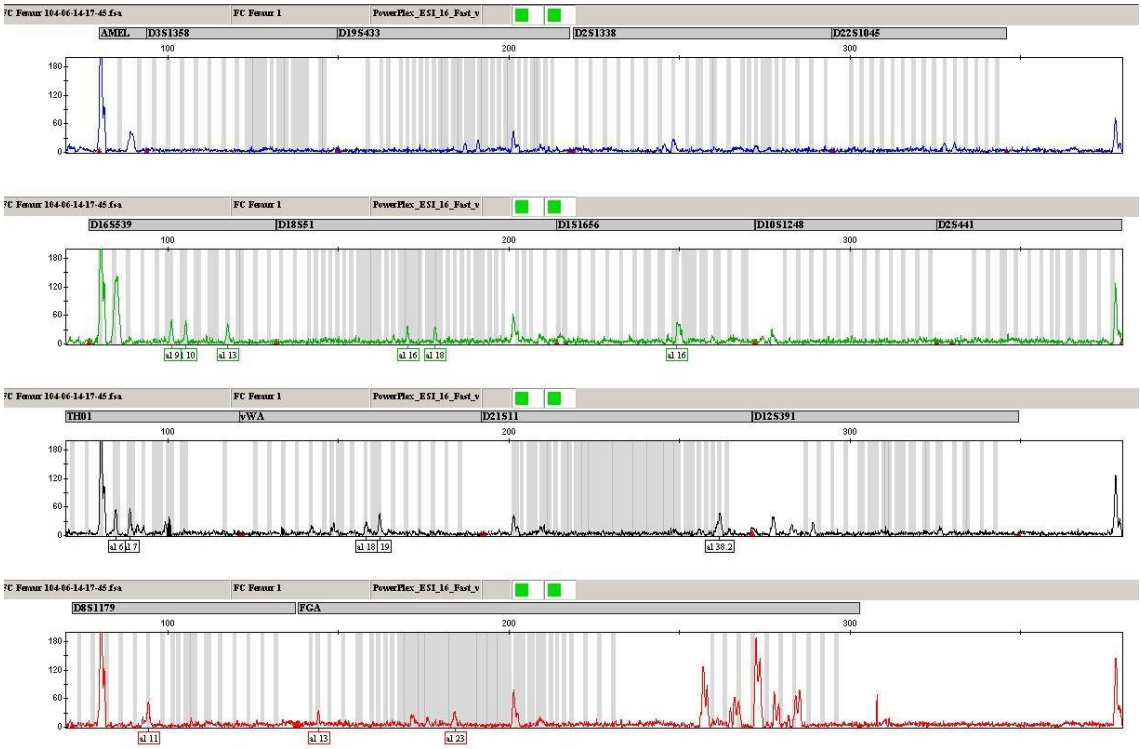

Figure B-11: Fin Cop Skeleton 1 femur electropherogram

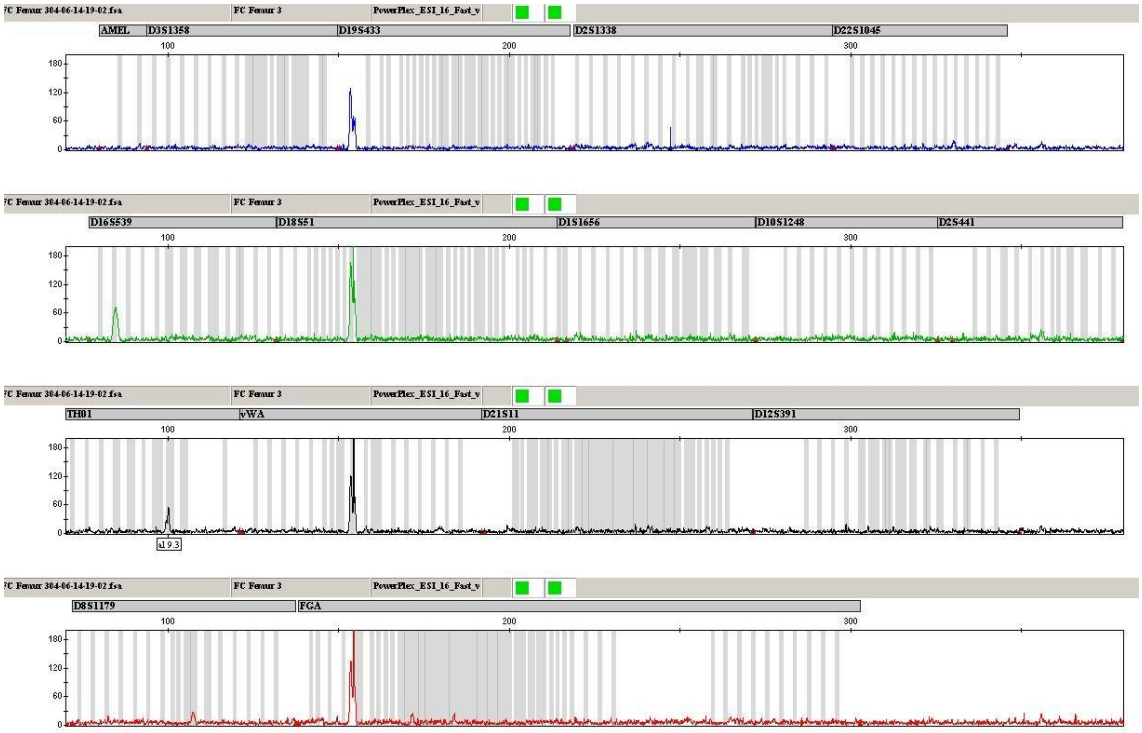

Figure B-12: Fin Cop Skeleton 3 femur electropherogram

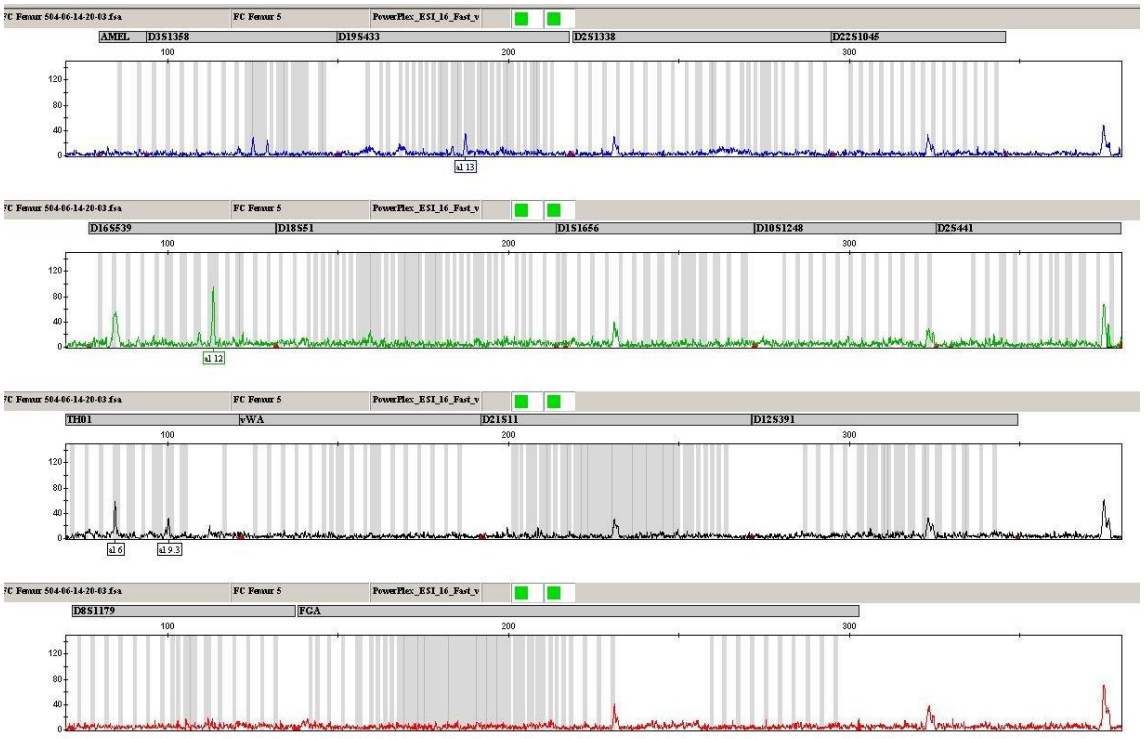

Figure B-13: Fin Cop Skeleton 5 femur electropherogram

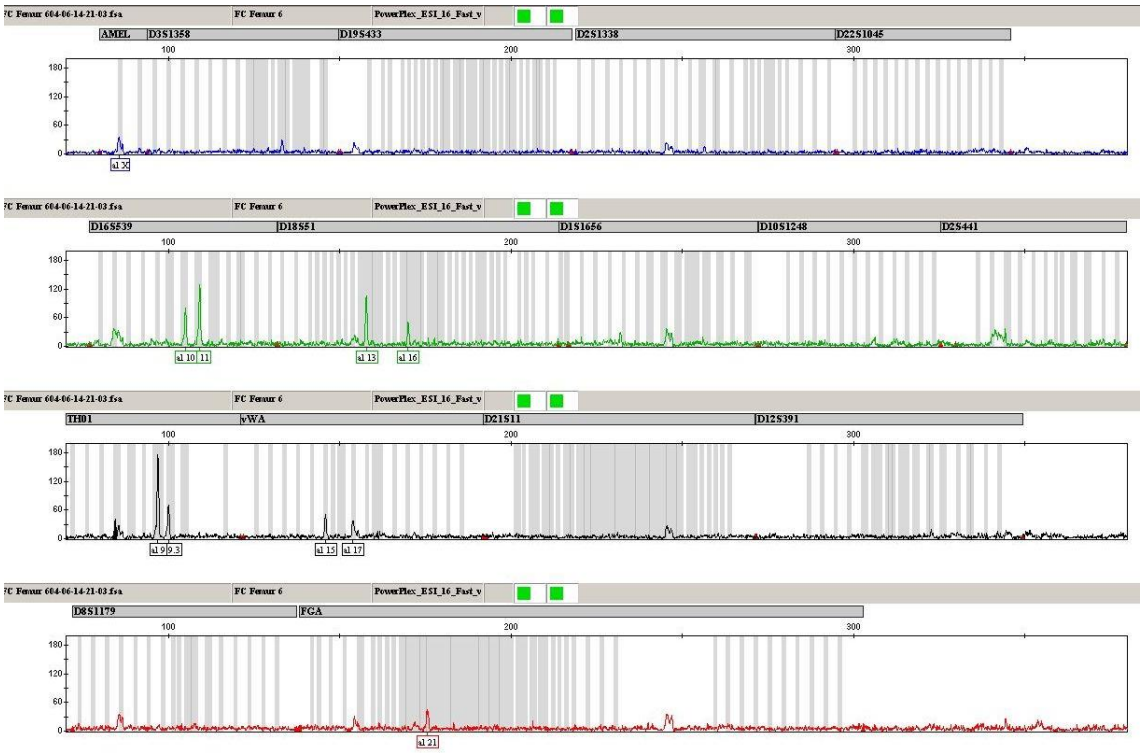

Figure B-14: Fin Cop Skeleton 6 femur electropherogram

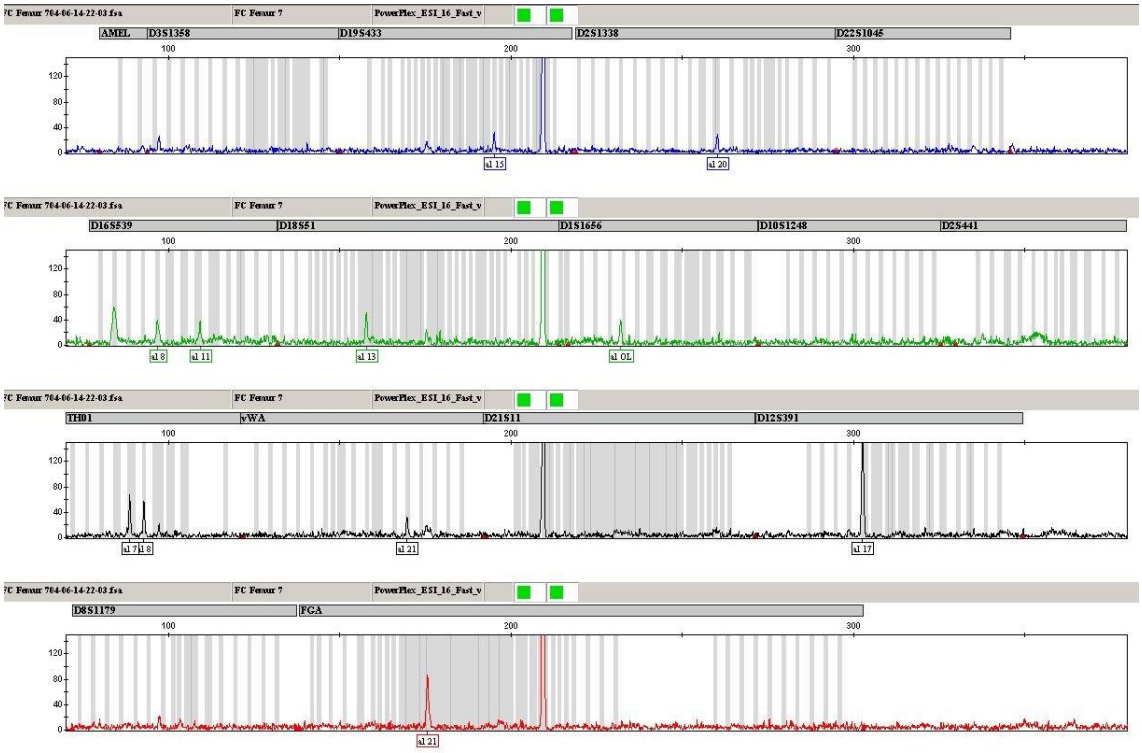

Figure B-15: Fin Cop Skeleton 7 femur electropherogram

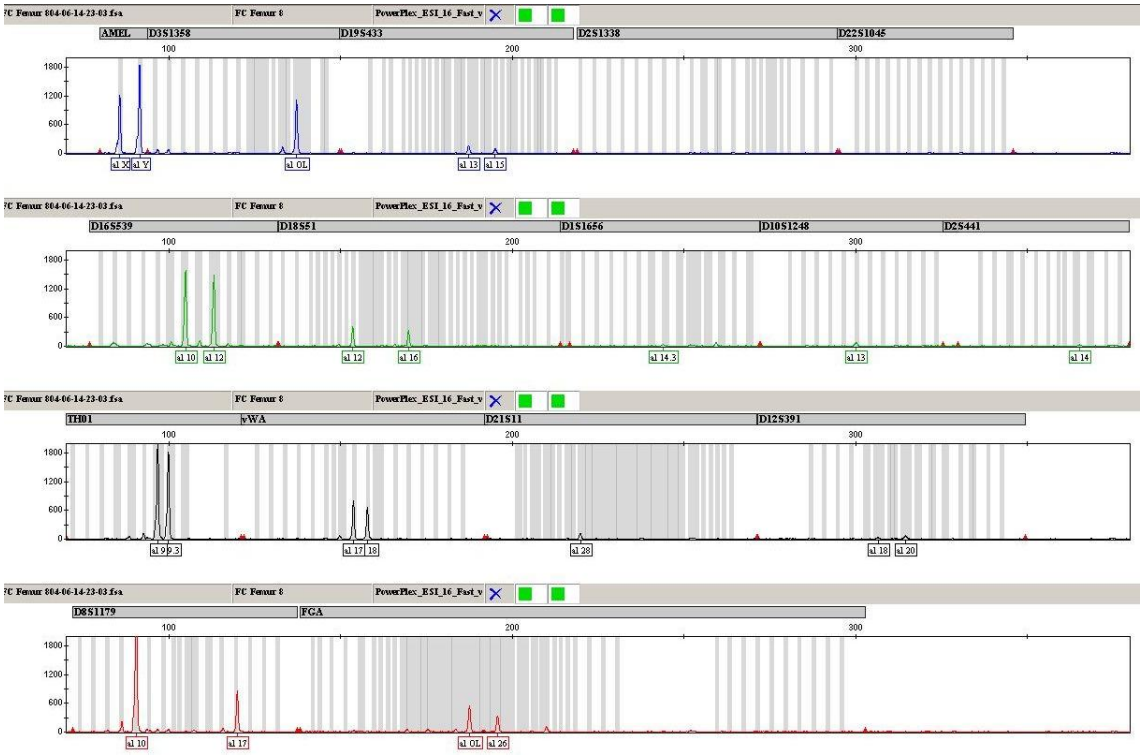

Figure B-16: Fin Cop Skeleton 8 femur electropherogram

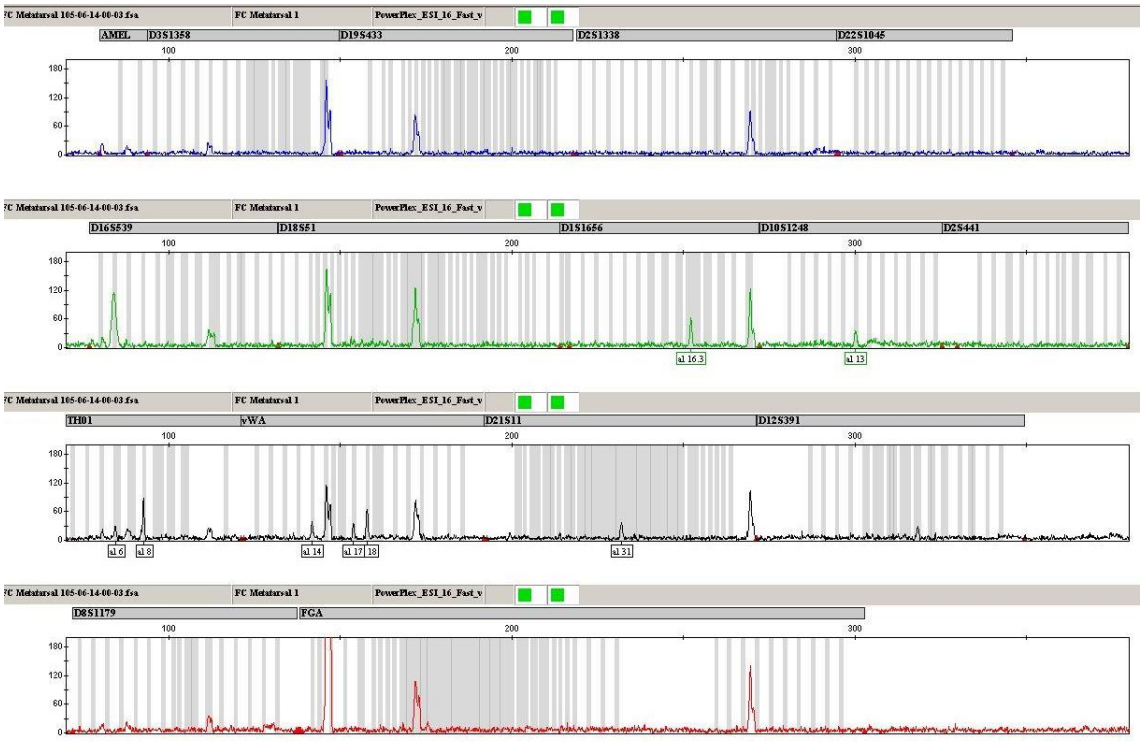

Figure B-17: Fin Cop Skeleton 1 metatarsal electropherogram

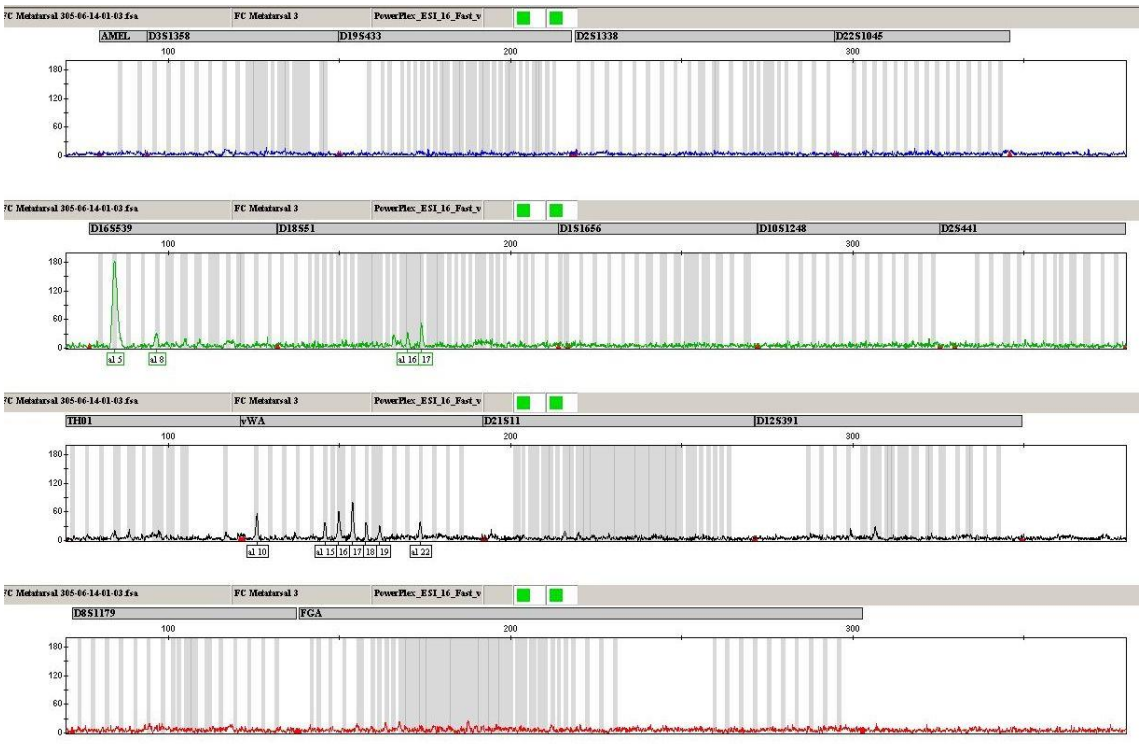

Figure B-18: Fin Cop Skeleton 3 metatarsal electropherogram

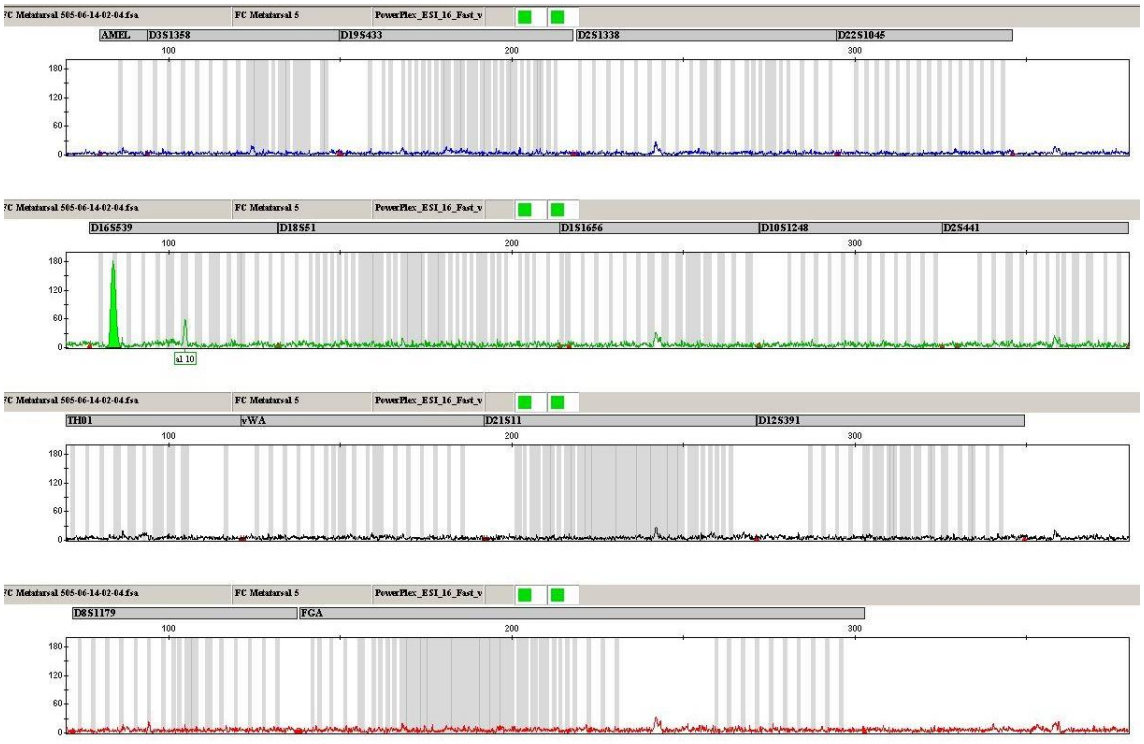

Figure B-19: Fin Cop Skeleton 5 metatarsal electropherogram

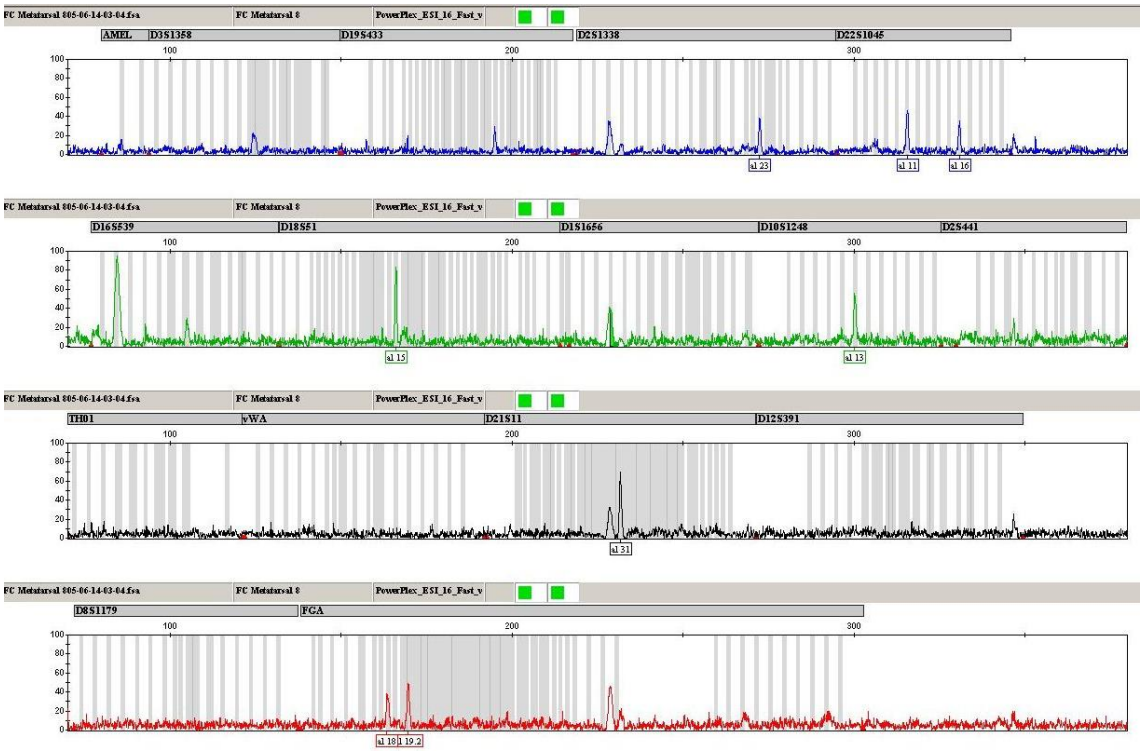

Figure B-20: Fin Cop Skeleton 8 metatarsal electropherogram

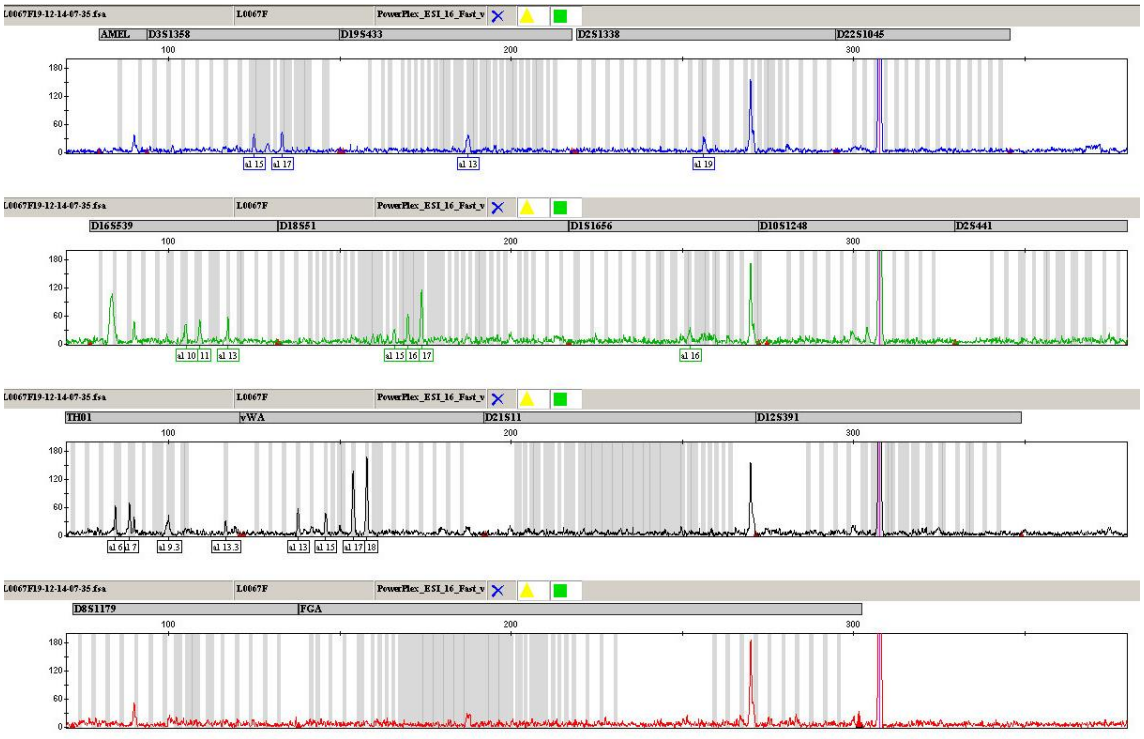

Figure B-21: Eriswell Skeleton 0067 femur electropherogram

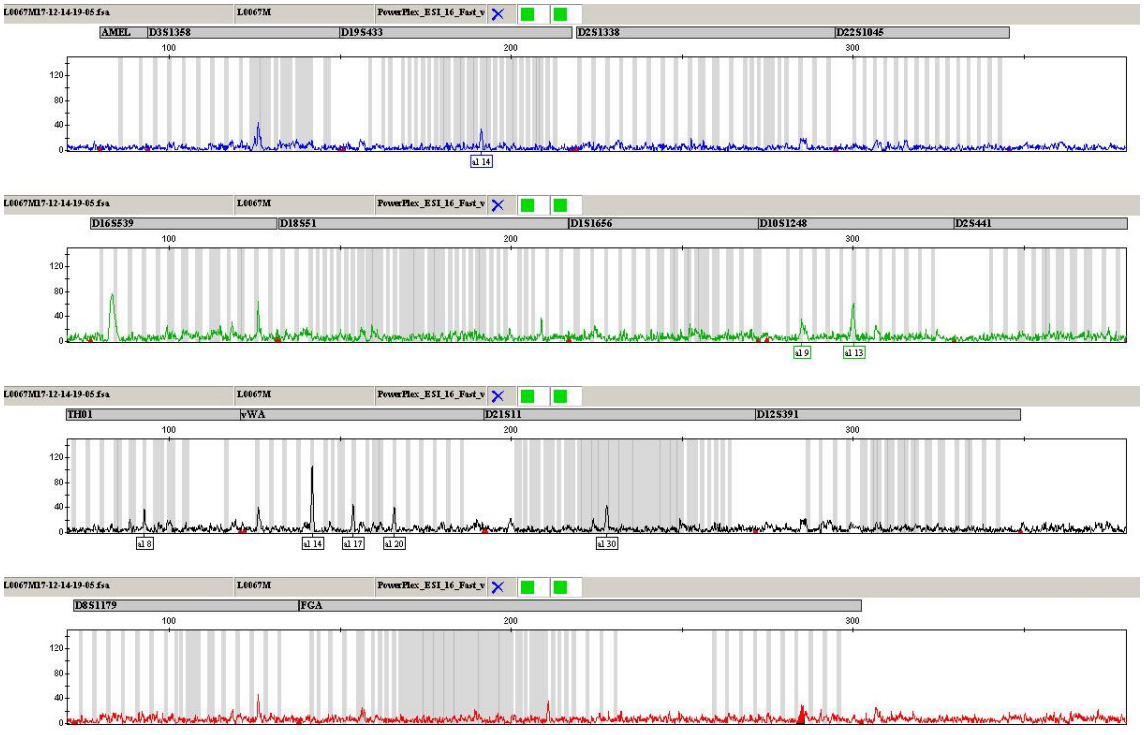

Figure B-22: Eriswell Skeleton 0067 metatarsal electropherogram

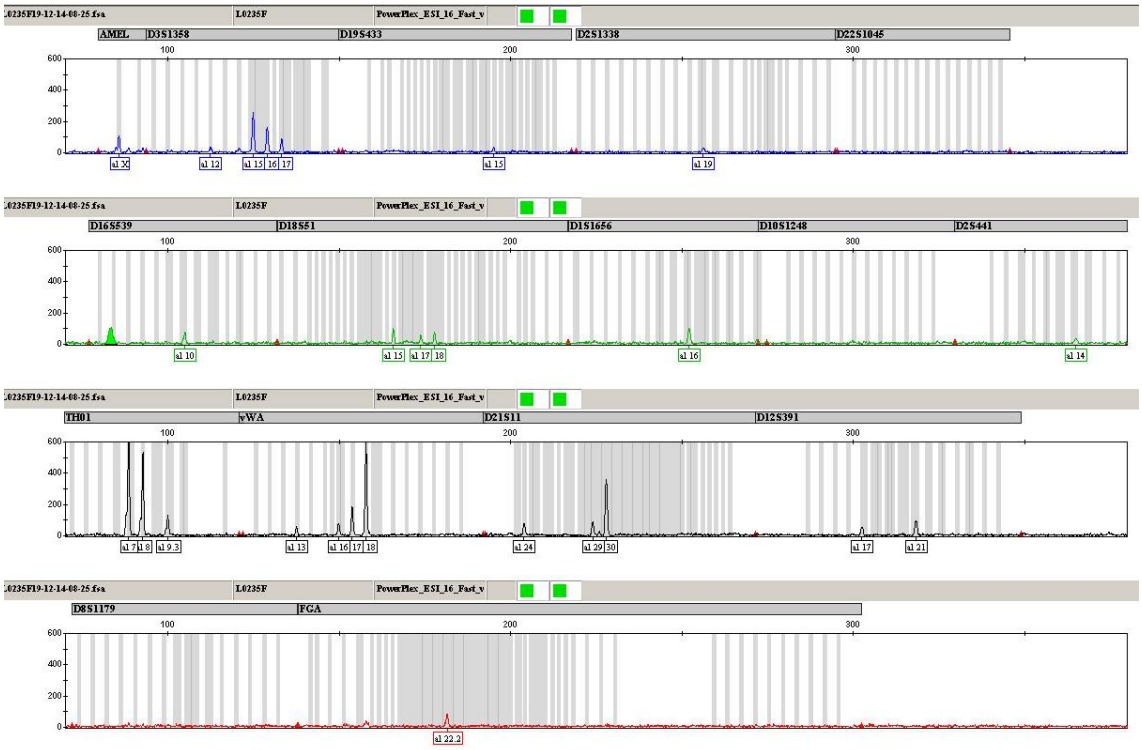

Figure B-23: Eriswell Skeleton 0235 femur electropherogram

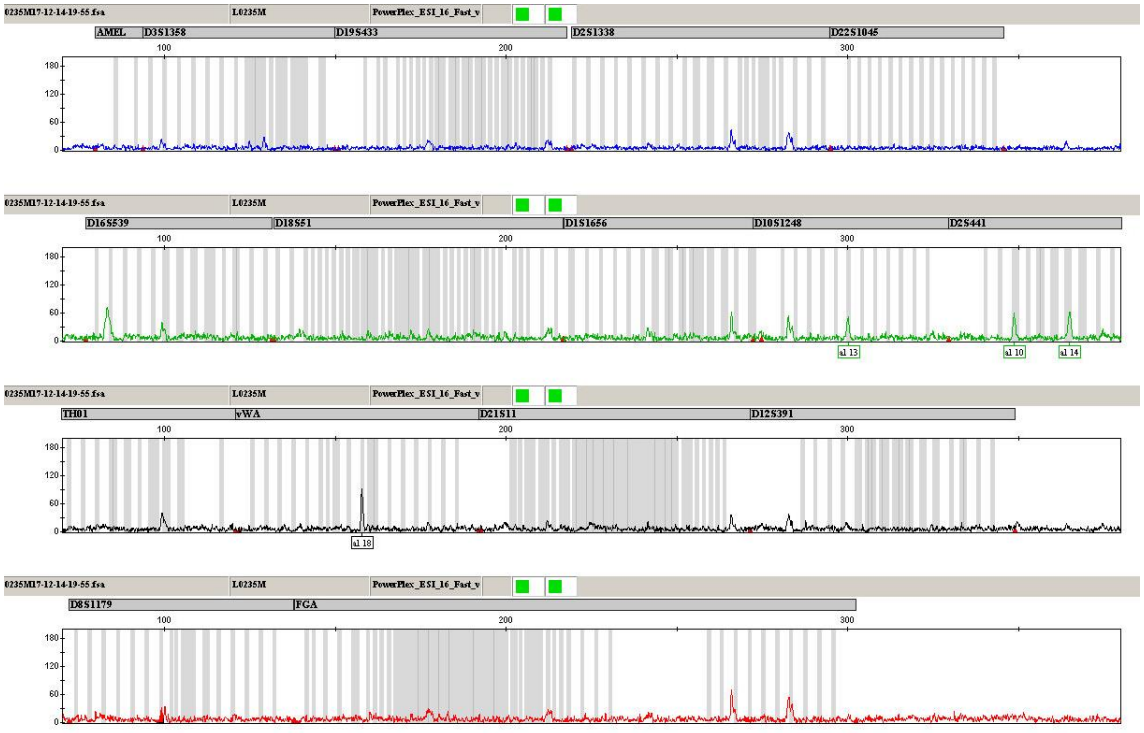

Figure B-24: Eriswell Skeleton 0235 metatarsal electropherogram

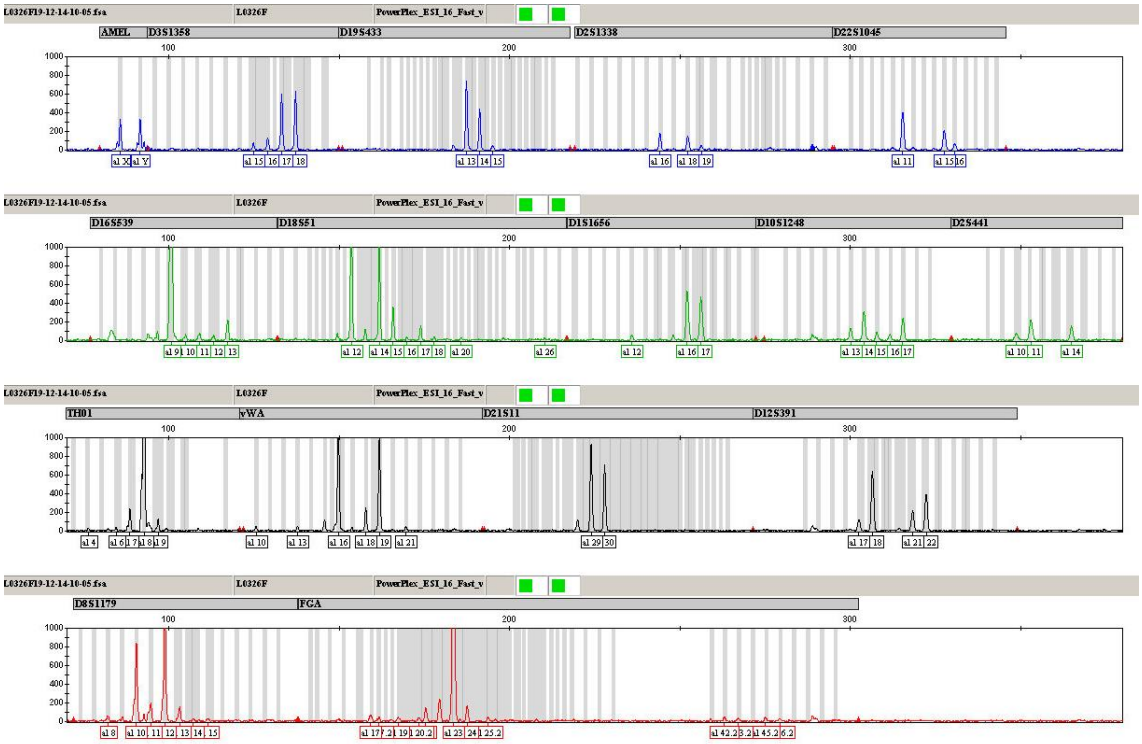

Figure B-25: Eriswell Skeleton 0326 femur electropherogram

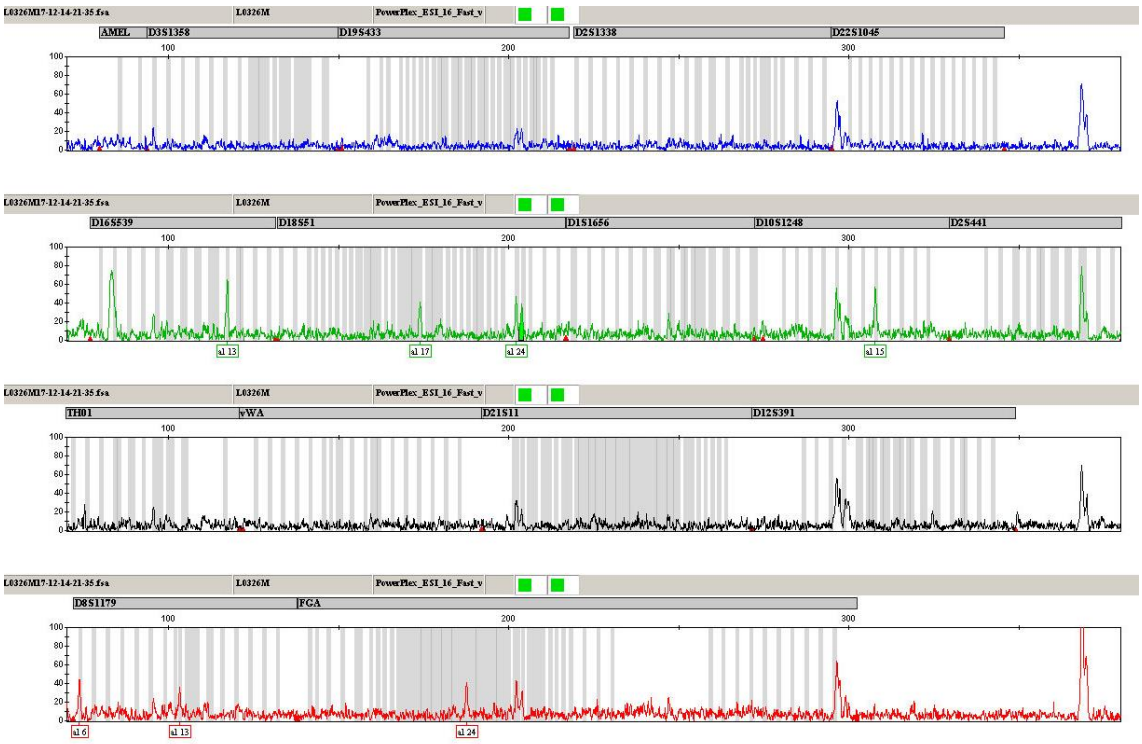

Figure B-26: Eriswell Skeleton 0326 metatarsal electropherogram

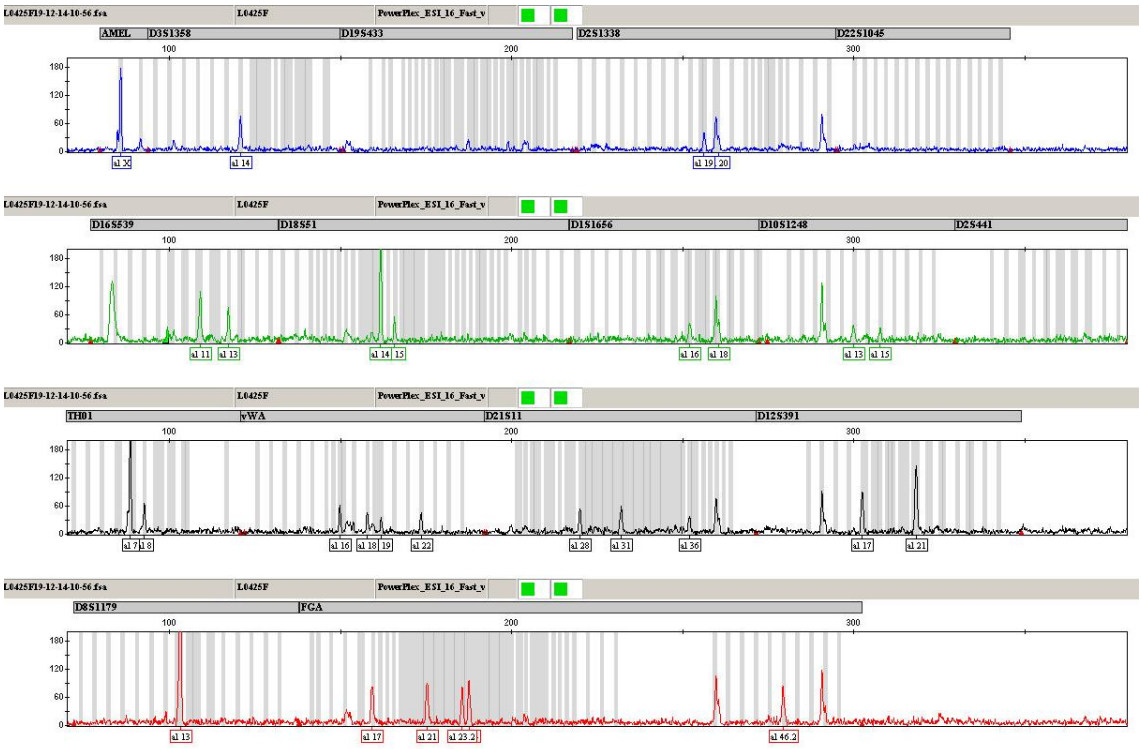

Figure B-27: Eriswell Skeleton 0425 femur electropherogram

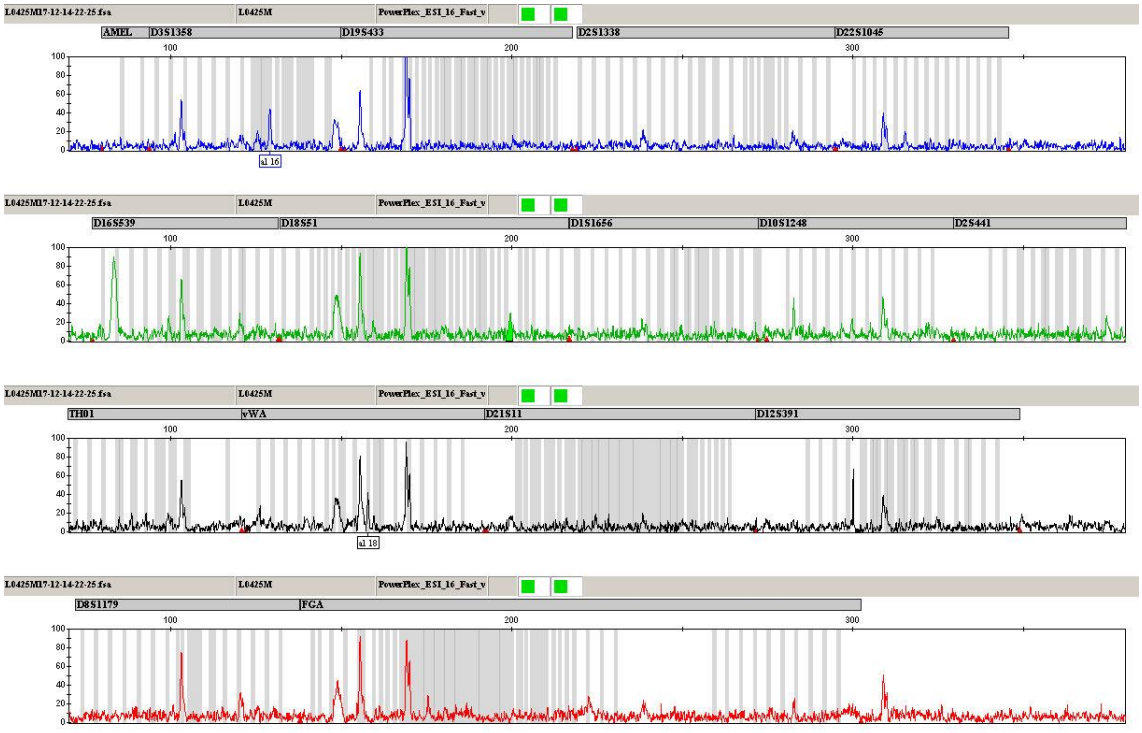

Figure B-28: Eriswell Skeleton 0425 metatarsal electropherogram

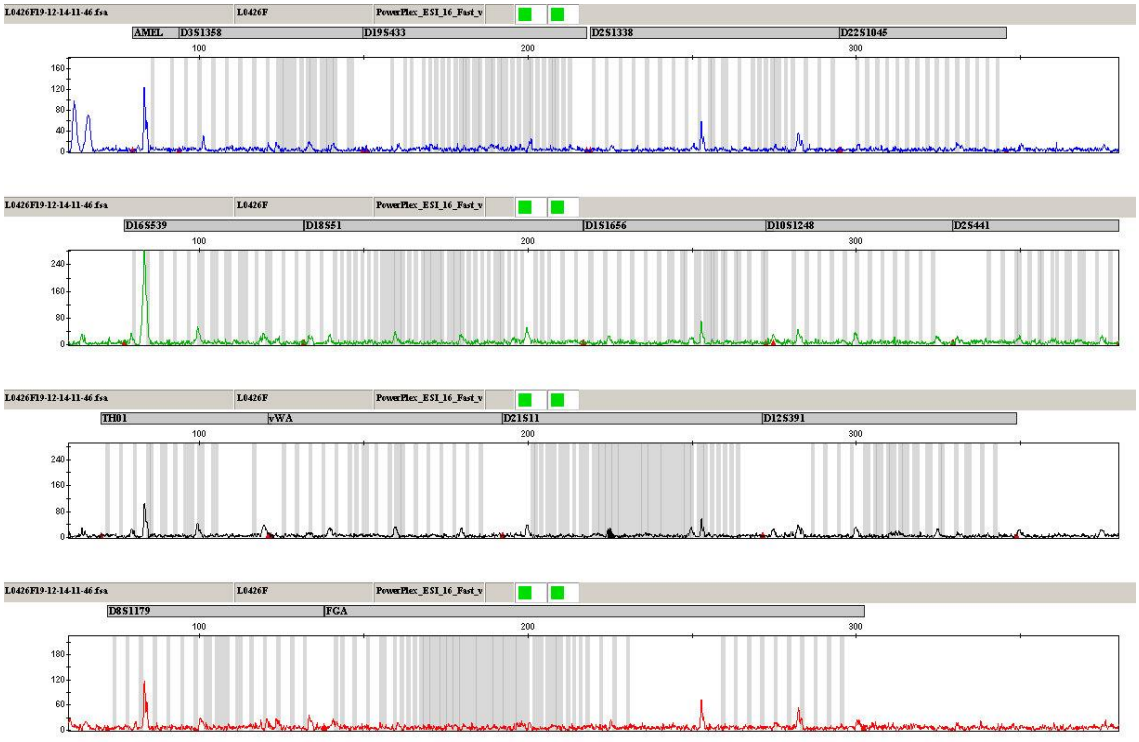

Figure B-29: Eriswell Skeleton 0426 femur electropherogram

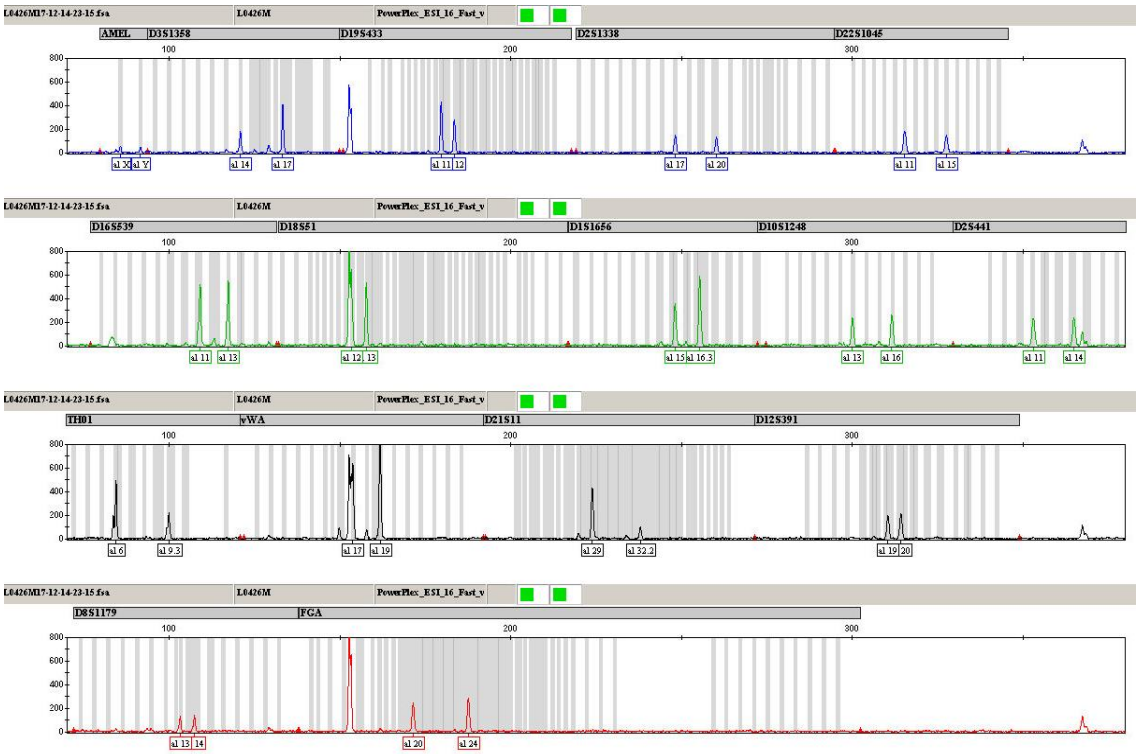

Figure B-30: Eriswell Skeleton 0426 metatarsal electropherogram

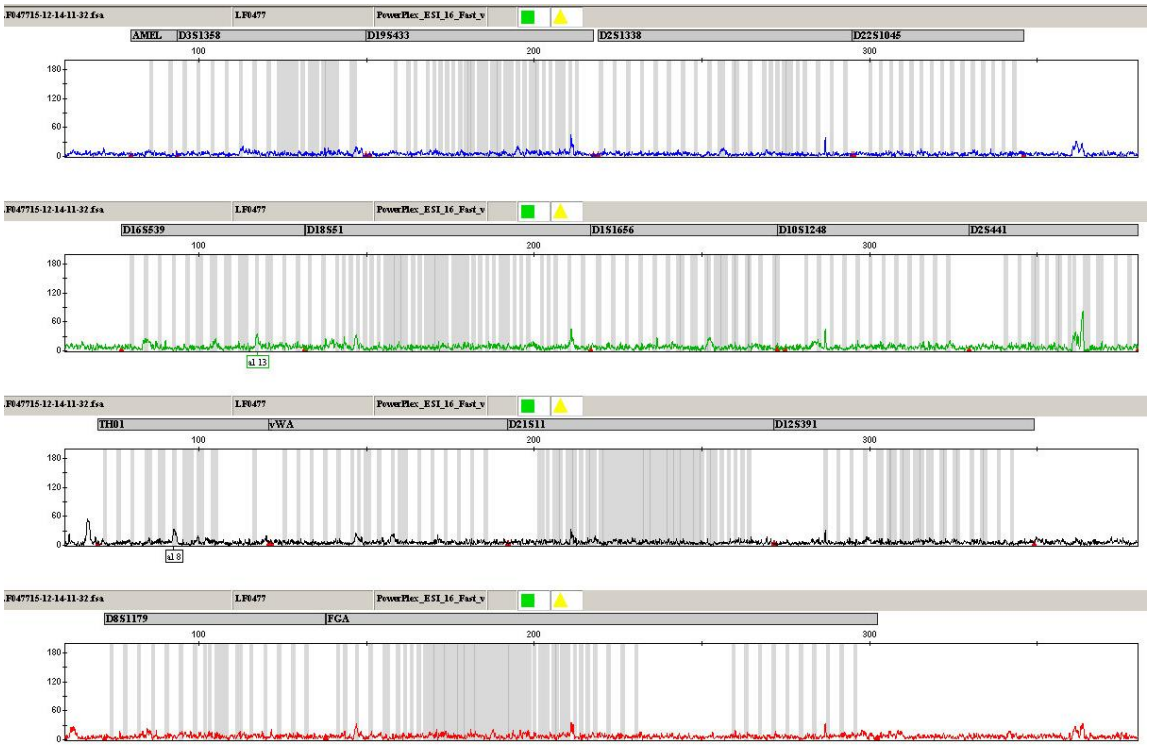

Figure B-31: Eriswell Skeleton 0477 femur electropherogram

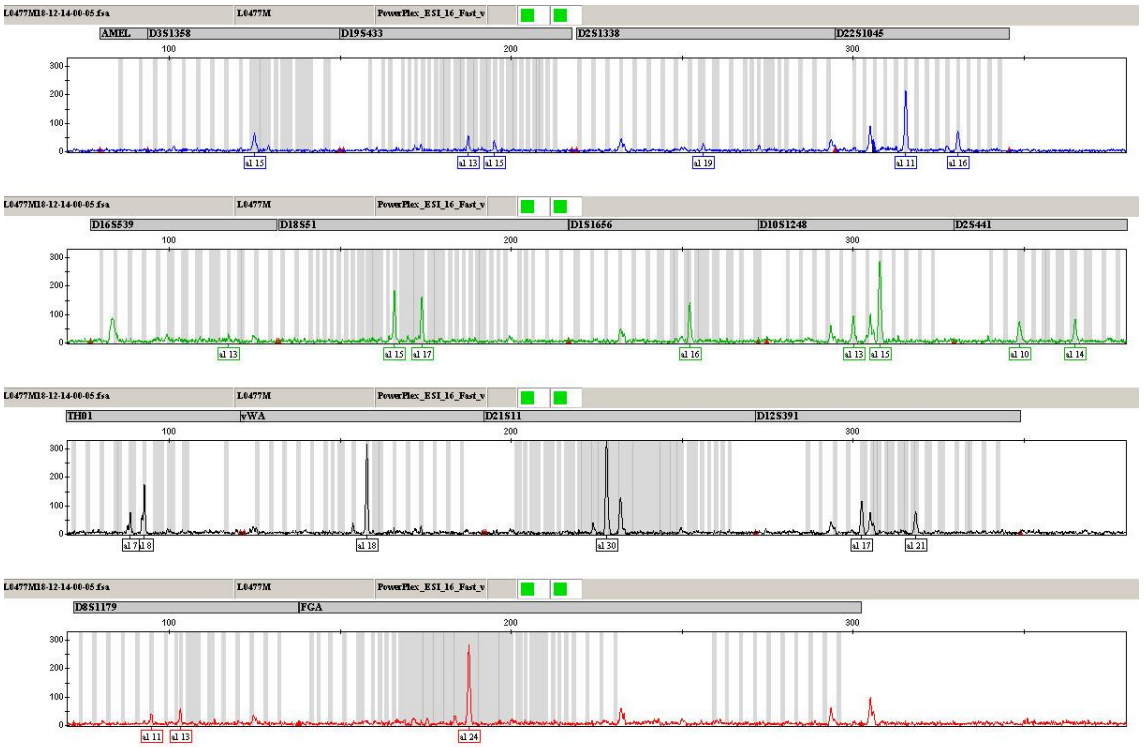

Figure B-32: Eriswell Skeleton 0477 metatarsal electropherogram

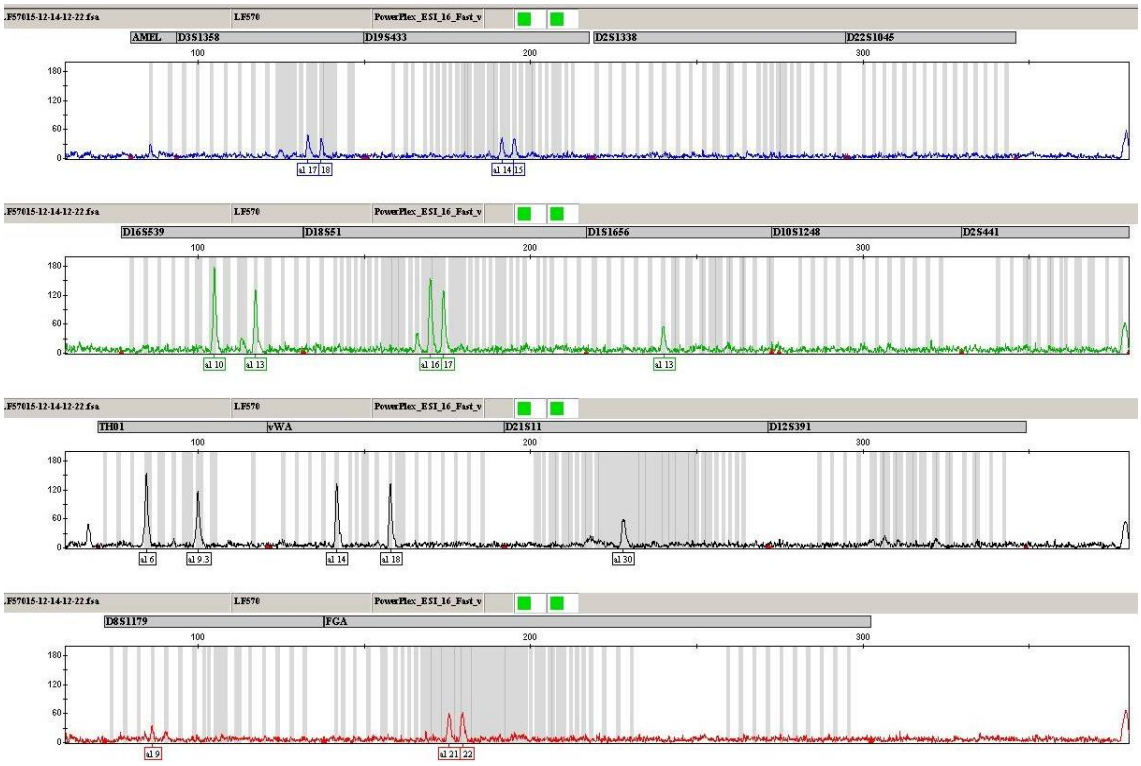

Figure B-33: Eriswell Skeleton 0570 femur electropherogram

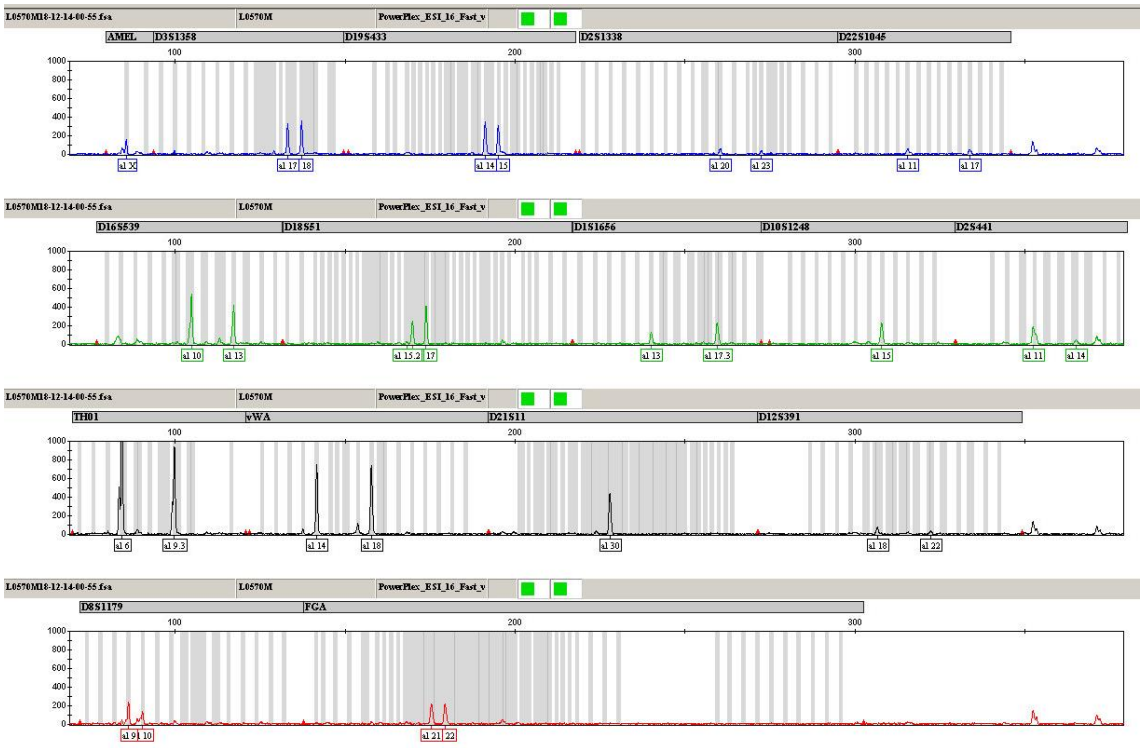

Figure B-34: Eriswell Skeleton 0570 metatarsal electropherogram

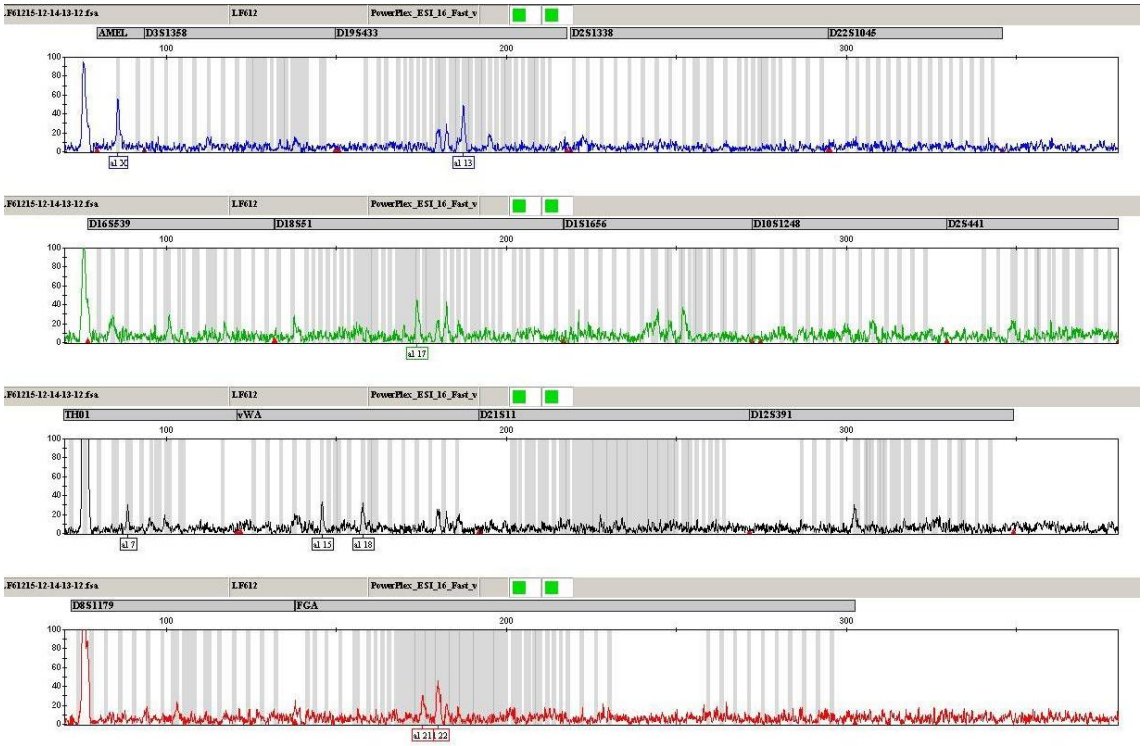

Figure B-35: Eriswell Skeleton 0612 femur electropherogram

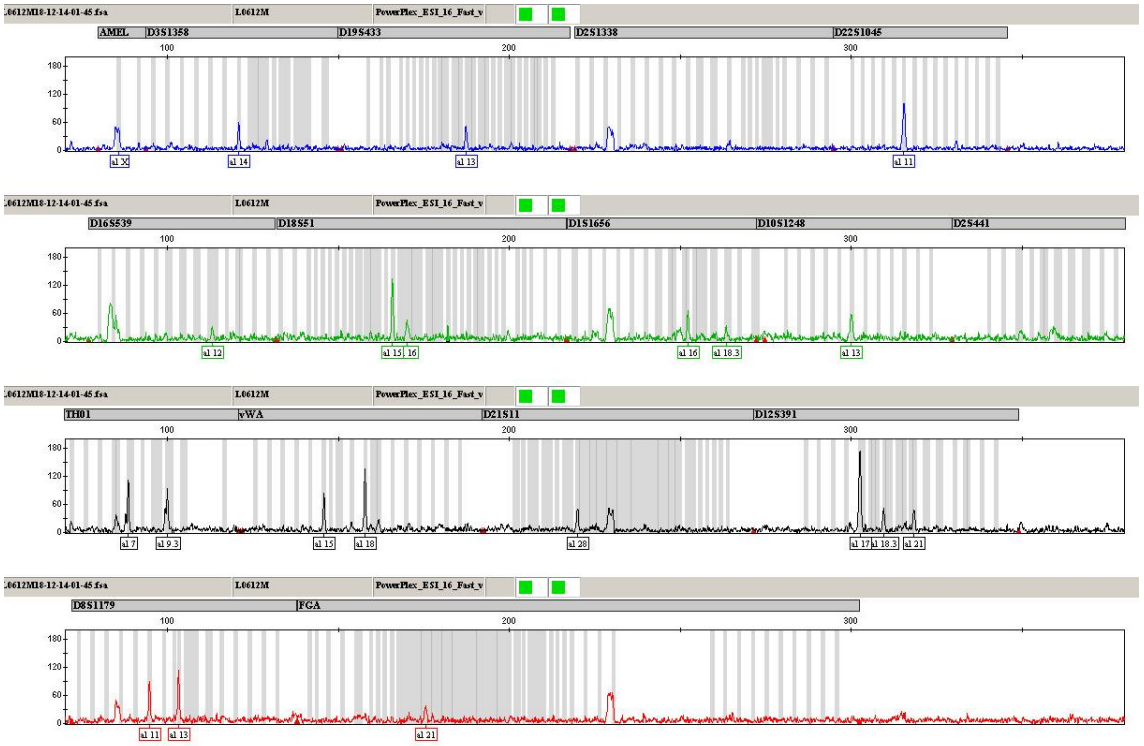

Figure B-36: Eriswell Skeleton 0612 metatarsal electropherogram

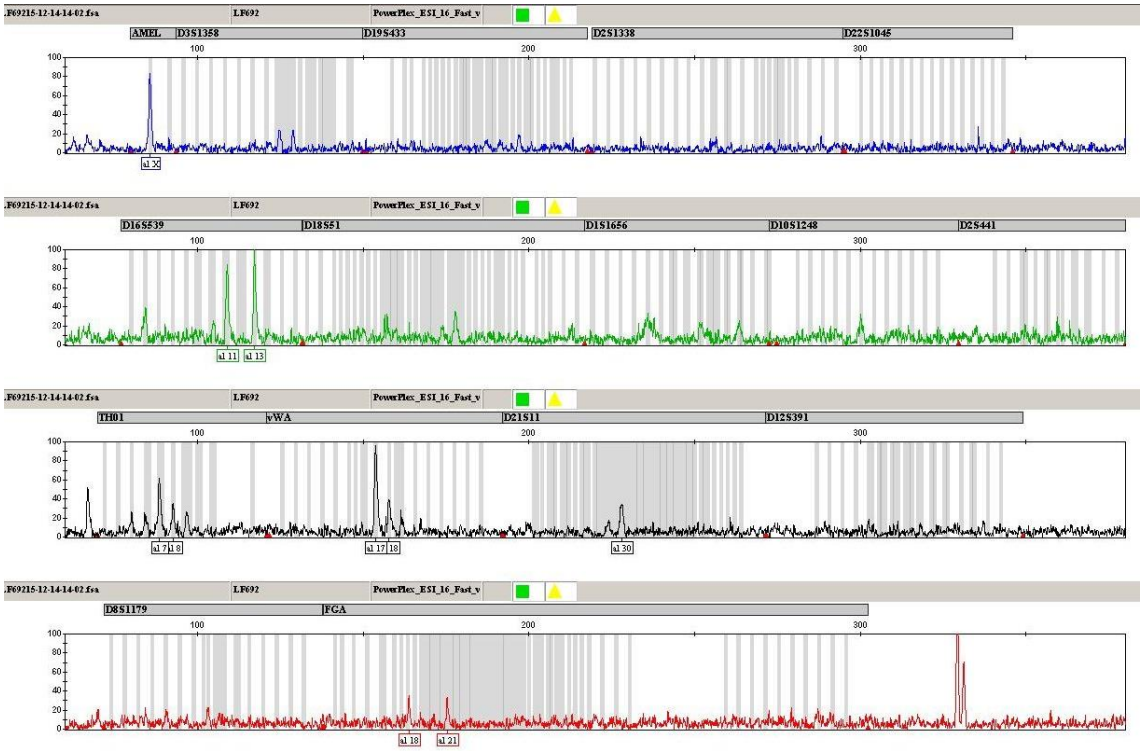

Figure B-37: Eriswell Skeleton 0692 femur electropherogram

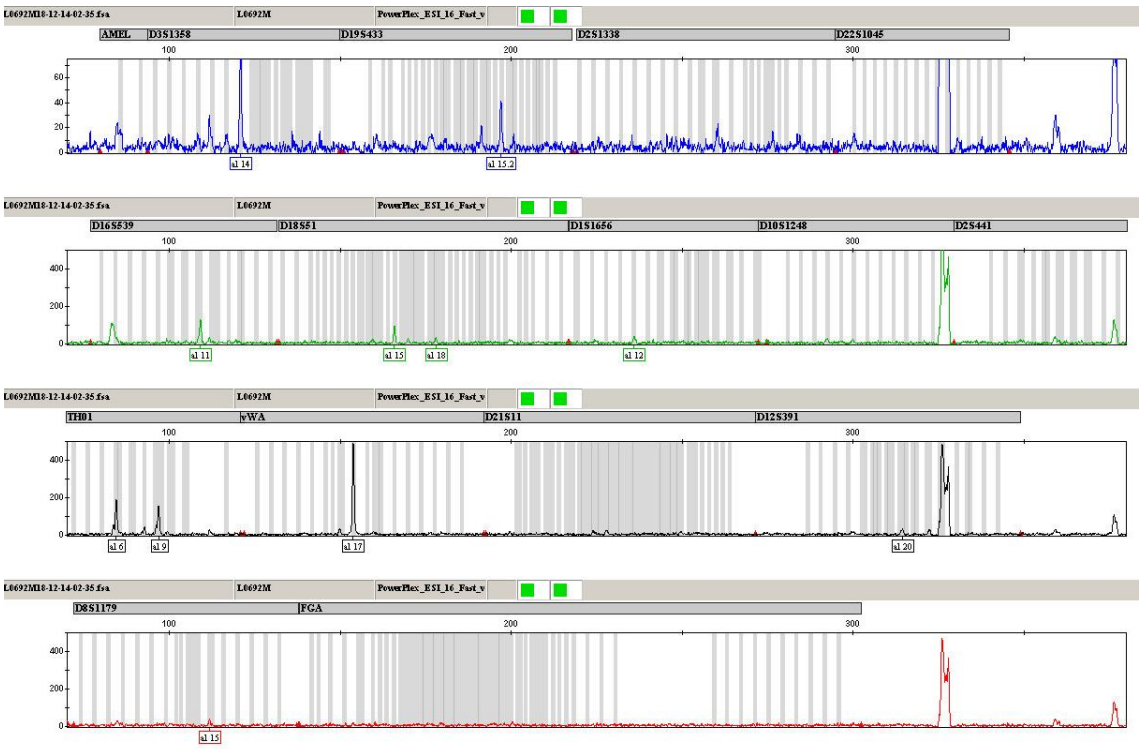

Figure B-38: Eriswell Skeleton 0692 metatarsal electropherogram

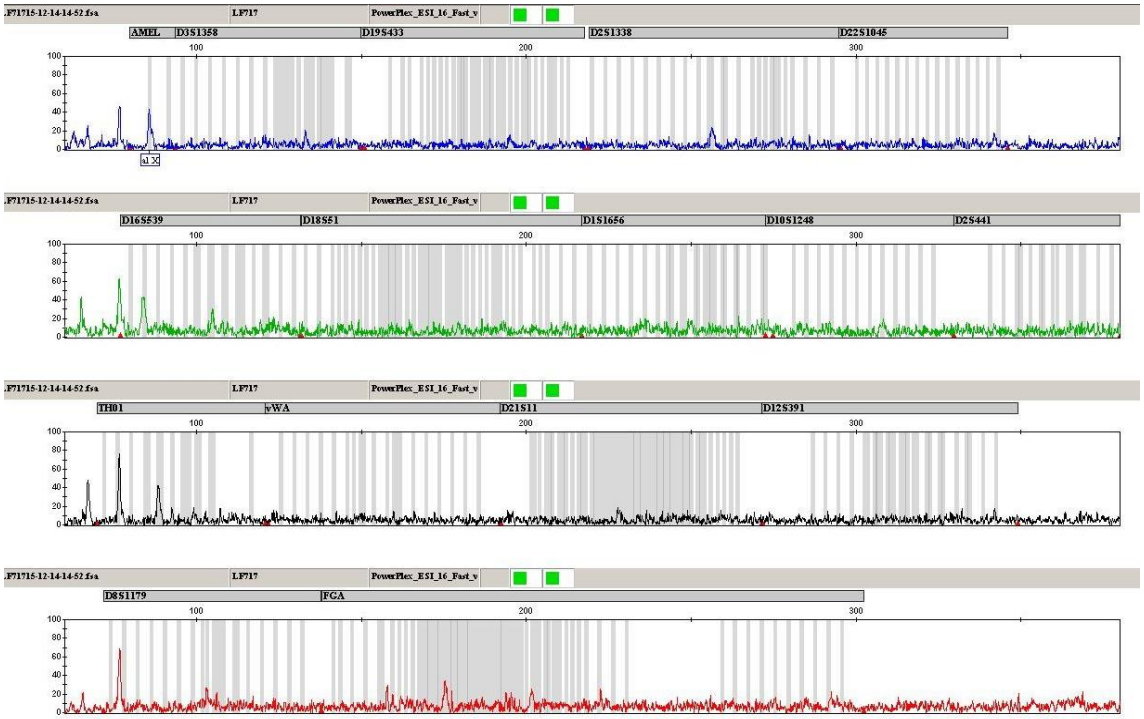

Figure B-39: Eriswell Skeleton 0717 femur electropherogram

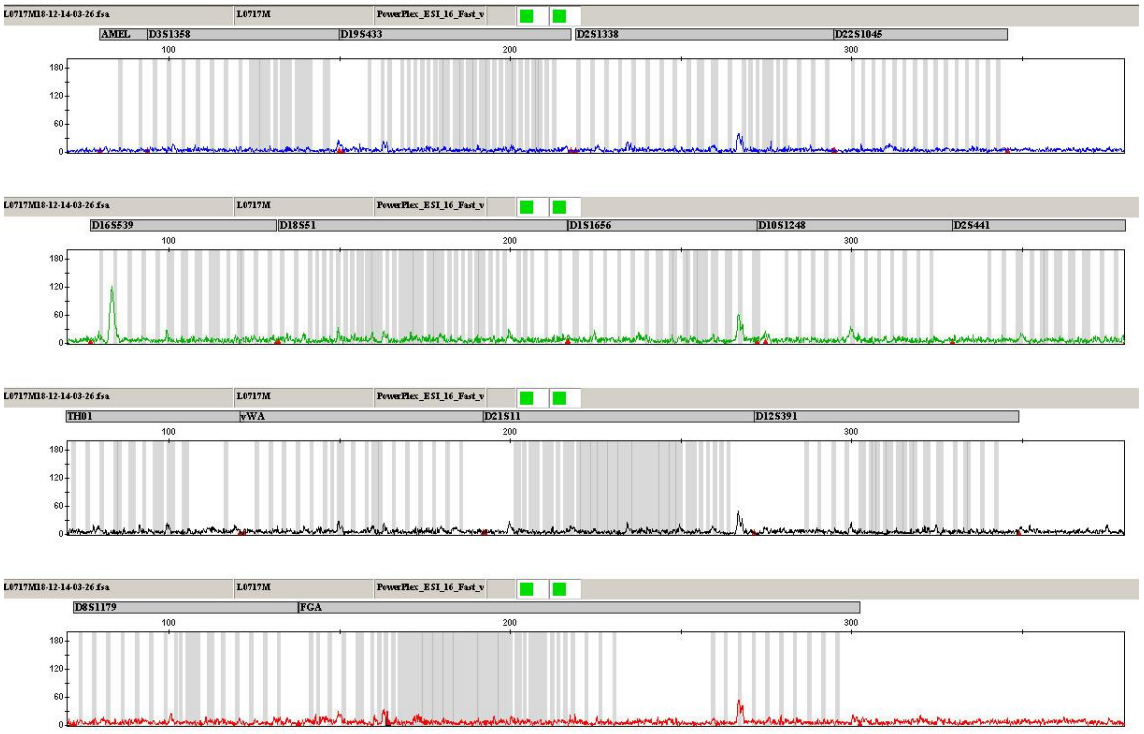

Figure B-40: Eriswell Skeleton 0717 metatarsal electropherogram

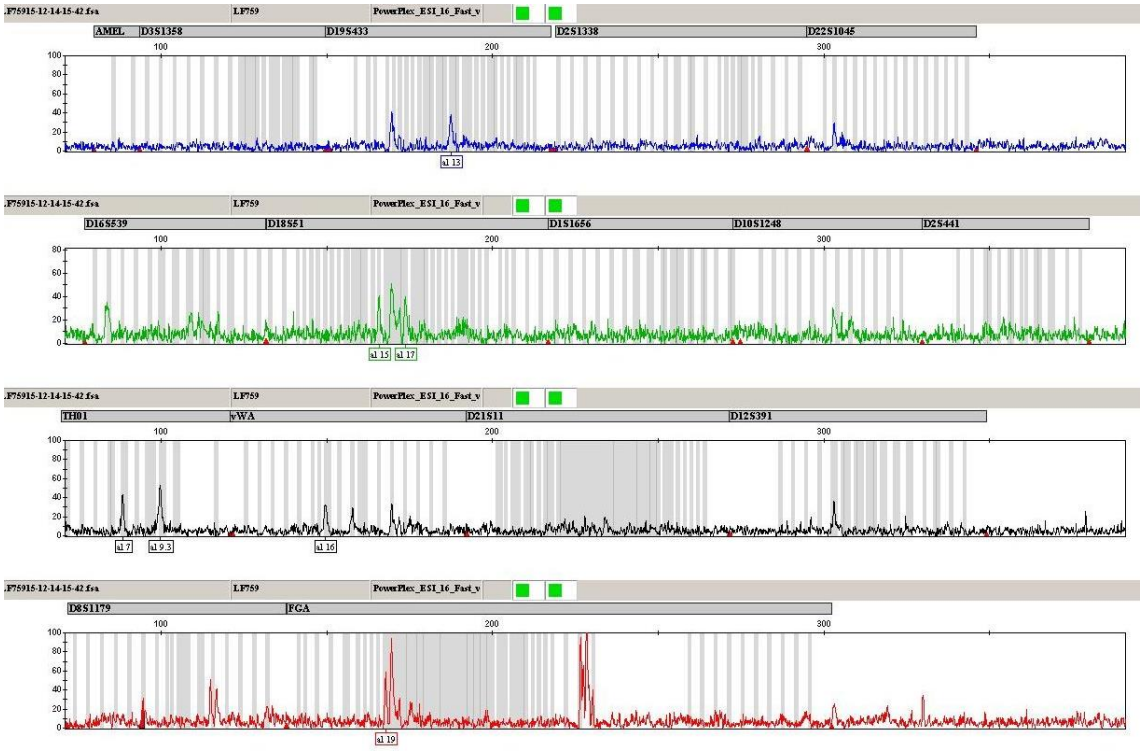

Figure B-41: Eriswell Skeleton 0759 femur electropherogram

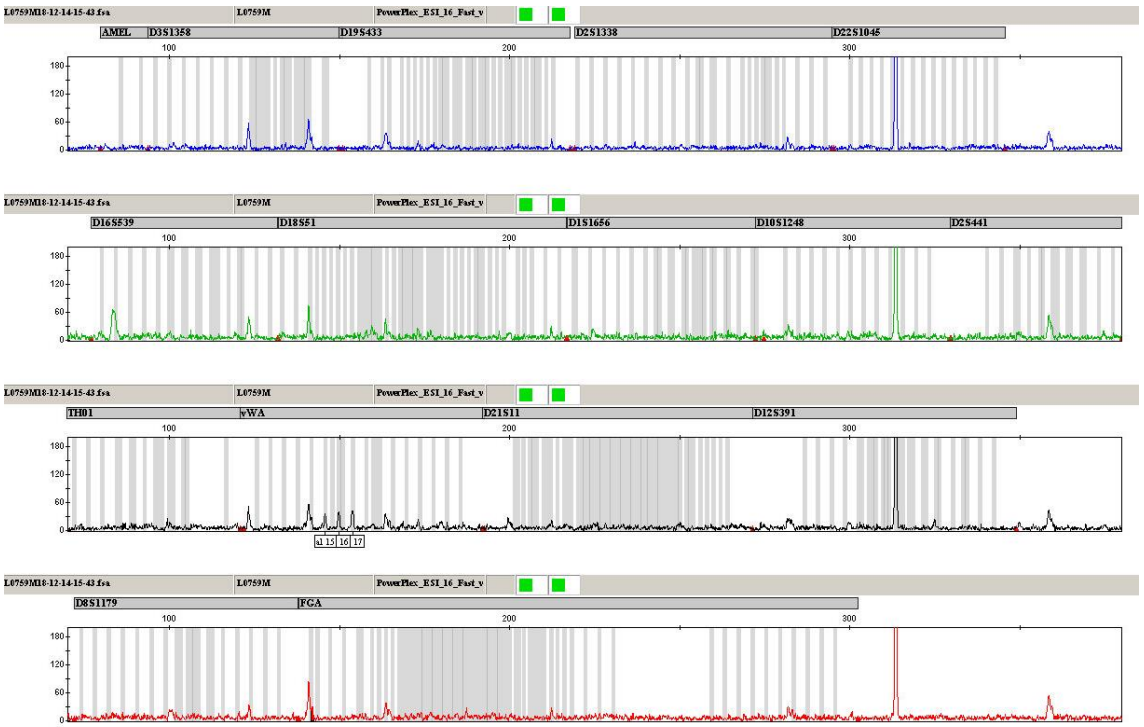

Figure B-42: Eriswell Skeleton 0759 metatarsal electropherogram

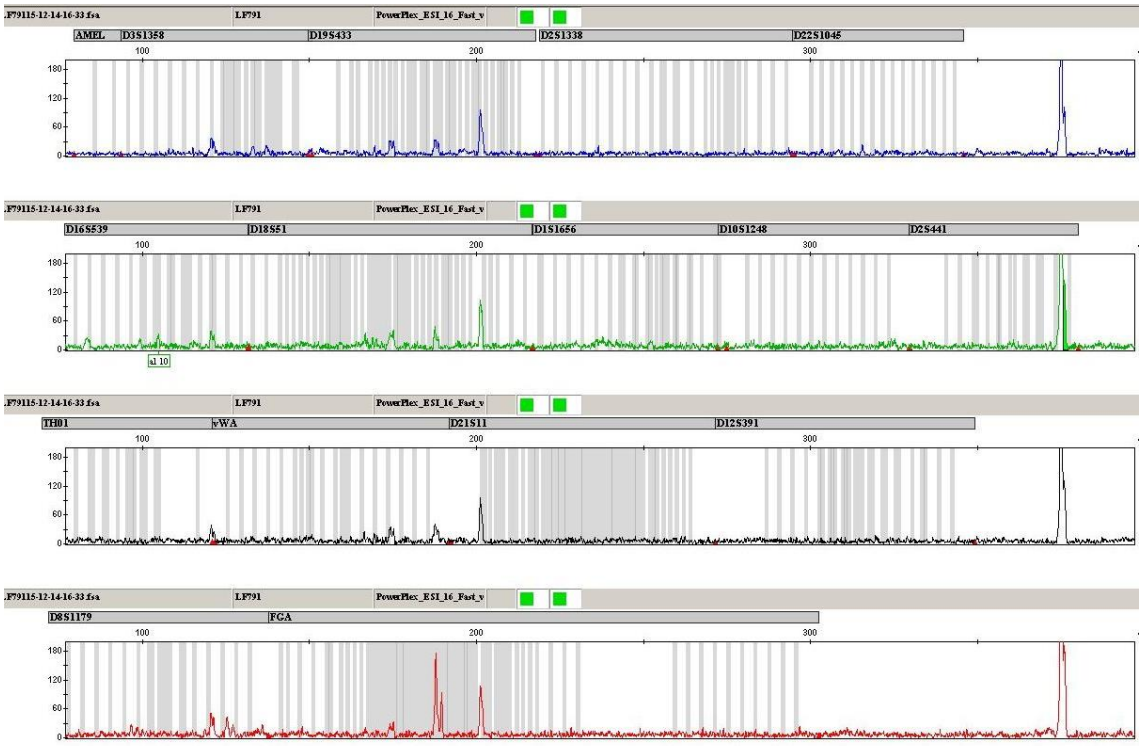

Figure B-43: Eriswell Skeleton 0791 femur electropherogram

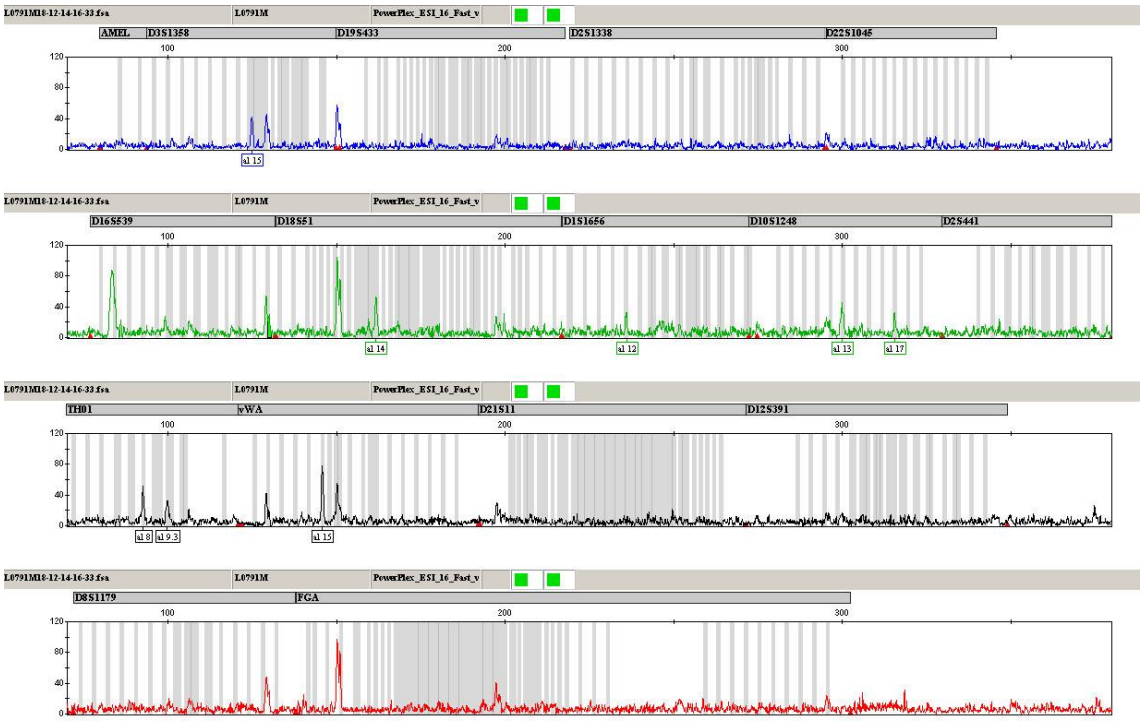

Figure B-44: Eriswell Skeleton 0791 metatarsal electropherogram

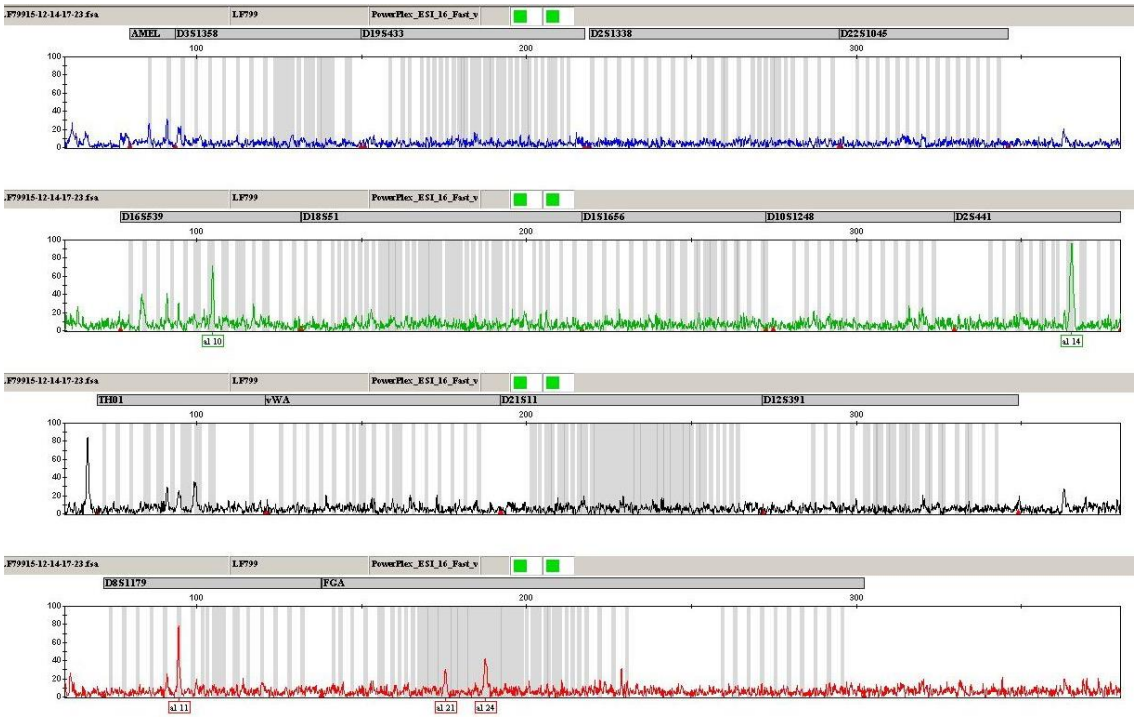

Figure B-45: Eriswell Skeleton 0799 femur electropherogram

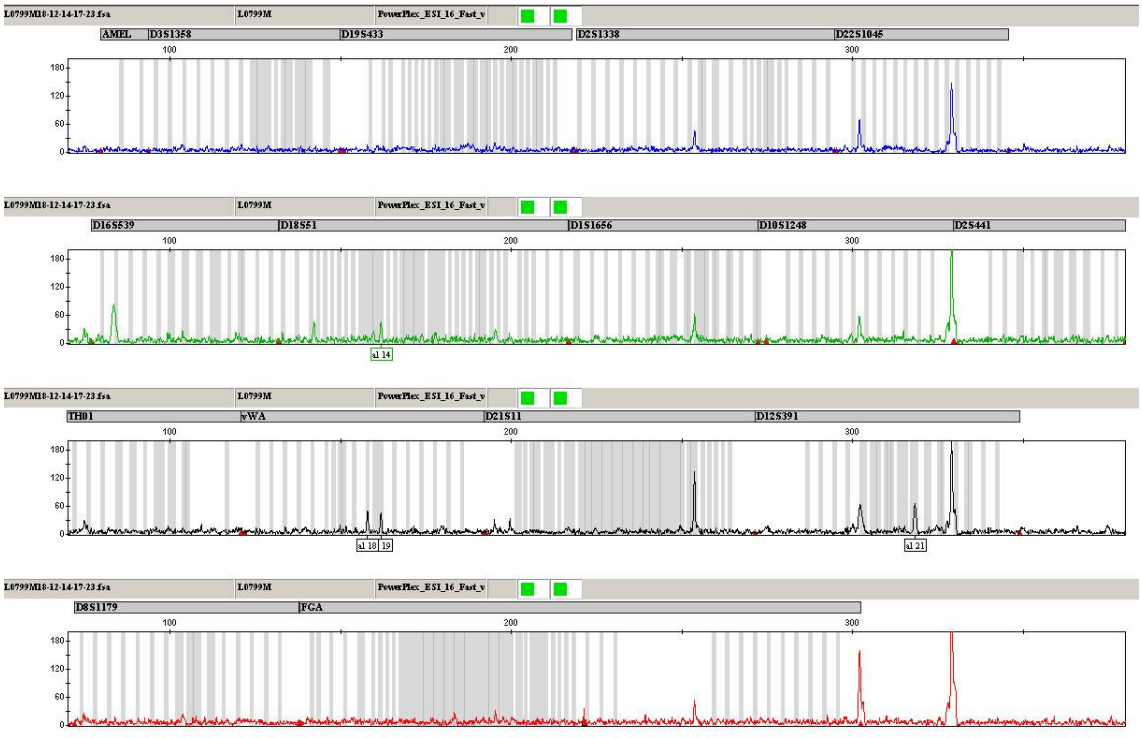

Figure B-46: Eriswell Skeleton 0799 metatarsal electropherogram

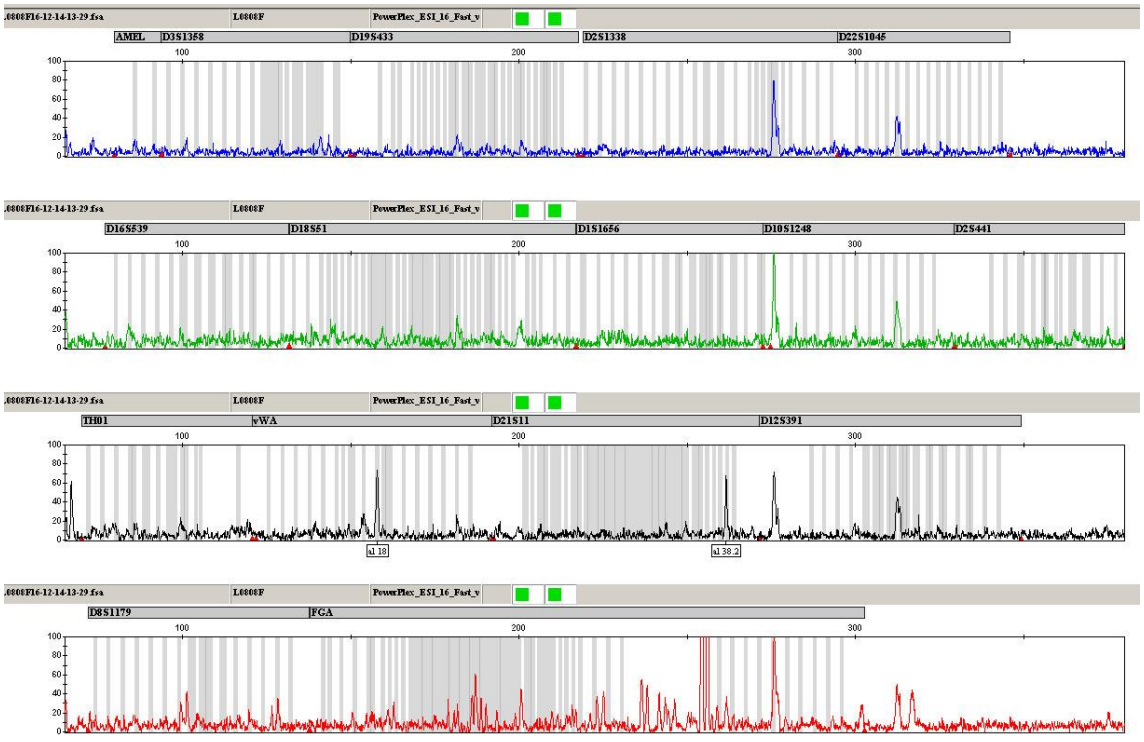

Figure B-47: Eriswell Skeleton 0808 femur electropherogram

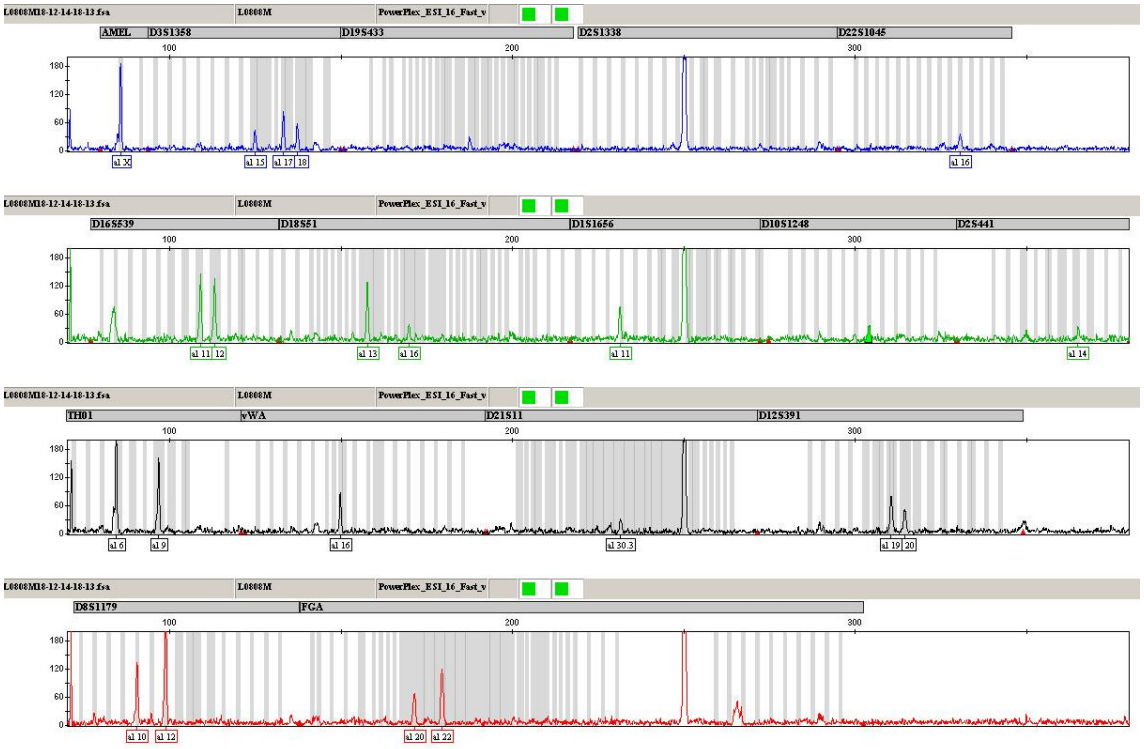

Figure B-48: Eriswell Skeleton 0808 metatarsal electropherogram

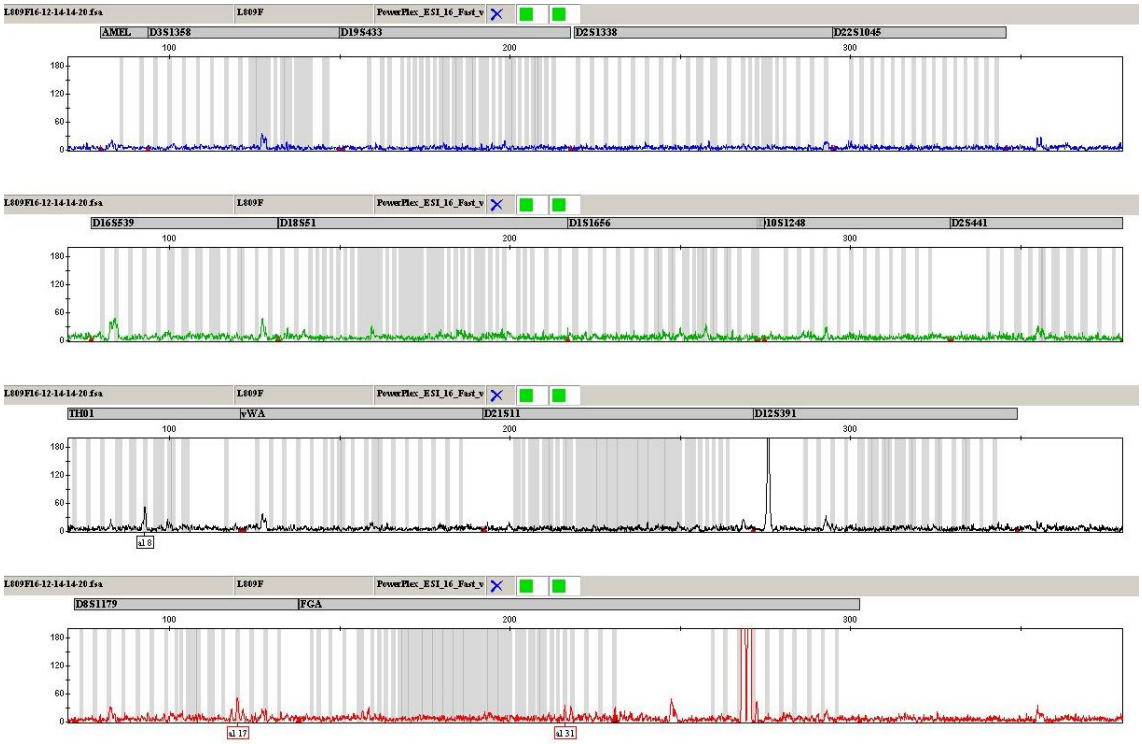

Figure B-49: Eriswell Skeleton 0809 femur electropherogram

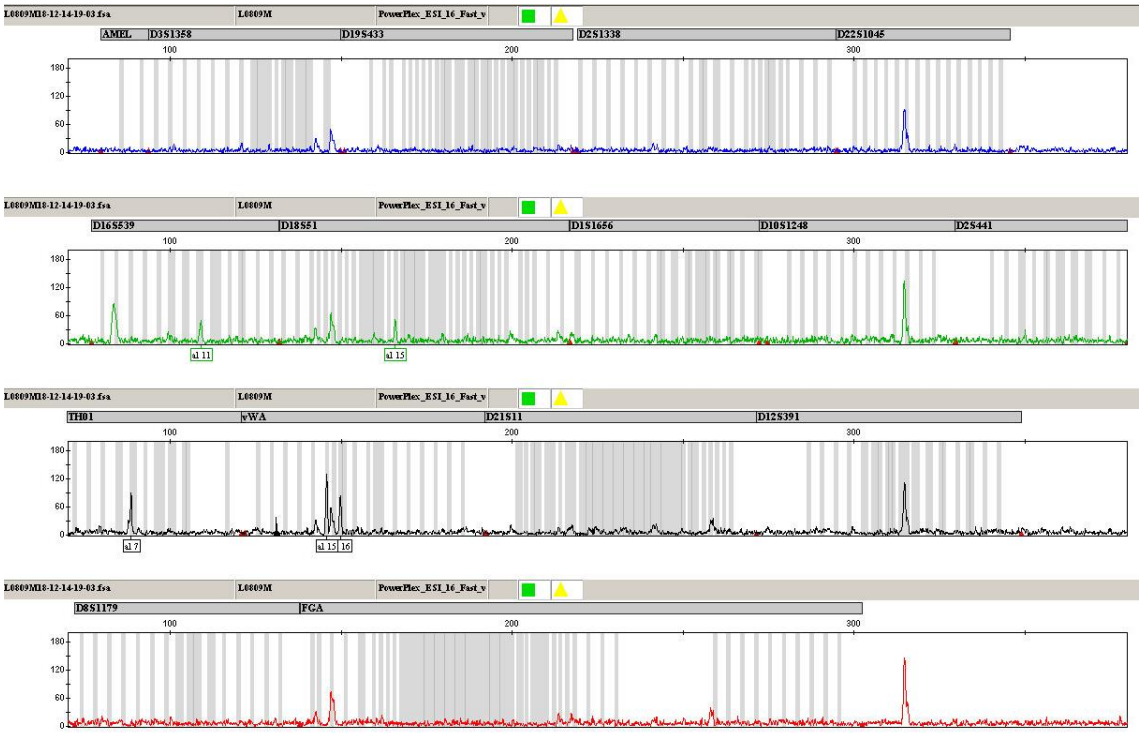

Figure B-50: Eriswell Skeleton 0809 metatarsal electropherogram

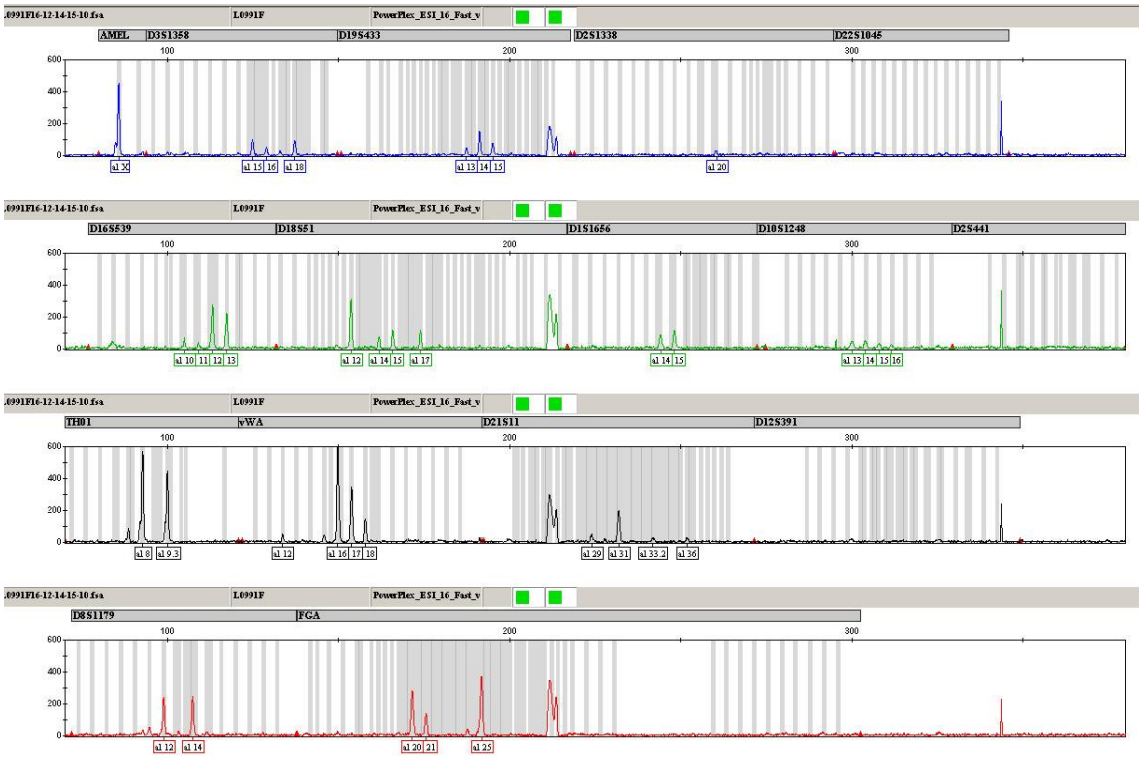

Figure B-51: Eriswell Skeleton 0991 femur electropherogram

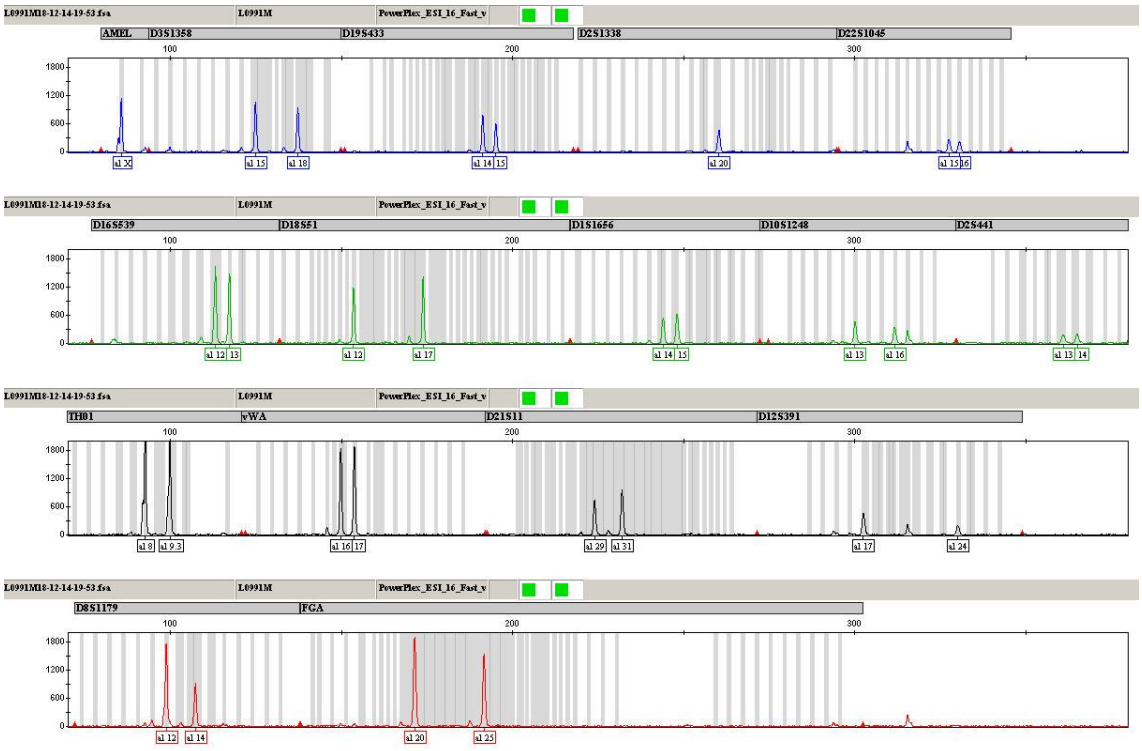

Figure B-52: Eriswell Skeleton 0991 metatarsal electropherogram

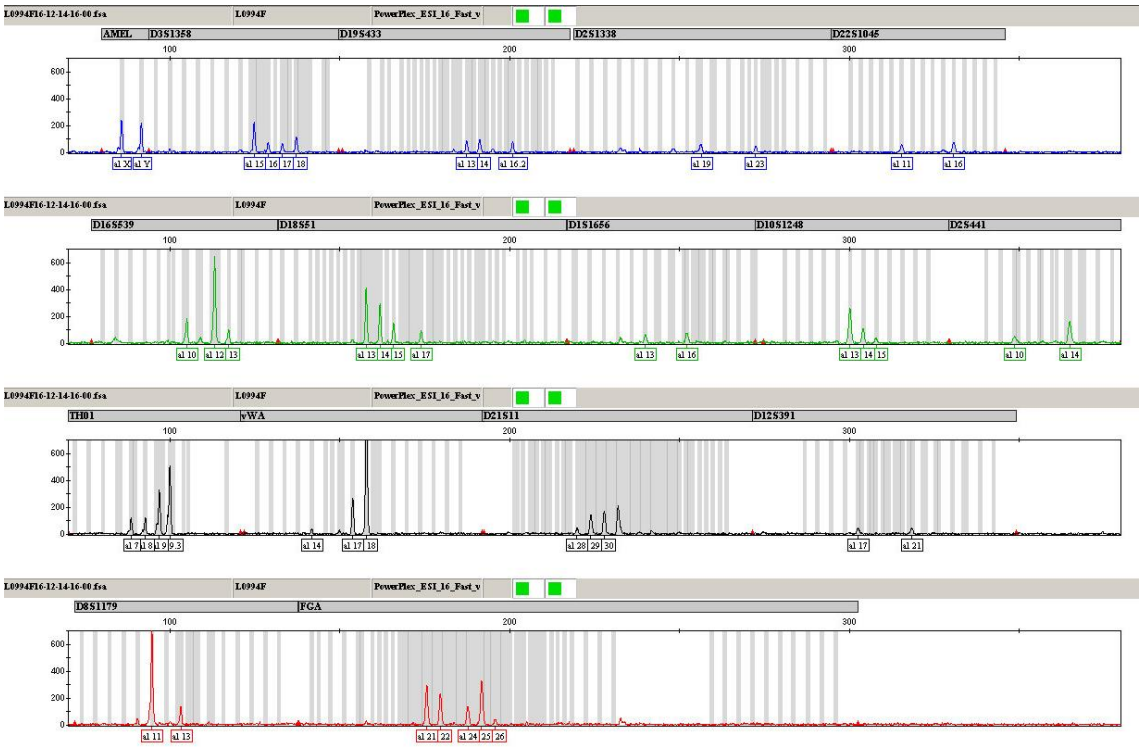

Figure B-53: Eriswell Skeleton 0994 femur electropherogram

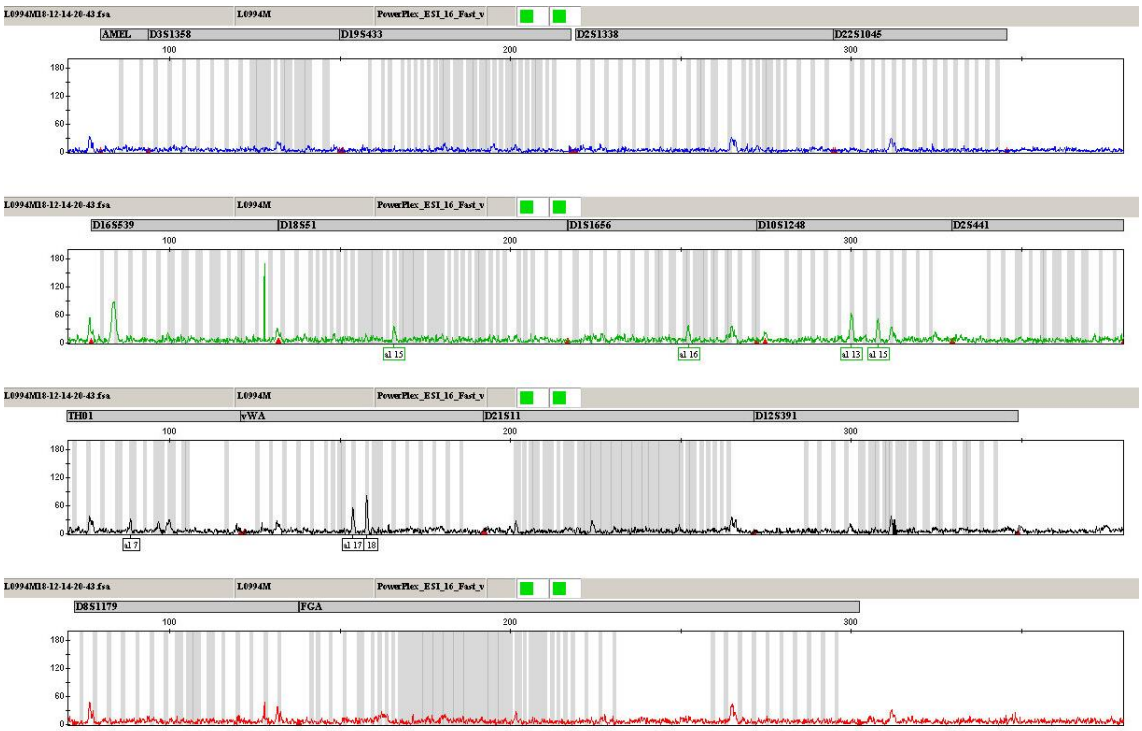

Figure B-54: Eriswell Skeleton 0994 metatarsal electropherogram

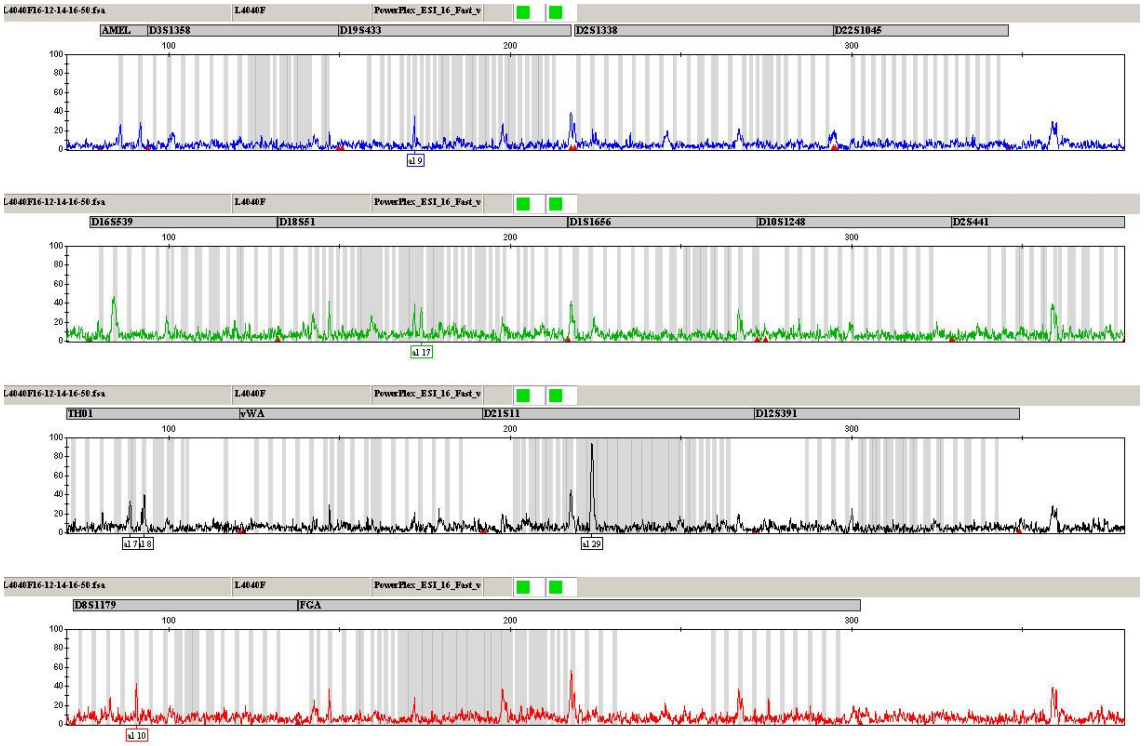

Figure B-55: Eriswell Skeleton 4040 femur electropherogram

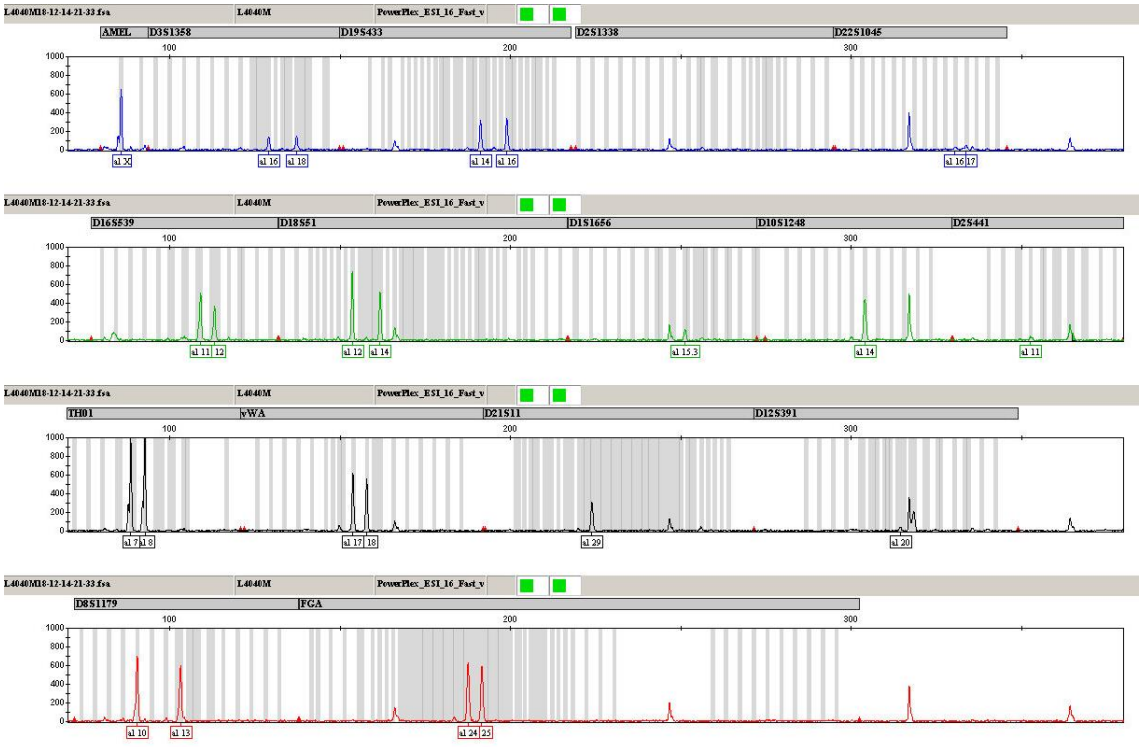

Figure B-56: Eriswell Skeleton 4040 metatarsal electropherogram

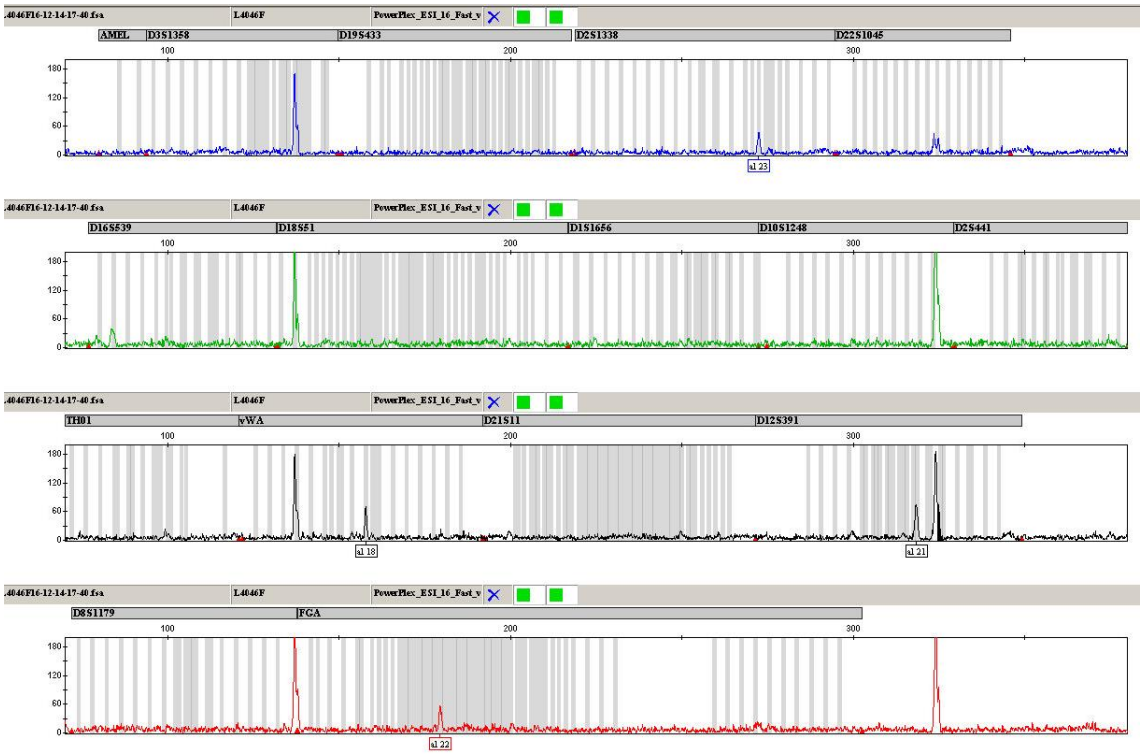

Figure B-57: Eriswell Skeleton 4046 femur electropherogram

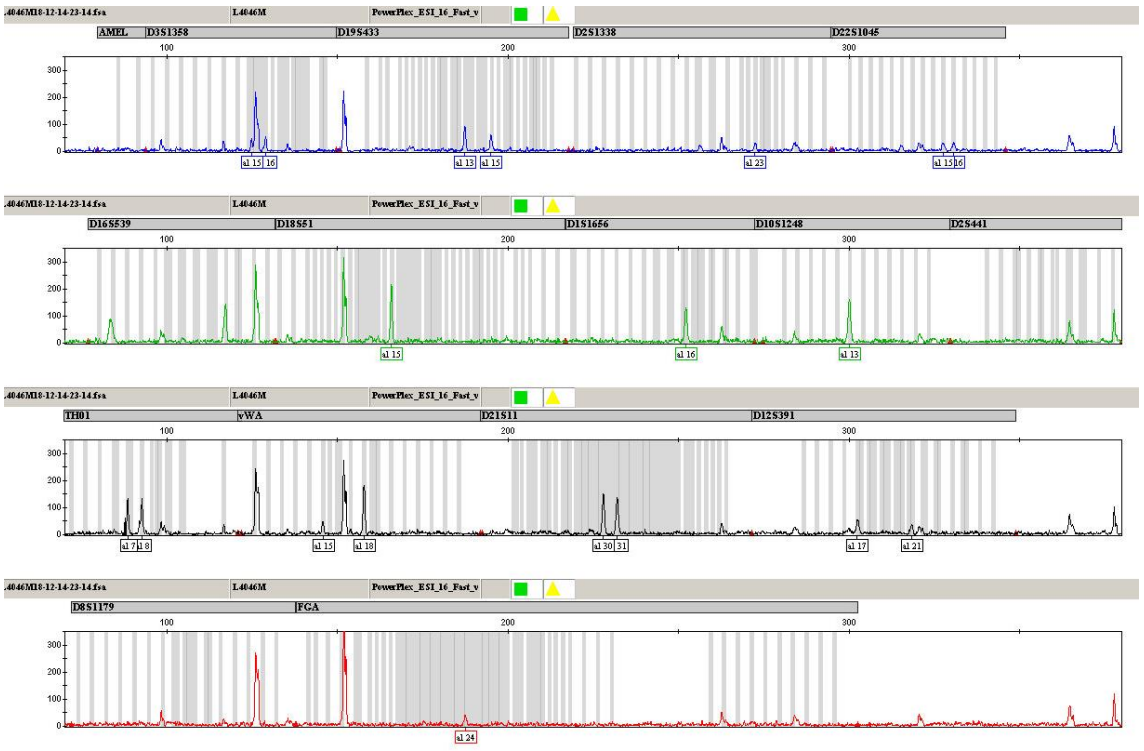

Figure B-58: Eriswell Skeleton 4046 metatarsal electropherogram

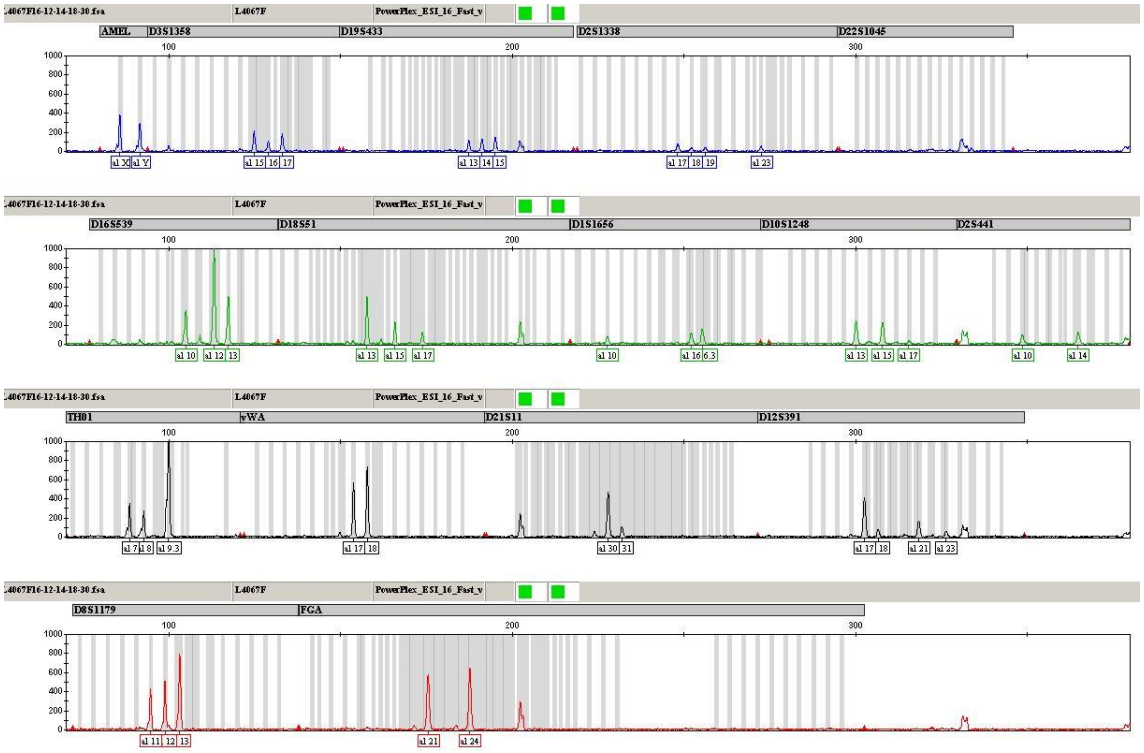

Figure B-59: Eriswell Skeleton 4067 femur electropherogram

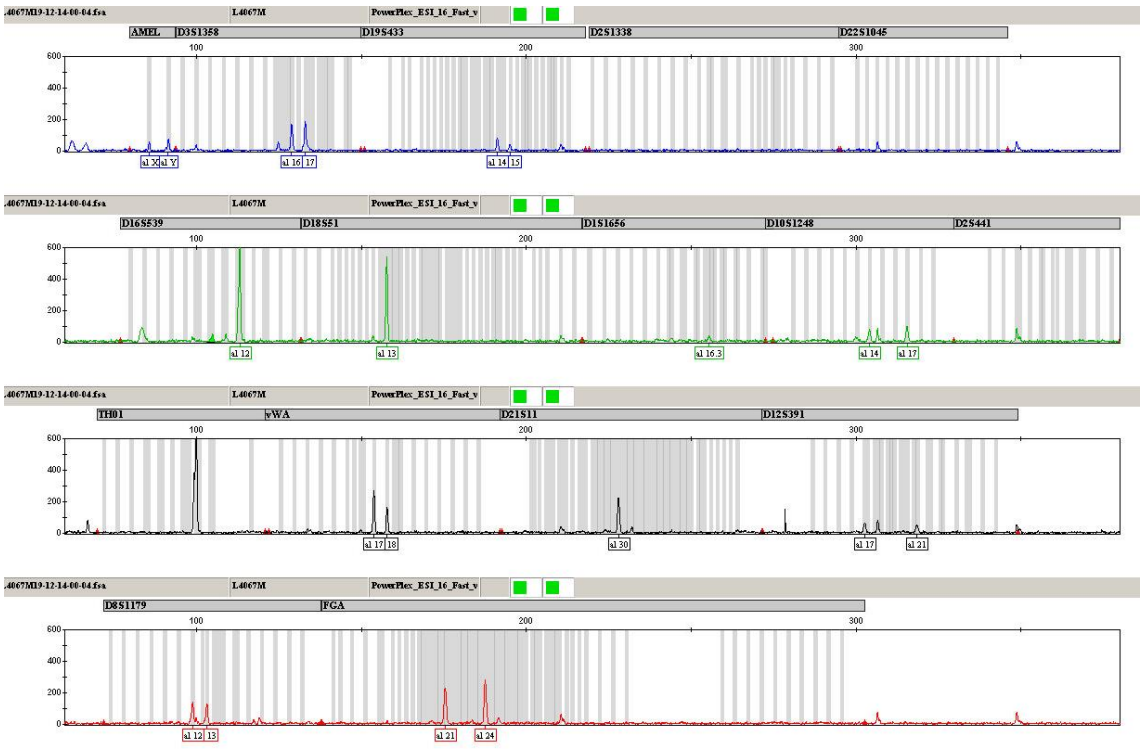

Figure B-60: Eriswell Skeleton 4067 metatarsal electropherogram

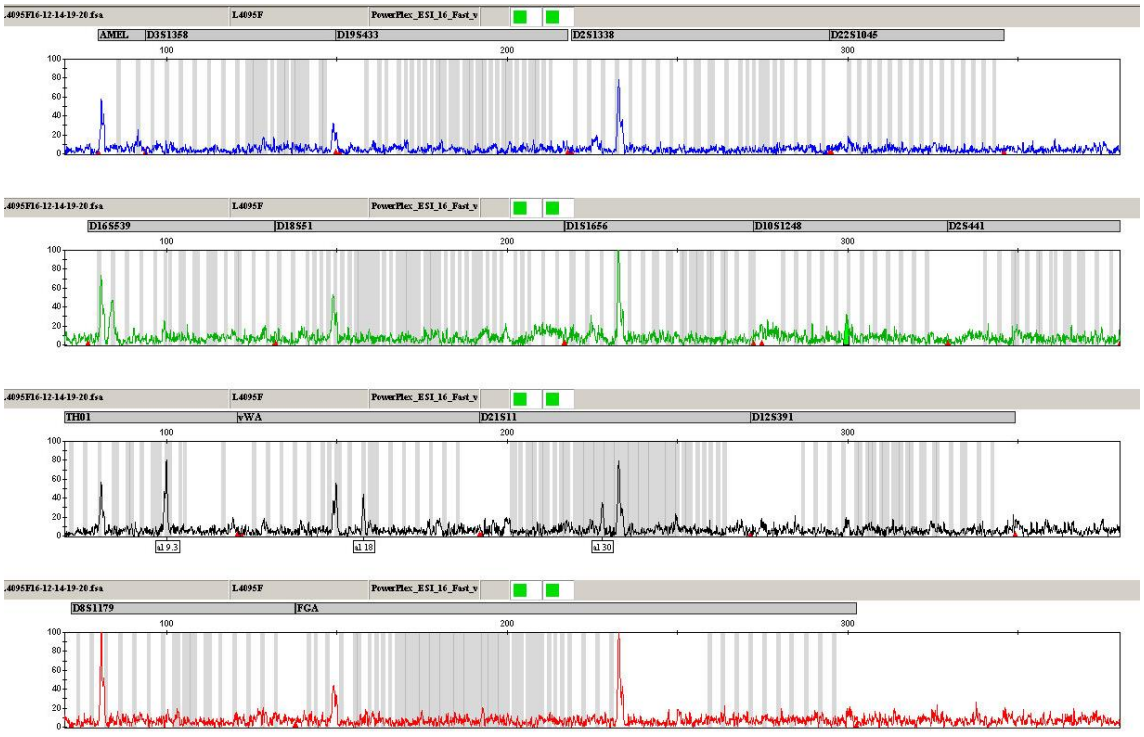

Figure B-61: Eriswell Skeleton 4095 femur electropherogram

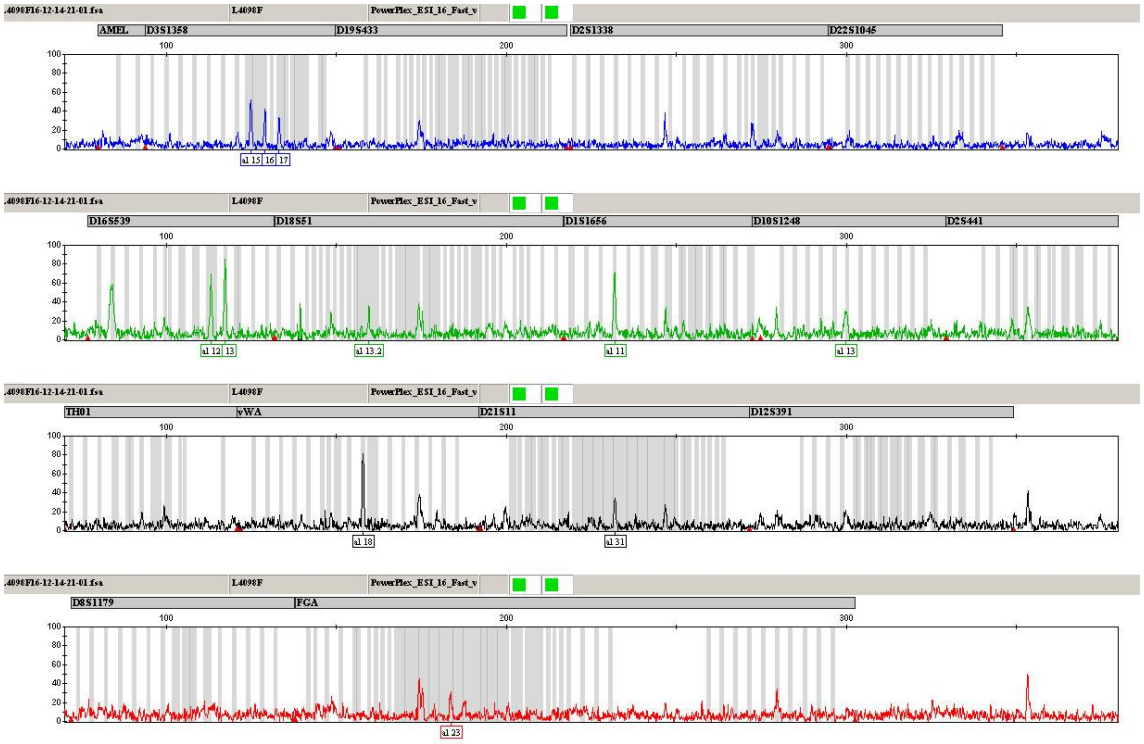

Figure B-62: Eriswell Skeleton 4098 femur electropherogram

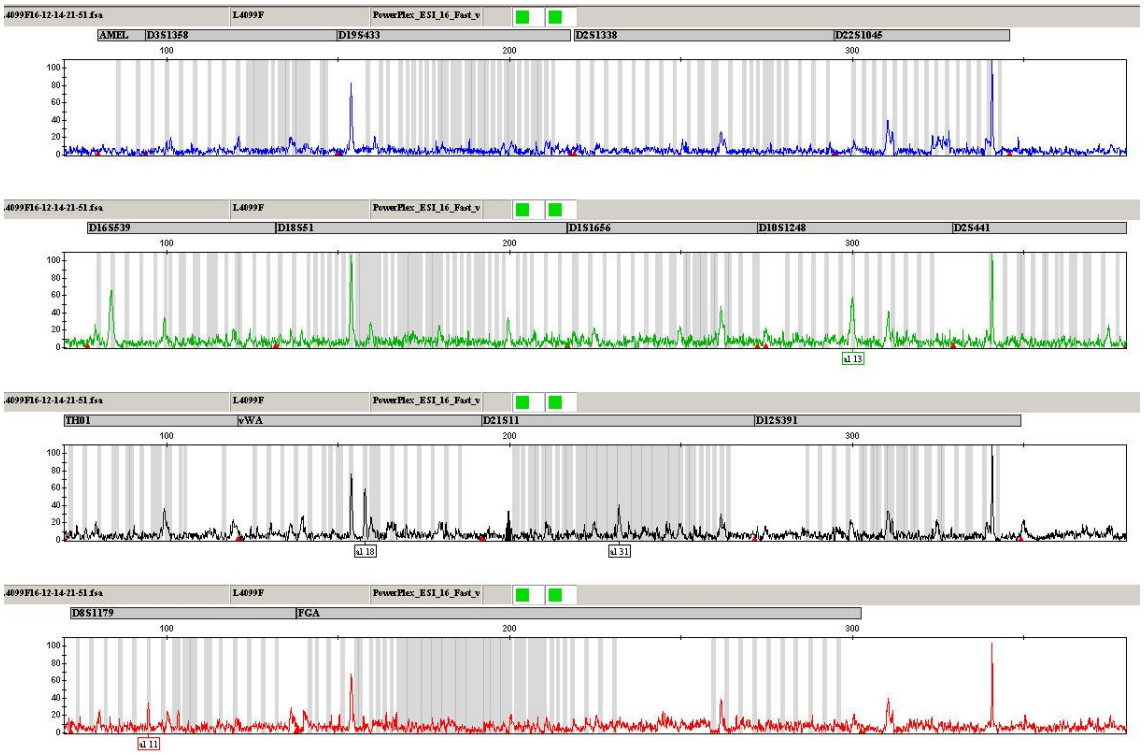

Figure B-63: Eriswell Skeleton 4099 femur electropherogram

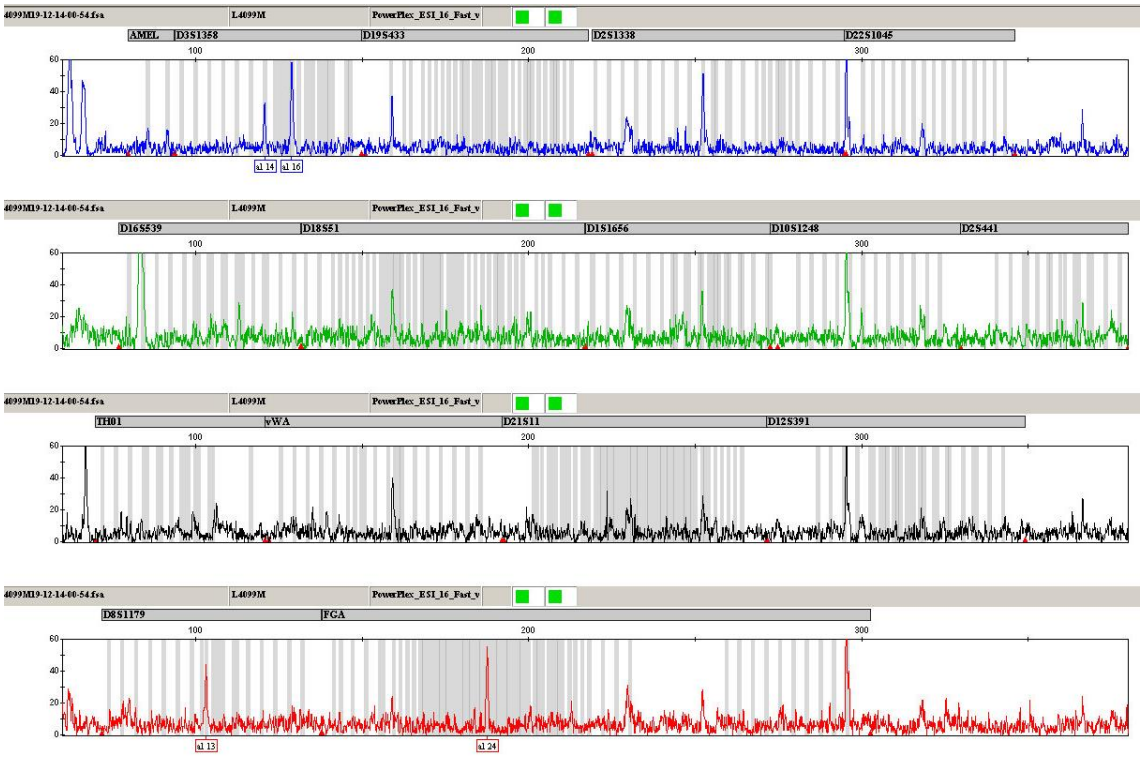

Figure B-64: Eriswell Skeleton 4099 metatarsal electropherogram

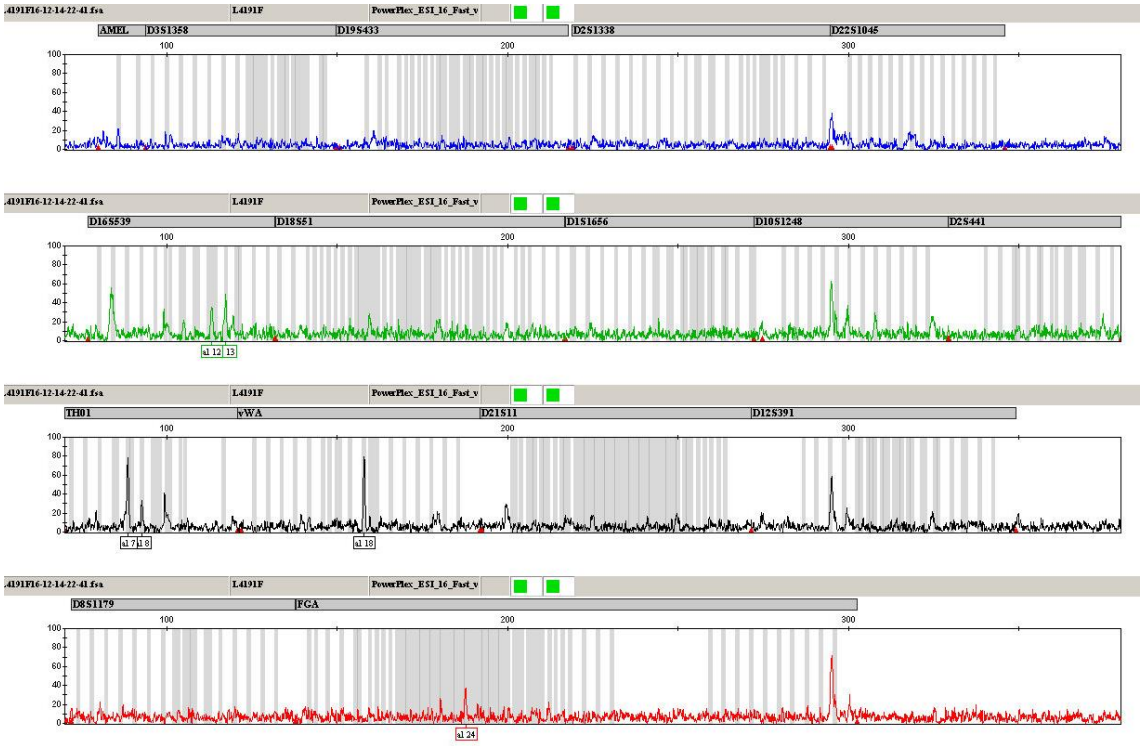

Figure B-65: Eriswell Skeleton 4191 femur electropherogram

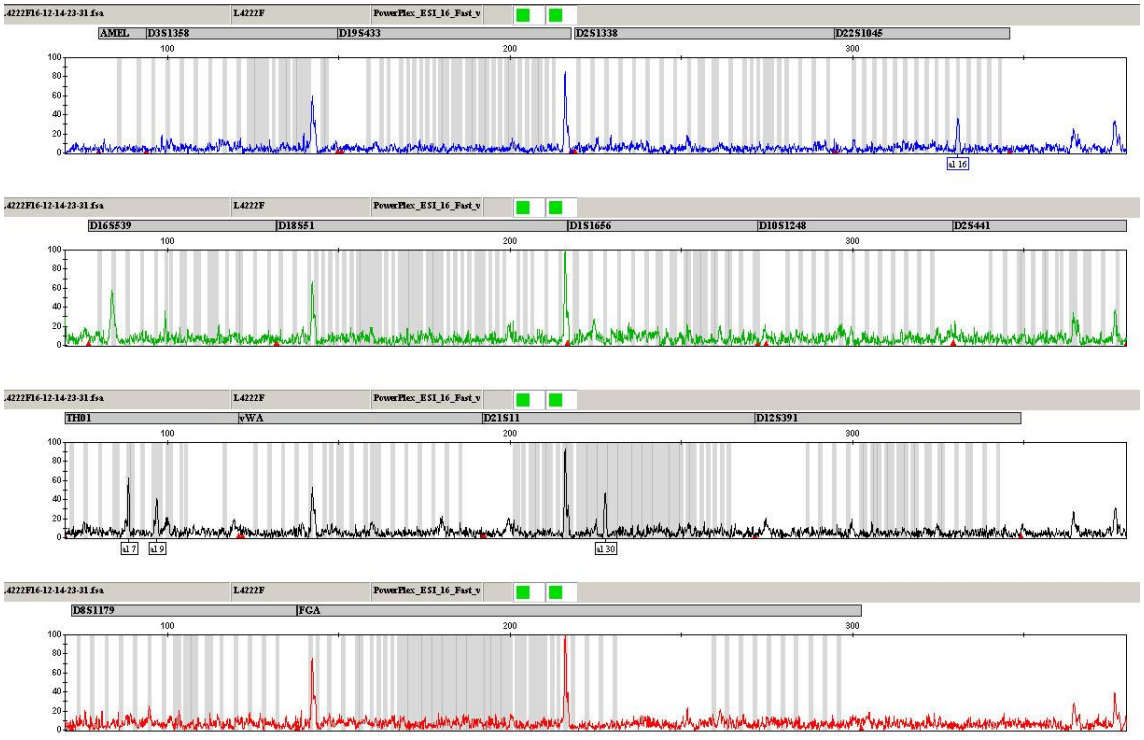

Figure B-66: Eriswell Skeleton 4222 femur electropherogram

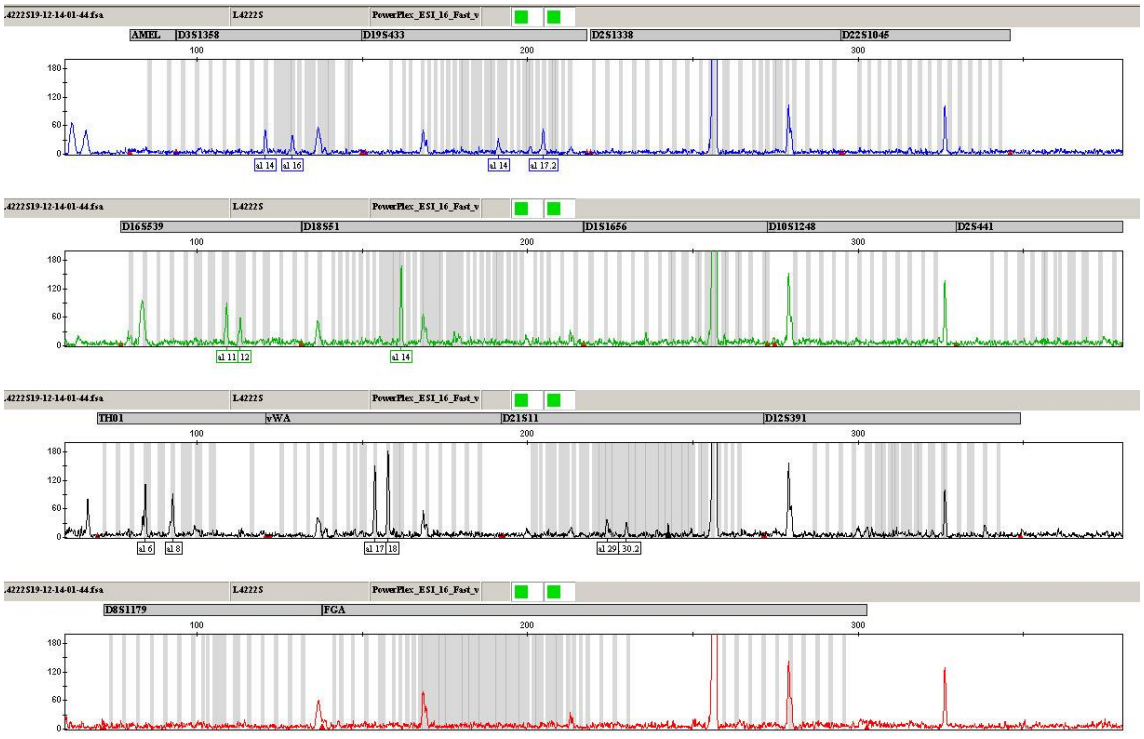

Figure B-67: Eriswell Skeleton 4222 sternum electropherogram

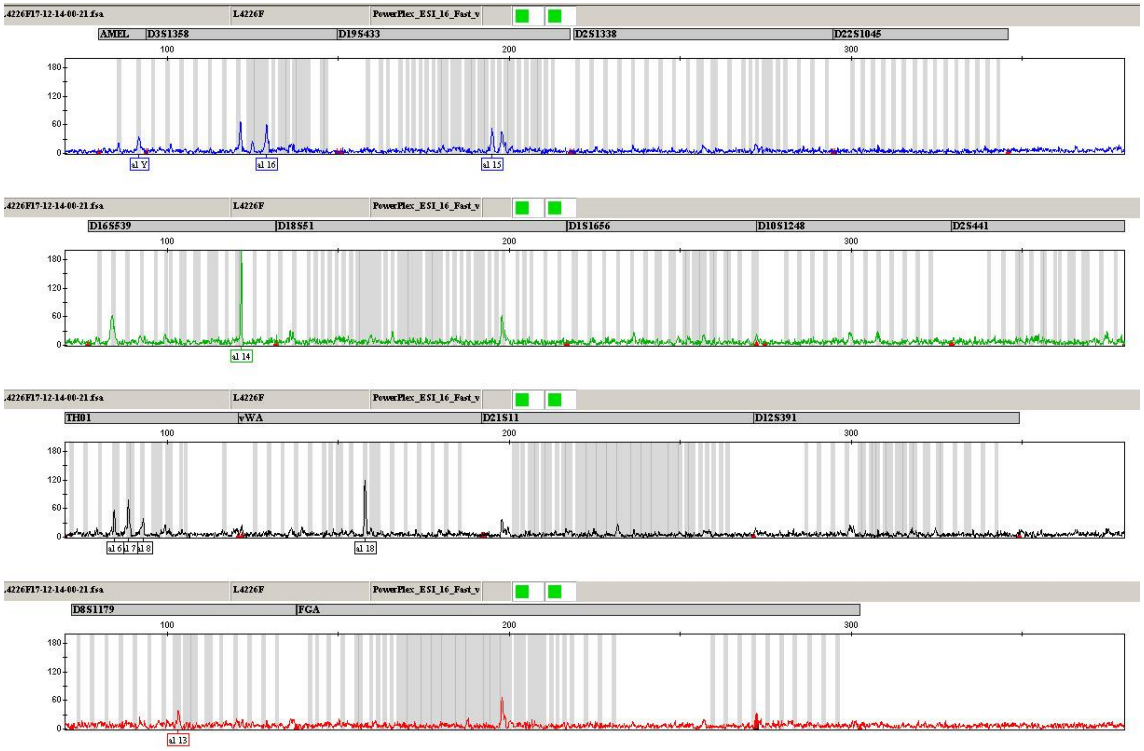

Figure B-68: Eriswell Skeleton 4226 femur electropherogram

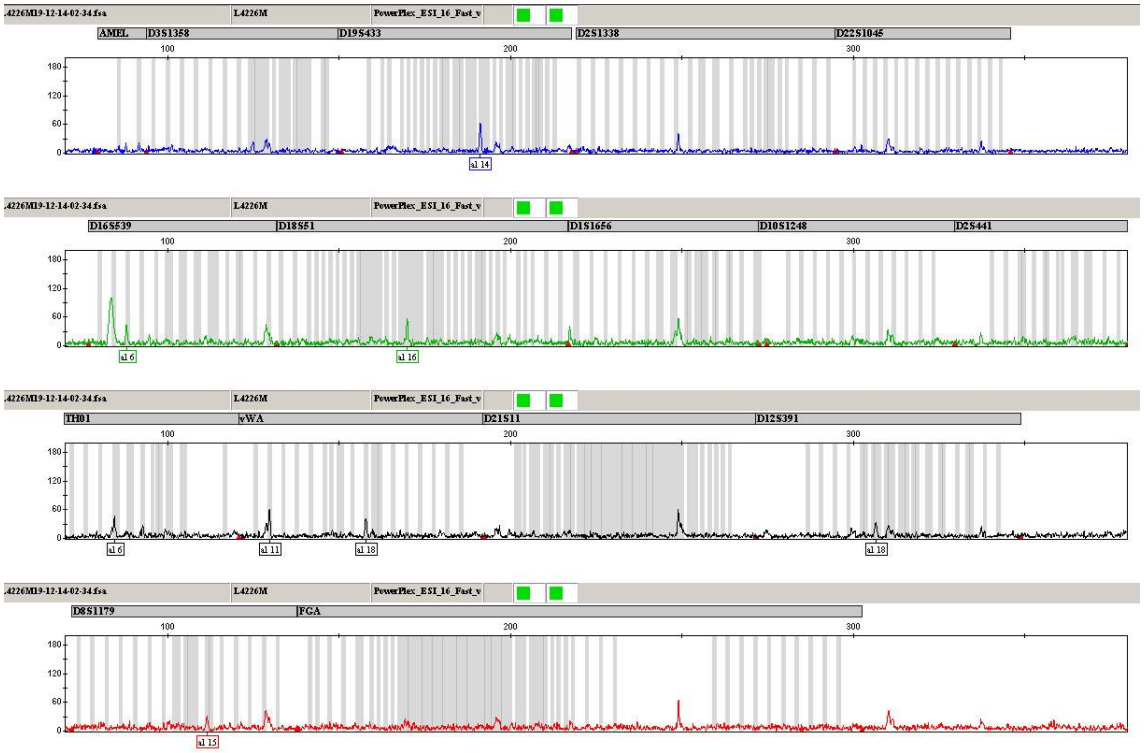

Figure B-69: Eriswell Skeleton 4226 metatarsal electropherogram

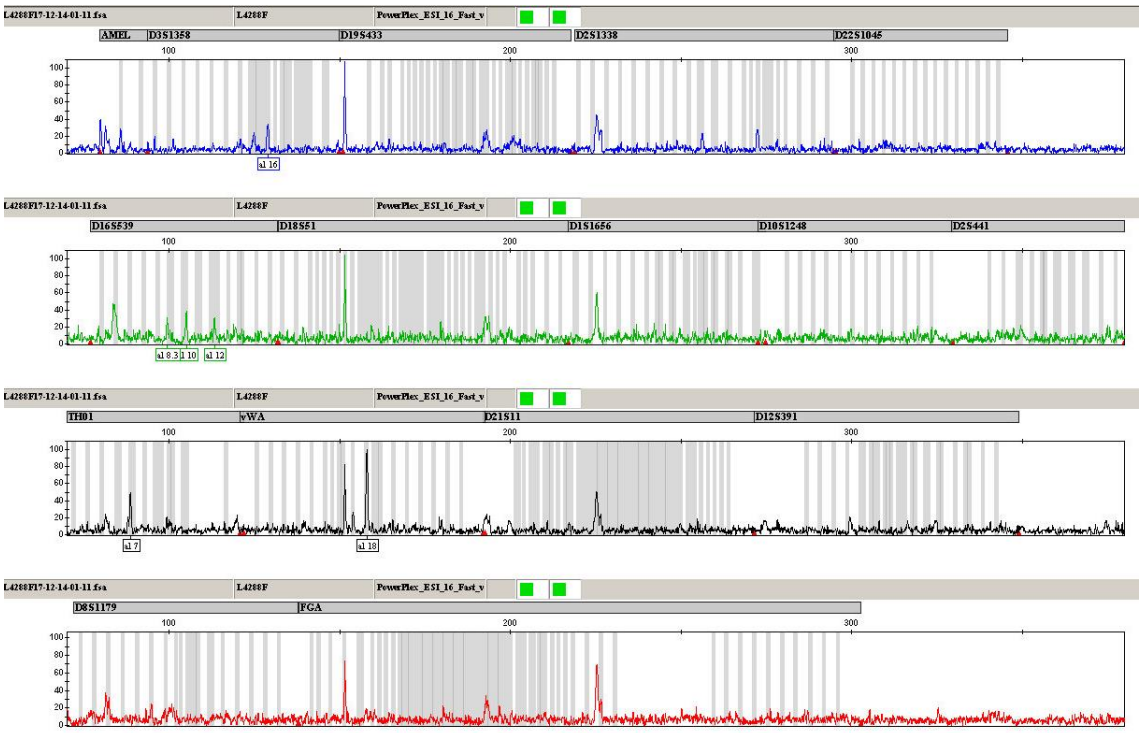

Figure B-70: Eriswell Skeleton 4288 femur electropherogram

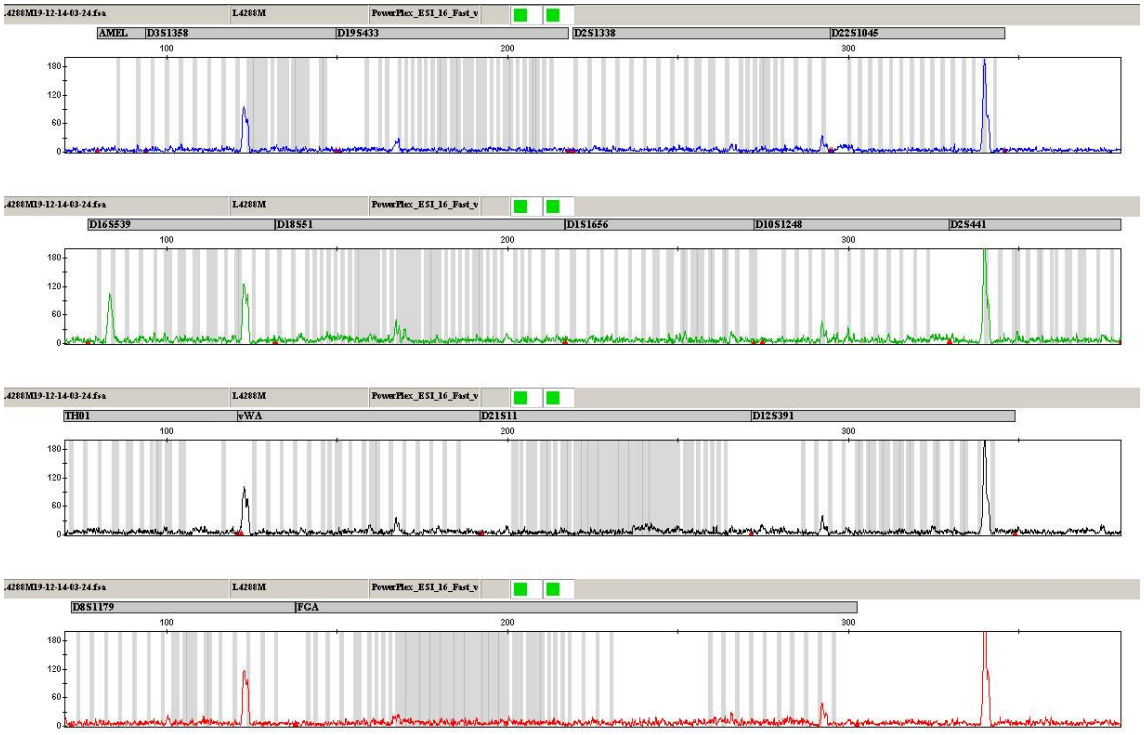

Figure B-71: Eriswell Skeleton 4288 metatarsal electropherogram

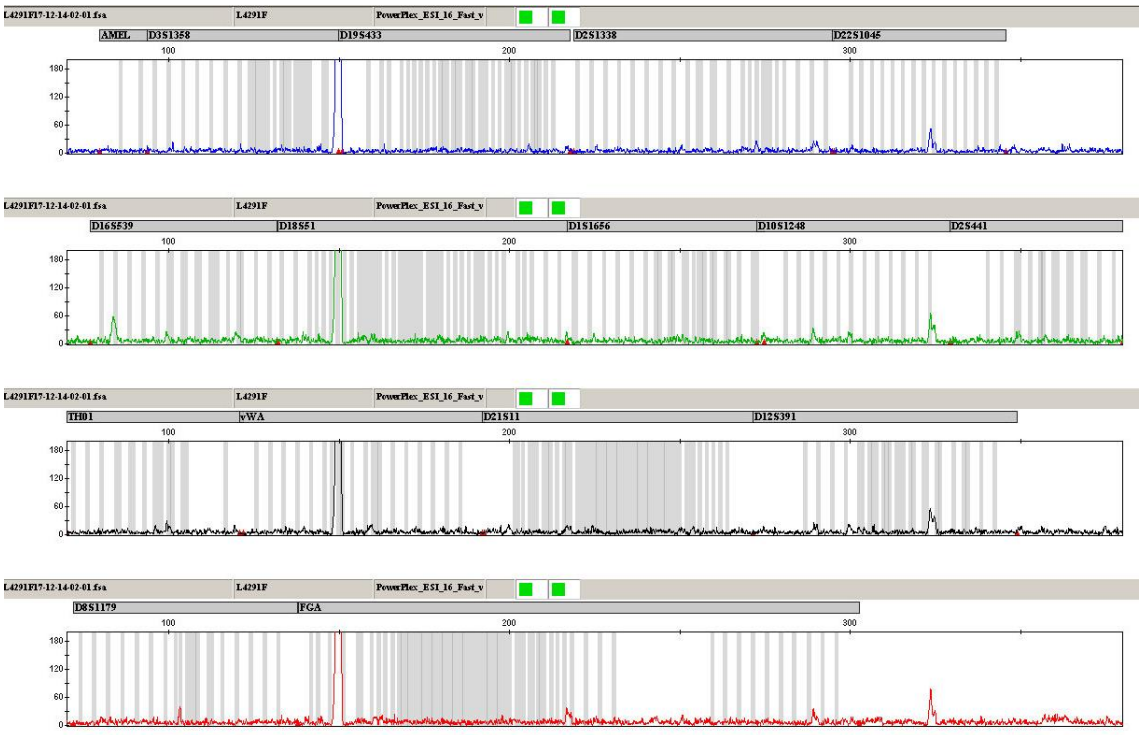

Figure B-72: Eriswell Skeleton 4291 femur electropherogram

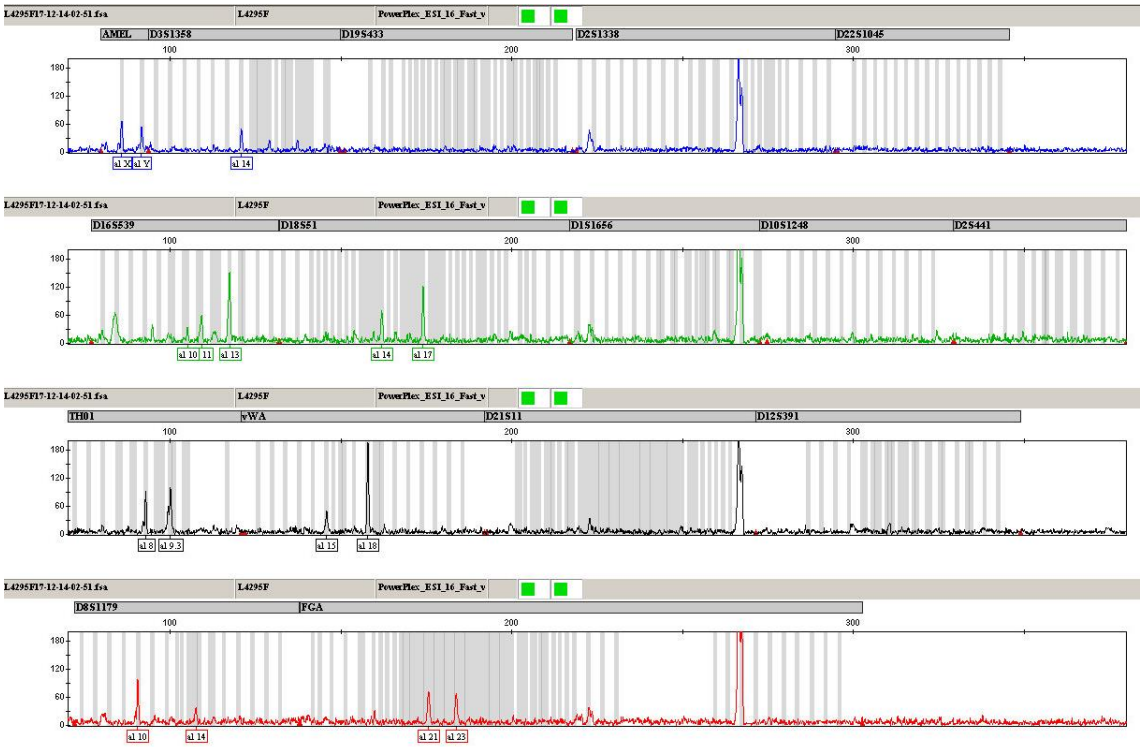

Figure B-73: Eriswell Skeleton 4295 femur electropherogram

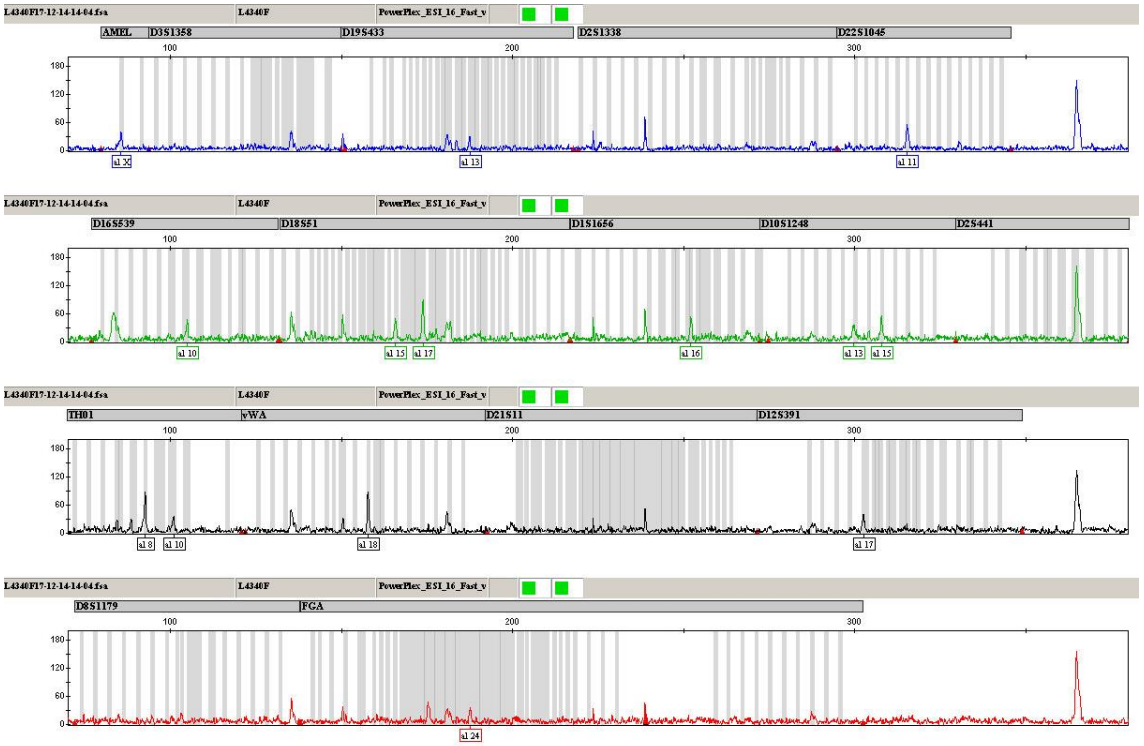

Figure B-74: Eriswell Skeleton 4340 femur electropherogram

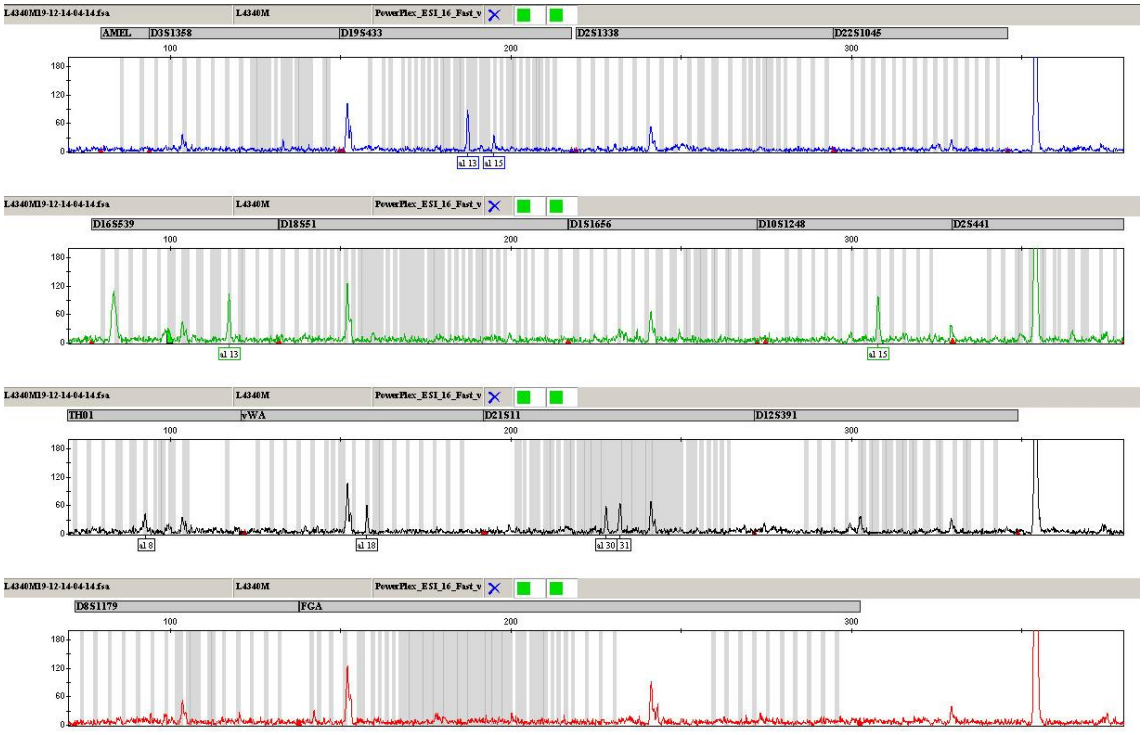

Figure B-75: Eriswell Skeleton 4340 metatarsal electropherogram

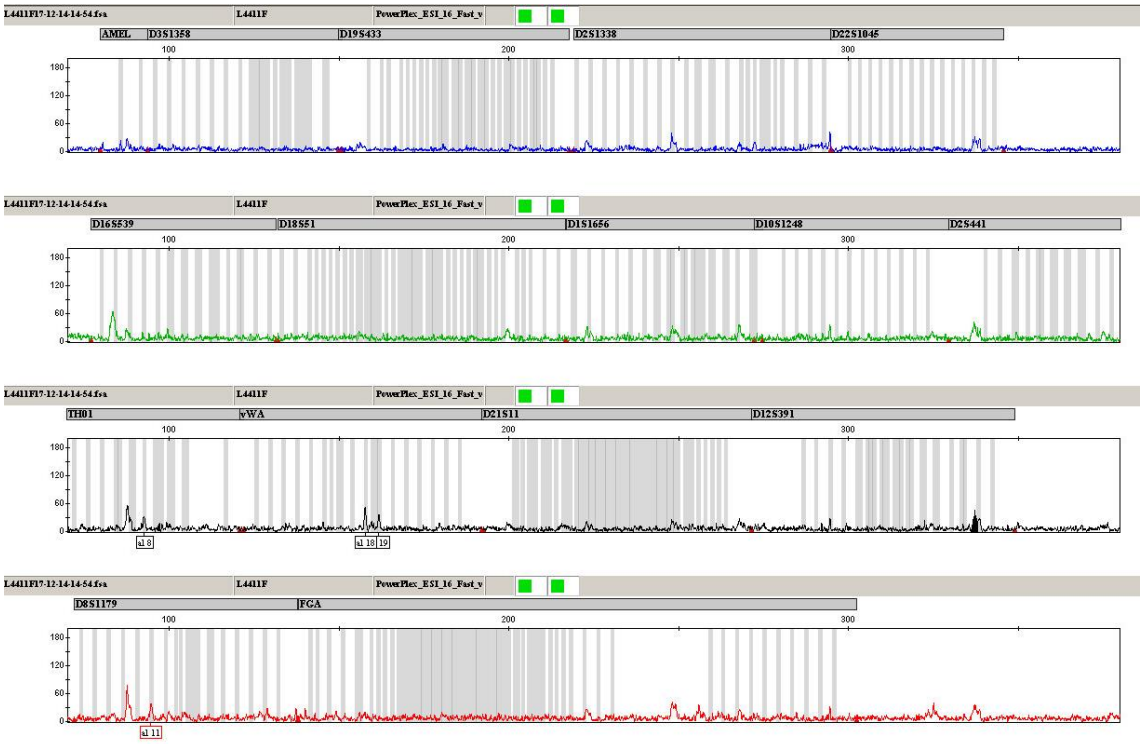

Figure B-76: Eriswell Skeleton 4411 femur electropherogram

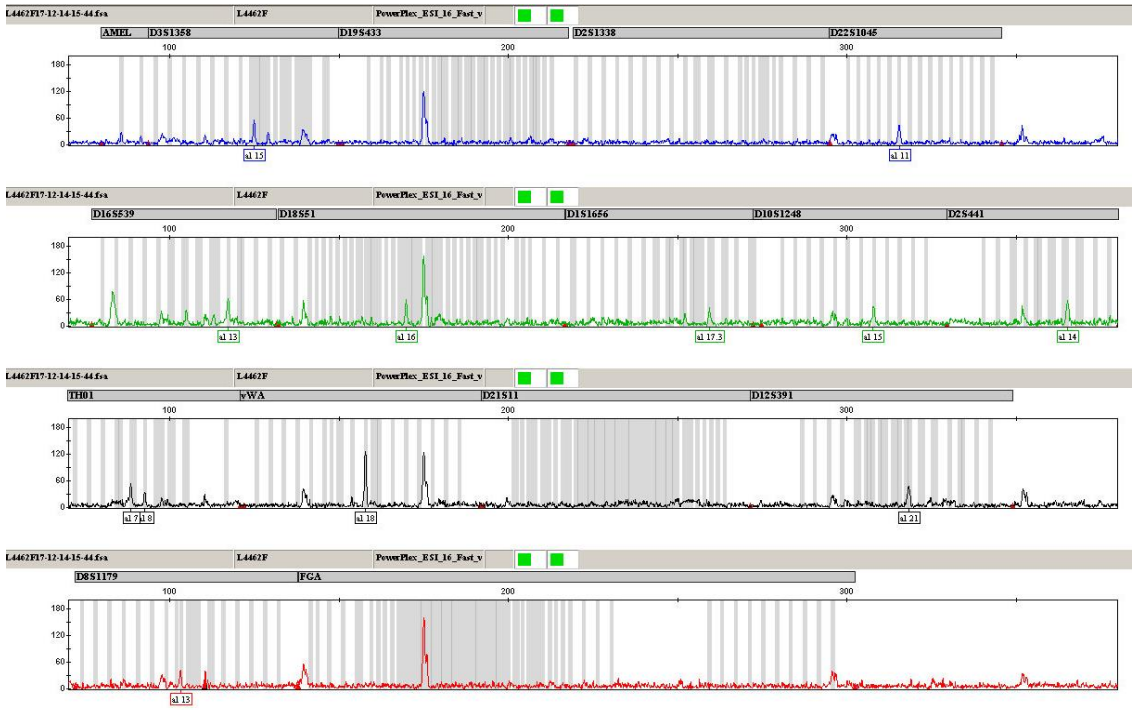

Figure B-77: Eriswell Skeleton 4462 femur electropherogram

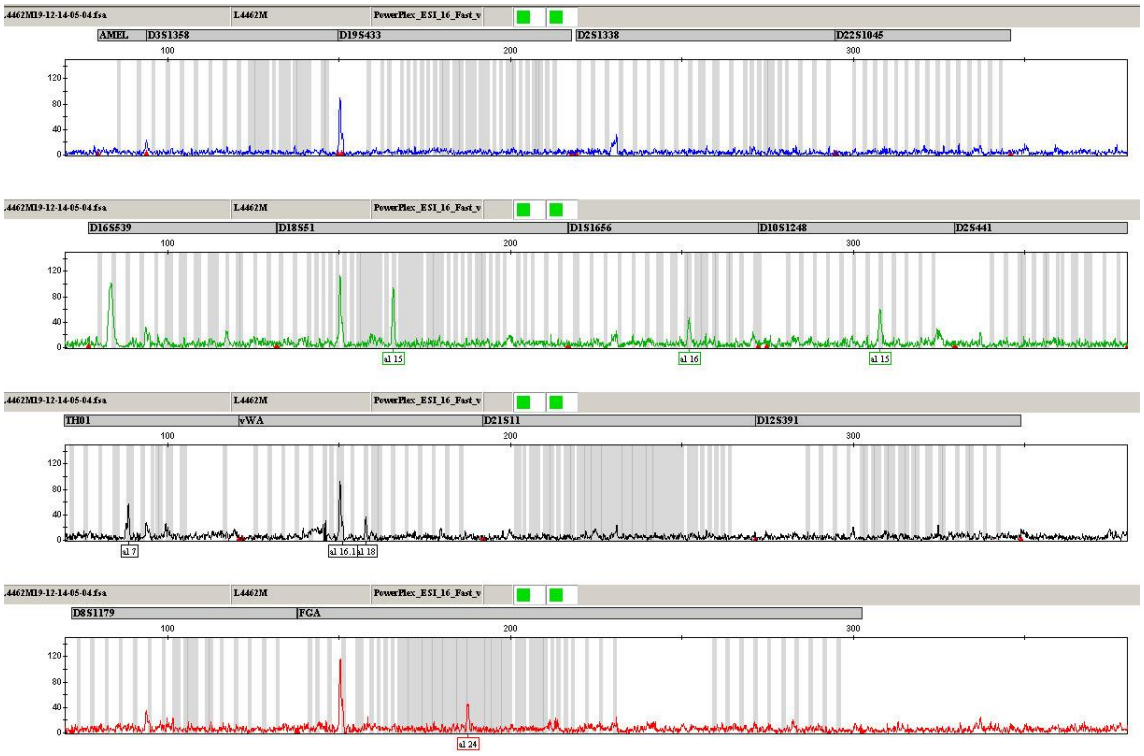

Figure B-78: Eriswell Skeleton 4462 metatarsal electropherogram

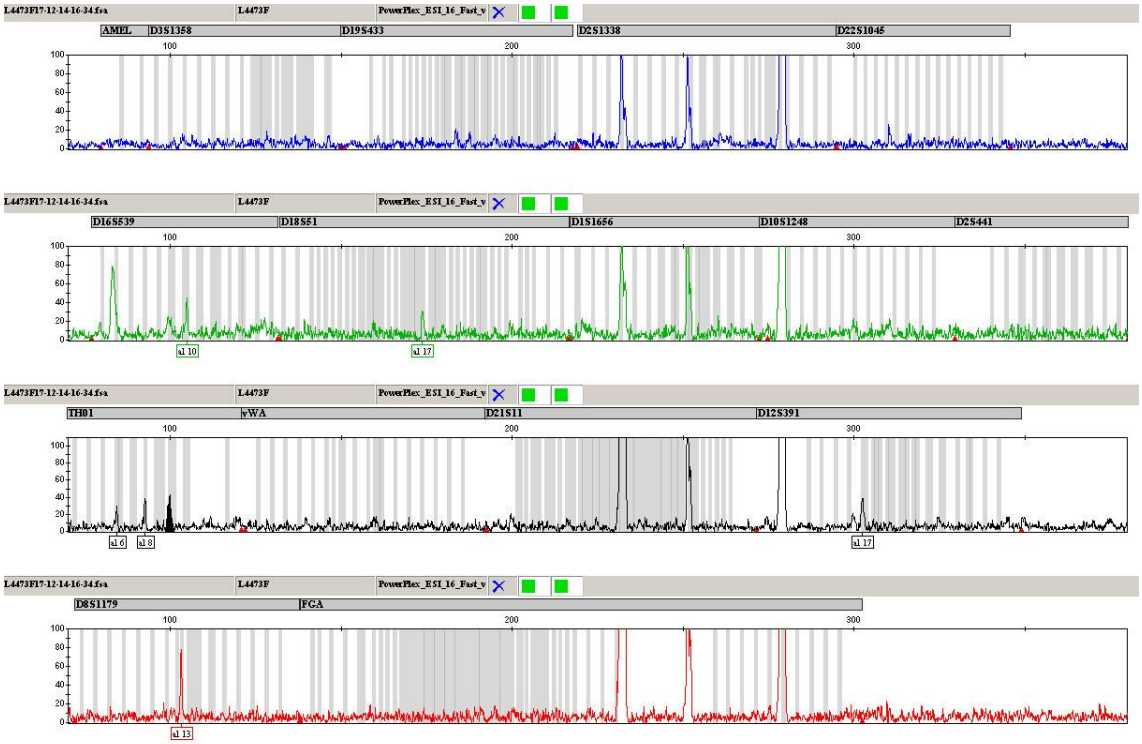

Figure B-79: Eriswell Skeleton 4473 femur electropherogram

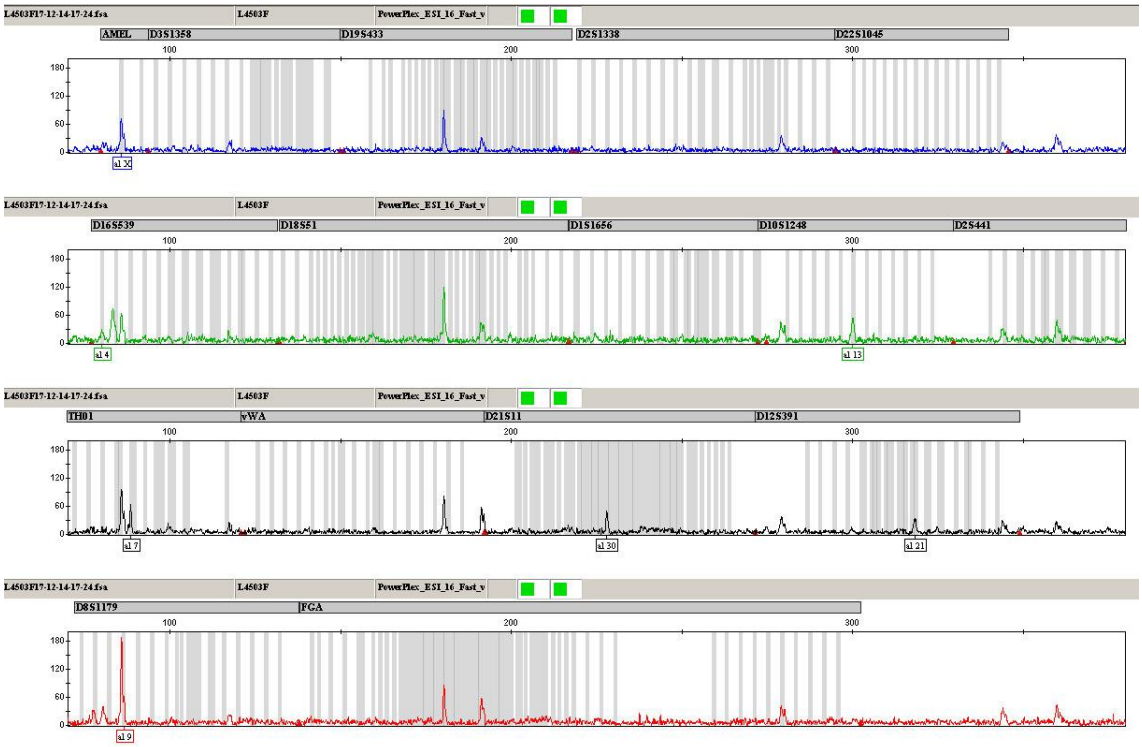

Figure B-80: Eriswell Skeleton 4503 femur electropherogram

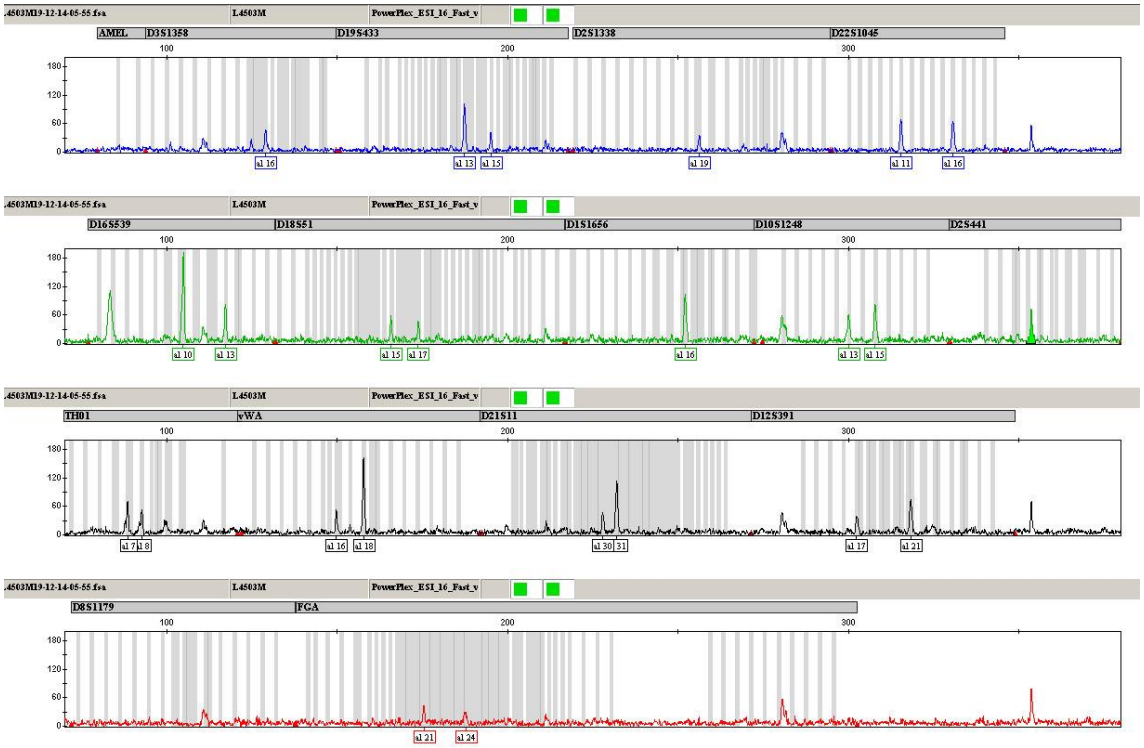

Figure B-81: Eriswell Skeleton 4503 metatarsal electropherogram

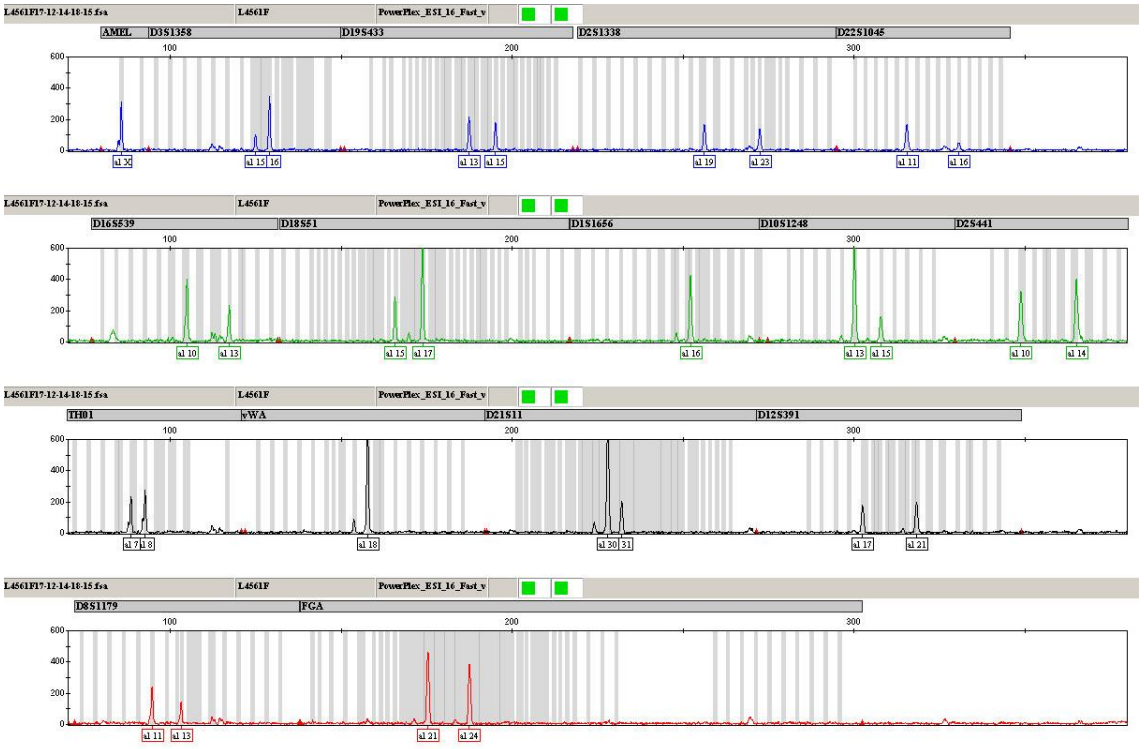

Figure B-82: Eriswell Skeleton 4561 femur electropherogram

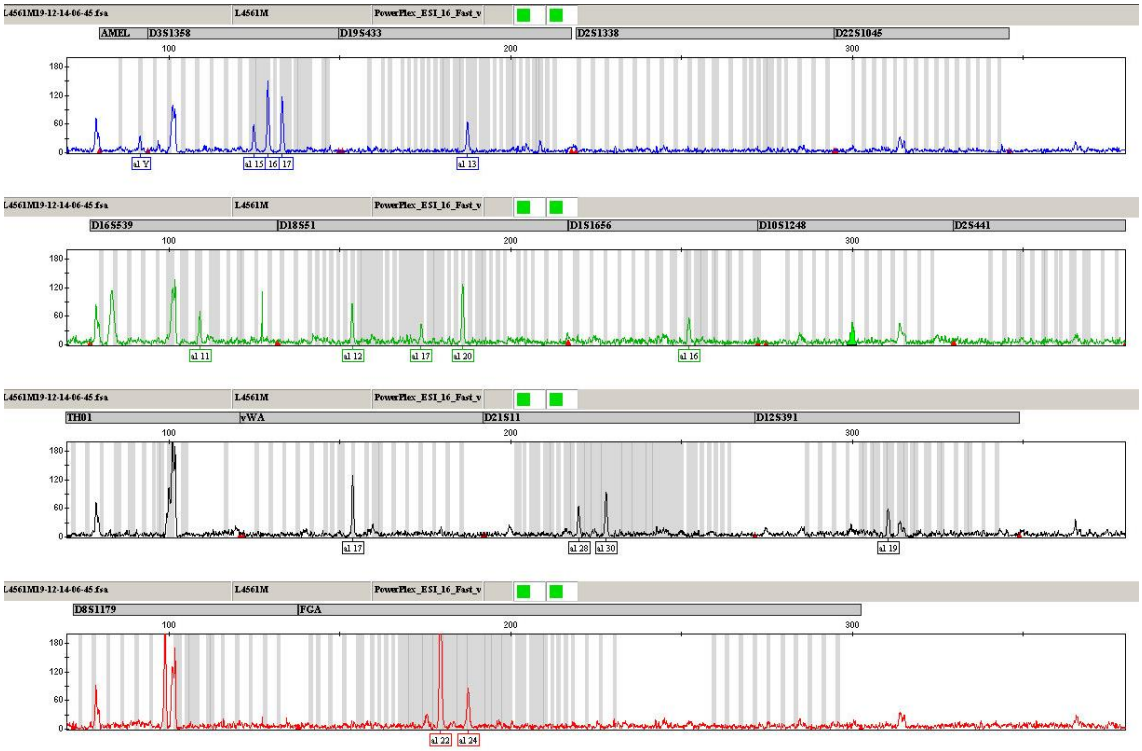

Figure B-83: Eriswell Skeleton 4561 metatarsal electropherogram

Appendix C : Recording sheets

Human Analogue Sample Sheet:

Burial environment:

Soil pH: Pre: Post:

Time duration:

Excavation observations:

Cutting observations:

SCE	Pre-burial			Post-burial			Post-surface Removal		
	L	a	b	L	a	b	L	a	b
Average									
Colour change									

EDTA:

Extractions:

	Date:	Weight:	Comments

PCRs:

Gels:

Human Remains Sample Sheet:

Burial environment:

Surface Observations:

SCE	Pre-surface Removal			Post-surface Removal		
	L	a	b	L	a	b
Average						
Colour change						

Weight:

EDTA:

Extractions:

	Date:	Weight:	Comments

PCRs:

Gels:

Fragment analysis:

Comments: